PB82-240219

Trace and Minor Element Reactions in Fluidized-Bed Combustion Processes

Westinghouse Research and Development Center
Pittsburgh, PA

Prepared for

Industrial Environmental Research Lab.
Research Triangle Park, NC

Jun 82

U.S. Department of Commerce
National Technical Information Service
NTIS

TECHNICAL REPORT DATA

(Please read Instructions on the reverse before completing)

1. REPORT NO. EPA-600/7-82-050

2. ORD Report

3. RECIPIENT'S ACCESSION NO. PB82 240219

4. TITLE AND SUBTITLE Trace and Minor Element Reactions in Fluidized-bed Combustion Processes

5. REPORT DATE June 1982

6. PERFORMING ORGANIZATION CODE

7. AUTHOR(S)
M.A. Alvin

8. PERFORMING ORGANIZATION REPORT NO.

9. PERFORMING ORGANIZATION NAME AND ADDRESS
Westinghouse Research and Development Center
1310 Beulah Road
Pittsburgh, Pennsylvania 15235

10. PROGRAM ELEMENT NO.

11. CONTRACT/GRANT NO.
68-02-3110, Task 5

12. SPONSORING AGENCY NAME AND ADDRESS
EPA, Office of Research and Development
Industrial Environmental Research Laboratory
Research Triangle Park, NC 27711

13. TYPE OF REPORT AND PERIOD COVERED
Task Final; 8/79-8/81

14. SPONSORING AGENCY CODE
EPA/600/13

15. SUPPLEMENTARY NOTES IERL-RTP project officer is John O. Milliken, Mail Drop 61, 191/541-7716.

16. ABSTRACT

The report gives results of thermodynamic equilibrium calculations for anticipated operating ranges for various fluidized-bed combustion (FBC) designs used to predict the potential volatility and interaction of 31 trace and minor elements contained in coal and sorbent feedstocks. The quantitative distribution of combustion products for trace and minor elements was predicted on the basis of assumptions concerning the multi-chemical reactions and interactions occurring throughout the FBC system. Predicted equilibrium concentrations for stack gas emissions and bottom ash material were correlated with in-field data for elemental partitioning. Potential pollutants of concern were identified based on discharge multimedia environmental goals (DMEGs). For the gaseous emissions stream, 13 elements were projected to exceed the DMEGs. For the solid waste stream, 15 elements were projected to exceed the land DMEGs. These predictions should be useful in identifying elements for sampling and analysis during future field testing of FBC emissions and solid waste. Further thermodynamic model refinements are recommended.

17. KEY WORDS AND DOCUMENT ANALYSIS

a. DESCRIPTORS		b. IDENTIFIERS/OPEN ENDED TERMS	c. COSATI Field/Group	
Pollution	Coal	Pollution Control	13B	08G,21D
Combustion	Sorbents	Stationary Sources	21B	11G
Fluidized Bed Processing	Reaction Kinetics		13H,07A	
	Volatility			20M
Trace Elements	Flue Gases		06A	
Chemical Analysis			07D	

18. DISTRIBUTION STATEMENT
Release to Public

19. SECURITY CLASS *(This Report)*
Unclassified

20. SECURITY CLASS *(This page)*
Unclassified

21. NO. OF PAGES
447

22. PRICE

PB82-240219

EPA [illegible]

EPA 600/7-82-050
June 1982

TRACE AND MINOR ELEMENT REACTIONS IN FLUIDIZED-BED COMBUSTION PROCESSES

by

M. A. Alvin

WESTINGHOUSE RESEARCH AND DEVELOPMENT CENTER
1310 Beulah Road
Pittsburgh, Pennsylvania 15235

Contract No. 68-02-3110 Task 5

EPA Project Officer: J. O. Milliken

Industrial Environmental Research Laboratory
Office of Environmental Engineering and Technology
Research Triangle Park, N.C. 27711

Prepared for:

U.S. ENVIRONMENTAL PROTECTION AGENCY
Office of Research and Development
Washington, D.C. 20460

REPRODUCED BY
NATIONAL TECHNICAL
INFORMATION SERVICE
U.S. DEPARTMENT OF COMMERCE
SPRINGFIELD, VA. 22161

NOTICE

Mention of trade names or commercial products does not consititute endorsement or recommendation for use.

ABSTRACT

In order to project the quantity and combustion product distribution for the trace and minor elements in coal and sorbent feedstock materials, one must define the multichemical reactions and interactions that occur throughout the fluidized-bed combustion (FBC) system. The potential volatility and the interaction of 27 trace and minor elements (Be, F, Hg, Pb, Co, Cr, Fe, Mo, Mn, Ni, Ti, Na, K, Br, B, P, Cu, V, Zn, Sb, Sn, Zr, As, Cd, Se, Ga, and Ge) with clay (Al, Si) and carbonate (Ca, Mg) constituents in the coal and sorbent were parametrically investigated on the basis of thermodynamic equilibrium calculations for anticipated operating ranges of different fluidized-bed combustor designs. The interactive calculations have defined $Al_2O_3 \cdot SiO_2$, $CaO \cdot MgO \cdot 2SiO_2$, $CaSiO_3$, Ca_2SiO_4, Mg_2SiO_4, $MgSiO_3$, $MgAl_2O_4$, $MgO \cdot Fe_2O_3$, $NiO \cdot Fe_2O_3$, $2NiO \cdot SiO_2$, $MnO \cdot Al_2O_3$, $Al_2O_3 \cdot TiO_2$, $3CaO \cdot TiO_2$, $CaO \cdot TiO_2$, $K_2Cr_2O_7$, $CoO \cdot Cr_2O_3$, $MgO \cdot Cr_2O_3$, $CaO \cdot MoO_3$, $MgO \cdot MoO_3$, $Mg_3(PO_4)_2$, $3CaO \cdot B_2O_5$, $xMgO \cdot V_2O_5$, $xCaO \cdot V_2O_5$, $xNaO \cdot V_2O_5$, $2Na_2O \cdot SiO_2$, $KAlSi_3O_8$, $BeAl_2O_4$, MgF_2, CaF_2, AlF_3, BeF_2, and FeF_3 as stable solids that have the potential to form during fluidized-bed combustion, thus minimizing the concentration of elements emitted from the stack. The equilibrium projections are correlated with in-field data that identify the elemental partitioning of stack-gas emissions and ash formations. The potential toxicity of the projected stack-gas emissions is also assessed.

Although release of volatiles from FBC systems is generally considered to be lower than release from conventional systems, on the basis of the thermodynamic model the concentrations of Be, F, Hg, Pb, Co, Br, Cu, As, Cd, and Se will exceed the accepted air minimum acute toxicity effluent (MATE) concentration for related species on a weight basis, if directly released from the combustor and emitted at the stack at ambient conditions for all process systems considered. The concentration of Cr

and P in the FBC effluent are also projected to exceed the reported air MATE level when combustion reactions with only C, H, N, O, S, and Cl are considered. These elements however, interact and complex with surrounding trace and minor constituents, minimizing their concentration within the FBC effluent to below the air MATE level. The volatility of Ge and its complexes is shown to depend on system pressure, and the off-gas Ge concentration is estimated to approach reported air MATE levels for atmospheric FBC operations. Similarly, the trace and minor element concentration in the resulting combustor solids is projected to exceed land MATE levels for related species containing Be, Co, Cr, Fe, Mn, Ni, Ti, V, Zn, Sb, Sn, Zr, and Ge. When Be and P interact with the surrounding trace and minor constituents, the concentrations of these elements within the resulting combustor solids are projected to exceed the reported land MATE levels.

The thermodynamic model serves as a guideline for projecting the potential of the various elements to form as possible pollutants in FBC systems. The elements that have been projected to exceed the accepted air and land MATE levels should be viewed only as potential FBC pollutants, with future efforts directed toward continuous monitoring of the FBC effluent streams for these species and chemical compounds.

TABLE OF CONTENTS

Page

1. INTRODUCTION 1

2. CONCLUSIONS 6

3. RECOMMENDATIONS 13

4. COMPOSITION OF FEEDSTOCK MATERIALS 15

5. TRACE AND MINOR ELEMENT BEHAVIOR DURING COMBUSTION 30

6. CRITERIA FOR THE SELECTION OF TRACE AND MINOR ELEMENTS USED IN THE PARAMETRIC EQUILIBRIUM INTERACTIVE PROJECTIONS 69

7. THERMODYNAMIC PROJECTIONS 82

Feedstock Trace and Minor Element Concentration 82
Fluidized-Bed Combustion Systems Design 84
The Chemical Equilibrium Calculation 90
Trace and Minor Element Reactions with Combustion Gases 100
    Beryllium 100
    Fluorine 101
    Mercury 105
    Lead 108
    Cobalt 113
    Chromium 116
    Iron 119
    Molybdenum 124
    Manganese 127
    Nickel 130
    Titanium 134
    Sodium 135
    Potassium 141

TABLE OF CONTENTS (Cont'd)

	Page
Aluminum	144
Silicon	149
Bromine	150
Boron	151
Phosphorus	156
Copper	159
Vanadium	162
Zinc	164
Antimony	168
Tin	172
Zirconium	172
Arsenic	176
Cadmium	179
Selenium	180
Gallium	183
Germanium	184
Summary of Trace and Minor Element Reactions in Fluidized-Bed Combustion Systems	187
Trace and Minor Element Interactions	205
C-H-N-O-S-Cl-Si-Al-K-Na	206
C-H-N-O-S-Cl-Si-Al-K-Na-Fe-Mn-Ni-Be	229
C-H-N-O-S-Cl-Si-Al-K-Na-Cr-Fe-Mo-Mn-Ti	241
C-H-N-O-S-Cl-Si-Al-K-Na-Ca-Mg-F-Be-Pb	250
C-H-N-O-S-Cl-Si-Al-K-Na-Ti-Mo-F-Be-Pb-Hg	260
C-H-N-O-S-Cl-Si-Al-K-Na-Ca-Mg-Fe-Ti-Ni	261
C-H-N-O-S-Cl-Si-Al-K-Na-Ca-Mg-Cr-Mn-Mo	262
C-H-N-O-S-Cl-Si-Al-K-Na-Co-Cr-Mg-Ni-Ca	262
C-H-N-O-S-Cl-Si-Al-K-Na-Ca-Mg-B-Br-V-P-Zn	264
C-H-N-O-S-Cl-Si-Al-K-Na-Br-F-Be-Hg-Pb-(Ca-Mg)	265
C-H-N-O-S-Cl-Si-Al-K-Na-Br-F-Fe-Mn-Ni	269

TABLE OF CONTENTS (Cont'd)

Page

C-H-N-O-S-Cl-Si-Al-K-Na-Br-F-Ti-B-P 271

C-H-N-O-S-Cl-Si-Al-K-Na-Br-F-Cu-Zn-Sb 271

C-H-N-O-S-Cl-Si-Al-K-Na-Br-F-Sn-Zr-As 274

C-H-N-O-S-Cl-Si-Al-K-Na-Br-F-Cd-Ga-Sb 274

C-H-N-O-S-Cl-Si-Al-K-Na-Br-F-Se-Mo-Pb 274

C-H-N-O-S-Cl-Si-Al-K-Na-Br-F-Ge-Co 278

C-H-N-O-S-Cl-Si-Al-K-Na-Zr-B-V 278

C-H-N-O-S-Cl-Si-Al-K-Na-Se-Pb-Ni-Cu-Sn 280

C-H-N-O-S-Cl-Si-Al-K-Na-Se-Cu-Ge-Cr-Fe 280

Comparison of the Equilibrium Product Distribution in Condensed and Gaseous Phases Formed During PFBC Using Eastern and Western U. S. Coals 280

Corrosive Condensate Formations in PFBC Systems 289

Combustion Gas Reactions with Cobalt- and Nickel-Based Alloys 297

Combustion Gas Reactions with Chromium-, Aluminum-, and Iron-Containing Alloys 303

Influence of Combustion Environments on Alloy-Deposit Reactions 310

Summary 322

8. SUMMARY OF THE TRACE AND MINOR ELEMENTAL INTERACTIONS - COMPARISON OF PROJECTED EMISSIONS AND PLANT DATA 326

Elemental Reactions and Interactions 326

Assessment of the Potential Toxicity of the Projected Trace and Minor Element Phases 332

Conventional Power Generating Systems 332

Fluidized-Bed Combustion Systems 334

Elemental Concentration in Ash Formations 338

Control Alternatives 352

TABLE OF CONTENTS (Cont'd)

Page

9. REFERENCES 355

APPENDIX

A. SUMMARY OF THE ELEMENTAL CONCENTRATIONS, CONSIDERED PHASES, AND EQUILIBRIUM REACTIONS 373

B. SOLUBILITY OF ALUMINOSILICATE COMPLEXES 397

C. CHEMICAL ANALYSIS OF TRACE AND MINOR ELEMENTS IN COMBUSTION PRODUCTS 400

LIST OF FIGURES

Page

1. Thermodynamics of Gettering Action of Aluminosilicates in Reducing Gaseous Potassium Emissions 26

2. Kaolin and Illite Crystal Structure and Potential Ion Exchange Sites 32

3. Phase Stability Diagram for $K_2O-Al_2O_3-SiO_2$ 36

4. Phase Stability Diagram for $Na_2O-Al_2O_3-SiO_2$ 37

5. Release of Na from Dolomite as a Function of Reaction Temperature 45

6. Release of K from Dolomite as a Function of Reaction Temperature 46

7. Alkali Concentration of Dolomites in ppm 52

8. Characterization by SEM of Tymochtee Dolomite Deposits in Fixed-Bed Pressurized Studies 53

9. Concentration of Trace and Minor Elements in Deposits from Glasshouse No. 10 and Tymochtee Dolomite Exposed to 1048 K and 825 kPa for 75 hr in 78% N_2/19.8% CO_2/2.2% O_2 54

10. Sodium and Potassium Concentration Retained in Geneva Dolomite after Exposure to Oxidizing and Reducing Gases 55

11. Alkali Concentration of Soluble and Insoluble Fractions of Chinook Coal Ash Fired at 1135 kPa in Simulated Fuel Gases 59

12. Particulate Material Deposited between 573 and 698 K from a 1023 K Fixed Bed of Chinook Coal Ash Exposed to 1114 kPa in 9.94% CO/16.1% CO_2/2.36% CH_4/23.4% H_2/42.2% N_2 for 5 Hours 60

13. Characterization by SEM of Tymochtee Dolomite/No. 10 Burgess Pigment Deposits in 1173 K Fixed-Bed Pressurized Studies 66

LIST OF FIGURES (Cont'd)

		Page
14.	Pressurized Fluidized-Bed Combustor Design for a 250 MW_e Combined-Cycle Plant	85
15.	Size Distributions for Ash in PFBC Systems	87
16.	Size Distributions for Sorbent Material in PFBC Systems	88
17.	Chemical Pathways in Fluidized-Bed Combustion Systems	89
18.	Combustion Gas Product Distribution for PFBC Systems Operating with 10% Excess Air and 90% Sulfur-Removal Efficiencies	94
19.	Combustion Gas Product Distribution for PFBC Systems Operating with 100% Excess Air and 90% Sulfur-Removal Efficiencies	95
20.	Combustion Gas Product Distribution for PFBC Systems Operating with 300% Excess Air and 90% Sulfur-Removal Efficiencies	96
21.	Combustion Gas Product Distribution for PFBC Systems Operating with 100% Excess Air and 0% Sulfur-Removal Efficiencies	97
22.	Combustion Gas Product Distribution for AFBC Systems Operating with 100% Excess Air and 0% Sulfur-Removal Efficiencies	98
23.	Percent Distribution of Solid $BeSO_4$ as a Function of Temperature and Pressure in a Fluidized-Bed Combustor Operating with 100% Excess Air and 90% Sulfur-Removal Efficiencies	102
24.	Percent Distribution of Solid BeO as a Function of Temperature and Pressure in a Fluidized-Bed Combustor Operating with 100% Excess Air and 90% Sulfur-Removal Efficiencies	102
25.	Percent Distribution of Gaseous $Be(OH)_2$ as a Function of Temperature and Pressure in a Fluidized-Bed Combustor Operating with 100% Excess Air and 90% Sulfur-Removal Efficiencies	103

LIST OF FIGURES (Cont'd)

Page

26. Percent Distribution of Gaseous $BeCl_2$ as a Function of Temperature and Pressure in a Fluidized-Bed Combustor Operating with 100% Excess Air and 90% Sulfur-Removal Efficiencies 103

27. Percent Distribution of Gaseous HF as a Function of Temperature and Pressure in a Fluidized-Bed Combustor Operating with 100% Excess Air and 90% Sulfur-Removal Efficiencies 104

28. Percent Distribution of Gaseous HSO_3F as a Function of Temperature and Pressure in a Fluidized-Bed Combustor Operating with 100% Excess Air and 90% Sulfur-Removal Efficiencies 104

29. Percent Distribution of Gaseous $HgCl_2$ as a Function of Temperature and Pressure in a Fluidized-Bed Combustor Operating with 100% Excess Air and 90% Sulfur-Removal Efficiencies 106

30. Percent Distribution of Gaseous Hg as a Function of Temperature and Pressure in a Fluidized-Bed Combustor Operating with 100% Excess Air and 90% Sulfur-Removal Efficiencies 106

31. Percent Distribution of Gaseous HgO as a Function of Temperature and Pressure in a Fluidized-Bed Combustor Operating with 100% Excess Air and 90% Sulfur-Removal Efficiencies 107

32. Percent Distribution of Feedstock Lead as a Function of Temperature and Pressure in a Fluidized-Bed Combustor Operating with 10% Excess Air and 90% Sulfur-Removal Efficiencies 109

33. Percent Distribution of Gaseous $PbCl_4$ as a Function of Temperature and Pressure in a Fluidized-Bed Combustor Operating with 100% Excess Air and 90% Sulfur-Removal Efficiencies 111

34. Percent Distribution of Gaseous $PbCl_2$ as a Function of Temperature and Pressure in a Fluidized-Bed Combustor Operating with 100% Excess Air and 90% Sulfur-Removal Efficiencies 111

LIST OF FIGURES (Cont'd)

Page

35. Percent Distribution of Gaseous PbCl as a Function of Temperature and Pressure in a Fluidized-Bed Combustor Operating with 100% Excess Air and 90% Sulfur-Removal Efficiencies 112

36. Percent Distribution of Gaseous PbO as a Function of Temperature and Pressure in a Fluidized-Bed Combustor Operating with 100% Excess Air and 90% Sulfur-Removal Efficiencies 112

37. Percent Distribution of Solid $CoSO_4$ as a Function of Temperature and Pressure in a Fluidized-Bed Combustor Operating with 100% Excess Air and 90% Sulfur-Removal Efficiencies 114

38. Percent Distribution of Solid Co_3O_4 as a Function of Temperature and Pressure in a Fluidized-Bed Combustor Operating with 100% Excess Air and 90% Sulfur-Removal Efficiencies 114

39. Percent Distribution of Solid CoO as a Function of Temperature and Pressure in a Fluidized-Bed Combustor Operating with 100% Excess Air and 90% Sulfur-Removal Efficiencies 115

40. Percent Distribution of Gaseous $CoCl_2$ as a Function of Temperature and Pressure in a Fluidized-Bed Combustor Operating with 100% Excess Air and 90% Sulfur-Removal Efficiencies 115

41. Percent Distribution of Solid CrO_2 as a Function of Temperature and Pressure in a Fluidized-Bed Combustor Operating with 100% Excess Air and 90% Sulfur-Removal Efficiencies 117

42. Percent Distribution of Solid Cr_2O_3 as a Function of Temperature and Pressure in a Fluidized-Bed Combustor Operating with 100% Excess Air and 90% Sulfur-Removal Efficiencies 117

43. Percent Distribution of Gaseous CrO_2Cl_2 as a Function of Temperature and Pressure in a Fluidized-Bed Combustor Operating with 100% Excess Air and 90% Sulfur-Removal Efficiencies 118

LIST OF FIGURES (Cont'd)

Page

44. Percent Distribution of Gaseous CrO_4H_2 as a Function of Temperature and Pressure in a Fluidized-Bed Combustor Operating with 100% Excess Air and 90% Sulfur-Removal Efficiencies 118

45. Percent Distribution of Gaseous CrO_2OH as a Function of Temperature and Pressure in a Fluidized-Bed Combustor Operating with 100% Excess Air and 90% Sulfur-Removal Efficiencies 120

46. Percent Distribution of Gaseous CrO_3 as a Function of Temperature and Pressure in a Fluidized-Bed Combustor Operating with 100% Excess Air and 90% Sulfur-Removal Efficiencies 120

47. Percent Distribution of Solid Fe_2O_3 as a Function of Temperature and Pressure in a Fluidized-Bed Combustor Operating with 100% Excess Air and 90% Sulfur-Removal Efficiencies 123

48. Percent Distribution of Solid $Fe_2(SO_4)_3$ as a Function of Temperature and Pressure in a Fluidized-Bed Combustor Operating with 100% Excess Air and 90% Sulfur-Removal Efficiencies 123

49. Percent Distribution of Solid MoO_3 as a Function of Temperature and Pressure in a Fluidized-Bed Combustor Operating with 100% Excess Air and 90% Sulfur-Removal Efficiencies 125

50. Percent Distribution of Gaseous $MoO_2(OH)_2$ as a Function of Temperature and Pressure in a Fluidized-Bed Combustor Operating with 100% Excess Air and 90% Sulfur-Removal Efficiencies 125

51. Percent Distribution of Gaseous MoO_2Cl_2 as a Function of Temperature and Pressure in a Fluidized-Bed Combustor Operating with 100% Excess Air and 90% Sulfur-Removal Efficiencies 126

52. Percent Distribution of Solid $MnSO_4$ as a Function of Temperature and Pressure in a Fluidized-Bed Combustor Operating with 100% Excess Air and 90% Sulfur-Removal Efficiencies 128

LIST OF FIGURES (Cont'd)

Page

53. Percent Distribution of Solid Mn_2O_3 as a Function of Temperature and Pressure in a Fluidized-Bed Combustor Operating with 100% Excess Air and 90% Sulfur-Removal Efficiencies 128

54. Percent Distribution of Solid Mn_3O_4 as a Function of Temperature and Pressure in a Fluidized-Bed Combustor Operating with 100% Excess Air and 90% Sulfur-Removal Efficiencies 129

55. Percent Distribution of Gaseous $MnCl_2$ as a Function of Temperature and Pressure in a Fluidized-Bed Combustor Operating with 100% Excess Air and 90% Sulfur-Removal Efficiencies 129

56. Percent Distribution of Solid $NiSO_4$ as a Function of Temperature and Pressure in a Fluidized-Bed Combustor Operating with 100% Excess Air and 90% Sulfur-Removal Efficiencies 131

57. Percent Distribution of Solid NiO as a Function of Temperature and Pressure in a Fluidized-Bed Combustor Operating with 100% Excess Air and 90% Sulfur-Removal Efficiencies 131

58. Percent Distribution of Gaseous $NiCl_2$ as a Function of Temperature and Pressure in a Fluidized-Bed Combustor Operating with 100% Excess Air and 90% Sulfur-Removal Efficiencies 132

59. Percent Distribution of Gaseous $Ni(OH)_2$ as a Function of Temperature and Pressure in a Fluidized-Bed Combustor Operating with 100% Excess Air and 90% Sulfur-Removal Efficiencies 132

60. Percent Distribution of Gaseous NiCl as a Function of Temperature and Pressure in a Fluidized-Bed Combustor Operating with 100% Excess Air and 90% Sulfur-Removal Efficiencies 133

61. Percent Distribution of Solid TiO_2 as a Function of Temperature and Pressure in a Fluidized-Bed Combustor Operating with 100% Excess Air and 90% Sulfur-Removal Efficiencies 133

LIST OF FIGURES (Cont'd)

		Page
62.	Equilibrium Pressure of NaOH(g) and NaCl(g) over Na_2SO_4(s) Exposed to Steam and HCl(g) under Fluidized-Bed Combustor Gas Phase Conditions	138
63.	Percent Distribution of Condensed $NaSO_4$ as a Function of Temperature and Pressure in a Fluidized-Bed Combustor Operating with 100% Excess Air and 90% Sulfur-Removal Efficiencies	139
64.	Percent Distribution of Gaseous NaCl as a Function of Temperature and Pressure in a Fluidized-Bed Combustor Operating with 100% Excess Air and 90% Sulfur-Removal Efficiencies	139
65.	Stability of Na_2SO_4 in a Fluidized-Bed Combustor Operating with 316% Excess Air at 1157 K and 404 kPa	140
66.	Stability of Na_2SO_4 in a Fluidized-Bed Combustor Operating with 316% Excess Air at 1157 K and 1114 kPa	140
67.	Percent Distribution of Solid K_2SO_4 as a Function of Temperature and Pressure in a Fluidized-Bed Combustor Operating with 100% Excess Air and 90% Sulfur-Removal Efficiencies	142
68.	Percent Distribution of Gaseous KCl as a Function of Temperature and Pressure in a Fluidized-Bed Combustor Operating with 100% Excess Air and 90% Sulfur-Removal Efficiencies	142
69.	Percent Distribution of Gaseous K_2SO_4 as a Function of Temperature and Pressure in a Fluidized-Bed Combustor Operating with 100% Excess Air and 90% Sulfur-Removal Efficiencies	143
70.	Percent Distribution of Gaseous KOH as a Function of Temperature and Pressure in a Fluidized-Bed Combustor Operating with 100% Excess Air and 90% Sulfur-Removal Efficiencies	143
71.	Stability of $Na_2SO_4 \cdot K_2SO_4$ Eutectic in a Fluidized-Bed Combustor Operating with 316% Excess Air at 1110 K and 404 kPa	145

LIST OF FIGURES (Cont'd)

Page

72. Percent Distribution of Solid Al_2O_3 as a Function of Temperature and Pressure in a Fluidized-Bed Combustor Operating with 100% Excess Air and 90% Sulfur-Removal Efficiencies 146

73. Percent Distribution of Solid $Al_2(SO_4)_3$ as a Function of Temperature and Pressure in a Fluidized-Bed Combustor Operating with 100% Excess Air and 90% Sulfur-Removal Efficiencies 146

74. Percent Distribution of Solid $Al_2O_3 \cdot H_2O$ as a Function of Temperature and Pressure in a Fluidized-Bed Combustor Operating with 100% Excess Air and 90% Sulfur-Removal Efficiencies 148

75. Percent Distribution of Solid $Al(OH)_3$ as a Function of Temperature and Pressure in a Fluidized-Bed Combustor Operating with 100% Excess Air and 90% Sulfur-Removal Efficiencies 148

76. Percent Distribution of Solid SiO_2 as a Function of Temperature and Pressure in a Fluidized-Bed Combustor Operating with 100% Excess Air and 90% Sulfur-Removal Efficiencies 150

77. Percent Distribution of Gaseous BrCl as a Function of Temperature and Pressure in a Fluidized-Bed Combustor Operating with 100% Excess Air and 90% Sulfur-Removal Efficiencies 152

78. Percent Distribution of Gaseous Br as a Function of Temperature and Pressure in a Fluidized-Bed Combustor Operating with 100% Excess Air and 90% Sulfur-Removal Efficiencies 152

79. Percent Distribution of Gaseous Br_2 as a Function of Temperature and Pressure in a Fluidized-Bed Combustor Operating with 100% Excess Air and 90% Sulfur-Removal Efficiencies 153

80. Percent Distribution of Gaseous BrH as a Function of Temperature and Pressure in a Fluidized-Bed Combustor Operating with 100% Excess Air and 90% Sulfur-Removal Efficiencies 153

LIST OF FIGURES (Cont'd)

Page

81. Percent Distribution of Solid H_3BO_3 as a Function of Temperature and Pressure in a Fluidized-Bed Combustor Operating with 100% Excess Air and 90% Sulfur-Removal Efficiencies 154

82. Percent Distribution of Solid HBO_2 as a Function of Temperature and Pressure in a Fluidized-Bed Combustor Operating with 100% Excess Air and 90% Sulfur-Removal Efficiencies 154

83. Percent Distribution of Gaseous H_3BO_3 as a Function of Temperature and Pressure in a Fluidized-Bed Combustor Operating with 100% Excess Air and 90% Sulfur-Removal Efficiencies 155

84. Percent Distribution of Gaseous HBO_2 as a Function of Temperature and Pressure in a Fluidized-Bed Combustor Operating with 100% Excess Air and 90% Sulfur-Removal Efficiencies 155

85. Percent Distribution of Condensed H_3PO_4 as a Function of Temperature and Pressure in a Fluidized-Bed Combustor Operating with 100% Excess Air and 90% Sulfur-Removal Efficiencies 157

86. Percent Distribution of Gaseous $(P_2O_5)_2$ as a Function of Temperature and Pressure in a Fluidized-Bed Combustor Operating with 100% Excess Air and 90% Sulfur-Removal Efficiencies 157

87. Percent Distribution of Gaseous PO_2 as a Function of Temperature and Pressure in a Fluidized-Bed Combustor Operating with 100% Excess Air and 90% Sulfur-Removal Efficiencies 158

88. Percent Distribution of Gaseous Cu_3Cl_3 as a Function of Temperature and Pressure in a Fluidized-Bed Combustor Operating with 100% Excess Air and 90% Sulfur-Removal Efficiencies 160

89. Percent Distribution of Gaseous CuCl as a Function of Temperature and Pressure in a Fluidized-Bed Combustor Operating with 100% Excess Air and 90% Sulfur-Removal Efficiencies 160

LIST OF FIGURES (Cont'd)

Page

90. Percent Distribution of Gaseous CuO as a Function of Temperature and Pressure in a Fluidized-Bed Combustor Operating with 100% Excess Air and 90% Sulfur-Removal Efficiencies 161

91. Percent Distribution of Solid $CuSO_4$ as a Function of Temperature and Pressure in a Fluidized-Bed Combustor Operating with 100% Excess Air and 90% Sulfur-Removal Efficiencies 161

92. Percent Distribution of Solid $CuO \cdot CuSO_4$ as a Function of Temperature and Pressure in a Fluidized-Bed Combustor Operating with 100% Excess Air and 90% Sulfur-Removal Efficiencies 162

93. Percent Distribution of Condensed V_2O_5 as a Function of Temperature and Pressure in a Fluidized-Bed Combustor Operating with 100% Excess Air and 90% Sulfur-Removal Efficiencies 163

94. Percent Distribution of Solid $ZnSO_4 \cdot H_2O$ as a Function of Temperature and Pressure in a Fluidized-Bed Combustor Operating with 100% Excess Air and 90% Sulfur-Removal Efficiencies 165

95. Percent Distribution of Solid $ZnSO_4 \cdot 7H_2O$ as a Function of Temperature and Pressure in a Fluidized-Bed Combustor Operating with 100% Excess Air and 90% Sulfur-Removal Efficiencies 165

96. Percent Distribution of Solid $ZnSO_4$ as a Function of Temperature and Pressure in a Fluidized-Bed Combustor Operating with 100% Excess Air and 90% Sulfur-Removal Efficiencies 166

97. Percent Distribution of Solid ZnO as a Function of Temperature and Pressure in a Fluidized-Bed Combustor Operating with 100% Excess Air and 90% Sulfur-Removal Efficiencies 166

98. Percent Distribution of Solid SbO_2 as a Function of Temperature and Pressure in a Fluidized-Bed Combustor Operating with 100% Excess Air and 90% Sulfur-Removal Efficiencies 169

LIST OF FIGURES (Cont'd)

Page

99. Percent Distribution of Gaseous SbO as a Function of Temperature and Pressure in a Fluidized-Bed Combustor Operating with 100% Excess Air and 90% Sulfur-Removal Efficiencies 169

100. Percent Distribution of Gaseous $SbCl_3$ as a Function of Temperature and Pressure in a Fluidized-Bed Combustor Operating with 100% Excess Air and 90% Sulfur-Removal Efficiencies 170

101. Percent Distribution of Gaseous SbCl as a Function of Temperature and Pressure in a Fluidized-Bed Combustor Operating with 100% Excess Air and 90% Sulfur-Removal Efficiencies 170

102. Percent Distribution of Solid SnO_2 as a Function of Temperature and Pressure in a Fluidized-Bed Combustor Operating with 100% Excess Air and 90% Sulfur-Removal Efficiencies 174

103. Percent Distribution of Gaseous SnO as a Function of Temperature and Pressure in a Fluidized-Bed Combustor Operating with 100% Excess Air and 90% Sulfur-Removal Efficiencies 174

104. Percent Distribution of Gaseous $SnCl_2$ as a Function of Temperature and Pressure in a Fluidized-Bed Combustor Operating with 100% Excess Air and 90% Sulfur-Removal Efficiencies 175

105. Percent Distribution of Solid ZrO_2 as a Function of Temperature and Pressure in a Fluidized-Bed Combustor Operating with 100% Excess Air and 90% Sulfur-Removal Efficiencies 175

106. Percent Distribution of Solid As_2O_5 as a Function of Temperature and Pressure in a Fluidized-Bed Combustor Operating with 100% Excess Air and 90% Sulfur-Removal Efficiencies 177

107. Percent Distribution of Gaseous AsCl as a Function of Temperature and Pressure in a Fluidized-Bed Combustor Operating with 100% Excess Air and 90% Sulfur-Removal Efficiencies 177

LIST OF FIGURES (Cont'd)

Page

108. Percent Distribution of Gaseous AsO as a Function of Temperature and Pressure in a Fluidized-Bed Combustor Operating with 100% Excess Air and 90% Sulfur-Removal Efficiencies 178

109. Percent Distribution of Gaseous $AsCl_3$ as a Function of Temperature and Pressure in a Fluidized-Bed Combustor Operating with 100% Excess Air and 90% Sulfur-Removal Efficiencies 178

110. Percent Distribution of Solid $CdSO_4$ as a Function of Temperature and Pressure in a Fluidized-Bed Combustor Operating with 100% Excess Air and 90% Sulfur-Removal Efficiencies 181

111. Percent Distribution of Gaseous CdO as a Function of Temperature and Pressure in a Fluidized-Bed Combustor Operating with 100% Excess Air and 90% Sulfur-Removal Efficiencies 181

112. Percent Distribution of Gaseous Cd as a Function of Temperature and Pressure in a Fluidized-Bed Combustor Operating with 100% Excess Air and 90% Sulfur-Removal Efficiencies 182

113. Percent Distribution of Gaseous CdCl as a Function of Temperature and Pressure in a Fluidized-Bed Combustor Operating with 100% Excess Air and 90% Sulfur-Removal Efficiencies 182

114. Percent Distribution of Gaseous SeO as a Function of Temperature and Pressure in a Fluidized-Bed Combustor Operating with 100% Excess Air and 90% Sulfur-Removal Efficiencies 183

115. Percent Distribution of Solid Ga_2O_3 as a Function of Temperature and Pressure in a Fluidized-Bed Combustor Operating with 100% Excess Air and 90% Sulfur-Removal Efficiencies 185

116. Percent Distribution of Gaseous GaCl as a Function of Temperature and Pressure in a Fluidized-Bed Combustor Operating with 100% Excess Air and 90% Sulfur-Removal Efficiencies 185

LIST OF FIGURES (Cont'd)

Page

117. Percent Distribution of Solid GeO_2 as a Function of Temperature and Pressure in a Fluidized-Bed Combustor Operating with 100% Excess Air and 90% Sulfur-Removal Efficiencies 186

118. Percent Distribution of Gaseous GeO as a Function of Temperature and Pressure in a Fluidized-Bed Combustor Operating with 100% Excess Air and 90% Sulfur-Removal Efficiencies 186

119. Gettering Activity of $KAlSi_3O_8$ in 100% Excess Air Fluidized-Bed Combustion Systems Operating at 1013 kPa Total Pressure 216

120. Three-Dimensional Display of Volatile and Condensed Potassium Phases in Fluidized-Bed Combustion Systems 221

121. Primary and Secondary Alkali Reactions during Combustion 230

122. Partial Pressure of Volatile Equilibrium Phases Formed in PFBC of C-H-N-O-S-Cl-Si-Al-K-Na-Br-F-Be-Hg-Pb in 100% Excess Air, 90% Sulfur Removal at 1013 kPa 266

123. Condensed Alkali Phases Formed as a Function of Temperature, Sulfur and Chlorine Content in 1013 kPa FBC Systems Operating with 100% Excess Air and 100% Sodium Release from Feedstock Materials 291

124. Condensed Alkali Phases Formed as a Function of Temperature, Sulfur and Chlorine Content in 1013 kPa FBC Systems Operating with 100% Excess Air and 1% Sodium Release from Feedstock Materials 293

125. Condensed Alkali and Vanadate Phases Formed as a Function of Temperature, Sulfur and Chlorine Content in 1013 kPa FBC Systems Operating with 100% Excess Air and 1% Sodium Release from Feedstock Materials 294

126. Composition of Sodium-Cobalt Complexes Formed as a Function of Temperature for 96% Sulfur-Removal, 405.2 kPa Systems 299

127. Composition of Sodium-Nickel Complexes Formed as a Function of Temperature for 96% Sulfur-Removal, 405.2 kPa Systems 299

LIST OF FIGURES (Cont'd)

Page

128. Equilibrium Phase Diagram for $Na_2SO_4 \cdot 47.8\%\ CoSO_4$ Eutectic as a Function of Temperature and Sulfur Activity at 405.2 kPa 316

129. Equilibrium Phase Diagram for $Na_2SO_4 \cdot 55\%\ NiSO_4$ Eutectic as a Function of Temperature and Sulfur Activity at 405.2 kPa 301

130. Pressure Dependence on the Cobalt Sulfate-Oxide Transition in the $Na_2SO_4 \cdot CoSO_4$ Eutectic for 96% Sulfur-Removal Systems as a Function of Temperature 304

131. Pressure Dependence on the Nickel Sulfate-Oxide Transition in the $Na_2SO_4 \cdot NiSO_4$ Eutectic for 96% Sulfur-Removal Systems as a Function of Temperature 304

132. Percent Volatilization of Solid Cr_2O_3 as a Function of Temperature and Pressure 306

133. Pressure Dependence on the Stability of $CoO \cdot Cr_2O_3$ Spinel in Na_2SO_4 for 96% Sulfur-Removal Systems as a Function of Temperature 308

134. Pressure Dependence on the Aluminum Sulfate-Oxide Transition in the $Na_2SO_4 \cdot Al_2(SO_4)_3$ Eutectic for 96% Sulfur-Removal Systems as a Function of Temperature 308

135. Equilibrium Phase Diagram for $Na_2SO_4 \cdot 17.6\%\ Al_2(SO_4)_3$ Eutectic as a Function of Temperature and Sulfur Activity at 405.2 kPa 309

136. Pressure Dependence on the Iron Sulfate-Oxide Transition in the $Na_2SO_4 \cdot Fe_2(SO_4)_3$ Eutectic for 96% Sulfur-Removal Systems as a Function of Temperature 311

137. Equilibrium Phase Diagram for $Na_2SO_4 \cdot 18\%\ Fe_2(SO_4)_3$ Eutectic as a Function of Temperature and Sulfur Activity at 405.2 kPa 312

138. Co/Ni/Cr/Al-O-S Phase Stability Diagram at 894 K 314

139. Co/Ni/Cr/Al-O-S Phase Stability Diagram at 1366 K 315

LIST OF FIGURES (Cont'd)

Page

140. Direct Interaction between Gaseous Alkali, Sulfur, and Oxygen with a Cobalt-Based Alloy Demonstrating the Resulting Equilibrium Phases at Temperatures of 1300 K and 950 K as a Function of Variable Oxygen Partial Pressures 316

141. Stability of Sodium Sulfate as a Function of Temperature and Pressure in Combustion Gases Containing Variable Concentrations of Sodium and Sulfur Oxides 320

142. Equilibrium Phase Diagram for Na_2SO_4·47.8% $CoSO_4$ Eutectic as a Function of Temperature and Sulfur Activity at 405.2 kPa in the Presence of 100% Chlorine Release from U.S. Mean Coals 323

143. Principal Reaction Pathways of Trace and Minor Elements during Combustion 327

LIST OF TABLES

Page

1. Minerals Identified in Coals 16

2. Classification of Trace and Minor Elements in Coal 19

3. Concentration of Trace and Minor Elements in Coals throughout the United States 20

4. Average Trace Element Concentration of Ash from U.S. Coals of Various Rank 21

5. Sulfur Variation in Coal throughout the United States 22

6. Analysis by Emission Spectroscopy of Trace Impurities in Selected U.S. Limestones and Dolomites 24

7. Concentration of Ca, Mg, Na, K, and Cl in Sorbent Materials 25

8. Concentration of Trace and Minor Elements in Kaolin, Pittsburgh Ash, Chinook Coal Ash, Renton Char, and Minnehaha Char as Determined by Emission Spectroscopy 28

9. Distribution of Alkali within Aluminosilicate Materials 29

10. Trace Element Concentration as a Function of Particle Size as Reported by Lyon 42

11. Trace Element Concentration as a Function of Particle Size as Reported by Cowherd 43

12. Trace Element Concentration as a Function of Particle Size as Reported by Cato 44

13. SEM Characterization of the Deposits Formed from the Release of Volatiles and Particulates from Dolomite 48

14. Total Micrograms of Trace and Minor Elements in Deposits from Fixed-Bed Reacted Sorbent Materials 49

LITS OF TABLES (Cont'd)

Page

15. Spark Source Mass Spectrometric Analysis of Deposits Formed as a Result of the Release of Volatiles and Particulates from Tymochtee Dolomite 50

16. Distribution of Alkali within Sorbents after Exposure to Oxiding or Reducing Gas Environments 51

17. SEM Characterization of Deposits Formed as a Result of the Release of Volatiles and Particulates from Coal Ash and Sorbent Materials 61

18. Distribution of Alkali in Chinook Coal Ash and Canaan Dolomite 63

19. SEM Characterization of Deposits Formed as a Result of the Release of Volatiles and Particulates from Coal Ash, Sorbent, and Aluminosilicate Materials 64

20. Preliminary List of OSHA Category 1 Confirmed Carcinogens Produced in Significant Quantities 73

21. Extract Concentration Levels Determining Hazardousness of Solid Waste 74

22. Pollutant Regulations 75

23. Carcinogenic Polycyclic Organic Materials 76

24. Criteria for Trace and Minor Element Selection for Fluidized-Bed Combustion Equilibrium Studies 77

25. Elemental Concentrations for Fluidized-Bed Combustion Calculations Using a U.S. Mean Coal 83

26. Summary of PFBC Parameters 86

27. C-H-N-O-S-Cl Species Considered in Fluidized-Bed Combustion Reactions 93

28. Sulfate → Oxide Transition Temperature of Iron in FBC Systems 121

29. Sodium Sulfate Liquid → Gas Transition Temperature as a Function of FBC Conditions 138

LIST OF TABLES (Cont'd)

Page

30. Potassium Sulfate Condensed Phase → Gas Transition Temperature as a Function of FBC Conditions 145

31. Zinc Sulfate → Oxide Transition Temperature as a Function of FBC Conditions 167

32. Gas/Solid Percent Distribution of Sb in 100% Excess Air, 90% Sulfur-Removal FBC Systems 171

33. Gas/Solid Percent Distribution of Sn in 10% Excess Air, 0% Sulfur-Removal FBC Systems 173

34. Summary of Trace and Minor Element Reactions in Fluidized-Bed Combustion Systems 188

35. Percent Distribution of Trace and Minor Elements in 10% Excess Air, 0% Sulfur-Removal, Fluidized-Bed Combustion Systems 191

36. Percent Distribution of Trace and Minor Elements in 10% Excess Air, 99% Sulfur-Removal, Fluidized-Bed Combustion Systems 193

37. Percent Distribution of Trace and Minor Elements in 100% Excess Air, 90% Sulfur-Removal, Fluidized-Bed Combustion Systems 195

38. Percent Distribution of Trace and Minor Elements in 100% Excess Air, 99% Sulfur-Removal, Fluidized-Bed Combustion Systems 197

39. Percent Distribution of Trace and Minor Elements in 300% Excess Air, 0% Sulfur-Removal, Fluidized-Bed Combustion Systems 199

40. Percent Distribution of Trace and Minor Elements in 300% Excess Air, 99% Sulfur-Removal, Fluidized-Bed Combustion Systems 201

41. Fluidized-Bed Combustion of C-H-N-O-S-Cl-Si-Al-K-Na for 100% Excess Air, 0% Sulfur-Removal, 1013 kPa Operations 209

42. Fluidized-Bed Combustion of C-H-N-O-S-Cl-Si-Al-K-Na for 100% Excess Air, 90% Sulfur-Removal, 1013 kPa Operations 210

LIST OF TABLES (Cont'd)

Page

43. Fluidized-Bed Combustion of C-H-N-O-S-Cl-Si-Al-K-Na for 100% Excess Air, 99% Sulfur-Removal, 1013 kPa Operations 211

44. Reevaluation of Fluidized-Bed Combustion of C-H-N-O-S-Cl-Si-Al-K-Na for 100% Excess Air, 0% Sulfur-Removal, 1013 kPa Operations 213

45. Reevaluation of Fluidized-Bed Combustion of C-H-N-O-S-Cl-Si-Al-K-Na for 100% Excess Air, 90% Sulfur-Removal, 1013 kPa Operations 214

46. Reevaluation of Fluidized-Bed Combustion of C-H-N-O-S-Cl-Si-Al-K-Na for 100% Excess Air, 99% Sulfur-Removal, 1013 kPa Operations 215

47. Decimal Distribution of Potassium Compounds in a Fluidized-Bed Combustion System Operating with 100% Excess Air and 0% Sulfur-Removal 217

48. Decimal Distribution of Potassium Compounds in a Fluidized-Bed Combustion System Operating with 100% Excess Air and 90% Sulfur-Removal 218

49. Decimal Distribution of Potassium Compounds in a Fluidized-Bed Combustion System Operating with 10% Excess Air and 0% Sulfur-Removal 219

50. Decimal Distribution of Potassium Compounds in a Fluidized-Bed Combustion System Operating with 10% Excess Air and 90% Sulfur-Removal 220

51. Fluidized-Bed Combustion of C-H-N-O-S-Cl-Si-Al-K-Na-Fe-Mn-Ni-Be for 100% Excess Air, 0% Sulfur-Removal, 1013 kPa Operations 231

52. Fluidized-Bed Combustion of C-H-N-O-S-Cl-Si-Al-K-Na-Fe-Mn-Ni-Be for 100% Excess Air, 90% Sulfur-Removal, 1013 kPa Operations 232

53. Fluidized-Bed Combustion of C-H-N-O-S-Cl-Si-Al-K-Na-Fe-Mn-Ni-Be for 100% Excess Air, 99% Sulfur-Removal, 1013 kPa Operations 233

LIST OF TABLES (Cont'd)

Page

54. Reevaluation of Fluidized-Bed Combustion of C-H-N-O-S-Cl-Si-Al-K-Na-Fe-Mn-Ni-Be for 100% Excess Air, 0% Sulfur-Removal, 1013 kPa Operations 239

55. Projected FBC Trace and Minor Species at 1200 K and 1013 kPa for 90% Sulfur Removal in 100% Excess Air 242

56. Fluidized-Bed Combustion of C-H-N-O-S-Cl-Si-Al-K-Na-Cr-Fe-Mo-Mn-Ti for 100% Excess Air, 0% Sulfur-Removal, 1013 kPa Operations 247

57. Fluidized-Bed Combustion of C-H-N-O-S-Cl-Si-Al-K-Na-Cr-Fe-Mo-Mn-Ti for 100% Excess Air, 90% Sulfur-Removal, 1013 kPa Operations 248

58. Fluidized-Bed Combustion of C-H-N-O-S-Cl-Si-Al-K-Na-Cr-Fe-Mo-Mn-Ti for 100% Excess Air, 99% Sulfur-Removal, 1013 kPa Operations 249

59. Fluidized-Bed Combustion of C-H-N-O-S-Cl-Si-Al-K-Na-Ca-Mg for 100% Excess Air, 0% Sulfur-Removal, 1013 kPa Operations 251

60. Fluidized-Bed Combustion of C-H-N-O-S-Cl-Si-Al-K-Na-Ca-Mg for 10% Excess Air, 0% Sulfur-Removal, 1013 kPa Operations 252

61. Fluidized-Bed Combustion of C-H-N-O-S-Cl-Si-Al-K-Na-Ca-Mg for 300% Excess Air, 0% Sulfur-Removal, 1013 kPa Operations 252

62. Summary of the Alkali, Carbonate, and Clay Constitutent Reactions 255

63. Comparison of Fluidized-Bed Combustion Systems Containing Carbonate Sorbents for Sulfur Removal with Projections for Reduced Sulfur Systems 258

64. Candidate Phases Considered in the C-H-N-O-S-Cl-Si-Al-K-Na-Ca-Mg-F-Pb Fluidized-Bed Combustion System 259

65. Resulting Active Phases as a Function of Temperature for C-H-N-O-S-Cl-Si-Al-K-Na-Ca-Mg-Fe-Ti-Ni 263

66. Resulting Active Phases as a Function of Temperature for C-H-N-O-S-Cl-Si-Al-K-Na-Ca-Mg-Cr-Mn-Mo 263

LIST OF TABLES (Cont'd)

Page

67. Comparison of the Percent Volatilization of Trace and Minor Elements in a Noninteractive and Interactive Fluidized-Bed Combustion System 265

68. Fluidized-Bed Combustion of C-H-N-O-S-Cl-Si-Al-K-Na-Br-F-Be-Hg-Pb-(Ca-Mg) - 100% Excess Air, 90% Sulfur-Removal, 1013 kPa Operations 267

69. Fluidized-Bed Combustion of C-H-N-O-S-Cl-Si-Al-K-Na-Br-F-Fe-Mn-Ni - 100% Excess Air, 90% Sulfur-Removal, 1013 kPa Operations 270

70. Fluidized-Bed Combustion of C-H-N-O-S-Cl-Si-Al-K-Na-Br-F-Ti-B-P - 100% Excess Air, 90% Sulfur-Removal, 1013 kPa Operations 272

71. Fluidized-Bed Combustion of C-H-N-O-S-Cl-Si-Al-K-Na-Br-F-Cu-Zn-Sb - 100% Excess Air, 90% Sulfur-Removal, 1013 kPa Operations 273

72. Fluidized-Bed Combustion of C-H-N-O-S-Cl-Si-Al-K-Na-Br-F-Sn-Zr-As - 100% Excess Air, 90% Sulfur-Removal, 1013 kPa Operations 275

73. Fluidized-Bed Combustion of C-H-N-O-S-Cl-Si-Al-K-Na-Br-F-Cd-Ga-Sb - 100% Excess Air, 90% Sulfur-Removal, 1013 kPa Operations 276

74. Fluidized-Bed Combustion of C-H-N-O-S-Cl-Si-Al-K-Na-Br-F-Se-Mo-Pb - 100% Excess Air, 90% Sulfur-Removal, 1013 kPa Operations 277

75. Fluidized-Bed Combustion of C-H-N-O-S-Cl-Si-Al-K-Na-Br-F-Ge-Co - 100% Excess Air, 90% Sulfur-Removal, 1013 kPa Operations 279

76. Fluidized-Bed Combustion of C-H-N-O-S-Cl-Si-Al-K-Na-Zr-B-V - 100% Excess Air, 90% Sulfur-Removal, 1013 kPa Operations 281

77. Fluidized-Bed Combustion of C-H-N-O-S-Cl-Si-Al-K-Na-Se-Pb-Ni-Cu-Sn - 100% Excess Air, 90% Sulfur-Removal, 1013 kPa Operations 282

LIST OF TABLES (Cont'd)

Page

78. Fluidized-Bed Combustion of C-H-N-O-S-Cl-Si-Al-K-Na-Se-Cu-Ge-Cr-Fe - 100% Excess Air, 90% Sulfur-Removal, 1013 kPa Operations 283

79. PFBC Projections for Minimum Trace and Minor Element Concentrations in Eastern Coals 285

80. PFBC Projections for Maximum Trace and Minor Element Concentrations in Eastern Coals 286

81. PFBC Projections for Minimum Trace and Minor Element Concentrations in Western Coals 287

82. PFBC Projections for Maximum Trace and Minor Element Concentrations in Western Coals 288

83. Mixed Sulfate Eutectic Compositions and Melt Temperatures 296

84. Alloy Composition 296

85. Trace Elements Exceeding MATE Values in Flue Gas and Solid Emissions from PFBC Systems, and Corresponding Projected Percent Elemental Volatilization 335

86. Projected Elemental Concentration in PFBC Effluent Gas and Solid Phases 336

ACKNOWLEDGMENT

We acknowledge the support and guidance of D. B. Henschel, and J. O. Milliken, who served as our EPA officers, and the efforts and contributions of the following Westinghouse personnel: R. W. Liebermann, who developed the free-energy minimization programs that form the basis of the trace element analysis; D. G. Faith, for the development of the three-dimensional plotting routines; D. R. Steele, for his assistance in the high-temperature, fixed-bed, pressurized bench-scale studies; A. Y. Ranadive, for his assistance in developing the particle profile model; and A. L. Wolfe, G. Gidick, R. C. Kuznicki, and T. A. Manion of the Analytical Chemistry and Physical Metallurgy Departments.

NOMENCLATURE

ANL	Argonne National Laboratory
ATP	adenosine triphosphate
CAFB	chemically active fluidized bed
CURL	Coal Utilization Research Laboratory, Leatherhead, UK
EDX	energy dispersive x-ray analysis
FBC	fluidized-bed combustion
ICP	inductively coupled plasma emission spectroscopy
LC_{LO}	lowest lethal concentration
LC_{50}	50 percent lethal concentration
LD_{50}	50 percent lethal dosage
MATE*	minimum acute toxicity effluent
METC	Morgantown Energy Technology Center
MMAD	mass median aerodynamic diameter
NAA	neutron activation analysis
NAAQS	first national primary and secondary National Ambient Air Quality Standards
NCB	National Coal Board, London, UK
NESHAP	National Emissions Standards for Hazardous Air Pollutants
NIOSH	National Institute for Occupational Safety and Health
OSHA	Occupational Safety & Health Administration
PAH	polynuclear aromatic hydrocarbon
PCB	polychlorinated biphenyl
PDU	process development unit
PER	Pope, Evans and Robbins
PFBC	pressurized fluidized-bed combustion
POM	polycyclic organic material
SEM	scanning electron microscopy
SSMS	spark source mass spectroscopy
TC_{LO}	lowest toxic concentration
TLV	threshold limit value
TWA	time weighted averages

---

*Since the time this report was prepared, IERL has recommended the use of DMEG (discharge multimedia environmental goals) as opposed to MATE. MATE, however, has been used throughout.

1. INTRODUCTION

The chemical distribution of trace and minor elements, particularly within ash fractions formed during combustion, has been demonstrated for conventional coal combustion systems. Fluidized-bed combustion (FBC), because of a lower combustion temperature, can minimize the concentration of potentially toxic and trace elements released in the stack-gas emissions, simultaneously enriching the elements in ash and slag formations. Particulate fines that escape cleaning systems are expected similarly to contain a lower concentration of the trace and minor elements on the particle surface than do conventional boiler fines.

In projecting the ultimate chemical fate of the elements in a combustion system, one must include the parameters of the trace and minor elemental concentration within coal and sorbent feed materials, the conditions of combustion, the percent of elemental release upon combustion as determined by the mineral structure of the feed materials, the combustion reaction kinetics, the system design, the gas/particle interactions and reactions, and the elemental partitioning mechanisms. The analytical characterization of gas and ash samples obtained at various locations in the fluidized-bed system provides valuable information on phase modifications that result from combustion of the feed materials. Thermodynamic equilibrium calculations principally delineate the stable phases that can form under specific operating conditions. When both analytic and thermodynamic data are assimilated, trace and minor element reaction mechanisms and pathways in the combustion system may be proposed.

The thermodynamic model projects the equilibrium composition for trace and minor elements in the FBC through calculations that minimize the Gibbs free energy for the polyphase system, using the techniques of

Geometric Programming, in addition to satisfying the mass conservation equations. The equilibrium product distribution for the reaction of fluorine (F), beryllium (Be), mercury (Hg), lead (Pb), cobalt (Co), chromium (Cr), iron (Fe), molybdenum (Mo), manganese (Mn), nickel (Ni), titanium (Ti), sodium (Na), potassium (K), bromine (Br), boron (B), phosphorous (P), copper (Cu), vanadium (V), zinc (Zn), antimony (Sb), tin (Sn), zirconium (Zr), arsenic (As), cadmium (Cd), selenium (Se), gallium (Ga), and germanium (Ge) with the major feedstock constituents - carbon (C), hydrogen (H), nitrogen (N), oxygen (O), sulfur (S), and chlorine (Cl) - and the interactions of these elements with the feedstock clay and carbonate constituents - aluminum (Al) and silicon (Si), calcium (Ca) and magnesium (Mg) - are presented for anticipated operating ranges of different FBC designs using a typical U.S. mean coal. With the exception of C, H, N, O, and S, the definition of trace and minor elements used throughout this text is based on the specific element's weight percent concentration within the feedstock material. Those elements with background levels greater than 0.01 wt % in the feedstock, e.g., Fe, Ti, Na, K, (Zn), Si, Al, Ca, and Mg, are defined as minor constituents, while the elements F, Be, Hg, Pb, Co, Cr, Mo, Mn, Ni, Br, B, P, Cu, V, Sb, Sn, Zr, As, Cd, Se, Ga, and Ge present at concentrations of less than 0.01 wt %, are considered trace constituents.

In defining the individual elemental reactions with combustion gases formed in the fluidized bed, we assumed the following:

- The elemental concentrations used in the equilibrium calculations are those typical of a U.S. mean coal.
- In the noninteractive FBC calculations each trace or minor element is considered to have the potential to react with C, H, N, O, S, and Cl from the feedstock or sorbent materials and will not remain bound within either the feedstock silicate, aluminosilicate, or carbonate matrix.

For the interactive FBC calculations, the elements considered are equally capable of reacting with all surrounding elements and are not considered as isolated chemical phases or complexes.

- For the noninteractive systems 100 percent of the projected gaseous phases are released from the bed into the effluent stream. Secondary interactions of the volatiles and solids in the bed, and the reactions of volatiles with elutriated ash fines, have not been considered in these calculations. Partitioning the gaseous trace and minor phases along particle surfaces (incompletely combusted coal particles, ash, char, etc.) as either a chemical reaction or a surface adsorption mechanism has also not been included in the noninteractive projections.
- The interactive system projects only the initial reaction of the trace and minor elements with clay and carbonate material in the combustor. Further reaction of the effluent volatiles with these entrained fines has not been considered in this study. It may, thus, seem unrealistic to assume that additional reactions along entrained ash particles or deposition reactions along cooler metal surfaces within the particle collection device or gas turbine do not occur. The interactions and deposition reactions, if equilibrium were attained, would minimize the concentration of volatiles escaping from the stack and would serve as a second approximation for the total projected concentration of the trace and minor elements in the stack gas effluent. Similarly, dilution by the expansion gases within the turbine, atmospheric diffusion and chemical reactions within the plume, rainout, washout, or dry deposition of volatile complexes from the

emitted aerosol, and meterological parameters will all modify, and possibly minimize, the concentration of trace and minor elements emitted at the stack.

- This study considers only the reactions of compounds for which thermodynamic data are available. We can reasonably assume that other compounds may form in the FBC system, but data for such compounds have not been cited in the literature, nor have estimates of their free energy, heats of formation, or molecular constants been made in this study. We believe that compounds not reported in the literature must be treated as less likely to result within the FBC than those for which data are available until future estimates prove this to the contrary.

- The reaction kinetics governing the reactions of trace, minor, or major species within combustion gases are unknown. The thermodynamic model utilizes the common assumption that, in high-temperature chemistry, equilibrium will be reached within the combustor, and the equilibrium product distribution will be characteristic of the process effluent.

The complexity of the trace and minor element interactions with the Al and Si clay lattice is illustrated in the solid phases formed either by ion exchange reactions or by physical absorption at the particle surface. The effect of FBC temperatures on the stability of the clay lattice is reviewed, and the thermodynamic equilibrium projections are correlated with analytical data obtained from both conventional boilers and FBC systems. The potential toxicity of the projected equilibrium phases and complexes resulting in either the solid waste streams or in the stack gases is also assessed on the basis of the minimum acute toxicity effluent concentrations (MATE) proposed by the Research Triangle Institute and on the current U.S. EPA regulations.

The MATE values used in this study describe a very approximate concentration of various elements and compounds in the air and land effluents that may be considered to evoke a minimal significant harmful response in exposed humans or in the environment. The air MATE value is based either on a time-weighted average for the element or compound threshold limit value (TLV) that has demonstrated acute or chronic effects on humans, including carcinogenic or suspect carcinogenic effects, and acute or chronic and oncogenic effects on animals; or on the National Institute for Occupational Safety and Health (NIOSH) recommendations for permissible element or compound concentrations in workroom areas. The reported air MATE level is based on the lower of these two values. When neither the TLV nor the NIOSH value is available, either the LD_{50} (50% lethal dosage), LC_{50} (lethal concentration of 50% of the animals tested), LC_{LO} (lowest lethal concentration reported), or TC_{LO} (lowest toxic concentration reported) are assumed. Land MATE values are established by stringent water MATE criteria in which it is assumed that 1000 g of soil may be leached entirely by 2 ℓ of water.

2. CONCLUSIONS

The chemical equilibrium model proposes numerous chemical pathways by which trace or minor elements react with and repartition within the clay lattice and carbonate structures of feedstock materials during combustion in the fluidized bed. At equilibrium the feedstock elements may be classified as constituents that

- Volatilize completely: Be, F, Hg, Pb, Mo, Br, B, P, Cu, As, Cd, and Se
- Volatilize partially: Co, Cr, Mn, Ni, and Sn
- Remain as stable solid complexes: Fe, Ti, Al, Si, V, Zn, Zr, and Ga.

This classification applies in the FBC, where 100 percent of the initial elemental concentration from a U.S. mean coal is assumed to be the maximum possible release from the carbon or clay matrix and without significant interactions between the trace and minor elements. The operating pressure within the combustor defines the volatility of the resulting Na, K, Sb, and Ge species: at ambient pressure these species volatilize completely, being emitted at 100 percent of the feedstock concentration into the effluent gases that leave the FBC; at 1520 kPa partial volatilization of these species is projected.

The thermodynamic model, however, provides a first-level approximation of the interactive phases formed at equilibrium, typifying the possible composition of the ash/spent sorbent particle. The phases projected to result within the ash or spent sorbent particle include manganese aluminate ($MnO \cdot Al_2O_3$), aluminum titanate ($Al_2O_3 \cdot TiO_2$), calcium metasilicate ($CaSiO_3$), calcium orthosilicate ($CaSiO_4$), magnesium aluminate ($MgAl_2O_4$), magnesium orthosilicate (Mg_2SiO_4), magnesium metasilicate ($MgSiO_3$), calcium magnesium silicate ($CaO \cdot MgO \cdot 2SiO_2$), calcium titanates ($CaO \cdot TiO_2$, $3CaO \cdot 2SiO_2$), calcium molybdate ($CaO \cdot MoO_3$), magnesium molybdate ($MgO \cdot MoO_3$), potassium aluminosilicate ($KAlSi_3O_8$), disodium silicate ($2Na_2O \cdot SiO_2$), nickel silicate ($2NiO \cdot SiO_2$), zirconium silicate ($ZrSiO_4$), and beryllium aluminate ($BeAl_2O_4$). In addition to the clay reactions, the interaction of the trace and minor constituents leads to the formation of stable solid compounds as cobalt chromate ($CoO \cdot Cr_2O_3$), potassium chromate ($K_2Cr_2O_7$), magnesium chromate ($MgO \cdot Cr_2O_3$), magnesium ferrate ($MgO \cdot Fe_2O_3$), nickel ferrate ($NiO \cdot Fe_2O_3$), magnesium phosphate ($Mg_3(PO_4)_2$), tricalcium borate ($3CaO \cdot B_2O_5$), and potentially corrosive vanadium complexes as magnesium vanadates ($MgO \cdot V_2O_5$, $2MgO \cdot V_2O_5$, $3MgO \cdot V_2O_5$), calcium vanadates ($2CaO \cdot V_2O_5$, $3CaO \cdot V_2O_5$), and sodium vanadates ($Na_2O \cdot V_2O_5$, $2Na_2O \cdot V_2O_5$, $3Na_2O \cdot V_2O_5$).

The thermodynamic projections also predict the formation of solid magnesium fluoride (MgF_2) and its conversion into solid calcium fluoride (CaF_2) in fluidized-bed combustors operating between 300 and 1000 K. The evolution of gaseous hydrogen fluoride (HF) is a function of the combustion temperature of either the clay fraction of the feedstock material (i.e., solid AlF_3 is stable between 300 to 500 K), the trace constituent association (i.e., solid BeF_2 and FeF_3, which are stable only between 300 and 400 K), or the stability of the carbonate-fluoride complexes (i.e., MgF_2 is stable from 300 to 600-700 K, and CaF_2 from 600-700 K to 900-1000 K).

The stability of the solid phases that result from the interaction of the trace or minor constituents is slightly reduced through the formation of the interactive fluoride and bromide volatile phases. These include: lead tetrafluoride (PbF_4), lead difluoride (PbF_2), lead monofluoride (PbF), sodium bromide (NaBr), monomeric and dimeric potassium bromide (KBr, K_2Br_2), zinc dibromide ($ZnBr_2$), beryllium difluoride (BeF_2), bromine monofluoride (BrF), beryllium chloride fluoride (BeClF), lead tetrabromide ($PbBr_4$), lead dibromide ($PbBr_2$), lead monobromide (PbBr), mercury dibromide ($HgBr_2$), aluminum oxydifluoride (AlF_2O), iron dibromide ($FeBr_2$), manganese dibromide ($MnBr_2$), nickel dibromide ($NiBr_2$), nickel monobromide (NiBr), nickel difluoride (NiF_2), boron oxide bromide (BOBr), copper monobromide (CuBr), copper monofluoride (CuF), tin dibromide ($SnBr_2$), arsenic trifluoride (AsF_3), cadmium monobromide (CdBr), gallium monobromide (GaBr), cadmium monofluoride (CdF), gallium monofluoride (GaF), and cobalt difluoride (CoF_2). These gaseous compounds, with the exception of the KBr, KBO_2, AsF_3 and CdBr are projected to be released at levels of less than 1 percent of the elemental feedstock concentration. These minor volatile phases, in addition to the gaseous trace and minor element chlorides, hydroxides, oxides, or nitrides, may be emitted directly from the stack or may become entrapped along the ash or carbonate particle surface through either a chemical reaction or a physical adsorption mechanism.

The thermodynamic model proposed volatile compounds of Be, F, Hg, Pb, Co, (Cr), Br, (P), Cu, As, Cd, (Ge), and Se, if directly released from the combustor and emitted at the stack at ambient conditions, will exceed the air minimum acute toxicity effluent (MATE) concentration for related species on a weight basis. The concentrations of Cr and P in the FBC effluent are also projected to exceed the reported air MATE level when combustion reactions with only C, H, N, O, S, and Cl are considered. These elements,however, interact and complex with surrounding trace and minor constituents, minimizing their concentration within the FBC effluent to below the air MATE level. The volatility of Ge and its complexes is shown to depend on system pressure, and the off-gas Ge concentration is estimated to approach reported air MATE levels for atmospheric operations. Similarly, the trace and minor element concentration in the resulting combustor solids is projected to exceed the land MATE levels for related species containing Be, Co, Cr, Fe, Mn, Ni, Ti, V, Zn, Sb, Sn, Zr, and Ge. When Be and P interact with the surrounding trace and minor constituents, the concentration of these elements within the resulting combustor solids are projected to exceed the reported land MATE levels. The interaction of the volatiles with entrained ash/spent sorbent fines, corrosion and deposition mechanisms within the FBC, stringent particle cleanup systems, dilution of the combustor effluent trace and minor element concentration in the turbine expansion gas, atmospheric diffusion and chemical reactions within the plume, rainout, washout, or dry deposition of the volatile complexes from the aerosol, and meterological parameters will minimize the ultimate concentration of the emitted trace and minor constituents. The influence of these phenomena on the final concentration of the FBC released phases will presumably be far below either the air or the land MATE concentration. For example, a 10-fold dilution of the flue gases will reduce the F, Pb, Co, Cr, Br, P, and Cu concentration to below the reported air MATE level. Similarly, a 100-fold dilution will render the Be, As, and Se flue gas concentration innocuous, and a 1000-fold dilution will achieve similar results for Hg and Cd. The projected model coal solids concentration will fall below accepted land MATE values if the Ge content is decreased 10-fold, the Be, Co, Ni, Sb, Sn, and Zr contents 100-fold, and the Cr, Fe, Mn, Ti, V, and Zn contents 1000-fold.

The projected thermodynamic off-gas Be concentration exceeds the reported Be emission level from stationary sources under Section 112 of the Clean Air Act in the National Ambient Air Quality Standards (NAAQS). Similarly, the equilibrium Hg concentration is below the emission level for sludge incineration. A qualitative relation between the thermodynamically projected emission level and federal regulations cannot be made at this time. New criteria and regulations for the trace and minor species concentrations are required in the National Emissions Standards for Hazardous Air Pollutants (NESHAP) prior to assessing the toxic pollutant characteristics of the estimated FBC effluent and solid products.

The validity of the equilibrium projections lies within the accuracy of the molecular constant data, heat of formation, and entropy values for each compound selected in the thermodynamic calculations. Delineation by chemical analysis of the silicate or aluminosilicate and carbonate phases that complex with the alkali and trace or minor elements throughout the entire FBC system is essential in order to correlate the thermodynamic projections with in-plant data. The clay fraction of the coal and the calcium fraction of the sorbent may remove the potentially toxic constituents in the emissions, either through chemical interactions as shown in the thermodynamic projections or through sorption by physical entrainment of the element on the ash or spent sorbent particle surface. The latter process may substantially reduce the volatile concentration of elements (i.e., Hg, Pb, P, Cu, Mo, Cd, Ge, Se, and As) that had been projected to be completely released from the stack if equilibrium were attained. An essential refinement to the trace and minor element emission model is to define kinetically the elemental partitioning as a function of particle composition and size in the various FBC systems.

The present thermodynamic model has the ability to define minute concentrations of stable equilibrium phases, all of which may be far below analytical limits. Phases that are projected as major constituents by the equilibrium model will indeed often be detected analytically. Although random, in-plant sampling of solids and off-gases does not provide a clear understanding of trace and minor element reaction mechanisms, the thermodynamic model for the generalized U.S. mean Illinois No. 6 feedstock is shown to complement many of the reported analytical results. In the 18 in. AFBC unit at the Morgantown Energy Technology Center (METC),bag-filter ash was shown to contain a very high concentration of calcium sulfate ($CaSO_4$), in addition to quartz (SiO_2). Minor phases of alpha iron oxide (α-Fe_2O_3) and traces of calcium oxide (CaO) were also detected within the bag-filter ash fraction. When compared to the carry-over of sulfated sorbent fines with ash, the unsulfated bed material when analyzed indicated the presence of CaO fines containing calcium carbonate ($CaCO_3$), and dark particles rich in quartz and iron oxide (Fe_2O_3).

The CPU-400 Process Development Unit (PDU) was originally constructed for the Environmental Protection Agency (EPA) to convert the heat energy of solid wastes to electrical energy by using an adiabatic

FBC/gas turbine cycle. The CPU ash when analyzed was shown to contain Ca, Si, S, Mg, and K in decreasing order of concentration. Discrete particles of $CaSO_4$, MgO, and Fe_2O_3 were observed in association with unsulfated $CaCO_3$ fines.

Analysis of the ash formed in the 32 cm pressurized unit of the Exxon miniplant at Linden, New Jersey, and of the Leatherhead Unit in England similarly indicated the presence of Ca, Al, Si, and S as major elements within the carry-over ash, with Mg, Ti, Fe, and K in minor or trace concentrations. The aluminosilicate phases of the ash particles that result from combustion of feedstock mineral inclusions are interspersed among the attrited sulfated sorbent fines.

The noninteractive and interactive thermodynamic equilibrium models project many of the phases identified by X-ray diffraction analysis. The equilibrium model assumes that the elemental constituents of the feedstock and sorbent initially exist as single entities, and the reaction products reflect the minimum free energy contribution within the polyphase system when all elements are permitted to interact and equilibrate. From quantitative calibration of the concentration of phases identified by x-ray diffraction analysis, it is evident that the quartz content within the FBC ash does not exceed 10 wt%. The remainder of the unidentified material is possibly composed of an amorphous mixture of the thermodynamically projected phases, interspersed with the trace and minor element phases.

Analysis of the PFBC flue gases at Leatherhead, England by the National Coal Board-Coal Utilization Research Laboratory (NCB-CURL) indicates that P, Cr, Cu, As, Se, and Pb exceed the air MATE level, similarly to the noninteractive thermodynamic estimates. In the NCB-CURL projections, however, the V, Fe, Ni, and Zn concentration in the flue gases exceeds the accepted air MATE, but the thermodynamic projections for flue gases from a model coal feed do not. The V, Fe, Ni, and Zn in the flue gases may actually be contributions from fines entrained in the effluent streams. Similarly, the NCB-CURL analytic data indicate that the concentration of V, Cr, Fe, Ni, Zn, and Mn in the solids exceeds the land MATE emission level and are comparable to the thermodynamic model. Although P, Cu, As, Se, Pb, and F were also chemically determined by NCB-CURL to exceed the land MATEs, at thermodynamic equilibrium these elements are projected as volatiles that in reality may have condensed along entrained ash fines prior to being emitted purely as volatiles in the stack gases. Correlation of the Exxon data for the Leatherhead process indicates agreement with the thermodynamic model in that Cr, As, and Be in the flue gases exceed the air MATE level, while V, Cr, Fe, Ni, Zn, and Mn in the solids exceed the reported land MATE levels.

The conservative thermodynamic model estimates should provide guidelines for monitoring trace and minor elements released in flue gases and solids during FBC of feedstocks with compositions similar to the model coal. On-line monitoring should be developed to determine the level of Be, F, Hg, Pb, Co, Cr, Br, P, Cu, As, Cd, Ge, and Se in the flue gases, and Be, Co, Cr, Fe, Mn, Ni, Ti, B, P, V, Zn, Sb, Sn, Zr, and Ge in solids formed during combustion.

3. RECOMMENDATIONS

- Increased efforts should be applied to the development of improved technology for actual sampling of gaseous and condensed phases in the high-temperature combustion region and for direct monitoring of the trace and minor element concentration in the effluent and solid streams and in the stack gases. Chemical analysis detailing the phase identification within the gas and solid products should be implemented on both a qualitative and quantitative level, so that the resulting FBC compounds can be compared with the equilibrium projected compositions. The thermodynamic model, if indicated, can then be modified to reflect preferred phase formations on the basis of the chemical kinetic data, and mass transfer considerations can be provided by the on-line analytical results. Refining the thermodynamic model in this manner will enhance confidence in the estimates of emission concentration of hazardous compounds from alternative combustion processes.

- To define the physical and chemical changes that occur within the organic and mineral matrix of the coal and sorbent particle during combustion, efforts should be extended to explore the possible volatilization-condensation or agglomeration-coagulation mechanism of particular elements and/or compounds from feedstock sources that result in ash and spent sorbent formations from various conventional or FBC processes. The chemical and physical processes that determine the rate and temperature at which volatiles are released from the feedstock and subsequently become associated with ash and spent sorbent matrices, through either displacement reactions or surface adsorption, should be established as a function of system parameters, reaction composition, and particle properties.

- The thermodynamic model should be extended to project critical locations within the FBC system (e.g., boiler, heat exchanger tube walls, gas turbine) where corrosion resulting from the deposition of melt phases and compounds is likely to occur. This type of model is contingent upon obtaining corrosive phase identification, thermodynamic molecular constants for the identified phases, and detailed mechanism and kinetic data that support the deposition products. With this type of model, alternative combustion designs could be explored that would minimize corrosive deposition and extend FBC system life.

4. COMPOSITION OF FEEDSTOCK MATERIALS

In addition to C, H, O, N, and S, the heterogeneous coal particle contains trace elements, mineral material, and hydrocarbon structures, with an empirical formula ranging from $C_{75}H_{140}O_{56}N_2S$ for a low-grade peat to $C_{240}H_{90}O_4NS$ in a high-grade anthracite seam. Numerous reports in the literature[1-11] have indicated that the major mineral constituents of coal are Si, Al, Ti, Ca, Mg, Fe, P, S, Na, and K. These mineral constituents exist either as aluminosilicate clays, sulfides or sulfates, carbonates, or silica, as shown in Table 1.[12]

The trace and minor elements can exist in more than one form in coal as a result of either synergism, diagenesis, or epigenesis that occurs during coalification.* The exact nature of the element's occurrence in the coal matrix may be an important factor in determining its behavior during combustion. Generally, the trace elements have been reported to be associated with either the aluminosilicate minerals (lithophilic) or the sulfide minerals (chalcophilic). Miller et al.,[14] correlated the trace element association of F with the clay aluminosilicate fraction, Be with the sulfide and sulfate fraction, and Hg with both the clay and sulfur fractions. In addition to the lithophilic and chalcophilic categories, Miller classified Mn and Mo as elements associated with either the carbonate or quartz fraction in coal and Cr with quartz. Gluskoter's[15] analysis of Illinois Basin Coals generalized the association of the trace and minor elements as either "organic,"

---

*Synergism - elements deposited from surface waters by living plants, or in dead organic material prior to coalification.

Diagenesis - elements introduced into the coal matrix during coalification.

Epigenesis - elements introduced into the coal matrix after coalification and consolidation of enclosing sediments by groundwater action.[13]

TABLE 1 - MINERALS IDENTIFIED IN COALS [12]

Dwg. 5592C87

Mineral	Chemical Formula
Clay Minerals	
Montmorillonite	$Al_2Si_4O_{10}(OH)_2 \cdot x\ H_2O$
Illite-sericite	$KAl_2(AlSi_3O_{10})\ (OH)_2$
Kaolinite	$Al_4Si_4O_{10}(OH)_8$
Halloysite	$Al_4Si_4O_{10}(OH)_8$
Chlorite (Prochlorite, Penninite)	$Mg_5Al(AlSi_3O_{10})\ (OH)_8$
Mixed-Layer Clay Minerals	
Sulfide Minerals	
Pyrite	FeS_2
Marcasite	FeS_2
Sphalerite	ZnS
Galena	PbS
Chalcopyrite	$CuFeS_2$
Pyrrhotite	$Fe_{1-x}\ S$
Arsenpyrite	$FeAsS$
Millerite	NiS
Carbonate Minerals	
Calcite	$CaCO_3$
Dolomite	$(Ca, Mg)CO_3$
Siderite	$FeCO_3$
Ankerite (Ferroan Dolomite)	$(Ca, Fe, Mg)CO_3$
Witherite	$BaCO_3$
Sulfate Minerals	
Barite	$BaSO_4$
Gypsum	$CaSO_4 \cdot 2H_2O$
Anhydrite	$CaSO_4$
Bassanite	$CaSO_4 \cdot 1/2H_2O$
Jarosite	$(Na, K)Fe_3(SO_4)_2(OH)_6$
Szomolnokite	$FeSO_4 \cdot H_2O$
Rozenite	$FeSO_4 \cdot 4H_2O$
Melanterite	$FeSO_4 \cdot 7H_2O$
Coquimbite	$Fe_2(SO)_3 \cdot 9H_2O$
Roemerite	$FeSO_4 \cdot Fe_2(SO_4)_3 \cdot 12H_2O$
Mirabilite	$Na_2SO_4 \cdot 10H_2O$

TABLE 1 (Continued)

Dwg. 5592C88

Minerals	Chemical Formula
Kieserite	$MgSO_4 \cdot H_2O$
Sideronatrite	$2Na_2O \cdot Fe_2O_3 \cdot 4SO_3 \cdot 7H_2O$
Chloride Minerals	
Halite	$NaCl$
Sylvite	KCl
Bischofite	$MgCl_2 \cdot 6H_2O$
Silicate Minerals	
Quartz	SiO_2
Biotite	$K(Mg, Fe)_3(AlSi_3O_{10})(OH)_2$
Zircon	$ZrSiO_4$
Tourmaline	$Na(Mg, Fe)_3Al_6(BO_3)_3(Si_6O_{18})(OH)_4$
Garnet	$(Fe, Ca, Mg)_3(Al, Fe)_2(SiO_4)_3$
Kyanite	Al_2SiO_5
Staurolite	$Al_4FeSi_2O_{10}(OH)_2$
Epidote	$Ca_2(Al, Fe)_3Si_3O_{12}(OH)$
Albite	$NaAlSi_3O_8$
Sanidine	$KAlSi_3O_8$
Orthoclase	$KAlSi_3O_8$
Augite	$Ca(Mg, Fe, Al)(Al, Si)_2O_6$
Hornblende	$NaCa_2(Mg, Fe, Al)_5(SiAl)_8O_{22}(OH)_2$
Topaz	$Al_2SiO_4(OH, F)_2$
Oxide and Hydroxide Minerals	
Hematite	Fe_2O_3
Magnetite	Fe_3O_4
Rutile	TiO_2
Limonite	$FeO \cdot OH \cdot nH_2O$
Goethite	$FeO \cdot OH$
Lepidocrocite	$FeO \cdot OH$
Diaspore	$AlO \cdot OH$
Phosphate Minerals	
Apatite (Fluorapatite)	$Ca_5(PO_4)_3(F, Cl, OH)$

"intermediate-organic," "intermediate-inorganic," and "inorganic." As illustrated in Table 2, Ge, Be, B, and Sb were classified within the organic group, with Ge having the highest organic affinity in each analysis. Zinc, Cd, Mn, As, Mo, and Fe were shown to be associated with the inorganic group, while Co, Ni, Cu, Cr, and Se were categorized as intermediate-organic affinity elements associated either with sulfide minerals or with organometallic compounds[*] as chelated species or as adsorbed cations. The trace elements associated with the organic fraction of the feedstock material are usually enriched in the smaller fly ash particles formed during combustion. Since these elements are entrapped within the organic matrix or chemically bonded as an organic complex, there is a greater probability that they will be transferred into the gas phase.

When coal and its resulting ash products are analyzed, they produce, because of their heterogeneous nature, a range of both trace and minor element concentrations that is the result of such factors as geographical location (Table 3), coal rank (Table 4), the chemical or physical association of the trace or minor elements within the hydroaromatic structure, and location within the field or quarry. Analysis also indicates variation in the sulfur content of coals mined throughout the United States (Table 5). These sulfur-rich coals, when used as fuels in FBC systems, produce hot combustion products containing sulfur dioxide (SO_2), hydrogen chloride (HCl) and volatile alkali metal species, in addition to ash. Through reaction of gaseous sulfur oxides (SO_x) and released alkali, potentially corrosive liquid deposition products, such as alkali sulfates or mixed sulfates, may be formed. In order to minimize the formation of the corrosive complexes and to produce a turbine expansion gas that meets sulfur emission regulations, several control options are available. These include: selection of low-sulfur

---

[*] [illegible] compounds in coal include: metal-porphyrin compounds, meta[illegible]ls, metallocenes, arene-carbonyls, metal-alkyls, organohydrides, and metal-chelates.

Dwg. 1712890

TABLE 2 - CLASSIFICATION OF TRACE AND MINOR ELEMENTS IN COAL[15]

Element	Classification
Be	Organic Affinity
F	Occurs in Apatite [$Ca_5(PO_4)_3(F, CO_3)$]
Hg	Inorganic Affinity, Sulfide Minerals
Pb	Chalcophilic; Occurs as Galena (PbS); Inorganic Affinity
Co	Sulfide Minerals/Organometallic Compounds/Chelated Species/Adsorbed Cations
Cr	Sulfide Minerals/Organometallic Compounds/Chelated Species/Adsorbed Cations
Fe	Inorganic Affinity; Sulfide Minerals
Mo	Inorganic Affinity; Sulfide Minerals
Mn	Inorganic Affinity as Carbonates; Mineral Matter
Ni	Sulfide Minerals/Organometallic Compounds/Chelated Species/Adsorbed Cations
Ti	Lithophilic; Organic/Inorganic Affinity
Na	Association with Chlorine; Possible Lithophilic Association
K	Lithophilic; Association with Chlorine
Al	Lithophilic
Si	Lithophilic
Br	Organic Affinity
B	Organic/Inorganic Affinity
P	Organic/Inogranic Affinity; Occurs in Apatite [$Ca_5(PO_4)_3(F, CO_3)$]
Cu	Sulfide Minerals/Organometallic Compounds/Chelated Species/Adsorbed Cations
V	Organic Affinity with Silicate Minerals; Partial Inorganic Affinity
Zn	Inorganic Affinity; Occurs as Sphalerite (ZnS)
Sb	Organic Affinity; Chalcophilic; Partial Inorganic Affinity
Sn	Possible Inorganic Affinity
Zr	Inorganic Affinity; Mineral Matter
As	Inorganic Affinity; Chalcophilic; Mineral Matter
Cd	Inorganic Affinity; Occurs as Solid Solution with Sphalerite
Se	Sulfide Minerals/Organometallic Compounds/Chelated Species/Adsorbed Cations
Ga	Organic/Inorganic Affinity
Ge	Organic Affinity; Chalcophilic; Inorganic Affinity is Possible

TABLE 3 - CONCENTRATION OF TRACE AND MINOR ELEMENTS IN COALS THROUGHOUT THE UNITED STATES (ARITHMETIC MEAN VALUES)[15]

Element	U. S. Mean Coal	Eastern United States	Illinois Basin	Western United States
Be	1.61 ppm	1.3 ppm	1.7 ppm	0.46 ppm
F	60.94 ppm	89 ppm	67 ppm	62 ppm
Hg	0.20 ppm	0.20 ppm	0.2 ppm	0.09 ppm
Pb	34.78 ppm	5.9 ppm	32 ppm	3.4 ppm
Co	9.57 ppm	9.8 ppm	7.3 ppm	1.8 ppm
Cr	13.75 ppm	20 ppm	18 ppm	9.0 ppm
Fe	1.92 %	1.5 %	2.0 %	0.53 %
Mo	7.54 ppm	4.6 ppm	8.1 ppm	2.1 ppm
Mn	49.40 ppm	18 ppm	53 ppm	49 ppm
Ni	21.07 ppm	15 ppm	21 ppm	5.0 ppm
Ti	0.07 %	0.09 %	0.06 %	0.05 %
Na	0.05 %	0.04 %	0.05 %	0.14 %
K	0.16 %	0.25 %	0.17 %	0.05 %
Al	1.29 %	1.7 %	1.2 %	1.0 %
Si	2.49 %	2.8 %	2.4 %	1.7 %
Br	15.42 ppm	12 ppm	13 ppm	4.7 ppm
B	102.21 ppm	42 ppm	110 ppm	56 ppm
P	71.10 ppm	150 ppm	64 ppm	130 ppm
Cu	15.16 ppm	18 ppm	14 ppm	10 ppm
V	32.71 ppm	38 ppm	32 ppm	14 ppm
Zn	272.29 ppm	25 ppm	250 ppm	7.0 ppm
Sb	1.26 ppm	1.6 ppm	1.3 ppm	0.58 ppm
Sn	4.79 ppm	2.0 ppm	3.8 ppm	1.9 ppm
Zr	72.46 ppm	45 ppm	47 ppm	33 ppm
As	14.02 ppm	25 ppm	0.03 ppm	2.3 ppm
Cd	2.52 ppm	0.24 ppm	2.2 ppm	0.18 ppm
Se	2.08 ppm	4.0 ppm	2.2 ppm	1.4 ppm
Ga	3.12 ppm	5.7 ppm	3.2 ppm	2.5 ppm
Ge	6.59 ppm	1.6 ppm	6.9 ppm	0.91 ppm

1712B88

Dwg. 5592C90

TABLE 4 - AVERAGE TRACE ELEMENT CONCENTRATION OF ASH FROM U.S. COALS OF VARIOUS RANK, ppm[16]

Element \ Rank	Anthracite Coal	Bituminous Coals			Lignite
		Low Volatility	Medium Volatility	High Volatility	
Be	9	16	13	17	6
F					
Hg					
Pb	81	89	96	183	80
Co	81	172	105	64	45
Cr	304	221	169	193	54
Fe					
Mo					
Mn	270	280	1432	170	688
Ni	220	141	263	154	129
Ti					
Na					
K					
Al					
Si					
Br					
B	90	123	218	770	1020
P					
Cu	405	379	313	293	655
V	248	278	390	249	125
Zn		231	195	310	
Sb					
Sn	962	92	75	171	156
Zr	688	458	326	411	245
As					
Cd					
Se					
Ga	42	41		40	23
Ge					
Representative Partial Structures	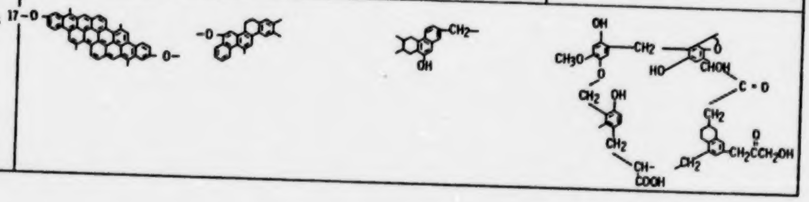				

17–O
O–
–O
CH2–
OH
OH
CH3O
CH2
O
HO
CHOH
O
C = O
CH2 OH
CH2
CH2
O
CH2CCH2OH
CH-
COOH
CH2

TABLE 5 - SULFUR VARIATION IN COAL THROUGHOUT THE UNITED STATES, WEIGHT PERCENT[15]

Dwg. 1714B29

	U.S. Mean Coal	Eastern United States	Illinois Basin	Western United States
Organic Sulfur	1.54 (0.37 - 3.09)*	0.92 (0.35 - 2.5)	1.6 (0.37 - 3.2)	0.53 (0.25 - 1.1)
Pyritic Sulfur	1.88 (0.29 - 3.78)	1.3 (0.04 - 2.6)	2.0 (0.29 - 4.6)	0.19 (0.01 - 1.2)
Sulfate Sulfur	0.09 (0.01 - 1.06)	0.10 (0.01 - 0.42)	0.1 (0.01 - 1.1)	0.04 (0.01 - 0.22)
Total Sulfur	3.51 (0.85 - 5.59)	2.3 (0.55 - 5.0)	3.6 (0.56 - 6.4)	0.76 (0.34 - 1.9)

* Parenthesis indicates minimum and maximum sulfur range

and low-alkali feedstock materials; pretreatment of the feedstock, which initially reduces the sulfur or alkali content or repartitions the alkali into stable, nonvolatile aluminosilicate phases; removal of gaseous SO_2 from the effluent streams by limestone or dolomite sorbents or through alkali-gettering reactions with ash or commercially produced clay additives. In the FBC process sorbent and gettering reactions by dolomite or limestone and aluminosilicate clay material not only contribute an additional load to the quantity of elutriated fines released from the bed, but also increase the trace and minor element concentrations in the effluent and subsequent stack-gas emissions.

Dolomite ideally contains 54.53 wt % calcium carbonate ($CaCO_3$) and 45.65 wt % magnesium carbonate ($MgCO_3$), while limestone is composed principally of $CaCO_3$. The proportions of the carbonates in dolomite vary within stone formations and with the purity of the material. High-purity dolomites generally contain 98 wt % total carbonates, although Keller[18] suggested that the trace element contaminant level in dolomite should not exceed the maximum level of 0.1 wt % for high-purity materials.

The presence of various trace impurities in dolomite and limestone may be attributed to the environmental conditions to which the stone was subjected during its formation. Water-carried salts, sands, clays, or silts are present as contaminant fluid inclusions and interspersed as strata between pure stone layers. Organic material from plants and soft-bodied animals is found embedded within rock crevices. During the diagenesis of the original sediment, movement of groundwater through the rock may have led to depletion of salts in the water by highly adsorbent clay mineral particles. The nature of the impurities and the concentration in which they exist cause variation in chemical composition and physical properties. Although there is no recent study of trace element concentrations and their distribution in limestone or dolomite, the maximum likely concentrations of some elements have been estimated by use of atomic emission data and neutron activation analysis data obtained by Exxon[19] and Argonne National Laboratories (ANL).[20] Several of the Westinghouse limestone or dolomite analyses[21-23] are shown in Tables 6 and 7.

Coupled with sulfur removal, gettering of released alkali from the feedstock coal and sorbents by commercial aluminosilicate clays or process development unit (PDU) chars and ashes provides an attractive technique for minimizing the total sulfur and alkali load in the effluent, consequently limiting the formation of gaseous SO_x and corrosive liquid alkali sulfate melts. Thermodynamically, the aluminosilicate materials have demonstrated 70 to 80 percent alkali removal through the formation of feldspar phases in systems typifying pressurized fluidized-bed combustion (PFBC) at equilibrium,[23] as shown in Figure 1. Current investigations at Westinghouse are being directed toward delineating the alkali

TABLE 6 - ANALYSIS BY EMISSION SPECTROSCOPY OF TRACE IMPURITIES IN SELECTED U.S. LIMESTONES AND DOLOMITES, wt %

Element	No. 10 Glasshouse 1337 (Ohio: Dolomite)[21]	Tymochtee (Ohio: Dolomite)[21]	CP & L (Texas: Limestone)[22]
Al	0.1	≥0.4	0.4
Ag	<0.0001	<0.0001	<0.0004
B	<0.0004	0.008	<0.004
Ba	–	–	0.0004
Be	–	–	<0.0004
Bi	<0.0004	<0.0004	<0.0004
Cd	<0.04	<0.04	<0.04
Co	<0.004	<0.004	<0.0004
Cr	<0.004	<0.004	<0.004
Cu	<0.0004	0.001	0.008
Fe	0.04	0.1	0.2
K*	0.0250	0.3700	0.116
Li	–	–	<0.0004
Mn	0.004	0.004	0.04
Mo	<0.004	<0.002	<0.004
Na*	0.0180	0.0329	0.014
Nb	<0.004	<0.004	<0.004
Ni	<0.0004	<0.0004	<0.004
P	–	–	<0.004
Pb	<0.004	<0.004	<0.0004
Sb	<0.004	<0.004	<0.004
Si	0.3	2.0	~2.0
Sn	<0.002	<0.002	<0.004
Sr	–	–	0.08
Ti	0.002	0.008	0.04
V	<0.004	<0.004	<0.004
Zn	0.02	<0.02	<0.004
Zr	<0.02	<0.004	<0.004

*Atomic Absorption

Dwg. 1712B91

TABLE 7 - CONCENTRATION OF Ca, Mg, Na, K AND Cl IN SORBENT MATERIALS

Concentration, Weight %

Sorbent	Location	Ca	Mg	Na			K			Cl
				Soluble*	Insoluble**	Total	Soluble	Insoluble	Total	
Canaan	Conn.	21. 91	12. 56	0. 0023	0. 0014	0. 0037	0. 0088	0. 0070	0. 0158	
Lehigh	Ill.	18. 07	10. 87	0. 0164	0. 0080	0. 0244	0. 0379	0. 6333	0. 6712	0. 028
Mt. Carroll	Ill.	21. 07	12. 32	0. 0158	0. 215	0. 0373	0. 0026	0. 2200	0. 2226	0.078
Thornton	Ill.	21. 44	12. 83	0. 2000	0. 0002	0. 2002	0. 0175	0. 0240	0. 0415	0. 120
Geneva	Ind.	21. 76	11. 61	0. 0167	0. 0010	0. 0177	0. 0038	0. 0178	0. 0216	0. 017
Salamonie	Ind.	21. 61	12. 97	0. 0163	0. 0005	0. 0168	0. 0069	0. 0051	0. 0120	
Cedarville	Mich.	21. 59	12. 73	0. 0325	0. 0006	0. 0331	0. 0258	0. 0168	0. 0426	0. 229
Drummond	Mich.	20. 95	12. 80	0. 0193	0. 0010	0. 0203	0. 0263	0. 0850	0. 1113	0. 098
Maybee	Mich.	18. 80	11. 32	0. 0216	0. 0012	0. 0228	0. 0213	0. 0340	0. 0553	
Ottawa Lake	Mich.	21. 07	12. 80	0. 0224	0. 0064	0. 0288	0. 0182	0. 1150	0. 1332	0. 033
Tymochtee	Ohio	19. 81	11. 80	0. 0179	0. 0150	0. 0329	0. 0450	0. 3250	0. 3700	0. 042
Glasshouse #10	Ohio	21. 08	12. 49	0. 0175	0. 0005	0. 0180	0. 0075	0. 0175	0. 0250	
General Portland	Texas	37. 5	–	0. 0058	0. 0016	0. 0074	0. 0221	0. 0372	0. 0593	
Parker Bros	Texas	37. 0	–	0. 0032	0. 0012	0. 0044	0. 0028	0. 0059	0. 0087	
McDonough Bros	Texas	38. 4	–	0. 0021	0. 0008	0. 0029	0. 0025	0. 0033	0. 0058	

* Alkali Soluble Phases - Chlorides, Carbonates, Water Glasses, Aluminosilicates and Feldspars. Sorbents are treated on a 1:1 Volumetric basis with HCl, followed by heating for one hour, then filtered

** Alkali Insoluble Phases - Amorphous Clays. Residue is heated in alcohol, followed by the addition of HF, heated for one hour, then perchloric acid is added and the entire sample brought to fuming

Dwg. 1712B92

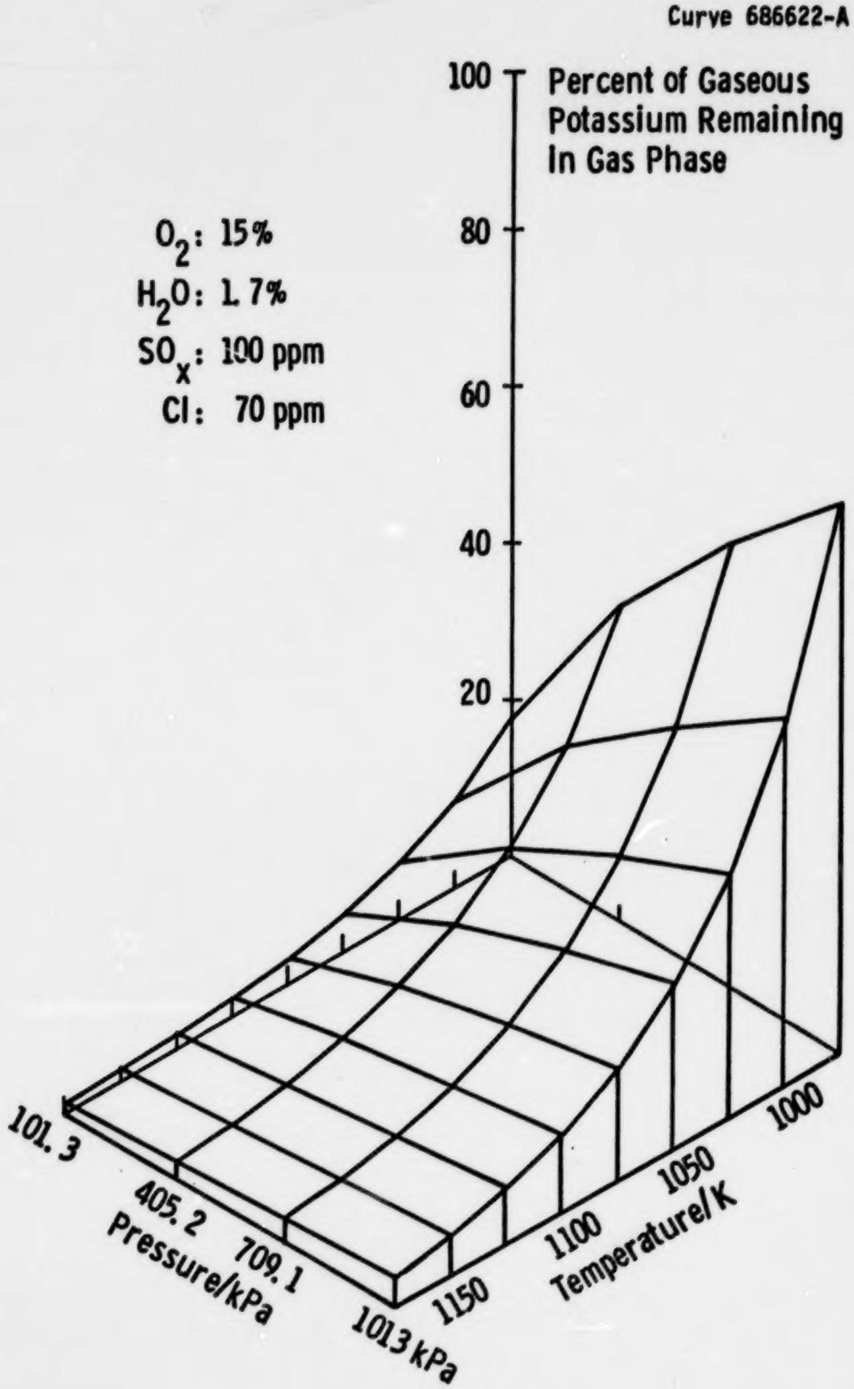

Figure 1 - Thermodynamics of Gettering Action of Aluminosilicates in Reducing Gaseous Potassium Emissions[23]

gettering mechanism as either a chemical or a sorption process for both combustion and gasification through fundamental chemical and kinetic data.[24,25] The potential for gettering trace and minor elements as aluminosilicate complexes will be demonstrated in the following sections of this report. Tables 8 and 9 illustrate the initial trace and minor element concentration in candidate getter materials. Through the reactions of the volatile trace and minor phases with attrited ash particles, the stack-gas concentration of the various volatile elements can be reduced.

TABLE 8 - CONCENTRATION OF TRACE AND MINOR ELEMENTS IN KAOLIN, PITTSBURGH ASH, CHINOOK COAL ASH, RENTON CHAR, AND MINNEHAHA CHAR AS DETERMINED BY EMISSION SPECTROSCOPY, wt %

Dwg. 1712B89

Element	Kaolin	Pgh Ash C117A[25]		Chinook Coal Ash	Renton Char[25]		Minnehaha Char[25]	
		As Received	Ashed*	As Received	As Received	Ashed	As Received	Ashed
Al	Major	Major	Major	Major	Major	Major	Major	Major
Ag	<0.001	<0.001	<0.00005	<0.0001	<0.001	0.00004	<0.001	0.00004
B	<0.001	0.003	0.005	~0.2	0.003	0.008	0.004	0.008
Ba	0.003	0.02	0.005	0.02	0.01	0.006	0.01	0.01
Be	<0.0001	0.00005	0.00005	0.001	0.0005	0.0002	0.0005	0.0002
Bi	<0.001	<0.001	<0.0005	<0.001	<0.001	<0.0002	<0.001	<0.0002
Ca	0.01	≥1.0	0.1	>1.0	0.1	>0.2	0.1	≥0.2
Cd	<0.003	<0.003	<0.005	<0.01	0.003	<0.002	<0.003	<0.002
Co	<0.001	0.001	0.002	0.002	<0.001	0.0006	<0.001	0.0006
Cr	0.003	0.003	0.005	0.003	0.002	0.002	0.002	0.002
Cu	0.002	0.003	0.005	0.004	0.001	0.002	0.001	0.002
Fe	0.05	≥1.0	>1.0	>>1.0	≥1.0	>1.0	≥1.0	>1.0
Ga	0.005	0.001	0.002	ND	<0.001	0.0006	<0.001	0.0006
Ge	<0.001	<0.001	<0.0005	ND	<0.001	0.0004	<0.001	0.001
K	ND[a]	ND	>1.0	>1.0	ND	>1.0	ND	>1.0
Li	0.003	0.003	0.005	0.008	0.002	0.002	0.002	0.004
Mg	0.003	0.05	0.1	>1.0	0.02	0.2	0.02	0.1
Mn	<0.001	0.02	0.02	0.01	0.002	0.006	0.002	0.006
Mo	<0.001	0.001	<0.0005	<0.001	<0.001	<0.0002	<0.001	<0.0002
Na	0.02	0.03	~0.5	0.1	0.02	~0.2	0.02	~0.2
Nb	<0.01	<0.01	<0.002	<0.001	<0.01	<0.0006	<0.01	<0.0006
Ni	0.001	0.002	0.005	0.01	0.001	0.002	0.001	0.002
Pb	<0.001	<0.001	<0.0005	0.004	<0.001	0.002	<0.001	0.002
Sb	<0.003	<0.003	<0.005	0.003	<0.003	<0.002	<0.003	<0.002
Si	>1.0	>1.0	Major	Major	>1.0	Major	>1.0	Major
Sn	<0.003	<0.003	<0.0005	0.03	<0.003	<0.0002	<0.003	<0.002
Sr	0.002	0.01	0.003	0.01	0.005	0.006	0.004	0.006
Ti	0.2	0.2	0.2	>1.0	0.08	0.1	0.07	0.06
V	0.005	0.006	0.005	0.03	0.003	0.002	0.003	0.002
Zn	<0.003	<0.003	0.003	0.02	<0.003	0.001	<0.003	0.001
Zr	<0.003	0.03	0.005	0.03	0.01	0.006	0.01	0.002

[a] ND — Not determined

* 600°C Muffle furnace ashing required to reduce the total carbon content to 1.2 weight percent

TABLE 9 - DISTRIBUTION OF ALKALI WITHIN ALUMINOSILICATE MATERIALS, wt %[25]

Material	Sodium			Potassium		
	Soluble	Insoluble	Total	Soluble	Insoluble	Total
Kaolin	0.027	0.029	0.056	0.002	0.050	0.052
Pittsburgh Ash	0.014	0.090	0.104	0.015	0.47	0.485
Chinook Coal Ash	0.202	0.059	0.261	1.003	0.753	1.756
Renton Char	0.017	0.048	0.065	0.069	0.34	0.409
Minnehaha Char	0.016	0.048	0.064	0.074	0.36	0.434

Dwg. 7721A10

5. TRACE AND MINOR ELEMENT BEHAVIOR DURING COMBUSTION

The fate of trace and minor elements during combustion depends not only on the affinity, concentration, and distribution of each element within the inorganic or organic-associated coal matrix, but also on process conditions such as temperature, heating rate, exposure time at elevated temperatures, the localized reducing or oxidizing environment surrounding the burning coal particle, and the solid waste control systems. During combustion, volatiles, including pyrolyzed organics, are released from the coal particle as either attached or detached flames, depending on the thermal properties of the coal and on the physical constraints of the system. The chemical transformations within the organic material during rapid heating and combustion are kinetically limited for particles smaller than 100 μm and diffusion limited for larger particles. Initially, conditions at the particle surface are reducing, with limited diffusion of oxygen through the boundary layer. Nonvolatiles may be trapped within the organic matrix, bonded in organic compounds (organometallics including chelates, metal carbonyls, etc.), or released directly into the effluent gas phase. The more volatile elements within the mineral matrix of the coal particle may vaporize either in their original or in their reduced state.

The coal particle fractures during combustion, in part because of internal burning, forming liquid ash droplet agglomerates. The ash agglomerates may expand through release of internal gases, forming hollow cenospheres, or may burst the particles into a shower of submicron particles. Alternatively, the cenospheres may coalesce with adjacent particles. Entrapped within the melted matrix of the cenosphere are volatile species, which undergo a secondary process and form an ashed-sphere packed with smaller spheres (plerosphere).

Not all of the trace elements contained in the coal particle may be volatilized during combustion. Under these conditions a sizeable portion becomes entrapped within the liquid matrix, where volatilization is diffusion limited. Similarly, nonvolatiles that are expected to result in the solid ash residues may be transferred into the effluent gas if associated with organic matter.

When the last combustible volatile species is consumed, the condition of the particle surface changes from a strongly reducing to a mildly oxidizing environment. Because of the percent of oxygen required for total combustion in the various process designs, most trace volatile elements, although not originally present within coal as oxides, exist in an oxidized state following combustion. Depending upon the boiling point of the trace oxides, various complexes may condense along entrained ash fines at various stages within the system. Elements forming chemical compounds with particularly high vapor pressures (Hg, Se) may be completely released from the stacks as gas phases.

Ultimately, the melted aluminosilicate fly ash matrix forms spherical particles consisting of andalusite ($Al_2O_3 \cdot SiO_2$) at combustion temperatures below 1200 K, which converts into a mullite structure ($3Al_2O_3 \cdot 2SiO_2$) as the operating temperature rises. The andalusite phase is structurally similar to that of the kaolin mineral group, which includes kaolinite ($Al_2O_3 \cdot 2SiO_2$), nacrite or dickite ($Al_2Si_2O_5[OH]_4$), allophane ($Al_2O_3 \cdot SiO_2$ or $Al_2O_3 \cdot 2SiO_2$), dehydrated halloysite or metahalloysite ($Al_2O_3 \cdot 2SiO_2 \cdot 2H_2O$), hydrated halloysite ($Al_2O_3 \cdot 2SiO_2 \cdot 4H_2O$), and anauxite ($Al_2O_3 \cdot SiO_2$). The kaolin layer[26] consists of a hexagonal network of silicon-oxygen tetrahedra with a superimposed layer of aluminum-oxygen or hydroxide octohedra that share oxygen atoms at the tetrahedral apex, as shown in Figure 2. The repeating Si-O/Al-O(OH) unit typifies the kaolinite structural unit in which the net change within the unit cell is balanced, permitting very little substitution within the lattice. Dickite and nacrite consist of structural units similar to those of kaolinite, differing only in the manner in which

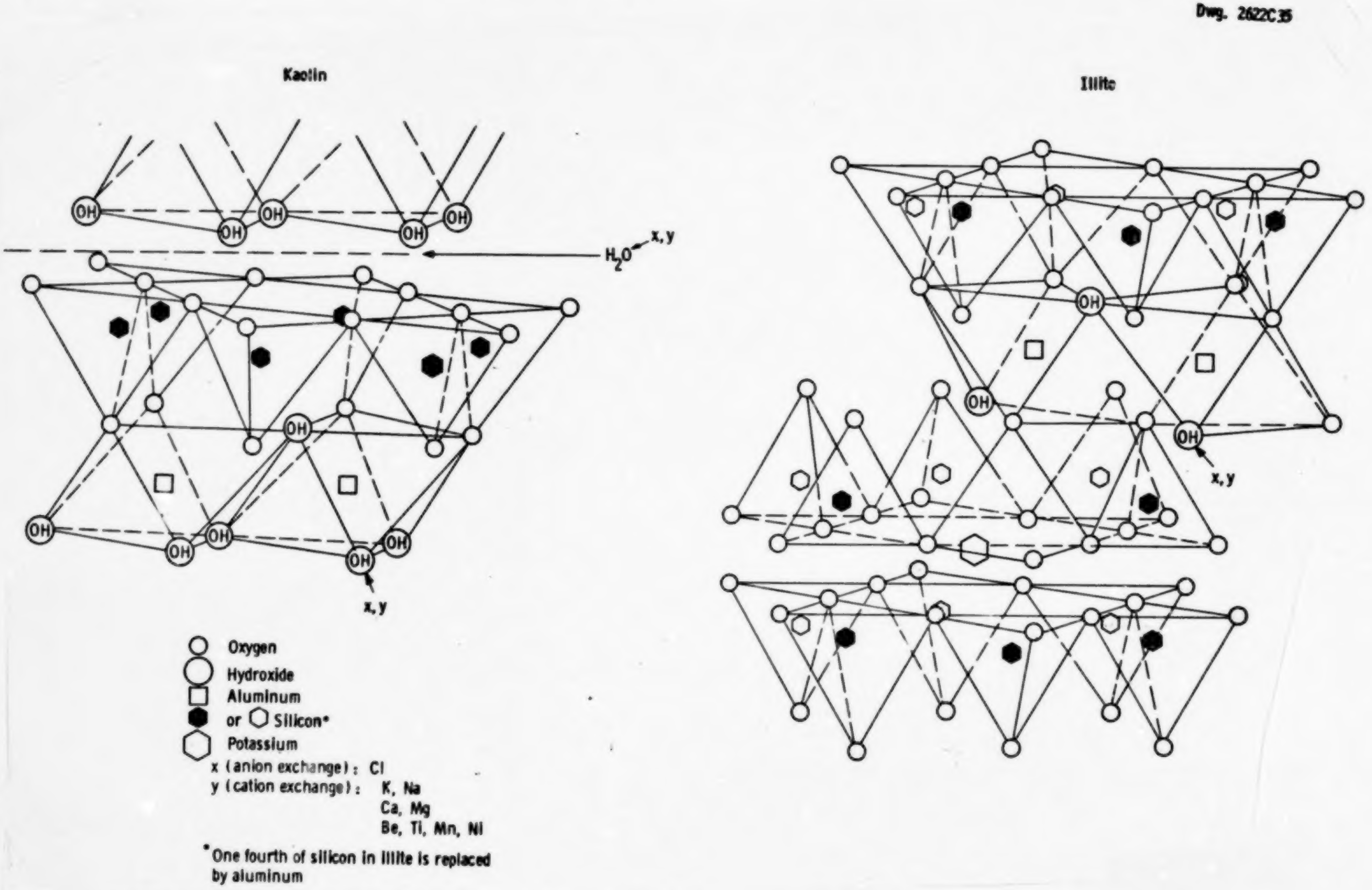

Dwg. 2622C35
Kaolin
Illite
OH
H2O
x,y
Oxygen
Hydroxide
Aluminum
or ⬡ Silicon*
Potassium
x (anion exchange): Cl
y (cation exchange): K, Na
Ca, Mg
Be, Ti, Mn, Ni
*One fourth of silicon in Illite is replaced by aluminum

Figure 2 - Kaolin and Illite Crystal Structure and Potential Ion Exchange Sites

the silicate units are stacked one above the other. Anauxite is a kaolinite mineral with an excess of silicon dioxide (SiO_2) in its structure. A hydrated form of kaolin, halloysite, consists of the kaolinite unit layer separated from adjacent unit layers by molecular layers of water.

In FBC kaolin undergoes a series of dehydration reactions and lattice rearrangements. These include:

- Shrinkage and loss of pore water, altering lattice dimensions at 373 to 423 K
- Oxidation of any organic material at 473 to 573 K. The rate of oxidation depends on the nature of the organic inclusion, the amount of oxygen and its ease of access through the mass of clay to the organic material, and the temperature of reaction.
- Beginning of pyrite oxidation at 673 to 773 K
- Removal of hydroxyl water from clay between 773 and 1173 K. The exact temperature depends on the size of the particle and the nature of the mineral. Kaolinite and halloysites generally lose the hydroxyl group abruptly between 723 and 933 K, changing but not completely destroying the mineral structure.
- Following hydroxyl loss, SiO_2 and alumina (Al_2O_3) are reactive in the temperature regime of 1223 to 1273 K. Alumina becomes readily soluble in acid and reacts with alkali and alkaline earths. The γ-Al_2O_3 phase forms as a transient complex between 1173 and 1273 K but is undetectable at or above 1373 K. Cristobalite, which forms from free amorphous SiO_2 at 1373 K, is not observed at temperatures from 1573 to 1673 K.

- Formation of mullite is observed at 1373 K. The complex conversion of kaolin into mullite is summarized in the following reaction series:

$$\underset{\text{kaolin}}{Al_2Si_2O_5(OH)_4(s)} \longrightarrow \underset{\text{metakaolin}}{Al_2Si_2O_7(s)} + 2H_2O(g)$$

$$\underset{\text{metakaolin}}{Al_2Si_2O_7(s)} \longrightarrow \underset{\text{alumina}}{\gamma\text{-}Al_2O_3(s)} + \underbrace{SiO_2(s) + Al_2O_3}_{\substack{\text{silica/cristobalite/}\\ \text{alumina solid solution}}}$$

$$\underset{\text{alumina}}{\gamma\text{-}Al_2O_3(s)} + \underset{\substack{\text{solid}\\ \text{solution}\\ \text{complex}}}{SiO_2\text{-}Al_2O_3} \longrightarrow \underset{\text{mullite}}{3Al_2O_3 \cdot 2SiO_2(s)}$$

In addition to the thermal decomposition of the unstable illite clays and the stoichiometric loss of SiO_2 from kaolinite, forming the mullite lattice, conversion of pyritic inclusions (FeS_2) in the feedstock to iron oxide (Fe_3O_4-magnetite, Fe_2O_3-hematite) occurs, releasing SO_2 during combustion. In the presence of oxygen and SO_2, calcite ($CaCO_3$) is sulfated, forming the anhydrite ($CaSO_4$) structure. In the absence of sulfur, carbon dioxide (CO_2) is released from the particle, forming calcium oxide (CaO). Additional reactions that can occur are the formation of anorthite ($CaAl_2Si_2O_8$) and/or gehlenite ($Ca_2Al_2SiO_2$) from the reaction between calcium and kaolinite in the fluidized bed.

Illite consists of layers, with a plane of octahedrally coordinated cations sandwiched between two inward-pointing sheets of $(SiAl)O_4$-linked tetrahedra. Generally, illites contain little or no interlayered water and are unaffected by heating. The dehydration of illite proceeds in a number of stages.[27]

- Adsorbed water on the particle surface and the small amount that may be interlayered with illite sheets is released rapidly below 383 K, gradually tapering off at temperatures of 623 K.
- Water formed by expulsion of hydroxide ions is rapidly removed between temperatures of 623 and 873 K.
- The remaining illite structure is disrupted at temperatures between 1123 and 1223 K.

The presence of a considerable number of potassium ions interlayered in the illite lattice prevents the entry into the structure not only of water, but also of other cations, attributing a low-cation exchange capacity to the material. The exchange that does occur is thought to take place at the crystal edge, as in kaolinite, where unsatisfied valences exist. In cation exchange reactions hydrogen in the exposed hydroxyl group is replaced by the reactant cation, while in an anion exchange reaction the complete hydroxyl group is displaced (see Figure 2). The presence of broken bonds around the edge of the clay particle, therefore, provides as many negative as positive charges that must be balanced in order to maintain the neutrality of either the kaolin or the illite structure. The unbalanced charges may be satisfied through interactions with the trace and minor elements K, Na, Ca, Mg, Be, Ti, Mn, and Ni, as will be shown in the FBC projections. The elements may also enter and be camouflaged in the clay lattice if the element has the same charge and ionic radius as the element being displaced. The element may be captured within the lattice if it has a similar ionic radius but a higher charge than the lattice element, or it may be admitted easily into the lattice if the element has a smaller or similar ionic radius and lower charge than the displaced ion. With the variation in the clay content in coal, multiple trace and minor solid phases result, depending on the ratio of Al and Si present in the reaction. The complexity of the resulting phases formed in the reaction of alkali with Al and Si is illustrated in Figures 3 and 4.

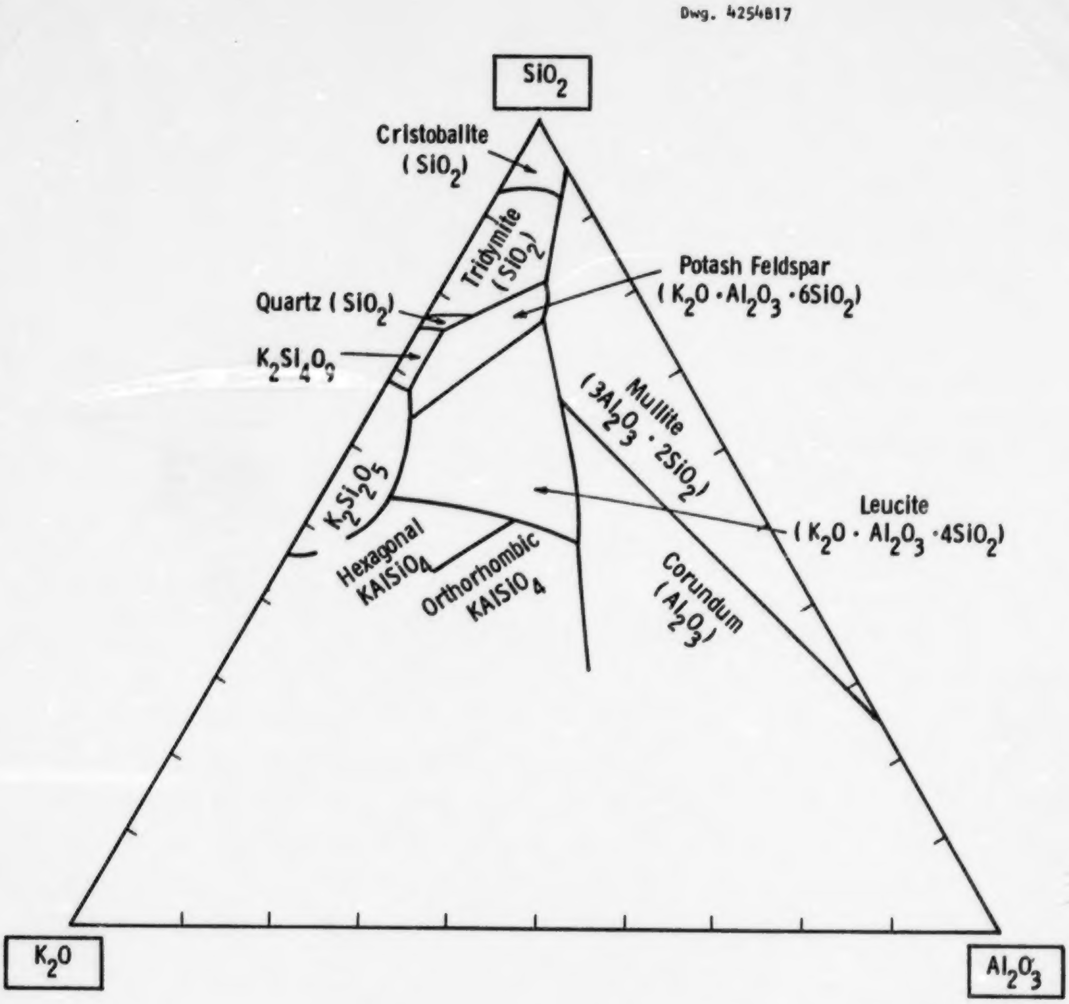
Dwg. 4254B17
SiO2
Cristobalite (SiO2)
Tridymite (SiO2)
Quartz (SiO2)
K2Si4O9
K2Si2O5
Potash Feldspar (K2O·Al2O3·6SiO2)
Mullite (3Al2O3·2SiO2)
Leucite (K2O·Al2O3·4SiO2)
Hexagonal KAlSiO4
Orthorhombic KAlSiO4
Corundum (Al2O3)
K2O
Al2O3

Figure 3 - Phase Stability Diagram for K_2O-Al_2O_3-SiO_2[28]

Dwg. 4254B16

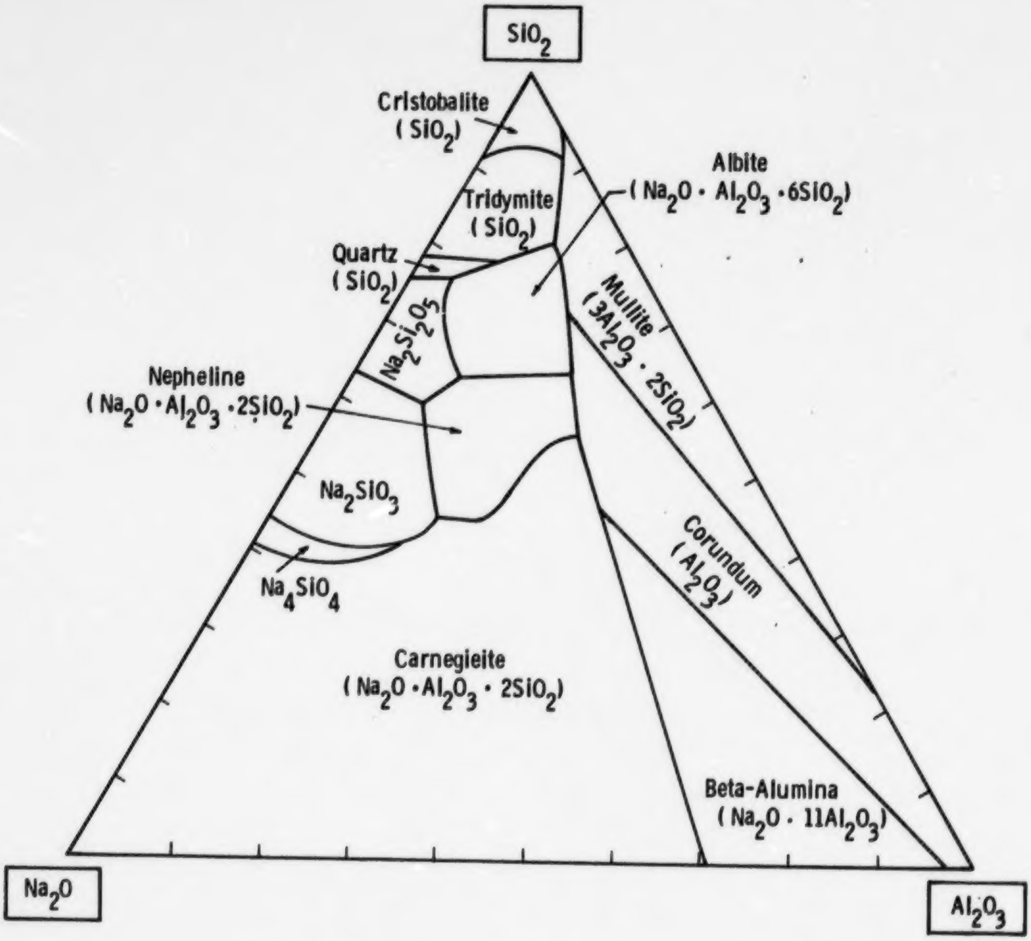
SiO$_2$
Cristobalite (SiO$_2$)
Tridymite (SiO$_2$)
Albite (Na$_2$O · Al$_2$O$_3$ · 6SiO$_2$)
Quartz (SiO$_2$)
Na$_2$Si$_2$O$_5$
Mullite (3Al$_2$O$_3$ · 2SiO$_2$)
Nepheline (Na$_2$O · Al$_2$O$_3$ · 2SiO$_2$)
Na$_2$SiO$_3$
Corundum (Al$_2$O$_3$)
Na$_4$SiO$_4$
Carnegieite (Na$_2$O · Al$_2$O$_3$ · 2SiO$_2$)
Beta-Alumina (Na$_2$O · 11Al$_2$O$_3$)
Na$_2$O
Al$_2$O$_3$

Figure 4 - Phase Stability Daigram for Na_2O-Al_2O_3-SiO_2[28]

The trace elements included in the mineral matrix are present at concentrations related to their isomorphous replacement of a major element or to the number of random inclusions in cavities or holes in the crystal lattice. The rules for substitution of a major element by a trace or minor element are generally related to ionic radii, charge, and the covalent character of the bond. For example, Ba, Rb, and Pb substitute for K; Cr for Fe; Y and Sr for Ca; Li and Ga for Mg; Ga for Al; Cd and In for Zn; and As for Cu.

As the aluminosilicate lattice undergoes dehydration and lattice rearrangement, the sulfide fraction in the coal particle oxidizes and the carbonates calcine, releasing gaseous SO_2 and CO_2 and forming supermicron and submicron ash particles. The supermicron residual ash is acknowledged to be from the burnout of the mineral residue in the single coal particle, while the submicron or condensation ash is thought to be produced by vaporization of metallic species that reoxidize and recondense.[29]

The spherical, glassy appearance of the supermicron ash particle implies its prior existence as a liquid or molten droplet, while the submicron ash particle appears to be an aggregate cluster of smaller particles rather than a discrete species. Sodium or potassium may vaporize directly and diffuse as a volatile from the burning coal particle surface. Silicon and refractory complexes may be reduced to more volatile suboxides or sulfides, which then enter the gas phase, diffusing from the burning surface. By this mechanism up to 1 percent of the Si, K, and Na in coal can vaporize and diffuse into the effluent gases. Reaction with surrounding gases may then lead to growth by coagulation or adherence at sticky sites along the entrained ash surface.

In a fluidized-bed combustor, of course, some of the process conditions can be much different from those that exist in a conventional boiler. The combustion temperature in a fluidized bed, for example, 1100 to 1200 K, is much lower than in a 1650 K conventional boiler. The mechanism and chemical fate of the trace elements in fluidized-bed systems, however, have not been delineated because of the limited data reported in the literature and currently can only reflect an extension to low-temperature operation data from the conventionally fired boiler systems. Lyon et al.,[1] proposed the following mechanism for the behavior of trace and minor elements during combustion in conventional coal-fired boilers:

- Complex aluminosilicates do not decompose, but melt and coalesce to form slag or boiler bottom ash and fly ash.*
- During the initial stages of combustion, a reducing environment probably exists within the coal particle and its immediate vicinity. Under these conditions the chemical bonding of metallic elements and sulfur in sulfide mineral inclusions or between the elements and the organic matrix may be broken, with the elements forming volatile species. If the elements are dispersed in the coal organic matrix, they initially become dispersed in the gas stream when coal is burned.
- Elements that initially are volatilized or dispersed in the flue gas stream may then be oxidized to form less volatile species that may then condense or be adsorbed on entrained particulates as the temperature of the flue gas drops.

---

*The distribution of ash between the bottom ash and fly ash fractions is a function of the burner type, coal type, ash fusion temperature, and the type of boiler bottom (wet or dry). For example, stoker-fired units emit the smallest proportions of fly ash, which is relatively coarse in nature; cyclone-units, which operate in excess of the ash melting temperature, produce 80 to 85 percent of the ash as a melted slag; pulverized units usually produce 65 to 80 percent fly ash and 20 to 35 percent bottom ash; wet bottom boilers are designed to process larger proportions of bottom ash than are dry bottom boiler designs.

- Since the slag is in contact with the flue gas for a short time and at a high temperature, condensation of volatiles on the slag is minimal.

Partitioning of the trace and minor elements in a conventional boiler results, according to this mechanism, between the volatile stack-gas emissions and the solid ash formation of either the slag or the fly ash. Lyon's[1] analysis of the ash and outlet gases at the Allen Steam Plant in Memphis, TN, indicates that the trace and minor elements can be classified as:

- Elements that readily incorporate into slag formations: Al, Co, Cr, Fe, K, Mn, Na, Si, Ti, V, and possibly Ni. These elements do not volatilize in the combustion zone, but form a melt of rather uniform composition, divided almost equally between the fly ash entering the electrostatic precipitator and the slag fraction. There is no apparent tendency to concentrate these elements on ash particles exiting from the electrostatic precipitator.
- Elements that concentrate in the inlet electrostatic precipitator fly ash instead of the slag and in the outlet electrostatic precipitator fly ash instead of the inlet electrostatic precipitator fly ash: As, Cd, Cu, Ga, Pb, Se, Zn, and, possibly, Mo. These elements volatilize on combustion. With the removal of the slag in the combustion zone, Pb has no opportunity to condense on the slag, but condenses or becomes adsorbed on the fly ash as the flue gas cools.
- Elements that remain completely in the gas phase: Hg, Cl, and Br.

Natusch et al.[30] proposed a volatilization-condensation or adsorption mechanism that accounted for the relation between the trace element concentration and the ash particle size. As the temperature of the flue gas decreases, volatiles condense and chemically react with or are absorbed onto the ash particle surface. Lyon,[1] Cowherd,[9] and Cato[10] have shown the concentration of the condensed element in a conventional boiler to be inversely proportional to the ash particle size, as shown in Tables 10 through 12. This finding would be expected, since the surface area increases as particle size decreases, thus increasing the concentration of condensed volatile material per unit area.

The volatile trace and minor elements emitted in the stack gases may be toxic. Cowherd et al.,[9] however, indicated that the concentration of emissions from conventional utility boilers at ground level is less than the corresponding threshold limit value (TLV) for the various inorganic trace and minor elements, with only the concentration of Be approaching the level of potential concern. Limited information is reported on potentially hazardous organic emissions. Polycyclic organic material (POM) and polychlorinated biphenyls (PCB) could possibly be formed within the combustor prior to complete oxidation.

Unlike the basic concepts that have been proposed for the release of trace and minor elements from coal particles during combustion and the subsequent formation of ash, release mechanisms for sorbent and getter materials projected for use in the FBC systems have not been reported. Release of alkali (Na and K) from candidate sorbents in 22.1% H_2, 19.4% CO, 18.2% CO_2, and 40.3% N_2 has been demonstrated by Yannopoulos, Toth, and Pebler[31] to be achieved within 10 to 20 minutes at projected desulfurizer temperatures of 1148 K. The flame emission spectroscopic technique used in their investigation indicated that alkali release was proportional to the alkali chloride content instead of to the alkali bound within the clay minerals and that alkali release increased with increasing reaction temperatures (Figures 5 and 6). Yannopoulos also demonstrated that release increased significantly during calcination of the dolomite.

TABLE 10 - TRACE ELEMENT CONCENTRATION AS A FUNCTION OF PARTICLE SIZE AS REPORTED BY LYON[1]

Dwg. 5592C82

LOCATION: The Allen Plant, Memphis, Tennessee

DESCRIPTION: The boilers are fed with crushed coal via a cyclone arrangement.

FUEL ANALYSIS: 9.5% moisture, 34% volatile matter, 43% fixed carbon, approximately 13% ash, and 3.4% sulfur (as fired).

ASH COLLECTION: Approximately 60% goes through the slag tank, while 40% is collected by electrostatic precipation.

Electrostatic Precipitator Inlet Fly Ash, ppm

	Microns						
Element	>15	14	9	6	4	3.5	1.4 - 0.5
Be							
F							
Hg							
Pb							
Al	99600	97100	100000	80000	105000	95000	92100
Co	56	49	45	50.6	67	65	83
Cr	433	240	250	320	420	490	634
Fe	181000	158000	140000	140000	160000	156000	174000
Mn	317	294	290	320	358	430	458
Mo	30	51	67	110	153	153	212
Ni							
Ti	5860	6350	6670	6810	8280	9510	9630
Na	3280	3400	3580	4100	3900	4110	4140
K	20300	23700	26800	28500	26600	30200	23600
Si							
Br							
B							
P							
Cu	<500	<650	<500	456	<500	<900	405
V	322	347	371	416	608	706	715
Zn	1140	1050	930	1100	1800	2200	1900
Sb	7.2	8.4	7.5	10	14	165	18
Sn							
Zr							
As	100	96	92	125	145	174	203
Cd							
Se	17	<50	26	<50	30	15	21
Ga	45	46	47	66	101	120	140
Ge							

Electrostatic Precipitator Outlet Fly Ash, ppm

	Microns		
Element	11 - 2.9	2.0 - 1.3	0.9 - 0.6
Be			
F			
Hg			
Pb			
Al	57000	99200	86000
Co	60	90	80
Cr	1100	1300	1000
Fe	143000	170000	77000
Mn	404	405	430
Mo	100	165	223
Ni			
Ti	6670	12000	12600
Na	3200	4000	4060
K	40000	39600	29700
Si			
Br			
B			
P			
Cu	<600	<800	<800
V	605	836	1060
Zn	1930	4000	3000
Sb	44	17	22
Sn	9	18	18
Zr			
As	180	73	110
Cd			
Se	150	104	82
Ga			
Ge			

TABLE 11 - TRACE ELEMENT CONCENTRATION AS A FUNCTION OF PARTICLE SIZE AS REPORTED BY COWHERD[9]

Dwg. 5592C86

LOCATION: Tennessee Valley Authority Widows Creek Steam Electric Generating Station-Unit 5

DESCRIPTION: The 125 MW utility boiler horizontally fired with pulverized coal was equipped with a mechanical fly ash collector. Sampled streams included: pulverized coal, furnace bottom ash, superheater ash, collection ash, and flue gases at the inlet and outlet of the fly ash collection.

FUEL ANALYSIS: 1,42% moisture, 34,28% volatile matter, 48,46% fixed carbon, 15,84% ash, and 3,47% sulfur (average weight percent reported values for the Appalachian coal)

ASH COLLECTION: Two four-bank multiclone units used for fly ash collection; V-type furnace bottom hoppers with water sluice for bottom ash sampling

Dust Collector Inlet Sample, ppm

	Microns				
Element	>3,96	2,35 - 3,96	1,61 - 2,35	0,87 - 1,61	0,56 - 0,87
Be	5,2	8,7	4,7	5,4	36,1
F					
Hg					
Pb	14,5	15,5	29,5	12,2	18,4
Al					
Co	26	30	28	58	75
Cr	251	458	1080	3080	4510
Fe	145000	155000	295000	121000	184000
Mn	149	274	189	569	654
Mo					
Ni	460	840	690	2460	689
Ti					
Na					
K					
Si					
Br					
B					
P					
Cu	147	261	152	564	2660
V	475	818	592	741	1550
Zn	791	1110	781	2670	4620
Sb					
Sn					
Zr					
As					
Cd	46	164	92	135	447
Se					
Ga					
Ge					

Dust Collector Outlet Sample, ppm

	Microns			
Element	> 2,87	1,16 - 1,69	0,61 - 1,16	0,39 - 0,61
Be	12,6	8,3	3,5	86
F				
Hg				
Pb	10,5	9,3	6,8	18,5
Al				
Co	55	48	67	218
Cr	347	577	709	1790
Fe	105000	93000	68000	185000
Mn	199	288	376	1560
Mo				
Ni	414	319	478	512
Ti				
Na				
K				
Si				
Br				
B				
P				
Cu	177	212	264	4500
V	630	500	680	1660
Zn	1780	2260	1880	4640
Sb				
Sn	630	500	680	1660
Zr				
As				
Cd	80	165	435	429
Se				
Ga				
Ge				

TABLE 12 - TRACE ELEMENT CONCENTRATIONS AS A FUNCTION OF PARTICLE SIZE AS REPORTED BY CATO[10]

Dwg. [illegible]

LOCATION: Fremont, Nebraska

DESCRIPTION: Boiler Number 6 at the Fremont Plant was an Erie City Iron Works water tube boiler with four Combustion Engineering gas - and coal - type RO burners

FUEL ANALYSIS: 6.85-7.65% moisture, 38.26-38.75% volatile matter, 43.07-43.58% fixed carbon, 10.18-10.79% ash, 1.03-1.28% sulfur.

ASH COLLECTION: Dust collector was a mechanical cyclone type. Collected materials include: bottom ash, dust collector ash, flue gas collector inlet and outlet.

Inlet to Dust Collector, ppm

	Microns					
Element	15	3.4	2.1	1.4	0.69	0.34
Be	2.9	4.2	2.6	3.6	9.1	< 10
F						
Hg						
Pb	10	270	260	570	300	560
Al						
Co	49	65	65	78	69	77
Cr	110	110	62	170	83	240
Fe						
Mn	1100	900	800	1000	1200	1300
Mo						
Ni	330	47	40	165	62	260
Ti	7700	8400	7000	6100	5400	<11000
Na						
K						
Si						
Br						
B						
P						
Cu	170	310	280	300	340	680
V	150	<850	<430	<760	<1400	<2800
Zn	180	400	440	540	580	850
Sb	<35	<130	<66	<120	<210	<430
Sn	1.4	4.0	3.0	3.0	3.3	140
Zr						
As						
Cd	3.9	5.0	5.2	5.4	4.5	8.6
Se						
Ga						
Ge						

Outlet from Dust Collector, ppm

	Microns					
Element	15	3.44	2.06	1.38	0.69	0.34
Be						
F						
Hg						
Pb	200	360	360	400	320	410
Co	63	66	62	57	97	1100
Cr	92	58	62	55	< 140	< 360
Fe						
Mn	1300	780	1000	1200	1400	1300
Mo						
Ni	76	78	71	77	310	340
Ti	6900	6600	5700	4800	<14000	< 36000
Na						
K						
Si						
Br						
B						
P						
Cu	260	250	280	300	280	520
V	<410	<390	<550	<1000	<3700	<9300
Zn	340	450	610	690	620	1000
Sb	<61	<59	<83	< 150	<560	<1400
Sn	2.2	3.3	4.4	5.7	10	900
Zr						
As						
Cd	3.9	4.6	7.1	9.1	8.3	12.
Se						
Ga						
Ge						

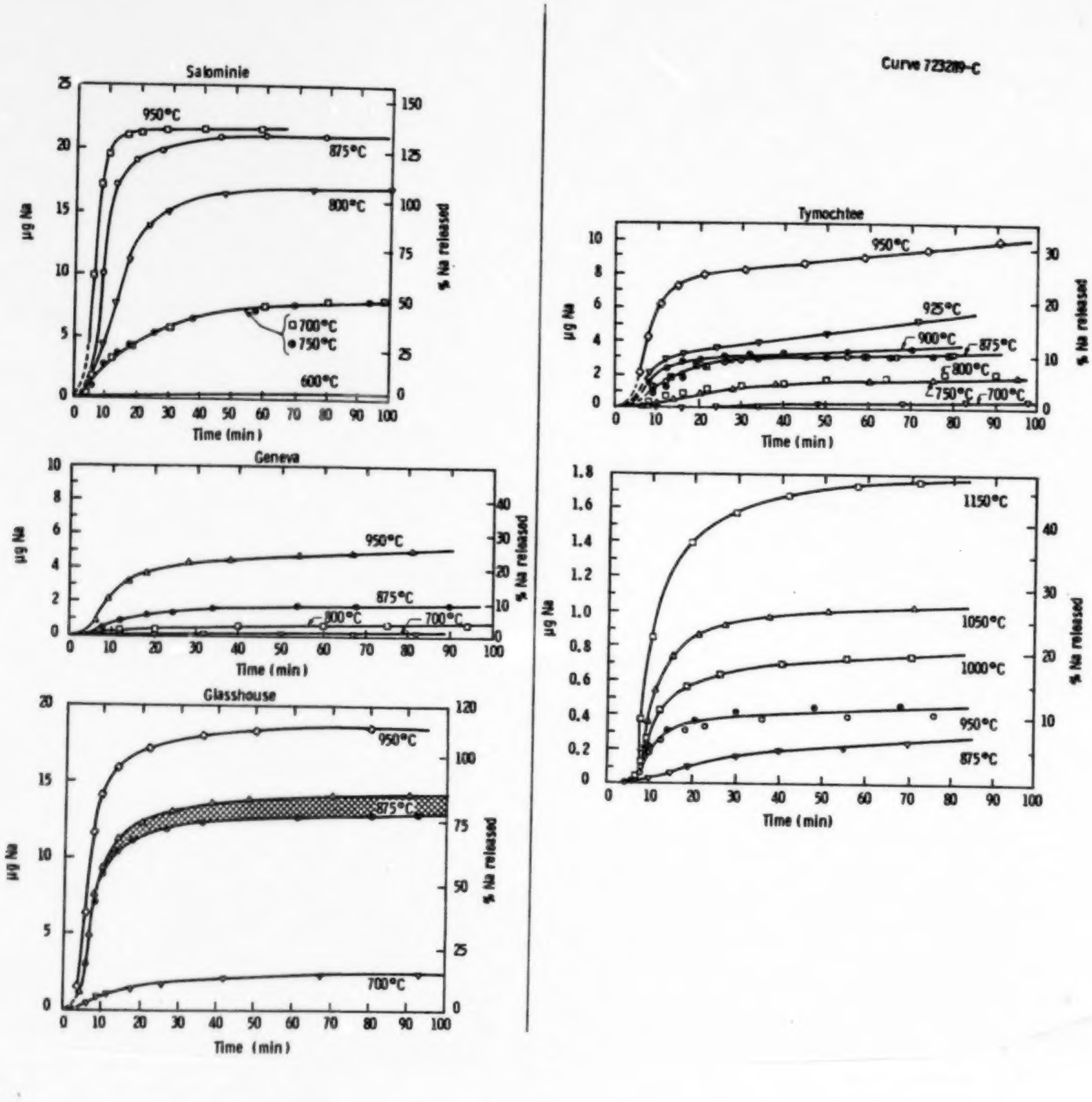

Figure 5 - Release of Na from Dolomite as a Function of Reaction Temperature[31]

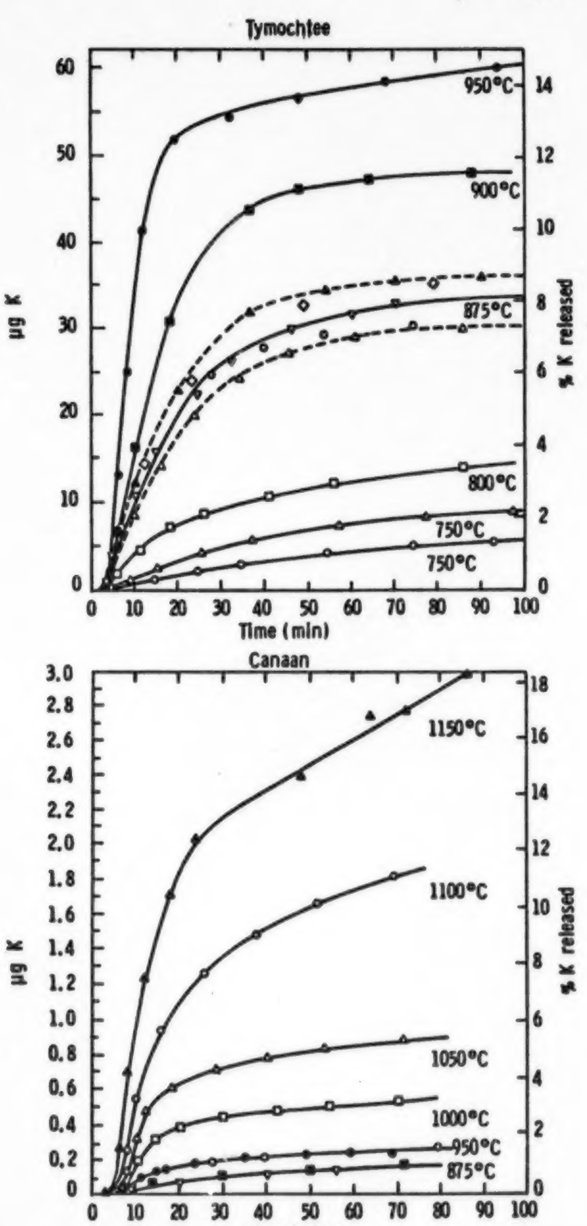

Figure 6 - Release of K from Dolomite as a Function of Reaction Temperature[31]

Preliminary, experimental, bench-scale studies at Westinghouse have exposed various dolomites and limestones to both oxidizing and reducing environments under pressure at temperatures between 1040 and 1150 K. Chemical characterization of condensed volatiles and impacted particulates and analysis of the reacted sorbents specifically for the retention concentration of Na and K are presented in Tables 13 through 16 and in Figures 7 through 10.

The composition of the material deposited varies greatly with temperature when sorbents are heated at pressure in an oxidizing gas environment (Table 13). Potassium and Cl predominate in most deposits, but Al, Si, S, Ca, or Mg are infrequently detected as major constituents. After 75 hours release from Salamonie dolomite is principally through attrition of the sorbent. Similarly, Geneva dolomite after 2 hours at 1048 K deposits Ca and Mg along the 963 to 508 K temperature gradient. Deposits of S predominate at temperatures below 508 K. The 2 hour reaction of Geneva dolomite at 1098 K enhances the release of Si and Al along the 1043 to 958 K temperature gradient and maintains release and deposition of the S-containing phase at the lower temperature zone (443-423 K). Increasing the Geneva dolomite reaction temperature to 1148 K no longer maintains deposition of the S phase at temperatures between 443-433 K but reverts to deposition by attrition of the Ca- and Mg-based sorbent.

Deposits from Glasshouse No. 10 dolomite heated either to 1098 or to 1148 K after 75 hours at pressure principally contain K and Cl. Deposition by attrition of the sorbent is not as prevalent in Glasshouse No. 10 dolomite as in the Salamonie or the Geneva materials. Silicon and Al infrequently result as the major constituents in the deposit.

Tymochtee dolomite, generally ranked as a high K-containing sorbent (Figure 7) releases the alkali, forming deposits composed principally of the alkali chloride phase. Silicon, Ca, and Al are also detected in the Tymochtee deposits, as shown in Figure 8.

TABLE 13 - SEM CHARACTERIZATION OF THE DEPOSITS FORMED FROM THE RELEASE OF VOLATILES AND PARTICULATES FROM DOLOMITE

Dwg. 2626C96

Test No.	Sorbent	Temp. (K)	Gas Composition	Time (Hours)	Pressure (kPa)	Composition of Deposits **							
HPR-13	Salamonie	1048	$N_2/CO_2/O_2$*	75	825	Al>Fe Cl>Na>Al>K>Ca Fe>Al Al	Ca>Mg>Al>Fe Ca>Mg>Fe Ca>Mg>Si>K>Cl	Ca>Si>Cl>K>Fe Ca>Mg>Fe Ca>Mg>Fe					
HPR-16	Geneva	1048	$N_2/CO_2/O_2$	2	825	963-873 K Ca>S>Mg Al>Fe>K S>Ca>Mg>Fe	873-723 K S>Ca>Mg Ca>Mg>S>Fe Ca>S>Mg>Fe	723-593 K Ca>Mg>S Ca>Mg>Si>S>Fe Al	593-508 K Ca>Mg>Fe Ca>Mg>Fe	508-458 K S>Ca>Cu S>Mg>Ca>Cu S>Ca>Fe	458-423 K S>Ca>Fe>Ni S>Al>Ca S>CaAl	≤423 K S>Al>Fe S>Al>K>Fe S>Al>K>Fe	
HPR-17	Geneva	1098	$N_2/CO_2/O_2$	2	825	1043-458 K Al Si>Al>K>Ti>Fe Al>Si>Ca>K>Ti						443-423 K S>Si>Al>Fe S>Al>K	
HPR-18	Geneva	1148	$N_2/CO_2/O_2$	2	825							443-423 K Ca>S>Mg>Cl Ca>S>Al>Fe Ca>Mg>S	
HPR-31	Glasshouse	1148	$N_2/CO_2/O_2$	75	825	1073-998 K Cl>K>Si>Fe Si>Cl≥K>Na>Fe Si>Cl>K>Na>Cr Si>Ca>K≥Cl>Mg≥Cr>Fe	998-863 K Si>>Cl≥K>>Cr>Fe Si>>Cl≥K>>Na>Cr>Fe Cl>K>Si>Ni>>Fe	863-693 K Cl≥K>Si>Na>>Fe Cl≥K>Na>Si Cl≥K>Na>Si Cl≥K>Si≥Na>Fe	693-573 K Cl>K>Na>Al>Fe Si>K≥Cl>Na>Cr Cl>Na≥Si≥K Mg>Cl≥K>Cr>Si	573-483 K Si>>S≥K≥Cl>>Cr>Fe Si>>S≥Cl≥K Si>>S≥K>Cr Si>>Ca≥Cr≥S≥Cl>Ni			
HPR-32	Glasshouse	1098	$N_2/CO_2/O_2$	75	825	948-873 K S>K≥Ca>Mg>Cl>Cr S>Ca>Al>Mg>Cr Al>Cl≥Ca≥K>Fe S≥Ca>Mg>Cl≥K>Cr>Fe Cl≥K>Al>Na S≥Ca>Cl≥K>Mg>Cr>Fe Cl>K>Ca≥Al≥Na>Fe	873-763 K Cl≥K>>Na≥Al Cl>K>Ca	763-633 K Cl>K>>Ca≥Al≥Na Cl≥K>Al≥Ca≥Na Cl≥K>Al≥Na	633-533 K Al≥Cl≥K>Ca Cl≥K>Al Al>Cl≥K>Fe Al>Cl≥K>Fe	533-463 K Al>Cl>Fe Al>Fe	463-418 K Al>Cl>Fe Ca>Mg>>Cl Al>Cl>Ca>>Fe Fe (low)	418-388 K Al>Cl≥Ca>Fe Al>>Fe≥Cl	<388 K Al>Fe Ca≥Mg>Cl>Fe Ca≥Mg>>Fe Ca Ca≥Si>K≥Fe Ca>>Mg>Cl
HPR-33	Glasshouse	1148	$N_2/CO_2/O_2$	75	825	1073-998 K low Fe Cl>Al>Na>K Al Al>Ti Cl>K>Na>Al (trace)	998-863 K K>Cl>Na>Al>Cr K>Cl>Na>Al>Cr Cl>Na>K>Al Cl>K>Na>Al	863-693 K Si≥Cl≥K>Al>Na>Cr>Ca Cl≥K>Al>Ca Al>Cl≥K Cl>K>Na>Ca Cl>K>Na>Al Cl>K>Na>Al Cl>K>Na>Al	693-563 K Cl>K>Na>Al Cl>K>Na>Al>Fe K>Na>Al>Cr	563-488 K Cl>K>Al Cl>K>Al>Cr≥Fe Cl>K>Al>Fe	488-433 K Cl>K>Al>Fe Al>Cl>K>Fe		
HPR-34	Tymochtee	1148	$N_2/CO_2/O_2$	75	825		883-753 K Cl>K>>Al K>Cl>S>Al>Cr		513-463 K Cl>K>Al>S(?) Cl>K>Cr>Al>S(?)>Fe	≤413 K Al>Cl≥K>>Ca; Si(?) K>Cl≥Al>S(?)>Cr≥Fe Al>K≥Cl>>Cr>Fe			
HPR-35	Tymochtee	1148	$N_2/CO_2/O_2$	75	825	933-823 K K>Ca>S>Cl>Cr>Al>Fe Cl>K>>Al>S(?)>>Cr Cl≥K>Ca≥S>Al>Cr>Fe Cl≥K>>Al Cl≥K>>Ca>Al; (S?)	823-713 K Cl≥K>>Al Cl≥K>>Al		473-443 K Si>Al>K≥Cl>Ca-Cr>Fe; (S?) S>Cr>Mg>Si~K≥Cl~Al>Cr	≤403 K Cl≥K>Al>Cr>Fe			

* 78% N_2/ 19.8% CO_2/ 2.2% O_2

**Composition in the Various Temperature Zones is Reported in Decreasing Order as Measured by EDAX

TABLE 14 - TOTAL MICROGRAMS OF TRACE AND MINOR ELEMENTS IN DEPOSITS FROM FIXED-BED REACTED SORBENT MATERIALS

Element	Glasshouse No. 10 1098K Fixed Bed	Glasshouse No. 10 1148K Fixed Bed	Tymochtee 1148K Fixed Bed
Na	86	144	173
K	280	176	1390
Ca	250	216	242
Mg	150	98	163
Cr	14	50	418
Cu	23	20	36
Fe	12	31	13
Si	22	17	56

Dwg. 1714B27

TABLE 15 - SPARK SOURCE MASS SPECTROMETRIC ANALYSIS OF DEPOSITS FORMED AS A RESULT OF THE RELEASE OF VOLATILES AND PARTICULATES FROM TYMOCHTEE DOLOMITE

Dwg. 1714B31

Elemental Constituent	HPR-34			HPR-35		
	Deposition Temp., K			Deposition Temp., K		
	883 - 753	513 - 463	≤ 413	823 - 713	473 - 443	≤ 503
K	47.000	24.000	44.000	42.000	34.000	32.000
Cl	47.000	71.000	23.000	42.000	54.000	11.000
S	00.370	00.300	03.100	00.580	01.000	13.500
Na	00.370	00.066	00.260	00.320	00.850	01.100
Rb	00.028	00.042	00.035	00.037	00.060	00.075
Br	00.003	00.069	00.064	00.016	00.100	00.110
Fe	00.002	00.010	00.032	00.011	00.054	00.050
Cr	00.120	00.550	00.460	00.240	00.240	01.300
Ca	00.005	00.009	00.038	00.120	00.090	00.250
Si	00.058	00.087	00.500	00.170	01.110	01.400
Al	00.006	00.015	00.044	00.018	00.110	00.310
F	00.009	00.005	00.110	00.054	00.056	00.200
B	00.022	00.056	00.290	00.090	00.410	00.540
C	00.220	01.030	15.000	06.200	02.500	21.000
O	04.900	03.500	13.000	07.700	05.300	16.000

[a] Concentration given in atomic percent.

TABLE 16 - DISTRIBUTION OF ALKALI WITHIN SORBENTS AFTER EXPOSURE TO OXIDIZING OR REDUCING GAS ENVIRONMENTS

Concentration, Weight %

Sorbent (Test No.)	Temp. (K)	Pressure (kPa)	Exposure Time (Hrs)	Gas Composition	Sorbent Weight Loss after Exposure	Na			K			Cl
						Soluble	Insoluble	Total	Soluble	Insoluble	Total	
Salamonie												
HPR-13	1048	825	2	N_2/20% CO_2*		0.0150	0.0003	0.0153	0.0055	> 0.0005	> 0.0060	~0.062
HPR-13B	1048	825	2	Fuel Gas**		0.0155	0.00025	0.01575	0.0050	> 0.0005	> 0.0055	~0.062
HPR-14	1098	825	2	N_2/20% CO_2		0.0165	0.0002	0.0167	0.0058	> 0.0005	> 0.0063	~0.057
HPR-14B	1098	825	2	Fuel Gas		0.0188	0.0001	0.0189	0.0100	0.0005	0.0105	~0.067
HPR-15	1148	825	2	N_2/20% CO_2		0.0175	0.00015	0.01765	0.0100	0.00025	0.01025	0.065
HPR-15B	1148	825	2	Fuel Gas		0.0198	0.00005	0.01985	0.0130	0.00005	0.01305	0.062
Geneva												
HPR-16	1148	825	2	N_2/20% CO_2	19.79%	0.0185	0.0019	0.0204	0.0283	0.0060	0.0343	0.018
HPR-17	1098	825	2	N_2/20% CO_2	21.59%	0.0165	0.0039	0.0204	0.0288	0.0055	0.0343	0.020
HPR-18	1148	825	2	N_2/20% CO_2	21.96%	0.0105	0.0080	0.0185	0.0233	0.0115	0.0348	0.016
HPR-22	1148	825	2	N_2/20% CO_2	21.55%	0.0145	0.0068	0.0213	0.0280	0.0090	0.0370	
HPR-23	1148	825	2	N_2/20% CO_2	21.09%	0.0178	0.0037	0.0212	0.0338	0.0062	0.0400	
HPR-24	1148	825	2	N_2/20% CO_2	20.64%	0.0148	0.0044	0.0192	0.0288	0.0079	0.0367	
HPR-19	1048	825	2	Fuel Gas	20.44%	0.0141	0.0080	0.0221	0.0200	0.0110	0.0310	
HPR-20	1098	825	2	Fuel Gas	22.45%	0.0080	0.0150	0.0230	0.0125	0.0163	0.0288	
HPR-21	1148	825	2	Fuel Gas	29.23%	0.0063	0.0230	0.0293	0.0125	0.0235	0.0360	
Glasshouse # 10												
HPR-25	1148	825	2	N_2/20% CO_2	23.61%	0.0190	0.0032	0.0222	0.0300	0.0100	0.0400	
HPR-26	1148	825	2	N_2/20% CO_2	23.31%	0.0200	0.0028	0.0228	0.0313	0.0120	0.0433	
HPR-27	1148	825	2	N_2/20% CO_2	23.36%	0.0184	0.0030	0.0214	0.0310	0.0108	0.0418	
HPR-29	1148	825	2	N_2/20% CO_2	23.32%	0.0201	0.0028	0.0229	0.0325	0.0118	0.0443	
HPR-30	1148	825	2	N_2/20% CO_2	23.57%	0.0188	0.0030	0.0218	0.0313	0.0095	0.0408	
HPR-31	1148	825	75	N_2/20% CO_2	23.57%	0.0087	0.0038	0.0125	0.0065	0.0064	0.0129	
HPR-32	1148	825	75	N_2/20% CO_2	23.15%	0.0156	0.0024	0.0180	0.0270	0.0111	0.0381	
HPR-33	1148	825	75	N_2/20% CO_2	23.29%	0.0175	0.0023	0.0198	0.0236	0.0099	0.0325	
Tymochtee												
HPR-34	1148	825	75	N_2/20% CO_2	26.63%	0.0304	0.0001	0.0305	0.2031	0.0042	0.2073	
HPR-35	1148	825	75	N_2/20% CO_2	29.35%	0.0300	0.0001	0.0301	0.1897	0.0089	0.1986	
HPR-36	1098	825	24	Fuel Gas***	28.19%	0.0337	0.0003	0.0340	0.2555	0.0186	0.2741	

* 78% N_2/19.8% CO_2/2.2% O_2

** 46.1% N_2/16.4% CO_2/ 10.0% CO/ 25% H_2/ 2.5% CH_4

*** 79.9% N_2/ 15.7% O_2/ 4.4% CO_2

Dwg. 2626C95

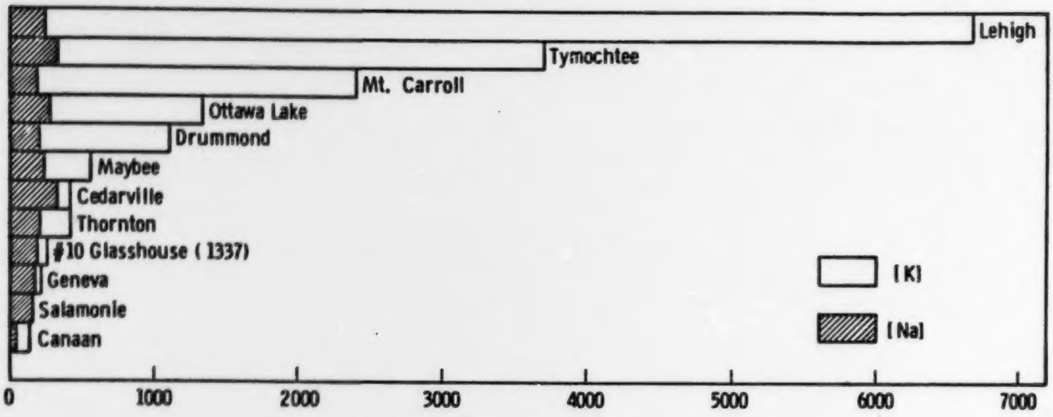

Figure 7 - Alkali Concentration of Dolomites in ppm

Comparison of the concentration of Na, K, Ca, Mg, Cr, Cu, Fe, and Si released and subsequently deposited along a 1025 to 400 K temperature gradient from a charge of Glasshouse No. 10 and Tymochtee dolomite exposed to 1048 K and 825 kPa for 75 hours in 78% N_2/19.8% CO_2/2.2% O_2 is presented in Figure 9. Potassium is present as the major alkali phase contained in the deposit, particularly at temperatures above 600 K. The relation of the deposition concentration to temperature for Ca, Mg, Cr, Cu, Fe, or Si is not as well defined in the Glasshouse No. 10 or the Tymochtee dolomite exposure. The concentrations of the various trace and minor elements as determined by emission spectroscopy that are not illustrated in Figure 7 are reported at concentrations of <0.5 μg within specific temperature zones.

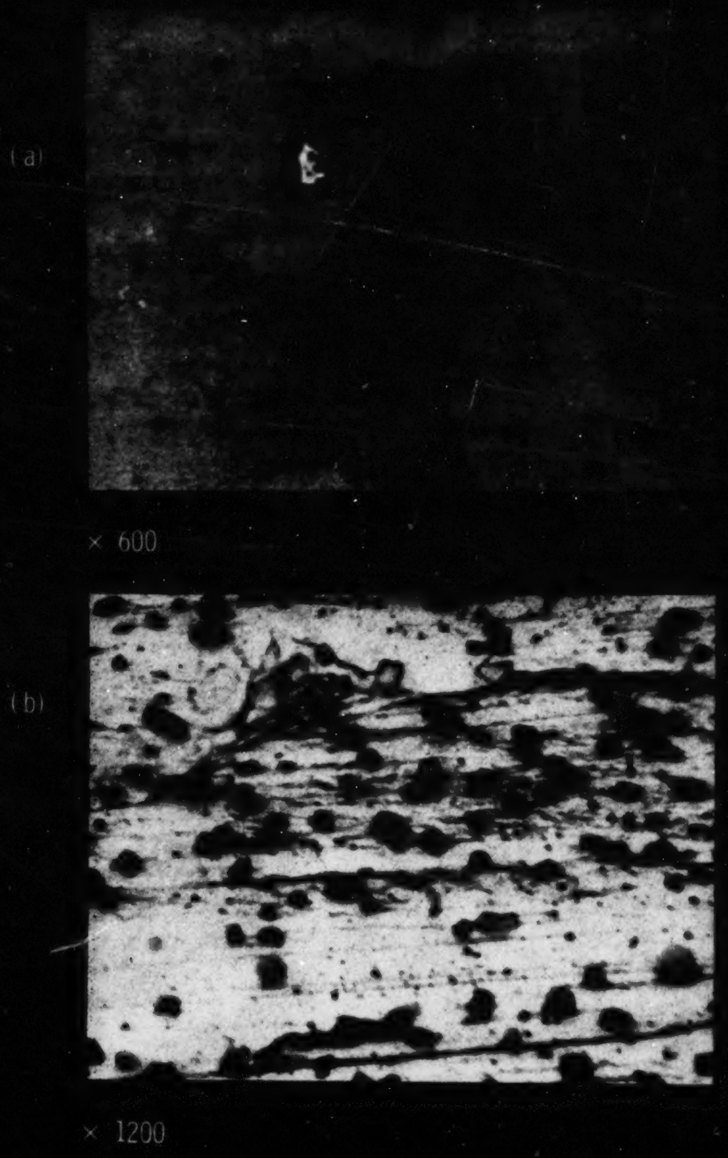

Reproduced from best available copy.

Figure 6 - Characterization by Scanning Electron Microscopy (SEM) of Tymochtee Dolomite Deposits in Fixed-Bed Pressurized Studies
(a) Impacted Particles at 1023-1123 K
Si > Ca > Mg > K > Fe
(b) Crystalline Formations at 798-903 K
Cl > K >> Al

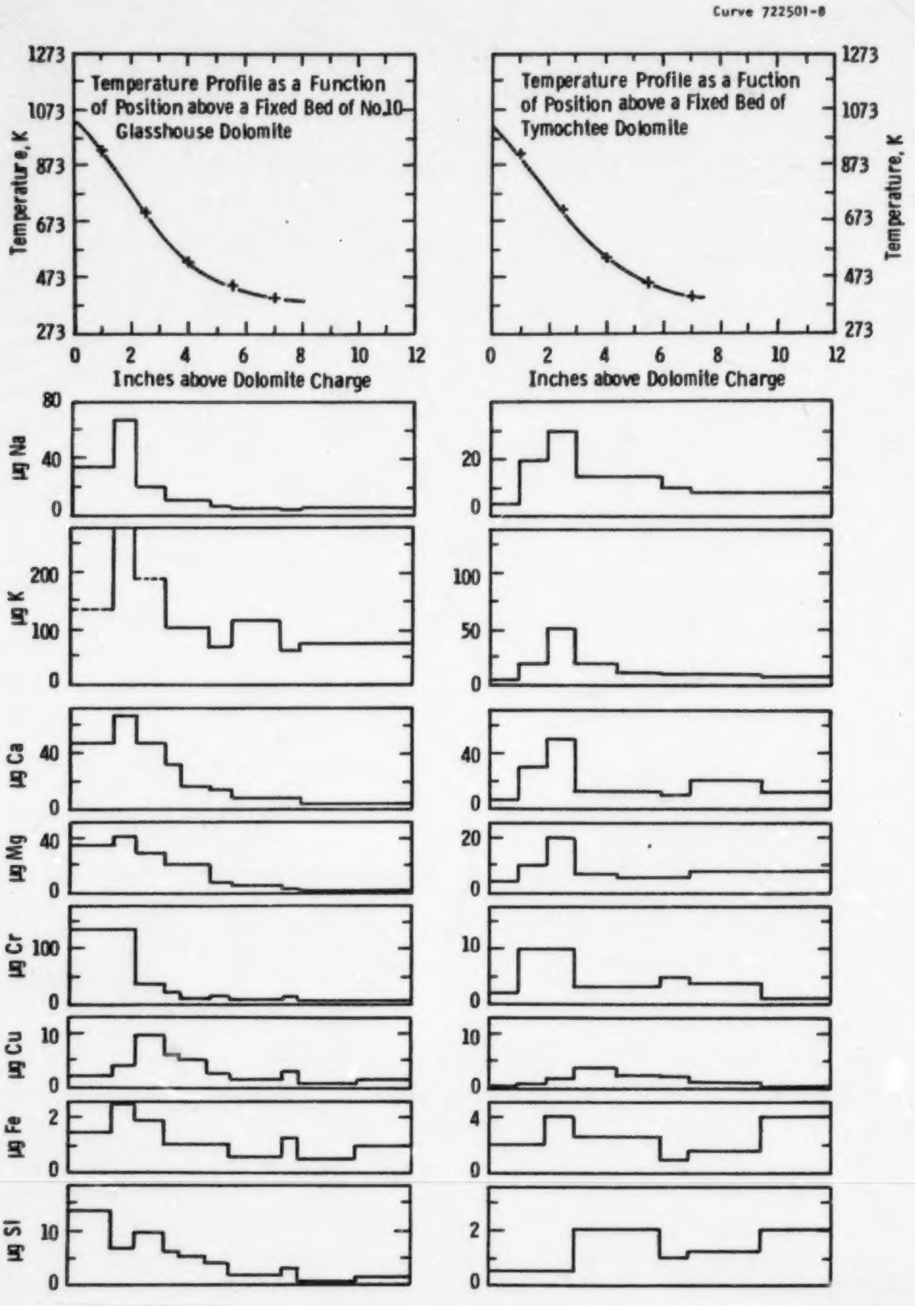

Figure 9 - Concentration of Trace and Minor Elements in Deposits from Glasshouse No. 10 and Tymochtee Dolomite Exposed to 1048 K and 825 kPa for 75 hr in 78% N_2/19.8% CO_2/2.2% O_2

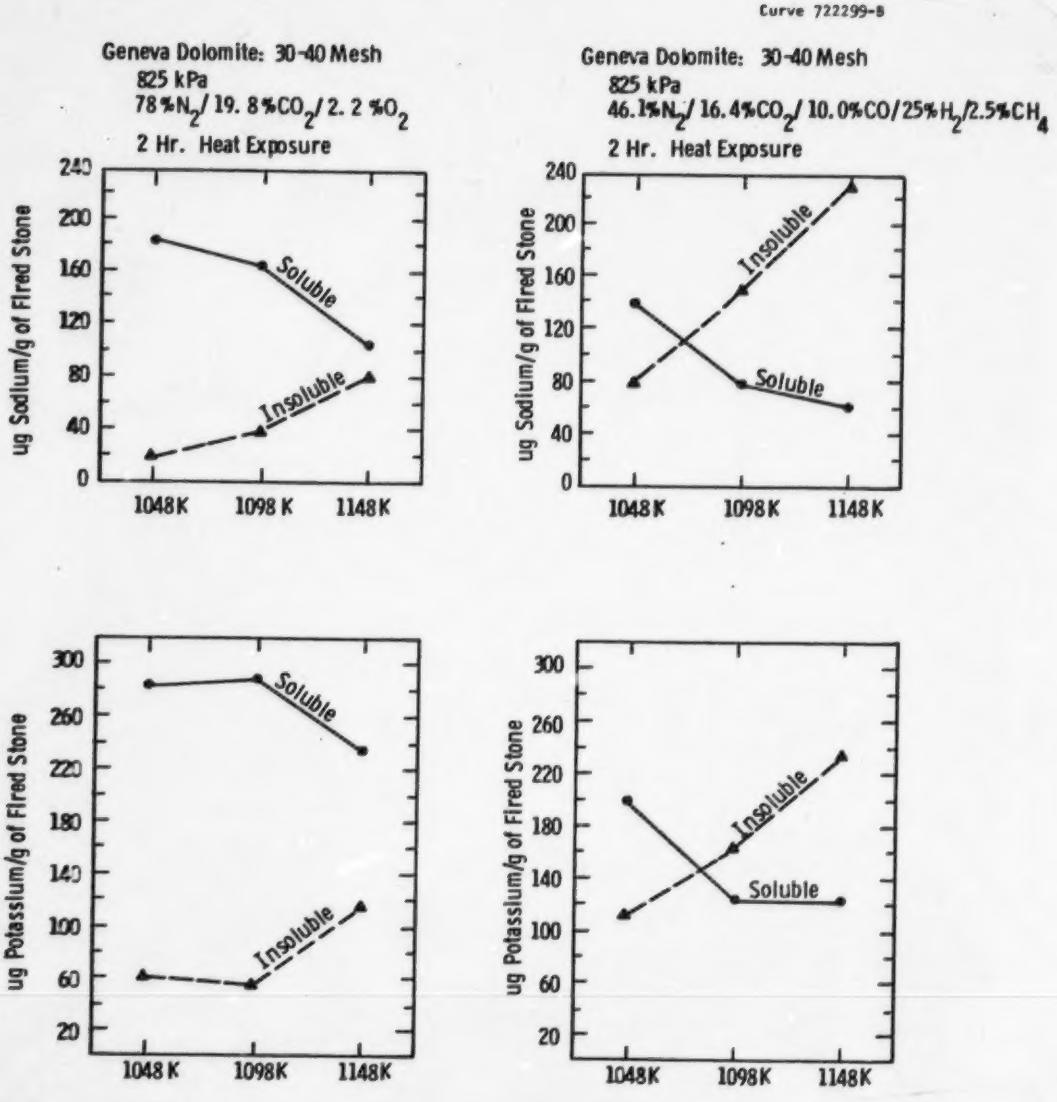

Figure 10 - Sodium and Potassium Concentration Retained in Geneva Dolomite after Exposure to Oxidizing and Reducing Gases

Since the alkali appear to be released and deposited at the highest concentration of all of the trace and minor elements in the sorbent materials, we attempted to demonstrate that variation of alkali release was dependent not only on the concentration within the original stone, but also on the sorbent exposure temperature. Table 14 summarizes the total concentration (μg) of Na, K, Ca, Mg, Cr, Cu, Fe, and Si deposited between temperatures of 1025 and 400 K from Glasshouse No. 10 and Tymochtee dolomite. The total concentration of Na deposited from a 40 g charge of Glasshouse No. 10 dolomite at a maximum internal fixed-bed temperature of 1098 K was 86 μg, approximately 0.1 wt % of the original Na content in the unreacted material. At higher internal bed temperatures, 1148 K, 144 μg of Na are deposited, representing approximately 1.7 wt % of the original Na content. Two hundred eighty μg of K, or 2.1 wt % of the original K concentration, are released from the 1098 K fixed bed of Glasshouse No. 10 dolomite (~3.25 times the deposited Na content), while only 176 μg or 1.3 wt % of the original K concentration form in the deposit from the 1148 K fixed bed.

Tymochtee dolomite, regarded as a relatively heavily alkali-contaminated stone, is expected to demonstrate greater alkali release than Glasshouse No. 10 dolomite. Deposits along the temperature gradient are significantly denser in the Tymochtee exposures. White crystalline formations, characterized as potassium chloride (KCl), result at 773 K. Analysis indicates that 1390 μg of K are deposited in toto (1.4 wt % of the original K content) from a 40 g fixed bed of Tymochtee dolomite heated at 1148 K for 75 hours, while 173 μg of Na (1.6 wt % of the original Na content) are present in the deposit. The same concentration order for deposited Na has resulted from two different sorbent materials, while an order-of-magnitude difference exists between the K deposits. This preliminary result indicates the possible variation in the original sorbent concentration and the nature of the contained phases.

The trace and minor element concentration present in the Tymochtee deposit was examined by spark source analysis. These results,* presented in Table 15, indicate that Na plays a minor role relative to K in the formation of deposits from sorbent materials. The principal trace constituents include K and Cl, independent of the deposition temperature, and portions of S (probably as sulfates) and C (probably as carbonates), increasing in concentration at lower temperatures (<500 K).

Alkali present in the sorbent may exist as chlorides, carbonates, free isolated ions, or in association with either a silicate, aluminate, or aluminosilicate clay phase. Exposure of the sorbent to high temperatures and pressures may induce volatilization of the alkali chloride phase or promote reactions with the clay lattice. Table 16 illustrates the results obtained from atomic adsorption analysis of the repartitioning of alkali within the soluble (chloride, carbonate, water glass, aluminosilicate or feldspar phases) and the insoluble fraction (amorphous clays) of Salamonie, Geneva, Glasshouse No. 10, and Tymochtee dolomites heated at temperatures of 1048 to 1148 K at 825 kPa for 2 to 75 hours in either an oxidizing or a reducing-gas environment. Variation in the internal bed temperature has no significant effect on the release of alkali from Salamonie dolomite after 2 hours of exposure to either an oxidizing or a reducing-gas environment. Alkali exchange, however, is indicated as a function of temperature, with the migration of both Na and K from insoluble clay lattice into the soluble fraction.

The partitioning of the alkali within Geneva dolomite is illustrated in Figure 10 as a function of temperature in both an oxidizing and a reducing gas environment. The migration of alkali in Geneva dolomite from the soluble to the insoluble fraction is observed. The transition temperature at which the insoluble phases exist as the principal alkali complex is dependent on the carrier gas. Temperatures in excess of 1148 K are required to drive the alkali into the nonvolatile, insoluble fraction for oxidizing systems. After two hours of reaction in a reducing environment, however, the insoluble alkali phases predominate at temperatures above 1080 K.

---

*Average concentration reported.

The repartitioning of Na in Glasshouse No. 10 dolomite tends to favor the insoluble complex formation upon exposure at 1148 K and 825 kPa in an oxidizing gas environment, while K preferentially repartitions into the soluble phase. The behavior of alkali in Tymochtee dolomite favors the formation for both soluble Na and K complexes under either an oxidizing or a reducing-gas environment. The mechanism of alkali exchange or repartitioning in sorbents exposed to FBC temperatures and pressures remains to be delineated.

Aluminosilicate materials have demonstrated that gettering of released alkali is feasible if thermodynamic equilibrium is achieved. Several bench-scale studies conducted at Westinghouse support this phenomenon and will be described in the following section. Once again, the aluminosilicate getters, either as commercially produced materials (kaolin, Burgess pigment, diatomaceous earth, silica gels, Attapulgus clay, activated bauxite, etc.) or as PDU ashes or chars, all contain and have the potential to contribute to the trace and minor element loading in the stack-gas effluent.

Heating Chinook coal ash at temperatures between 1023 and 1223 K for five hours causes a migration of the alkali from the soluble into the insoluble fraction under reducing conditions, as shown in Figure 11. Analysis by scanning electron microscopy (SEM) of material deposited as a function of temperature from Chinook coal ash indicates that deposition resulted from the impact of 6 to 32 μm particles, as opposed to the condensation of released volatiles (Figure 12). Table 17 illustrates the chemical composition as detected by EDX/SEM (energy dispersive x-ray analysis) of individual particles in relation to the temperature at

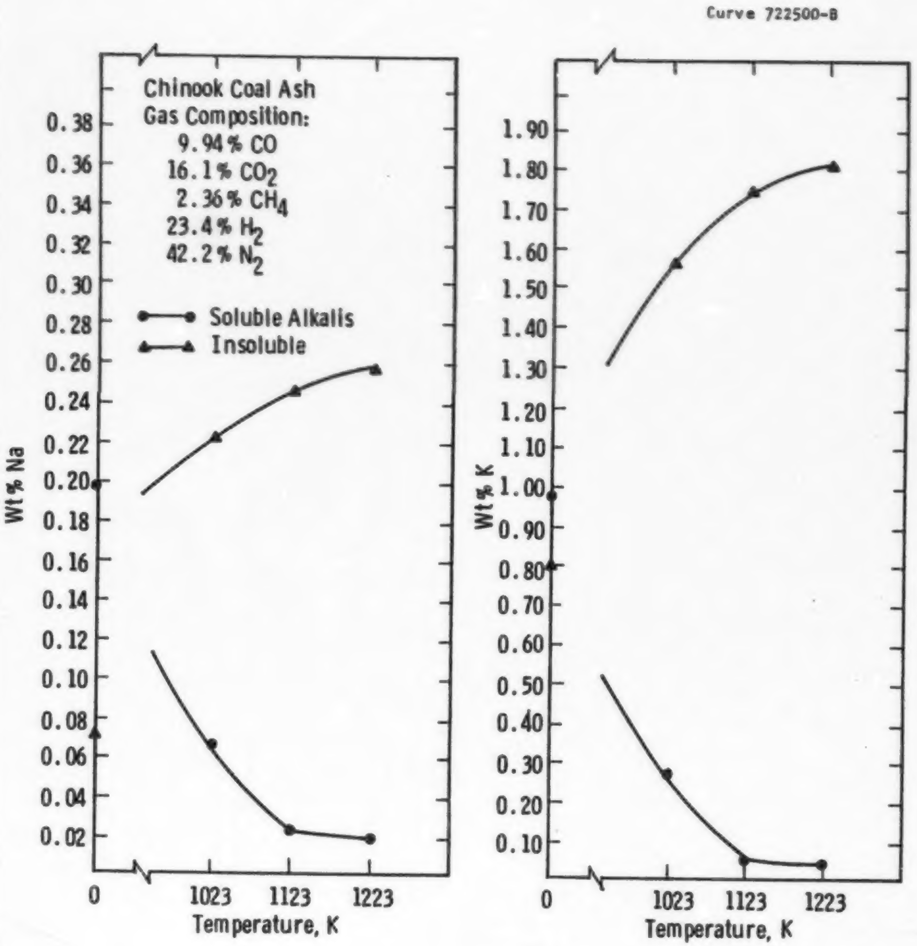

Figure 11 - Alkali Concentration of Soluble and Insoluble Fractions of Chinook Coal Ash Fired at 1135 kPa in Simulated Fuel Gases

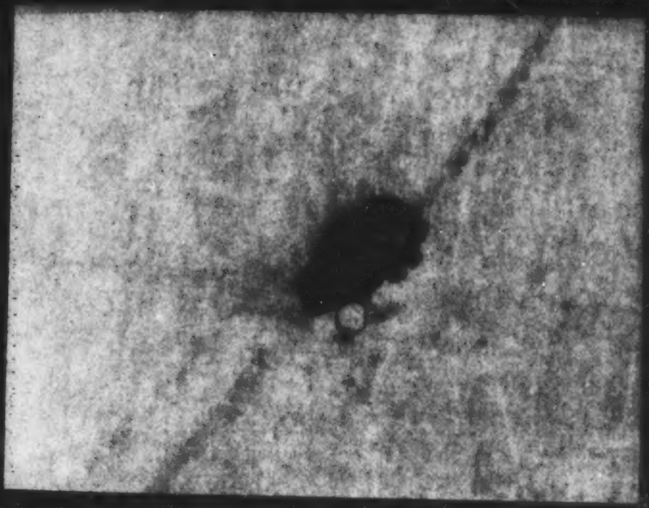

Si > Al > K > Fe × 1000

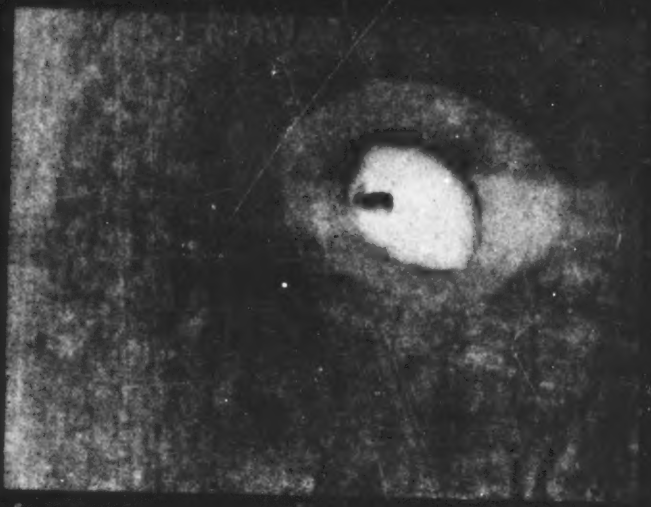

Cl > S > K × 1000

Figure 12 - Particulate Material Deposited between 573 and 698K from a 1023 K Fixed Bed of Chinook Coal Ash exposed to 1114 KPa in 9.94% CO/16.1% CO_2/2.36% CH_4/23.4% H_2/42.2% N_2 for 5 Hours

TABLE 17 - SEM CHARACTERIZATION OF DEPOSITS FORMED AS A RESULT OF THE RELEASE OF VOLATILES AND PARTICULATES FROM COAL ASH AND SORBENT MATERIALS

Experiment Number	Charge	Temp. °K	Gas Composition	Time (hrs)	Pressure kPa	Composition of Deposits				
HPR - 42	Chinook Coal Ash	1023	9.94 % CO 16.1 % CO_2 2.36 % CH_4 23.4 % H_2 42.2 % N_2	5	1132	473-573 K: Cl>Si>K Si>Fe>Cl =K	573-698 K: Si>Al>K>Fe Cl>Si>K Cl>Si>K	698-873 K: Al = Si>K>Fe Si>Al>Fe>K Si>Ti		
HPR-43	Chinook Coal Ash	1123	9.94 % CO 16.1 % CO_2 2.36 % CH_4 23.4 % H_2 42.2 % N_2	5	1132	583-683 K: S>Fe>Si>K >Ca Al>Zn (Na) >Cl>K>Fe Si>Al>Fe> K>Ca	683-823 K: Si>Al>K>Fe S>Fe>K>Si Ca>V>Cr S>Fe>Si>K Mg>Ca>V >Cr S>Fe>Si>K Mg>Ca>V >Cr S>Mg>Si>Fe> K>Ca>Cr	893-1053 K: Si>K>Fe Si≥Al>K>Fe Si>Al>K>Fe		
HPR-44	Chinook Coal Ash	1223	9.94 % CO 16.1 % CO_2 2.36 % CH_4 23.4 % H_2 42.2 % N_2	5	1132	553-648 K: Si>Al>Fe> K>Ti Si>Al>K > Fe>Ti	648-753 K: Si>Al>S>Fe> K>Ca	753-908 K: Si>K	908-1123 K: Si>Al>K>Fe Si>Al>K>Fe Si>Al>K>Fe	1123-1223 K: Si>Al>K Al Si>Al>K
HPR-47(B)	Chinook Coal Ash + Canaan Dolomite	1223	9.94 % CO 16.1 % CO_2 2.36 % CH_4 23.4 % H_2 42.2 % N_2	5	1132	1223-1248 K: Mg>Ca>Si	1248-1263 K: Ca>Si>Mg Ca>Si>Mg Ca			

Dwg. 2626C98

impact. The composition of the majority of the particles is Si > Al > Fe > x (x = K, Cl, Ti, Mg, Ca, Cr), in addition to S- and Cl-rich particles.

Exposure of Chinook coal ash and Canaan dolomite to temperatures of 1223 K at pressure to the reducing-gas environment causes the alkali to migrate from the soluble to the insoluble fraction in the ash (Table 18). A slight net gain over the background alkali content in the ash is observed after heating but is not defined as a function of temperature. Heating may affect the way in which the alkalis are bound in the clay structure through lattice rearrangements and dehydration reactions. Under these conditions both Na and K may be released from the amorphous clay lattice, resulting in a less tightly bound aluminosilicate or feldspar structure. Temperature does not promote the migration of Na between phases in Canaan dolomite, but favors instead the volatilization from the soluble fraction. Conversely, K is released from both the soluble and insoluble complexes under these conditions. The release of 0.0142 wt % Na and 0.0204 wt % K from the Canaan dolomite is proposed as contributing to the increase over the background alkali content in the Chinook coal ash analysis. Delineation of the phase responsible for gettering the released sorbent alkali cannot be made at this time.

Minimal deposition was observed when Chinook coal ash and Canaan dolomite were exposed to temperatures of 1123 to 1223 K and at pressure of 1013 to 1132 kPa for five hours. Scanning electron microscopy characterization of the deposits is presented in Tables 17 and 19. In the hottest zone of the temperature gradient, the deposit consists of 4 to 40 μm particles composed of Ca and Si. As particles strike cooler regions of the gradient, the composition of the material shifts to a Si and Al complex.

When Chinook coal ash is used to getter alkali released from Geneva dolomite after five hours of reaction in an oxidizing environment (19.8% CO_2, 2.2% O_2, and 78% N_2) at 1223 K, alkali migrate from the soluble to

TABLE 18 - DISTRIBUTION OF ALKALI IN CHINOOK COAL ASH AND CANAAN DOLOMITE

Dwg. 1714B28

Material	Sodium, wt%			Potassium, wt%		
	Soluble	Insoluble	Total	Soluble	Insoluble	Total
Unreacted Chinook Coal Ash	0.202	0.054	0.256	0.992	0.753	1.745
Reacted Chinook Coal Ash	0.021	0.242	0.263	0.041	1.814	1.855
Unreacted Canaan Dolomite	0.016	0.0008	0.0168	0.0074	0.016	0.0234
Reacted Canaan Dolomite	0.0018	0.0011	0.0029	0.0017	0.0013	0.0030

the insoluble ash fraction, exactly the effect demonstrated under reducing conditions at lower temperatures. Exposure of the ash with the dolomite at 1223 K increases the total Na and K concentration in the ash by 60 and 1100 ppm, respectively. Analysis by emission spectroscopy of the ash material before and after heating indicates that:

- Heating causes release of the following elements:

Ba	200 ppm
Co	10 ppm
Cu	20 ppm
Li	20 ppm
Mn	300 ppm
Sn	200 ppm
Sr	100 ppm
Zr	100 ppm

TABLE 19 - SEM CHARACTERIZATION OF DEPOSITS FORMED AS A RESULT OF THE RELEASE OF VOLATILES AND PARTICULATES FROM COAL ASH, SORBENT AND ALUMINOSILICATE MATERIALS

Experiment Number	Charge	Temp. °K	Gas Composition	Time (hrs)	Pressure kPa	Composition of Deposits
HPR-46 (B)	Chinook Coal Ash + Canaan Dolomite	1123	9.94 % CO 16.1 % CO_2 2.36 % CH_4 23.4 % H_2 42.2 % N_2	5	1013	1123-1148 K Si>Mg>>Ca Al>Si>K>Ca Si>Mg>>Fe Si>Ca>Mg 1148-1173 K Ca>Si Ca>>Si>K>Mg>Cl>Fe>Ti Si>Al>K = Na>Ca Si>Al>Mg
HPR-47	Chinook Coal Ash + Canaan Dolomite	1223	9.94 % CO 16.1 % CO_2 2.36 % CH_4 23.4 % H_2 42.2 % N_2	5	1013	1073-1248 K Si>Al>Ca>Ti=K Si>Ca>Mg Si>Al>>Ti 1248-1298 K Al>Cl Al
HPR-51	Tymochtee Dolomite	1073	9.94 % CO 16.1 % CO_2 2.36 % CH_4 23.4 % H_2 42.2 % N_2	5	1013	673-798 K K>Si>Fe>Cl>Ca Ca>>Mg>Si-Cl>K>Fe Cl>K>Al>Fe 798-903 K Cl-K>>Al Cl-K>>Al>Fe>Ni Cl-K>Al>>Fe Si>Ca>Mg>K>Cl>Fe 1023-1123 K Si>K>Fe Si>Ca>Mg>>Fe Si>>K-Ca>Fe Al>>K>Cr>Fe Si>K>>Fe Si>>Ca>Mg>K>Fe Si>Ca>Mg>K>Fe Si>K>Ti Si>>Mg>K Fe>>K
HPR-52	Tymochtee Dolomite + #10 Pigment	1173	9.94 % CO 16.1 % CO_2 2.36 % CH_4 23.4 % H_2 42.2 % N_2	5	1013	633-733 K Si>>K>Fe Al Ca>>Mg>Cl>K>Fe Fe>S>Cl>Cr>Al>K>Ca>Ni 853-973 K Cl>>Ni>Al Fe>>Cl>S Fe>>Al 1093-1173 K Cl>>Al Cl>Al>>Ca Si>>K>Fe Cl>Al>Ca-Fe Cl>>Fe>Al Al>>Cl>Fe>K>Cr>Ca Cl>>Fe>Al Al>>Cl>Fe Cl>>Fe>Ni>Al>Si>Cr

Dwg. 2626C93

- No net gain of any element except Na or K results from the combination of Chinook coal ash and Geneva dolomite during gettering.

Heating Geneva dolomite to 1223 K promotes the release of both alkalis, while a net gain in the following trace elements was observed:

B	~260 ppm
Fe	2000 ppm
Mn	400 ppm
Ti	40 ppm.

Emissions from the Chinook coal ash/Geneva dolomite fixed bed were minimal. The impacted deposited particles observed under SEM, however, varied from 34 x 26 μm to 106 x 116 μm and were composed principally of Si and/or S.

Release of trace and minor elements from Tymochtee dolomite produces deposits rich in Cl and K, or Si and K, Ca, or Mg. When the highly alkali-contaminated sorbent is heated to temperatures of 1173 K with No. 10 Burgess pigment, a Cl- and Al-rich deposit forms at 1173 to 1093 K. At the same time, the concentration of K is reduced in the deposits formed from the dolomite/pigment charge. Figure 13 illustrates that deposition is a function of condensation and nucleation, rather than of the particle impact that had been observed in the Chinook coal ash and dolomite exposures.

Delineation of the gettering mechanism of kaolin and PDU chars and ashes is currently being conducted at Westinghouse in an attempt to demonstrate removal simultaneously of volatile alkali and of particulates at high temperature for a pressurized gasification system.[25] In view of the data presented earlier in this section, results from the gasification studies may simulate the combustion gettering reaction at higher

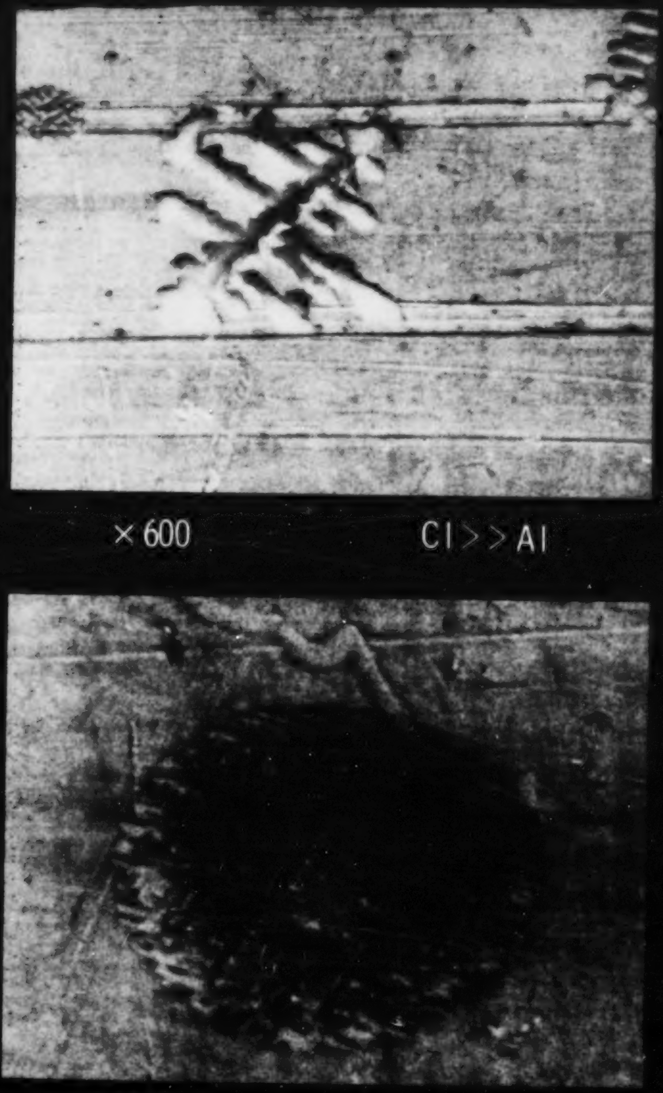
×600
Cl>>Al
×1200
Cl>Al>>Ca

Figure 13 - Characterization by SEM of Tymochtee Dolomite/No. 10 Burgess Pigment Deposits in 1173 K Fixed-Bed Pressurized Studies

temperatures. From these investigations we find that no substantial alkali is lost because of volatilization from the materials exposed to temperatures of 930 to 1170 K. As the exposure temperature increases, the background soluble Na and K content decreases, while the concentration of the insoluble phase of these constituents increases. The reverse trend is observed for kaolin. The sodium chloride (NaCl) gettering reaction of these materials appears to be both time and temperature dependent. Once the insoluble alkali-active sites are saturated, further gettering and simultaneous loss of K are controlled by the soluble constituents. Identification by X-ray diffraction indicates that the reaction of NaCl with the aluminosilicate produces carnegieite, $NaAlSiO_4$. Identification of the alkali within the amorphous clay lattice has not been determined. The proposed low-temperature gettering reaction is through a chemisorption process in which NaCl loosely binds to the aluminosilicate lattice as a substitution reaction between the hexagonal network of Si-O-tetrahedra and aluminum-O/OH octahedra (Figure 2):

$$NaCl(g) + Al_2Si_2O_5(OH_4)^*(s) \longrightarrow Na(Cl)\text{-}Al_2O_3 \cdot 2SiO_2(s) + 2H_2O(g)$$

or, in a displacement reaction where Na cationically replaces H in exposed OH groups,

$$NaCl(g) + Al_2Si_2O_5(OH_4)(s) \longrightarrow Al_2SiO_5(O(H,Na))_4(s) + HCl(g) \quad .$$

Proposed high-temperature reactions include

$$NaCl(g) + \left[\begin{array}{c} Al_2Si_2O_7(s) \\ \text{or} \\ \gamma\text{-}Al_2O_3\text{-}SiO_2 \end{array}\right] \longrightarrow \text{alkali amorphous complex} \quad .$$

---

*Kaolin.

Potassium was observed to be released from the aluminosilicate lattice only when NaCl was present in the buffer gas. Preliminary experimental data indicate that background potassium is displaced by volatile sodium in select phases within the getter materials.

Argonne[32] demonstrated that diatomaceous earth through a chemical reaction, and activated bauxite through surface adsorption, removed gaseous alkali metal compounds from the hot flue gas (1073-1153 K) in bench-scale exposures that simulated the pressurized fluidized-bed combustors for proposed combined-cycle power generation. The detailed mechanisms of lattice dehydration and disorientation within the ash particle need not be repeated for the combustion reaction of the commercial or PDU materials.

Although in neither the Westinghouse nor the ANL studies was the trace and minor element behavior monitored during the gettering reaction, it is evident that a complex series of physical changes and chemical reactions are occurring in the simple bench-scale studies. In assessing the environmental impact of the FBC process, the chemical fate of the trace and minor elements in the coal, sorbent, and getter materials during combustion needs to be determined. The data presented in the preceeding section illustrate the many possible reactions likely to occur simultaneously within the combustor. Kinetic models of these reactions are needed to calculate the rate of product distribution of chemical species and compounds formed as a function of the process operating conditions. This would permit quantification of the concentration and type of chemical compounds emitted in the solid or gaseous effluents from the plant. Since the kinetics of the chemical reactions in coal, sorbent, or getter materials are unknown, it is possible to fall back on the common assumption used in high-temperature chemistry, that, as a first-level approximation, thermodynamic equilibrium will be reached in the bed and that the thermodynamic product distribution will be characteristic of the process effluent.

6. CRITERIA FOR THE SELECTION OF TRACE AND MINOR ELEMENTS USED IN THE PARAMETRIC EQUILIBRIUM INTERACTIVE PROJECTIONS

Coal combustion and other industrial processes are major sources of the release of pollutants into the atmosphere, either as gas constituents or as solid particles and liquid phases. The emitted particles are assessed as potential health hazards when the quantity released approaches toxic levels. A consideration of the existing chemical state and physical form of the particle emissions is necessary in order to evaluate the minimum allowable toxicity concentration.

Toxicity of a substance, as defined by the National Institute for Occupational Safety and Health (NIOSH),[33] is that state which: demonstrates carcinogenic or neoplasmic effects on the organism; induces permanent genetic modifications; and/or produces irritation or death to the exposed organism. Potentially dangerous forms of pollutants arise when toxic trace elements (Be, Cd, As, Se, Pb, Sb, Hg, Tl, V) are mobilized by association with airborne particles. The suspended particles, existing as heterogeneous mixtures of compounds, are dispersed by wind action or become resident in the atmosphere until removed through rain or agglomeration into larger particles. A primary pollutant may be present in a nontoxic state but, given suitable conditions, will participate in reactions that yield a secondary toxic pollutant. This process is illustrated by the photochemical smog effect where the reaction of water vapor with acid anhydrides produce corrosive acid aerosols. Ambient air containing photochemical smogs show deleterious effects to existing life by the formation of peroxyacyl nitrates, oxides, and nitrogen compounds.

The concentration of trace metals has been shown to increase continuously with the inverse particle diameter. In the assessment of the toxicity level of trace element concentration, therefore, particle size is of major concern. Upon inhalation large particles are deposited in the nasal, pharyngial, and bronchial regions of the respiratory tract. The particles are then removed through cilial action to regions of the stomach where 5 to 15 percent of the trace element is adsorbed. Particles that exhibit diameters smaller than 1 μm are deposited primarily in the alveolar regions of the lungs, where the adsorption efficiency reaches 50 to 80 percent. From the lung the submicron particle gains entrance into the bloodstream. Toxic trace elements such as As, Hg, or Se interfere with normal metabolism through methylation reactions in critical biological pathways. Similarly, stable chelates such as V^{5+}, Zr^{4+}, Hg, Tl, and Pb disrupt anabolic and catabolic processes.

Conventional power plant studies conducted by Natusch[30] indicate that approximately 91 percent of the fly ash material retained contains particles with diameters greater than 40 μm, thus removing the large, bulk emission products preferentially and allowing the release of the smaller, toxic, trace-element-bearing particles. The trace elements are concentrated in the release of small fly ash particles because of the volatilization of the element in the high-temperature, coal combustion zones. There the volatile product may recondense or preferentially adsorb onto larger available surfaces produced by previously existing smaller particles. It becomes a vital problem when the emitted particle is within the respirable size range and contains biologically active compounds. Most living organisms do not possess metabolic systems for the removal of toxic trace elements. It is of major concern, therefore, that toxic emissions be limited to the lowest possible tolerance level for the sustenance of eco- and biosystems.

Carpenter,[34] demonstrated that the mass median aerodynamic diameter (MMAD) of particles released by conventional cleanup systems ranged between 2.2 and 2.8 μm, while the MMAD of aerosols from FBC exhaust systems was found to be slightly larger. The composition of the aerosols, as Weissman[35] showed, varied greatly in the trace, minor, and major element concentrations, possibly because of the variation in the combustion operating conditions and/or of the difference in the attached gas-cleaning devices. Ash particles in the clean gas streams of the experimental low-Btu gasifier unit at Morgantown Energy Technology Center (METC) were similar to FBC and conventional combustor fly ash in the As, Be, Bi, Cd, Cr, Co, I, Mo, Ni, Se, and Tl concentration. The ash formed in the METC unit, however, had a higher concentration of Br, Cl, Mn, Sn, and Zr. Weissman[36] concluded, in general, that the potential toxicity of trace elements emitted from an FBC, when normalized to the input heating value for the system, was equal to or lower than emissions from the conventional plant.

Biochemical studies conducted by Sheridan[37] have shown that the respirable intake of V depresses cholesterol and phospholipid synthesis and accumulates in bone. Although the metabolic pathways leading to the production of cholesterol and phospholipids are entirely different, the intake of V induces a replacement of the required phosphate ion in intermediate steps producing phospholipids and appears to act as an uncoupler in the oxidative phosphorylation in the adenosine triphosphate (ATP) synthesis producing cholesterol.

Fluidized-bed combustion ash was shown by Hill[38] to induce activation of immune complement, while ash from the two conventional combustion plants did not. This activation facilitates the release of vasoactive and chemotactic fragments, as well as peptides and lysosomal enzymes from macrophages essential to the immunological defense systems.

Some bag-filtered ash fractions of the atmospheric FBC unit at METC were found to contain an extractable isomer of methylphenanthrene, which was defined by Ames testing as mutagenic.[39] The isomer was not detectable as ash fractions collected at the FBC stack. Since the mutagenicity of the ash varied with samples from the same coal type, Clark suggested that operating conditions determine the mutagenicity within ash formations. From the results reported by Royer et al.,[40] aza-arenes, which represented a small percentage of the organic effluent by weight produced in the low-Btu gasifier at METC, might also be responsible for mutagenic activity. Hill[41] demonstrated, further, that lower molecular-weight aromatic compounds of coal tars may be more cytotoxic than higher molecular-weight compounds.

Determination of potentially toxic hydrocarbons and polyaromatic hydrocarbons, in addition to the inorganic phases and complexes formed during FBC, requires extensive investigation. Tables 20 to 22 illustrate an abbreviated Occupational Safety and Health Administration (OSHA) Category 1 preliminary listing of compounds that are confirmed as carcinogens when produced in significant quantities for various feedstock-contained elements; the extracted concentration levels that determine the hazardousness of As, Cd, Cr, Pb, Hg, Se, and Ag in solid wastes; and the regulatory concentrations permitted for selected pollutants in air. A summary of known carcinogenic POM is shown in Table 23.

The elemental concentration for a U.S. mean coal is illustrated in Table 24, in addition to the MATE[42] level for air proposed for fossil energy processes. The ratio of the MATE level to that of the elemental concentration defines a minimum tolerance release in stack-gas emissions for FBC processes burning a mean U.S. coal. Included in the category of 0.001 to 0.01 percent minimum elemental release from feedstock materials are As, as metallic arsenic, arsenic trioxide (As_2O_3), and arsine (AsH_3); and Ni as nickel carbonyl ($Ni(CO)_4$) and nickel sulfide (Ni_3S_2). If the released percentage for the above phases exceeds 0.1 percent of the initial feedstock concentration, removal of As or Ni would be required in order to minimize the potentially toxic level of stack-gas emissions. In addition, Be, Cr, Ni, and Zn ions; Pb as lead oxide (PbO), lead sulfide (PbS), arsenate, and/or fume; P as phosphine (PH_3); Se as elemental selenium (Se) or selenium hydride (SeH_2); and Zn as zinc chloride ($ZnCl_2$), as shown in the MATE/[coal] ratio, should not exceed 0.1 percent release from feedstock materials in order to maintain a minimum emission tolerance. Similarly, Co, Cu, F, V, and Zr ions; boron

TABLE 20 - PRELIMINARY LIST OF OSHA CATEGORY 1 CONFIRMED CARCINOGENS PRODUCED IN SIGNIFICANT QUANTITIES[43]

Arsenic Acid (Calcium and Lead Salts)
Arsenious Acid (Disodium and Potassium Salt)
Arsenic Trioxide
Beryl
Beryllium
Beryllium Hydrogen Phosphate
Beryllium Oxide
Beryllium Sulfate
Beryllium Sulfate, Tetrahydrate
Cadmium
Cadmium Chloride
Cadmium Oxide
Cadmium Sulfate
Cadmium Sulfate, Tetrahydrate
Chromic Acid (Calcium Salt; Lead (2+) Salt)
Chromic Acid ((3+) Salt; Dipotassium and Disodium Salt)
Chromium Chromate
Chromium (III) and (VI) Oxide
Dichromic Acid, Disodium Salt
Hematite
Lead Chromate (VI) Oxide
Lead (II) Phosphate
Nickel
Nickel Carbonyl
Nickel (II) Oxide, Dust, Sulfide

Dwg. 1713B78

TABLE 21 - EXTRACT CONCENTRATION LEVELS DETERMINING HAZARDOUSNESS OF SOLID WASTE[43]

Dwg. 7726A73

	Extract Level, Milligrams/Liter
As	0.50
Cd	0.10
Cr	0.50
Pb	0.50
Hg	0.02
Se	0.10
Ag	0.50

oxide (B_2O_3); Br^-; Ge as germane (GeH_4); Ni as nickel oxide (NiO); P as orthophosphoric acid (H_3PO_4) and phosphoric pentasulfide (P_2S_5); Sn as tin chloride ($SnCl_4$); and Zn as zinc oxide (ZnO), should remain within 0.1 to 1.0 percent release, with Sb, B, Fe, Mn, Mo ions; Sb as antimony hydride (SbH_3); Br as bromine hydride (HBr); Co as cobalt chloride ($CoCl_2$); Fe as iron pentacarbonyl ($Fe(CO)_5$); and Si as silicane (SiH_4) within 1 to 10 percent release for minimum toxic emission levels.

In order to define the trace and minor elements to be used in the parametric thermodynamic equilibrium calculations, we have considered those elements whose concentration levels in typical feedstock materials are known,[12] the MATE level,[42] the quantity of analytical data cited for the specific element in either the feedstock material, the resulting ash fractions, or the effluent streams,[1-10,44-64] and the availability of

TABLE 22 - POLLUTANT REGULATIONS[43]

Dwg. 1713B76

Pollutant	Regulation	Value (Air)
Be	NIOSH	2 μg/m^3
	OSHA	2 μg/m^3
	NESHAP	10 g/24 hr
F$^-$	NIOSH	2.5 mg/m^3
	OSHA	2.5 mg/m^3
Hg and Compounds	NIOSH	0.05 mg/m^3 TWA
	OSHA	0.1 mg/m^3
Lead and Compounds	NAAQS	1.5 μg/m^3
	NIOSH	0.15 mg/m^3
	OSHA	50 μg/m^3
Cr and Compounds	NIOSH	1 μg/m^3
	OSHA	100 μg/m^3
Ni and Compounds	NIOSH	0.15 mg/m^3
	OSHA	1 mg/m^3
Zn and Compounds	NIOSH (ZnO)	5 mg/m^3
	OSHA (ZnO)	5 mg/m^3
As	NIOSH	2 μg/m^3
	OSHA	10 μg/m^3
Cd and Compounds	OSHA	0.1 mg/m^3
	NIOSH	0.040 mg/m^3 TWA
Se and Compounds	OSHA	0.2 mg/m^3

NIOSH - National Institute for Occupational Safety and Health
OSHA - Occupational Safety and Health Administration
NESHAP - National Emission Standards for Hazardous Air Pollutants
NAAQA - National Ambient Air Quality Standards
TWA - Time Weighted Averages

TABLE 23 - CARCINOGENIC POLYCYCLIC ORGANIC MATERIALS[10]

Dwg. 1714B26

Compound	Structure
1. 7, 12 Dimethylbenz [a] - anthracene	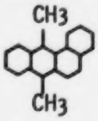
2. Dibenz [a, h] anthracene	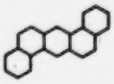
3. Benzo [c] phenanthrene	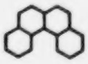
4. 3 Methylcholanthrene	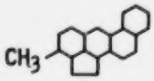
5. Benzo [a] pyrene	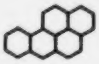
6. Dibenzo [a, h] pyrene	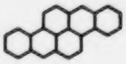
7. Dibenzo [a, i] pyrene	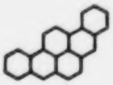
8. Dibenzo [c, g] carbazole	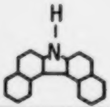

TABLE 24

CRITERIA FOR TRACE AND MINOR ELEMENT SELECTION FOR FLUIDIZED-BED COMBUSTION EQUILIBRIUM STUDIES

Element		US Mean Coal Concentration, ppm	Minimum Acute Toxicity Effluent Levels (MATE)		Parametric Studies	Thermochemical Data Base	Comments
			Air, μg/m³ (ppm)	Land, μg/g			
Actinium	Ac						Insufficient Data
Aluminum	Al	1.29%	Al^{+3} 5.30E3 Al_2O_3 1.00E4	2.00E0 3.00E2	1978-9		Previously Studied; Interactive Systems
Americium	Am						Insufficient Data
Antimony	Sb	1.26	Sb 5.00E2 SbH_3 5.00E2	4.00E-1 4.00E-1		SbH_3, SbN, Sb_2O_5, Sb_2O_4, Sb_2O_3, SbO_2, SbO, Sb_2S_3, $SbCl_3$, $SbCl_2$, Sb_4, Sb_2, $SbBr_3$, Sb	Currently Reported
Argon	Ar						Insufficient Data; Inert
Arsenic	As	14.02	As 2.00E0 As_2O_3 2.00E0 AsH_3 2.00E0	1.00E-1 1.00E-1 1.00E-1		AsH_3, AsH, AsN, As_2O_5, As_2O_3, AsO, $AsCl_3$, AsCl, As_4, As_2, $AsBr_3$, As	Currently Reported
Astatine	At						Insufficient Data
Barium	Ba	(100-500)	Ba 5.00E2 $BaCl_2$ 7.59E2 $Ba(NO_3)_2$ 9.52E2	2.20E0		$BaCO_3$, $Ba(OH)_2$, Ba(OH), BaH, $BaSO_4$, BaO, BaS, $BaCl_2$, BaCl, Ba	
Berkelium	Bk						Insufficient Data
Beryllium	Be	1.61	Be and Compounds, 2.0E0	3.00E-2	1978		Previously Studied
Bismuth	Bi		Bi^{+3} 7.92E5	2.38E4		BiH, Bi_2O_3, BiO, Bi_2S_3, BiCl, Bi_2, Bi	
Boron	B	102.21	B 9.00E4 B_2O_3 1.00E4	2.00E0 3.00E2		B_4C, BC, $B_{10}H_{14}$, B_5H_9, $B_3H_6N_3$, B_2H_6, $B_2(OH)_4$, KBH_4, $NaBH_4$, $(HBO_3)_3$, $B_3O_3H_3$, H_3BO_3, BH_3, BH_2O_3, BH_2, HBO_2, HBO, HBS, BCl_2H, BH, BN, $K_2B_8O_{13}$, $K_2O\ 3B_2O_3$, $B_6Na_2O_{10}$, $K_2O.2B_2O_3$, $B_4K_2O_7$, $Na_2B_4O_7$, $(BOCl)_3$, B_2O_3, KBO_2, $NaBO_2$, B_2O_2, BO_2, BOCl, B_2O, BO, BS, B_2Cl_4, BCl_3, BCl_2, BBrCl, BCl, B_2, B, BBr_2Cl	Currently Reported
Bromine	Br	15.42	Br_2 7.00E2 HBr 1.00E4	1.00E0 3.00E2		CH_3Br, CH_2Br_2, $CHBr_3$, CBrN, CCl_3Br, CCl_2Br_2, $CClBr_3$, CBr_4, CBr_3, CBr_2, CBr, NH_4Br, BBr_2H, BrH, NOBr, BrN, $SOBr_2$, BOBr, BrO, $BBrCl_2$, BrCl, K_2Br_2, KBr, Na_2Br_2, NaBr, Br_3, BBr_2, Br_2	Currently Reported
Cadmium	Cd	2.52	Cd 8.80E0	4.00E-3		CdH, $CdSO_4$, CdO, CdS, $CdCl_2$, CdCl, CdSb, CdBr, Cd, Cd_2	Currently Reported
Calcium	Ca	0.77%	Ca^{+2} 1.62E4 CaO 5.00E3	3.20E1 9.00E0	1978-9		Previously Studied; Interactive
Californium	Cf						Insufficient Data
Carbon	C	70.28%					Inclusive
Cerium	Ce	(11-25)	Ce^{+4} 3.66E4; Ce^{+3} 1.28E3 CeO_2 4.50E4 $CeCl_3$ 2.25E3	1.10E3, 3.84E1 1.35E3 6.76E1		CeO_2, CeO, NaI-CeI_3, Ce_2, CeI_2, CeI_3, CeI, Ce	
Cesium	Cs	(0.42-2.0)	Cs^+ 8.19E4	2.46E3			Insufficient Data
Chlorine	Cl	0.14%	Cl_2	2.00E-2			Inclusive
Chromium	Cr	13.75	Cr Insoluble 1.00E3 Cr Salts Soluble 5.00E2 Cr Chromates 9.55E0 Cr VI Oxide 1.10E1	5.00E-1 5.00E-1 2.86E-1 3.30E-1	1978		Previously Studied
Cobalt	Co	9.57	Co Fume 1.00E2 $CoCl_2$ 1.60E3 $Co(CO)_4$ 1.40E5 CoS 3.15E3 $Co(NO_3)_2$ 2.70E2 CoO 2.36E3	3.00E0 4.80E1 4.20E3 9.46E1 8.10E0 7.08E1	1978		Previously Studied

( ) Indicate Range for Eastern United States, Illinois Basin and Western United States Coals

Dwg. 2621C92

TABLE 24 (Continued)

Dwg. 2623C93

Element		US Mean Coal Concentration, ppm	Minimum Acute Toxicity Effluent Levels (MATE) Air, $\mu g/m^3$ (ppm)	Land, $\mu g/g$	Parametric Studies	Thermochemical Data Base	Comments
Columbium	Nb		Nb 2.17E8 $NbCl_5$ 6.30E4				Insufficient Data
Copper	Cu	16.16	Complexed Copper 3.52E3 Cu Fume 2.00E2 Cu Salts, Dust 1.00E3 CuCN	1.06E2 2.00E-1		CuCN, $Cu(OH)_2$, CuH, CuO-$CuSO_4$ $CuSO_4$, CuO_2, CuO, Cu_2S, CuS, Cu_3Cl_3, $CuCl_2$, CuCl, Cu_2, Cu	Currently Reported
Curium	Cm						Insufficient Data
Dysprosium	Dy	(0.63 - 2.3)	$DyCl_3$ 1.58E4	4.62E2			Insufficient Data
Einsteinium	Es						Insufficient Data
Erbium	Er						Insufficient Data
Europium	Eu	(0.20 - 0.52)					Insufficient Data
Fermium	Fm						Insufficient Data
Fluorine	F	60.94	HF 2.00E3	6.00E1	1978		Previously Studied
Francium	Fr						Insufficient Data
Gadolinium	Gd						Insufficient Data
Gallium	Ga	3.12	Ga 4.95E3	1.49E1		Ga_2C_2, Ga_2O_3, GaO, GaCl, GaI, AuGa, Ga,	Currently Reported
Germanium	Ge	6.59	Ge^{+4} 2.34E4 GeH_4 6.00E2	7.03E2 1.80E1		GeH, GeO_2, GeO, GeS, GeCl, Ge	Currently Reported
Gold	Au					AuH, $AuCl_3$, AuCl, AuGa, AuI, Au_2, Au	
Hafnium	Hf	(0.54 - 1.2)	Hf 5.00E2	1.50E0		HfC, HfN, HfO_2, HfO, $HfCl_4$, $HfCl_3$ $HfCl_2$, HfI_4, Hf	
Helium	He						Insufficient Data; Inert
Holmium	Ho						Insufficient Data
Hydrogen	H	4.95%					Inclusive
Indium	In	(0.1 - 0.23)	In and Compounds 1.00E2	3.00E0			Insufficient Data
Iodine	I	(0.52 - 1.7)	I_2 1.00E3	3.00E1		CH_3I, CH_2I_2, CHI_3, ICN, CI_4, NH_4I, HI, NOI, IO, ICl, K_2I_2, KI, Na_2I_2 NaI, I_2, I	
Iridium	Ir						Insufficient Data
Iron	Fe	1.92%	Fe Soluble Salts 1.00E3 FeO Fume 5.00E3 $Fe(CO)_5$ 7.00E2 Fe_2O_3 Fe_3O_4 9.30E3	5.00E-1 2.10E1 2.00E2 3.80E1	1978		Previously Studied
Krypton	Kr						Insufficient Data; Inert
Lanthanum	La	(5.2 - 15)	La^+ 1.07E5			La_2O_3, LaO, $LaCl_3$, La, LaC_2	
Lawrencium	Lr						Insufficient Data
Lead	Pb	34.78	PbO 2.00E2 PbS 1.90E2 Pb Arsenate 1.90E2 Pb Inorganic Fume 1.90E2	6.00E0 1.00E-1 1.00E-1 1.00E-1	1978		Previously Studied
Lithium	Li		Li^+ 1.70E1	5.1E-1		Li_2C_2, $LiCO_3$, $Li_2O_2H_2$, LiOH, LiH, LiON, Li_3N, LiN, $LiClO_4$, Li_2O_2, LiClO, LiNaO, Li_2O, LiO_2, LiO, $(LiCl)_3$, $(LiCl)_2$ LiCl, LiK, LiNa, LiI, Li_2I_2, Li	
Lutetium	Lu	(0.07 - 0.22)					Insufficient Data
Magnesium	Mg	0.09%	Mg^{+2} 3.22E4 MgO 1.00E4	3.66E1 3.00E2	1978-9		Previously Studied; Interactive Systems
Manganese	Mn	49.40	Mn 5.00E3	2.00E-1	1978		Previously Studied
Mendelevium	Md						Insufficient Data
Mercury	Hg	0.20	Alkyl Mercury 1.0E1 $HgCl_2$	4.00E-7 1.00E-1	1978		Previously Studied
Molybdenum	Mo	7.54	Mo Soluble 5.00E3 Mo Insoluble 1.00E4	1.40E1 3.00E2	1978		Previously Studied
Neodymium	Nd						Insufficient Data
Neon	Ne						Insufficient Data; Inert
Neptunium	Np						Insufficient Data

TABLE 24 (Continued)

Dwg. 2621C94

Element		US Mean Coal Concentration, ppm	Minimum Acute Toxicity Effluent Levels (MATE)		Parametric Studies	Thermochemical Data Base	Comments
			Air, $\mu g/m^3$ (ppm)	Land, $\mu g/g$			
Nickel	Ni	21.07	Ni Soluble 1.00E2 Ni $(CO)_4$ 7.00E0 Ni_3S_2 1.50E1 NiO 9.00E2	2.00E-2 2.10E-1 4.50E-1 2.70E0	1978		Previously Studied
Niobium	Nb		Nb	6.50E2			Insufficient Data
Nitrogen	N	1.30%					Inclusive
Nobelium	No						Insufficient Data
Osmium	Os						Insufficient Data
Oxygen	O	8.60%					Inclusive
Palladium	Pd						Insufficient Data
Phosphorus	P	71.10	H_3PO_4 1.00E3 PH_3 4.00E2 P_2S_5 1.00E3	9.00E0 1.20E1 3.00E1		HCP, CP, H_3PO_4, H_3P, H_2P, PH, P_3N_5, PN, $(P_2O_5)_2$, P_4O_{10}, P_4O_6, PO_2, $POCl_3$, PO, P_4S_3, $PSCl_3$, PS, PCl_5, PCl_3, PCl, P_4, P_2, P	Currently Reported
Platinum	Pt		Pt Soluble Salts 2.00E0	6.00E-2			Insufficient Data
Plutonium	Pu						Insufficient Data
Polonium	Po						Insufficient Data
Potassium	K	0.16%	K^+ 5.73E4 KOH 2.00E4	1.72E3 6.00E1	1978-9		Interactive Systems
Praseodymium	Pr		Pr^{+3} 5.14E4 $PrCl_3$ 9.00E4	1.54E3 2.70E3			Insufficient Data
Promethium	Pm						Insufficient Data
Protactinium	Pa						Insufficient Data
Radium	Ra						Insufficient Data
Radon	Rn						Insufficient Data; Inert
Rhenium	Re						Insufficient Data
Rhodium	Rh		Rh Fume, Dust 1.00E2 Rh Soluble Salts 1.00E0	3.00E0 3.00E-2			Insufficient Data
Rubidium	Rb	(4.6-22)	Rb^+ 1.21E5	3.64E3			Insufficient Data
Ruthenium	Ru						Insufficient Data
Samarium	Sm	(0.61-2.61)	Sm^{+3} 5.26E4 $SmCl_3$ 9.00E4	1.58E3 2.70E3		Sm_2O_3, Sm_2, Sm	
Scandium	Sc	(1.8-5.1)	Sc^{+3} 5.36E4	1.61E3		Sc_2O_3, ScO, $ScCl_3$, ScCl, Sc_2, Sc, Sc_2I_6, Sc_2, ScI_3, ScI_2, ScI, Sc	
Selenium	Se	2.08	Se 1.08E1 H_2Se 1.08E1	5.00E-2 5.00E-2		CSe, H_2Se, HSe, NSe, SeO, Se_2, Se	Currently Reported
Silicon	Si	2.49%	Si 1.00E4 SiH_4 7.00E2 SiC 1.00E4	2.10E1	1978-9		Previously Studied; Interactive Systems
Silver	Ag	(0.02-0.03)	Ag Metal and Soluble 1.00E1	5.00E-2			Insufficient Data
Sodium	Na	0.05%	Na^+ 5.31E4 NaOH 2.00E3	9.00E1 6.00E1	1978-9		Interactive Systems
Strontium	Sr	(35-260)	Sr^{+2} 3.07E3	9.22E1		$SrCO_3$, $Sr(OH)_2$, SrOH, $SrSO_4$, SrO, SrS, $SrCl_2$, SrCl, $SrBr_2$, SrBr, Sr	
Sulfur	S						Inclusive
Tantalum	Ta	(0.15-0.33)	Ta 5.00E3	1.50E2		TaC, Ta_2N, TaN, Ta_2O_5, TaO_2Cl, TaO_2, $TaOCl_3$, TaO, $TaCl_5$, $TaCl_4$, $TaCl_3$, $TaCl_{2.5}$, Ta, Ta_2C	
Technetium	Tc						Insufficient Data
Tellurium	Te		Te 1.00E2	3.00E0			Insufficient Data
Terbium	Tb	(0.21-0.34)					Insufficient Data
Thallium	Tl	(0.66)	Tl 1.00E2	5.00E-1			Insufficient Data

TABLE 24 (Continued)

Dwg. 2621C95

Element		US Mean Coal Concentration, ppm	Minimum Acute Toxicity Effluent Levels (MATE)		Parametric Studies	Thermochemical Data Base	Comments
			Air, µg/m³ (ppm)	Land, µg/g			
Thorium	Th	(2.1-4.5)	Th^{+4} 4.19E2 $ThCl_4$ 6.75E2	1.26E0 2.02E1		ThC_2, ThC, Th_3N_4, $Th(SO_4)_2$, ThO_2, $ThOCl_2$, ThO, $ThCl_4$, $ThCl_3$, $ThCl_2$, Th	
Thulium	Tm						Insufficient Data
Tin	Sn	4.79	Organotin 1.00E2 SnO 1.00E4 $SnCl_4$ 2.07E3	2.00E0 3.00E0		SnH_4, SnH, Sn, SnO_2, SnO, SnS_2, SnS, $SnCl_4$, $SnCl_2$, SnCl, Sn_2, Sn	Currently Reported
Titanium	Ti	0.07%	Ti^{+4} 2.53E2 $TiCl_4$, TiO_2 1.00E4	2.00E0 2.0E1, 2.0E2	1978		Previously Studied
Tungsten	W	(0.69-0.82)	W Soluble 1.00E3 W Insoluble 5.00E3	3.00E1 1.50E2		$W(CO)_6$, W_2C, WC, H_2WO_4, $(WO_3)_4$, $(WO_3)_3$, W_3O_8, $(WO_3)_2$, Na_2WO_4, $Na_2O{\cdot}WO_3$, WO_3, $WO_{2.96}$, $WO_{2.72}$, $WOCl_2$, WO_2, $WOCl_4$, WO, W_2Cl_{10}, WCl_6, WCl_5, WCl_4, WCl_3, WCl, W	
Uranium	U	(1.2-1.5)	U 2.00E2	6.00E0		$UC_{1.93}$, $UC_{1.9}$, UC, UH_3, U_4O_9, U_3O_8, UO_2Cl_2, UO_2, $UOCl_3$, $UOCl_2$, UOCl, UO, US_2, US, UCl_6, UCl_5, UCl_4, UCl_3, U	
Vanadium	V	32.71	V, V_2O_5 5.00E2	3.00E-1		V_2C, $VC_{.8}$, VN, $VN_{.465}$, $3Na_2O{\cdot}V_2O_5$, $2Na_2O{\cdot}V_2O_5$, $Na_2O{\cdot}V_2O_5$, V_2O_4, V_2O_3, VO_2, $VOCl_3$, VO, VCl_4, VCl_3, VCl_2, V, V_2O_5	Currently Reported
Xenon	Xe					Insufficient Data; Inert	
Ytterbium	Yb	(0.38-0.83)				Insufficient Data	
Yttrium	Y		Y 1.00E3	3.00E1		Insufficient Data	
Zinc	Zn	272.29	Zn 6.75E2 $ZnCl_2$ 1.00E3 ZnO 5.00E3	1.00E0		$ZnCO_3$, $ZnSO_4{\cdot}7H_2O$, $ZnSO_4{\cdot}6H_2O$, $ZnSO_4{\cdot}H_2O$, $ZnSO_4$, ZnO, ZnS, $ZnCl_2$, ZnCl, Zn_2, Zn	Currently Reported
Zirconium	Zr	72.46	Zr 5.00E3	1.50E1		ZrC_4, ZrC, ZrN, ZrO_2, ZrO, $ZrCl_4$, $ZrCl_3$, $ZrCl_2$, ZrCl, Zr	Currently Reported

thermodynamic data for the compounds or phases that are likely to form in the FBC system. In view of the above considerations, the elements Be, F, Hg, Pb, Co, Cr, Fe, Mo, Mn, Ni, Ti, Na, K, Al, Si, Br, B, P, Cu, V, Zn, Sb, Sn, Zr, As, Cd, Se, Ga, and Ge were selected. Future investigations that define the product distribution of the elements Sc, Th, U, I, Li, Ta, W, Sr, Ba, La, Ce, Au, Hf, and Sm in either simple combustion reactions or in interactive systems will require updating the thermodynamic data base and/or defining the concentration in the feedstock materials.

7. THERMODYNAMIC PROJECTIONS

FEEDSTOCK TRACE AND MINOR ELEMENT CONCENTRATION

Previous investigations[21,65,66] that explored the fate of trace and minor elements in FBC systems have utilized the chemical composition of a typical U.S. mean coal.[11] A complete chemical characterization for sorbent and getter materials has not been documented to date, and, therefore, the contribution of a representative sorbent and getter trace element concentration cannot be included in the final combustion concentration for trace or minor elements. If sufficient data were documented, reporting comprehensive elemental analysis for sorbent and getter materials, one would expect a negligible contribution of the sorbents' and getters' trace and minor element concentration in the total (coal plus sorbent and getter) concentration and, subsequently, a negligible impact on the calculated emission level. Estimates of the maximum likely concentration for particular elements by atomic emission data and from neutron activation analysis obtained by the Exxon Research and Engineering Company[19] and ANL[20] are included in the final concentration for the elements Be, F, Hg, and Pb. Our approach has been to demonstrate the product distribution of F, Be, Hg, Pb, Co, Cr, Fe, Mo, Mn, Ni, Ti, Na, K, Al, Si, Br, B, P, Cu, V, Zn, Sb, Sn, Zr, As, Cd, Se, Ga, and Ge in gaseous and condensed complexes, formed at combustor temperatures and pressure, for various fuel:air combustion ratios and sulfur removal capabilities, using a 4 percent S coal. A composite profile of the number of moles for each key element when 100 g of coal are combusted with 27.6 g of sorbent is illustrated in Table 25. The first-order emission estimate, emphasizing the potential chemical interactions and product distribution at equilibrium, was then determined for FBC operations with 100 percent excess air at 1013 kPa. A final series of equilibrium calculations was made to illustrate variation in the

TABLE 25 - ELEMENTAL CONCENTRATIONS FOR FLUIDIZED-BED COMBUSTION CALCULATIONS USING A U.S. MEAN COAL

Dwg. 1714B30

Element	Moles Fed to the Fluidized Bed/ 100 g Coal Burned with 27.6 g Sorbent	
C	6.1563	
H	4.9107	
N	(57.4186)	(10% excess air)
	104.3977	100% excess air
	(208.7947)	(300% excess air)
O	(16.7038)	(10% excess air)
	29.1919	100% excess air
	(56.9430)	(300% excess air)
S	0.12480	0% sulfur removal
	0.01248	90% sulfur removal
	0.00125	99% sulfur removal
Be *	3.921E-5	
F *	4.457E-4	
Hg *	2.016E-7	
Pb *	4.033E-5	
Co	1.524E-5	
Cr	2.610E-5	
Fe	0.0344	
Mo	7.859E-6	
Mn	8.992E-5	
Ni	3.580E-5	
Ti	0.0015	
Cl	9.455E-3	
Na	4.311E-3	
K	8.451E-3	
Al	0.0478	
Si	0.0851	
Br	19.298E-6	
B	9.454E-4	
P	2.295E-4	
Cu	2.380E-5	
V	6.421E-5	
Zn	4.165E-4	
Sb	1.035E-6	
Sn	4.036E-6	
Zr	7.943E-5	
As	1.871E-5	
Cd	2.242E-6	
Se	2.634E-6	
Ga	4.475E-6	
Ge	9.078E-6	
Ca	0.1513 (sorbent)	
Mg	0.1499 (sorbent)	

* Coal and sorbent feed concentrations

projected trace and minor product distribution for the combustion of eastern and western coals.

FLUIDIZED-BED COMBUSTION SYSTEMS DESIGN

During coal combustion, incombustible material that originates in the mineral content remains in the combustor as either slag or bottom ash or is released into the flue gas stream as fly ash, part of which is emitted from the stack into the atmosphere as particulate matter of various sizes. In order to estimate the emission concentration of gaseous and condensed species released during FBC, a conceptual plant design is required. Figure 14 schematically illustrates a typical PFBC design for a 250 MW_e, combined-cycle system in which the combustor operates at temperatures between 1100 and 1300 K, at 1013 kPa, with 100 percent excess air and 90 percent S removal capabilities (Ca:S = 2). Table 26 summarizes the PFBC parameters for this design, following the particulate loadings of ash and sorbent materials from the bed, through a recycle cyclone, and then onto a primary cyclone and secondary fabric-filter device, prior to expansion in the gas turbine. Figures 15 and 16 illustrate the projected size distribution of ash and spent sorbent fines at each location within the system. The combined particulate loading projection of 0.0097 g/m^3 at the gas turbine entrance estimates that 45 to 50 percent of the entrained ash and sorbent fines are larger than 1 μm but do not exceed 10 to 15 μm in diameter.

In general, particle size distribution leaving the combustor is primarily a function of the combustion temperature, the coal size distribution, the chemical and physical properties of the feedstock, and the combustion facility design. The size distribution may vary continuously from the furnace to the low-temperature particulate collection devices because of particle growth (agglomeration, coagulation, condensation, etc.) or the loss of heavier particles.

Complex condensation or nucleation reactions (Figure 17) of combustion gases containing volatile trace and minor element phases with the

Dwg. 7721A79

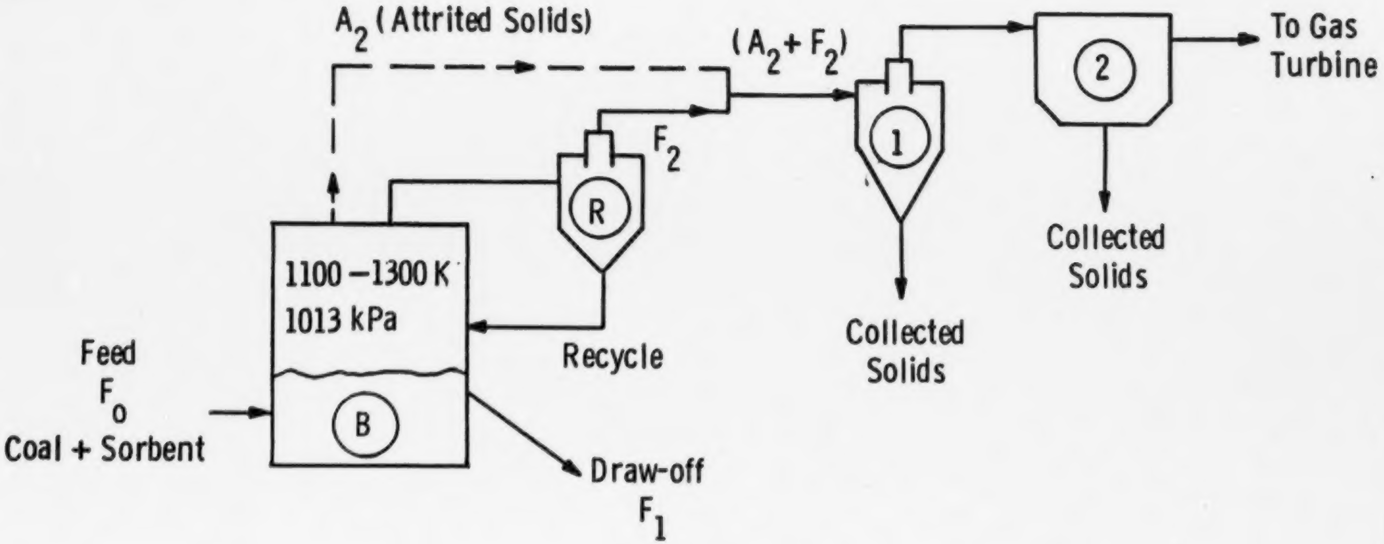
A_2 (Attrited Solids)
$(A_2 + F_2)$
To Gas Turbine
F_2
R
1
2
1100 – 1300 K
1013 kPa
Feed
F_0
Coal + Sorbent
B
Recycle
Collected Solids
Collected Solids
Draw-off
F_1

B = Fluidized Bed Combustor

R = Recycle Cyclone

1 = First Collection Device – "Cyclone"

2 = Second Collection Device – "Fabric Filter"

Figure 14 - Pressurized Fluidized-Bed Combustor Design for a 250 MW_e Combined-Cycle Plant

TABLE 26 - SUMMARY OF PFBC PARAMETERS

	Sorbent	Ash*	Total
Feed F_0,g/s	6482.1	1514.7	7996.8
Draw-off F_1, g/s	3489	184.6	3673.6
Draw-off as % of Feed	53.83	12.19	45.94
Attrited A_2,g/s	2698.1	528.9	3227
Elutriated E,g/s	295.02	801.2	1096.2
Carry-over(A_2 + E), g/s	2993.12	1330.1	4323.2
Attrited as % of Carry-over	90.1	39.8	74.6
Elutriated as % of Carry-over	9.9	60.2	25.4
Overhead,g/s	45420.8	1963.8	47384.6
Recycle,g/s	42427.7	633.7	43061.4
Emitted Grain Loading,gr/scf	6.07 (13.89)	2.7 (6.17)	8.8 (20.06)
First Device Exit,g/s	714.8	149.5	864.3
First Device Grain Loading	1.45 (3.32)	0.3 (0.69)	1.75 (4.0)
First Device Efficiency	76.1	88.8	80
Second Device Exit,g/s	1.75	0.35	2.10
Second Device Grain Loading	0.0036 (0.0081)	0.007 (0.0016)	1.0106 (0.0097)
Second Device Efficiency	99.8	99.8	99.8

Superficial Velocity: 5 ft/sec
Expanded Bed Height: 15 ft
Bed Voidage: 0.33
Bed Cross Section: 653 ft^2
Attrition Rate for Sorbent: 2% of Bed Wt Per Hour

* Coal

** Figures in parenthesis refer to g/m^3

Dwg. 7721A80

Curve 722644-B

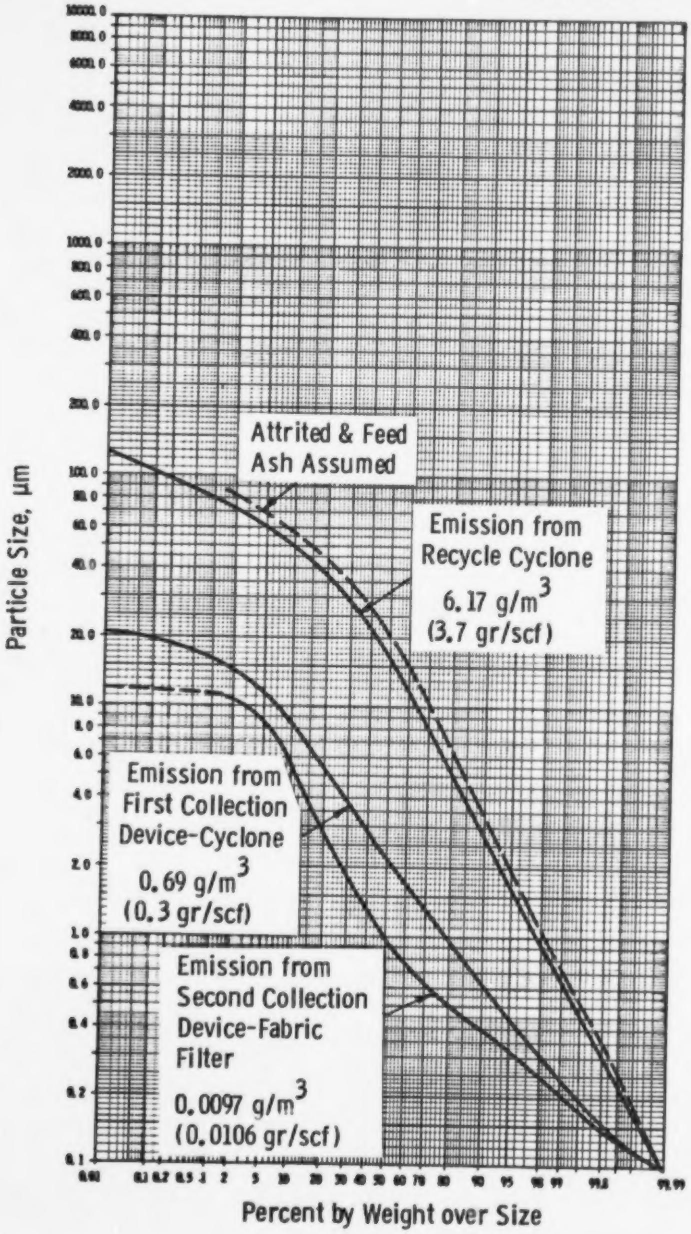

Figure 15 - Size Distributions for the Ash in PFBC Systems

Curve 722643-B

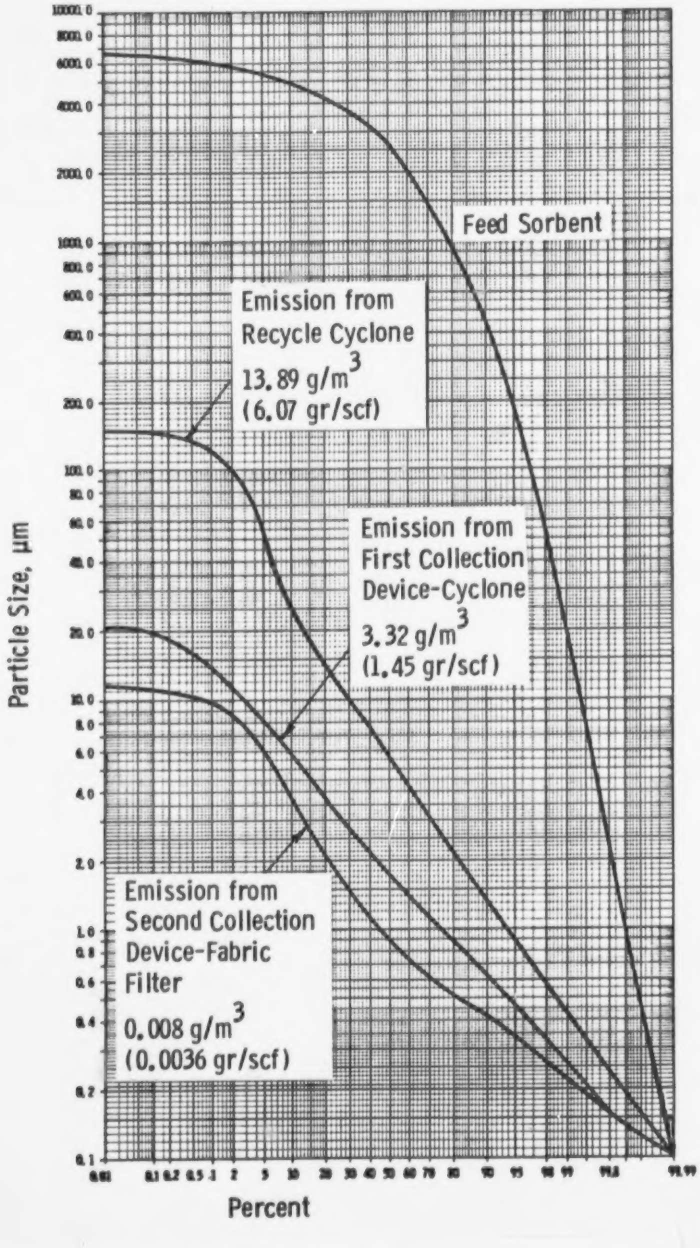

Figure 16 - Size Distributions for Sorbent Material in PFBC Systems

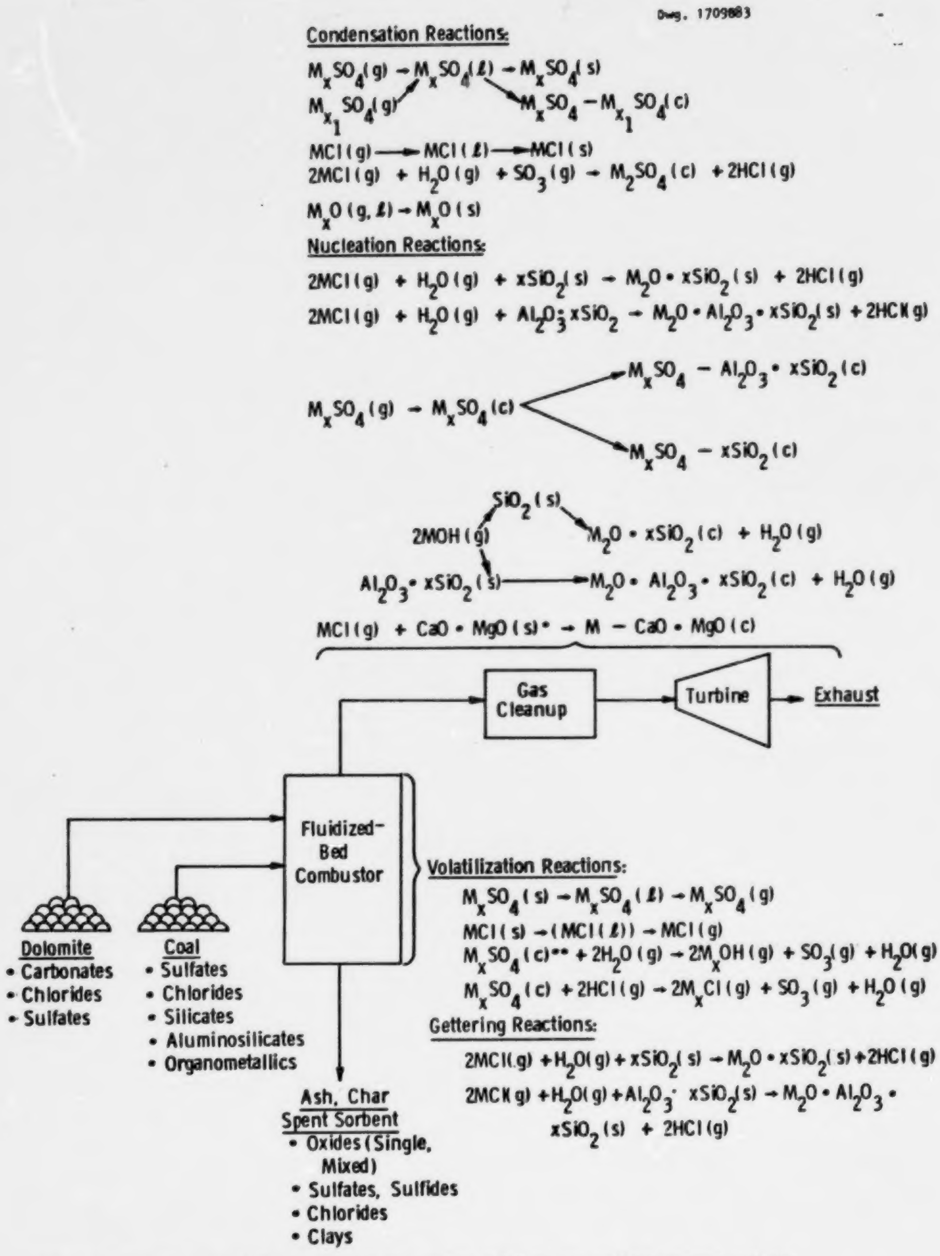
Dwg. 1709B83
Condensation Reactions:
$M_xSO_4(g) \rightarrow M_xSO_4(\ell) \rightarrow M_xSO_4(s)$
$M_{x_1}SO_4(g)$
$M_xSO_4 - M_{x_1}SO_4(c)$
$MCl(g) \rightarrow MCl(\ell) \rightarrow MCl(s)$
$2MCl(g) + H_2O(g) + SO_3(g) \rightarrow M_2SO_4(c) + 2HCl(g)$
$M_xO(g,\ell) \rightarrow M_xO(s)$
Nucleation Reactions:
$2MCl(g) + H_2O(g) + xSiO_2(s) \rightarrow M_2O \cdot xSiO_2(s) + 2HCl(g)$
$2MCl(g) + H_2O(g) + Al_2O_3 \cdot xSiO_2 \rightarrow M_2O \cdot Al_2O_3 \cdot xSiO_2(s) + 2HCl(g)$
$M_xSO_4(g) \rightarrow M_xSO_4(c)$
$M_xSO_4 - Al_2O_3 \cdot xSiO_2(c)$
$M_xSO_4 - xSiO_2(c)$
$SiO_2(s)$
$2MOH(g)$
$M_2O \cdot xSiO_2(c) + H_2O(g)$
$Al_2O_3 \cdot xSiO_2(s)$
$M_2O \cdot Al_2O_3 \cdot xSiO_2(c) + H_2O(g)$
$MCl(g) + CaO \cdot MgO(s)^* \rightarrow M - CaO \cdot MgO(c)$
Gas Cleanup
Turbine
Exhaust
Fluidized-Bed Combustor
Volatilization Reactions:
$M_xSO_4(s) \rightarrow M_xSO_4(\ell) \rightarrow M_xSO_4(g)$
$MCl(s) \rightarrow (MCl(\ell)) \rightarrow MCl(g)$
$M_xSO_4(c)^{**} + 2H_2O(g) \rightarrow 2M_xOH(g) + SO_3(g) + H_2O(g)$
$M_xSO_4(c) + 2HCl(g) \rightarrow 2M_xCl(g) + SO_3(g) + H_2O(g)$
Gettering Reactions:
$2MCl(g) + H_2O(g) + xSiO_2(s) \rightarrow M_2O \cdot xSiO_2(s) + 2HCl(g)$
$2MCl(g) + H_2O(g) + Al_2O_3 \cdot xSiO_2(s) \rightarrow M_2O \cdot Al_2O_3 \cdot xSiO_2(s) + 2HCl(g)$
Dolomite
• Carbonates
• Chlorides
• Sulfates
Coal
• Sulfates
• Chlorides
• Silicates
• Aluminosilicates
• Organometallics
Ash, Char
Spent Sorbent
• Oxides (Single, Mixed)
• Sulfates, Sulfides
• Chlorides
• Clays

$^*CaO \cdot MgO$ = Representative of either half- or fully calcined, or sulfated sorbent material

$^{**}(c)$ = condensed = solid + liquid

Figure 17 - Chemical Pathways in Fluidized-Bed Combustion Systems

entrained ash or sorbent particles may occur before the gases are emitted from the stack. These phenomena may lead to the formation of particulate emissions that are potentially toxic in nature. Delineation of the reaction mechanisms requires definition of the gas phase chemistry, knowledge of the principal chemical reactions of the volatiles with either the aluminosilicate ash or the spent sorbent material, and kinetic data defining the rate of formation for the resulting complexes. Using a kinetic model approach, we could calculate the product distribution of the chemical species and phases as a function of the process operating conditions. This would then permit quanitification of the concentration and chemical identification of the compound emitted in either the solid or the gaseous effluents from the plant. Since the kinetics for the trace and minor element reactions in combustion are unknown, it is possible to fall back on a common assumption used in high-temperature chemistry that, as a first-level approximation, thermodynamic equilibrium is reached in the fluidized bed and the equilibrium product distribution will be characteristic of the process effluent. On this basis a brief overview of the techniques used in projecting the elemental product distribution in the gas, liquid, and/or solid phases released from the FBC will be presented.

THE CHEMICAL EQUILIBRIUM CALCULATION

The equilibrium composition for trace element FBC conditions is calculated by minimizing the Gibbs free energy of the polyphase system, using the techniques of Geometric Programming,[67] in addition to satisfying the mass conservation equations.

The Gibbs free energy (G) of a multicomponent system is represented by a summation over the mixture chemical species; in other words,

$$G = \sum_i n_i G_i \quad ,$$

where $G_i = \mu_i$ is the molar chemical potential, and n_i is the number of moles of the i^{th} species. The molar chemical potential is expressed as

$$\mu_i = \mu_i^o + \delta(RT \ln P_i) \quad ,$$

where for a gaseous species $\delta = 1.0$, and for a condensed species $\delta = 0$. In the above equation P_i is the partial pressure of the gaseous species, T is the gas temperature, R is the universal gas constant, and μ_i^o is the species's chemical potential at unit fugacity. The species's chemical potential is expressed as:

$$\mu_i^o = H_i^o - TS_i^o \quad ,$$

where H_i^o (molar enthalpy) and S_i^o (molar entropy) are the species's standard thermochemical properties, which are functions of the species standard specific heat, $C_{p,i}^o$. In other words:

$$H_i^o(T) = \int_{T_r}^{T_o} C_{p,i}^o dT + \Delta H_f^o(T_r)$$

and

$$S_i(T) = \int_o^T \frac{C_{p,i}^o dT}{T} \quad ,$$

where ΔH_f^o is the standard heat of formation for the compound at the reference temperature (T_r) of 298.15 K.

The chemical equilibrium program determines the value of n_i for each species in all possible solid, liquid, or gaseous phases, given the species's standard thermochemical data as reported in the literature,[68-78] the total gas pressure, and the mass constraints on the system. Note that this study considers only the reactions of compounds for which thermodynamic data are available. We can reasonably assume that other compounds may form in the fluid-bed system, but data for such compounds have not been cited in the literature, nor have estimates of their free energy, heats of formation, or molecular constants been made in this study. We believe that compounds not reported in the literature are less likely to form than are those for which data are cited.

Table 27 illustrates the major combustion gas species for which thermodynamic data are available. The data for each species have been reduced and used as input for the chemical equilibrium calculations. The resulting product distribution in phases formed from the equilibrium reactions of C, H, N, O, S, and Cl in a typical U.S. mean coal as a function of temperature are presented in Figures 18 through 22. The principal volatile phases formed in the fluidized-bed combustor include N_2, O_2, CO_2, and H_2O, in addition to the formation of sulfur and nitrogen oxides, and chlorine complexes. Increasing the excess air content for combustion from 10 to 100 percent reduces the partial pressure of the volatile sulfur phases (SO_2, SO_3, and H_2SO_4) while enhancing the partial pressure of the nitrogen-containing phases (NO, NO_2, N_2O, HNO_3, HNO_2, and NOCl). Operating at 90 percent S-removal efficiencies through the addition of sorbent materials to the bed minimizes the partial pressure of SO_2, SO_3, and H_2SO_4; and reducing the total pressure of the system from 1520 to 101.3 kPa reduces the partial pressure of all volatile phases.

The trace and minor species and phases considered in the noninteractive equilibrium calculations are presented in Appendix A. In defining the individual elemental reactions with combustion gases formed in

TABLE 27 - C-H-N-O-S-Cl SPECIES CONSIDERED IN FLUIDIZED-BED COMBUSTION REACTIONS

Gases				Solids/Liquids
C	C_2Cl_6	HCl	N	C
CCl	C_2H	HNO	NH	
CCl_2	C_2H_2	HNO_3	NH_2	
CCl_2O	C_2H_4	HO	NH_3	
CCl_3	C_2H_4O	HO_2	NO	
CCl_4	C_2N	HS	NO_2	
CH	C_2N_2	H_2	NO_3	
CHN	C_2O	H_2O	NS	
CHNO	C_3	H_2S	N_2	
CHO	C_3O_2	H_2SO_4	N_2H_2	
CH_2	C_4	O	N_2H_4	
CH_2O	C_4N_2	O_2	N_2O	
CH_3	CS	O_3	N_2O_3	
CH_4	COS	S	N_2O_4	
CN	Cl	S_2	N_2O_5	
CHN	ClHO	S_3		
CN_2	ClO	S_8		
CO	ClO_2	SO		
CO_2	Cl_2	SO_2		
C_2	Cl_2O	SO_3		
C_2Cl_4	H	S_2O		

Dwg. 1714B32

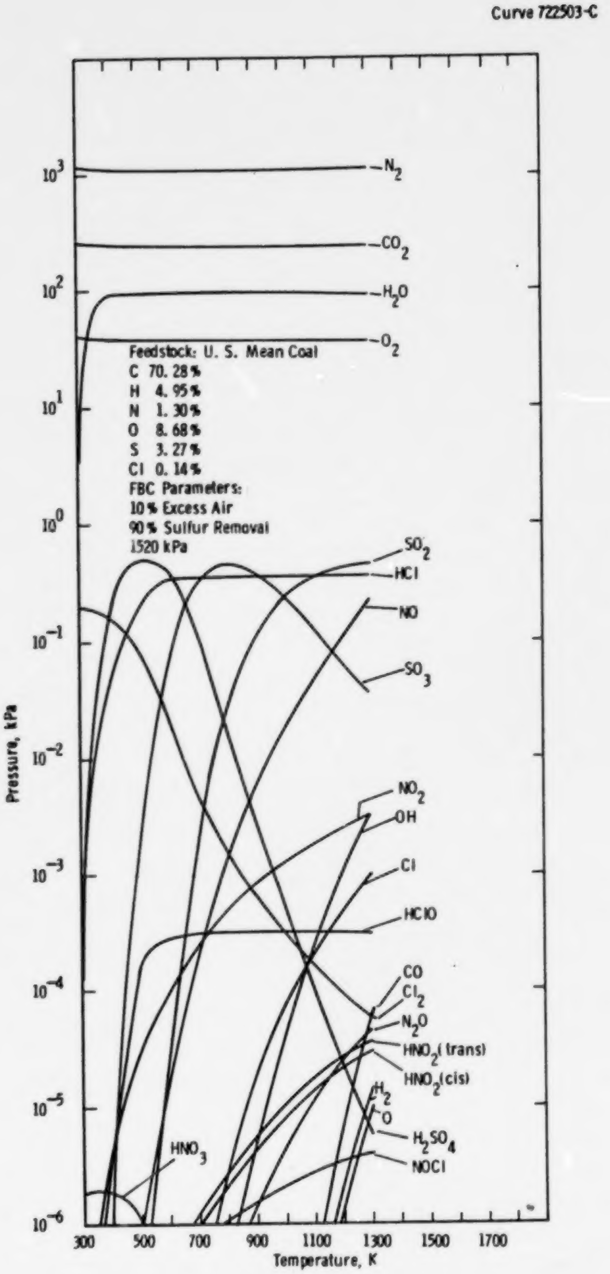

Figure 18 - Combustion Gas Product Distribution for PFBC Systems Operating with 10% Excess Air and 90% Sulfur-Removal Efficiencies

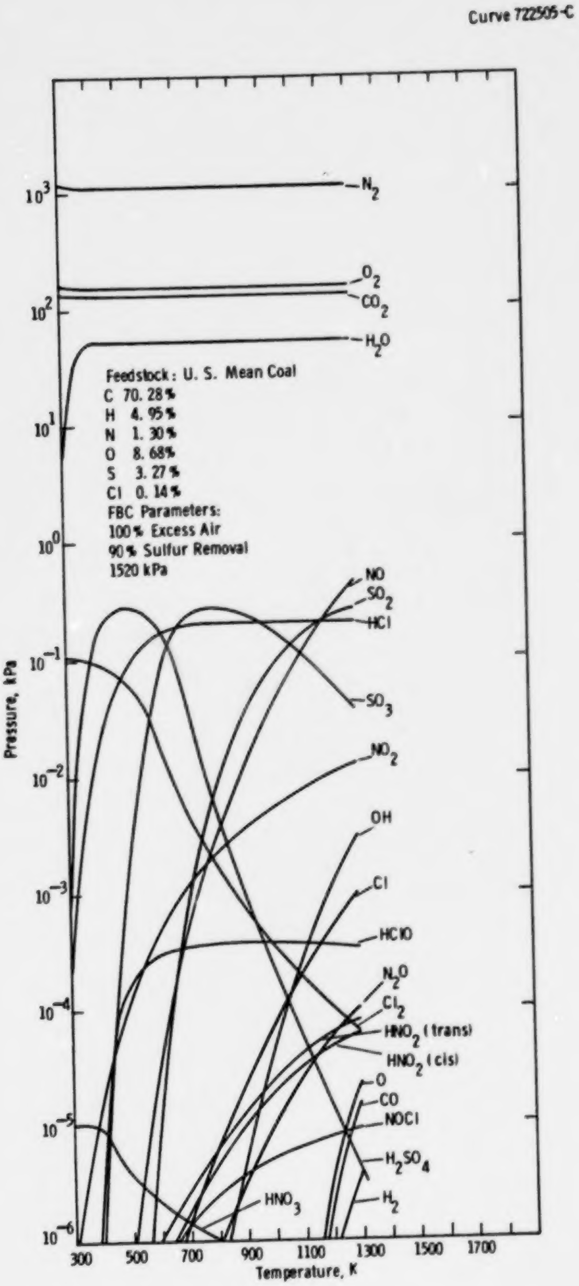

Figure 19 - Combustion Gas Product Distribution for PFBC Systems Operating with 100% Excess Air and 90% Sulfur-Removal Efficiencies

Curve 722502-C

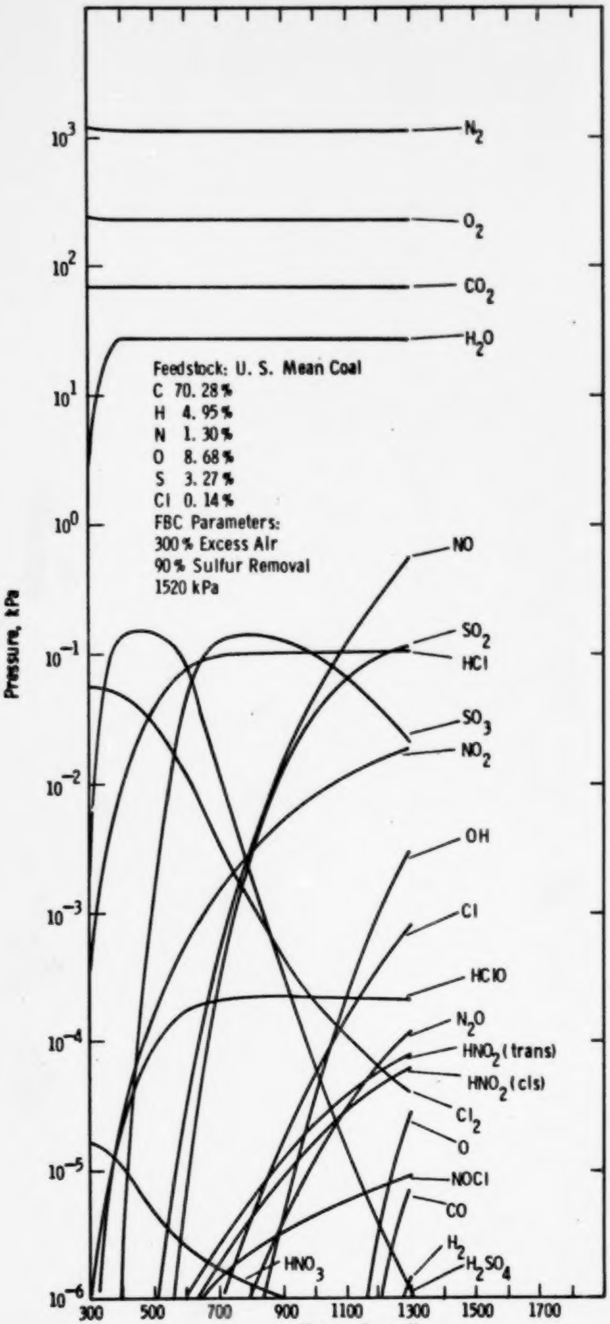

Figure 20 - Combustion Gas Product Distribution for PFBC Systems Operating with 300% Excess Air and 90% Sulfur-Removal Efficiencies

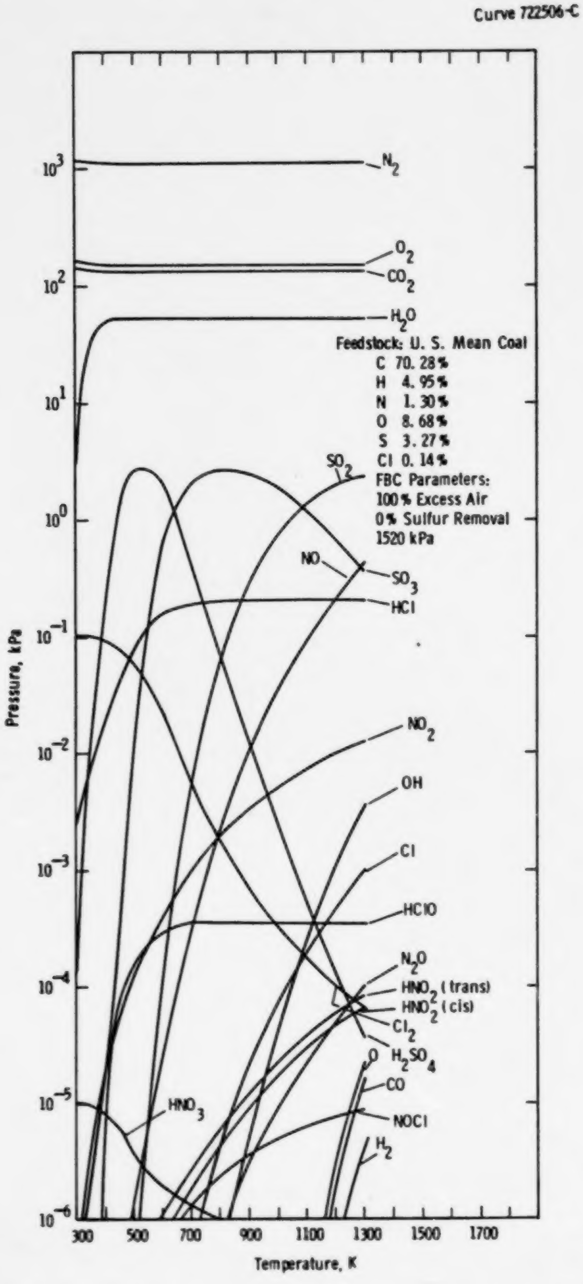

Figure 21 - Combustion Gas Product Distribution for PFBC Systems Operating with 100% Excess Air and 0% Sulfur-Removal Efficiencies

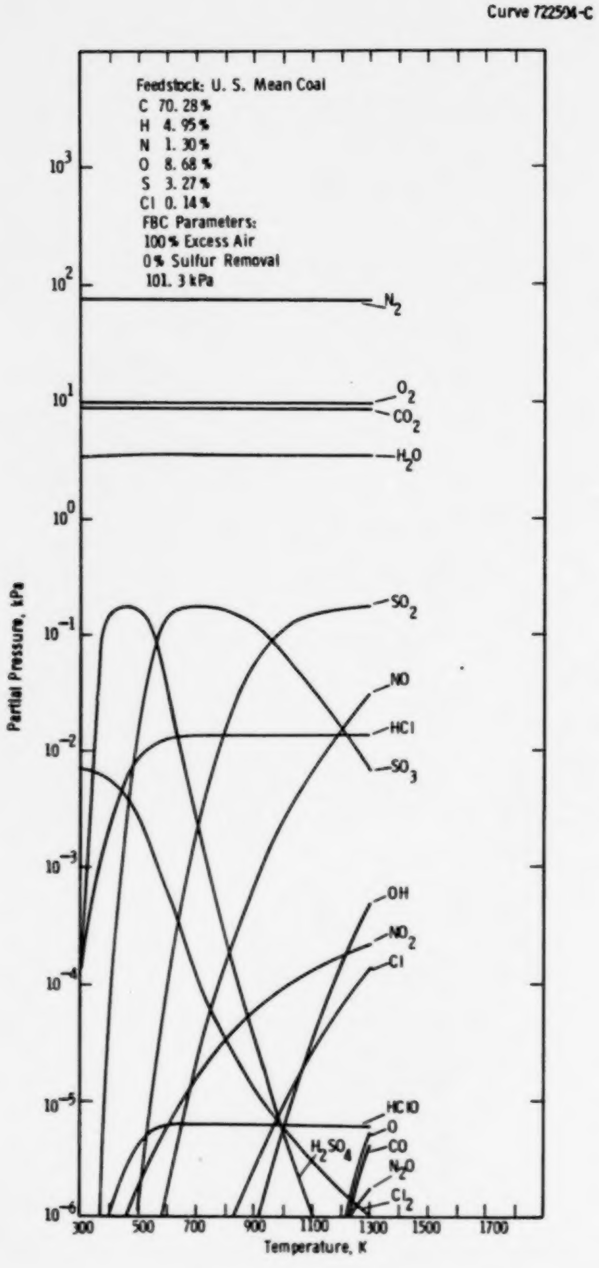

Figure 22 - Combustion Gas Product Distribution For AFBC Systems Operating with 100% Excess Air and 0% Sulfur-Removal Efficiencies

the fluidized bed, we made a series of simple, noninteractive, equilibrium calculations involving C-H-N-O-S-Cl-X (X represents the specific trace or minor element). The following assumptions were used throughout this series:

- The elemental concentrations used in the equilibrium calculations are those typical of a U.S. mean coal.[11]
- In the FBC calculations each trace or minor element is considered to have the potential to react with C-H-N-O-S-Cl from the feedstock or sorbent materials and will not remain bound as either a silicate or aluminosilicate clay constituent. The ash projected to form within the bed results from the interaction of the feedstock-contained Al and Si.
- One hundred percent of the projected gaseous phases are released from the bed into the effluent stream. Secondary interactions of the volatiles and solids in the bed and volatiles with elutriated ash fines are not considered in these calculations. Partitioning the gaseous trace and minor phases along the particle surfaces (either incompletely combusted coal particles, ash, char, etc.) as either a chemical reaction or a surface adsorption mechanism is also not included in the preliminary noninteractive projections.
- The reaction kinetics governing the reactions of trace, minor, or major species with combustion gases are unknown.

The chemical reaction of each element will be reviewed individually in the following subsections in order to illustrate the major, minor, or trace phases and complexes that are likely to form with combustion gases. The principal phases projected for a simple combustion system will be included in the interactive equilibrium calculations where numerous complex reactions are likely to occur simultaneously.

TRACE AND MINOR ELEMENT REACTIONS WITH COMBUSTION GASES

Beryllium

In the fluidized bed Be reacts with O_2 and sulfur oxides (SO_x), forming solid beryllium sulfate ($BeSO_4$) at temperatures of 300 to 700 K and pressure between 101.3 and 1520 kPa for 0 to 90 percent S-removal systems. At temperatures greater than 700 to 800 K, $BeSO_4(s)$ dissociates, forming solid beryllium oxide (BeO) and gaseous O_2 and SO_2,* as shown by the following reaction:

$$BeSO_4(s) \xrightarrow{700\text{-}800\ K} BeO(s) + SO_2\ (g) + 1/2\ O_2(g)\quad . \qquad (1)$$

Beryllium oxide in FBC systems then reacts with water vapor, forming the stable $Be(OH)_2$ phase at high temperatures:

$$BeO(s) + H_2O(g) \xrightarrow{>1100\ K} Be(OH)_2(g)\quad . \qquad (2)$$

With 99 percent S-removal efficiencies, $BeSO_4$ is no longer projected to form as a stable solid in the low-temperature regions of the fluidized-bed combustor. The principal reaction under these conditions is the direct formation of solid BeO from the elemental concentration contained within the coal matrix.

Independent of the S-removal efficiencies or fuel:air ratio during combustion, operating temperatures greater than 1300 K introduce additional gaseous interactions, forming trace levels of volatile chlorides.

---

*Throughout this study reactions are written as $X + 1/2\ O_2 + SO_2$, as opposed to $X + SO_3$.

A level of 0.01 percent of the initial Be feedstock concentration exists as gaseous beryllium dichloride ($BeCl_2$), possibly as a result of the following reaction:

$$Be(OH)_2(g) + 2HCl(g) \xrightarrow{>1300\ K} BeCl_2(g) + 2H_2O(g) \quad . \qquad (3)$$

Three-dimensional plots of the major solid and gaseous stable equilibrium Be species formed as a function of temperature and pressure in a fluidized bed operating at 100 percent excess air and 90 percent S-removal efficiencies are illustrated in Figures 23 through 26. The reaction of Be with the clay constituents, Al and Si, and trace or minor elements will be presented in the interactive discussion.

Fluorine

The principal reaction of F in the fluidized-bed combustor leads to the formation of gaseous hydrogen fluoride (HF) (Figure 27), with fluorosulfuric acid (HSO_3F) projected to form as a trace volatile phase at concentrations less than 0.5 percent of the initial feedstock at temperatures less than 1000 K (Figure 28). At typical combustor operating temperatures the HSO_3F phase completely dissociates, with 100 percent of the feedstock F present in the effluent as HF. The dissociation can be written as:

$$HSO_3F(g) \xrightarrow{>1000\ K} HF(g) + SO_2(g) + 1/2\ O_2(g) \quad . \qquad (4)$$

This reaction is governed not only by the level at which F and S are present in the combustor, but also by the operating temperature and pressure. As the concentration of S in the FBC effluent is reduced (i.e., 99 percent S-removal efficiencies), the production of volatile HSO_3F is minimized. Under these conditions F complexes primarily with hydrogen. Similarly, atmospheric operations diminish the stability of the volatile HSO_3F phase at low temperature. Conversion into gaseous HF for a 100 percent excess air, 90 percent S-removal system operating

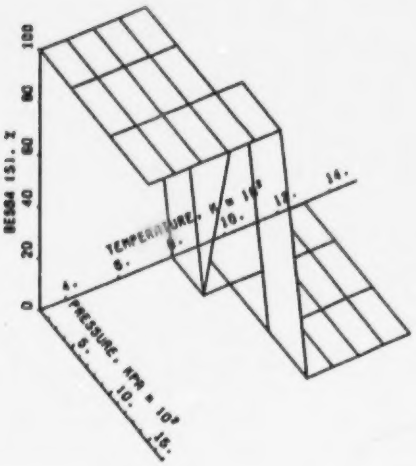

Figure 23 - Percent Distribution of Solid $BeSO_4$ as a Function of Temperature and Pressure in a Fluidized-Bed Combustor Operating with 100% Excess Air and 90% Sulfur-Removal Efficiencies

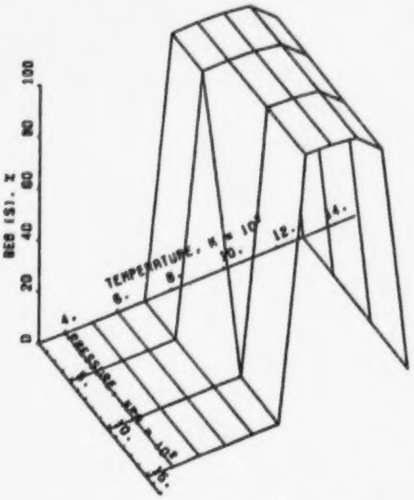

Figure 24 - Percent Distribution of Solid BeO as a Function of Temperature and Pressure in a Fluidized-Bed Combustor Operating with 100% Excess Air and 90% Sulfur-Removal Efficiencies

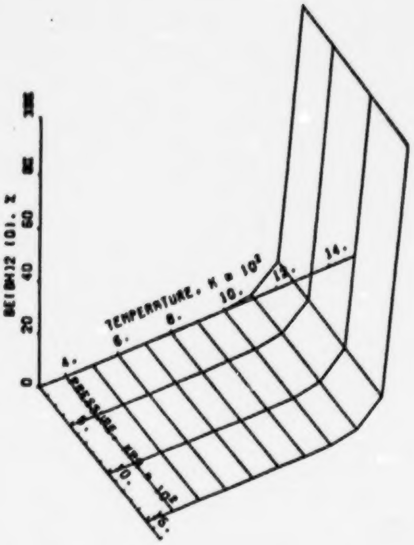

Figure 25 - Percent Distribution of Gaseous $Be(OH)_2$ as a Function of Temperature and Pressure in a Fluidized-Bed Combustor Operating with 100% Excess Air and 90% Sulfur-Removal Efficiencies

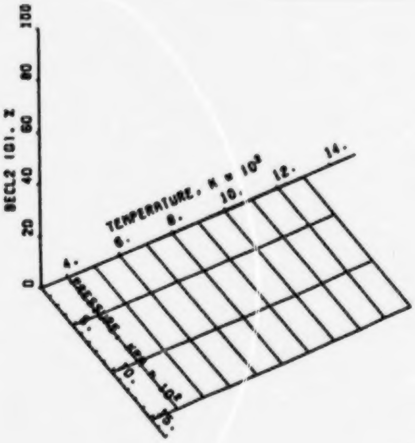

Figure 26 - Percent Distribution of Gaseous $BeCl_2$ as a Function of Temperature and Pressure in a Fluidized-Bed Combustor Operating with 100% Excess Air and 90% Sulfur-Removal Efficiencies

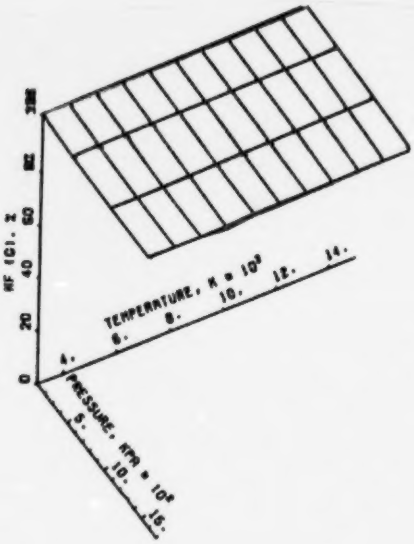

Figure 27 - Percent Distribution of Gaseous HF as a Function of Temperature and Pressure in a Fluidized-Bed Combustor Operating with 100% Excess Air and 90% Sulfur-Removal Efficiencies

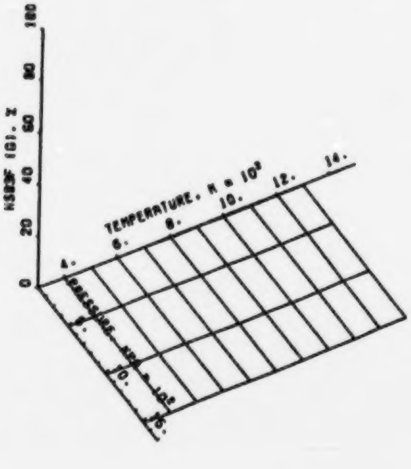

Figure 28 - Percent Distribution of Gaseous HSO_3F as a Function of Temperature and Pressure in a Fluidized-Bed Combustor Operating with 100% Excess Air and 90% Sulfur-Removal Efficiencies

at 101.3 kPa is achieved at temperatures between 700 to 800 K; at 1520 kPa temperatures between 900 and 1000 K are required. The interaction of F with the volatile alkalis (Na and K) and the attrited sorbent particles containing Ca and Mg form additional stable phases. These interactions will be presented in a later discussion.

Mercury

The reaction of Hg with FBC gases produces volatile species of mercuric chloride ($HgCl_2$), mercury monoxide (HgO), and monoatomic mercury (Hg), in systems containing 100 and 300 percent excess air. Fluidized-bed combustion systems operating at 10 percent excess air additionally form diatomic mercury (Hg_2), mercury chloride (HgCl), mercurous chloride (Hg_2Cl_2), and mercury monohydride (HgH).

Mercuric chloride is the favored trace Hg compound that forms at low temperatures, as shown in Figures 29 through 31. Mercuric chloride gas is stable below 900 K; above this temperature chlorine is released from the complex, producing gaseous Hg and HgO, as shown in the following reactions:

$$HgCl_2(g) \xrightarrow{>900\ K} Hg(g) + 2\ Cl^{-*}(g) \qquad (5)$$

$$Hg(g) + 1/2\ O_2(g) \xrightarrow{>900\ K} HgO(g)\ . \qquad (6)$$

At reduced pressures and elevated temperatures removal of $HgCl_2$ from the gas phase is enhanced. Similarly, reduction of the S concentration in fluid-bed gases further reduces the partial pressure of the

---

*$Cl_2(g)$ at low temperatures; $2Cl^-(g)$ at high temperatures.

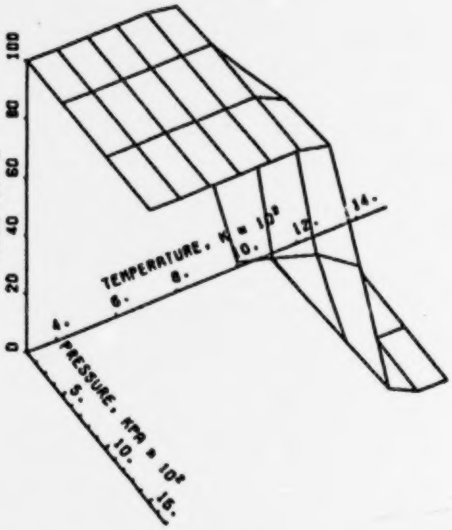

Figure 29 - Percent Distribution of Gaseous $HgCl_2$ as a Function of Temperature and Pressure in a Fluidized-Bed Combustor Operating with 100% Excess Air and 90% Sulfur-Removal Efficiencies

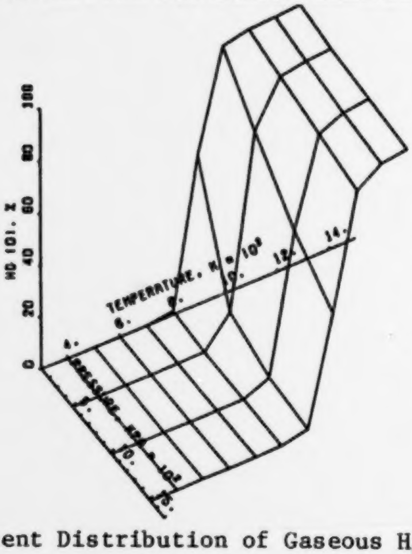

Figure 30 - Percent Distribution of Gaseous Hg as a Function of Temperature and Pressure in a Fluidized-Bed Combustor Operating with 100% Excess Air and 90% Sulfur-Removal Efficiencies

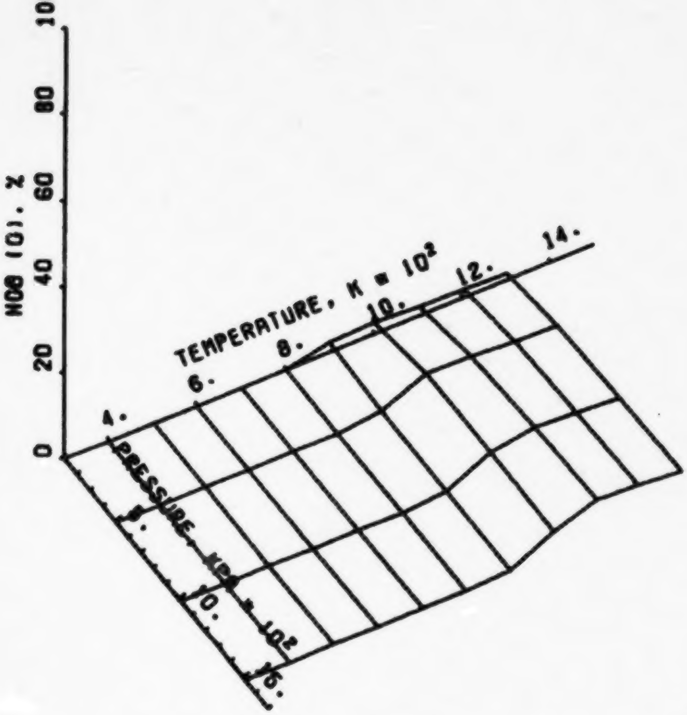

Figure 31 - Percent Distribution of Gaseous HgO as a Function of Temperature and Pressure in a Fluidized-Bed Combustor Operating with 100% Excess Air and 90% Sulfur-Removal Efficiencies

$HgCl_2$ due to the increased O_2 partial pressure in the system. This is illustrated by comparison of the partial pressure of $HgCl_2$ at 1200 K:

	System Total Pressure	
Sulfur Removal, %	1520 kPa	101.3 kPa
0	3.802×10^{-8} kPa	2.080×10^{-11} kPa
99	1.134×10^{-11} kPa	8.297×10^{-15} kPa

Trace levels ($<10^{-10}$ kPa) of $Hg_2(g)$ and $HgCl(g)$ are projected to form in the fluidized-bed combustor. Reduction in the concentration of S to 99 percent removal efficiencies produces greater partial pressures of Hg_2 and HgCl at low temperatures than in the 0 or 90 percent S-removal systems. Equivalence in the partial pressure exerted by gaseous Hg_2 for the 0, 90, or 99 percent S-removal system is reached at elevated temperatures. Gaseous HgCl is not detected in systems containing 300 percent excess air.

Solids and sulfate compounds of Hg are not projected to form stable phases in the fluidized-bed combustor at equilibrium. Mercury released as a gas should not condense in the cooling stages of the process. Complete volatilization of Hg from the coal, sorbent, or getter is projected with emission from the stack in the form of volatile oxides or chlorides.

Lead

The volatile compounds lead tetrachloride ($PbCl_4$), lead dichloride ($PbCl_2$), lead chloride (PbCl), lead oxide (PbO), and monoatomic lead (Pb), are projected to form when Pb is released from the feedstock materials and reacts with FBC gases. Over the temperature range of 300 to 1300 K, $(Pb)Cl_4$ is the predominant gaseous trace compound under pressurized conditions. For atmospheric fluidized-bed combustion (AFBC), PbO is the projected volatile phase favored when operating temperatures exceed 1150 K, as shown in Figure 32. Conversion between the volatile tetrachloride and oxide phases is through the following reaction:

$$PbCl_4(g) + 2H_2O(g) \longrightarrow Pb(g) + 4HCl(g) + O_2(g) \quad . \quad (7)$$

Reducing the S level (i.e., 99 percent S-removal efficiencies) increases the partial pressure of O_2, limiting the formation of gaseous $PbCl_4$ at low pressures when the temperature is greater than 1000 K. Between 1000 and 1100 K $PbCl_4$ releases chlorine, reducing the concentration of $PbCl_4$

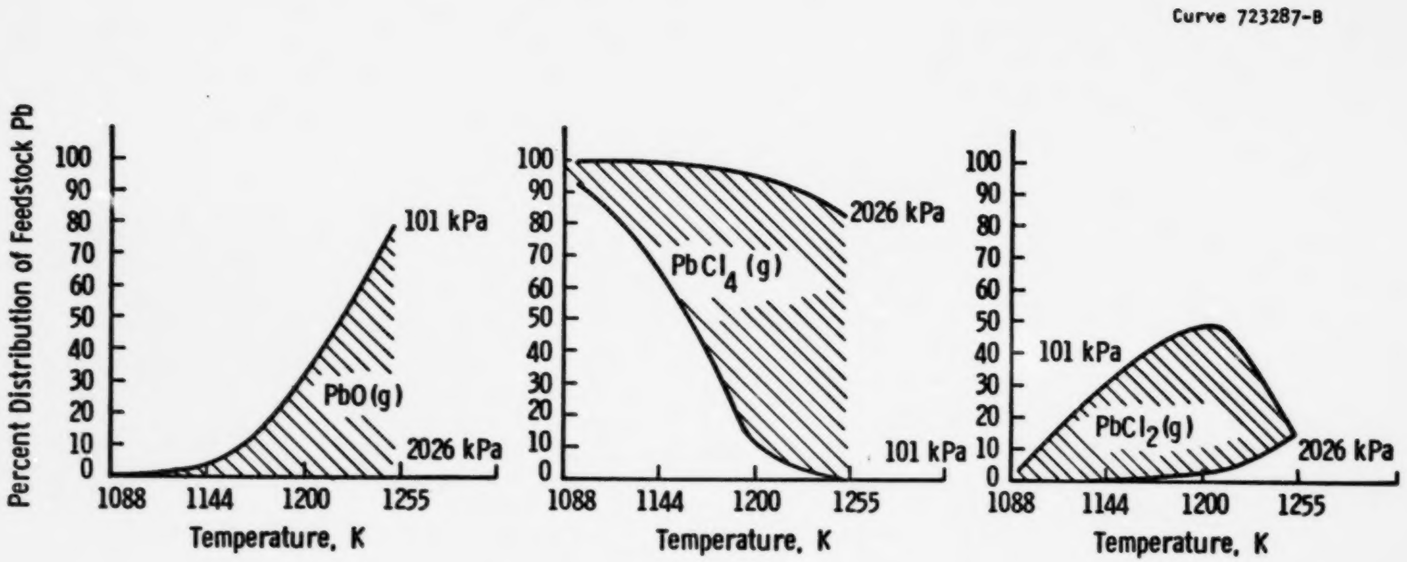

Figure 32 - Percent Distribution of Feedstock Lead as a Function of Temperature and Pressure in a Fluidized-Bed Combustor Operating with 10% Excess Air and 90% Sulfur-Removal Efficiencies

in the effluent stream while increasing the volatile $PbCl_2$ content (reaction 8):

$$PbCl_4(g) \xrightarrow{1000-1000\ K} PbCl_2(g) + 2\ Cl^-(g) \quad . \qquad (8)$$

Reduction of the operating pressure at elevated temperatures causes a further dissociation of chlorine from the $PbCl_2$ phase, forming gaseous PbCl (reaction 9):

$$PbCl_2(g) \longrightarrow PbCl(g) + Cl^-(g) \quad . \qquad (9)$$

Reducing the S level from 0 to 90 percent produces only a slight increase in the resulting partial pressure of PbO, but a dramatic increase is projected when the combustor operates at 99 percent S-removal efficiency. At 1200 K and 1520 kPa the partial pressure of PbO for combustion in 10 and 100 percent excess air is as follows:

	Excess Air	
Sulfur Removal, %	10%	100%
0	1.290×10^{-7} kPa	1.070×10^{-7} kPa
90	1.394×10^{-7} kPa	1.281×10^{-7} kPa
99	1.579×10^{-3} kPa	9.015×10^{-4} kPa

Condensation of the volatile Pb phases illustrated in Figures 33 through 36 may result along entrained particulate matter as it passes through the cooler parts of the system. Similarly, deposition of solid PbO or $PbCl_2$ may result at temperatures below 1151 and 774 K, respectively.

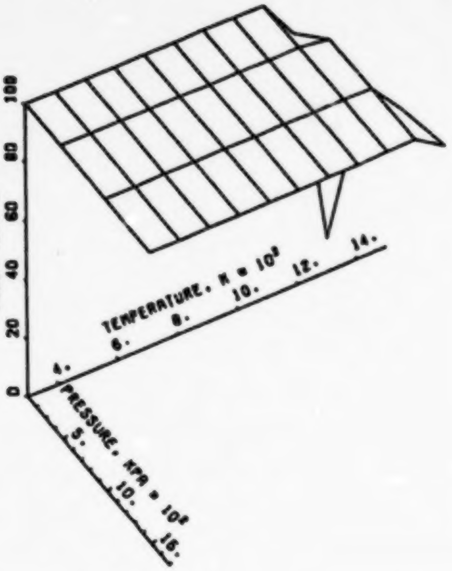

Figure 33 - Percent Distribution of Gaseous $PbCl_4$ as a Function of Temperature and Pressure in a Fluidized-Bed Combustor Operating with 100% Excess Air and 90% Sulfur-Removal Efficiencies

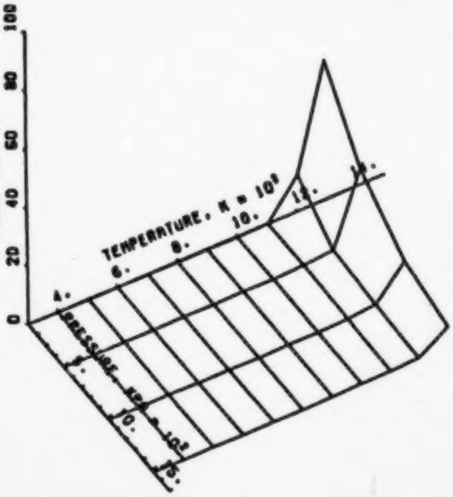

Figure 34 - Percent Distribution of Gaseous $PbCl_2$ as a Function of Temperature and Pressure in a Fluidized-Bed Combustor Operating with 100% Excess Air and 90% Sulfur-Removal Efficiencies

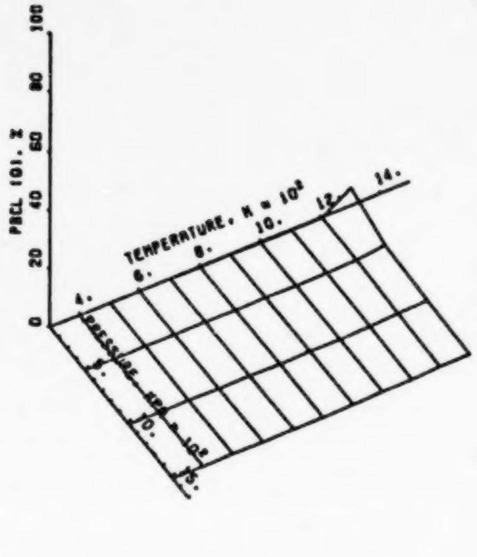

Figure 35 - Percent Distribution of Gaseous PbCl as a Function of Temperature and Pressure in a Fluidized-Bed Combustor Operating with 100% Excess Air and 90% Sulfur-Removal Efficiencies

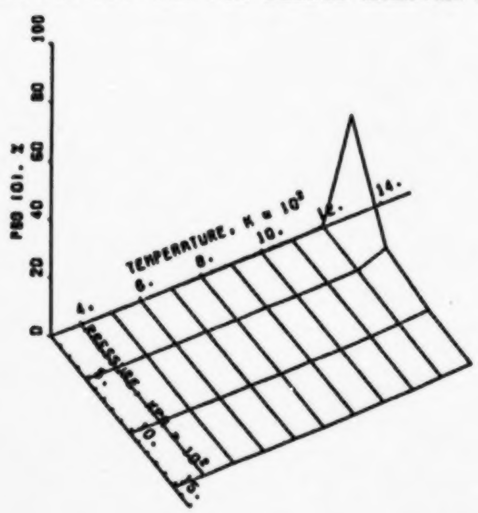

Figure 36 - Percent Distribution of Gaseous PbO as a Function of Temperature and Pressure in a Fluidized-Bed Combustor Operating with 100% Excess Air and 90% Sulfur-Removal Efficiencies

Cobalt

Solid cobalt sulfate ($CoSO_4$) and cobalt oxides (CoO and Co_3O_4) are formed in FBC systems operating at 10, 100, and 300 percent excess air. The major chemical reactions include

$$3CoSO_4(s) + 1/2\ O_2(g) \longrightarrow Co_3O_4(s) + 3SO_2(g) + 3/2\ O_2(g) \qquad (10)$$

$$CoSO_4(s) \longrightarrow CoO(s) + SO_2(g) + 1/2\ O_2(g) \qquad (11)$$

$$Co_3O_4(s) \longrightarrow 3CoO(s) + 1/2\ O_2(g)\ . \qquad (12)$$

The transition of $CoSO_4$ to CoO occurs in three successive decomposition reactions as the temperature of the system is increased. Cobalt sulfate releases SO_2 and O_2, forming Co_3O_4 at temperatures of 1000 to 1100 K for 10 percent excess air, 900 to 1100 K for 100 percent excess air, and 900 to 1000 K for 300 percent excess air for 0 percent S-removal conditions. In 90 percent S-removal systems the temperature at which $CoSO_4$ is stable is further reduced to between 900 and 1000 K for 10 percent and 100 percent excess air, and to between 800 to 900 K for 300 percent excess air. Initially, the decomposition product is Co_3O_4, followed by the formation of a mixture of Co_3O_4 and CoO, and finally complete conversion to CoO as the temperature of the system is increased. The oxide transition as a function of temperature and pressure is illustrated three-dimensionally in Figures 37 to 39 for combustion with 100 percent excess air and 90 percent S-removal capabilities.

The major gaseous phase formed in equilibrium with the $CoSO_4$/Co_3O_4/CoO solids is cobalt dichloride ($CoCl_2$), exerting a partial pressure of 10^{-4} kPa (10^{-6} atm) at FBC bed temperatures (Figure 40). Depending on the operating system temperature, the following reactions occur:

$$CoSO_4(s) + 2HCl(g) \longrightarrow CoCl_2(g) + H_2SO_4(g) \qquad (13)$$

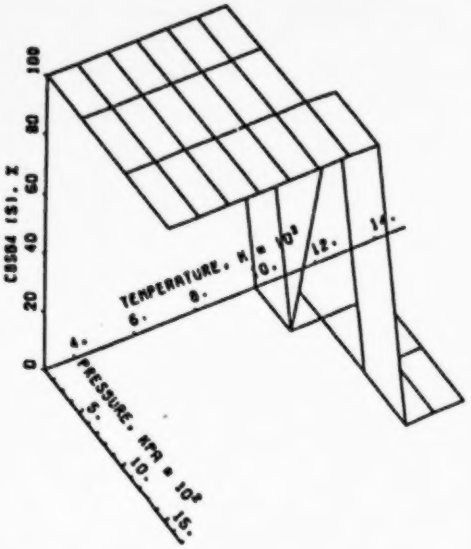

Figure 37 - Percent Distribution of Solid $CoSO_4$ as a Function of Temperature and Pressure in a Fluidized-Bed Combustor Operating with 100% Excess Air and 90% Sulfur-Removal Efficiencies

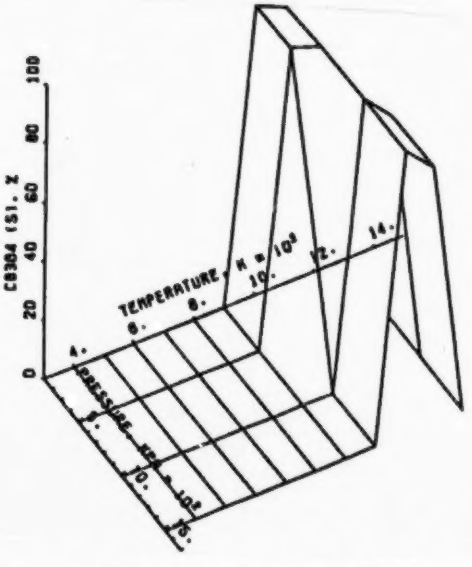

Figure 38 - Percent Distribution of Solid Co_3O_4 as a Function of Temperature and Pressure in a Fluidized-Bed Combustor Operating with 100% Excess Air and 90% Sulfur-Removal Efficiencies

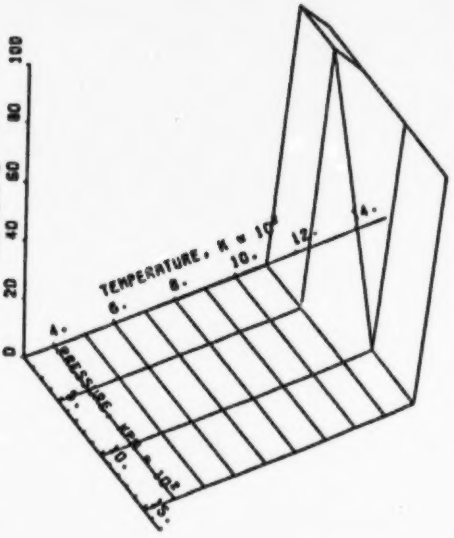

Figure 39 - Percent Distribution of Solid CoO as a Function of Temperature and Pressure in a Fluidized-Bed Combustor Operating with 100% Excess Air and 90% Sulfur-Removal Efficiencies

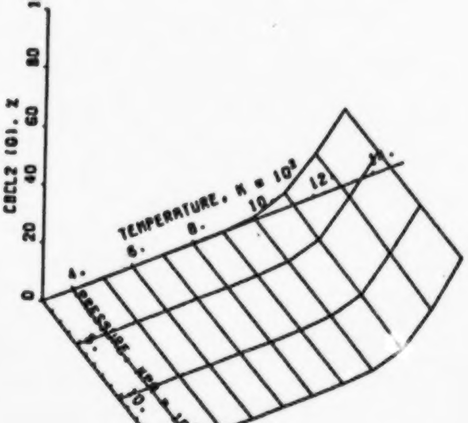

Figure 40 - Percent Distribution of Gaseous $CoCl_2$ as a Function of Temperature and Pressure in a Fluidized-Bed Combustor Operating with 100% Excess Air and 90% Sulfur-Removal Efficiencies

$$Co_3O_4(s) + 6HCl(g) \longrightarrow 3CoCl_2(g) + 3H_2O(g) + 1/2\ O_2(g) \quad (14)$$

$$CoO(s) + Cl_2(g) \longrightarrow CoCl_2(g) + 1/2\ O_2(g)\ . \quad (15)$$

Further reaction of $CoCl_2$ with chlorine yields cobalt trichloride ($CoCl_3$):

$$2CoCl_2(g) + Cl_2(g) \longrightarrow 2CoCl_3(g)\ . \quad (16)$$

Trace quantities of the cobalt dichloride dimer (Co_2Cl_4) are formed at high combustion temperatures, in addition to cobalt monochloride (CoCl).

Data for cobalt hydroxides, oxychlorides, and oxide compounds are not contained in the present data file. Consideration should be given to the possible formation of these compounds when thermodynamic data become available.

The mechanisms of nucleation or condensation of gaseous Co phases may occur in the effluent stream. Solid emissions from the bed, however, are projected to contain Co as either $CoSO_4$, Co_3O_4, or CoO, depending on the combustor operating temperature and pressure.

Chromium

In the oxidizing combustor environment, Cr contained in the feedstock is projected to form solid chromium dioxide (CrO_2) at temperatures of 300 K (Figure 41). Reaction of the feedstock Cr with combustion gases at 400 to 1300 K and ambient pressure leads to the formation of chromium oxide (Cr_2O_3) (Figure 42). Pressurized operations enhance volatilization of Cr_2O_3 between 400 and 800 K through the reaction of gaseous HCl, forming the volatile chromium oxychloride phase (CrO_2Cl_2) (reaction 17 and Figure 43):

$$Cr_2O_3(s) + 4HCl(g) + 3/2\ O_2(g) \longrightarrow 2CrO_2Cl_2(g) + 2H_2O(g)\ . \quad (17)$$

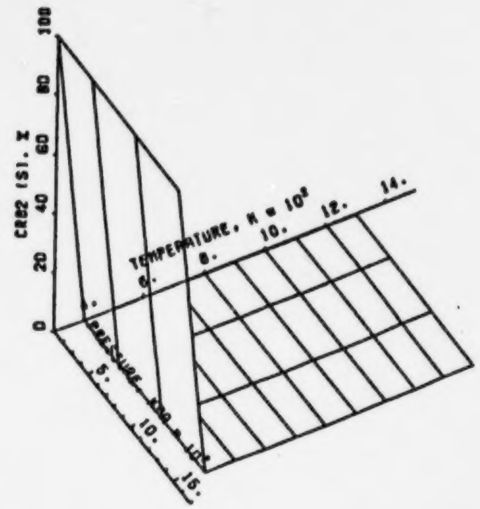

Figure 41 - Percent Distribution of Solid CrO_2 as a Function of Temperature and Pressure in a Fluidized-Bed Combustor Operating with 100% Excess Air and 90% Sulfur-Removal Efficiencies

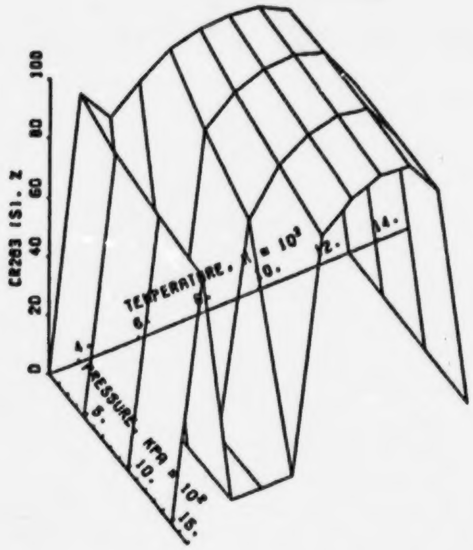

Figure 42 - Percent Distribution of Solid Cr_2O_3 as a Function of Temperature and Pressure in a Fluidized-Bed Combustor Operating with 100% Excess Air and 90% Sulfur-Removal Efficiencies

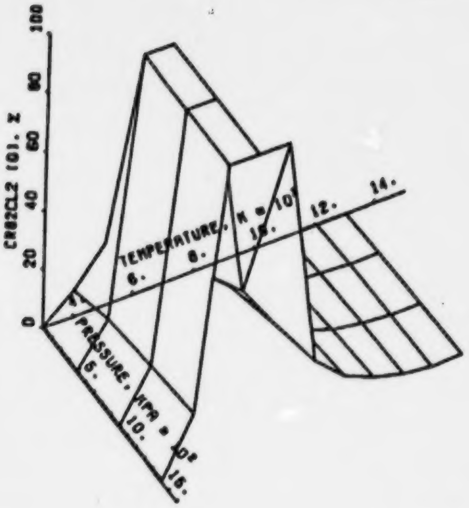

Figure 43 - Percent Distribution of Gaseous CrO_2Cl_2 as a Function of Temperature and Pressure in a Fluidized-Bed Combustor Operating with 100% Excess Air and 90% Sulfur-Removal Efficiencies

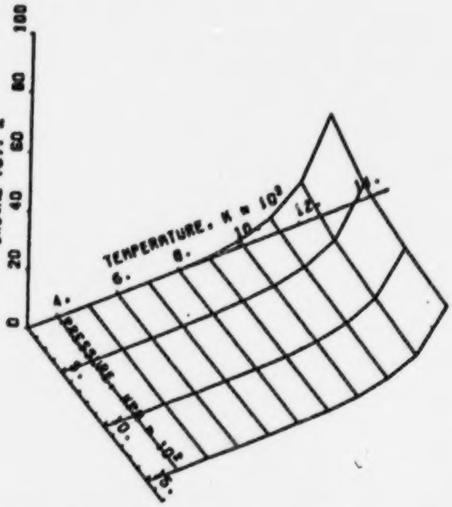

Figure 44 - Percent Distribution of Gaseous CrO_4H_2 as a Function of Temperature and Pressure in a Fluidized-Bed Combustor Operating with 100% Excess Air and 90% Sulfur-Removal Efficiencies

At FBC operating temperatures higher than 800 K, the solid Cr_2O_3 phase is once again projected to form as the major Cr complex in equilibrium with volatile dihydroxy-dioxy-chromium VI (CrO_4H_2), hydroxy-dioxy-chromium V (CrO_2OH), and chromium trioxide (CrO_3) (Figures 44-46). In addition to these major Cr volatiles, which exert maximum partial pressures of approximately 10^{-4} kPa, trace levels of volatile chromium oxides and chlorides as CrO_2, CrO, $CrCl_3$, $CrCl_2$, and $CrCl_4$ are projected to form at partial pressures less than 10^{-6} kPa in a 1200 K fluidized-bed combustor.

In the presence of S, conversion to the solid sulfate by the reaction

$$Cr_2O_3(s) + 3SO_2(g) + 3/2\ O_2(g) \longrightarrow Cr_2(SO_4)_3(s) \qquad (18)$$

is not projected for conditions existing in the fluidized bed. Ash formed from combustion within the bed and fines released into the effluent streams are projected to contain Cr as solid Cr_2O_3, in addition to the emissions of volatile oxy-hydroxy, oxychloride, and oxide species.

Iron

The principal reaction of Fe in FBC systems is the formation of hematite (Fe_2O_3) and diiron trisulfate ($Fe_2(SO_4)_3$). The relative concentration and stability of each compound is dependent on the concentration of S and the operating temperature and pressure of the system, as shown in Table 28. Hematite is the stable solid Fe complex in fluidized-bed systems operating at temperatures of 1088 to 1173 K; transition into magnetite (Fe_3O_4) would result when combustion temperature exceeds 1735 K (reaction 19):

$$6Fe_2O_3(s) \longrightarrow 4Fe_3O_4(s) + O_2(g)\ . \qquad (19)$$

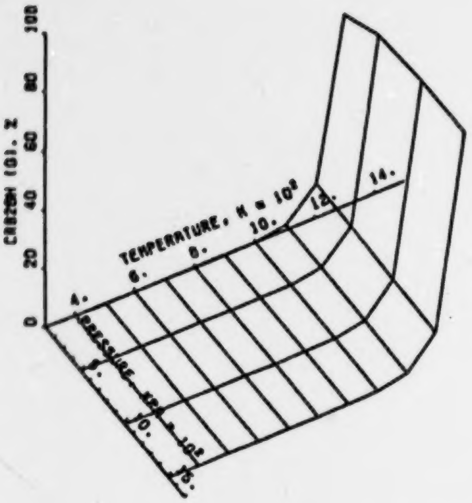

Figure 45 - Percent Distribution of Gaseous CrO_2OH as a Function of Temperature and Pressure in a Fluidized-Bed Combustor Operating with 100% Excess Air and 90% Sulfur-Removal Efficiencies

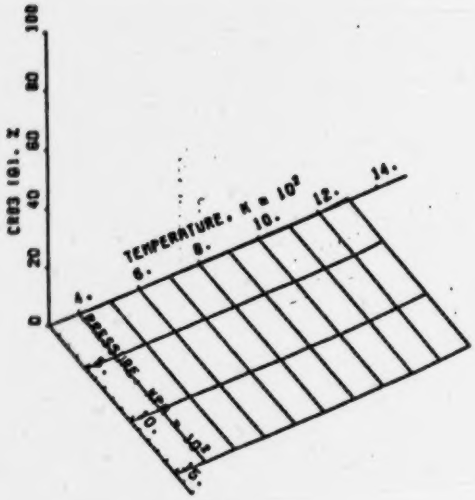

Figure 46 - Percent Distribution of Gaseous CrO_3 as a Function of Temperature and Pressure in a Fluidized-Bed Combustor Operating with 100% Excess Air and 90% Sulfur-Removal Efficiencies

The reaction of Fe with S released from the combustion of coal produces $Fe_2(SO_4)_3$ at low temperatures in the fluidized bed:

$$Fe_2O_3(s) + 3SO_2(g) + 3/2\ O_2(g) \longrightarrow Fe_2(SO_4)_3(s) \qquad (20)$$

or

$$Fe_2O_3(s) + 3H_2SO_4(g) \longrightarrow Fe_2(SO_4)_3(s) + 3H_2O(g) \quad . \qquad (21)$$

Solids Fe_2O_3 would be present, for example, in fluidized-bed combustion systems operating with 0 percent S removal and temperatures exceeding 900 K. Below 900 K, 100 percent of the feedstock iron content is projected to react with S, forming solid $Fe_2(SO_4)_3$. In the 90 percent S-removal systems considered in this study, Fe_2O_3 is the stable major phase formed at fluidizing temperatures and within cooler regimes,

TABLE 28 - SULFATE → OXIDE TRANSITION TEMPERATURE OF IRON IN FBC SYSTEMS

$$Fe_2(SO_4)_3\,(s) \longrightarrow Fe_2O_3\,(s) + 3SO_2\,(g) + 3/2O_2\,(g)$$

Sulfate → Oxide Transition Temperature

Combustion Conditions Pressure (kPa)	100% Excess Air 0% Sulfur Removal	100% Excess Air 90% Sulfur Removal	100% Excess Air 99% Sulfur Removal
101	790 - 820K	750 - 760K	670 - 680K
505	840 - 870K	790 - 800K	710 - 720K
1013	860 - 890K	810 - 820K	720 - 750K
1520	880 - 900K	820 - 830K	730 - 760K
2026	890 - 910K	830 - 840K	740 - 770K

Dwg. 1714822

with $Fe_2(SO_4)_3(s)$ present as a secondary phase that is stable within the temperature range from 300 K to between 800 and 900 K (Figures 47 and 48). Although FBC temperatures are well above 900 K, this lower temperature could be experienced by particles carried out of the bed into the cooler flue gas zones.

In a typical U.S. mean coal the major volatile compounds, iron dihydroxide ($Fe(OH)_2$), iron dichloride ($FeCl_2$), and iron trichloride ($FeCl_3$), form at pressures of 10^{-7} kPa (10^{-9} atm). These volatile phases can escape as stack-gas emissions, condense and deposit as Fe_2O_3 or $Fe_2(SO_4)_3$ on cooler metal surfaces, or nucleate along the surface of entrained flue gas ash particles. The possible series of reactions that could occur are illustrated below:

$$2Fe(OH)_2(g) + 1/2\ O_2(g) \longrightarrow Fe_2O_3(s) + 2H_2O(g) \qquad (22)$$

or

$$2Fe(OH)_2(g) + 2O_2(g) + 3SO_2(g) \longrightarrow Fe_2(SO_4)_3(s) + 2H_2O(g)$$

$$2FeCl_2(g) + 2H_2O(g) + 1/2\ O_2(g) \longrightarrow Fe_2O_3(s) + 4HCl(g) \qquad (23)$$

or

$$2FeCl_2(g) + 2H_2O(g) + 2O_2(g) + 3SO_2(g) \longrightarrow Fe_2(SO_4)_3(s) + 4HCl(g)$$

$$2FeCl_3(g) + 3H_2O(g) \longrightarrow Fe_2O_3(s) + 6HCl(g) \qquad (24)$$

or

$$2FeCl_3(g) + 3H_2O(g) + 3SO_2(g) + 3/2O_2(g) \longrightarrow Fe_2(SO_4)_3(s) + 6HCl(g)$$

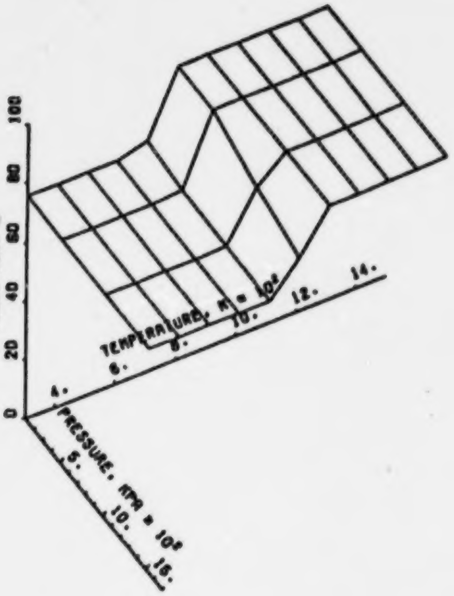

Figure 47 - Percent Distribution of Solid Fe_2O_3 as a Function of Temperature and Pressure in a Fluidized-Bed Combustor Operating with 100% Excess Air and 90% Sulfur-Removal Efficiencies

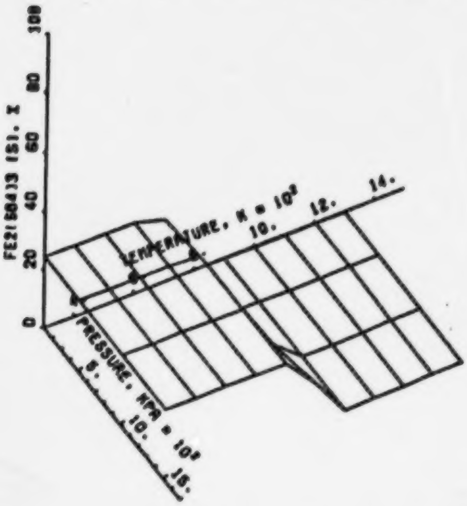

Figure 48 - Percent Distribution of Solid $Fe_2(SO_4)_3$ as a Function of Temperature and Pressure in a Fluidized-Bed Combustor Operating with 100% Excess Air and 90% Sulfur-Removal Efficiencies

Trace FeO, Fe_2Cl_4, FeCl, and $(Fe_2Cl_3)_2$, in addition to the major volatile compounds, are also projected to be thermodynamically stable. These trace phases do not exert partial pressures greater than 10^{-14} kPa (10^{-16} atm) at combustion temperatures of 1200 K.

Molybdenum

When considering the fate of Mo in the combustion of coal, it is reasonable to propose that stable oxides will be formed. From the thermodynamic calculations molybdenum trioxide (MoO_3) is projected to form as the stable solid equilibrium product between 273 and 600 K, as shown in Figure 49. Volatilization of the compound should begin when the system temperature exceeds 600 K and is enhanced in the presence of water vapor at high temperatures, according to the reaction:

$$MoO_3(s) + H_2O(g) \longrightarrow MoO_2(OH)_2(g) \quad . \qquad (25)$$

Fluidized-bed combustion gases containing chlorine enhance volatilization of solid MoO_3 through the formation of the dioxydichloride complex (MoO_2Cl_2), as shown in reactions 26 and 27:

$$MoO_3(s) + 2HCl(g) \longrightarrow MoO_2Cl_2(g) + H_2O(g) \qquad (26)$$

$$MoO_3(s) + Cl_2(g) \longrightarrow MoO_2Cl_2(g) + 1/2\ O_2(g) \quad . \qquad (27)$$

With the feedstock Mo concentration of 7.54 ppm assumed for this study, the partial pressures of molybdenum dioxydihydroxide ($MoO_2(OH)_2$) and MoO_2Cl_2 are thermodynamically projected to be as high as 10^{-13} and 10^{-16} kPa (10^{-15} and 10^{-18} atm), respectively, at the fluidized-bed temperature. The percent distribution of Mo between the dioxydihydroxy and dioxydichloride phases as a function of operating temperature and pressure in the 100 percent excess air, 90 percent S-removal, fluidized-bed combustor is shown in Figures 50 and 51.

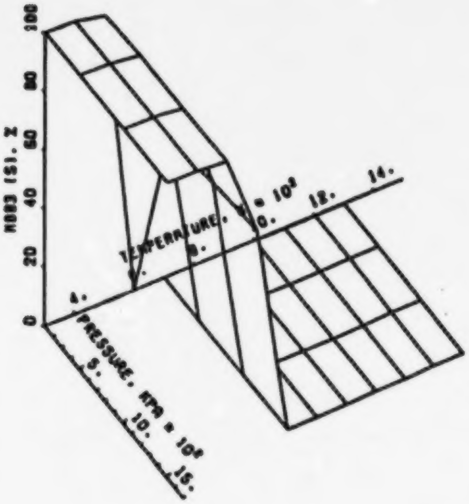

Figure 49 - Percent Distribution of Solid MoO_3 as a Function of Temperature and Pressure in a Fluidized-Bed Combustor Operating with 100% Excess Air and 90% Sulfur-Removal Efficiencies

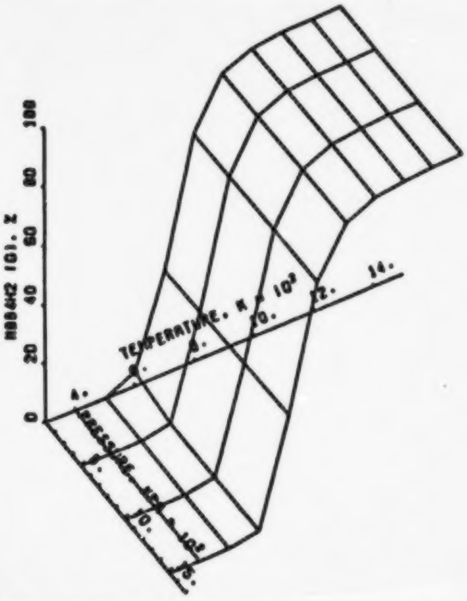

Figure 50 - Percent Distribution of Gaseous $MoO_2(OH)_2$ as a Function of Temperature and Pressure in a Fluidized-Bed Combustor Operating with 100% Excess Air and 90% Sulfur-Removal Efficiencies

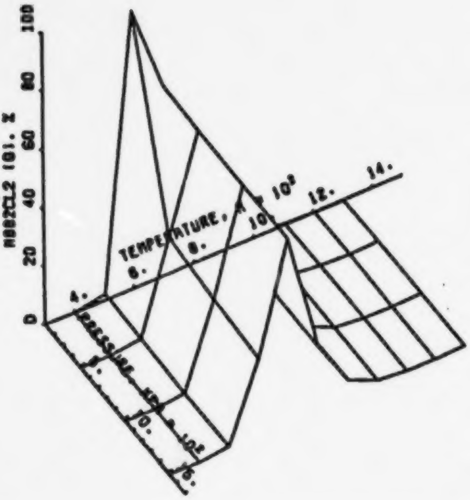

Figure 51 - Percent Distribution of Gaseous MoO_2Cl_2 as a Function of Temperature and Pressure in a Fluidized-Bed Combustor Operating with 100% Excess Air and 90% Sulfur-Removal Efficiencies

Gas phases projected to be formed as trace complexes include molybdenum trioxide (MoO_3,) molybdenum dioxide (MoO_2), molybdenum tetrachloride ($MoCl_4$), molybdenum pentachloride ($MoCl_5$), molybdenum monoxide (MoO), and molybdenum hexachloride ($MoCl_6$).

In conclusion, the parametric calculations projected complete volatilization of Mo contained in the feedstock material. The ultimate fate of gaseous Mo complexes would appear to be release in the stack gas emissions. Condensation of Mo along cooled metal surfaces or nucleation along entrained ash particles should be considered as potential mechanisms that would minimize the concentration of Mo in the stack gases. The current thermodynamic model has not taken into account potential removal sites in the process design.

Manganese

The thermochemical equilibrium reaction of Mn with FBC gases containing S and HCl leads to the formation of solid manganese sulfate ($MnSO_4$) and/or manganese oxides (Mn_2O_3 and Mn_3O_4). At temperatures below 900 K, $MnSO_4$ is the stable solid form in both 0 and 90 percent S-removal conditions. As the temperature is increased to 1100 K at 10 percent excess air, and 1200 K at 100 percent and 300 percent excess air, $MnSO_4(s)$ is converted to $Mn_2O_3(s)$ by the reaction

$$2MnSO_4(s) + 1/2\ O_2(g) \longrightarrow Mn_2O_3(s) + 2SO_2(g) + O_2(g) \quad . \qquad (28)$$

At temperatures greater than 1200 K, $Mn_2O_3(s)$ releases oxygen, forming solid Mn_3O_4:

$$3Mn_2O_3(s) \longrightarrow 2Mn_3O_4(s) + 1/2\ O_2(g) \quad . \qquad (29)$$

Figures 52-54 illustrate the sulfate ⟶ oxide transition for solid Mn complexes as a function of temperature and pressure in the 100 percent excess air, 90 percent S-removal fluidized-bed combustor.

The principal gaseous Mn compound projected to be formed in equilibrium with the Mn sulfate or oxide solid is manganese dichloride ($MnCl_2$) (Figure 55). At 1200 K operational temperatures the partial pressure exerted by the innocuous volatile $MnCl_2$ complex is approximately 10^{-4} kPa (10^{-6} atm). Additional gaseous phases of manganese chloride (MnCl), manganese oxide (MnO), and Mn are present at trace levels (10^{-12} kPa [$<10^{-14}$ atm]). Data for manganese hydroxides, oxides, and oxychlorides are not considered in the present data file and, hence, are not included in the current study.

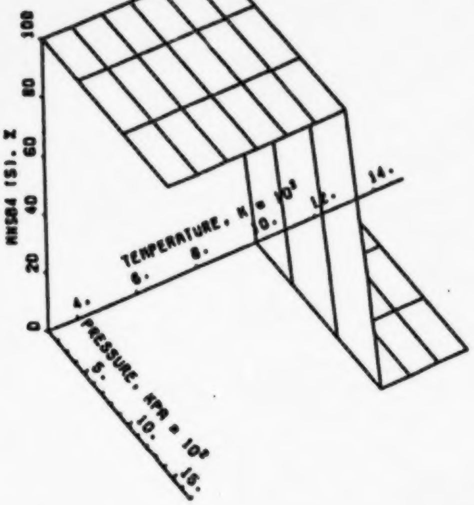

Figure 52 - Percent Distribution of Solid $MnSO_4$ as a Function of Temperature and Pressure in a Fluidized-Bed Combustor Operating with 100% Excess Air and 90% Sulfur-Removal Efficiencies

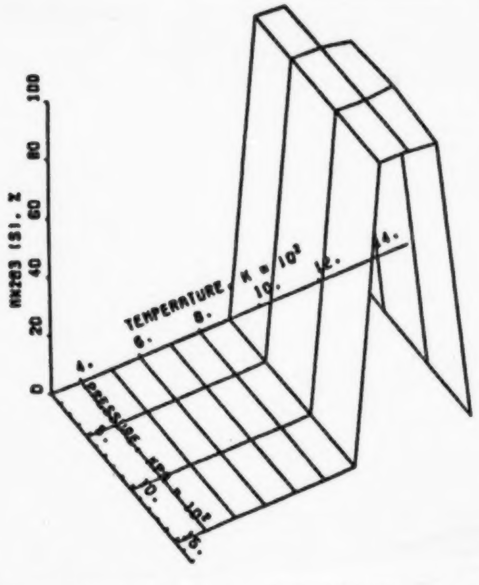

Figure 53 - Percent Distribution of Solid Mn_2O_3 as a Function of Temperature and Pressure in a Fluidized-Bed Combustor Operating with 100% Excess Air and 90% Sulfur-Removal Efficiencies

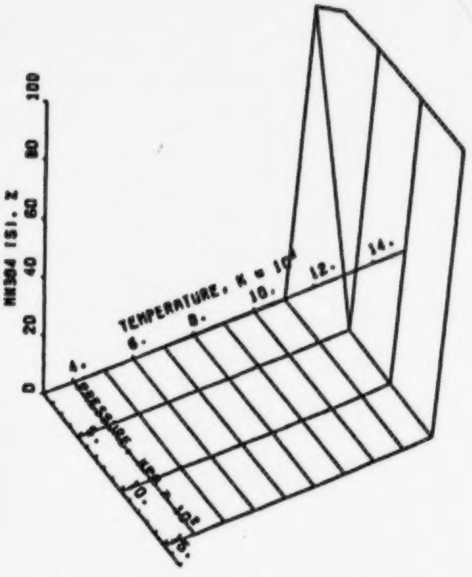

Figure 54 - Percent Distribution of Solid Mn_3O_4 as a Function of Temperature and Pressure in a Fluidized-Bed Combustor Operating with 100% Excess Air and 90% Sulfur-Removal Efficiencies

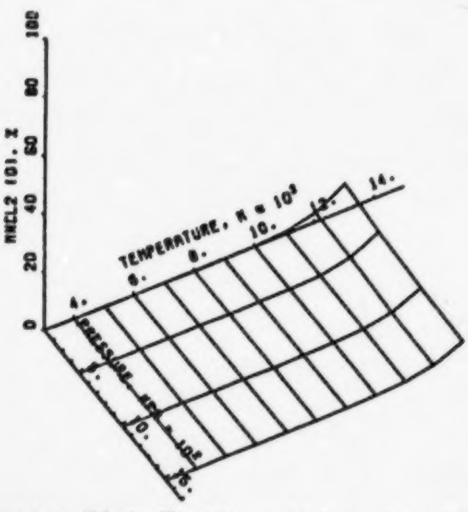

Figure 55 - Percent Distribution of Gaseous $MnCl_2$ as a Function of Temperature and Pressure in a Fluidized-Bed Combustor Operating with 100% Excess Air and 90% Sulfur-Removal Efficiencies

Nickel

The formation of stable nickel oxides and sulfate solids in the fluidized bed is dependent on the system parameters of temperature, pressure, excess air, and sulfur content. The major chemical equilibrium reactions of Ni in the fluidized bed include

$$NiO(s) \xrightarrow{t > 1100\ K} NiO(g) \tag{30}$$

$$NiSO_4(s) \xrightarrow{t = 800\ to\ 1000K} NiO(s) + SO_2(g) + 1/2\ O_2(g) \tag{31}$$

$$NiSO_4(s) + 2HCl(g) \longrightarrow NiCl_2(g) + H_2SO_4(g) \tag{32}$$

$$NiO(s) + 2HCl(g) \longrightarrow NiCl_2(g) + H_2O(g) \tag{33}$$

$$NiSO_4(s) + H_2O(g) \longrightarrow Ni(OH)_2(g) + SO_2(g) + 1/2\ O_2(g) \tag{34}$$

$$NiO(s) + H_2O(g) \longrightarrow Ni(OH)_2(g)\quad . \tag{35}$$

With 0 percent S-removal, nickel sulfate ($NiSO_4(s)$) is projected to be present at temperatures between 1000 and 1100 K for pressures of 506.5, 1013.6, and 1520.4 kPa (5, 10, and 15 atm), prior to the conversion of the solid complex into nickel oxide (NiO) (reaction 31). The temperature of the sulfate/oxide conversion, however, is between 900 and 1000 K for atmospheric, 0 percent S-removal systems. Within the bed, therefore, the major chemical phase of Ni at equilibrium should be that of the oxide (Figures 56 and 57).

The major volatile Ni species projected to form over $NiSO_4(s)$ or NiO(s) is nickel dichloride ($NiCl_2$) (Figure 58). The partial pressures exerted by the chloride are approximately 10^{-4} kPa (10^{-6} atm) at the fluidized-bed temperature. Secondary gaseous phases projected to form include nickel hydroxide ($Ni(OH)_2$) (Figure 59), nickel chloride (NiCl) (Figure 60), NiO, Ni, and nickel hydride (NiH). These gaseous phases

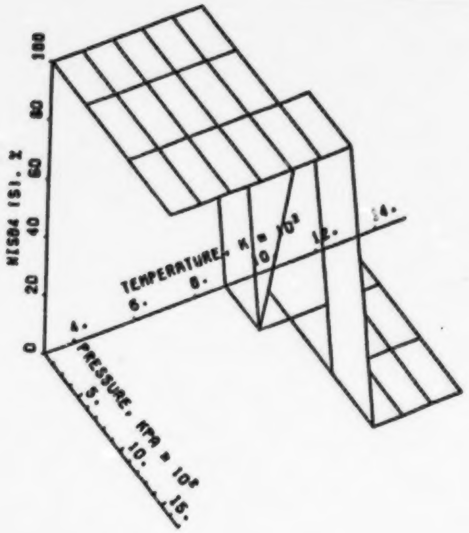

Figure 56 - Percent Distribution of Solid $NiSO_4$ as a Function of Temperature and Pressure in a Fluidized-Bed Combustor Operating with 100% Excess Air and 90% Sulfur-Removal Efficiencies

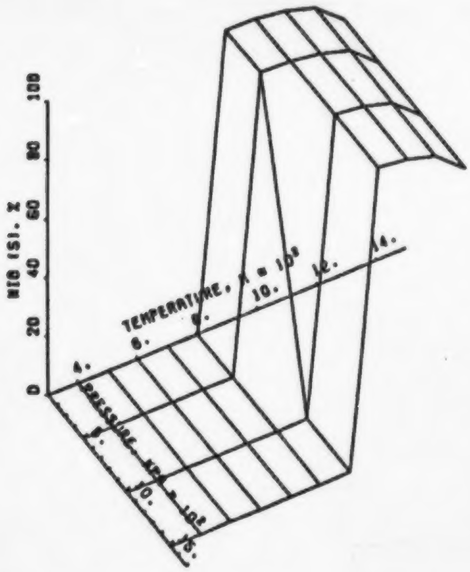

Figure 57 - Percent Distribution of Solid NiO as a Function of Temperature and Pressure in a Fluidized-Bed Combustor Operating with 100% Excess Air and 90% Sulfur-Removal Efficiencies

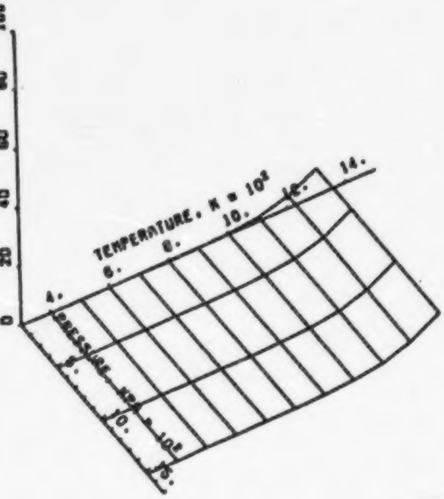

Figure 58 - Percent Distribution of Gaseous $NiCl_2$ as a Function of Temperature and Pressure in a Fluidized-Bed Combustor Operating with 100% Excess Air and 90% Sulfur-Removal Efficiencies

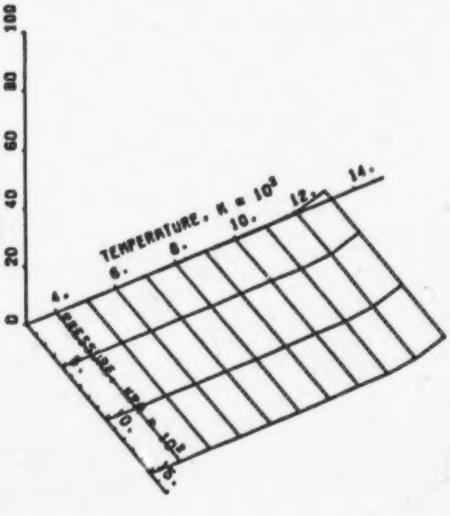

Figure 59 - Percent Distribution of Gaseous $Ni(OH)_2$ as a Function of Temperature and Pressure in a Fluidized-Bed Combustor Operating with 100% Excess Air and 90% Sulfur-Removal Efficiencies

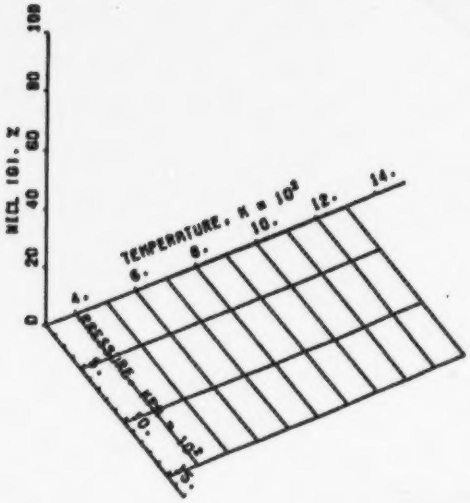

Figure 60 - Percent Distribution of Gaseous NiCl as a Function of Temperature and Pressure in a Fluidized-Bed Combustor Operating with 100% Excess Air and 90% Sulfur-Removal Efficiencies

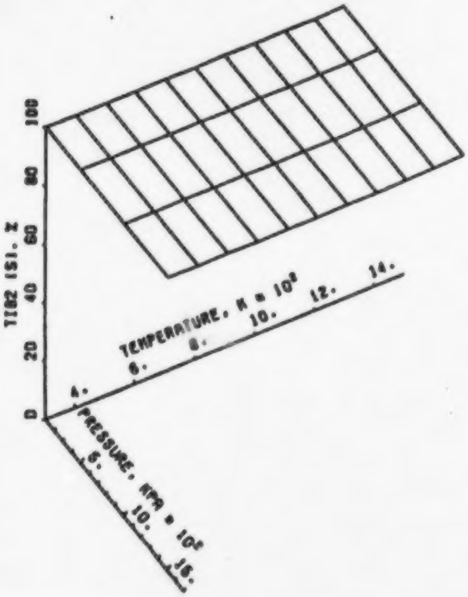

Figure 61 - Percent Distribution of Solid TiO_2 as a Function of Temperature and Pressure in a Fluidized-Bed Combustor Operating with 100% Excess Air and 90% Sulfur-Removal Efficiencies

are not considered potentially toxic, even if the concentration in the stack gases were to approach the level of 100 percent release of the feedstock nickel concentration during combustion. Nickel carbonyl ($Ni(CO)_4$) is considered the most toxic of all the nickel compounds[42] but is not projected to form in the effluent combustion streams.

Titanium

The projected equilibrium reaction of Ti in FBC systems is the formation of rutile (TiO_2) as a stable solid under the various temperature, pressure, excess oxygen, and S-removal conditions (Figure 61). The major gaseous Ti compounds projected to form in equilibrium with rutile as trace volatiles are titanium oxydichloride ($TiOCl_2$), titanium tetrachloride ($TiCl_4$), and titanium dioxide (TiO_2). The formation of these gaseous complexes results from the following equilibrium reactions:

$$TiO_2(s) + 2HCl(g) \xrightarrow{t > 1000\ K} TiOCl_2(g) + H_2O(g) \qquad (36)$$

$$TiCl_4(g) + 1/2\ O_2(g) \xrightarrow{t > 1000\ K} TiOCl_2(g) + 2Cl^-(g) \qquad (37)$$

$$TiO_2(s) + 4HCl(g) \xrightarrow{t < 1000\ K} TiCl_4(g) + 2H_2O(g) \qquad (38)$$

$$TiO_2(s) \longrightarrow TiO_2(g)\ . \qquad (39)$$

With variation in pressure at temperatures in excess of 1000 K and at 10 percent excess air, the partial pressure of $TiOCl_2$ is projected to be greater than $TiCl_4$ and TiO_2. In systems operating at 100 percent excess air and 1013.6 to 1520.4 kPa (10-15 atm), the partial pressures of the resulting gases should be similar to those of the 10 percent excess air system ($ppTiOCl_2 > ppTiCl_4 > ppTiO_2$). If the total system pressure were decreased to 101.3 kPa (1 atm), $TiOCl_2$ would be the major gaseous phase, with the partial pressure of TiO_2 exceeding the partial pressures of $TiCl_4$. Increasing the excess air content to 300 percent favors the formation of $TiOCl_2 > TiO_2 > TiCl_4$ at all system pressures. The partial pressures of none of the projected volatile species exceed 10^{-15} kPa (10^{-17} atm).

When the temperature of the fluidized-bed system is less than 1000 K, the predominant gaseous phase is thermodynamically projected to be $TiCl_4$. These reactions apply for both 0 and 90 percent S-removal systems. Variation in the S content should not appreciably affect the resulting partial pressure of each gas phase. The slight decrease in the partial pressure of each compound at 90 percent S removal, if monitored, would not be detectably different from that of the 0 percent S-removal system. Solid S-Ti compounds are not expected to form in the FBC system.

A similarity has been demonstrated in the degree of volatilization of titanium and iron oxide solids formed in the fluidized-bed combustor. The principal volatile phases likely to be formed include chloride complexes, exerting generally insignificant partial pressures over the stable solid oxides.

Sodium

The reaction of Na with FBC gases containing SO_x and chlorides leads to the formation of liquid melt deposits when the combustor or downstream passage temperatures exceed 1157 K. The preliminary equilibrium projections assume 100 percent release of the feedstock-contained Na for reaction with the combustion gases. It will become evident in the interactive calculations where Si and Al are present that alkali silicates and aluminosilicates are more thermodynamically stable than the simple solid sulfate/volatile chloride equilibrium.

In PFBC solid or liquid sodium sulfate (Na_2SO_4) is projected to form as the major Na complex. Reducing the system pressure enhances volatilization of Na as sodium chloride (NaCl), with the formation of sodium hydroxide (NaOH) and Na_2SO_4 as minor phases, and the hydroxide and chloride dimers ($Na_2O_2H_2$ and Na_2Cl_2) as trace species. Figure 62 shows the equilibrium pressures of NaCl(g) and NaOH(g) over Na_2SO_4(s) under combustion conditions. The critical level above which HCl(g) will cause release of Na as NaCl(g) from Na_2SO_4(s) faster than vaporization of the compound occurs is shown to be log p_{HCl} ~-5.4, or p_{HCl} = 4.05 x 10^{-4} kPa, which corresponds to an HCl(g) level of 400 ppb by volume. In the combustor the gaseous HCl level may be orders of magnitude higher unless efforts are taken either to use a low-chlorine coal, to remove the chlorine in a pretreatment step, or to cause chlorine and sodium to react and form more stable, nonvolatile complexes.

Once released as the volatile chloride from the combustor, reactions with water vapor and gaseous SO_x promote the formation of Na_2SO_4, as shown in reaction 40:

$$2NaCl(g) + H_2O(g) + SO_2(g) + 1/2\ O_2(g) \longrightarrow Na_2SO_4(s,l,g) + 2HCl(g) \quad . \qquad (40)$$

The nature of the sulfate complex is dependent upon the reaction temperature and pressure and the concentration of the volatile constituents that share in the reaction. Simultaneously, reactions of the volatile hydroxide phase with SO_x promote the formation of the sulfate complex (reaction 41):

$$2NaOH(g) + SO_2(g) + 1/2\ O_2(g) \longrightarrow Na_2SO_4(s,l,g) + H_2O(g) \quad . \qquad (41)$$

Deposition of the Na_2SO_4 phase, through either condensation directly from the combustion gases or nucleation along ash fines, promotes hot corrosive attack or catastrophic oxidation of underlying metal surfaces. The corrosive attack of the alloy may result from the introduction of sulfur into the alloy, or it may be due to an oxide ion activity gradient established in the deposit. It is generally agreed that the presence of Na_2SO_4 is a prerequisite for sulfidation attack. Thus, it is essential to avoid the formation of the liquid metal sulfate melt in order to minimize corrosion, either by selecting low-alkali and -S feedstock materials or pretreating (by either devolatilization or water/dilute acid washings) unacceptable materials. Similarly, minimization of the alkali and S complexes emitted from the combustor through the addition of getter and sorbent material reduces the potential for liquid melt deposition downstream in cooler regions in the combustion system, particularly in the turbine. Getter and sorbent materials selected for these processes must also contribute minimally to the alkali and S loading in the combustor. Alternatively, operating the combustor at temperatures below the liquid melt formation or cooling the product combustion gases minimizes the potential for the formation of the corrosive sulfate melt, but these procedures would reduce the overall plant operating efficiency. Similarly, maintaining the operational temperatures above the liquid phase temperatures throughout the entire system (Table 29), although minimizing hot corrosive attack of alloy surfaces by the sulfate, would require additional development of high-temperature materials.

Figures 63 and 64 illustrate the percent distribution of Na in the condensed sulfate and volatile chloride phases formed during the combustion of a U.S. mean coal in a 100 percent excess air and 90 percent S-removal system. The shaded and hatched regions of the three-dimensional plot illustrate operational temperatures and pressures where the liquid sulfate melt is projected to form. In order to illustrate the complex chemistry involved in the Na reactions with combustion gases, simple phase diagrams were generated that depicted the relation of Na, Cl, and SO_x in the formation of the liquid sulfate melt at 1157 K for both 404 and 1114 kPa operations (Figures 65 and 66). Deposition of the liquid is projected to the right of each SO_x tolerance concentration, while conditions representative of Na and Cl levels to the left of

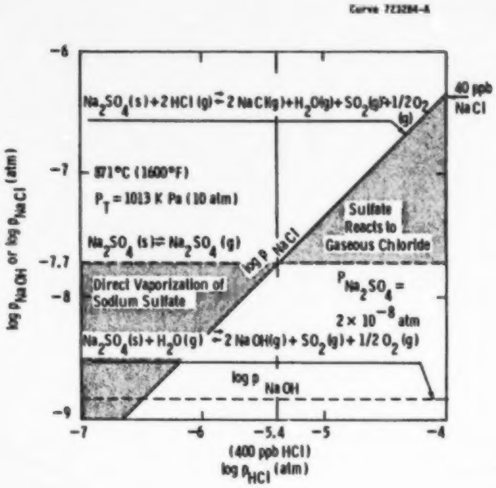

Figure 62 - Equilibrium Pressures of NaOH(g) and NaCl(g) over $Na_2SO_4(s)$ Exposed to Steam and HCl(g) under Fluidized-Bed Combustor Gas Phase Conditions

TABLE 29 - SODIUM SULFATE LIQUID ⟶ GAS TRANSITION TEMPERATURE AS A FUNCTION OF FBC CONDITIONS

Dwg. 1714B23

$$Na_2SO_4\,(I,s) \xrightarrow{980K} Na_2SO_4\,(\delta,s)$$

$$Na_2SO_4\,(\delta,s) \xrightarrow{1157K} Na_2SO_4\,(l)$$

Na_2SO_4 Liquid ⟶ Gas Transition Temperature

Combustion Conditions / Pressure (kPa)	100% Excess Air 0% Sulfur Removal	100% Excess Air 90% Sulfur Removal	100% Excess Air 99% Sulfur Removal
101	1300 - 1310K	1250 - 1260K	1200 - 1210K
505	1400 - 1410K	1340 - 1350K	1290 - 1300K
1013	1450 - 1460K	1390 - 1400K	1330 - 1340K
1520	1480 - 1490K	1420 - 1430K	1360 - 1370K
2026	1500 - 1510K	1440 - 1450K	1370 - 1380K

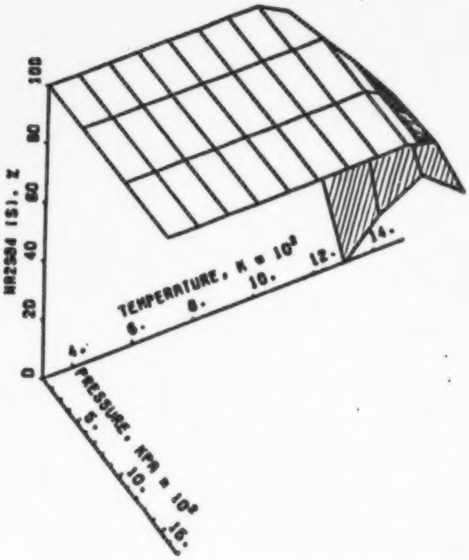

Figure 63 - Percent Distribution of Condensed Na_2SO_4 as a Function of Temperature and Pressure in a Fluidized-Bed Combustor Operating with 100% Excess Air and 90% Sulfur-Removal Efficiencies

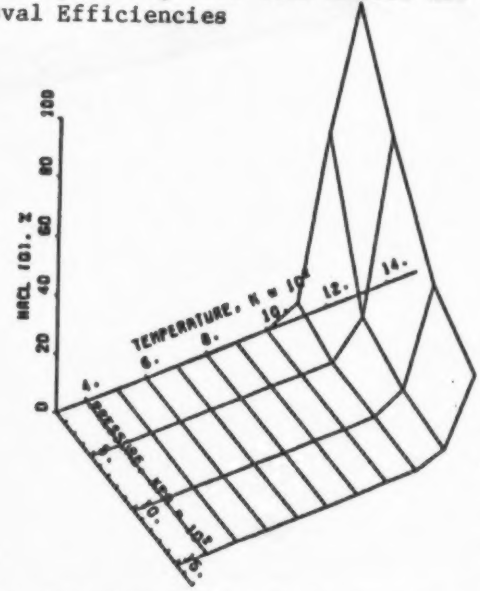

Figure 64 - Percent Distribution of Gaseous NaCl as a Function of Temperature and Pressure in a Fluidized-Bed Combustor Operating with 100% Excess Air and 90% Sulfur-Removal Efficiencies

Curve 723283-A

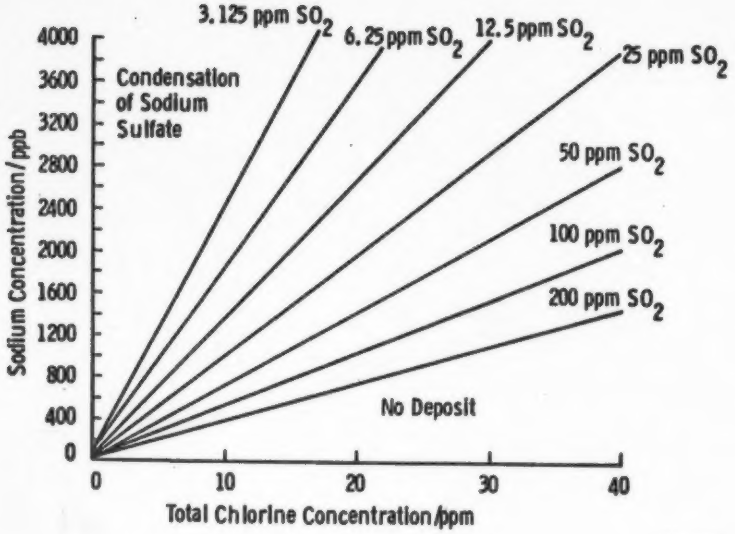

Figure 65 - Stability of Na_2SO_4 in a Fluidized-Bed Combustor Operating with 316% Excess Air at 1157 K and 404 kPa[23]

Curve 723285-A

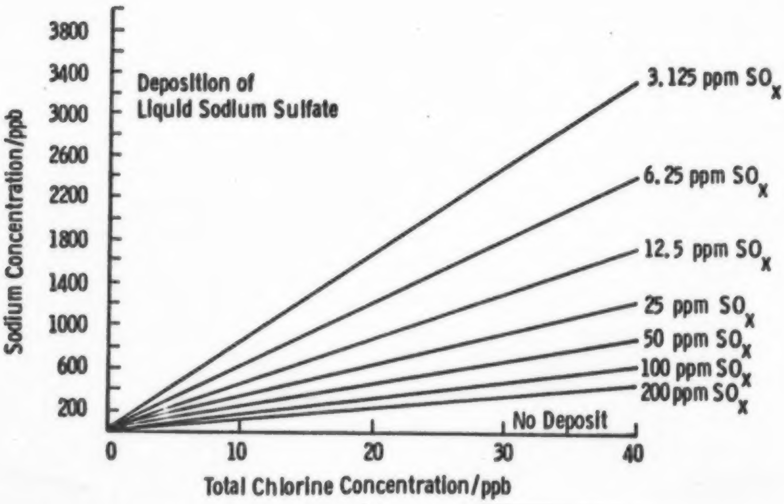

Figure 66 - Stability of Na_2SO_4 in a Fluidized-Bed Combustor Operating with 316% Excess air at 1157 K and 1114 kPa[23]

the sulfate tolerance project solid deposition. The boundary conditions for "no deposit" are a strong function of the total Cl concentration and SO_x concentration for the particular Na content in the feedstock. Conditions that avoid the liquid Na_2SO_4 melt formation at 101 or 404 kPa pressures can lead to melt formations in 1114 kPa operations. For example, 25 ppm Cl, 200 ppm SO_x, and 800 ppb Na is a safe combination for avoiding liquid deposition at 404 kPa, while 300 ppb Na leads to liquid deposition at 1114 kPa.

Potassium

Similarly to the reactions of Na with combustion gases, K forms a stable solid sulfate complex (K_2SO_4), in the PFBC (Figure 67), while ambient operations enhance the production of the volatile chloride (KCl), sulfate (K_2SO_4), and hydroxide (KOH) phases (Figures 68-70). Deposition of the corrosive sulfate liquid is not expected in the current FBC design, since operational temperatures do not exceed the melt temperature of 1334 K for the sulfate complex (Table 30).

Potassium competes with the Na present in the combustion gases for gaseous HCl. In this context volatilization of K lowers the Na release when KCl forms. In addition, K_2SO_4 is significantly more volatile than Na_2SO_4. If both Na_2SO_4 and K_2SO_4 form as a solid solution within the fluidized-bed, however, release of the alkalis is expected to be less than the calculated projection based on no condensed phase interaction. For no condensed phase interaction, the K concentration in the gas phase ranges from 1 to 15 ppm. The concentration decreases with pressure and increases with lower SO_x levels and with higher temperatures. Because the formation of KCl(g) removes HCl(g) from the combustion gas, the release of K, therefore, lowers the NaCl concentration in the effluent.

Formation of the mixed alkali sulfate eutectic either within the FBC or through the reaction of volatile alkali chlorides with SO_x,

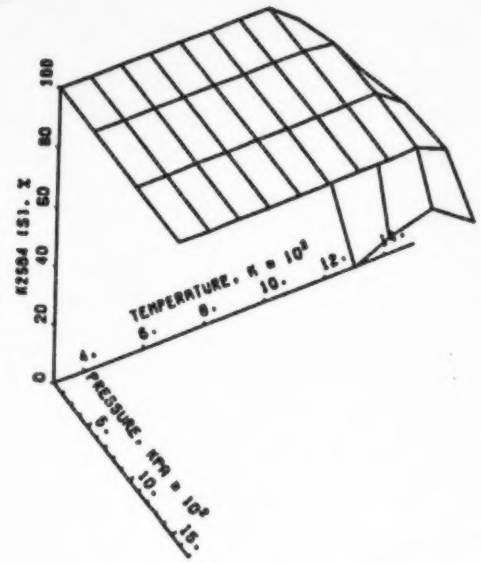

Figure 67 - Percent Distribution of Solid K_2SO_4 as a Function of Temperature and Pressure in a Fluidized-Bed Combustor Operating with 100% Excess Air and 90% Sulfur-Removal Efficiencies

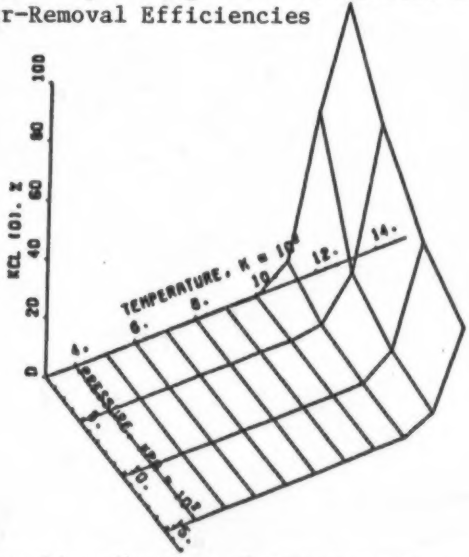

Figure 68 - Percent Distribution of Gaseous KCl as a Function of Temperature and Pressure in a Fluidized-Bed Combustor Operating with 100% Excess Air and 90% Sulfur-Removal Efficiencies

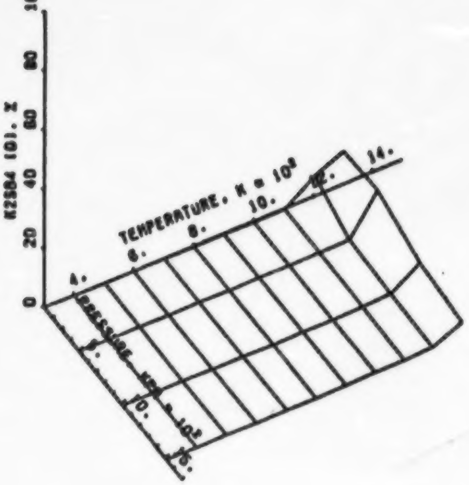

Figure 69 - Percent Distribution of Gaseous K_2SO_4 as a Function of Temperature and Pressure in a Fluidized-Bed Combustor Operating with 100% Excess Air and 90% Sulfur-Removal Efficiencies

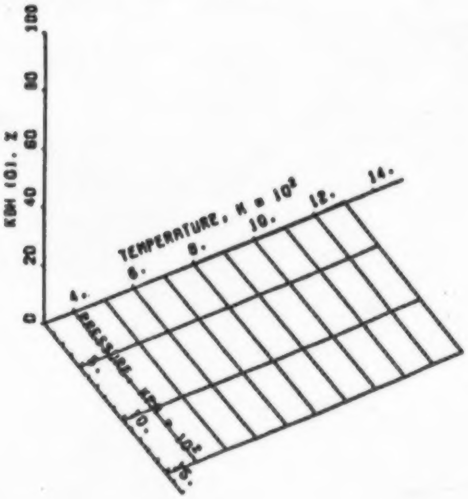

Figure 70 - Percent Distribution of Gaseous KOH as a Function of Temperature and Pressure in a Fluidized-Bed Combustor Operating with 100% Excess Air and 90% Sulfur-Removal Efficiencies

followed by condensation and deposition, is critically dependent on the concentration of alkali. Figure 71 illustrates the eutectic stability (T_m $Na_2SO_4 \cdot K_2SO_4$ = 1110 K) as a function of Na, Cl, and SO_x concentrations for combustion in 316 percent excess air at 404 kPa. Comparison of Figures 65 and 71 shows that in combustion systems containing 25 ppm Cl and 1000 ppb Na, a SO_x tolerance of less than 200 ppm minimizes the sulfate melt formation, while less than 3 ppm SO_x are required under similar conditions to minimize the formation of the mixed sulfate eutectic.

Aluminum

The major chemical reaction of Al in FBC systems at equilibrium is the formation of aluminum oxide ($Al_2O_3(s)$). Temperatures within the various fluidized-bed coal combustion processes do not exceed the oxide melt temperature of 2327 K. Aluminum oxide, therefore, is expected to be stable as a solid, principally within the temperature range of 273 to 1200 K for S-free processes. With 90 percent S removal in systems utilizing a 3.27-4.00 percent S coal (Figures 72 and 73), the resultant SO_x concentration in the effluent gas is sufficient at equilibrium to convert 80 percent of the $Al_2O_3(s)$ to aluminum sulfate ($Al_2(SO_4)_3(s)$), if operational temperatures are below 800 K as shown in reaction 42:

$$Al_2O_3(s) + 3SO_2(g) + 3/2\ O_2(g) \longrightarrow Al_2(SO_4)_3(s)\ . \qquad (42)$$

For 0 percent S-removal systems, where the maximum S content has been released into the combustion stream, Al_2O_3 is no longer projected to be present as a stable solid phase below 900 K, because of the total conversion of alumina into the solid sulfate phase. The temperature of the oxide $\longrightarrow$ sulfate transition is a function of the total pressure of the system and S content.

Hydrated forms of alumina projected to be thermodynamically stable at temperatures between 300 and 400 K include $Al_2O_3 \cdot H_2O$ and $Al(OH)_3$

TABLE 30 - POTASSIUM SULFATE CONDENSED PHASE ⟶ GAS TRANSITION TEMPERATURE AS A FUNCTION OF FBC CONDITIONS

$$K_2SO_4\ (s) \xrightarrow{1342K} K_2SO_4\ (l)$$

K_2SO_4 Condensed → Gas Transition Temperature

Combustion Conditions / Pressure (kPa)	100% Excess Air 0% Sulfur Removal	100% Excess Air 90% Sulfur Removal	100% Excess Air 99% Sulfur Removal
101	1250 - 1260K	1160 - 1170K	1180 - 1190K
505	1340 - 1350K	1260 - 1270K	1260 - 1270K
1013	1380 - 1390K	1310 - 1320K	1310 - 1320K
1520	1410 - 1420K	1340 - 1350K	1330 - 1340K
2026	1430 - 1440K	1360 - 1370K	1350 - 1360K

Dwg. 1714824

Curve 723286-A

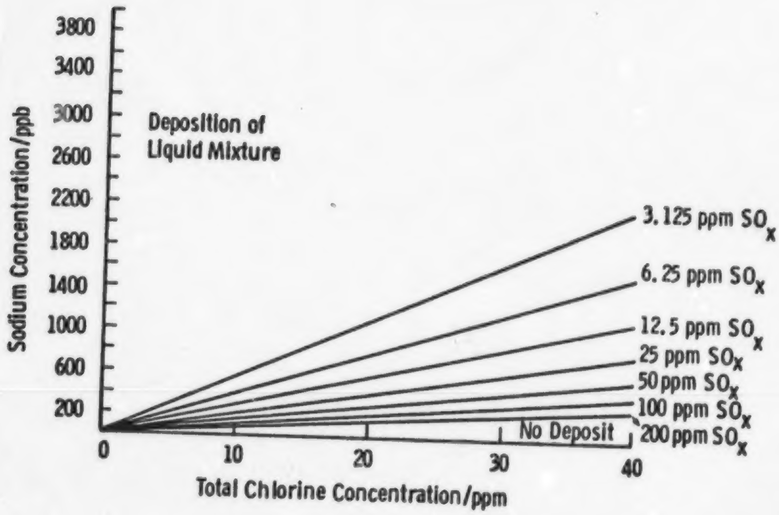

Figure 71 - Stability of $Na_2SO_4 \cdot K_2SO_4$ Eutectic in a Fluidized-Bed Combustor Operating with 316% Excess Air at 1110 K and 404 kPa[23]

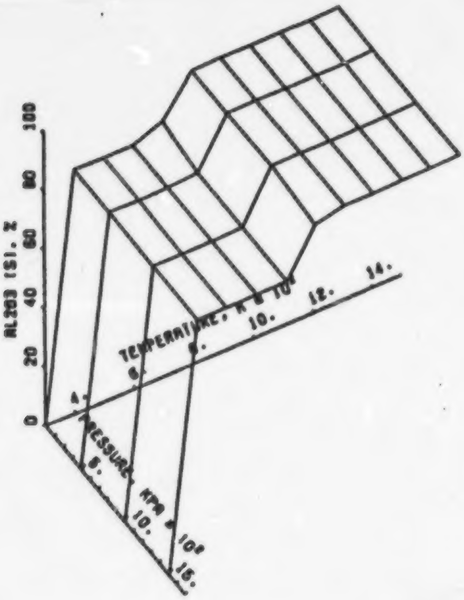

Figure 72 - Percent Distribution of Solid Al_2O_3 as a Function of Temperature and Pressure in a Fluidized-Bed Combustor Operating with 100% Excess Air and 90% Sulfur-Removal Efficiencies

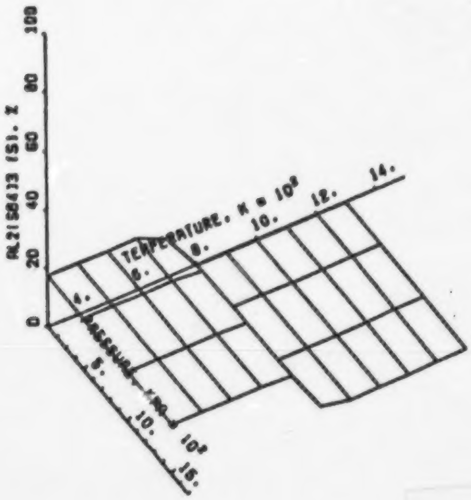

Figure 73 - Percent Distribution of Solid $Al_2(SO_4)_3$ as a Function of Temperature and Pressure in a Fluidized-Bed Combustor Operating with 100% Excess Air and 90% Sulfur-Removal Efficiencies

(Figures 74 and 75). If equilibrium were attained, the $Al_2(SO_4)_3$ particle would release SO_2 and O_2 and react with gaseous water vapor to form the hydrated alumina complex, as shown in reactions 43 and 44:

$$Al_2(SO_4)_3(s) + H_2O(g) \xrightarrow{101\ kPa} Al_2O_3 \cdot H_2O(s) + 3SO_2(g) + 3/2\ O_2(g) \tag{43}$$

$$Al_2(SO_4)_3(s) + 3H_2O(g) \xrightarrow{>101\ kPa} 2Al(OH)_3(s) + 3SO_2(g) + 3/2\ O_2(g)\ . \tag{44}$$

No major volatile compounds are projected to form over the Al_2O_3 (major phase)/$Al_2(SO_4)_3$ (potential minor phase) solids at fluidized-bed operating temperatures. Insignificant traces of gaseous aluminum trichloride ($AlCl_3$), aluminum oxychloride (AlOCl), aluminum dichloride ($AlCl_2$), aluminum dioxide (AlO_2), aluminum monoxyhydride (AlOH), aluminum monochloride (AlCl), aluminum monoxide (AlO), and aluminum trichloride dimer (Al_2Cl_6) are thermodynamically projected to exist in equilibrium with the solids at partial pressures of 10^{-12} kPa and below. The reaction of hydrogen chloride (HCl) with Al_2O_3 influences the formation of the volatile aluminum phases, as shown in reactions 45 and 46:

$$Al_2O_3(s) + 6HCl(g) \longrightarrow 2AlCl_3(g) + 3H_2O(g) \tag{45}$$

$$Al_2O_3(s) + 2HCl(g) \longrightarrow 2AlOCl(g) + H_2O(g)\ . \tag{46}$$

In summary, the parametric calculations demonstrate that, at fluidization temperatures, aluminum released from the combustion of coal will primarily exist as the solid oxide. An alternate phase, the most probable of which is the sulfate, has the potential to form through the reaction of aluminum with gaseous SO_x, if equilibrium is attained

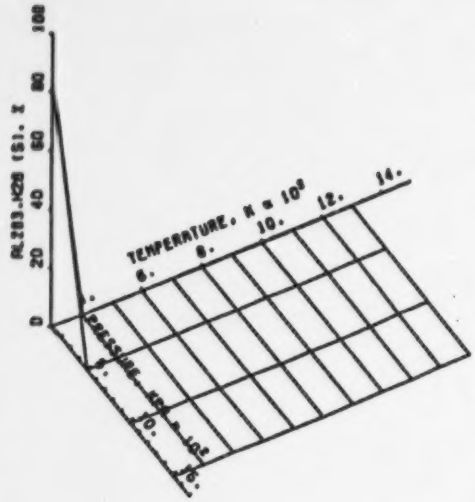

Figure 74 - Percent Distribution of Solid $Al_2O_3 \cdot H_2O$ as a Function of Temperature and Pressure in a Fluidized-Bed Combustor Operating with 100% Excess Air and 90% Sulfur-Removal Efficiencies

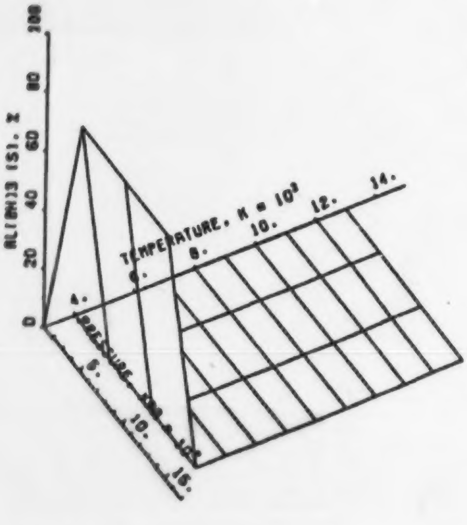

Figure 75 - Percent Distribution of Solid $Al(OH)_3$ as a Function of Temperature and Pressure in a Fluidized-Bed Combustor Operating with 100% Excess Air and 90% Sulfur-Removal Efficiencies

locally within the bed where fluidization temperatures have decreased to below 800 K. The major chemical composition of the fines carried over in the oxidizing gas streams from the bed into the cyclone are, therefore, projected to be an oxide phase. Conversion of the fines and subsequent stack-gas emission of the oxide to the sulfate is not expected.

Silicon

At equilibrium in FBC systems, quartz (SiO_2) forms between temperatures of 300 and 1000 K. The trigonal or hexagonal quartz lattice is converted into the cubic cristobalite (SiO_2) lattice at combustion temperatures that exceed 1000 K (shaded area of Figure 76). The major volatile phases formed in equilibrium with solid quartz and cristobalite at partial pressures less than 10^{-13} kPa are gaseous silicon dioxide (SiO_2) and silicon tetrachloride ($SiCl_4$), as shown in the following reactions:

$$SiO_2(c) \longrightarrow SiO_2(g) \tag{47}$$

$$SiO_2(c) + 4HCl(g) \longrightarrow SiCl_4(g) + 2H_2O(g) \ . \tag{48}$$

A reduction in the total pressure of the FBC system decreases the partial pressure of gaseous $SiCl_4$ while increasing the partial pressure of gaseous SiO_2, as shown by the reaction

$$SiCl_4(g) + 2H_2O(g) \longrightarrow SiO_2(g) + 4HCl(g) \ . \tag{49}$$

Calculations for the various excess air systems indicate that as the O_2 content increases, the partial pressure of gaseous $SiCl_4$ decreases. Numerous reactions of the alkali and trace elements with Si are projected to form additional stable solid complexes in the combustor. These reactions will be presented in the elemental interaction discussion that follows the basic reaction chemistry of the trace and minor feedstock constituents.

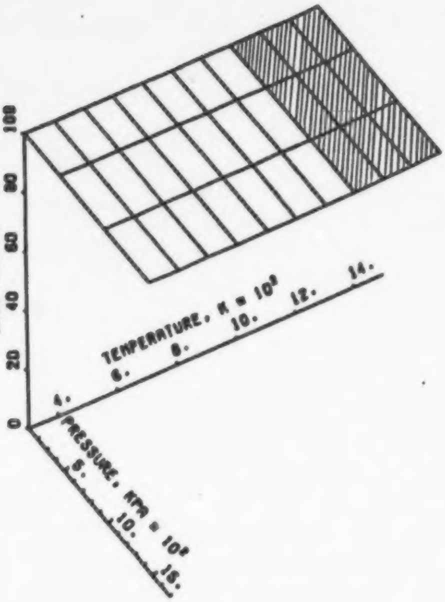

Figure 76 - Percent Distribution of Solid SiO_2 as a Function of Temperature and Pressure in a Fluidized-Bed Combustor Operating with 100% Excess Air and 90% Sulfur-Removal Efficiencies

Bromine

The principal chemical reaction of Br at equilibrium in FBC leads to the formation of numerous volatile chloride (BrCl), hydride (BrH), oxide (BrO), nitrosyl (BrNO), nitride (BrN), carbon-associated (CBr_3, CBr_2, $CClBr_3$, CCl_2Br_2, CH_2Br_2), sulfuryl ($SOBr_2$), cyanogen (CBrN), and mono- and diatomic (Br, Br_2) phases. Variation in the excess air content and gaseous S concentration in the combustor directly affects the resulting partial pressures of the BrNO, BrO, and $SOBr_2$ phases. The partial pressures exerted by BrNO and BrO increase as a function of the excess air content, while the partial pressures of the remaining volatile phases are reduced as a result of dilution by the increased excess air content. Reduction in the FBC gas S content decreases the partial pressure exerted by $SOBr_2$. The distribution of the feedstock-contained

Br in the major volatile complexes formed as a function of temperature and pressure in a 100 percent excess air, 90 percent S-removal combustion system is illustrated in Figures 77 through 80.

Solid or condensed Br phases are not expected to form at equilibrium because of the relatively low melting, boiling, and dissociation temperatures for the various complexes. Emission at the stack, therefore, is estimated at 100 percent release of the feedstock-contained Br to the environment, with minimal depletion of the total content through gas/particulate interaction. Gordon[79] demonstrated an enrichment of 0.16 to 0.17 of the Br concentration on suspended ash particles in stacks over the Br concentration in the feedstock coal. Although Br appears to remain essentially in the vapor phase, additional chemical analyses are required to determine the Br concentration in various ash particle sizes and the volatile Br concentration in the stack gases.

Boron

The principal reaction of B with combustion gases containing C, H, N, O, S, and Cl is the formation of solid boric acid (H_3BO_3) and metaboric acid (HBO_2), at temperatures between 300 and 500 K, prior to complete volatilization of these complexes (Figures 81 and 82). Gaseous H_3BO_3 exists as the major volatile phase at temperatures between 400 and 1200 K, whereupon H_2O is released and gaseous HBO_2 is formed, as shown in reaction 50:

$$H_3BO_3(g) \xrightarrow{>1200\text{ K}} HBO_2(g) + H_2O(g) \ . \qquad (50)$$

Figures 83 and 84 illustrate three-dimensionally the distribution of B in the resulting equilibrium volatile phases. Minor volatile phases include trimeric metaboric acid ($(HBO_2)_3$) and boron dioxide (BO_2).

The solid H_3BO_3 phase is unaffected by changes in the S content of the combustion gas and to variation in the percentage of excess air used for combustion. Similarly, the partial pressure of the volatiles is unaffected by the combustion gas S content. An increase in the partial

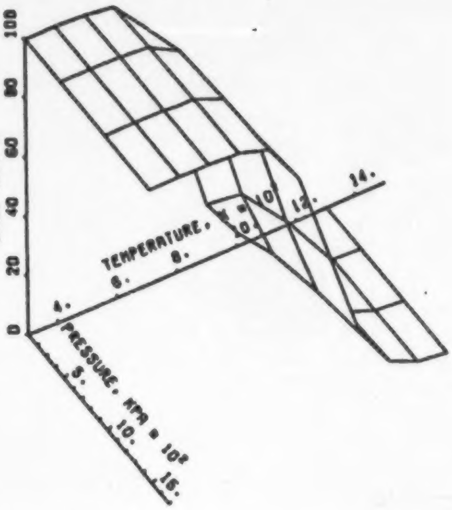

Figure 77 - Percent Distribution of Gaseous BrCl as a Function of Temperature and Pressure in a Fluidized-Bed Combustor Operating with 100% Excess Air and 90% Sulfur-Removal Efficiencies

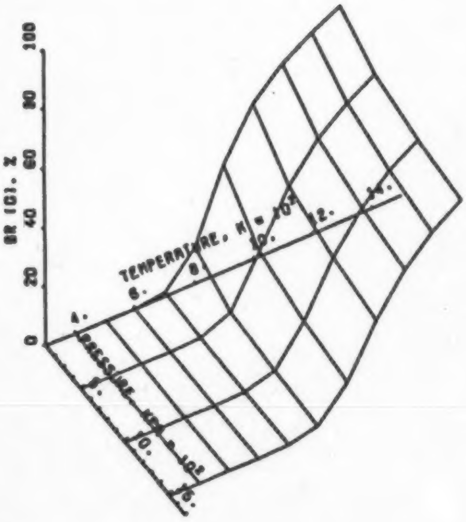

Figure 78 - Percent Distribution of Gaseous Br as a Function of Temperature and Pressure in a Fluidized-Bed Combustor Operating with 100% Excess Air and 90% Sulfur-Removal Efficiencies

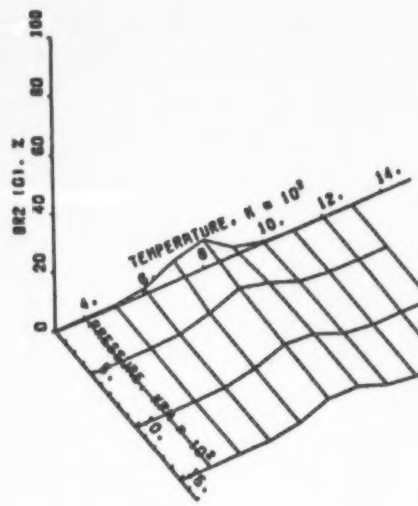

Figure 79 - Percent Distribution of Gaseous Br_2 as a Function of Temperature and Pressure in a Fluidized-Bed Combustor Operating with 100% Excess Air and 90% Sulfur-Removal Efficiencies

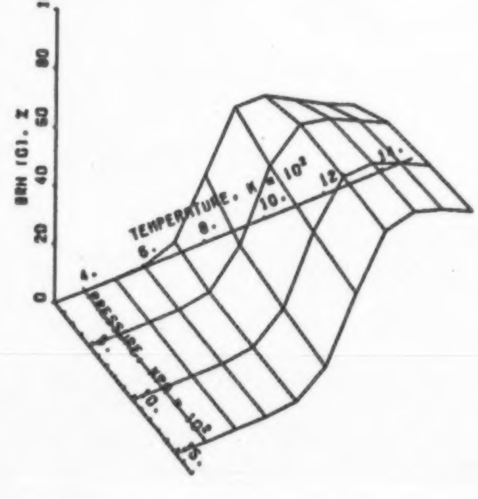

Figure 80 - Percent Distribution of Gaseous BrH as a Function of Temperature and Pressure in a Fluidized-Bed Combustor Operating with 100% Excess Air and 90% Sulfur-Removal Efficiencies

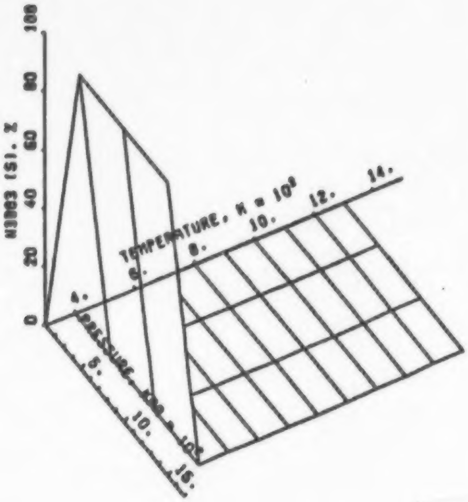

Figure 81 - Percent Distribution of Solid H_3BO_3 as a Function of Temperature and Pressure in a Fluidized-Bed Combustor Operating with 100% Excess Air and 90% Sulfur-Removal Efficiencies

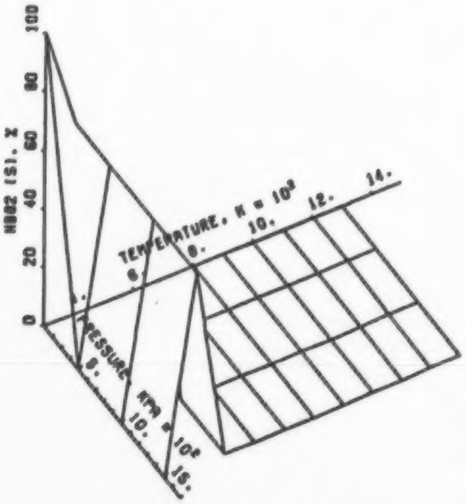

Figure 82 - Percent Distribution of Solid HBO_2 as a Function of Temperature and Pressure in a Fluidized-Bed Combustor Operating with 100% Excess Air and 90% Sulfur-Removal Efficiencies

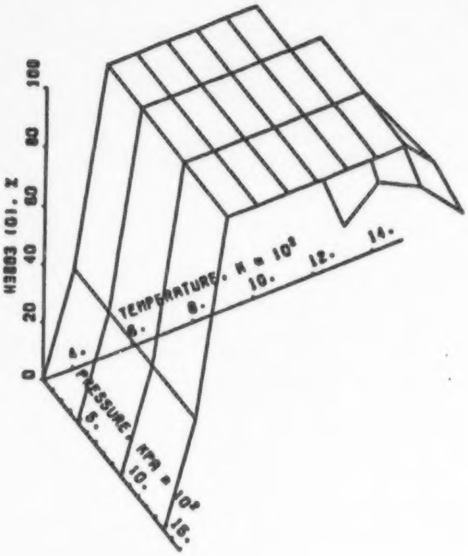

Figure 83 - Percent Distribution of Gaseous H_3BO_3 as a Function of Temperature and Pressure in a Fluidized-Bed Combustor Operating with 100% Excess Air and 90% Sulfur-Removal Efficiencies

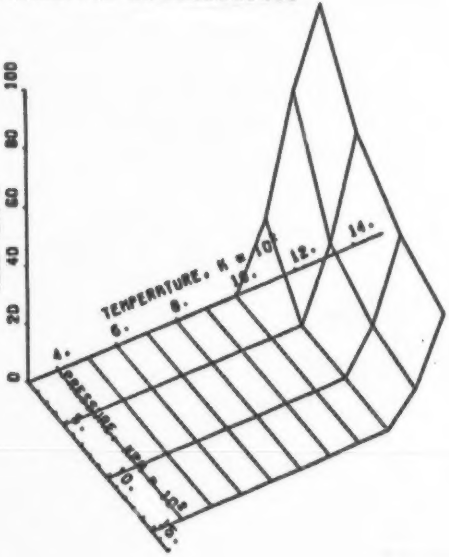

Figure 84 - Percent Distribution of Gaseous HBO_2 as a Function of Temperature and Pressure in a Fluidized-Bed Combustor Operating with 100% Excess Air and 90% Sulfur-Removal Efficiencies

pressures is generally noted at 300 K for the metaborate and dioxide phases when the percentage of excess air is increased, and a reduction in the partial pressure of both the borate and metaborate phases results at elevated temperatures.

The initial equilibrium study indicates the potential for 100 percent volatilization of B when coal is combusted at temperatures of 1300 K. As Torrey[80] reported, B tends to be concentrated in the ash with minimum release to the environment. The equilibrium projected volatile phases may interact with particles entrained in the gas stream, minimizing the percentage of volatile B in stack-gas emissions. Cox et al.,[81] proposed the existence of two chemical states of B in ash: a boron fly ash complex that is 50 percent leachable by water and a nearly insoluble bottom ash boron phase. Interactive studies of B with clay and carbonate constituents will define the possible partitioning of B in various solid phases formed in the fluidized-bed combustor.

Phosphorus

In FBC systems the principal chemical reaction of P with C, H, N, O, S, and Cl leads to the formation of solid orthophosphoric acid (H_3PO_4) below operating temperatures of 316 K, liquid H_3PO_4 from 316 K to between 600 and 900 K (shaded area in Figure 85), and volatile oxides at elevated temperatures (Figures 86 and 87). Volatile oxychlorides, chlorides, and hydrides of P exist only as secondary and minor phases.

The stability of liquid orthophosphoric acid is reduced to lower temperatures when the excess air content required for combustion is increased from 10 to 300 percent. This is particularly evident in the 1520 kPa operations: at 10 percent excess air $H_3PO_4(l)$ forms between 316 K and 800 to 900 K, at 100 percent excess air between 316 K and 700 to 800 K, and at 300 percent excess air between 316 K and 600 to 800 K. Increasing the excess air content simultaneously increases the partial

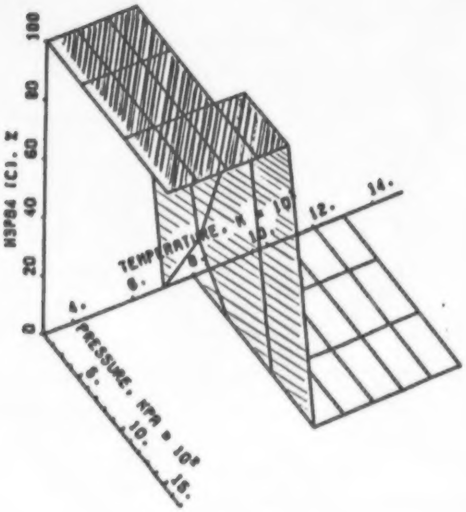

Figure 85 - Percent Distribution of Condensed H_3PO_4 as a Function of Temperature and Pressure in a Fluidized-Bed Combustor Operating with 100% Excess Air and 90% Sulfur-Removal Efficiencies

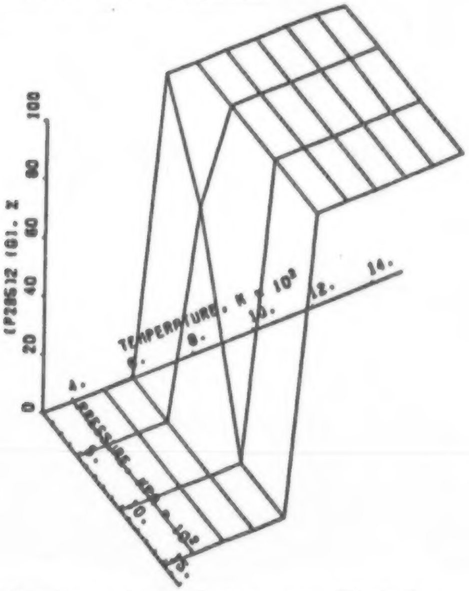

Figure 86 - Percent Distribution of Gaseous $(P_2O_5)_2$ as a Function of Temperature and Pressure in a Fluidized-Bed Combustor Operating with 100% Excess Air and 90% Sulfur Removal Efficiencies

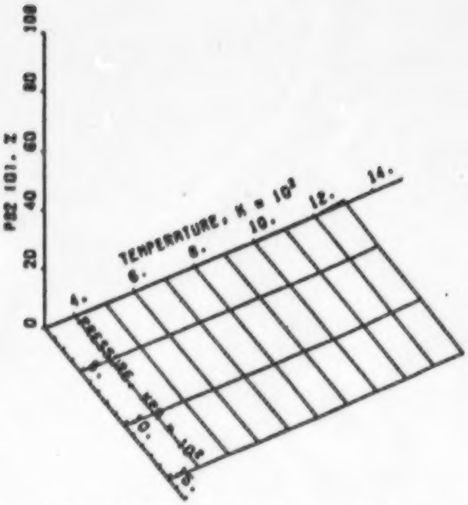

Figure 87 - Percent Distribution of Gaseous PO_2 as a Function of Temperature and Pressure in a Fluidized-Bed Combustor Operating with 100% Excess Air and 90% Sulfur-Removal Efficiencies

pressure of the resulting volatile oxide phases for operations below 800 K, while at higher fluidized-bed operating temperatures the partial pressures of the volatile P oxides is reduced. The formation of gaseous phosphorus oxychlorides, chlorides, and hydrides at partial pressures greater than 10^{-35} kPa results within the 800 to 1300 K temperature regime. As the combustion systems operate with increased concentrations of excess air, the partial pressure for each gaseous phase is projected to decrease. Minimal variation is evident in the number of moles of condensed H_3PO_4 and the partial pressures of the volatile P phases formed in the various S-containing combustion systems. The principal chemical reactions of P in the fluidized bed include:

$$H_3PO_4(s) \xrightarrow{>316\ K} H_3PO_4(l) \qquad (51)$$

and

$$4H_3PO_4(l) \xrightarrow{316\ to\ 800\text{-}900\ K} (P_2O_5)_2(g) + 6H_2O(g) \quad . \qquad (52)$$

These simple reactions are modified when Mg is present.

Copper

Complete volatilization of feedstock Cu is projected in FBC systems operating at temperatures greater than 1100 K. The principal volatile phases formed in the combustor include copper monochloride (CuCl and the trimer, Cu_3Cl_3) and copper monoxide (CuO) (Figures 88-90), with trace formations of gaseous copper hydride, sulfide, and metal species (CuH, CuS, Cu_2, Cu).

A reduction in the fluidized-bed operating temperature to below 1000 K enhances the formation of copper monoxide (CuO), copper oxide-sulfate ($CuO \cdot CuSO_4$), and copper sulfate ($CuSO_4$), depending on the concentration of S in the system. The reaction series that defines the oxide/sulfate transition as a function of temperature can be written as follows:

$$\begin{tikzcd} 2CuSO_4(s) \arrow[r] & CuO \cdot CuSO_4(s) + SO_2(g) + 1/2\ O_2(g) \arrow[d] \\ & 2CuO(s) + SO_2(g) + 1/2\ O_2(g). \end{tikzcd} \qquad (53)$$

For combustion in 100 percent excess air with 90 percent S-removal efficiencies, only $CuSO_4$ and $CuO \cdot CuSO_4$ are projected to form as stable solids (Figures 91 and 92). The solid CuO phase is unstable under these conditions and directly volatilizes. These complexes may be released from the bed with entrained ash particles prior to complete volatilization. The solids released or the condensation/adsorption of volatile copper phases on entrained ash in cooler flue gas regimes was demonstrated in the data reported by Lyon[1] in which Cu was shown to incorporate poorly into slag formations of the conventional coal-fired systems while generally concentrating on the inlet electrostatic precipitator fly ash. Either phenomenon will further reduce the Cu concentration emitted from the stacks.

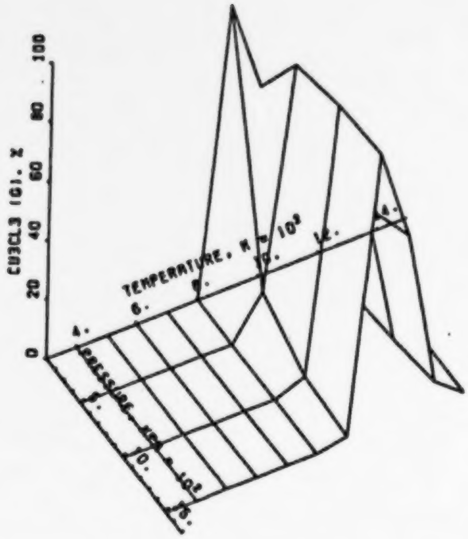

Figure 88 - Percent Distribution of Gaseous Cu_3Cl_3 as a Function of Temperature and Pressure in a Fluidized-Bed Combustor Operating with 100% Excess Air and 90% Sulfur-Removal Efficiencies

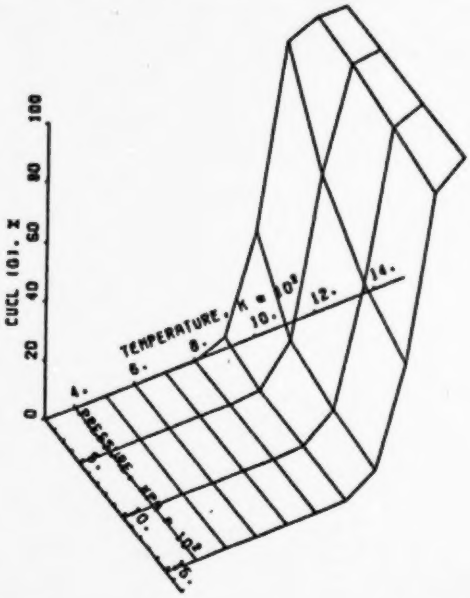

Figure 89 - Percent Distribution of Gaseous CuCl as a Function of Temperature and Pressure in a Fluidized-Bed Combustor Operating with 100% Excess Air and 90% Sulfur-Removal Efficiencies

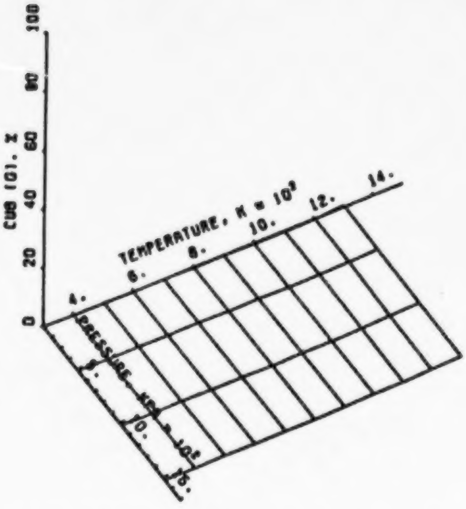

Figure 90 - Percent Distribution of Gaseous CuO as a Function of Temperature and Pressure in a Fluidized-Bed Combustor Operating with 100% Excess Air and 90% Sulfur-Removal Efficiencies

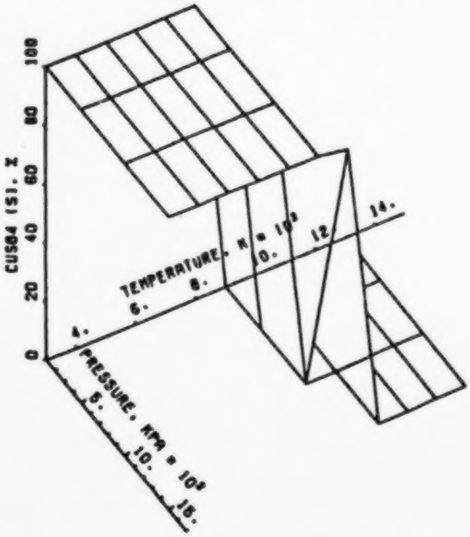

Figure 91 - Percent Distribution of Solid $CuSO_4$ as a Function of Temperature and Pressure in a Fluidized-Bed Combustor Operating with 100% Excess Air and 90% Sulfur-Removal Efficiencies

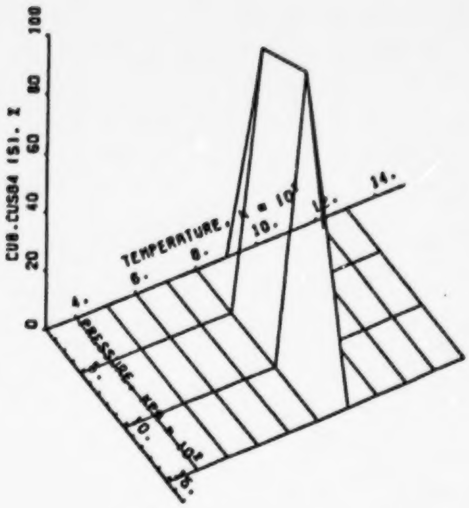

Figure 92 - Percent Distribution of Solid CuO•CuSO$_4$ as a Function of Temperature and Pressure in a Fluidized-Bed Combustor Operating with 100% Excess Air and 90% Sulfur-Removal Efficiencies

Vanadium

Divanadium pentoxide (V_2O_5) is projected to form as a stable solid phase at equilibrium in the FBC system at temperatures between 300 and 943 K. Operation at higher temperatures enhances the formation of a liquid V_2O_5 melt (Figure 93). Conversion of V_2O_5 into solid divanadium tetroxide (V_2O_4) or divanadium trioxide (V_2O_3), which have sufficiently higher melting temperatures (1818 K and 2340 K, respectively) than does the V_2O_5 complex, is not projected even in combustion systems operating with a low excess air content.

Volatilization of less than 0.2 percent of the feedstock V results in the formation of vanadium oxychloride, ($VOCl_3$), vanadium tetrachloride (VCl_4), vanadium oxides (VO and VO_2), and nitride (VN) complexes. A reduction in the partial pressure of the gaseous V complexes results

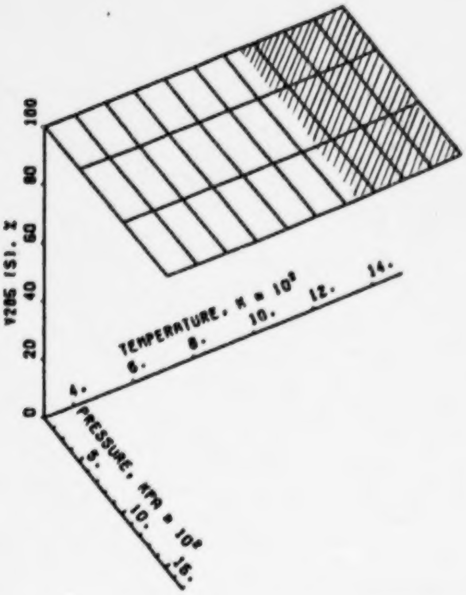

Figure 93 - Percent Distribution of Condensed V_2O_5 as a Function of Temperature and Pressure in a Fluidized-Bed Combustor Operating with 100% Excess Air and 90% Sulfur-Removal Efficiencies

as the excess air content of the FBC system increases. Reduction in the total gaseous S content does not significantly modify the resulting partial pressures of the volatile and condensed V phases.

Within the combustor V reacts locally with Na or Mg to form high melting temperature vanadate compounds. These reactions will be discussed in the parametric interactive projections of this report.

Zinc

Feedstock Zn during combustion in a fluidized bed undergoes a series of dehydration reactions that are dependent on the combustor operating temperature. These include:

$$ZnSO_4 \cdot 7H_2O(s) \xrightarrow{300-400\ K} ZnSO_4 \cdot H_2O(s) + 6H_2O(g) \qquad (54)$$

$$ZnSO_4 \cdot H_2O(s) \xrightarrow{400-500\ K} ZnSO_4(s) + H_2O(g) \qquad (55)$$

$$ZnSO_4(s) \xrightarrow{500-1200\ K} ZnO(s) + SO_2(g) + 1/2\ O_2(g) \quad . \qquad (56)$$

Reference to Figures 94 through 97 will illustrate the dehydration and sulfate/oxide transition as a function of temperature and pressure for the reaction of Zn in a 100 percent excess air, 90 percent S-removal FBC system. Table 31 defines the sulfate ⟶ oxide transition temperature as a function of S removal. This transition occurs through an oxysulfate intermediate,* the formula of which apparently varies as a function of temperature. For example:

$$5ZnSO_4(s) \xrightarrow{1113-1173\ K} 3ZnSO_4 \cdot 2ZnO(s) + 2SO_2(g) + O_2(g) \qquad (57)$$

and,

$$3ZnSO_4 \cdot 2ZnO(s) \xrightarrow{1233-1293\ K} 5ZnO(s) + 3SO_2(g) + 3/2\ O_2(g). \qquad (58)$$

The concentration of S present in the combustion gases directly influences the formation and stability of the solid sulfate phases. At reduced operating temperatures, and as the concentration of excess air increases in the FBC system, the hydrated $ZnSO_4$ complexes are stable, particularly, in the 101 kPa system. Dehydration of the sulfate is

---

*Thermodynamic data for the oxysulfate intermediate is not included in the present data base.

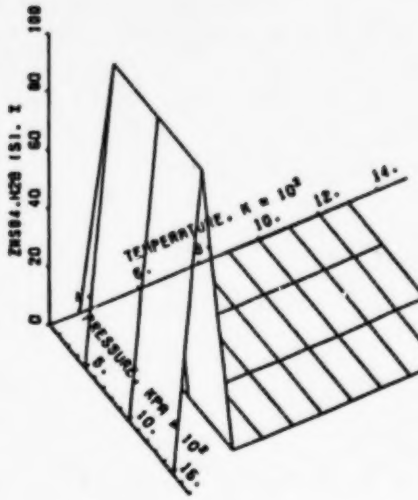

Figure 94 - Percent Distribution of Solid $ZnSO_4 \cdot H_2O$ as a Function of Temperature and Pressure in a Fluidized-Bed Combustor Operating with 100% Excess Air and 90% Sulfur-Removal Efficiencies

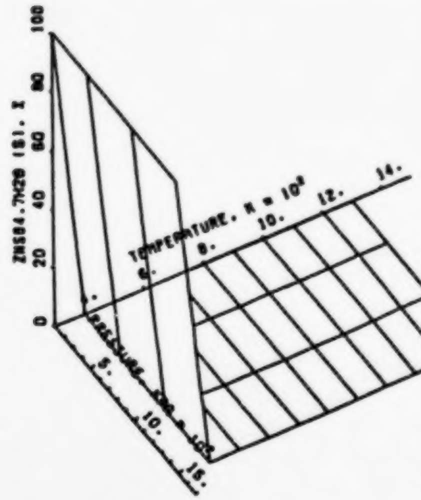

Figure 95 - Percent Distribution of Solid $ZnSO_4 \cdot 7H_2O$ as a Function of Temperature and Pressure in a Fluidized-Bed Combustor Operating with 100% Excess Air and 90% Sulfur-Removal Efficiencies

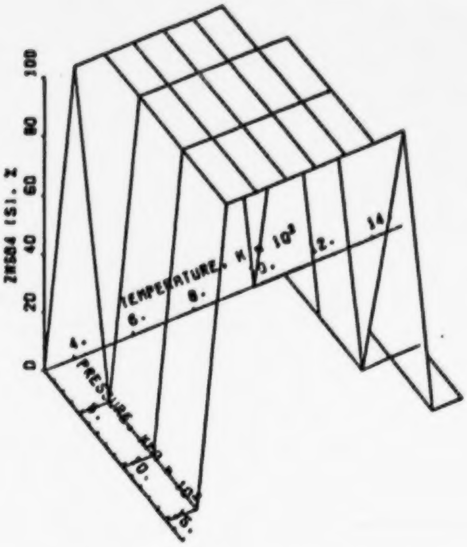

Figure 96 - Percent Distribution of Solid $ZnSO_4$ as a Function of Temperature and Pressure in a Fluidized-Bed Combustor Operating with 100% Excess Air and 90% Sulfur-Removal Efficiencies

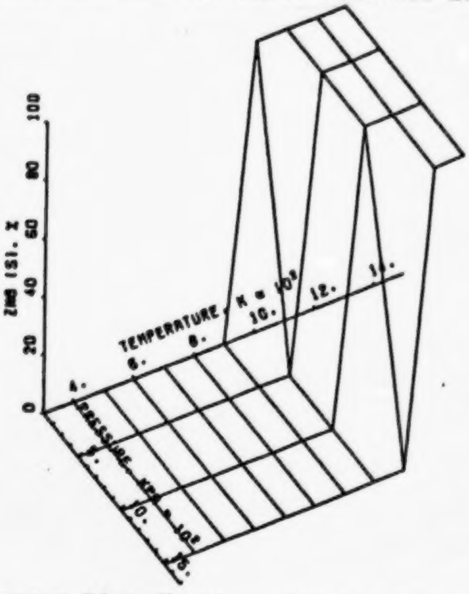

Figure 97 - Percent Distribution of Solid ZnO as a Function of Temperature and Pressure in a Fluidized-Bed Combustor Operating with 100% Excess Air and 90% Sulfur-Removal Efficiencies

TABLE 31 - ZINC SULFATE → OXIDE TRANSITION TEMPERATURE AS A FUNCTION OF FBC CONDITIONS

Dwg. 1714B25

$$ZnSO_4\,(s) \longrightarrow ZnO\,(s) + SO_2\,(g) + 1/2O_2\,(g)$$

Sulfate → Oxide Transition Temperature

Combustion Conditions Pressure (kPa)	100% Excess Air 0% Sulfur Removal	100% Excess Air 90% Sulfur Removal	100% Excess Air 99% Sulfur Removal
101	1050 - 1060K	990 - 1000K	910 - 920K
505	1130 - 1140K	1050 - 1060K	960 - 970K
1013	1160 - 1170K	1080 - 1090K	990 - 1000K
1520	1190 - 1200K	1100 - 1110K	1000 - 1010K
2026	1200 - 1210K	1120 - 1130K	1010 - 1030K

complete between 400 and 500 K for 10 percent excess air systems but reduces to temperatures of 300 and 400 K for 300 percent excess air systems with similar operating pressures and S-removal efficiencies.

Volatilization of less than 1 percent of the Zn feedstock content can be expected at combustor temperatures. The principal volatile phases include mono- and diatomic zinc (Zn and Zn_2), chlorides (ZnCl), hydrides (ZnH), and sulfides (ZnS). With increased S-removal efficiency in the combustor, the partial pressures of the resulting volatiles, with the exception of ZnS, increase at lower temperatures, but they decrease slightly as combustion temperatures approach 1300 K. The reverse trend is projected for the partial pressure of the ZnS phase. Increasing the excess air content in the system reduces the partial pressures of all volatile Zn phases.

Antimony

The principal chemical form of Sb in the combustor is that of solid antimony dioxide (SbO_2). Although unexpected, the solid dioxide satisfies the mass conservation equations while minimizing the total free energy of the polyphase system. Under atmospheric operations SbO_2 remains as a stable solid phase to temperatures between 1200 and 1300 K, whereupon complete volatilization of Sb into gaseous antimony monoxide (SbO) and chlorides ($SbCl_3$ and SbCl) occurs (Figures 98 through 101). In pressurized systems the oxide is stable as a solid at operating temperatures exceeding 1300 K.

A transition reaction is detected in the major volatile Sb complexes. At temperatures below 1200 K Sb exists as gaseous $SbCl_3$ and SbO. With complete volatilization of the solid dioxide at elevated operating temperatures, the gaseous trichloride is projected to dissociate into the monochloride complex (SbCl) with SbO as the principal gaseous phase (Table 32).

Variation in the air:fuel ratio slightly increases the stability of the SbO_2 solid at the combustor temperature. In 10 percent excess air and 0 percent S removal, 1520 kPa systems, 95.12 percent of the initial feedstock Sb is projected to exist as SbO_2. For the 1520 kPa, 300 percent excess air, and 0 percent S-removal combustor, 96.54 percent is projected. As expected, the percentage of Sb in gaseous SbO tends to increase for combustion with a higher air:fuel ratio.

Although 4 to 100 percent of the feedstock Sb is projected to volatilize at FBC temperatures of 1200 to 1300 K in an atmospheric system and between 0.5 to 4.9 percent for 1520 kPa operation, the emission level lies far below the MATE level.

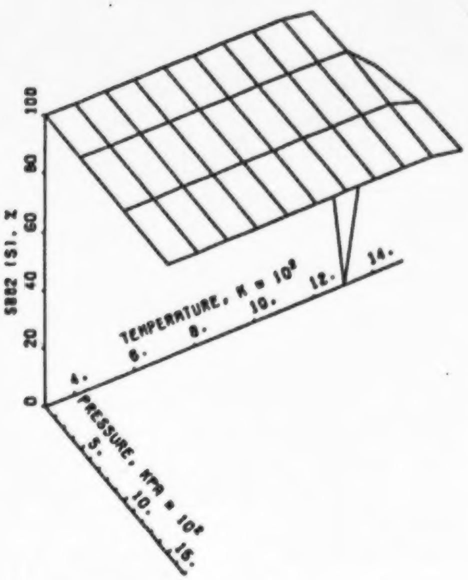

Figure 98 - Percent Distribution of Solid SbO_2 as a Function of Temperature and Pressure in a Fluidized-Bed Combustor Operating with 100% Excess Air and 90% Sulfur-Removal Efficiencies

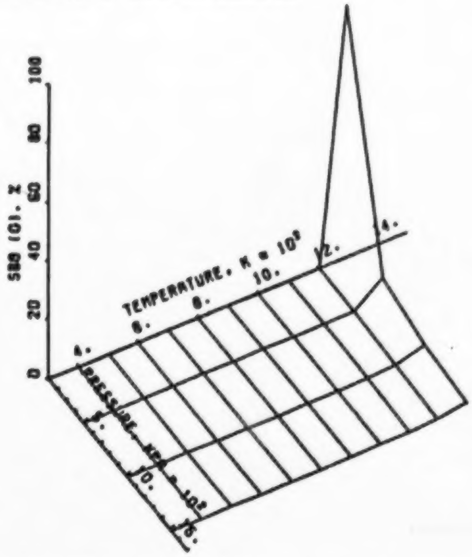

Figure 99 - Percent Distribution of Gaseous SbO as a Function of Temperature and Pressure in a Fluidized-Bed Combustor Operating with 100% Excess Air and 90% Sulfur-Remove Efficiencies

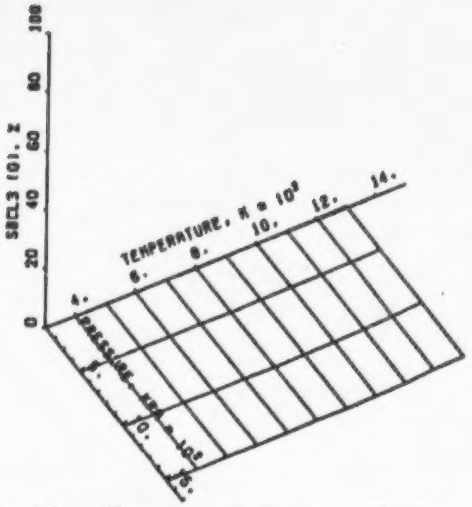

Figure 100 - Percent Distribution of Gaseous $SbCl_3$ as a Function of Temperature and Pressure in a Fluidized-Bed Combustor Operating with 100% Excess Air and 90% Sulfur-Removal Efficiencies

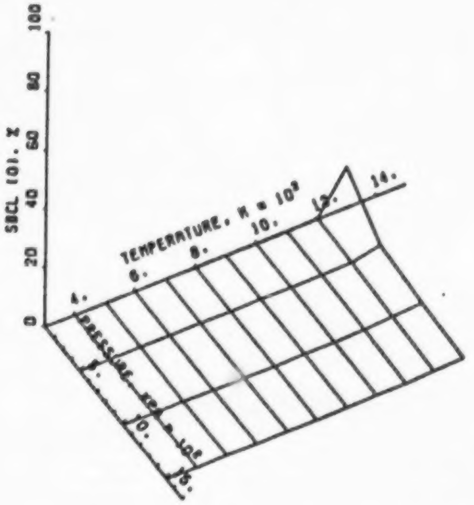

Figure 101 - Percent Distribution of Gaseous SbCl as a Function of Temperature and Pressure in a Fluidized-Bed Combustor Operating with 100% Excess Air and 90% Sulfur-Removal Efficiencies

TABLE 32 - GAS/SOLID PERCENT DISTRIBUTION OF Sb IN 100%
EXCESS AIR, 90% SULFUR REMOVAL FBC SYSTEMS

```
COMPOUND:SBO2 (S)
         \
TEMP.\PRESSURE  (KPA)
 (K)    \    101.3      506.5      1013.0      1519.5
  300        100.0      100.0      100.0       100.0
  400        100.0      100.0      100.0       100.0
  500       100.0       100.0      100.0       100.0
  600       100.0       100.0      100.0       100.0
  700       100.0       100.0       99.99       99.99
  800         99.99      99.98      99.98       99.97
  900         99.96      99.94      99.92       99.92
 1000         99.90      99.86      99.83       99.81
 1100         99.79      99.71      99.66       99.62
 1200         97.92      99.33      99.35       99.31
 1300          0.0       89.97      95.70       97.10
COMPOUND:SBCL3 (G)
         \
TEMP.\PRESSURE  (KPA)
 (K)    \    101.3      506.5      1013.0      1519.5
  300        0.0          0.0         0.0        0.0
  400        0.0          0.0         0.0        0.0
  500        0.0          0.0         0.0        0.0
  600        0.0          0.0         0.0        0.0
  700        0.0          0.0         0.1        0.01
  800        0.01         0.02        0.2        0.03
  900        0.04         0.06        0.7        0.08
 1000        0.10         0.14       0.17        0.19
 1100        0.19         0.29       0.34        0.38
 1200        0.33         0.49       0.59        0.65
 1300        0.51         0.76       0.91        1.00
COMPOUND:SBO (G)
         \
TEMP.\PRESSURE  (KPA)
 (K)    \    101.3      506.5      1013.0      1519.5
  300        0.0         0.0         0.0         0.0
  400        0.0         0.0         0.0         0.0
  500        0.0         0.0         0.0         0.0
  600        0.0         0.0         0.0         0.0
  700        0.0         0.0         0.0         0.0
  800        0.0         0.0         0.0         0.0
  900        0.0         0.0         0.0         0.0
 1000        0.0         0.0         0.0         0.0
 1100        0.01        0.0         0.0         0.0
 1200        1.32        0.12        0.04        0.02
 1300       85.69        7.45        2.63        1.43
COMPOUND:SBCL (G)
         \
TEMP.\PRESSURE  (KPA)
 (K)    \    101.3      506.5      1013.0      1519.5
  300        0.0         0.0         0.0         0.0
  400        0.0         0.0         0.0         0.0
  500        0.0         0.0         0.0         0.0
  600        0.0         0.0         0.0         0.0
  700        0.0         0.0         0.0         0.0
  800        0.0         0.0         0.0         0.0
  900        0.0         0.0         0.0         0.0
 1000        0.0         0.0         0.0         0.0
 1100        0.01        0.0         0.0         0.0
 1200        0.42        0.06        0.02        0.02
 1300       13.80        1.81        0.76        0.46
```

Tin

Solid tin IV dioxide (SnO_2, cussiterite) is the principal chemical phase of Sn projected to form in FBC. As shown in Table 33 in atmospheric systems, 3 percent of the feedstock-contained Sn is projected to volatilize at 1300 K as either gaseous tin oxide (SnO) or tin dichloride ($SnCl_2$), while at 1520 kPa the extent of volatilization of solid SnO_2 is less than 1 percent.

Neither the solid → gas volatilization reaction nor the partitioning of Sn in either of the volatile complexes is projected to change significantly when the air:fuel ratio or S-removal capacity is varied. Figures 102 through 104 illustrate the percent distribution of Sn in the solid and volatile phases formed as a function of temperature and pressure for combustion of a U.S. mean coal in 100 percent excess air with 90 percent S removal.

Zirconium

In the fluidized bed-combustor, Zr exists principally as solid zirconium dioxide (ZrO_2) (Figure 105). Partial pressures less than 10^{-34} kPa are projected for volatile phases as zirconium tetrachloride ($ZrCl_4$), which are formed in equilibrium with the solid oxide at combustion temperatures of 1300 K. Variations in the air:fuel ratio or S-removal capability do not affect the stability of the Zr solid. With 100 percent of the initial feedstock Zr present in the combustor solids and with ~0 percent Zr projected to exist in the gas phase, there is no need for concern about the potential toxicity of emitted gaseous Zr complexes.

Review of the Exxon data[45] indicates that the concentration of B, P, Cu, Zn, and Sb is lower in the ash analyses than is the elemental concentration in the feedstock material. The concentrations of Br and Zr are shown to increase, while no relation between the feedstock and ash V and Sn content is detected.

TABLE 33 - GAS/SOLID PERCENT DISTRIBUTION OF Sn IN 10% EXCESS AIR, 0% SULFUR REMOVAL FBC SYSTEMS

```
COMPOUND:SNO2 (S)
   \
TEMP.\PRESSURE (KPA)
 (K)   \   101.3      506.5     1013.0     1519.5
  300     100.0      100.0      100.0      100.0
  400     100.0      100.0      100.0      100.0
  500     100.0      100.0      100.0      100.0
  600     100.0      100.0      100.0      100.0
  700     100.0      100.0      100.0      100.0
  800     100.0      100.0      100.0      100.0
  900     100.0      100.0      100.0      100.0
 1000     100.0      100.0      100.0      100.0
 1100     199.99      99.99     100.0      100.0
 1200      99.96      99.95      99.96      99.97
 1300      97.10      97.56      99.63      99.72
COMPOUND:SNCL2 (G)
   \
TEMP.\PRESSURE (KPA)
 (K)   \   101.3      506.5     1013.0     1519.5
  300       0.0        0.0        0.0        0.0
  400       0.0        0.0        0.0        0.0
  500       0.0        0.0        0.0        0.0
  600       0.0        0.0        0.0        0.0
  700       0.0        0.0        0.0        0.0
  800       0.0        0.0        0.0        0.0
  900       0.0        0.0        0.0        0.0
 1000       0.0        0.0        0.0        0.0
 1100       0.01       0.01       0.0        0.0
 1200       0.01       0.05       0.04       0.03
 1300       0.95       2.27       0.31       0.25
COMPOUND:SNO (G)
   \
TEMP.\PRESSURE (KPA)
 (K)   \   101.3      506.5     1013.0     1519.5
  300       0.0        0.0        0.0        0.0
  400       0.0        0.0        0.0        0.0
  500       0.0        0.0        0.0        0.0
  600       0.0        0.0        0.0        0.0
  700       0.0        0.0        0.0        0.0
  800       0.0        0.0        0.0        0.0
  900       0.0        0.0        0.0        0.0
 1000       0.0        0.0        0.0        0.0
 1100       0.0        0.0        0.0        0.0
 1200       0.03       0.0        0.0        0.0
 1300       1.95       0.17       0.06       0.03
```

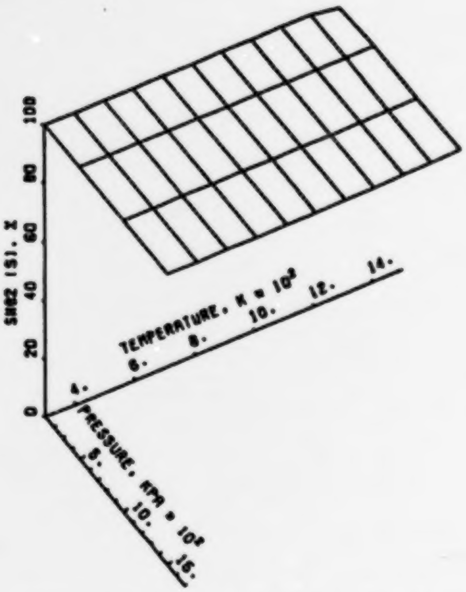

Figure 102 - Percent Distribution of Solid SnO_2 as a Function of Temperature and Pressure in a Fluidized-Bed Combustor Operating with 100% Excess Air and 90% Sulfur-Removal Efficiencies

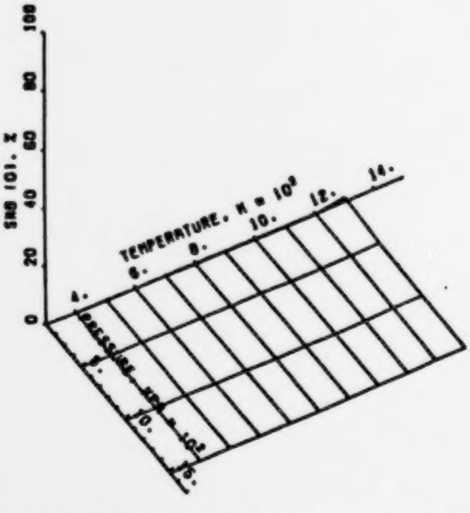

Figure 103 - Percent Distribution of Gaseous SnO as a Function of Temperature and Pressure in a Fluidized-Bed Combustor Operating with 100% Excess Air and 90% Sulfur-Removal Efficiencies

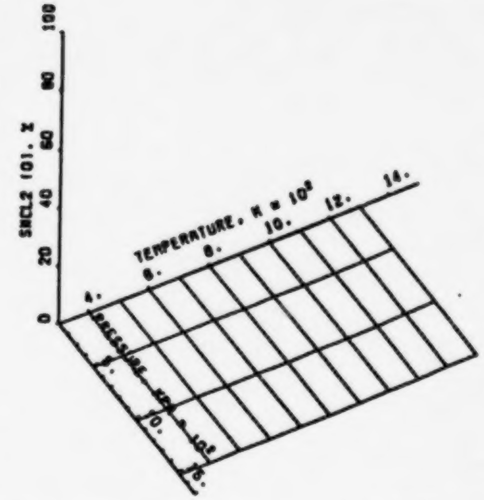

Figure 104 - Percent Distribution of Gaseous $SnCl_2$ as a Function of Temperature and Pressure in a Fluidized-Bed Combustor Operating with 100% Excess Air and 90% Sulfur-Removal Efficiencies

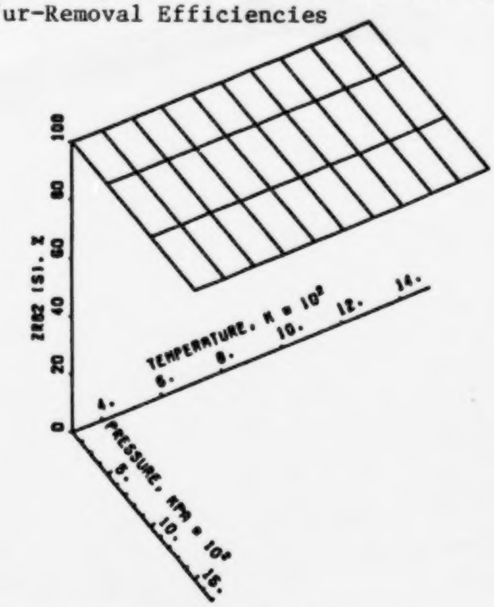

Figure 105 - Percent Distribution of Solid ZrO_2 as a Function of Temperature and Pressure in a Fluidized-Bed Combustor Operating with 100% Excess Air and 90% Sulfur-Removal Efficiencies

Although thermodynamically B, P, and Br were projected to volatilize completely during combustion, retention of these elements within ash fractions results possibly from a "reaction" of the gaseous complexes and the ash surface. Chemical determination of the elements in either the clay or nonclay fractions would indicate whether the retained concentration resulted from either a gas-solid reaction or a physical adsorption mechanism. The concentration of Sb is lower in the Exxon ash analyses than in the feedstock, implying that volatilization has occurred. This volatilization was projected at equilibrium for an AFBC operating between 1200 and 1300 K. Thermodynamically, the projected concentration of Cu and Zn in the ash is expected to be comparable to the concentration in the feedstock material. The Exxon data, however, indicate a 30 to 50 percent decrease in the concentration of Cu and Zn in the resulting ash phases. Variations in the level of V and Sn are noted in the Exxon ash when it is compared with the feedstock; this may be indicative of the nonhomogeneity of trace and minor elements in the resulting ash.

Arsenic

Basic chemical reactions of As as the coal particle is heated include the initial formation of solid arsenic pentoxide (As_2O_5) between temperatures of 300 and 1000 to 1100 K for AFBC and 300 and 1100 to 1200 K for PFBC systems (Figure 106). As the combustion temperature is increased, complete volatilization of As results, as shown by the reaction

$$As_2O_5(s) + 2HCl(g) \longrightarrow 2AsCl(g) + H_2O(g) + 2O_2(g). \qquad (59)$$

At FBC temperatures, arsenic exists principally as the gaseous chloride phase (AsCl), in addition to the oxide (AsO) and trichloride ($AsCl_3$) complexes (Figures 107-109).

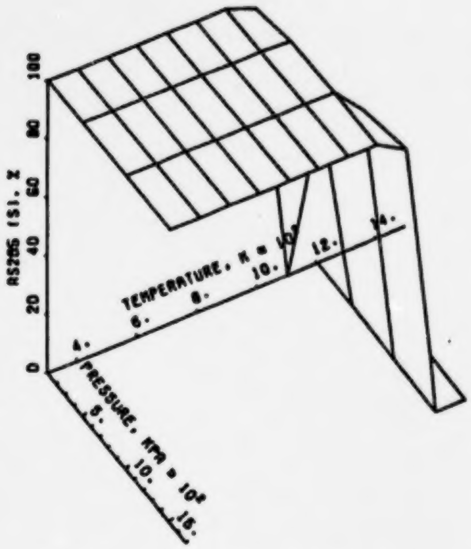

Figure 106 - Percent Distribution of Solid As_2O_5 as a Function of Temperature and Pressure in a Fluidized-Bed Combustor Operating with 100% Excess Air and 90% Sulfur-Removal Efficiencies

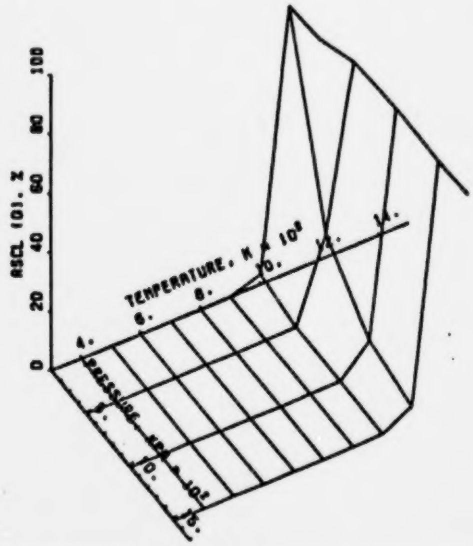

Figure 107 - Percent Distribution of Gaseous AsCl as a Function of Temperature and Pressure in a Fluidized-Bed Combustor Operating with 100% Excess Air and 90% Sulfur-Removal Efficiencies

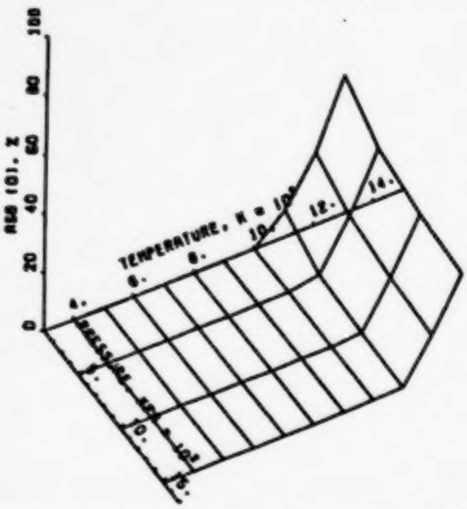

Figure 108 - Percent Distribution of Gaseous AsO as a Function of Temperature and Pressure in a Fluidized-Bed Combustor Operating with 100% Excess Air and 90% Sulfur-Removal Efficiencies

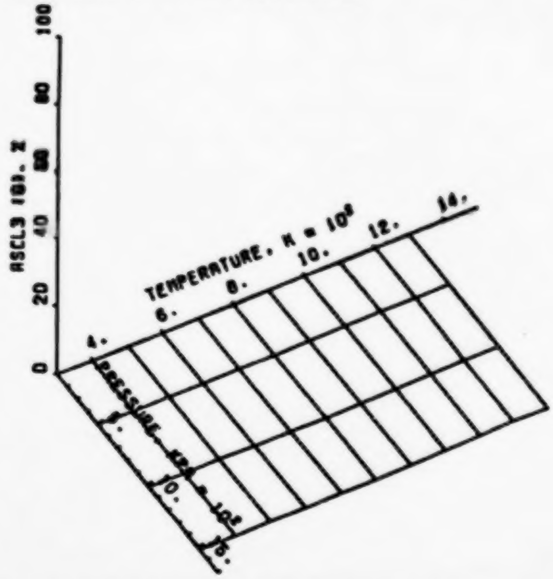

Figure 109 - Percent Distribution of Gaseous $AsCl_3$ as a Function of Temperature and Pressure in a Fluidized-Bed Combustor Operating with 100% Excess Air and 90% Sulfur-Removal Efficiencies

Minor variation in the percent distribution in each phase is observed for combustion in 0 to 300 percent excess air for 0 to 99 percent S-removal systems.

In comparing the inlet fly ash As concentration with that of bottom ash and outlet fly ash formed in the Allen Steam Plant in Tennessee, Ray[16] demonstrated that enrichment of As occurs in the ash particle as it migrates from the combustor through cooler regions of the gas stream. As a result of volatilization, the gaseous As phases may subsequently recondense partially or completely or be discharged at the stack as volatiles. Condensation of As in cooler effluent streams may result where locally high concentrations of As are in contact with elutriated fines. Ray proposes that

> Condensation occurs by nucleation or by deposition on previously formed particles. Since the residence times between volatilization and condensation are relatively low, nucleation will produce relatively small particles.
>
> Deposition occurs on the particle surface and is, therefore dependent on particle surface area. Since surface area is greater for finer particles, small particulates display increased concentrations of elements which tend to recondense.

Cadmium

Cadmium, in 90 and 99 percent S-removal AFBC systems operating between 300 and 900 to 1000 K, and between 300 and 1000 to 1100 K in pressurized systems, exists as solid cadmium sulfate ($CdSO_4$). For 0 percent S-removal systems conversion of the solid sulfate into the volatile oxide, as shown by the reaction

$$CdSO_4(s) \longrightarrow CdO(g) + SO_2(g) + 1/2\ O_2(g) \quad , \qquad (60)$$

for AFBC and PFBC systems occurs between 1000 and 1100 K. Volatilization of the coal-contained Cd, therefore, is complete at FBC temperatures, with cadmium oxide (CdO) forming as the principal volatile phase. Additional volatile cadmium phases include the free ion (Cd) and cadmium chloride (CdCl). Figures 110 through 113 illustrate the percent distribution of Cd within the various condensed and volatile phases formed in a FBC operating with 100 percent excess air and 90 percent S-removal efficiencies.

Similarly to As, Cd was shown by Ray[16] to be enriched along the ash particles as they travel from the combustor into cooler effluent streams. The enrichment mechanism by which Cd concentrates along the entrained fines remains to be delineated.

Selenium

Similarly to Cd, Se in the fluidized bed is projected to volatilize completely as a gaseous SeO (Figure 114), with no apparent solids formed at low operating temperatures. Although thermodynamic data are unavailable for various solid Se phases, it is unlikely that solid Se complexes would result. For example, the melting temperature of Se(s) is reported[82] as 490 K and of SeO_3(s) as 391 K, while SeO_2(s) sublimes between 613 and 623 K, and H_3SeO_3(s) dissociates at 343 K.

The partial pressure of the volatile oxide in a 1300 K AFBC and PFBC is projected at 10^{-6} kPa and 10^{-4} kPa, respectively. In addition to the volatile oxide, selenium hydride (SeH) exerts a partial pressure of 10^{-11} kPa at 1300 K in AFBC systems and partial pressures of 10^{-10} kPa in 1520 kPa systems.

Similarly to As and Cd, feedstock Se volatilizes within the combustor and has the potential to condense along elutriated fines through nucleation or deposition mechanisms. These mechanisms promote depletion of the volatile content released at the stack but enhance the concentration within the fines.

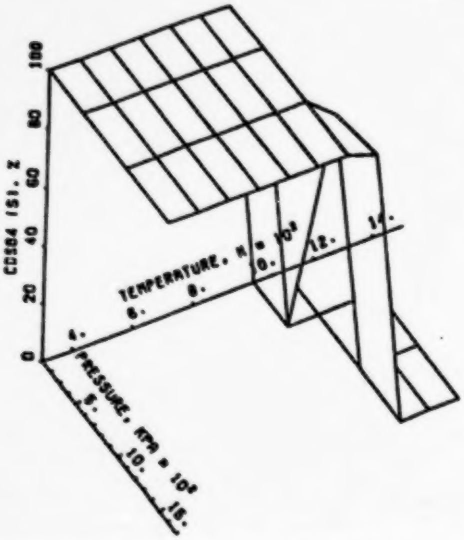

Figure 110 - Percent Distribution of Solid $CdSO_4$ as a Function of Temperature and Pressure in a Fluidized-Bed Combustor Operating with 100% Excess Air and 90% Sulfur-Removal Efficiencies

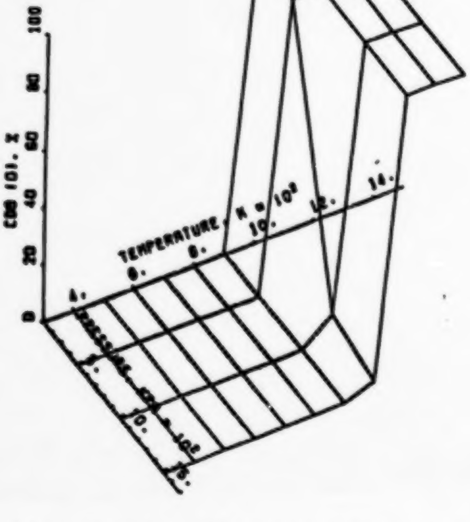

Figure 111 - Percent Distribution of Gaseous CdO as a Function of Temperature and Pressure in a Fluidized-Bed Combustor Operating with 100% Excess Air and 90% Sulfur-Removal Efficiencies

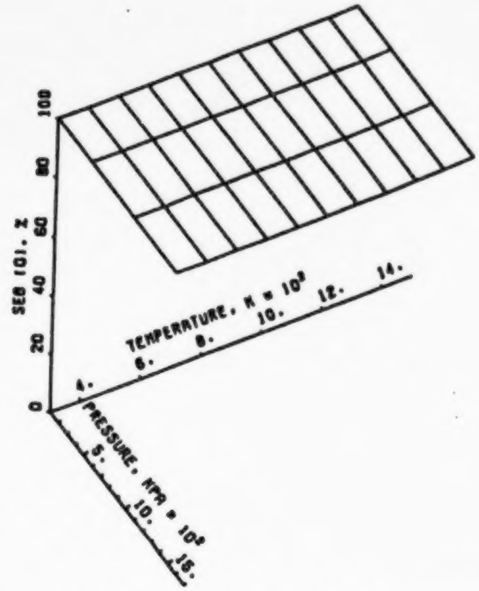

Figure 114 - Percent Distribution of Gaseous SeO as a Function of Temperature and Pressure in a Fluidized-Bed Combustor Operating with 100% Excess Air and 90% Sulfur-Removal Efficiencies

Gallium

The equilibrium product distribution of Ga was projected in 101.3 to 1520 kPa FBC systems operating at 10 and 300 percent excess air with 0 or 90 percent S-removal efficiencies, and at 100 percent excess air with 90 and 99 percent S-removal capabilities. Review of the literature and additional updating of the thermodynamic data base for Ga complexes was not attempted. The projected equilibrium reactions, therefore, should be regarded as potential reactions involving select compounds (see Appendix A). Alternate reactions forming complexes that were not included in the data base may also be possible.

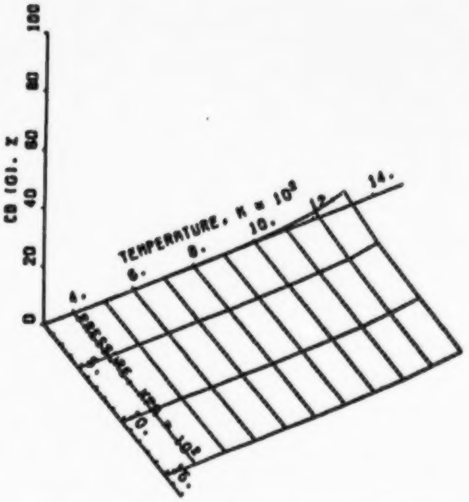

Figure 112 - Percent Distribution of Gaseous Cd as a Function of Temperature and Pressure in a Fluidized-Bed Combustor Operating with 100% Excess Air and 90% Sulfur-Removal Efficiencies

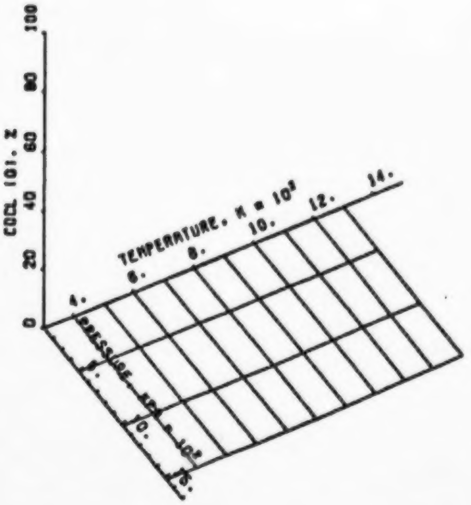

Figure 113 - Percent Distribution of Gaseous CdCl as a Function of Temperature and Pressure in a Fluidized-Bed Combustor Operating with 100% Excess Air and 90% Sulfur-Removal Efficiencies

In the combustor the principal chemical form of Ga is solid gallium sesquioxide (Ga_2O_3). In both AFBC and PFBC Ga_2O_3 exists as the major Ga species between 300 and 1300 K, with less than 1 percent volatilization of the initial feedstock concentration at 1300 K (Figure 115). Variation in the fluidized-bed operating parameters (i.e., air:fuel ratio, S-removal) does not significantly affect the stability of the solid sesquioxide.

The predominant gaseous species that exists in equilibrium with the solid sesquioxide is gallium chloride (GaCl) (Figure 116). Pressurized operations diminish conversion into the volatile Ga phase, maintaining the stability of the solid sesquioxide at higher operating temperatures. The principal equilibrium reaction between the condensed and volatile species may be written as

$$Ga_2O_3(s) + 2HCl(g) \longrightarrow 2GaCl(g) + H_2O(g) + O_2(g) \quad . \qquad (61)$$

Germanium

Germanium in the AFBC exists as solid germanium dioxide (GeO_2), with less than 1 percent volatilization of the initial feedstock concentration below 1100 to 1200 K. The temperature regime for less than 1 percent volatilization is extended to between 1200 and 1300 K for 1519.5 kPa (15 atm) operations. Complete conversion of solid GeO_2 to gaseous germanium monoxide (GeO) occurs at 1300 K in AFBC designs, as shown in reaction 62:

$$GeO_2(s) \longrightarrow GeO(g) + 1/2\ O_2(g) \quad . \qquad (62)$$

The percent distribution of Ge in the solid oxide and gaseous phases as a function of operating pressure and temperature for combustion of a U.S. mean coal with 100 percent excess air and 90 percent S-removal efficiencies is shown in Figures 117 and 118. Although the equilibrium calculations are based on a reaction with a limited number of species,

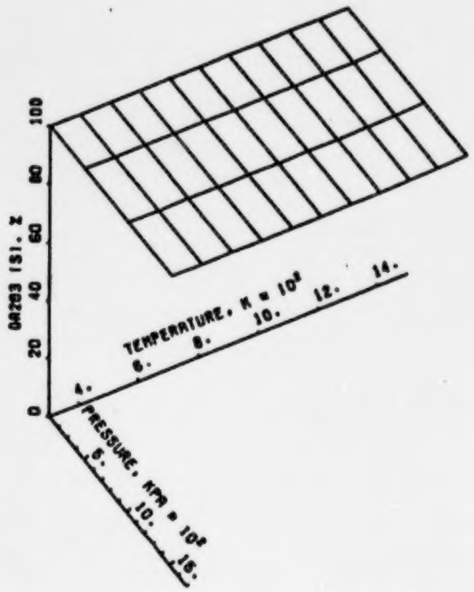

Figure 115 - Percent Distribution of Solid Ga_2O_3 as a Function of Temperature and Pressure in a Fluidized-Bed Combustor Operating with 100% Excess Air and 90% Sulfur-Removal Efficiencies

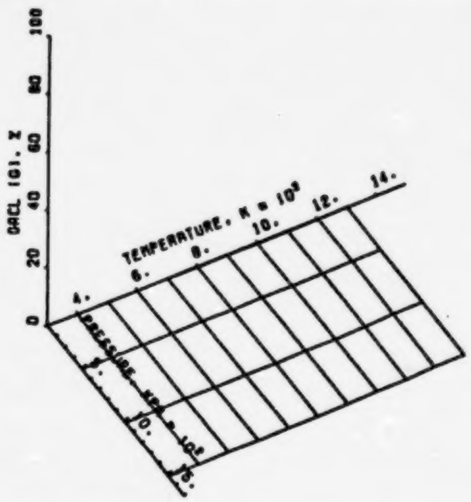

Figure 116 - Percent Distribution of Gaseous GaCl as a Function of Temperature and Pressure in a Fluidized-Bed Combustor Operating with 100% Excess Air and 90% Sulfur-Removal Efficiencies

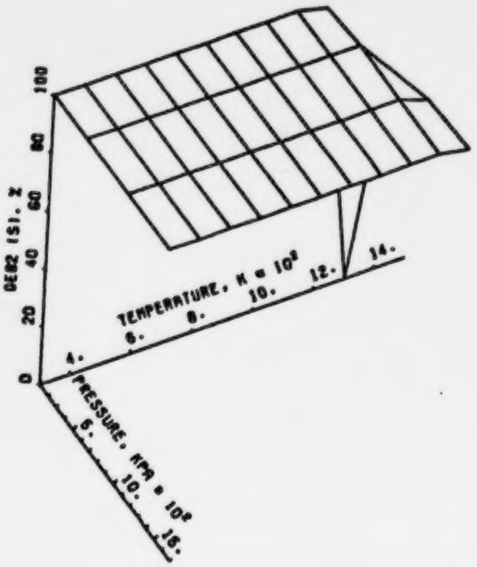

Figure 117 - Percent Distribution of Solid GeO_2 as a Function of Temperature and Pressure in a Fluidized-Bed Combustor Operating with 100% Excess Air and 90% Sulfur-Removal Efficiencies

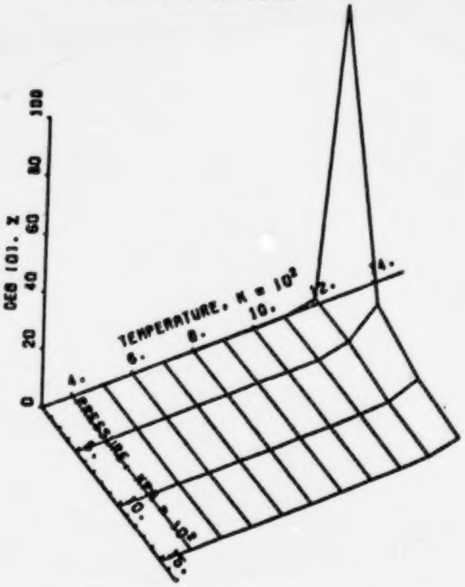

Figure 118 - Percent Distribution of Gaseous GeO as a Function of Temperature and Pressure in a Fluidized-Bed Combustor Operating with 100% Excess Air and 90% Sulfur-Removal Efficiencies

the projected results should be regarded as candidate reactions that are subject to change when new data supporting additional phases and complexes are included in the equilibrium mixture.

SUMMARY OF TRACE AND MINOR ELEMENT REACTIONS IN FLUIDIZED-BED COMBUSTION SYSTEMS

The equilibrium projections of the trace and minor element reactions with combustion products containing carbon, hydrogen, nitrogen, oxygen, sulfur, and chlorine are summarized in Table 34. The feedstock elements may be classified as constituents that:

- Volatilize completely: Be, F, Hg, Pb, Mo, Br, B, P, Cu, As, Cd, and Se
- Volatilize partially: Co, Cr, Mn, Ni, and Sn
- Remain as stable solid complexes: Fe, Ti, Al, Si, V, Zn, Zr, and Ga

in FBC where 100 percent of the initial elemental concentration was released from the carbon or clay matrix and no significant interaction between the trace or minor elements occurred. The operating pressure within the combustor defines the volatility of the resulting Na, K, Sb, and Ge species: at ambient pressures these species volatilize completely and are emitted at 100 percent of the feedstock concentration into the effluent gases leaving the FBC, while at 1520 kPa operations partial volatilization of the feedstock Na, K, Sb, and Ge is projected. The percent distribution of the trace and minor elements within the condensed and gaseous phases formed in various combustion systems operating at temperatures of 1100 to 1300 K at 101 and 1520 kPa is illustrated in Tables 35 through 40.

The volatile elements Be, F, Hg, Pb, Mo, Br, B, P, Cu, As, Cd, Se, Na, K, Sb, and Ge can be divided into those elements that will not condense on cooling (Hg and Br, in addition to Cl); and those that will

TABLE 34 - SUMMARY OF TRACE AND MINOR ELEMENT REACTIONS IN FLUIDIZED-BED COMBUSTION SYSTEMS

Dwg. 5592C83

Element	Coal Wt %/ppm	Condensed Phases	Sulfate/Oxide Conversion Reactions	Temperature Range for the Formation of Stable Oxide Solids	Volatile Phases*	Percent Volatilization at 1300K		Comment[83]
						101kPa	1520kPa	
Be	1.61 ppm	$BeSO_4$	$BeSO_4(s) \xrightarrow{700-900K} BeO(s) + SO_2(g) + 1/2O_2(g)$	BeO (700-1200K)	$Be(OH)_2$	100	100	· Be is not well absorbed but is retained in the lungs and mobilized slowly. · At present, it is not clear whether exposure to Be compounds increases the incidence of carcinomas in humans.
F	60.94 ppm	-	-	-	HF, HSO_3F	100	100	· Chronic fluoride poisoning has been observed in livestock when water contains 10 to 15 mg/l of flouride. · Fluoride may be transformed by some organisms into far more toxic organic fluorides.
Hg	0.20 ppm	-	-	-	Hg, $HgCl_2$, HgO Hg_2, HgCl	100	100	· Exposure to Hg vapor results in absorption by the lungs, with secondary amounts taken into the skin. · All organic forms are toxic to man, particularly the alkyl form. · Mercurials accumulate and are retained in the nervous system, causing poisoning.
Pb	34.78 ppm	-	-	-	$PbCl_4$, $PbCl_2$, PbO, PbCl	100	100	· Toxic effects on humans include hemolytic and renal poisoning. · Of the lead ingested, 5 to 10% is absorbed, and about 37% of the inhaled lead remains in the lungs. Once absorbed, lead accumulates primarily in the bones.
Co	9.57 ppm	$CoSO_4$, Co_3O_4, CoO	$3CoSO_4(s) + 1/2O_2(g) \xrightarrow{900-1100K} Co_3O_4(s) + 3SO_2(g) + 3/2O_2(g)$	Co_3O_4(1100-1300K)	$CoCl_2$, $CoCl_3$, Co_2Cl_4, CoCl	26	27	· Significant retention of Co by humans does not occur. · No reported toxic effects of Co to humans.
Cr	13.75 ppm	Cr_2O_3	$Cr_2O_3(s)$	Cr_2O_3(300-1200K)	CrO_4H_2, CrO_2Cl_2, CrO_2OH, CrO_3, CrO_2, $CrCl_3$, $CrCl_2$, $CrCl_4$, CrO, CrCl, Cr	28-100	25-100	· Even in its most soluble form Cr is not absorbed by mammals. · The presence of Cr in the trivalent state does not produce adverse effects in humans. Occupational lung cancer may however be associated with the hexavalent chromium state.
Fe	1.92%	Fe_2O_3, $Fe_2(SO_4)_3$	$Fe_2(SO_4)_3(s) \xrightarrow{800-900K} Fe_2O_3(s) + 3SO_2(g) + 3/2O_2(g)$	Fe_2O_3(900-1300K)	$FeCl_2$, $Fe(OH)_2$ $FeCl_3$, FeO Fe_2Cl_4, FeCl, $(FeCl_3)_2$, Fe	0	0	· Because Fe is hemostatically controlled, it is not toxic to man.
Mo	7.54 ppm	MoO_3	$MoO_3(s)$	MoO_3 (300-700K)	MoO_4H_2, MoO_2Cl_2, MoO_3, MoO_2, $MoCl_4$, MoO, $MoCl_5$, $MoCl_6$	100	100	· No data is available documenting Mo toxicity in man due to industrial exposure.

TABLE 34 (Continued)

Dwg. 5992C84

Element	Coal Wt %/ppm	Condensed Phases	Sulfate/Oxide Conversion Reactions	Temperature Range for the Formation of Stable Oxide Solids	Volatile Phases*	Percent Volatilization at 1300K		Comment[83]
						101kPa	1520kPa	
Mn	49.40 ppm	$MnSO_4$, Mn_2O_3, Mn_3O_4	$2MnSO_4(s) + 1/2O_2(g) \xrightarrow{800\text{-}900K} Mn_2O_3(s) + 2SO_3(g) + O_2(g)$	Mn_2O_3(1000-1200K)	$MnCl_2$, MnCl, MnO, Mn	8-12	5-8	•Mn is a required cofactor for a number of mammalian enzymes. •Mn is generally nontoxic to man, except from chronic inhalation of MnO_2 during occupational exposure over long periods of time.
Ni	21.07 ppm	$NiSO_4$, NiO	$NiSO_4(s) \xrightarrow{800\text{-}1000K} NiO(s) + SO_2(g) + 1/2O_2(g)$	NiO (1000-1200K)	$NiCl_2$, $Ni(OH)_2$, NiCl, NiO, Ni NiH	13	13	•Nickel carbonyl, $Ni(CO)_4$, is the most toxic of all Ni compounds to man, causing death after exposure of 30 ug/g for 30 minutes. •$Ni(CO)_4$ is implicated as a respiratory carcinogen. •When inhaled or absorbed through the skin Ni as a particulate air pollutant is deleterious to humans and mammals.
Ti	0.07%	TiO_2	$TiO_2(s)$	TiO_2(300-1200K)	$TiOCl_2$, $TiCl_3$, $TiCl_2$, TiCl, $TiCl_4$, TiOCl, TiO_2, TiO	0	0	•Metals, salts, and oxides of Ti are all nontoxic to man, and in most cases considered physically inert.
Na	0.05%	Na_2SO_4	Volatilization of Sulfate	-	NaCl, NaOH, Na_2SO_4	100	6-92	•No reported toxic effect. •Formation of corrosive liquid melts at combustion temperatures.
K	.0.16%	K_2SO_4	Volatilization of Sulfate	-	KCl, KOH, K_2SO_4	100	10-80	•No reported toxic effect.
Al	.1.29%	Al_2O_3, $Al_2(SO_4)_3$	$Al_2(SO_4)_3(s) \xrightarrow{700\text{-}800K} Al_2O_3(s) + 3SO_2(g) + 3/2O_2(g)$	Al_2O_3(800-1300K)	$AlCl_3$, AlOCl, $AlCl_2$, AlOH, AlCl, AlO, Al_3Cl_6	0	0	•Only massive oral doses of Al are expected to be toxic to mammals.
Si	2.49%	SiO_2	$SiO_2(s)$	300-1300K	$SiCl_4$, $SiCl_3$, $SiCl_2$, SiCl, SiO_2, SiO	0	0	•No reported toxic effect.
Br	15.42 ppm	-	-	-	BrH, Br_2, Br, BrCl, BrO, NOBr	100	100	•No reported toxic effect.
B	102.21 ppm	H_3BO_3, HBO_2	-	-	BHO_2, H_3BO_3, $(HBO_2)_3$, BO_2	100	100	•Concentrations of B as high as 30 mg/ℓ of water are not harmful to man.
P	71.10 ppm	H_3PO_4	-	-	$(P_2O_5)_2$, PO_2	100	100	•No reported toxic effect. •Low melting temperature liquids.
Cu	15.16 ppm	CuO, $CuSO_4$ $CuO \cdot CuSO_4$	$2CuSO_4(s) \xrightarrow{>1078K} CuO(s) + SO(g) + 1/2O_2(g)$	CuO(s) directly volatilizes	CuCl, CuO Cu_3Cl_3, Cu, Cu_2, CuS, CuH	100	100	•No reported toxic effect.
V	32.71 ppm	V_2O_5	$V_2O_5(s,l)$	$V_2O_5(s)$ (300-943K) $V_2O_5(l)$ (943-1300K)	$VOCl_3$, VO_2, VCl_4, VO, V, VN	0.03	0.03	•Toxicity of V is largely confined to the respiratory tract. •V may have a catalytic effect on the oxidation of atmospheric sulfur dioxide to sulfur trioxides. SO_3 then dissolved in water, forms sulfuric acid or sulfates. •Liquid melt formations at combustion temperatures induce corrosive attack.

TABLE 34 (Continued)

Dwg. 5592C85

Element	Coal Wt %/ppm	Condensed Phases	Sulfate/Oxide Conversion Reactions	Temperature Range for the Formation of Stable Oxide Solids	Volatile Phases*	Percent Volatilization at 1300K		Comment[83]
						101kPa	1520kPa	
Zn	272.29 ppm	$ZnSO_4 \cdot 7H_2O$, $ZnSO_4 \cdot H_2O$ $ZnSO_4 \cdot ZnO$	$ZnSO_{4}(s) \xrightarrow{500-1200K} ZnO(s) + SO_2(g) + 1/2O_2(g)$	500-1200K	Zn, ZnCl, Zn_2, ZnS, ZnH	0.3-0.5	0.01-0.10	· Zn is antagonistic to the detrimental effects of Cd. · Zn oxide fumes induce fever in man which disappears within 24 to 48 hours.
Sb	1.26 ppm	SbO_2	$SbO_2(s)$	300-1300K	SbCl, $SbCl_3$, Sb	100	3-5	· Possible relationship between Sb and pulmonary carcinogenesis based on abnormal enzyme formations. · Sb is also implicated in heart disease.
Sn	4.79 ppm	SnO_2	$SnO_2(s)$	300-1300K	SnO, $SnCl_2$, $SnCl_4$	2-3	0.1-0.3	· Ingested inorganic Sn is not absorbed in humans but concentrates in the liver and kidneys. · Inhaled inorganic tin remains in the lungs, whereas organic tin may enter the blood stream and accumulate in the liver.
Zr	72.46 ppm	ZrO_2	$ZrO_2(s)$	300-1300K	$ZrCl_4$	0	0	· No reported toxic effect.
As	14.02 ppm	As_2O_5	$As_2O_5(s)$	300 to 1000-1200K	AsCl, AsO, AsN, $AsCl_3$	100	100	· Toxicity of As in humans depends upon the chemical form. · Organic arsenic compounds are considerably more toxic than inorganic forms. · Toxic effects on humans include poisoning of the oxidative phosphorylation system, and as carcinogens.
Cd	2.52 ppm	$CdSO_4$	$CdSO_4(s) \xrightarrow{900-1100K} CdO(g) + SO_2(g) + 1/2O_2(g)$	300 to 900-1000K	CdO, Cd, CdCl	100	100	· Toxic effects on humans include hypertension, pulmonary emphysema, and carcinoma formation in the lungs.
Se	2.08 ppm	-	-	-	SeO	100	100	· Toxic effects on humans include degeneration of the liver and kidney, cancer of the liver, and pneumonia.
Ga	3.12 ppm	Ga_2O_3	$Ga_2O_3(s)$	300-1300K	GaCl	0.5-0.6	0.03-0.04	· There are no reported adverse effects of Ga in humans following industrial exposure. · Exposure to excessive Ga concentrations include tumor formation, neuro muscular poisoning, and kidney damage.
Ge	6.59 ppm	GeO_2	$GeO_2(s)$	300-1300K	GeO	100	2-4	· Toxicity of Ge and its compounds is low in mammals even when present at very high levels.

* Major Volatile Phases Are Reported Initially.

TABLE 35 - PERCENT DISTRIBUTION OF TRACE AND MINOR ELEMENTS IN 10% EXCESS AIR, 0% SULFUR-REMOVAL, FLUIDIZED-BED COMBUSTION SYSTEMS

	1100K		1200K		1300K	
COMPOUND	1ATM	15ATM	1ATM	15ATM	1ATM	15ATM
BEO (S)	97.92	97.92	89.62	89.62	---	---
BE(OH)2 (G)	2.08	2.08	10.38	10.38	99.99	99.99
BECL2 (G)	---	---	---	---	0.01	0.01
HF (G)	100.	100.	100.	100.	100.	100.
HGO (G)	1.12	3.98	0.94	3.50	0.80	3.02
HGCL2 (G)	0.09	4.91	0.01	0.47	---	0.06
HG (G)	98.79	91.11	99.05	96.03	99.20	96.92
HGCL (G)	---	---	---	---	---	---
PBO (G)	---	---	0.60	---	23.03	0.21
PBCL4 (G)	99.61	99.99	83.64	99.67	11.47	91.87
PBCL2 (G)	0.39	0.01	15.34	0.33	56.82	7.77
PBCL (G)	---	---	0.42	---	8.53	0.15
PB (G)	---	---	---	---	0.15	---
CO3O4 (S)	92.61	---	---	---	---	---
COO (S)	---	---	84.77	84.76	73.56	73.31
COSO4 (S)	---	97.80	---	---	---	---
COCL2 (G)	7.39	2.20	15.23	15.23	26.44	26.69
CR2O3 (S)	97.15	96.64	91.41	92.51	72.12	75.65
CRO3 (G)	---	---	0.02	0.01	0.12	0.06
CRO2CL2 (G)	0.23	1.73	0.17	1.26	0.13	0.96
CRO4H2 (G)	1.99	1.00	4.40	2.23	8.66	4.39
CRO2OH (G)	0.63	0.63	4.00	3.99	18.97	18.94
FE2O3 (S)	100.	100.	100.	100.	100.	100.
MOO2CL2 (G)	0.71	0.71	0.30	0.03	0.14	0.15
MOO3 (G)	---	---	0.01	---	0.03	---
H2MOO4 (G)	99.29	99.29	99.69	99.70	99.83	99.85
MN2O3 (S)	---	99.20	---	---	---	---
MN3O4 (S)	98.60	---	95.43	97.08	87.85	92.18
MNCL2 (G)	1.40	0.80	4.57	2.92	12.15	7.82
NIO (S)	98.19	98.19	94.91	94.91	86.61	86.52
NI(OH)2 (G)	0.10	0.10	0.73	0.73	3.92	3.92
NICL2 (G)	1.71	1.71	4.36	4.36	9.46	9.56
NICL (G)	---	---	---	---	0.01	---
TIO2 (C)	100.	100.	100.	100.	100.	100.
NA2SO4 (C)	98.63	100.	81.34	100.	---	93.67
NACL (G)	1.37	---	18.66	---	100.	6.33
NA2CL2 (G)	---	---	---	---	---	---
NA2SO4 (G)	---	---	---	---	---	---
NAOH (G)	---	---	---	---	---	---
K2SO4 (S)	98.21	100.	74.49	99.06	---	89.54
KCL (S)	---	---	---	---	---	---
K2CL2 (G)	---	---	---	---	---	---
KCL (G)	1.79	---	21.45	0.94	73.60	8.13
K2SO4 (G)	---	---	4.06	---	26.07	2.33
KOH (G)	---	---	---	---	0.33	---
AL2O3 (S)	100.	100.	100.	100.	100.	100.
SIO2 (C)	100.	100.	100.	100.	100.	100.

TABLE 35 (Continued)

```
----------------------------------------------------------------------
BRH (G)       // 53.28 /  66.25 //  47.19/  62.76 // 41.87 / 41.97
BRO (G)       //  0.01 /   0.03 //  0.01 /   0.03 //  0.02 /  0.02
BRCL (G)      //  0.94 /   4.49 //  0.33 /   1.71 //  0.14 /  0.14
BR (G)        // 45.69 /  28.77 // 52.45 /  35.38 // 57.97 / 58.13
BR2 (G)       //  0.04 /   0.23 //  0.01 /   0.06 //  ---  /  ---
NOBR (G)      //  ---  /    0.01//  ---  /   0.01 //  ---  /  ---
----------------------------------------------------------------------
(HBO2)3 (G)   //  0.05 /  0.06  //  0.01 /  0.05  //  ---  /  0.03
H3BO3 (G)     // 84.67 / 98.77  // 52.41 / 94.20  // 20.73 / 79.62
BHO2 (G)      // 13.72 /  1.07  // 47.19 /  5.65  // 79.24 / 20.29
BO2 (G)       // ---   /  ---   //  ---  /  ---   //  ---  /  ---
----------------------------------------------------------------------
(P2O5)2 (G)   // 99.98 / 99.98  // 99.93 / 99.97  // 98.83 / 99.90
PO2 (G)       //  ---  /  ---   //  0.05 /  0.03  //  1.15 /  0.08
----------------------------------------------------------------------
CU3CL3 (G)    // 11.00 / 72.60  //  0.14 / 17.90  //  ---  /  0.60
CUCL (G)      // 89.00 / 27.40  // 99.85 / 82.08  // 99.76 / 99.28
CUO (G)       //  ---  /  ---   //  0.01 /  0.02  //  0.24 /  0.12
----------------------------------------------------------------------
V2O5 (L)      // 99.98 / 99.73  // 99.99 / 99.75  // 99.98 / 99.77
VOCL3 (G)     //  0.02 /  0.09  //  0.01 /  0.05  //  0.01 /  0.03
VO2 (G)       // ---   /  ---   //  ---  /  ---   //  0.01 /  ---
----------------------------------------------------------------------
ZNO (S)       // 99.99 /  ---   // 99.99 / 99.99  // 99.56 / 99.99
ZNSO4 (S)     //  ---  /100.    //  ---  /  ---   //  ---  /  ---
ZN (G)        //  ---  /  ---   //  0.01 /  ---   //  0.43 /  ---
ZNCL (G)      //  ---  /  ---   //  ---  /  ---   //  ---  /  ---
----------------------------------------------------------------------
SBO2 (S)      // 99.59 / 99.26  // 96.69 / 98.66  //  ---  / 95.12
SBO (G)       //  0.01 /  ---   //  1.63 /  0.03  // 75.23 /  1.77
SBCL3 (G)     //  0.38 /  0.74  //  0.65 /  1.28  //  0.72 /  1.98
SBCL (G)      //  0.02 /  ---   //  1.03 /  0.03  // 24.04 /  1.12
SB (G)        //  ---  /  ---   //  ---  /  ---   //  0.01 /  ---
----------------------------------------------------------------------
SNO2 (S)      // 99.99 /100.    // 99.96 / 99.97  // 97.10 / 99.72
SNCL2 (G)     //  0.01 /  ---   //  0.01 /  0.03  //  0.95 /  0.25
SNO (G)       //  ---  /  ---   //  0.03 /  ---   //  1.95 /  0.03
----------------------------------------------------------------------
ZRO2 (S)      //100.    /100.    //100.    /100.    //100.    /100.
----------------------------------------------------------------------
AS2O5 (S)     //  ---  / 79.08  //  ---  /  ---   //  ---  /  ---
ASO (G)       //  4.93 / 10.51  // 14.21 /  7.73  // 30.83 / 18.38
ASCL3 (G)     //  0.08 /  0.95  //  0.01 /  0.32  //  ---  /  0.03
ASCL (G)      // 94.99 / 19.46  // 85.78 / 91.95  // 69.16 / 81.59
ASN (G)       //  ---  /  ---   //  ---  /  ---   //  0.01 /  ---
----------------------------------------------------------------------
CDO (G)       // 97.14 / 98.92  // 93.93 / 98.11  // 88.60 / 96.58
CDCL (G)      //  0.19 /  0.37  //  0.14 /  0.29  //  0.11 /  0.24
CD (G)        //  2.67 /  0.71  //  5.93 /  1.60  // 11.29 /  3.18
----------------------------------------------------------------------
SEO (G)       //100.    /100.    //100.    /100.    //100.    /100.
----------------------------------------------------------------------
GA2O3 (S)     //100.    /100.    // 99.97 /100.    // 99.34 / 99.96
GACL (G)      //  ---  /  ---   //  0.03 /  ---   //  0.66 /  0.04
----------------------------------------------------------------------
GEO2 (S)      // 99.97 /100.    // 96.80 / 99.94  //  ---  / 97.33
GEO (G)       //  0.03 /  ---   //  3.20 /  0.06  //100.    /  2.67
```

TABLE 36 - PERCENT DISTRIBUTION OF TRACE AND MINOR ELEMENTS IN 10% EXCESS AIR, 99% SULFUR-REMOVAL, FLUIDIZED-BED COMBUSTION SYSTEMS

	1100K		1200K		1300K	
COMPOUND	1ATM	15ATM	1ATM	15ATM	1ATM	15ATM
BEO (S)	97.92	97.92	89.62	89.62	---	---
BE(OH)2 (G)	2.08	2.08	10.38	10.38	99.99	99.99
BECL2 (G)	---	---	---	---	0.01	0.01
HF (G)	100.	100.	100.	100.	100.	100.
HGO (G)	1.20	4.27	1.00	3.76	0.86	3.24
HGCL2 (G)	0.10	5.26	0.01	0.50	---	0.07
HG (G)	98.70	90.47	98.99	95.74	99.14	96.69
HGCL (G)	---	---	---	---	---	---
PBO (G)	---	---	0.56	---	22.92	0.20
PBCL4 (G)	99.64	99.99	84.58	99.70	12.22	92.38
PBCL2 (G)	0.36	0.01	14.47	0.30	56.53	7.28
PBCL (G)	---	---	0.39	---	8.19	0.14
PB (G)	---	---	---	---	0.14	---
CO3O4 (S)	92.78	95.41	---	---	---	---
COO (S)	---	---	84.77	84.76	75.58	73.31
COSO4 (S)	---	---	---	---	---	---
COCL2 (G)	7.22	4.59	15.23	15.24	26.42	26.69
CR2O3 (S)	96.85	96.25	90.61	91.81	69.78	73.66
CRO3 (G)	---	---	0.02	0.01	0.14	0.07
CRO2CL2 (G)	0.26	1.95	0.19	1.41	0.14	1.07
CRO4H2 (G)	2.21	1.12	4.89	2.48	9.61	4.88
CRO2OH (G)	0.68	0.68	4.29	4.29	20.33	20.32
FE2O3 (S)	100.	100.	100.	100.	100.	100.
MOO2CL2 (G)	0.71	0.71	0.30	0.30	0.14	0.15
MOO3 (G)	---	---	0.01	---	0.03	---
H2MOO4 (G)	99.29	99.29	99.69	99.70	99.83	99.85
MN2O3 (S)	---	99.23	---	---	---	---
MN3O4 (S)	98.63	---	95.53	97.15	88.13	92.37
MNCL2 (G)	1.37	0.77	4.47	2.85	11.87	7.64
NIO (S)	98.19	98.19	94.91	94.91	86.61	86.52
NI(OH)2 (G)	0.10	0.10	0.73	0.73	3.92	3.92
NICL2 (G)	1.71	1.71	4.36	4.36	9.46	9.56
NICL (G)	---	---	---	---	0.01	---
TIO2 (C)	100.	100.	100.	100.	100.	100.
NA2SO4 (C)	54.77	57.99	---	57.99	---	33.32
NACL (G)	42.26	25.63	97.40	36.49	100.	66.68
NA2CL2 (G)	2.97	16.38	2.60	5.52	---	---
NA2SO4 (G)	---	---	---	---	---	---
NAOH (G)	---	---	---	---	---	---
K2SO4 (S)	29.58	29.58	10.26	29.58	---	22.81
KCL (S)	---	9.14	---	---	---	---
K2CL2 (G)	7.41	29.06	2.45	15.86	---	6.20
KCL (G)	63.01	32.22	83.04	54.56	96.27	68.66
K2SO4 (G)	---	---	4.07	---	2.67	2.33
KOH (G)	---	---	0.18	---	1.06	---
AL2O3 (S)	100.	100.	100.	100.	100.	100.
SIO2 (C)	100.	100.	100.	100.	100.	100.

TABLE 36 (Continued)

```
--------------------------------------------------------------------------
BRH (G)        // 52.37 / 65.31   // 46.31 / 61.86   // 41.03 / 57.36
BRO (G)        //  0.01 /  0.03   //  0.01 /  0.04   //  0.02 /  0.05
BRCL (G)       //  0.99 /  4.77   //  0.35 /  1.81   // 14.17 /  0.77
BR (G)         // 46.55 / 29.50   // 53.30 / 36.17   // 58.81 / 41.78
BR2 (G)        //  0.04 /  0.48   //  0.01 /  0.06   //  ---  /  0.02
NOBR (G)       //  ---  /  ---    //  ---  /  0.01   //  ---  /  0.01
--------------------------------------------------------------------------
(HBO2)3 (G)    //  0.54 /  0.06   //  0.14 /  0.05   //  0.01 /  0.03
H3BO3 (G)      // 84.66 / 98.76   // 52.41 / 94.18   // 20.73 / 79.61
BHO2 (G)       // 13.72 /  1.07   // 47.19 /  5.65   // 79.24 / 20.29
BO2 (G)        //  ---  /  ---    //  ---  /  ---    //  ---  /  ---
--------------------------------------------------------------------------
(P2O5)2 (G)    // 99.98 / 99.98   // 99.93 / 99.98   // 98.88 / 99.91
PO2 (G)        //  ---  /  ---    //  0.05 /  ---    //  1.11 /  0.07
--------------------------------------------------------------------------
CU3CL3 (G)     //  2.11 / 61.90   //  0.05 /  7.98   //  ---  /  0.19
CUCL (G)       // 97.88 / 38.10   // 99.84 / 91.97   // 99.50 / 99.57
CUO (G)        //  0.01 /  ---    //  0.11 /  0.05   //  0.48 /  0.24
--------------------------------------------------------------------------
V2O5 (L)       // 99.98 / 99.92   // 99.99 / 99.95   // 99.98 / 99.96
VOCL3 (G)      //  0.02 /  0.08   //  0.01 /  0.05   //  0.01 /  0.03
VO2 (G)        //  ---  /  ---    //  ---  /  ---    //  0.01 /  ---
--------------------------------------------------------------------------
ZNO (S)        // 99.99 / 99.99   // 99.98 / 99.99   // 99.59 / 99.98
ZNSO4 (S)      //  ---  /  ---    //  ---  /  ---    //  ---  /  ---
ZN (G)         //  ---  /  ---    //  0.01 /  ---    //  0.40 /  0.01
ZNCL (G)       //  ---  /  ---    //  ---  /  ---    //  ---  /  ---
--------------------------------------------------------------------------
SBO2 (S)       // 99.60 / 99.28   // 96.92 / 98.70   //  0.00 / 95.43
SBO (G)        //  0.01 /  ---    //  1.53 /  0.03   // 75.84 /  1.65
SBCL3 (G)      //  0.37 /  0.72   //  0.63 /  1.24   //  0.76 /  1.91
SBCL (G)       //  0.02 /  ---    //  0.93 /  0.03   // 23.40 /  1.01
SB (G)         //  ---  /  ---    //  ---  /  ---    //  ---  /  ---
--------------------------------------------------------------------------
SNO2 (S)       // 99.99 /100.     // 99.87 / 99.97   // 97.29 / 99.74
SNCL2 (G)      //  0.01 /  ---    //  0.11 /  0.03   //  0.89 /  0.23
SNO (G)        //  ---  /  ---    //  0.02 /  ---    //  1.82 /  0.03
--------------------------------------------------------------------------
ZRO2 (S)       //100.    /100.    //100.    /100.    //100.    /100.
--------------------------------------------------------------------------
ASO (G)        //  5.10 /  0.46   // 14.63 /  7.99   // 31.58 / 18.91
ASCL3 (G)      //  0.09 /  0.88   //  0.01 /  0.34   //  ---  /  0.03
ASCL (G)       // 94.81 / 16.66   // 85.35 / 91.67   // 68.42 / 81.06
ASN (G)        //  ---  /  ---    //  ---  /  ---    //  ---  /  ---
AS2O5 (S)      //  ---  / 82.00   //  ---  /  ---    //  ---  /  ---
--------------------------------------------------------------------------
CDO (G)        // 97.32 / 98.98   // 94.31 / 98.22   // 89.28 / 96.80
CDCL (G)       //  0.18 /  0.36   //  0.14 /  0.28   //  0.11 /  0.23
CD (G)         //  2.50 /  0.66   //  5.55 /  1.50   // 10.61 /  2.97
--------------------------------------------------------------------------
SEO (G)        //100.    /100.    //100.    /100.    //100.    /100.
--------------------------------------------------------------------------
GA2O3 (S)      //100.    /100.    // 99.97 /100.     // 99.38 / 99.96
GACL (G)       //  ---  /  ---    //  0.03 /  ---    //  0.62 /  0.04
--------------------------------------------------------------------------
GEO2 (S)       // 99.97 /100.     // 97.02 / 99.95   //  ---  / 97.51
GEO (G)        //  0.03 /  ---    //  2.98 /  0.05   //100.    /  2.49
```

TABLE 37 - PERCENT DISTRIBUTION OF TRACE AND MINOR ELEMENTS IN 100% EXCESS AIR, 90% SULFUR-REMOVAL, FLUIDIZED-BED COMBUSTION SYSTEMS

	1100K		1200K		1300K	
COMPOUND	1ATM	15ATM	1ATM	15ATM	1ATM	15ATM
BEO (S)	97.92	97.92	89.62	89.62	---	---
BE(OH)2 (G)	2.08	2.08	10.38	10.38	99.99	99.99
BECL2 (G)	---	---	---	---	0.01	0.01
HF (G)	100.	100.	100.	100.	100.	100.
HGO (G)	2.43	8.30	2.03	7.39	1.74	6.41
HGCL2 (G)	0.11	5.76	0.10	0.56	---	0.07
HG (G)	97.46	85.94	97.96	92.05	98.26	93.52
HGCL (G)	---	---	---	---	---	---
PBO (G)	---	---	0.88	---	34.42	0.30
PBCL4 (G)	99.70	99.99	86.02	99.74	11.69	93.21
PBCL2 (G)	0.30	0.01	12.78	0.26	47.36	6.38
PBCL (G)	---	---	0.32	---	6.43	---
PB (G)	---	---	---	---	0.10	---
CO304 (S)	94.32	96.38	---	86.95	---	---
COO (S)	---	---	84.77	---	73.81	73.31
COSO4 (S)	---	---	---	---	---	---
COCL2 (G)	5.68	3.62	15.23	13.05	26.19	26.69
CR2O3 (S)	90.93	89.16	73.38	76.87	---	---
CRO3 (G)	0.01	---	0.09	0.05	0.83	0.49
CRO2CL2 (G)	0.75	5.70	0.54	4.12	0.47	4.26
CRO4H2 (G)	6.46	3.29	14.30	7.27	33.22	19.52
CRO2OH (G)	1.85	1.85	11.69	11.69	65.48	75.73
FE2O3 (S)	100.	100.	100.	100.	100.	100.
MOO2CL2 (G)	0.71	0.71	0.30	0.30	0.14	0.14
MOO3 (G)	---	---	0.01	---	0.06	0.01
H2MOO4 (G)	99.29	99.29	99.69	99.70	99.80	99.85
MN2O3 (S)	98.94	99.46	---	97.98	---	---
MN3O4 (S)	---	---	96.48	---	90.73	93.99
MNCL2 (G)	1.06	0.54	3.52	2.02	9.27	6.01
NIO (S)	98.19	98.19	94.91	94.91	86.70	86.52
NI(OH)2 (G)	0.10	0.01	0.73	0.73	3.91	3.92
NICL2 (G)	1.71	1.71	4.36	4.36	9.38	9.56
NICL (G)	---	---	---	---	0.01	---
TIO2 (C)	100.	100.	100.	100.	100.	100.
NA2SO4 (C)	94.24	99.99	40.66	96.83	---	75.74
NACL (G)	5.76	0.01	59.34	3.17	100.	24.26
NA2CL2 (G)	---	---	---	---	---	---
NA2SO4 (G)	---	---	---	---	---	---
NAOH (G)	---	---	---	---	---	---
K2SO4 (S)	92.04	100.	37.02	95.57	---	66.95
KCL (S)	---	---	---	---	---	---
K2CL2 (G)	---	---	0.61	---	---	---
KCL (G)	-7.96	---	55.14	4.43	88.06	28.90
K2SO4 (G)	---	---	7.23	---	11.30	4.15
KOH (G)	---	---	---	---	0.64	---
AL2O3 (S)	100.	100.	100.	100.	100.	100.
SIO2 (C)	100.	100.	100.	100.	100.	100.

TABLE 37 (Continued)

```
------------------------------------------------------------------------------
BRH (G)         // 35.62 / 49.60   // 31.18 / 45.79   // 26.74 / 41.98
BRO (G)         //  0.03 /  0.08   //  0.04 /  0.11   //  0.05 /  0.14
BRCL (G)        //  0.77 /  7.31   //  0.48 /  4.24   //  0.19 /  1.16
BR (G)          // 63.74 / 42.70   // 68.42 / 50.52   // 73.10 / 58.33
BR2 (G)         //  ---  /  0.56   //  ---  /  ---    //  ---  /  ---
NOBR (G)        //  ---  /  0.03   //  ---  /  0.02   //  ---  /  0.02
------------------------------------------------------------------------------
(HBO2)3 (G)     //  0.69 /  0.98   //  0.09 /  0.08   //  ---  /  0.04
H3BO3 (G)       // 76.03 / 97.79   // 38.36 / 90.12   // 12.83 / 68.76
BHO2 (G)        // 21.89 /  1.88   // 61.36 /  9.61   // 87.14 / 31.13
BO2 (G)         //  ---  /  ---    //  ---  /  ---    //  0.02 /  ---
------------------------------------------------------------------------------
(P2O5)2 (G)     // 99.99 /100.     // 99.93 / 99.97   // 98.78 / 99.90
PO2 (G)         //  ---  /  ---    //  0.05 /  ---    //  1.19 /  0.08
------------------------------------------------------------------------------
CU3CL3 (G)      //  2.11 / 62.0    //  0.05 /  7.99   //  ---  /  0.19
CUCL (G)        // 97.88 / 38.0    // 99.84 / 91.96   // 99.50 / 99.56
CUO (G)         //  0.01 /  ---    //  0.11 /  0.05   //  0.48 /  0.25
------------------------------------------------------------------------------
V2O5 (L)        // 99.98 / 99.94   // 99.99 / 99.96   // 99.97 / 99.97
VOCL3 (G)       //  0.02 /  0.06   //  0.01 /  0.04   //  0.01 /  0.03
VO2 (G)         //  ---  /  ---    //  ---  /  ---    //  0.02 /  ---
------------------------------------------------------------------------------
ZNO (S)         // 99.96 /  ---    // 99.99 / 99.97   // 99.65 / 99.99
ZNSO4 (S)       //  ---  /100.     //  ---  /  ---    //  ---  /  ---
ZN (G)          //  ---  /  ---    //  ---  /  ---    //  0.35 /  0.01
ZNCL (G)        //  ---  /  ---    //  ---  /  ---    //  ---  /  ---
------------------------------------------------------------------------------
SBO2 (S)        // 99.79 / 99.62   // 97.92 / 99.31   //  ---  / 97.10
SBO (G)         //  0.01 /  ---    //  1.32 /  0.02   // 85.69 /  1.43
SBCL3 (G)       //  0.19 /  0.38   //  0.33 /  0.65   //  0.51 /  1.00
SBCL (G)        //  0.01 /  ---    //  0.42 /  0.01   // 13.80 /  0.46
SB (G)          //  ---  /  ---    //  ---  /  ---    //  ---  /  ---
------------------------------------------------------------------------------
SNO2 (S)        // 99.99 /100.     // 99.93 / 99.99   // 97.99 / 99.86
SNCL2 (G)       //  0.01 /  ---    //  0.05 /  0.01   //  0.43 /  0.11
SNO (G)         //  ---  /  ---    //  0.02 /  ---    //  1.58 /  0.03
------------------------------------------------------------------------------
ZRO2 (S)        //100.   /100.     //100.   /100.     //100.   /100.
------------------------------------------------------------------------------
AS2O5 (S)       //  ---  / 94.09   //  ---  /  ---    //  ---  /  ---
ASO (G)         //  9.29 /  0.28   // 24.64 / 14.20   // 46.92 / 30.78
ASCL3 (G)       //  0.10 /  0.32   //  0.01 /  0.36   //  ---  /  0.03
ASCL (G)        // 90.61 /  5.31   // 75.35 / 85.44   // 53.08 / 69.19
ASN (G)         //  ---  /  ---    //  ---  /  ---    //  ---  /  ---
------------------------------------------------------------------------------
CDO (G)         // 98.67 / 99.49   // 97.13 / 99.11   // 94.46 / 98.40
CDCL (G)        //  0.09 /  0.19   //  0.08 /  0.15   //  0.06 /  0.22
CD (G)          //  1.24 /  0.32   //  2.79 /  0.74   //  5.48 /  1.48
------------------------------------------------------------------------------
SEO (G)         //100.   /100.     //100.   /100.     //100.   /100.
------------------------------------------------------------------------------
GA2O3 (S)       //100.   /100.     // 99.98 /100.     // 99.60 / 99.97
GACL (G)        //  ---  /  ---    //  0.02 /  ---    //  0.40 /  0.03
------------------------------------------------------------------------------
GEO2 (S)        // 99.97 /100.     // 97.41 / 99.96   //  ---  / 97.84
GEO (G)         //  0.03 /  ---    //  2.59 /  0.04   //100.   /  2.16
```

TABLE 38 - PERCENT DISTRIBUTION OF TRACE AND MINOR ELEMENTS IN 100% EXCESS AIR, 99% SULFUR-REMOVAL, FLUIDIZED-BED COMBUSTION SYSTEMS

COMPOUND	1100K		1200K		1300K	
	1ATM	15ATM	1ATM	15ATM	1ATM	15ATM
BEO (S)	97.92	97.92	89.62	89.62	---	---
BE(OH)2 (G)	2.08	2.08	10.38	10.38	99.99	99.99
BECL2 (G)	---	---	---	---	0.01	0.01
HF (G)	100.	100.	100.	100.	100.	100.
HGO (G)	2.43	8.31	2.03	7.40	1.74	6.42
HGCL2 (G)	0.11	5.76	0.01	0.56	---	0.07
HG (G)	97.46	85.93	97.96	92.04	98.26	93.51
HGCL (G)	---	---	---	---	---	---
PBO (G)	---	---	0.88	---	34.42	0.30
PBCL4 (G)	99.70	99.99	86.03	99.74	11.70	93.22
PBCL2 (G)	0.30	0.01	12.77	0.26	47.35	6.37
PBCL (G)	---	---	0.32	---	6.42	0.11
PB (G)	---	---	---	---	0.11	---
CO304 (S)	94.32	96.38	---	86.96	---	---
COO (S)	---	---	84.77	---	73.81	73.31
COSO4 (S)	---	---	---	---	---	---
COCL2 (G)	5.68	3.62	15.23	13.04	26.19	26.69
CR2O3 (S)	90.91	89.15	73.35	76.84	---	---
CRO3 (G)	0.01	---	0.09	0.05	0.83	0.49
CRO2CL2 (G)	0.75	5.71	0.54	4.13	0.47	4.26
CRO4H2 (G)	6.48	3.29	14.32	7.28	33.23	19.53
CRO2OH (G)	1.85	1.85	11.70	11.70	65.47	75.72
FE2O3 (S)	100.	100.	100.	100.	100.	100.
MOO2CL2 (G)	0.71	0.71	0.30	0.30	0.14	0.15
MOO3 (G)	---	---	0.01	---	0.06	---
H2MOO4 (G)	99.29	99.29	99.69	99.70	99.80	99.85
MN2O3 (S)	98.94	---	---	97.98	---	---
MN3O4 (S)	---	99.46	96.48	---	90.74	93.99
MNCL2 (G)	1.06	0.54	3.52	2.02	9.26	6.01
NIO (S)	98.19	98.19	94.91	94.91	86.70	86.52
NI(OH)2 (G)	0.10	0.10	0.73	0.73	3.91	3.92
NICL2 (G)	1.71	1.71	4.36	4.36	9.38	9.56
NICL (G)	---	---	---	---	0.01	---
TIO2 (C)	100.	100.	100.	100.	100.	100.
NA2SO4 (C)	53.87	57.99	---	57.99	---	25.89
NACL (G)	46.13	29.65	100.	38.54	100.	71.49
NA2CL2 (G)	---	12.35	---	3.46	---	2.62
NA2SO4 (G)	---	---	---	---	---	---
NAOH (G)	---	0.01	---	0.01	---	---
K2SO4 (S)	29.58	29.58	4.78	29.58	---	19.70
KCL (S)	---	---	---	---	---	---
K2CL2 (G)	4.57	28.15	1.51	10.69	---	3.87
KCL (G)	65.85	42.27	86.79	59.73	96.03	72.28
K2SO4 (G)	---	---	7.23	---	2.93	4.15
KOH (G)	---	---	---	---	1.04	---
AL2O3 (S)	100.	100.	100.	100.	100.	100.
SIO2 (C)	100.	100.	100.	100.	100.	100.

TABLE 38 (Continued)

BRH (G)	35.63	49.54	31.20	45.85	26.77	41.29
BRO (G)	---	0.08	---	0.11	0.05	0.14
BRCL (G)	0.77	7.29	0.48	2.75	0.19	1.14
BR (G)	63.76	42.67	68.48	51.14	73.20	57.37
BR2 (G)	---	0.56	---	0.07	---	0.02
NOBR (G)	---	---	---	0.02	---	0.02
(HBO2)3 (G)	0.69	0.09	0.09	0.08	---	---
H3BO3 (G)	76.03	97.83	38.36	90.13	12.83	68.76
BHO2 (G)	21.89	1.88	61.36	9.61	87.14	31.13
BO2 (G)	---	---	---	---	0.02	---
(P2O5)2 (G)	99.97	99.99	99.92	99.99	98.79	99.92
PO2 (G)	---	---	0.05	---	1.19	0.08
CU3CL3 (G)	2.11	61.90	0.05	7.98	---	0.19
CUCL (G)	98.01	38.10	99.94	92.00	99.57	99.64
CUO (G)	0.01	---	0.11	0.02	0.48	0.17
V2O5 (L)	99.98	99.93	100.	99.96	99.98	99.97
VOCL3 (G)	0.02	0.06	---	0.04	---	0.03
VO2 (G)	---	---	---	---	0.02	---
ZNO (S)	100.	99.99	99.99	100.	99.44	99.99
ZNSO4 (S)	---	---	---	---	---	---
ZN (G)	---	---	0.01	---	0.05	0.01
ZNCL (G)	---	---	---	---	---	---
SBO2 (S)	99.79	99.62	97.92	99.31		97.11
SBO (G)	0.01	---	1.32	0.02		1.43
SBCL3 (G)	0.19	0.38	0.33	0.65		1.00
SBCL (G)	0.01	---	0.42	0.01		0.46
SB (G)	---	---	---	---		---
SNO2 (S)	100.	100.	99.92	99.99	97.99	99.86
SNCL2 (G)	---	---	0.06	0.01	0.43	0.11
SNO (G)	---	---	0.02	---	1.58	0.03
ZRO2 (S)	100.	100.	100.	100.	100.	100.
AS2O5 (S)	---	94.10	---	---	---	---
ASO (G)	9.29	0.28	24.65	14.20	46.93	30.79
ASCL3 (G)	0.10	0.32	0.01	0.37	---	0.03
ASCL (G)	90.61	5.30	75.34	85.43	53.07	69.18
ASN (G)	---	---	---	---	---	---
CDO (G)	98.67	99.49	97.14	99.12	94.46	98.40
CDCL (G)	0.09	0.19	0.07	0.15	0.06	0.12
CD (G)	1.24	0.32	2.79	0.73	5.48	1.48
SEO (G)	100.	100.	100.	100.	100.	100.
GA2O3 (S)	100.	100.	99.98	100.	99.60	99.97
GACL (G)	---	---	0.02	---	0.40	0.03
GEO2 (S)	99.97	100.	97.41	99.96	---	97.84
GEO (G)	0.03	---	2.59	0.04	100.	2.16

TABLE 39 - PERCENT DISTRIBUTION OF TRACE AND MINOR ELEMENTS IN 300% EXCESS AIR, 0% SULFUR-REMOVAL, FLUIDIZED-BED COMBUSTION SYSTEMS

	1100K		1200K		1300K	
COMPOUND	1ATM	15ATM	1ATM	15ATM	1ATM	15ATM
BEO (S)	97.92	97.92	89.62	89.62	---	---
BE(OH)2 (G)	2.08	2.08	10.38	10.38	99.99	99.99
BECL2 (G)	---	---	---	---	0.01	0.01
HF (G)	100.	100.	100.	100.	100.	100.
HGO (G)	2.94	10.13	2.46	8.86	2.11	7.69
HGCL2 (G)	0.07	3.56	0.01	0.34	---	0.05
HG (G)	96.99	86.31	97.53	90.80	97.89	92.26
HGCL (G)	---	---	---	---	---	---
PBO (G)	---	---	2.56	0.01	52.16	0.93
PBCL4 (G)	99.50	99.99	78.04	99.58	5.43	88.98
PBCL2 (G)	0.50	0.01	18.80	0.41	36.02	9.88
PBCL (G)	---	---	0.60	---	6.26	0.21
PB (G)	---	---	---	---	0.13	---
CO3O4 (S)	94.67	96.61	---	87.77	---	---
COO (S)	---	---	84.77	---	74.08	73.31
COSO4 (S)	---	---	---	---	---	---
COCL2 (G)	5.33	3.39	15.23	12.23	25.92	26.69
CR2O3 (S)	87.17	84.81	59.92	64.68	---	---
CRO3 (G)	0.02	0.01	0.24	0.12	1.37	0.79
CRO2CL2 (G)	1.00	7.63	0.73	5.52	0.40	3.52
CRO4H2 (G)	8.66	4.40	19.16	9.73	27.99	16.11
CRO2OH (G)	3.15	3.15	19.95	19.95	70.24	79.58
FE2O3 (S)	100.	100.	100.	100.	100.	100.
MOO2CL2 (G)	0.71	0.71	0.30	0.30	0.14	0.14
MOO3 (G)	---	---	0.02	---	0.12	0.01
H2MOO4 (G)	99.29	99.29	99.68	99.70	99.74	99.85
MN2O3 (S)	99.04	99.51	---	98.16	---	94.48
MN3O4 (S)	---	---	96.70	---	91.41	---
MNCL2 (G)	0.96	0.49	3.30	1.84	8.59	5.52
NIO (S)	98.19	98.19	94.91	94.91	86.79	86.52
NI(OH)2 (G)	0.10	0.10	0.73	0.73	3.92	3.92
NICL2 (G)	1.71	1.71	4.36	4.36	9.28	9.56
NICL (G)	---	---	---	---	0.01	---
TIO2 (C)	100.	100.	100.	100.	100.	100.
NA2SO4 (C)	100.	100.	62.68	100.	---	86.23
NACL (G)	---	---	37.32	---	100.	13.77
NA2CL2 (G)	---	---	---	---	---	---
NA2SO4 (G)	---	---	---	---	---	---
NAOH (G)	---	---	---	---	---	---
K2SO4 (S)	95.99	100.	14.24	97.80	---	75.04
KCL (S)	---	---	---	---	---	---
K2CL2 (G)	---	---	---	---	---	---
KCL (G)	4.01	---	38.38	2.20	76.32	16.79
K2SO4 (G)	---	---	14.24	---	23.68	8.17
KOH (G)	---	---	---	---	---	---
AL2O3 (S)	100.	100.	100.	100.	100.	100.
SIO2 (C)	100.	100.	100.	100.	100.	100.

TABLE 39 (Continued)

BRH (G)	27.29	39.56	22.66	35.48	19.08	31.40
BRO (G)	---	1.24	---	0.45	0.06	0.19
BRCL (G)	1.28	7.15	0.42	7.27	0.16	1.04
BR (G)	71.54	52.70	76.96	60.09	80.74	67.49
BR2 (G)	---	0.44	---	0.78	---	---
NOBR (G)	---	---	---	0.09	---	---
(HBO2)3 (G)	0.08	0.17	0.05	0.12	---	0.03
H3BO3 (G)	62.35	95.81	24.05	82.31	6.95	52.79
BHO2 (G)	35.39	3.62	75.81	17.30	93.02	47.10
BO2 (G)	---	---	---	---	0.03	---
(P2O5)2 (G)	99.99	99.99	99.86	99.94	98.15	99.82
PO2 (G)	---	---	0.08	0.01	1.79	0.12
CU3CL3 (G)	0.08	45.91	0.01	2.44	---	0.05
CUCL (G)	99.91	54.19	99.82	97.47	99.25	99.57
CUO (G)	0.01	---	0.17	0.09	0.75	0.38
V2O5 (L)	99.99	99.95	99.99	99.97	99.99	99.98
VOCL3 (G)	0.01	0.05	0.01	0.03	0.01	0.02
VO2 (G)	---	---	---	---	---	---
ZNO (S)	100.	100.	99.99	99.99	99.42	99.99
ZNSO4 (S)	---	---	---	---	---	---
ZN (G)	---	---	---	---	0.03	---
ZNCL (G)	---	---	---	---	---	---
SBO2 (S)	99.86	99.76	97.20	99.53	---	96.54
SBO (G)	0.02	---	2.15	0.04	90.42	2.33
SBCL3 (G)	0.12	0.24	0.21	0.42	0.21	0.65
SBCL (G)	---	---	0.44	0.01	9.36	0.48
SB (G)	---	---	---	---	---	---
SNO2 (S)	100.	100.	99.92	99.99	97.08	99.87
SNCL2 (G)	---	---	0.05	0.01	0.35	0.09
SNO (G)	---	---	0.03	---	2.57	0.04
ZRO2 (S)	100.	100.	100.	100.	100.	100.
AS2O5 (S)	---	94.35	---	---	---	---
ASO (G)	13.68	0.41	33.61	20.41	57.90	40.77
ASCL3 (G)	0.06	0.19	---	0.21	---	0.02
ASCL (G)	86.26	5.05	66.39	79.38	42.10	59.21
ASN (G)	---	---	---	---	---	---
CDO (G)	98.85	99.49	97.60	99.20	95.37	98.63
CDCL (G)	0.12	0.24	0.09	0.20	0.07	0.15
CD (G)	1.02	0.27	2.31	0.60	4.56	1.22
SEO (G)	100.	100.	100.	100.	100.	100.
GA2O3 (S)	100.	100.	99.98	100.	99.54	99.97
GACL (G)	---	---	0.02	---	0.46	0.03
GEO2 (S)	99.96	100.	95.80	99.93	---	96.50
GEO (G)	0.04	---	4.20	0.07	100.	3.50

TABLE 40 - PERCENT DISTRIBUTION OF TRACE AND MINOR ELEMENTS IN 300% EXCESS AIR, 99% SULFUR-REMOVAL, FLUIDIZED-BED COMBUSTION SYSTEMS

	1100K		1200K		1300K	
COMPOUND	1ATM	15ATM	1ATM	15ATM	1ATM	15ATM
BEO (S)	97.92	97.92	89.62	89.62	---	---
BE(OH)2 (G)	2.08	2.08	10.38	10.38	99.99	99.99
BECL2 (G)	---	---	---	---	0.01	0.01
HF (G)	100.	100.	100.	100.	100.	100.
HGO (G)	2.95	10.16	2.46	8.88	2.11	7.71
HGCL2 (G)	0.07	3.57	0.01	0.03	---	0.05
HG (G)	96.98	86.27	97.53	90.79	97.89	92.24
HGCL (G)	---	---	---	---	---	---
PBO (G)	---	---	2.56	---	52.15	0.92
PBCL4 (G)	99.51	99.99	78.08	99.58	5.44	89.01
PBCL2 (G)	0.49	0.01	18.76	0.42	36.03	9.85
PBCL (G)	---	---	0.60	---	6.25	0.22
PB (G)	---	---	---	---	0.13	---
CO3O4 (S)	94.68	96.61	---	87.79	---	---
COO (S)	---	---	84.77	---	74.08	73.31
COSO4 (S)	---	---	---	---	---	---
COCL2 (G)	5.32	3.39	15.23	12.21	25.92	26.69
CR2O3 (S)	87.11	84.74	59.76	64.53	---	---
CRO3 (G)	0.02	0.01	0.25	0.13	1.37	0.79
CRO2CL2 (G)	1.01	7.67	0.73	5.55	0.40	3.52
CRO4H2 (G)	8.70	4.42	19.25	9.78	28.01	16.13
CRO2OH (G)	3.16	3.16	20.01	20.01	70.22	79.56
FE2O3 (S)	100.	100.	100.	100.	100.	100.
MOO2CL2 (G)	0.71	0.71	0.30	0.30	0.14	0.14
MOO3 (G)	---	---	0.02	---	0.12	0.01
H2MOO4 (G)	99.29	99.29	99.68	99.70	99.74	99.85
MN2O3 (S)	99.04	99.51	---	98.17	---	94.49
MN3O4 (S)	---	---	96.71	---	91.41	---
MNCL2 (G)	0.96	0.49	3.29	1.83	8.59	5.51
NIO (S)	98.19	98.19	94.91	94.91	86.79	86.52
NI(OH)2 (G)	0.10	0.10	0.73	0.73	3.92	3.92
NICL2 (G)	1.71	1.71	4.36	4.36	9.28	9.56
NICL (G)	---	---	---	---	0.01	---
TIO2 (C)	100.	100.	100.	100.	100.	100.
NA2SO4 (C)	48.22	57.99	---	58.00	---	8.38
NACL (G)	51.78	38.44	100.	42.00	100.	91.62
NA2CL2 (G)	---	3.57	---	---	---	---
NA2SO4 (G)	---	---	---	---	---	---
NAOH (G)	---	---	---	---	---	---
K2SO4 (S)	29.58	29.58	---	29.58	---	9.70
KCL (S)	---	---	---	---	---	---
K2CL2 (G)	---	20.16	---	6.26	---	---
KCL (G)	70.42	50.26	91.53	64.16	97.62	82.13
K2SO4 (G)	---	---	8.47	---	2.38	8.17
KOH (G)	---	---	---	---	---	---
AL2O3 (S)	100.	100.	100.	100.	100.	100.
SIO2 (C)	100.	100.	100.	100.	100.	100.

TABLE 40 (Continued)

```
-------------------------------------------------------------------------------
BRH (G)        // 27.17 / 39.59   // 22.65 / 35.48   // 19.09 / 31.37
BRO (G)        //  ---  /  0.12   //  ---  /  0.16   //  0.06 /  0.19
BRCL (G)       //  1.27 /  7.18   //  0.42 /  4.11   //  0.16 /  1.04
BR (G)         // 71.36 / 52.83   // 77.03 / 60.19   // 80.88 / 67.54
BR2 (G)        //  ---  /  0.44   //  ---  /  ---    //  ---  /  ---
NOBR (G)       //  ---  /  0.04   //  ---  /  ---    //  ---  /  ---
-------------------------------------------------------------------------------
(HBO2)3 (G)    // 0.75  /  0.17   //  0.05 /  0.12   //  ---  /  0.03
H3BO3 (G)      // 62.35 / 95.81   // 24.05 / 82.31   //  6.96 / 52.79
BHO2 (G)       // 35.39 /  3.63   // 75.81 / 17.30   // 93.12 / 47.11
BO2 (G)        //  ---  /  ---    //  ---  /  ---    //  0.03 /  ---
-------------------------------------------------------------------------------
(P2O5)2 (G)    // 99.97 / 99.99   // 99.87 / 99.95   // 98.16 / 99.83
PO2 (G)        //  ---  /  ---    //  0.08 /  0.01   //  1.79 /  0.12
-------------------------------------------------------------------------------
CU3CL3 (G)     //  0.08 / 46.01   //  0.01 /  2.26   //  ---  /  0.05
CUCL (G)       // 99.91 / 53.99   // 99.88 / 97.65   // 99.30 / 99.57
CUO (G)        //  0.01 /  ---    //  0.11 /  0.09   //  0.70 /  0.38
-------------------------------------------------------------------------------
V2O5 (L)       // 99.99 / 99.95   // 99.99 / 99.97   // 99.99 / 99.98
VOCL3 (G)      //  0.01 /  0.05   //  0.01 /  0.03   //  0.01 /  0.02
VO2 (G)        //  ---  /  ---    //  ---  /  ---    //  ---  /  ---
-------------------------------------------------------------------------------
ZNO (S)        //100.   / 99.99   // 99.99 /100.     // 99.44 / 99.99
ZNSO4 (S)      //  ---  /  ---    //  ---  /  ---    //  ---  /  ---
ZN (G)         //  ---  /  ---    //  0.01 /  ---    //  0.05 /  0.01
ZNCL (G)       //  ---  /  ---    //  ---  /  ---    //  ---  /  ---
-------------------------------------------------------------------------------
SBO2 (S)       // 99.86 / 99.76   // 97.21 / 99.53   //  ---  / 96.56
SBO (G)        //  0.02 /  ---    //  2.14 /  0.37   // 90.44 /  2.32
SBCL3 (G)      //  0.12 /  0.24   //  0.21 /  0.42   //  0.21 /  0.65
SBCL (G)       //  ---  /  ---    //  0.44 /  0.02   //  9.35 /  0.48
SB (G)         //  ---  /  ---    //  ---  /  ---    //  ---  /  ---
-------------------------------------------------------------------------------
SNO2 (S)       // 100.  /100.     // 99.93 / 99.99   // 97.09 / 99.87
SNCL2 (G)      //  ---  /  ---    //  0.04 /  0.01   //  0.35 /  0.09
SNO (G)        //  ---  /  ---    //  0.03 /  ---    //  2.56 /  0.04
-------------------------------------------------------------------------------
ZRO2 (S)       //100.    /100.    //100.    /100.    //100.    /100.
-------------------------------------------------------------------------------
AS2O5 (S)      //  ---  / 94.39   //  ---  /  ---    //  ---  /  ---
ASO (G)        // 13.70 /  0.41   // 33.64 / 20.44   // 57.94 / 40.81
ASCL3 (G)      //  0.06 /  0.19   //  ---  /  0.21   //  ---  /  0.02
ASCL (G)       // 86.24 /  5.01   // 66.36 / 79.35   // 42.06 / 59.17
ASN (G)        //  ---  /  ---    //  ---  /  ---    //  ---  /  ---
-------------------------------------------------------------------------------
CDO (G)        // 98.86 / 99.49   // 97.60 / 99.20   // 95.38 / 98.63
CDCL (G)       //  0.12 /  0.24   //  0.10 /  0.20   //  0.08 /  0.16
CD (G)         //  1.02 /  0.26   //  2.30 /  0.60   //  4.56 /  1.21
-------------------------------------------------------------------------------
SEO (G)        //100.    /100.    //100.    /100.    //100.    /100.
-------------------------------------------------------------------------------
GA2O3 (S)      //100.   /100.     // 99.98 /100.     // 99.54 / 99.97
GACL (G)       //  ---  /  ---    //  0.02 /  ---    //  0.46 /  0.03
-------------------------------------------------------------------------------
GEO2 (S)       // 99.96 /100.     // 95.81 / 99.93   //  ---  / 96.51
GEO (G)        //  0.04 /  ---    //  4.19 /  0.07   //100.   /  3.49
```

(Be, F, Pb, Mo, B, P, Cu, As, Cd, Se, Na, K, Sb, and Ge). In the simple, noninteractive equilibrium system condensates of BeO or $BeSO_4$, CaF_2 or MgF_2,* PbO,** MoO_3, H_3BO_3 or HBO_2, H_3PO_4, CuO or $CuSO_4$, As_2O_5, CdO or $CdSO_4$, SeO,** Na_2SO_4 or NaCl, K_2SO_4 or KCl, SbO_2, and GeO_2 are likely to form as the effluent gas temperature cools.

Localized SO_2 partial pressures may enhance the transition of CoO/Co_3O_4, Fe_2O_3, MnO_2/Mn_3O_4, NiO, Al_2O_3, or ZnO fume or ash-associated phases into sulfate complexes as the aerosol droplets or particulates migrate into the cooler regimes of the FBC system. Formed as stable solid oxides within the combustor, Cr_2O_3, TiO_2, SiO_2, SnO_2, ZrO_2, and Ga_2O_3 will not undergo further reaction downstream with combustion gas constituents. Vanadium, projected to form a liquid melt at combustion temperatures ($V_2O_5(l)$), may condense as droplets at temperatures lower than 963 K, nucleate along entrained ash, forming sticky, potentially corrosive sites, or enter into additional trace or minor element reactions. Similar to the corrosive melt formation of V_2O_5 at FBC temperatures, formation of Na as a liquid sulfate (Na_2SO_4) is projected at FBC temperatures higher than 1157 K, as well as reaction with solid K_2SO_4 to form a low melting temperature eutectic. Both of these effects are potentially corrosive and deleterious to hardware life. In the simple combustion gas reactions, P is projected to form liquid H_3PO_4 at temperatures below 800 K. If directly deposited on the alloy surface, the liquid may cause catastrophic corrosive attack through accelerated oxidation of the protective oxide layer on the exposed metal surface.

The parametric equilibrium projections have used the equilibrium model to indicate the maximum concentration of the various elements in resulting volatile or condensed phases leaving the combustor. Preliminary interactions that attempt to illustrate the in-bed partitioning of the trace and minor elements through the formation of stable in-bed solid phases are presented in the following section. These interactions, if equilibrium were attained, would minimize the concentration of volatiles escaping from the bed and would serve as a second approximation for the total concentration emitted from the stack. It may seem unrealistic to assume that additional reactions along entrained ash particles do not occur, nor deposition reactions along cooler metal surfaces within either the particle collector devices or the gas turbine. Evaluation of these reactions will demonstrate further minimization of the trace and/or minor element concentration permitted to escape at the stack.

---

*Will be demonstrated in the following interactive reaction systems.

**Although not thermodynamically projected, it is possible that PbO and SeO are likely to form within the FBC system at reduced temperatures.

The validity of the interactive thermodynamic equilibrium projections lies within the accuracy of the molecular constant data and heats of formation and the entropy values for each compound used in the calculations. Delineation by chemical analysis of the silicate or aluminosilicate phase that complexes with either the alkali, trace, or minor elements in the ash, the spent sorbent, or the getter materials is essential in order to correlate the thermodynamic projections with in-plant data. It is apparent that the clay or ash fraction of the feedstock act as potential constituents for emission removal either through chemical interactions or through sorption by physical entrapment of the elements on the ash, spent sorbent, or alkali getter particle surface. A refinement to the thermodynamic equilibrium model is the identification of in-plant complexes and phases, kinetic data for these reactions, definition of the elemental partitioning as a function of particle type and size, and correlation with system design.

Analytical measurements have shown that the trace elements and their compounds preferentially concentrate on ash particles with diameters less than 10 μm.[84] If the particles are inhaled, their retention in the lung increases as a function of decreasing particle size.

Although many trace elements are essential for man's metabolic processes, these elements, if present in excess concentrations, may decrease the availability and utilization of other required elements, inducing a toxic effect. For example, excess Cd negates the Ca balance in man; Se protects against Hg toxicity; and Hg, Cu, and Cd protect against Se toxicity. An imbalance of the trace metal concentration, thus, perturbs the synergism of the various metabolic reactions and processes.[85,86]

Trace elements, if absorbed into the bloodstream, may interfere with normal metabolic process by inhibiting or stimulating enzymes or may damage organs and cause or encourage cancerous growth. Lead, As, organic and inorganic Hg, and Cd have been reported to induce chromosomal aberrations and teratogenicity, while immunological responses are impaired by excess concentrations of Pb, Cd, or Be.[86] It is clear that delineation of the possible mechanisms by which trace elements released during combustion are adsorbed onto entrained ash particles and of the dose-effect relationship and threshold concentration at which these elements are potentially hazardous to man needs to be established.

TRACE AND MINOR ELEMENT INTERACTIONS

An understanding of the individual trace and minor element reactions in the fluidized bed is essential prior to defining multichemical reactions that are likely to occur throughout the FBC system. The interactions of the trace and minor elements with clay (Al, Si) or carbonate (Ca, Mg) constituents will be examined in detail in this section in order to determine the ultimate reaction of the elements in forming either volatile stack-gas emission phases or solid, ashlike complexes. Due to the size limitation in the main chemical equilibrium program (15 elements, 200 compounds), several subsystems have been selected for study. These include:

(1) C-H-N-O-S-Cl-Si-Al-K-Na

(2) C-H-N-O-S-Cl-Si-Al-K-Na-Fe-Mn-Ni-Be

(3) C-H-N-O-S-Cl-Si-Al-K-Na-Cr-Fe-Mo-Mn-Ti
(4) C-H-N-O-S-Cl-Si-Al-K-Na-Ca-Mg-F-Be-Pb
(5) C-H-N-O-S-Cl-Si-Al-K-Na-Ti-Mo-F-Be-Pb-Hg
(6) C-H-N-O-S-Cl-Si-Al-K-Na-Ca-Mg-Fe-Ti-Ni
(7) C-H-N-O-S-Cl-Si-Al-K-Na-Ca-Mg-Cr-Mn-Mo
(8) C-H-N-O-S-Cl-Si-Al-K-Na-Co-Cr-Mg-Ni-Ca
(9) C-H-N-O-S-Cl-Si-Al-K-Na-Ca-Mg-B-Br-V-P-Zn
(10) C-H-N-O-S-Cl-Si-Al-K-Na-Br-F-Be-Hg-Pb-(Ca-Mg)
(11) C-H-N-O-S-Cl-Si-Al-K-Na-Br-F-Fe-Mn-Ni
(12) C-H-N-O-S-Cl-Si-Al-K-Na-Br-F-Ti-B-P
(13) C-H-N-O-S-Cl-Si-Al-K-Na-Br-F-Cu-Zn-Sb
(14) C-H-N-O-S-Cl-Si-Al-K-Na-Br-F-Sn-Zr-As
(15) C-H-N-O-S-Cl-Si-Al-K-Na-Br-F-Cd-Ga-Sb
(16) C-H-N-O-S-Cl-Si-Al-K-Na-Br-F-Se-Mo-Pb
(17) C-H-N-O-S-Cl-Si-Al-K-Na-Br-F-Ge-Co
(18) C-H-N-O-S-Cl-Si-Al-K-Na-Zr-B-V
(19) C-H-N-O-S-Cl-Si-Al-K-Na-Se-Pb-Ni-Cu-Sn
(20) C-H-N-O-S-Cl-Si-Al-K-Na-Se-Cu-Ge-Cr-Fe.

As in the simple elemental reaction projections with combustion gas constituents, the composition as reported by Ruch and Gluskoter[11] is used to define the relative elemental concentration. Again, we have assumed that 100 percent of the feedstock element concentration is reacted and that none remains bound within either an organic or clay lattice during combustion. Recombination of the feedstock initial phases and compounds are projected in the resulting product solids, condensates, and volatiles formed from combustion of a 4 percent S U.S. mean coal with a steady-state SO_x value in the effluent corresponding to 0, 90, and 99 percent S removal at 300 to 1200-1300 K and 1013 kPa.

C-H-N-O-S-Cl-Si-Al-K-Na

When Si, Al, Na, and K are present in FBC systems with 100 percent S release from a 4 percent S coal, at 1300 K, SiO_2 (cristobalite), aluminosilicate* ($Al_2O_3 \cdot SiO_2$), potassium sulfate (K_2SO_4), and disodium silicate ($2NaO \cdot SiO_2$) are projected to form. The formation of these compounds results from a series of reactions that includes:

$$SiO_2(s)\ (\text{quartz}) \xrightarrow{1000\text{–}1100\ K} SiO_2(s)\ (\text{cristobalite}) \qquad (63)$$

$$KAl(SO_4)_2 \cdot 12H_2O(c) \xrightarrow{300\text{–}400\ K} KAl(SO_4)_2(c) + 12H_2O(g) \qquad (64)$$

$$2KAl(SO_4)_2(c) + SiO_2(c) \xrightarrow{800\text{–}1000\ K} Al_2O_3 \cdot SiO_2(c) + K_2SO_4(c) + 3SO_2(g) + 3/2\ O_2(g) \qquad (65)$$

$$Al_2(SO_4)_3(s) + SiO_2(s) \xrightarrow{700\text{–}800\ K} Al_2O_3 \cdot SiO_2(c) + 3SO_2(g) + 3/2\ O_2(g) \qquad (66)$$

$2Na_2O \cdot SiO_2$ -- stable at all fluidized-bed temperatures and pressures.

The above reactions are modified for systems in which 90 percent of the S content is removed: SiO_2 remains as either quartz or cristobalite; hydrated potassium aluminum sulfate ($KAl(SO_4)_2 \cdot 12H_2O$) releases water at 300 to 400 K, forming solid $KAl(SO_4)_2$; $KAl(SO_4)_2$ reacts with SiO_2 at 700 to 900 K to form $Al_2O_3 \cdot SiO_2(s)$ and $K_2SO_4(s)$; and $2Na_2O \cdot SiO_2$ is present as a solid. At low temperatures aluminum hydroxide ($Al(OH)_3(s)$) and potassium chloride ($KCl(s)$) are formed in the fluidized-bed system. Reaction with SiO_2 and SO_x, respectively, at temperatures between 300 and 400 K, forms $Al_2O_3 \cdot SiO_2(s)$ and $K_2SO_4(s)$ by reactions 67 through 69:

$$2Al(OH)_3(s) + SiO_2(s) \xrightarrow{300\text{–}400\ K} Al_2O_3 \cdot SiO_2(s) + 3H_2O(g) \qquad (67)$$

---

*Andalusite

$$2KCl(s) + H_2SO_4(g) \xrightarrow{300\text{–}400\ K} K_2SO_4(s) + 2HCl(g) \qquad (68)$$

$$2KCl(s) + SO_2(g) + O_2(g) \xrightarrow{300\text{–}400\ K} K_2SO_4(s) + Cl_2(g) \quad . \qquad (69)$$

A continued reduction in the S content of the FBC gas, as for systems operating at 99 percent S removal, further modifies the composition of the resulting solid phases with respect to temperature. The $KAl(SO_4)_2 \cdot 12H_2O$ reacts with SiO_2 at 300 K to form K_2SO_4, aluminum trisulfate ($Al_2(SO_4)_3$), H_2O, and gaseous SO_2. Solid KCl is stable between temperatures of 300 and 900 to 1100 K, whereupon reaction with O_2 and SO_x converts the alkali chloride into solid K_2SO_4. The stability of SiO_2 and $2Na_2O \cdot SiO_2$ is unaffected by the reduction in the total S content. Tables 41 through 43 summarize the resulting moles of solids, or condensed phases and partial pressures in kPa, of gaseous constituents from FBC reactions of Si, Al, Na, and K in 0, 90, and 99 percent S-removal systems operating at 100 percent excess air and at 1013 kPa (10 atm) total pressure.

The major volatile phases formed over the solid aluminosilicates are potassium hydroxide (KOH), K_2SO_4, and KCl. The partial pressure exerted by the comparable Na, Al, or Si phases are less than 10^{-13} kPa (10^{-15} atm) at temperatures of 1200 K and are subsequently reduced at lower temperatures. In all S-removal systems the effect of an increase in the excess air content decreases the partial pressure of gaseous KOH and KCl but does not affect the partial pressure of K_2SO_4. A reduction in the total pressure of the system decreases the partial pressure of KOH and KCl at low temperatures while increasing the partial pressure at high temperatures.

Note that the above projections favor the formation of K as $KAl(SO_4)_2 \cdot 12H_2O$, $KAl(SO_4)2$, or K_2SO_4. Data for the potassium aluminosilicate complex $KAlSi_3O_8$ considered in these thermodynamic projections

TABLE 41 - FLUIDIZED-BED COMBUSTION OF C-H-N-O-S-Cl-Si-Al-K-Na FOR 100% EXCESS AIR, 0% SULFUR-REMOVAL, 1013 kPa OPERATIONS

TEMP.\COMPOUND (K) \	QUARTZ (S)	CRISTOBALITE SIO2 (S)	KCL (S)	KAL(SO4)2. 12H2O (S)	AL(OH)3 (S)
300	.8293-01	.0000	.0000	.8451-02	.0000
400	.8293-01	.0000	.0000	.0000	.0000
500	.8293-01	.0000	.0000	.0000	.0000
600	.8293-01	.0000	.0000	.0000	.0000
700	.8293-01	.0000	.0000	.0000	.0000
800	.8293-01	.0000	.0000	.0000	.0000
900	.6325-01	.0000	.0000	.0000	.0000
1000	.5903-01	.0000	.0000	.0000	.0000
1100	.0000	.5903-01	.0000	.0000	.0000
1200	.0000	.5903-01	.0000	.0000	.0000

TEMP.\COMPOUND (K) \	KAL(SO4)2 (S)	AL2O3. SIO2 (S)	K2SO4 (S)	2NA2O. SIO2 (S)	KALSI3O8 (S)
300	.0000	.0000	.0000	.2155-02	.0000
400	.8450-02	.0000	.0000	.2155-02	.0000
500	.8450-02	.0000	.0000	.2155-02	.0000
600	.8450-02	.0000	.0000	.2155-02	.0000
700	.8450-02	.0000	.0000	.2155-02	.0000
800	.8450-02	.0000	.0000	.2155-02	.0000
900	.8450-02	.1968-01	.0000	.2155-02	.0000
1000	.0000	.2390-01	.4225-02	.2155-02	.0000
1100	.0000	.2390-01	.4217-02	.2155-02	.0000
1200	.0000	.2390-01	.4113-02	.2155-02	.0000

TEMP.\COMPOUND (K) \	AL2(SO4)3 (S)	KOH (G)	K2SO4 (G)	KCL (G)
300	.1968-01	.0000	.0000	.0000
400	.1968-01	.0000	.0000	.5948-28
500	.1968-01	.7180-32	.1338-27	.1056-20
600	.1968-01	.4265-25	.5641-21	.5459-16
700	.1968-01	.6232-20	.2857-16	.1957-12
800	.1968-01	.6472-16	.9048-13	.1155-09
900	.0000	.5631-12	.3844-08	.1041-06
1000	.0000	.3099-09	.1403-05	.9284-05
1100	.0000	.2839-07	.3368-04	.1892-03
1200	.0000	.1320-05	.4545-03	.2454-02

(S) or (C) - solid or condensed phases in moles
(G) - gas phases in kPa

TABLE 42 - FLUIDIZED-BED COMBUSTION OF C-H-N-O-S-Cl-Si-Al-K-Na FOR 100% EXCESS AIR, 90% SULFUR-REMOVAL, 1013 kPA OPERATIONS

TEMP.\COMPOUND (K) \	QUARTZ (S)	CRISTOBALITE SIO2 (S)	KCL (S)	KAL(SO4)2. 12H2O (S)	AL(OH)3 (S)
300	.8293-01	.0000	.2211-02	.6240-02	.4157-01
400	.6127-01	.0000	.0000	.0000	.0000
500	.6127-01	.0000	.0000	.0000	.0000
600	.6127-01	.0000	.0000	.0000	.0000
700	.6127-01	.0000	.0000	.0000	.0000
800	.6127-01	.0000	.0000	.0000	.0000
900	.5903-01	.0000	.0000	.0000	.0000
1000	.5903-01	.0000	.0000	.0000	.0000
1100	.0000	.5903-01	.0000	.0000	.0000
1200	.0000	.5903-01	.0000	.0000	.0000

TEMP.\COMPOUND (K) \	KAL(SO4)2 (S)	AL2O3. SIO2 (S)	K2SO4 (S)	2NA2O. SIO2 (S)	KALSI3O8 (S)
300	.0000	.0000	.0000	.2155-02	.0000
400	.5503-02	.2115-01	.1474-02	.2155-02	.0000
500	.5503-02	.2115-01	.1474-02	.2155-02	.0000
600	.5503-02	.2115-01	.1474-02	.2155-02	.0000
700	.5488-02	.2116-01	.1481-02	.2155-02	.0000
800	.4486-02	.2166-01	.1982-02	.2155-02	.0000
900	.0000	.2390-01	.4225-02	.2156-02	.0000
1000	.0000	.2390-01	.4224-02	.2156-02	.0000
1100	.0000	.2390-01	.4199-02	.2156-02	.0000
1200	.0000	.2390-01	.3901-02	.2155-02	.0000

TEMP.\COMPOUND (K) \	AL2(SO4)3 (S)	KOH (G)	K2SO4 (G)	KCL (G)
300	.0000	.0000	.0000	.3336-28
400	.0000	.3014-33	.3139-30	.2852-19
500	.0000	.2704-25	.9056-22	.3910-14
600	.0000	.5286-20	.3563-16	.6675-11
700	.0000	.3101-16	.3229-12	.9762-09
800	.0000	.2014-13	.2737-09	.3596-07
900	.0000	.5406-11	.2719-07	.1004-05
1000	.0000	.1182-08	.1403-05	.3540-04
1100	.0000	.1081-06	.3368-04	.7172-03
1200	.0000	.4940-05	.4545-03	.6947-02

TABLE 43 - FLUIDIZED-BED COMBUSTION OF C-H-N-O-S-Cl-Si-Al-K-Na FOR 100% EXCESS AIR, 99% SULFUR-REMOVAL, 1013 kPa OPERATIONS

TEMP.\COMPOUND (K) \	QUARTZ (S)	CRISTOBALITE SIO2 (S)	KCL (S)	KAL(SO4)2. 12H2O (S)	AL(OH)3 (S)
300	.8293-01	.0000	.7826-02	.6250-03	.4719-01
400	.5903-01	.0000	.5951-02	.0000	.0000
500	.5903-01	.0000	.5951-02	.0000	.0000
600	.5903-01	.0000	.5951-02	.0000	.0000
700	.5903-01	.0000	.5950-02	.0000	.0000
800	.5903-01	.0000	.5949-02	.0000	.0000
900	.5903-01	.0000	.5896-02	.0000	.0000
1000	.5903-01	.0000	.5064-02	.0000	.0000
1100	.0000	.5903-01	.0000	.0000	.0000
1200	.0000	.5903-01	.0000	.0000	.0000

TEMP.\COMPOUND (K) \	KAL(SO4)2 (S)	AL2O3. SIO2 (S)	K2SO4 (S)	2NA2O. SIO2 (S)	KALSI3O8 (S)
300	.0000	.0000	.0000	.2155-02	.0000
400	.0000	.2390-01	.1250-02	.2155-02	.0000
500	.0000	.2390-01	.1250-02	.2155-02	.0000
600	.0000	.2390-01	.1250-02	.2155-02	.0000
700	.0000	.2390-01	.1250-02	.2155-02	.0000
800	.0000	.2390-01	.1250-02	.2155-02	.0000
900	.0000	.2390-01	.1250-02	.2155-02	.0000
1000	.0000	.2390-01	.1250-02	.2155-02	.0000
1100	.0000	.2390-01	.1248-02	.2155-02	.0000
1200	.0000	.2390-01	.1207-02	.2155-02	.0000

TEMP.\COMPOUND (K) \	AL2(SO4)3 (S)	KOH (G)	K2SO4 (G)	KCL (G)
300	.0000	.0000	.0000	.3336-28
400	.0000	.2569-32	.3139-30	.1431-18
500	.0000	.1058-23	.9056-22	.7813-13
600	.0000	.9261-18	.3563-16	.4865-09
700	.0000	.1968-13	.3229-12	.2366-06
800	.0000	.3515-16	.2737-09	.2345-04
900	.0000	.1168-07	.2719-07	.8066-03
1000	.0000	.1189-05	.1403-05	.1322-01
1100	.0000	.3588-04	.3368-04	.8881-01
1200	.0000	.1276-03	.4545-03	.8902-01

were based on the heat of formation, entropy, and molecular constants cited by Barin and Knacke.[71] Robie and Waldbaum[77] report similar data for the $KAlSi_3O_8$ complex but indicate that the heat of formation of the complex is 159 kJ/mole (38 kcal/mole) more negative than the Barin and Knacke data. The C-H-N-O-S-Cl-Si-Al-Na-K fluidized-bed systems were reevaluated using the Robie data, and, as shown in Tables 44 through 46, the activity of the alkali aluminosilicate phase as a getter material is extended to lower operating temperatures when the partial pressure of S in the combustion gas is reduced (1100-1200 K for 0 percent S removal, 1000-1100 K for 90 percent S removal, and 500-600 K for 99 percent S removal -- see Figure 119). As the concentration of K increases in the formation of the stable $KAlSi_3O_8$ complex, K_2SO_4 is removed from the system, as shown by the reaction

$$K_2SO_4(s) + Al_2O_3 \cdot SiO_2(s) + 5SiO_2(s) \longrightarrow 2KAlSi_3O_8(s) + SO_2(g) + 1/2\ O_2(g). \qquad (70)$$

Unreacted andalusite ($Al_2O_3 \cdot SiO_2$) is stable in the FBC system up to temperatures of 1200 to 1300 K, whereupon conversion into a mullite clay lattice occurs:

$$3\ Al_2O_3 \cdot SiO_2(s) \longrightarrow 3Al_2O_3 \cdot 2SiO_2(s) + SiO_2(s). \qquad (71)$$

Significant emphasis in the interactive section has been given not only to the alkali-clay, but also to the trace and minor element-clay reactions. In equilibrium with the solids are volatile chlorides, sulfates, and hydroxides exerting partial pressures dependent on both the pressure and temperature of the fluidized-bed system. Tables 47 through 50 illustrate the decimal distribution in the condensed and volatile alkali phases for 100 and 10 percent excess air, 0 and 90 percent S-removal, FBC systems. The results are graphically displayed in the three-dimensional plots of Figure 120.

TABLE 44 - REEVALUATION OF FLUIDIZED-BED COMBUSTION OF C-H-N-O-S-Cl-Si-Al-K-Na FOR 100% EXCESS AIR, 0% SULFUR-REMOVAL, 1013 kPa OPERATIONS

TEMP.\COMPOUND (K) \	QUARTZ (S)	CRISTOBALITE SIO2 (S)	KCL (S)	KAL(SO4)2 12H2O (S)	AL(OH)3 (S)
300	.8295-01	.0000	.0000	.8451-02	.0000
400	.8295-01	.0000	.0000	.0000	.0000
500	.8295-01	.0000	.0000	.0000	.0000
600	.8295-01	.0000	.0000	.0000	.0000
700	.8295-01	.0000	.0000	.0000	.0000
800	.8295-01	.0000	.0000	.0000	.0000
900	.6327-01	.0000	.0000	.0000	.0000
1000	.5904-01	.0000	.0000	.0000	.0000
1100	.0000	.5904-01	.0000	.0000	.0000
1200	.0000	.3809-01	.0000	.0000	.0000

TEMP.\COMPOUND (K) \	KAL(SO4)2 (S)	AL2O3. SIO2 (S)	K2SO4 (S)	2NA2O. SIO2 (S)	KALSI3O8 (S)
300	.0000	.0000	.0000	.2155-02	.0000
400	.8451-02	.0000	.0000	.2155-02	.0000
500	.8451-02	.0000	.0000	.2155-02	.0000
600	.8451-02	.0000	.0000	.2155-02	.0000
700	.8451-02	.0000	.0000	.2155-02	.0000
800	.8451-02	.0000	.0000	.2155-02	.0000
900	.8451-02	.1968-01	.0000	.2155-02	.0000
1000	.0000	.2391-01	.4225-02	.2155-02	.0000
1100	.0000	.2391-01	.4217-02	.2155-02	.0000
1200	.0000	.1972-01	.0000	.2155-02	.8377-02

TEMP.\COMPOUND (K) \	AL2(SO4)3 (S)	KOH (G)	K2SO4 (G)	KCL (G)
300	.1968-01	.0000	.0000	.1433-17
400	.1968-01	.0000	.0000	.5948-28
500	.1968-01	.7180-32	.1338-27	.1056-20
600	.1968-01	.4265-25	.5641-21	.5465-16
700	.1968-01	.6230-21	.2857-16	.1958-12
800	.1968-01	.6474-16	.9048-13	.1154-09
900	.0000	.5622-13	.3838-08	.1046-06
1000	.0000	.3099-09	.1403-06	.9296-05
1100	.0000	.2839-07	.3368-04	.1894-03
1200	.0000	.5105-06	.7035-04	.9610-03

TABLE 45 - REEVALUATION OF FLUIDIZED-BED COMBUSTION OF C-H-N-O-S-Cl-Si-Al-K-Na FOR 100% EXCESS AIR, 90% SULFUR-REMOVAL, 1013 kPa OPERATIONS

TEMP.\COMPOUND (K) \	QUARTZ (S)	CRISTOBALITE SIO2 (S)	KCL (S)	KAL(SO4)2 12H2O (S)	AL(OH)3 (S)
300	.8295-01	.0000	.2211-02	.6240-02	.4157-01
400	.6179-01	.0000	.0000	.0000	.0000
500	.6179-01	.0000	.0000	.0000	.0000
600	.6179-01	.0000	.0000	.0000	.0000
700	.6178-01	.0000	.0000	.0000	.0000
800	.6128-01	.0000	.0000	.0000	.0000
900	.5904-01	.0000	.0000	.0000	.0000
1000	.5904-01	.0000	.0000	.0000	.0000
1100	.0000	.3796-01	.0000	.0000	.0000
1200	.0000	.3808-01	.0000	.0000	.0000

TEMP.\COMPOUND (K) \	KAL(SO4)2 (S)	AL2O3. SIO2 (S)	K2SO4 (S)	2NA2O. SIO2 (S)	KALSI3O8 (S)
300	.0000	.0000	.0000	.2155-02	.0000
400	.5503-02	.2115-01	.1474-02	.2155-02	.0000
500	.5503-02	.2115-01	.1474-02	.2155-02	.0000
600	.5503-02	.2115-01	.1474-02	.2155-02	.0000
700	.5488-02	.2116-01	.1481-02	.2155-02	.0000
800	.4486-02	.2166-01	.1982-02	.2155-02	.0000
900	.0000	.2391-01	.4225-02	.2155-02	.0000
1000	.0000	.2391-01	.4224-02	.2155-02	.0000
1100	.0000	.1969-01	.0000	.2155-02	.8432-02
1200	.0000	.1971-01	.0000	.2155-02	.8385-02

TEMP.\COMPOUND (K) \	AL2(SO4)3 (S)	KOH (G)	K2SO4 (G)	KCL (G)
300	.0000	.0000	.0000	.3336-28
400	.0000	.3014-33	.3139-30	.2852-19
500	.0000	.2704-25	.9056-22	.3911-14
600	.0000	.5286-20	.3563-16	.6681-11
700	.0000	.3101-16	.3229-12	.9775-09
800	.0000	.2014-13	.2737-09	.3600-07
900	.0000	.5406-11	.2719-07	.1006-05
1000	.0000	.1182-08	.1403-05	.3546-04
1100	.0000	.3976-07	.6872-05	.2651-03
1200	.0000	.5103-06	.7083-05	.9609-03

TABLE 46 - REEVALUATION OF FLUIDIZED-BED COMBUSTION OF C-H-N-O-S-Cl-Si-Al-K-Na FOR 100% EXCESS AIR, 99% SULFUR-REMOVAL, 1013 kPa OPERATIONS

TEMP.\COMPOUND (K) \	QUARTZ (S)	CRISTOBALITE SIO2 (S)	KCL (S)	KAL(SO4)2 12H2O (S)	AL(OH)3 (S)
300	.8294-01	.0000	.7826-02	.6250-03	.4719-01
400	.5904-01	.0000	.5951-02	.0000	.0000
500	.5904-01	.0000	.5951-02	.0000	.0000
600	.5000-01	.0000	.2334-02	.0000	.0000
700	.4416-01	.0000	.0000	.0000	.0000
800	.4415-01	.0000	.0000	.0000	.0000
900	.4363-01	.0000	.0000	.0000	.0000
1000	.3792-01	.0000	.0000	.0000	.0000
1100	.0000	.3796-01	.0000	.0000	.0000
1200	.0000	.3807-01	.0000	.0000	.0000

TEMP.\COMPOUND (K) \	KAL(SO4)2 (S)	AL2O3. SIO2 (S)	K2SO4 (S)	2NA2O. SIO2 (S)	KALSI3O8 (S)
300	.0000	.0000	.0000	.2155-02	.0000
400	.0000	.2391-01	.1250-02	.2155-02	.0000
500	.0000	.2391-01	.1250-02	.2155-02	.0000
600	.0000	.2210-01	.1250-02	.2155-02	.3616-02
700	.0000	.2093-01	.1250-02	.2155-02	.5950-02
800	.0000	.2093-01	.1247-02	.2155-02	.5956-02
900	.0000	.2082-01	.1144-02	.2155-02	.6162-02
1000	.0000	.1968-01	.0000	.2155-02	.8447-02
1100	.0000	.1969-01	.0000	.2155-02	.8433-02
1200	.0000	.1971-01	.0000	.2155-02	.8386-02

TEMP.\COMPOUND (K) \	AL2(SO4)3 (S)	KOH (G)	K2SO4 (G)	KCL (G)
300	.0000	.0000	.0000	.3356-28
400	.0000	.2568-32	.3139-30	.1431-18
500	.0000	.1058-23	.1002-20	.7813-13
600	.0000	.4906-18	.3563-16	.4865-09
700	.0000	.1268-14	.3229-12	.3996-07
800	.0000	.4664-12	.2737-09	.8337-06
900	.0000	.4764-10	.2719-07	.8864-05
1000	.0000	.1939-08	.5717-06	.5816-04
1100	.0000	.3976-07	.6886-06	.2651-03
1200	.0000	.5103-06	.7099-06	.9609-03

Dwg.1703853

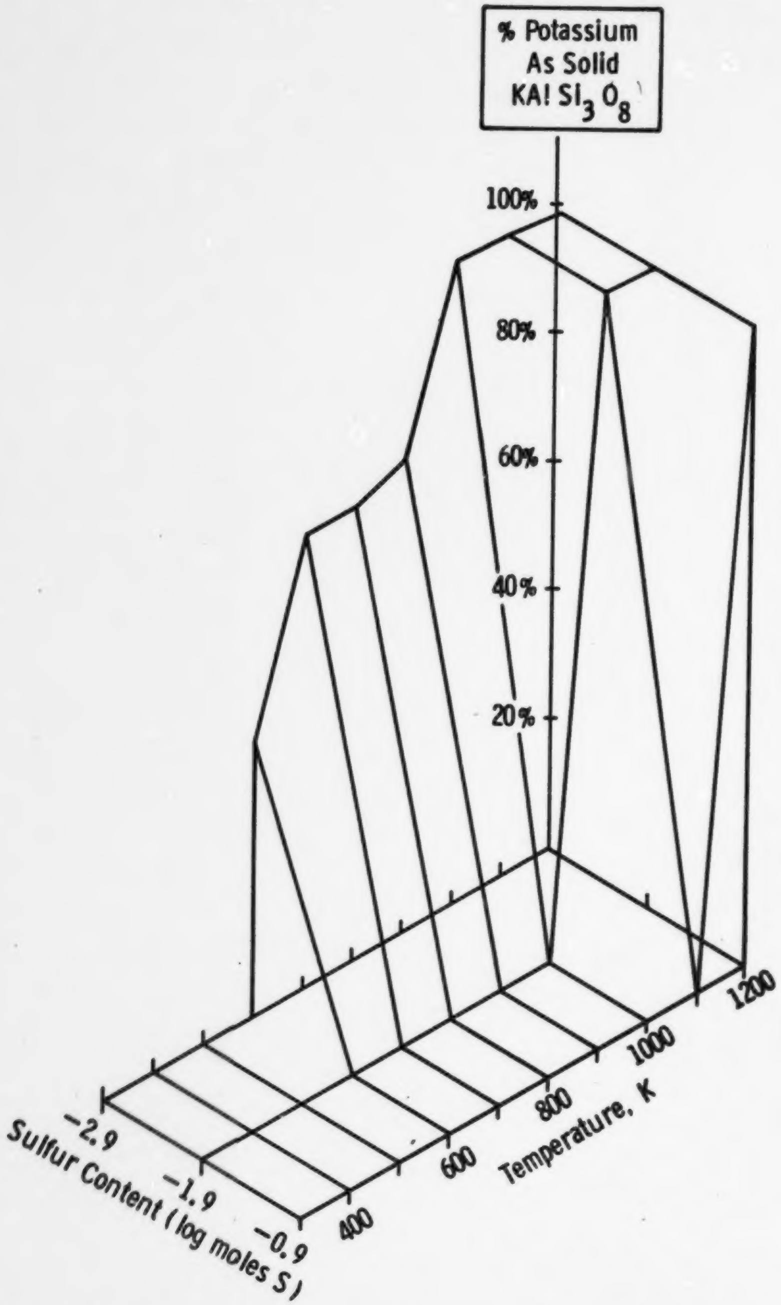

Figure 119 - Gettering Activity of $KAlSi_3O_8$ in 100% Excess Air Fluidized-Bed Combustion Systems Operating at 1013 kPa (10 atm) Total Pressure (-0.9 = 0% Sulfur Removal, -1.9 = 90% Sulfur Removal, -2.9 = 99% Sulfur Removal)

TABLE 47 - DECIMAL DISTRIBUTION OF POTASSIUM COMPOUNDS IN A FLUIDIZED-BED COMBUSTION SYSTEM OPERATING WITH 100% EXCESS AIR AND 0% SULFUR-REMOVAL

```
Temp     KALSI308 (S)
 (K)\ KPA 1518            1013            505             101
1300   .9801+00       .9762+00       .9673+00       .9309+00
1200   .9925+00       .9913+00       .9884+00       .9759+00
1100   .0000+00       .0000+00       .0000+00       .9929+00
1000   .0000+00       .0000+00       .0000+00       .0000+00
 900   .0000+00       .0000+00       .0000+00       .0000+00

         K2SO4 (S)
      KPA 1518            1013            505             101
1300   .0000+00       .0000+00       .0000+00       .0000+00
1200   .0000+00       .0000+00       .0000+00       .0000+00
1100   .9987+00       .9980+00       .9956+00       .0000+00
1000   .9999+00       .9999+00       .9998+00       .9988+00
 900   .1000+01       .1000+01       .1000+01       .1000+01

         KOH (G)
      KPA 1518            1013            505             101
1300   .2919-04       .3575-04       .5057-04       .1131-03
1200   .3305-05       .4048-05       .5725-05       .1280-04
1100   .1414-06       .2252-06       .5042-06       .9973-06
1000   .1584-08       .2456-08       .5258-08       .3259-07
 900   .1546-11       .4455-11       .2788-10       .1267-09

         K2SO4 (G)
      KPA 1518            1013            505             101
1300   .1288-02       .1078-02       .7880-03       .3690-03
1200   .1306-02       .1116-02       .8404-03       .4115-03
1100   .3561-03       .5341-03       .1068-02       .4669-03
1000   .1483-04       .2224-04       .4448-04       .2224-03
 900   .1124-07       .6084-07       .1132-05       .4311-05

         KCL (G)
      KPA 1518            1013            505             101
1300   .1863-01       .2272-01       .3184-01       .6858-01
1200   .6232-02       .7622-02       .1075-01       .2372-01
1100   .9438-03       .1502-02       .3358-02       .6623-02
1000   .4750-04       .7370-04       .1579-03       .9787-03
 900   .2873-06       .8290-06       .5195-05       .2366-04

         KCN (G)
      KPA 1518            1013            505             101
1300   .3520-24       .4771-24       .8020-24       .2681-23
1200   .4464-27       .6048-27       .1017-26       .3396-26
1100   .9434-31       .1661-30       .4419-30       .1305-29
1000   .0000+00       .0000+00       .0000+00       .7254-34
 900   .0000+00       .0000+00       .0000+00       .0000+00

         HK (G)
      KPA 1518            1013            505             101
1300   .2339-15       .3509-15       .7017-15       .3508-14
1200   .1722-17       .2582-17       .5164-17       .2581-16
1100   .2914-20       .5681-20       .1798-19       .7949-19
1000   .6763-24       .1284-23       .3887-23       .5384-22
 900   .5776-29       .2039-28       .1804-27       .1831-26

         KO  (G)
      KPA 1518            1013            505             101
1300   .2990-09       .4053-09       .6817-09       .2280-08
1200   .8552-11       .1159-10       .1950-10       .6521-10
1100   .7166-13       .1263-12       .3363-12       .9951-12
1000   .1128-15       .1937-15       .4931-15       .4573-14
 900   .9952-20       .3174-19       .2362-18       .1606-17

         K (G)
      KPA 1518            1013            505             101
1300   .8498-09       .1411-08       .3355-08       .2508-07
1200   .2121-10       .3520-10       .8372-10       .6259-09
1100   .1514-12       .3266-12       .1230-11       .8131-11
1000   .1967-15       .4133-15       .1488-14       .3083-13
 900   .1371-19       .5355-19       .5635-18       .8560-17
```

TABLE 48 - DECIMAL DISTRIBUTION OF POTASSIUM COMPOUNDS IN A FLUIDIZED-BED COMBUSTION SYSTEM OPERATING WITH 100% EXCESS AIR AND 90% SULFUR-REMOVAL

Temp (K)\KPA	1518	1013	505	101
KALSI308 (S)				
1300	.9812+00	.9771+00	.9680+00	.9313+00
1200	.9936+00	.9923+00	.9892+00	.9762+00
1100	.9982+00	.9978+00	.9969+00	.9933+00
1000	.0000+00	.0000+00	.0000+00	.9985+00
900	.0000+00	.0000+00	.0000+00	.0000+00
K2SO4 (S)				
1300	.0000+00	.0000+00	.0000+00	.0000+00
1200	.0000+00	.0000+00	.0000+00	.0000+00
1100	.0000+00	.0000+00	.0000+00	.0000+00
1000	.9998+00	.9997+00	.9994+00	.0000+00
900	.1000+01	.1000+01	.1000+01	.9999+00
KOH (G)				
1300	.2919-04	.3576-04	.5057-04	.1131-03
1200	.3306-05	.4049-05	.5726-05	.1280-04
1100	.2575-06	.3154-06	.4460-06	.9973-06
1000	.6046-08	.9374-08	.2006-07	.4864-07
900	.2827-10	.4288-10	.8792-10	.4836-09
K2SO4 (G)				
1300	.1298-03	.1086-03	.7940-04	.3719-04
1200	.1315-03	.1124-03	.8464-04	.4146-04
1100	.1228-03	.1090-03	.8704-04	.4702-04
1000	.1483-04	.2225-04	.4450-04	.5155-04
900	.2875-06	.4313-06	.8626-06	.4313-05
KCL (G)				
1300	.1863-01	.2272-01	.3184-01	.6858-01
1200	.6232-02	.7623-02	.1075-01	.2372-01
1100	.1717-02	.2103-02	.2972-02	.6623-02
1000	.1813-03	.2812-03	.6019-03	.1460-02
900	.5253-05	.7977-05	.1638-04	.9030-04
KCN (G)				
1300	.3446-24	.4671-24	.7855-24	.2626-23
1200	.4365-27	.5917-27	.9950-27	.3326-26
1100	.1676-30	.2271-30	.3820-30	.1277-29
1000	.0000+00	.0000+00	.0000+00	.1057-33
900	.0000+00	.0000+00	.0000+00	.0000+00
HK (G)				
1300	.2320-15	.3480-15	.6959-15	.3480-14
1200	.1707-17	.2560-17	.5120-17	.2560-16
1100	.5255-20	.7882-20	.1576-19	.7881-19
1000	.2555-23	.4851-23	.1468-22	.7958-22
900	.1044-27	.1940-27	.5626-27	.6919-26
KO (G)				
1300	.3003-09	.4071-09	.6846-09	.2289-08
1200	.8592-11	.1165-10	.1959-10	.6549-10
1100	.1311-12	.1777-12	.2989-12	.9995-12
1000	.4331-15	.7432-15	.1891-14	.6858-14
900	.1831-18	.3073-18	.7494-18	.6163-17
K (G)				
1300	.8463-09	.1405-08	.3341-08	.2498-07
1200	.2112-10	.3506-10	.8338-10	.6234-09
1100	.2743-12	.4554-12	.1083-11	.8097-11
1000	.7470-15	.1570-14	.5649-14	.4580-13
900	.2494-18	.5127-18	.1768-17	.3252-16

TABLE 49 - DECIMAL DISTRIBUTION OF POTASSIUM COMPOUNDS IN A FLUIDIZED-BED COMBUSTION SYSTEM OPERATING WITH 10% EXCESS AIR AND 0% SULFUR-REMOVAL

KALSI308 (S)

Temp (K)\KPA	1518	1013	505	101
1300	.9853+00	.9823+00	.9755+00	.9473+00
1200	.9947+00	.9937+00	.9915+00	.9819+00
1100	.0000+00	.0000+00	.9973+00	.9948+00
1000	.0000+00	.0000+00	.0000+00	.0000+00
900	.0000+00	.0000+00	.0000+00	.0000+00

K2SO4 (S)

KPA	1518	1013	505	101
1300	.0000+00	.0000+00	.0000+00	.0000+00
1200	.0000+00	.0000+00	.0000+00	.0000+00
1100	.9991+00	.9986+00	.0000+00	.0000+00
1000	.1000+01	.9999+00	.9999+00	.9991+00
900	.0000+00	.0000+00	.0000+00	.1000+01

KAL(SO4)2 (S)

KPA	1518	1013	505	101
1300	.0000+00	.0000+00	.0000+00	.0000+00
1200	.0000+00	.0000+00	.0000+00	.0000+00
1100	.0000+00	.0000+00	.0000+00	.0000+00
1000	.0000+00	.0000+00	.0000+00	.0000+00
900	.1000+01	.1000+01	.1000+01	.0000+00

KOH (G)

KPA	1518	1013	505	101
1300	.2189-04	.2681-04	.3791-04	.8478-04
1200	.2478-05	.3035-05	.4293-05	.9599-05
1100	.1055-06	.1710-06	.3344-06	.7477-06
1000	.1062-08	.1681-08	.3729-08	.2493-07
900	.4864-12	.1471-11	.1016-10	.8531-10

K2SO4 (G)

KPA	1518	1013	505	101
1300	.5968-03	.4930-03	.3541-03	.1617-03
1200	.6483-03	.5418-03	.3952-03	.1845-03
1100	.2001-03	.3002-03	.4489-03	.2211-03
1000	.8332-05	.1250-04	.2500-04	.1250-03
900	.1717-08	.9996-08	.2157-06	.2423-05

KCL (G)

KPA	1518	1013	505	101
1300	.1406-01	.1717-01	.2412-01	.5246-01
1200	.4687-02	.5735-02	.8092-02	.1792-01
1100	.7053-03	.1143-02	.2232-02	.4979-02
1000	.3191-04	.5052-04	.1121-03	.7494-03
900	.9079-07	.2747-06	.1898-05	.1595-04

KCN (G)

KPA	1518	1013	505	101
1300	.2903-23	.3930-23	.6599-23	.2202-22
1200	.3695-26	.4997-26	.8380-26	.2790-25
1100	.7877-30	.1408-29	.3245-29	.1075-28
1000	.0000+00	.0000+00	.6285-34	.6180-33
900	.0000+00	.0000+00	.0000+00	.0000+00

HK (G)

KPA	1518	1013	505	101
1300	.4096-15	.6142-15	.1228-14	.6133-14
1200	.3020-17	.4526-17	.9041-17	.4513-16
1100	.5113-20	.1013-19	.2793-19	.1392-18
1000	.1076-23	.2082-23	.6509-23	.9667-22
900	.4368-29	.1616-28	.1573-27	.2926-26

KO (G)

(K)\KPA	1518	1013	505	101
1300	.1100-09	.1491-09	.2509-09	.8392-09
1200	.3143-11	.4262-11	.7173-11	.2401-10
1100	.2613-13	.4692-13	.1093-12	.3661-12
1000	.3681-16	.6456-16	.1706-15	.1712-14
900	.1514-20	.5071-20	.4171-19	.5264-18

K (G)

KPA	1518	1013	505	101
1300	.7301-09	.1212-08	.2881-08	.2153-07
1200	.1823-10	.3026-10	.7192-10	.5373-09
1100	.1298-12	.2850-12	.9357-12	.6985-11
1000	.1523-15	.3264-15	.1216-14	.2709-13
900	.5013-20	.2053-19	.2381-18	.6657-17

TABLE 50 - DECIMAL DISTRIBUTION OF POTASSIUM COMPOUNDS IN A FLUIDIZED-BED COMBUSTION SYSTEM OPERATING WITH 10% EXCESS AIR AND 90% SULFUR-REMOVAL

KALSI308 (S)

Temp (K)\KPA	1518	1013	505	101
1300	.9859+00	.9828+00	.9758+00	.9474+00
1200	.9952+00	.9942+00	.9919+00	.9820+00
1100	.9986+00	.9984+00	.9977+00	.9950+00
1000	.0000+00	.0000+00	.0000+00	.9989+00
900	.0000+00	.0000+00	.0000+00	.0000+00

K2S04 (S)

KPA	1518	1013	505	101
1300	.0000+00	.0000+00	.0000+00	.0000+00
1200	.0000+00	.0000+00	.0000+00	.0000+00
1100	.0000+00	.0000+00	.0000+00	.0000+00
1000	.9999+00	.9998+00	.9996+00	.0000+00
900	.1000+01	.1000+01	.1000+01	.9999+00

KOH (G)

KPA	1518	1013	505	101
1300	.2189-04	.2681-04	.3791-04	.8478-04
1200	.2478-05	.3035-05	.4293-05	.9599-05
1100	.1931-06	.2365-06	.3344-06	.7477-06
1000	.3969-08	.6271-08	.1387-07	.3647-07
900	.1689-10	.2588-10	.5423-10	.3187-09

K2S04 (G)

KPA	1518	1013	505	101
1300	.6400-04	.5290-04	.3801-04	.1737-04
1200	.6935-04	.5800-04	.4236-04	.1981-04
1100	.7373-04	.6328-04	.4793-04	.2369-04
1000	.8338-05	.1251-04	.2501-04	.2951-04
900	.1616-06	.2424-06	.4849-06	.2424-05

KCL (G)

KPA	1518	1013	505	101
1300	.1406-01	.1717-01	.2412-01	.5246-01
1200	.4687-02	.5735-02	.8092-02	.1792-01
1100	.1290-02	.1579-02	.2232-02	.4979-02
1000	.1192-03	.1884-03	.4169-03	.1096-02
900	.3150-05	.4830-05	.1013-04	.5959-04

KCN (G)

KPA	1518	1013	505	101
1300	.2408-23	.3263-23	.5487-23	.1834-22
1200	.3048-26	.4130-26	.6944-26	.2321-25
1100	.1171-29	.1586-29	.2666-29	.8907-29
1000	.4097-34	.7162-34	.1883-33	.7377-33
900	.0000+00	.0000+00	.0000+00	.0000+00

HK (G)

KPA	1518	1013	505	101
1300	.3802-15	.5702-15	.1140-14	.5701-14
1200	.2796-17	.4194-17	.8387-17	.4193-16
1100	.8610-20	.1291-19	.2582-19	.1291-18
1000	.3670-23	.7101-23	.2221-22	.1304-21
900	.1366-27	.2564-27	.7596-27	.9978-26

KO (G)

KPA	1518	1013	505	101
1300	.1142-09	.1548-09	.2603-09	.8704-09
1200	.3267-11	.4429-11	.7449-11	.2491-10
1100	.4986-13	.6758-13	.1137-12	.3802-12
1000	.1441-15	.2520-15	.6629-15	.2608-14
900	.5541-19	.9399-19	.2342-18	.2059-17

K (G)

KPA	1518	1013	505	101
1300	.7034-09	.1168-08	.2777-08	.2076-07
1200	.1755-10	.2913-10	.6928-10	.5179-07
1100	.2280-12	.3784-12	.8999-12	.6727-11
1000	.5438-15	.1165-14	.4332-14	.3806-13
900	.1653-18	.3433-18	.1210-17	.2377-16

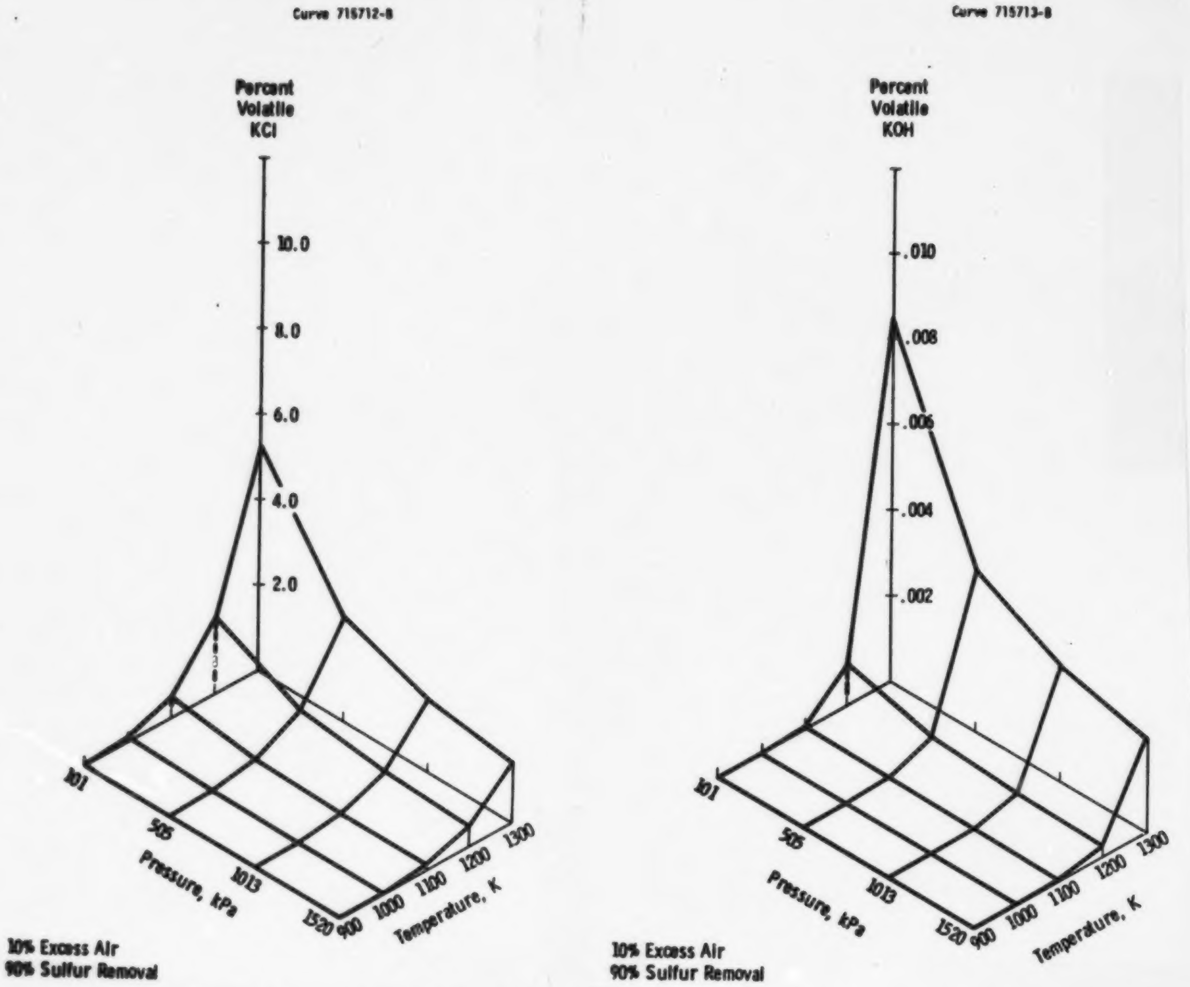

Figure 120 - Three-Dimensional Display of Volatile and Condensed Potassium Phases in Fluidized-Bed Combustion Systems

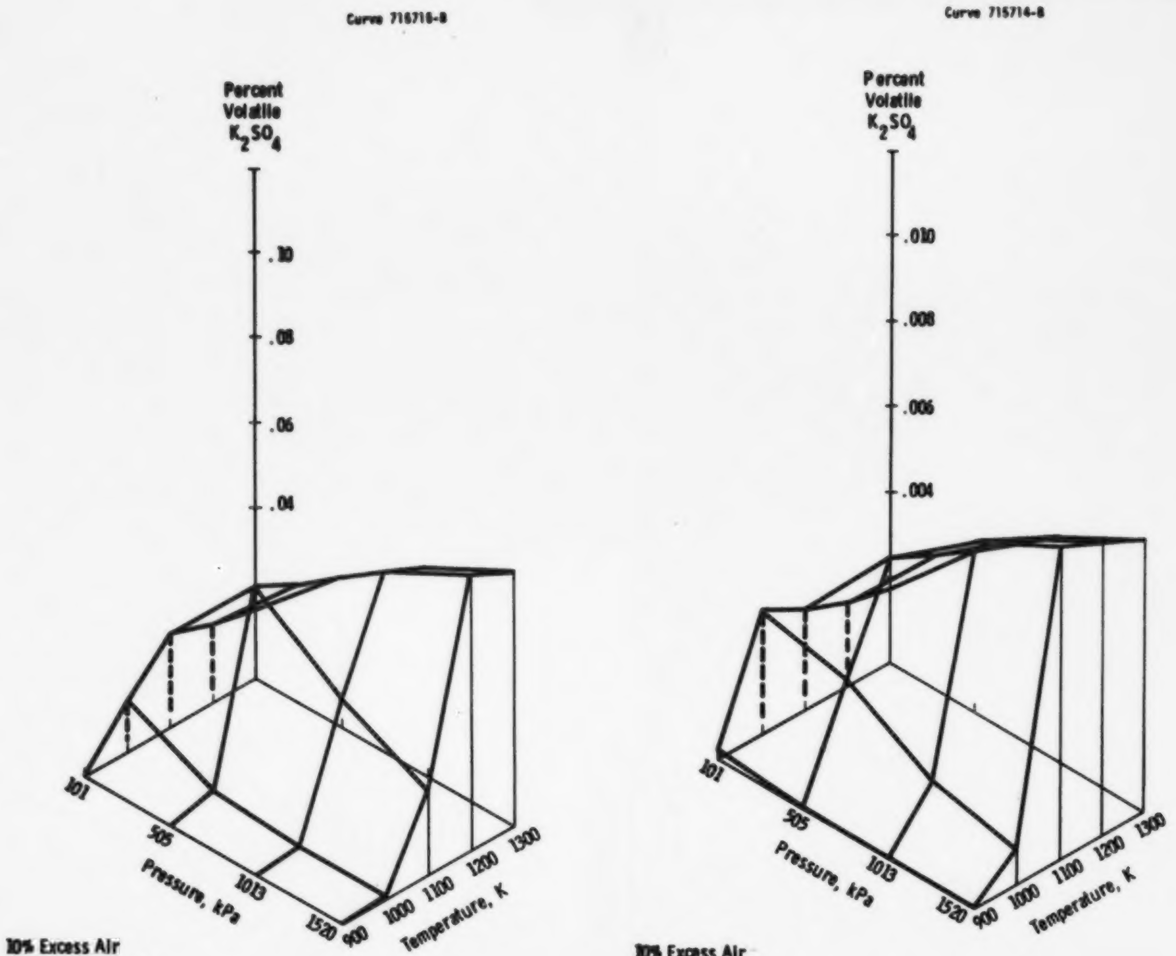

10% Excess Air
0% Sulfur Removal

10% Excess Air
90% Sulfur Removal

Figure 120 - Three-Dimensional Display of Volatile and Condensed Potassium Phases in Fluidized-Bed Combustion Systems (Continued)

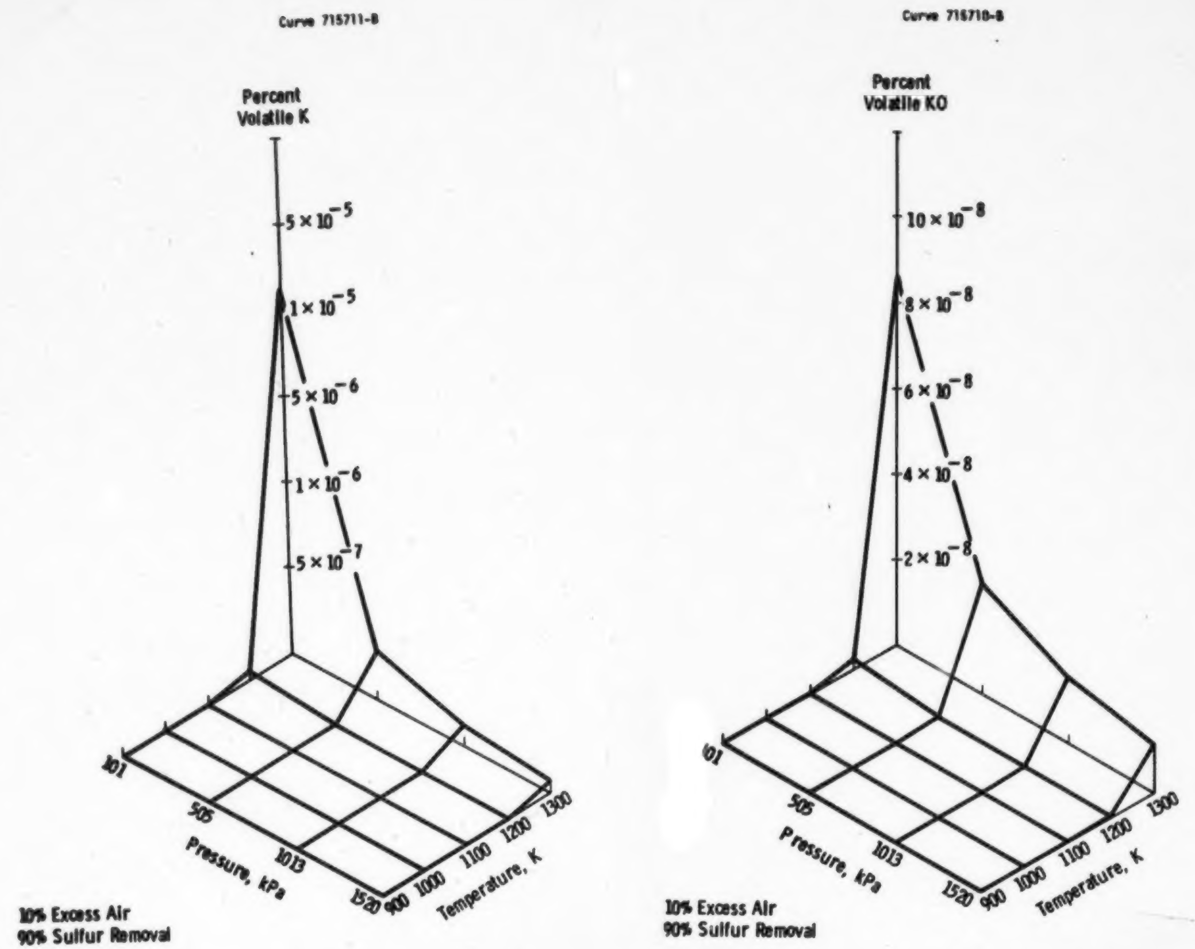

Figure 120 - Three-Dimensional Display of Volatile and Condensed Potassium Phases in Fluidized-Bed Combustion Systems (Continued)

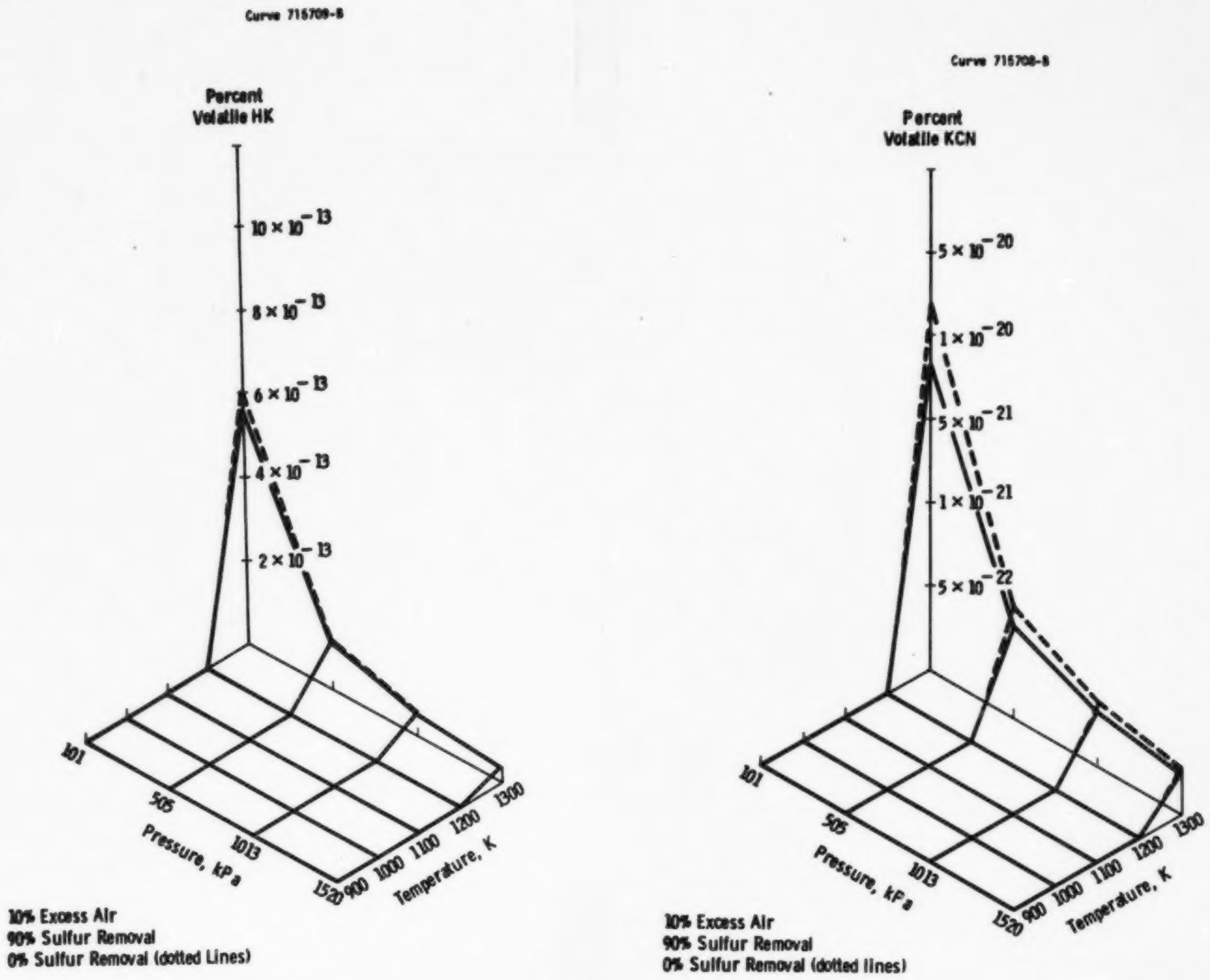

Figure 120 - Three-Dimensional Display of Volatile and Condensed Potassium Phases in Fluidized-Bed Combustion Systems (Continued)

Curve 715718-B

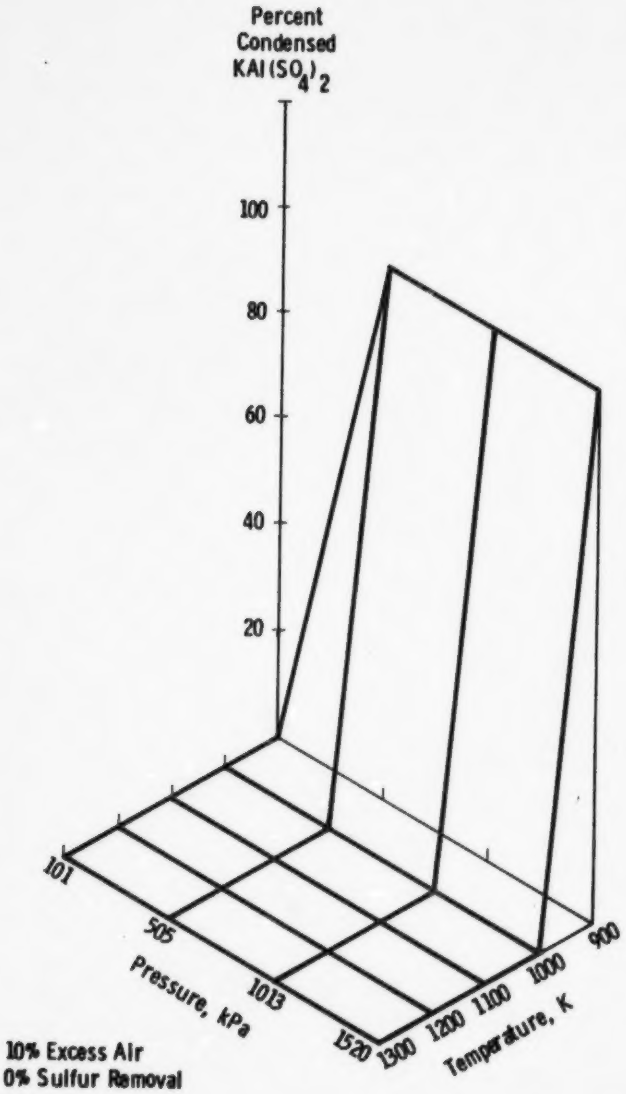

Figure 120 - Three-Dimensional Display of Volatile and Condensed Potassium Phases in Fluidized-Bed Combustion Systems (Continued)

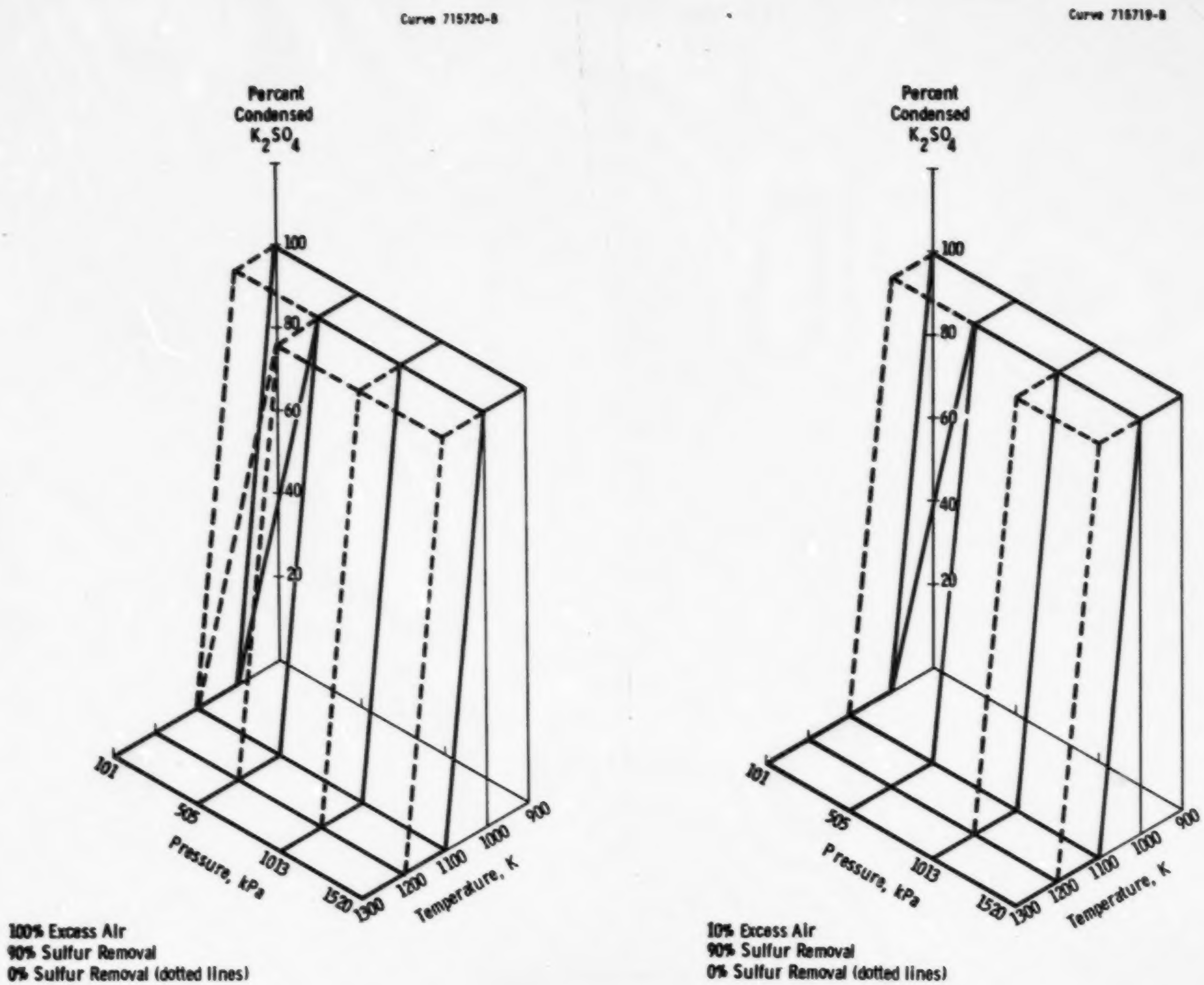

Figure 120 - Three-Dimensional Display of Volatile and Condensed Potassium Phases in Fluidized-Bed Combustion Systems (Continued)

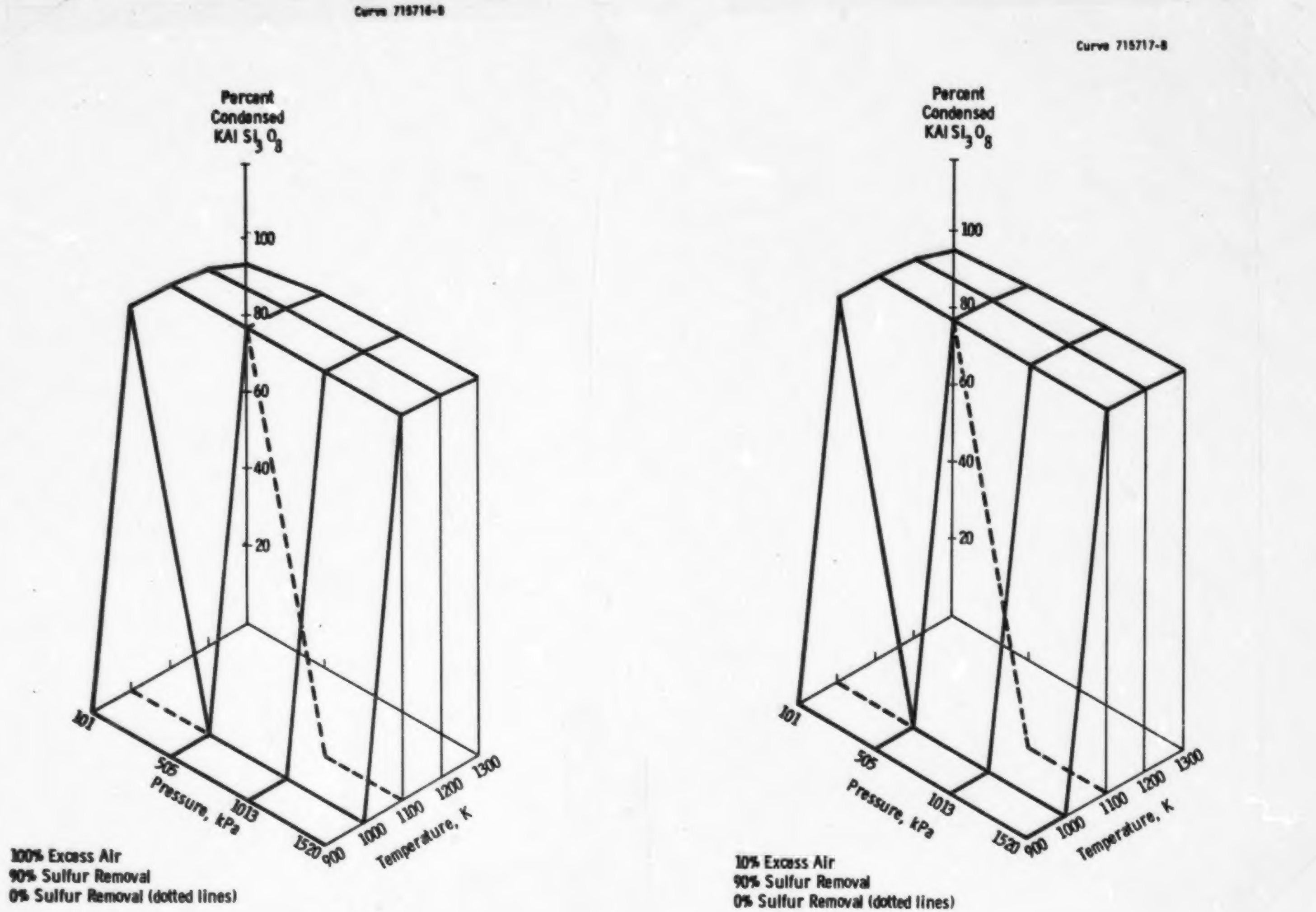

Figure 120 - Three-Dimensional Display of Volatile and Condensed Potassium Phases in Fluidized-Bed Combustion Systems (Continued)

Although the resulting partial pressures of the volatile Na phases in the FBC system are projected to be below 10^{-30} kPa (~10^{-28} atm), traces of gaseous NaCl are expected to be formed in equilibrium with the water glass ($2Na_2O \cdot SiO_2$)* complex. Reaction of gaseous NaCl with SO_2 may then lead to the formation of the corrosive liquid melt, Na_2SO_4, at temperatures above 1157 K or a mixed eutectic phase, $Na_2SO_4 \cdot K_2SO_4$, at temperatures above 1110 K.

Thermodynamically, the solid sodium water glass phase has been projected to form as a stable FBC ash phase, although additional low-melting temperature, highly viscous, mixed silicates may result between $2Na_2O \cdot SiO_2$ and free silica. These silicates could then promote the formation of liquidus phases that aggregate particulate fines, forming adhering deposits along alloy surfaces.

The volatilities of the mineral-type alkali compounds (i.e., mixed silicates) are unknown but are likely to be substantially lower than those projected for either the alkali chlorides or sulfates formed in the combustor. Rerelease of the alkali from the mineral phases in ash fines elutriated from the bed, when water vapor and/or gaseous HCl are present in the combustion gases, leads to formation of gaseous alkali chlorides and hydroxides, as shown for Na in reactions 72 and 73:

$$2Na_2O \cdot SiO_2(s) + 4HCl(g) \longrightarrow 4NaCl(g) + SiO_2(s) + 2H_2O(g) \qquad (72)$$

$$2Na_2O \cdot SiO_2(s) + 2H_2O(g) \longrightarrow 4NaOH(g) + SiO_2(s) \qquad (73)$$

---

*Similar in structure to the potassium feldspar complex, the sodium feldspar, $NaAlSi_3O_8$, is not projected to form as a stable solid in the fluidized-bed combustor when a U.S. mean coal is utilized as the feedstock material.

One can diagram these complex, simultaneous reactions in which gaseous vapors or fumes and ashlike fines containing alkali are formed, as shown in Figure 121, where an initial partitioning results and where secondary reactions proceed as functions of reaction kinetics, of the composition of the clay-contained phase, and of the operating parameters in the FBC system. Similar reactions of the trace and minor elements with ash may occur in the FBC effluent streams.

C-H-N-O-S-Cl-Si-Al-K-Na-Fe-Mn-Ni-Be

Tables 51 through 53 summarize the product distribution for the active gaseous and condensed phases formed in the C-H-N-O-S-Cl-Si-Al-K-Na-Fe-Mn-Ni-Be FBC system. At bed temperatures of 1200 K and at 1013 kPa (10 atm) total pressure the major solids formed in a 0 percent S-removal system are SiO_2 (cristobalite), $Al_2O_3 \cdot SiO_2$, $2Na_2O \cdot SiO_2$, K_2SO_4, manganese sesquioxide (Mn_2O_3), iron oxide (Fe_2O_3), beryllium aluminate ($BeAl_2O_4$), and nickel ferrate ($NiO \cdot Fe_2O_3$). The major volatiles exerting partial pressures greater than 10^{-10} kPa (10^{-12} atm) are KCl, K_2SO_4, nickel hydroxide ($Ni(OH)_2$), beryllium hydroxide ($Be(OH)_2$), beryllium chloride ($BeCl_2$), nickel chloride ($NiCl_2$), and manganese chloride ($MnCl_2$). A complex series of chemical reactions is involved in this system as the temperature is increased from 300 to 1200 K. These include:

$$SiO_2(s) \text{ (quartz)} \xrightarrow{1000\text{-}1100 \text{ K}} SiO_2(s) \text{ (cristobalite)} \qquad (74)$$

$$KAl(SO_4)_2 \cdot 12H_2O(s) \xrightarrow{300\text{-}400 \text{ K}} KAl(SO_4)_2(s) + 12H_2O(g) \qquad (75)$$

Dwg. 7727A22

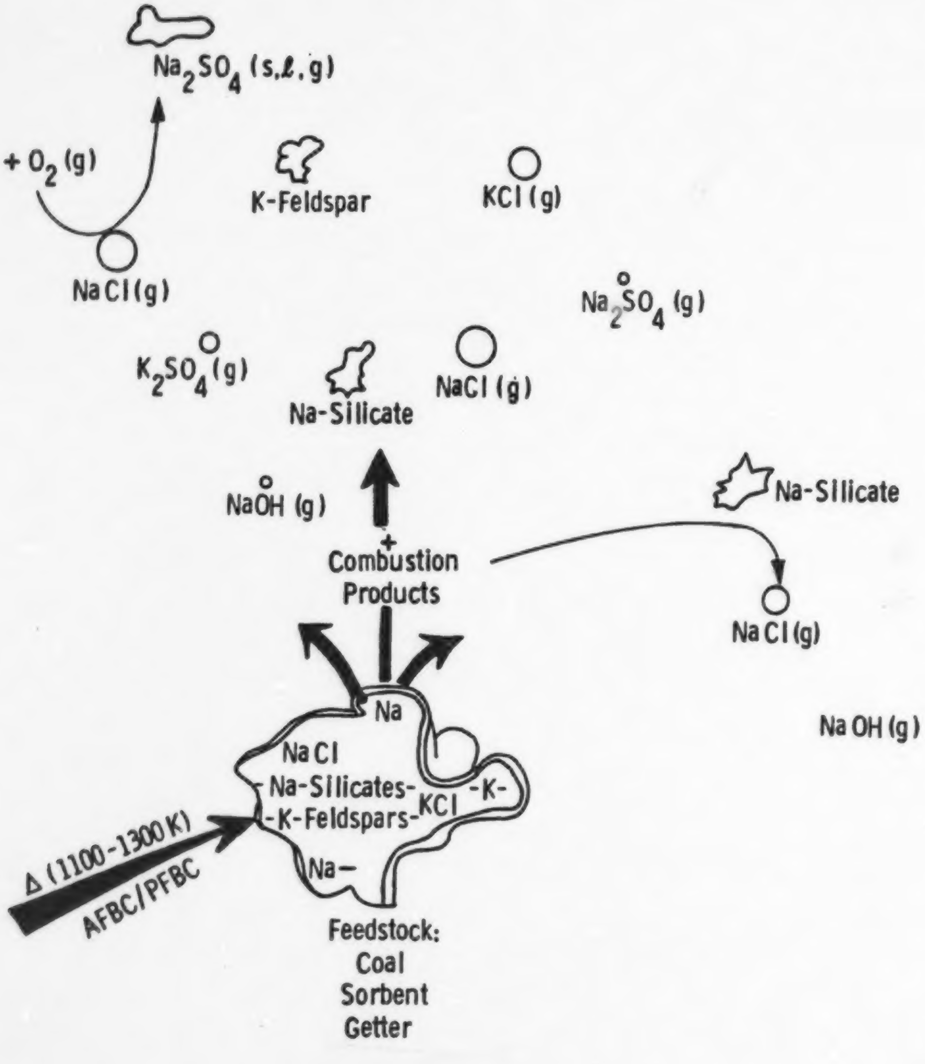

Na_2SO_4 (s,ℓ,g)
SO_2(g) + O_2(g)
K-Feldspar
KCl (g)
NaCl(g)
Na_2SO_4 (g)
K_2SO_4(g)
Na-Silicate
NaCl (g)
NaOH (g)
Na-Silicate
+ Combustion Products
NaCl(g)
NaOH (g)
Na
NaCl
Na-Silicates-
-K-Feldspars-
KCl
-K-
Na—
Δ (1100-1300 K)
AFBC/PFBC
Feedstock:
Coal
Sorbent
Getter

Figure 121 - Primary and Secondary Alkali Reactions during Combustion

TABLE 51 - FLUIDIZED-BED COMBUSTION OF C-H-N-O-S-Cl-Si-Al-K-Na-Fe-Mn-Ni-Be FOR 100% EXCESS AIR, 0% SULFUR-REMOVAL, 1013 kPa OPERATIONS

TEMP.\COMPOUND (K) \	QUARTZ (S)	CRISTOBALITE SIO2 (S)	KAL(SO4)2. 12H2O (S)	AL(OH)3 (S)	KAL(SO4)2 (S)
300	.8294-01	.0000	.8451-02	.1857-02	.0000
400	.8204-01	.0000	.0000	.0000	.8450-02
500	.8200-01	.0000	.0000	.0000	.8450-02
600	.8200-01	.0000	.0000	.0000	.8450-02
700	.8183-01	.0000	.0000	.0000	.8450-02
800	.7466-01	.0000	.0000	.0000	.8450-02
900	.6326-01	.0000	.0000	.0000	.8450-02
1000	.5904-01	.0000	.0000	.0000	.0000
1100	.0000	.5904-01	.0000	.0000	.0000
1200	.0000	.5904-01	.0000	.0000	.0000

TEMP.\COMPOUND (K) \	AL2SIO5 (S)	2NA2O. SIO2 (S)	AL2(SO4)3 (S)	FE2(SO4)3 (S)	NISO4 (S)
300	.0000	.2155-02	.1875-01	.1719-01	.3583-04
400	.9069-03	.2155-02	.1873-01	.1719-01	.3574-04
500	.9454-03	.2155-02	.1873-01	.1719-01	.3577-04
600	.9480-03	.2155-02	.1873-01	.1719-01	.3578-04
700	.1112-02	.2155-02	.1857-01	.1719-01	.3578-04
800	.8283-02	.2155-02	.1140-01	.1719-01	.3577-04
900	.1968-01	.2155-02	.0000	.0000	.3579-04
1000	.2390-01	.2155-02	.0000	.0000	.3567-04
1100	.2390-01	.2155-02	.0000	.0000	.0000
1200	.2390-01	.2155-02	.0000	.0000	.0000

TEMP.\COMPOUND (K) \	BESO4 (A)	BESO4 (B)	MNSO4 (S)	MNO2 (S)	BEAL2O4 (S)
300	.3921-04	.0000	.0000	.8994-04	.0000
400	.3921-04	.0000	.8994-04	.0000	.0000
500	.3921-04	.0000	.8992-04	.0000	.0000
600	.3921-04	.0000	.8992-04	.0000	.0000
700	.3921-04	.0000	.8992-04	.0000	.0000
800	.0000	.3921-04	.8992-04	.0000	.0000
900	.0000	.0000	.8992-04	.0000	.3921-04
1000	.0000	.0000	.0000	.0000	.3919-04
1100	.0000	.0000	.0000	.0000	.3904-04
1200	.0000	.0000	.0000	.0000	.3829-04

TEMP.\COMPOUND (K) \	K2SO4 (S)	MN2O3 (S)	FE2O3 (S)	NIO. FE2O3 (S)	NI2SIO4 (S)
300	.0000	.0000	.0000	.0000	.0000
400	.0000	.0000	.0000	.0000	.0000
500	.0000	.0000	.0000	.0000	.0000
600	.0000	.0000	.0000	.0000	.0000
700	.0000	.0000	.0000	.0000	.0000
800	.0000	.0000	.0000	.0000	.0000
900	.0000	.0000	.1719-01	.0000	.0000
1000	.4225-02	.4493-04	.1719-01	.0000	.0000
1100	.4217-02	.4473-04	.1716-01	.3539-04	.0000
1200	.4113-02	.4402-04	.1716-01	.3476-04	.0000

TEMP.\COMPOUND (K) \	KCL (G)	K2SO4 (G)	NI(OH)2 (G)	NICL2 (G)	MNCL2 (G)
300	.0000	.0000	.0000	.2988-32	.1916-33
400	.3608-24	.0000	.9494-31	.4058-22	.2615-22
500	.5101-18	.1338-27	.1350-23	.1284-16	.7699-17
600	.4223-14	.5641-21	.7820-19	.2748-13	.1518-13
700	.1942-12	.2857-16	.1964-15	.3711-11	.1891-11
800	.1721-09	.9048-13	.6944-13	.1233-09	.5817-10
900	.1047-06	.3850-08	.2938-10	.7941-08	.3481-08
1000	.9289-05	.1403-05	.1422-07	.8396-06	.1604-05
1100	.1892-03	.3368-04	.3002-06	.5071-05	.8002-05
1200	.2455-02	.4545-03	.2229-05	.1270-04	.2896-04

TEMP.\COMPOUND (K) \	BE(OH)2 (G)	BECL2 (G)
300	.0000	.0000
400	.6847-28	.0000
500	.6285-21	.3689-27
600	.3783-16	.1399-21
700	.4588-12	.3408-17
800	.1108-08	.1158-13
900	.2936-07	.3799-12
1000	.3488-06	.5221-11
1100	.2583-05	.4291-10
1200	.1377-04	.2450-09

TABLE 52 - FLUIDIZED-BED COMBUSTION OF C-H-N-O-S-Cl-Si-Al-K-Na-Fe-Mn-Ni-Be FOR 100% EXCESS AIR, 90% SULFUR-REMOVAL, 1013 kPa OPERATIONS

```
      \
TEMP.\COMPOUND        CRISTOBALITE KAL(SO4)2.
 (K)  \   QUARTZ (S)    SIO2 (S)     12H2O (S)    AL(OH)3 (S) KAL(SO4)2 (S)
  300     .8295-01     .0000        .6240-02     .4157-01     .0000
  400     .6182-01     .0000        .0000        .0000        .5479-02
  500     .6178-01     .0000        .0000        .0000        .5479-02
  600     .6175-01     .0000        .0000        .0000        .5419-02
  700     .6175-01     .0000        .0000        .0000        .5404-02
  800     .6124-01     .0000        .0000        .0000        .4403-02
  900     .5904-01     .0000        .0000        .0000        .0000
 1000     .5904-01     .0000        .0000        .0000        .0000
 1100     .0000        .5904-01     .0000        .0000        .0000
 1200     .0000        .5904-01     .0000        .0000        .0000
      \
TEMP.\COMPOUND         2NA2O.
 (K)  \   AL2SIO5 (S)    SIO2 (S) AL2(SO4)3 (S)FE2(SO4)3 (S) NISO4 (S)
  300     .0000        .2155-02     .0000        .0000        .0000
  400     .2113-01     .2155-02     .0000        .0000        .3584-04
  500     .2117-01     .2155-02     .0000        .0000        .3582-04
  600     .2120-01     .2155-02     .0000        .0000        .3582-04
  700     .2120-01     .2155-02     .0000        .0000        .3583-04
  800     .2170-01     .2155-02     .0000        .0000        .3581-04
  900     .2391-01     .2155-02     .0000        .0000        .3580-04
 1000     .2391-01     .2155-02     .0000        .0000        .0000
 1100     .2391-01     .2155-02     .0000        .0000        .0000
 1200     .2391-01     .2155-02     .0000        .0000        .0000
      \
TEMP.\COMPOUND
 (K)  \   BESO4 (A)     BESO4 (B)     MNSO4 (S)     MNO2 (S)    BEAL2O4 (S)
  300     .3921-04     .0000         .0000         .8992-04    .0000
  400     .0000        .0000         .0000         .8993-04    .3921-04
  500     .0000        .0000         .0000         .8993-04    .3921-04
  600     .0000        .0000         .8993-04      .0000       .3921-04
  700     .0000        .0000         .8991-04      .0000       .3921-04
  800     .0000        .0000         .8992-04      .0000       .3921-04
  900     .0000        .0000         .8996-04      .0000       .3921-04
 1000     .0000        .0000         .0000         .0000       .3919-04
 1100     .0000        .0000         .0000         .0000       .3904-04
 1200     .0000        .0000         .0000         .0000       .3829-04
      \
TEMP.\COMPOUND                                     NIO.
 (K)  \   K2SO4 (S)     MN2O3 (S)     FE2O3 (S)     FE2O3 (S)   NI2SIO4 (S)
  300     .0000        .0000         .1719-01      .0000       .0000
  400     .0000        .0000         .1719-01      .0000       .0000
  500     .0000        .0000         .1719-01      .0000       .0000
  600     .1516-02     .0000         .1719-01      .0000       .0000
  700     .1523-02     .0000         .1719-01      .0000       .0000
  800     .2024-02     .0000         .1719-01      .0000       .0000
  900     .4225-02     .0000         .1719-01      .0000       .0000
 1000     .4224-02     .4493-04      .1715-01      .3563-04    .0000
 1100     .4199-02     .4472-04      .1716-01      .3538-04    .0000
 1200     .3901-02     .4411-04      .1716-01      .3481-04    .0000
      \
TEMP.\COMPOUND
 (K)  \   KCL (C)       NICL2 (C)
  300     .2211-02     .3582-04
  400     .0000        .0000
  500     .0000        .0000
  600     .0000        .0000
  700     .0000        .0000
  800     .0000        .0000
  900     .0000        .0000
 1000     .0000        .0000
 1100     .0000        .0000
 1200     .0000        .0000
      \
TEMP.\COMPOUND
 (K)  \   KCL (G)       K2SO4 (G)     NI(OH)2 (G) NICL2 (G)     MNCL2 (G)
  300     .3336-28     .0000         .0000        .3489-28     .1417-33
  400     .2854-19     .3139-30      .2672-28     .1131-19     .2644-22
  500     .3912-14     .9056-22      .1182-21     .1116-14     .8122-16
  600     .6678-11     .3563-16      .3108-17     .1088-11     .6011-12
  700     .9765-09     .3229-12      .4397-14     .8298-10     .4230-10
  800     .3596-07     .2737-09      .1002-11     .1778-08     .8389-09
  900     .1012-05     .2719-07      .3889-09     .1051-06     .4608-07
 1000     .3541-04     .1403-05      .2716-07     .1602-05     .1594-05
 1100     .7174-03     .3368-04      .3001-06     .5031-05     .7901-05
 1200     .8772-02     .4545-03      .2229-05     .1157-04     .2627-04
      \
TEMP.\COMPOUND
 (K)  \   BE(OH)2 (G) BECL2 (G)
  300     .6670-29   .0000
  400     .9469-21   .1003-28
  500     .6736-16   .3816-22
  600     .1171-12   .4202-18
  700     .2428-10   .1792-15
  800     .1324-08   .1383-13
  900     .2934-07   .3795-12
 1000     .3487-06   .5218-11
 1100     .2587-05   .4289-10
 1200     .1376-04   .2450-09
```

TABLE 53 - FLUIDIZED-BED COMBUSTION OF C-H-N-O-S-Cl-Si-Al-K-Na-Fe-Mn-Ni-Be FOR 100% EXCESS AIR, 99% SULFUR-REMOVAL. 1013 kPa OPERATIONS

TEMP. \ COMPOUND (K) \	QUARTZ (S)	CRISTOBALITE SIO2 (S)	KAL(SO4)2. 12H2O (S)	AL(OH)3 (S)	KAL(SO4)2 (S)
300	.8295-01	.0000	.6250-03	.4719-01	.0000
400	.5908-01	.0000	.0000	.0000	.0000
500	.5902-01	.0000	.0000	.0000	.0000
600	.5902-01	.0000	.0000	.0000	.0000
700	.5902-01	.0000	.0000	.0000	.0000
800	.5904-01	.0000	.0000	.0000	.0000
900	.5904-01	.0000	.0000	.0000	.0000
1000	.5904-01	.0000	.0000	.0000	.0000
1100	.0000	.5904-01	.0000	.0000	.0000
1200	.0000	.5913-01	.0000	.0000	.0000

TEMP. \ COMPOUND (K) \	AL2SIO5 (S)	2NA2O. SIO2 (S)	AL2(SO4)3 (S)	FE2(SO4)3 (S)	NISO4 (S)
300	.0000	.2155-02	.0000	.0000	.0000
400	.2387-01	.2155-02	.0000	.0000	.0000
500	.2391-01	.2155-02	.0000	.0000	.3582-04
600	.2391-01	.2155-02	.0000	.0000	.0000
700	.2391-01	.2155-02	.0000	.0000	.0000
800	.2391-01	.2155-02	.0000	.0000	.0000
900	.2391-01	.2155-02	.0000	.0000	.0000
1000	.2391-01	.2155-02	.0000	.0000	.0000
1100	.2391-01	.2155-02	.0000	.0000	.0000
1200	.2382-01	.2155-02	.0000	.0000	.0000

TEMP. \ COMPOUND (K) \	BESO4 (A)	BESO4 (B)	MNSO4 (S)	MNO2 (S)	BEAL2O4 (S)
300	.3921-04	.0000	.0000	.8990-04	.0000
400	.0000	.0000	.0000	.8996-04	.3921-04
500	.0000	.0000	.0000	.8993-04	.3921-04
600	.0000	.0000	.0000	.8993-04	.3921-04
700	.0000	.0000	.0000	.8993-04	.3921-04
800	.0000	.0000	.0000	.0000	.3921-04
900	.0000	.0000	.0000	.0000	.3921-04
1000	.0000	.0000	.0000	.0000	.3921-04
1100	.0000	.0000	.0000	.0000	.3919-04
1200	.0000	.0000	.0000	.0000	.3904-04
					.3829-04

TEMP. \ COMPOUND (K) \	K2SO4 (S)	MN2O3 (S)	FE2O3 (S)	NIO. FE2O3 (S)	NI2SIO4 (S)
300	.0000	.0000	.1719-01	.0000	.0000
400	.1214-02	.0000	.1719-01	.0000	.0000
500	.1250-02	.0000	.1719-01	.0000	.1788-04
600	.1250-02	.0000	.1719-01	.0000	.1790-04
700	.1250-02	.0000	.1719-01	.0000	.1790-04
800	.1250-02	.4496-04	.1715-01	.3579-04	.0000
900	.1250-02	.4496-04	.1715-01	.3572-04	.0000
1000	.1250-02	.4498-04	.1715-01	.3574-04	.0000
1100	.1248-02	.4495-04	.1715-01	.3569-04	.0000
1200	.1207-02	.0000	.1715-01	.3553-04	.0000

TEMP. \ COMPOUND (K) \	KCL (S)	NICL2 (S)	MNO. AL2O3 (S)
300	.7826-02	.3579-04	.0000
400	.6022-02	.0000	.0000
500	.5951-02	.0000	.0000
600	.5951-02	.0000	.0000
700	.5951-02	.0000	.0000
800	.5949-02	.0000	.0000
900	.5897-02	.0000	.0000
1000	.0000 *	.0000	.0000
1100	.0000	.0000	.0000
1200	.0000	.0000	.8980-04

TEMP. \ COMPOUND (K) \	KCL (G)	K2SO4 (G)	NI(OH)2 (G)	NICL2 (G)	MNCL2 (G)
300	.3336-28	.0000	.0000	.3489-28	.3047-34
400	.1431-18	.3139-30	.1982-26	.2843-18	.8949-23
500	.7813-13	.9056-22	.4509-19	.1110-12	.2116-16
600	.4865-09	.3563-16	.4594-15	.2784-10	.1297-12
700	.2366-06	.3229-12	.3222-12	.8862-09	.4024-10
800	.2345-04	.2737-09	.3541-10	.8776-08	.2378-08
900	.8066-03	.2719-07	.1433-08	.5347-07	.2983-07
1000	.8879-01*	.1403-05	.2719-07	.2207-06	.2195-06
1100	.8877-01	.3368-04	.3004-06	.6995-06	.1098-05
1200	.8906-01	.4545-03	.2231-05	.1790-05	.2626-05

TEMP. \ COMPOUND (K) \	BE(OH)2 (G)	BECL2 (G)	KOH (G)
300	.6671-29	.0000	.0000
400	.9467-21	.1001-28	.2596-32
500	.6734-16	.3812-22	.1058-23
600	.1172-12	.4199-18	.9259-18
700	.2427-10	.1792-15	.1968-13*
800	.1324-08	.1383-13	.3515-10
900	.2934-07	.3795-12	.1168-07
1000	.3486-06	.5218-11	.7991-05
1100	.2587-05	.4289-10	.3589-04
1200	.1376-04	.2449-09	.1276-03

* ESTIMATED VALUES

$$2KAl(SO_4)_2(s) \xrightarrow{900-1000\ K} K_2SO_4(s) + Al_2O_3(s) + 3SO_2(g) + 3/2\ O_2(g) \quad (76)$$

$$2Al(OH)_3(s) + SiO_2(s) \xrightarrow{300-400\ K} Al_2O_3 \cdot SiO_2(s) + 3H_2O(g) \quad (77)$$

$$2Na_2O \cdot SiO_2 \text{ -- stable from 300-1200 K} \quad (78)$$

$$Al_2(SO_4)_3(s) + SiO_2(s) \xrightarrow{700-900\ K} Al_2O_3 \cdot SiO_2(s) + 3SO_2(g) + 3/2\ O_2(g) \quad (79)$$

$$Fe_2(SO_4)_3(s) \xrightarrow{800-900\ K} Fe_2O_3(s) + 3SO_2(g) + 3/2\ O_2(g) \quad (80)$$

$$NiSO_4(s) + Fe_2O_3(s) \xrightarrow{1000-1100\ K} NiO \cdot Fe_2O_3(s) + SO_2(g) + 1/2\ O_2(g) \quad (81)$$

$$Be(OH)_2(s) + Al_2O_3(s) \xrightarrow{300-400\ K} BeAl_2O_4(s) + H_2O(g) \quad (82)$$

$$\alpha\text{-}BeSO_4(s) + Al_2O_3(s) \xrightarrow{300-1200\ K} BeAl_2O_4(s) + SO_2(g) + 1/2\ O_2(g) \quad (83)$$

$$BeAl_2O_4(s) + H_2O(g) \longrightarrow Be(OH)_2(g) + Al_2O_3(s) \quad (84)$$

$$Al_2O_3(s) + SiO_2(s) \xrightarrow{600\ K} Al_2O_3 \cdot SiO_2(s) \quad (85)$$

$$MnO_2(s) + SO_2(g) \xrightarrow{300-400\ K} MnSO_4(s) \quad (86)$$

$$2MnSO_4(s) + 1/2\ O_2(g) \xrightarrow{900-1000\ K} Mn_2O_3(s) + 2SO_2(g) + O_2(g) \quad (87)$$

A reduction in the total S content of the system alters the chemical equilibrium in the FBC system. Unlike those at 0 percent S removal, operations at 90 percent S removal reduce the temperature range of stability of the $KAl(SO_4)_2(s)$ complex. At 90 percent S removal $KAl(SO_4)_2(s)$ is converted into $K_2SO_4(s)$ and alumina ($Al_2O_3(s)$) at 600 to 700 K, while at 0 percent S removal this reaction results only when the system temperature approaches 900 to 1000 K. Free $K_2SO_4(s)$, therefore, is stable in fluidized-bed, 90 percent S-removal systems at much lower temperatures than those that would form if the total S content of the coal were present.

In 90 percent S-removal systems the reaction forming $Al_2O_3 \cdot SiO_2$ occurs between 300 and 400 K, whereas in the 0 percent S-removal system temperatures of 1000 K are required prior to the formation of an equivalent concentration. No change is noted for the compound $2Na_2O \cdot SiO_2$ when the concentration of free S is reduced; in the 90 percent S-removal systems, however, neither $Al_2(SO_4)_3$ nor iron trisulfate ($Fe_2(SO_4)_3$) form as stable solids. Aluminum reacts with Si to form the $Al_2O_3 \cdot SiO_2$ complex, while Fe forms as solid Fe_2O_3.

At temperatures of 300 K, Ni reacts with Cl to form $NiCl_2(s)$. As the system temperature increases, nickel sulfate ($NiSO_4(s)$) results, as shown in the following reaction:

$$NiCl_2(s) + H_2SO_4(g) \longrightarrow NiSO_4(s) + 2HCl(g) \quad . \qquad (88)$$

A reduction in the S content lowers the temperature of stability for solid $NiSO_4$ to between 900 and 1000 K, prior to its conversion into $NiO \cdot Fe_2O_3(s)$. At 0 percent S removal solid $NiSO_4$ is present at temperatures of 1000 to 1100 K.

Alpha-beryllium sulfate (α-$BeSO_4$) is stable as a solid between temperatures of 300 and 700 to 800 K in the 100 percent excess air, 0 percent S-removal fluidized-bed combustor. At operating temperatures exceeding 700 K conversion into beryllium aluminate ($BeAl_2O_4$) results, as shown in reaction 83. Conversion into $BeAl_2O_4$ is achieved in the FBC at temperatures between 300 and 400 K with 90 and 99 percent S-removal efficiencies. Beryllium remains complexed with Al as the stable aluminate phase at temperatures of 1200 K, where only 2.4 percent of the initial Be feedstock content volatilizes as gaseous beryllium hydroxide ($Be(OH)_2$).

Limiting the S content in the combustor effluent gases enhances the sulfate $\longrightarrow$ oxide transition of solid Mn. Manganese dioxide (MnO_2), is formed as a stable solid phase between 300 and 500 K prior to its conversion into the manganese sulfate ($MnSO_4$) solid phase. This reaction in 0 percent S-removal systems occurs between 300 and 400 K. Final conversion of the $MnSO_4(s)$ into $Mn_2O_3(s)$ occurs between 900 and 1000 K for both systems.

The equilibrium calculations indicate that solid KCl is formed in 90 percent S-removal systems at temperatures of 300 K and at pressures between 101 and 1013 kPa (1 and 10 atm). The 0 percent S-removal system favors the formation not of KCl, but of potassium aluminum sulfate complexes.

The partial pressures of the major volatile compounds are virtually equivalent at combustion temperatures of 1100 K for both S systems. At lower temperatures the reduction in the S content increases the partial pressures of the major volatile phases, while decreasing the stability of the solid S phases. At combustion temperatures of 1200 K, the solids formed at equilibrium for 90 percent S removal are identical to those formed at 0 percent S removal.

Reduction of the total S content in FBC systems to that of 99 percent S removal is sufficient to prevent the formation of solid sulfates ($KAl(SO_4)_2$, $Al_2(SO_4)_3$, $Fe(SO_4)_3$, and $MnSO_4$). The conversion of quartz into cristobalite at 1000 to 1100 K, the reaction of $KAl(SO_4)_2 \cdot 12H_2O$ and $Al(OH)_3$ to form K_2SO_4 and $Al_2O_3 \cdot SiO_2$, respectively, and the stability of $Al_2O_3 \cdot SiO_2$ and $2Na_2O \cdot SiO_2$ over 300 to 1200 K are similar to those previously described. Beryllium forms the alpha sulfate solid under reduced S partial pressures and converts into $BeAl_2O_4$ at temperatures exceeding 400 K.

The major differences that result when S is removed by sorbent material are in the K, Be, Ni, and Mn reactions. Solid KCl is formed between 300 and 900 K, while solid K_2SO_4 is stable between 400 and 1200 K. In the 90 percent S-removal systems K reacts with Al and S to form $KAl(SO_4)_2$.

Beryllium exists primarily as alpha or beta sulfate below 900 K in 0 percent S-removal systems; these phases, however, are stable only at temperatures of 300 to 400 K in the combustor with 90 or 99 percent S-removal efficiencies. Conversion into the stable aluminate complex results at elevated operating temperatures.

At bed temperatures of 300 K, solid $NiCl_2$ is formed. Conversion into $NiSO_4$ results at 400 K, which then reacts with quartz to yield nickel silicate (Ni_2SiO_4) by the reaction

$$2NiSO_4(s) + SiO_2(s) \xrightarrow{400\text{–}500\ K} Ni_2SiO_4(s) + 2SO_2(g) + O_2(g) \quad . \qquad (89)$$

As the temperature of the system is increased to 700 or 800 K, Ni_2SiO_4 reacts with Fe_2O_3 to form solid $NiO{\cdot}Fe_2O_3$ by the reaction

$$Ni_2SiO_4(s) + 2Fe_2O_3(s) \xrightarrow{700\text{–}800\ K} 2\ NiO{\cdot}Fe_2O_3(s) + SiO_2(s) \quad , \qquad (90)$$

which remains stable at combustion temperatures of 1200 K.

Manganese at low temperatures in 99 percent S-removal systems forms $MnO_2(s)$ rather than $MnSO_4$. Conversion of MnO_2 into Mn_2O_3 results between 700 and 800 K. A final reaction of Mn with Al occurs at 1100 to 1200 K to form manganese aluminate ($MnO{\cdot}Al_2O_3(s)$) by the reaction

$$\begin{aligned} Mn_2O_3(s) + 2\ Al_2O_3{\cdot}SiO_2(s) &\xrightarrow{1100\text{–}1200\ K} 2\ MnO{\cdot}Al_2O_3(s) \\ &\quad + 2SiO_2(s) + 1/2\ O_2(g) \quad . \qquad (91) \end{aligned}$$

The solid phases formed in 99 percent S-removal FBC systems operating at 1200 K are SiO_2 (cristobalite), $Al_2O_3 \cdot SiO_2$, $2Na_2O \cdot SiO_2$, K_2SO_4, Fe_2O_3, $NiO \cdot Fe_2O_3$, $BeAl_2O_4$, and $MnO \cdot Al_2O_3$. In addition to the major volatile phases, $MnCl_2$, KCl, K_2SO_4, $Ni(OH)_2$, $Be(OH)_2$, $BeCl_2$, and $NiCl_2$, KOH is formed at equilibrium in 99 percent S-removal systems.

Equilibrium calculations using the Robie and Waldbaum data[77] for the phase $KAlSi_3O_8$ were repeated for the C-H-N-O-S-Cl-Si-Al-K-Na-Fe-Mn-Ni-Be FBC systems. Table 54 indicates the resulting solid, liquid, and gaseous phases for operations at 100 percent excess air, 0 percent S removal at 1013 kPa (10 atm) total pressure for temperatures from 900 to 1300 K. Comparison of these results with those obtained using the Barin and Knacke[71] data for $KAlSi_3O_8$ show that the system is modified at the higher temperatures by the following reaction:

$$K_2SO_4(s) + Al_2O_3 \cdot SiO_2(s) + 5SiO_2(s) \xrightarrow{1100\text{-}1200\ K} 2\ KAlSi_3O_8(s) + SO_2(g) + 1/2\ O_2(g) \ . \qquad (92)$$

Between 1100 and 1200 K, 100 percent of the solid K_2SO_4 phase reacts with 35 percent of the solid SiO_2 phase and 18 percent of the solid $Al_2O_3 \cdot SiO_2$ to form the alkali aluminosilicate ($KAlSi_3O_8$). At temperatures of 1200 to 1300 K, 1.5 percent of $KAlSi_3O_8$ releases $SiO_2(s)$, and 100 percent of the remaining $Al_2O_3 \cdot SiO_2(s)$ present at 1200 K is converted to mullite ($3Al_2O_3 \cdot 2SiO_2(s)$), with an increase in the total concentration of $SiO_2(s)$ in the system. The gettering activity of the $KAlSi_3O_8$ is shown to be 98.5 percent effective for the K content in the feed materials for temperatures of 1200 to 1300 K.

Comparison of the projections using the Robie and Waldbaum[77] and Barin and Knacke[71] data for the remaining trace and minor solid or gaseous phases shows virtually little change between projected combustion systems.

The reduction of S in the FBC gases minimizes the stability of $MnSO_4$, $NiSO_4$, $KAl(SO_4)_2$, and K_2SO_4 in the system. With a lower

TABLE 54 - REEVALUATION OF FLUIDIZED-BED COMBUSTION OF C-H-N-O-S-Cl-Si-Al-K-Na-Fe-Mn-Ni-Be FOR 100% EXCESS AIR, 0% SULFUR-REMOVAL, 1013 kPa OPERATIONS

```
    \
TEMP.\COMPOUND         CRISTOBALITE  KAL(SO4)2.
 (K)  \  QUARTZ (S)     SIO2 (S)      12H2O (S)    AL(OH)3 (S)  KAL(SO4)2 (S)
  900     .6325-01      .0000         .0000        .0000        .8450-02
 1000     .5903-01      .0000         .0000        .0000        .0000
 1100     .0000         .5903-01      .0000        .0000        .0000
 1200     .0000         .3818-01      .0000        .0000        .0000
 1300     .0000         .4506-01      .0000        .0000        .0000
    \
TEMP.\COMPOUND          2NA2O.
 (K)  \  AL2SIO5 (S)     SIO2 (S)    AL2(SO4)3 (S) FE2(SO4)3 (S) NISO4 (S)
  900     .1968-01      .2155-02      .0000        .0000        .3580-04
 1000     .2390-01      .2155-02      .0000        .0000        .3574-04
 1100     .2390-01      .2155-02      .0000        .0000        .0000
 1200     .1963-01      .2155-02      .0000        .0000        .0000
 1300     .0000         .2155-02      .0000        .0000        .0000
    \
TEMP.\COMPOUND
 (K)  \  BESO4 (A)     BESO4 (B)     MNSO4 (S)     MNO2 (S)     BEAL2O4 (S)
  900     .0000         .0000         .8990-04     .0000        .3921-04
 1000     .0000         .0000         .0000        .0000        .3919-04
 1100     .0000         .0000         .0000        .0000        .3904-04
 1200     .0000         .0000         .0000        .0000        .3829-04
    \
TEMP.\COMPOUND                                     NIO.
 (K)  \  K2SO4 (S)     MN2O3 (S)     FE2O3 (S)      FE2O3 (S)   NI2SIO4 (S)
  900     .0000         .0000         .1719-01     .0000        .0000
 1000     .4225-02      .4490-04      .1719-01     .0000        .0000
 1100     .4217-02      .4469-04      .1715-01     .3538-04     .0000
 1200     .0000         .4432-04      .1716-01     .3478-04     .0000
 1300     .0000         .0000         .1716-01     .3311-04     .0000
    \
TEMP.\COMPOUND         3AL2O3        MNO.
 (K)  \ KALSI3O8 (S)    2SIO2 (S)    AL2O3 (S)     KCL (G)      K2SO4 (G)
  900     .0000         .0000         .0000        .1045-06     .3852-08
 1000     .0000         .0000         .0000        .9288-05     .1398-05
 1100     .0000         .0000         .0000        .1892-03     .3368-04
 1200     .8377-02      .0000         .0000        .9594-03     .7028-04
 1300     .8250-02      .6564-02      .8733-04     .2858-02     .6788-04
    \
TEMP.\COMPOUND
 (K)  \  NI(OH)2 (G)  BE(OH)2 (G)   NICL2 (G)     MNCL2 (G)    FE(OH)2 (G)
  900     .2939-10      .2936-07      .7917-08     .3472-08     .7879-12
 1000     .1422-07      .3488-06      .8396-06     .1604-05     .5481-10
 1100     .3002-06      .2583-05      .5071-05     .8002-04     .1742-08
 1200     .2229-05      .1377-04      .1298-04     .1904-04     .3088-06
    \
TEMP.\COMPOUND
 (K)  \  KOH (G)       FECL2 (G)
  900     .5638-12      .1537-09
 1000     .3099-09      .2204-08
 1100     .2841-07      .1876-07
 1200     .5106-06      .1079-06
 1300     .4509-05      .4563-06
```

concentration of S available for reaction with Mn, Ni, and K to form solid sulfate phases, alternate reactions occur as a function of temperature. For example, in systems operating with 100 percent excess air, the reaction

$$2MnSO_4(s) \longrightarrow Mn_2O_3(s) + 2SO_2(g) + 1/2\ O_2(g) \qquad (93)$$

occurs at 900 to 1000 K for 0 percent and 90 percent S removal. With 99 percent S removal the solid $MnSO_4$ phase is not expected to form at any temperature. Similarly, the reaction

$$NiSO_4(s) + Fe_2O_3(s) \longrightarrow NiO \cdot Fe_2O_3(s) + SO_2(g) + 1/2\ O_2(g) \quad (94)$$

occurs at 1000 to 1100 K for 0 percent S-removal, at 900 to 1000 K for 90 percent S-removal, and at temperatures less than 700 K for 99 percent S removal systems. The formation of $KAl(SO_4)_2$ as a stable solid phase exists at temperatures of 900 to 1000 K for 0 percent S-removal and at 800 to 900 K for 90 percent S-removal but does not form at any temperature for a 99 percent S-removal system. Potassium sulfate reacts with $Al_2O_3 \cdot SiO_2$ and excess Si to form $KAlSi_3O_8$,* as shown by the reaction

$$K_2SO_4(s) + Al_2O_3 \cdot SiO_2(s) + 5SiO_2(s) \longrightarrow 2\ KAlSi_3O_8(s) \qquad (95)$$

$$+ SO_2(g) + 1/2\ O_2(g).$$

The stability of the K_2SO_4 phase is dependent on the total S content of the system. At 0 percent sulfur removal reaction 95 proceeds at temperatures between 1100 and 1200 K, while at 90 percent S removal the reaction temperature is lowered to 1000 or 1100 K and, for 99 percent S removal to 500 or 700 K. The efficiency of the $Al_2O_3 \cdot SiO_2$ to act as an effective gettering material therefore, is dependent on the partial pressure of SO_2 and the K content of the combustion system.

---

*Robie and Waldbaum data for $KAlSi_3O_8$

Comparison of the thermodynamic projections using the Robie and Waldbaum data for the $KAlSi_3O_8$ phase as opposed to the Barin and Knacke data indicates once again the potential in forming an efficient gettering material for K-laden combustion gases at reduced S partial pressures. The Barin and Knacke data do not predict the gettering activity of the aluminosilicates present in the system in which either potassium silicate (K_2SiO_3) or $KAlSi_3O_8$ form but project deposition of the solid K_2SO_4 or $KAl(SO_4)_2$ phase.

Projections of the percent volatilization for the minor and trace elements are shown in Table 55 for a 90 percent S-removal, 100 percent excess air, 1013 kPa FBC system operating at 1200 K. Comparison of these data with the projections for the isolated trace and minor systems indicates that the interaction with the clay constituents reduces the volatility of Mn, Ni and Be by 64, 52, and 97 percent, respectively.* The elements Si, Al, Na, K, and Fe remain virtually as solid phases.

C-H-N-O-S-Cl-Si-Al-K-Na-Cr-Fe-Mo-Mn-Ti

Coals deficient in Ni or Be may form a series of reactions that are different from those that have been described. Consideration is now given to the coal combustion reactions of C-H-N-O-S-Cl-Si-Al-K-Na-Cr-Fe-Mo-Ni and Ti. Solids formed at 1200 K and 1013 kPa (10 atm) total pressure in 0 percent S-removal systems include SiO_2 (cristobalite), $Al_2O_3 \cdot SiO_2$, $Al_2O_3 \cdot TiO_2$, $MnO \cdot Al_2O_3$, Cr_2O_3, K_2SO_4, and $2Na_2O \cdot SiO_2$.

The following reactions summarize the equilibrium phases that result as a function of temperature in FBC systems:

$$SiO_2(s)(quartz) \xrightarrow{1000-1100\ K} SiO_2(s)(cristobalite) \qquad (96)$$

---

*Noninteractive Systems 2.2% Mn, 5.05% Ni, and 100% Be of the original feed content volatilize at 1200 K.

TABLE 55 - PROJECTED FBC TRACE AND MINOR SPECIES AT 1200 K AND 1013 kPa FOR 90% SULFUR REMOVAL IN 100% EXCESS AIR

Element	Coal wt %, ppm	Condensed Phases	Volatile Phases	Percent Volatilization at 1200 K
Si	2.39%	SiO_2, $Al_2O_3 \cdot SiO_2$, $2Na_2O \cdot SiO_2$, $KAlSi_3O_8$	--	0%
Al	1.29%	$Al_2O_3 \cdot SiO_2$, $KAlSi_3O_8$ $MnO \cdot Al_2O_3$	--	0%
K	0.16%	$KAlSi_3O_8$	KCl, K_2SO_4, KOH	0.77%
Na	0.05%	$2Na_2O \cdot SiO_2$	--	0%
Fe	1.92%	Fe_2O_3,$NiO \cdot Fe_2O_3$	$FeCl_2$, $Fe(OH)_2$	~0%
Mn	49.40 ppm	Mn_2O_3,$MnO \cdot Al_2O_3$	$MnCl_2$	1.4%
Ni	21.07 ppm	$NiO \cdot Fe_2O_3$	$Ni(OH)_2$, $NiCl_2$	2.6%
Be	1.61 ppm	$BeAl_2O_4$	$Be(OH)_2$	2.4%

$$KAl(SO_4)_2\cdot 12H_2O(s) \xrightarrow{300\text{-}400\ K} KAl(SO_4)_2(s) + 12H_2O(g) \tag{97}$$

$$2KAl(SO_4)_2(s) \xrightarrow{900\text{-}1000\ K} K_2SO_4(s) + Al_2O_3(s) + 3SO_2(g) + 3/2\ O_2(g) \tag{98}$$

$$K_2SO_4(s) + Al_2O_3\cdot SiO_2(s) + 5SiO_2(s) \longrightarrow 2\ KAlSi_3O_8(s) + SO_2(g) + 1/2\ O_2(g) \tag{99}$$

$$2Al(OH)_3(s) + TiO_2(s) \xrightarrow{300\text{-}400\ K} Al_2O_3\cdot TiO_2(s) + 3H_2O(g) \tag{100}$$

$$Al_2(SO_4)_3(s) + SiO_2(s) \xrightarrow{700\text{-}900\ K} Al_2O_3\cdot SiO_2(s) + 3SO_2(g) + 3/2\ O_2(g) \tag{101}$$

$$TiO_2(s) + Al_2O_3(s) \xrightarrow{700\text{-}800\ K} Al_2O_3\cdot TiO_2(s) \tag{102}$$

$$MnO_2(s) + SO_2(g) \xrightarrow{300\text{-}400\ K} MnSO_4(s) \tag{103}$$

$$2MnSO_4(s) \xrightarrow{900\text{-}1000\ K} Mn_2O_3(s) + 2SO_2(g) + 1/2\ O_2(g) \tag{104}$$

$$Mn_2O_3(s) + 2Al_2O_3(s) \xrightarrow{1100\text{-}1200\ K} 2\ MnO\cdot Al_2O_3(s) + 1/2\ O_2(g) \tag{105}$$

$$Fe_2(SO_4)_3(s) \xrightarrow{800\text{-}900\ K} Fe_2O_3(s) + 3SO_2(g) + 3/2\ O_2(g) \tag{106}$$

$$\left.\begin{array}{l} Cr_2O_3(s) \\ \\ \\ 2Na_2O\cdot SiO_2(s) \end{array}\right\} \text{stable from 300-1200 K}$$

$$MoO_3(s) + H_2O(g) \xrightarrow{>700\ K} MoO_4H_2(g)\ . \qquad (107)$$

Aluminum is distributed at high temperatures between solid phases of Si, Ti, and Mn. There is little difference between the alkali and clay metal reactions of this system and those of the previous system. The addition of Cr produces a solid chromium oxide (Cr_2O_3) phase between 300 and 1200 K. Molybdenum volatilizes at temperatures above 700 K in the presence of water vapor. The omission of Be from the equilibrium calculation is not expected to have a major effect on the resulting products. Instead, Be, if included, is expected to form $BeAl_2O_4(s)$ between 300 and 400 K and to partially volatilize in the presence of water vapor, forming gaseous $Be(OH)_2$ at operating temperatures of 1200 K, as previously discussed.

The major gaseous trace phases at 1200 K that exert partial pressures greater than 10^{-8} kPa (10^{-10} atm) are $MnCl_2$, iron chloride ($FeCl_2$), molybdenum hydroxide (MoO_4H_2), molybdenum oxychloride (MoO_2Cl_2), chromium hydroxides ($CrO_2(OH)_2$, CrO_2OH), chromium oxychloride (CrO_2Cl_2), chromium oxide (CrO_3), KCl, KOH, and K_2SO_4. The various phases are formed by the reactions of the stable solid phases with water vapor or gaseous hydrogen chloride (HCl).

Reduction in the S content, as in both 90 and 99 percent S-removal systems, does not affect the following reactions:

- Conversion of quartz to cristobalite at 1000-1100 K
- Dehydration of $KAl(SO_4)_2 \cdot 12H_2O(s)$
- Removal of $Al(OH)_3(s)$ at temperatures greater than 400 K
- Stable formation of $2Na_2O \cdot SiO_2$ between 300 and 1200 K
- Formation of $MnO \cdot Al_2O_3$ at 1200 K.

Sulfur reduction, however, does modify many of the remaining trace reactions, which include:

- Removal of $Al_2(SO_4)_3(s)$ and $Fe_2(SO_4)_3(s)$. As the $Fe_2(SO_4)_3$ solid is depleted in the system, Fe_2O_3 is formed. Thus, 99 percent S-removal systems contain a greater concentration of Fe_2O_3 at low temperatures than do 0 percent S-removal systems.
- Reduction in the formation of $KAl(SO_4)_2(s)$ to lower temperatures in 90 percent S-removal systems and complete removal in 99 percent S-removal systems.
- Enhanced formation of $Al_2O_3 \cdot SiO_2(s)$ as the gaseous S content decreases.
- Reduction in S limits the formation of solid $MnSO_4$, thus enhancing the formation of MnO_2, principally at lower temperatures.
- The formation of an aluminum titanium oxide ($Al_2O_3 \cdot TiO_2(s)$) is enhanced at lower temperatures when S is removed from FBC systems. Similarly, solid titanium oxide (TiO_2) is not formed at temperatures exceeding 400 K in either 90 or 99 percent S-removal systems because of the preferred formation of $Al_2O_3 \cdot TiO_2$.
- Solid KCl is formed at low temperatures when S is limited. In 90 percent S-removal systems sufficient S is present to cause the formation of $K_2SO_4(s)$ at elevated temperatures. In 99 percent S-removal systems both K_2SO_4 and KCl exist simultaneously, with a greater distribution of K in the solid chloride phase.

- Reduction in the total S content frees the K that reacted to form $K_2SO_4(s)$ for reaction with Cr to form potassium chromate ($K_2Cr_2O_7(s)$) by the reaction

$$K_2SO_4(s) + Cr_2O_3(s) + 3/2\ O_2(g) \xrightarrow{>800\ K} K_2Cr_2O_7(s) + SO_2(g) + 1/2\ O_2(g)\ . \qquad (108)$$

The major volatile gaseous phases that are formed in equilibrium with the FBC gas solids are

- Chlorides: $MnCl_2$, $FeCl_3$, $FeCl_2$, and KCl
- Oxychlorides: MoO_2Cl_2, CrO_2Cl_2
- Oxides: MoO_3, CrO_3
- Hydroxides: MoO_4H_2, $CrO_2(OH)_2$, CrO_2OH, and KOH
- Sulfates: K_2SO_4.

Interconversion of the hydroxide and oxychloride gaseous phases of Cr and Mo are detected at temperatures below 800 K, as shown by the following reactions:

Chromium

$$Cr_2O_3(s) + 4HCl(g) + 3/2\ O_2(g) \longrightarrow 2CrO_2Cl_2(g) + 2H_2O(g) \qquad (109)$$

$$CrO_2Cl_2(g) + H_2O(g) + 1/2\ O_2(g) \longrightarrow CrO_2(OH)_2(g) + Cl_2(g) \qquad (110)$$

$$CrO_2Cl_2(g) + H_2O(g) \longrightarrow CrO_2OH(g) + HCl(g) + Cl_2(g) \qquad (111)$$

Molybdenum

$$MoO_3(s) + 2HCl(g) \longrightarrow MoO_2Cl_2(g) + H_2O(g) \qquad (112)$$

$$MoO_2Cl_2(g) + H_2O(g) + 1/2\ O_2(g) \longrightarrow MoO_4H_2(g) + Cl_2(g) \qquad (113)$$

Tables 56 through 58 illustrate the resulting moles of solids and partial pressures (kPa) of gaseous phases for the Cr, Fe, Mo, Mn, and Ti complexes formed as a function of temperature for the three S-removal systems considered.

TABLE 56 - FLUIDIZED-BED COMBUSTION OF C-H-N-O-S-Cl-Si-Al-K-Na-Cr-Fe-Mo-Mn-Ti FOR 100% EXCESS AIR, 0% SULFUR-REMOVAL, 1013 kPa OPERATIONS

TEMP.\COMPOUND (K)	CR2O3 (S)	RUTILE TIO2 (S)	AL2O3. TIO2 (S)	MNO. AL2O3 (S)	MNO2 (S)
300	.1293-04**	.1460-02	.0000	.0000	.8994-04
400	.1081-04	.5266-03	.9334-03	.0000	.0000
500	.5797-05	.5264-03	.9336-03	.0000	.0000
600*	.7476-05	.3875-03	.1094-02	.0000	.0000
700	.9155-05	.2486-03	.1255-02	.0000	.0000
800	.1077-04	.0000	.1460-02	.0000	.0000
900	.1124-04	.0000	.1460-02	.0000	.0000
1000	.1047-04	.0000	.1460-02	.0000	.0000
1100	.7677-05	.0000	.1460-02	.0000	.0000
1200	.9745-06	.0000	.1460-02	.8870-04	.0000

TEMP.\COMPOUND (K)	MNSO4 (S)	MN2O3 (S)	FE2(SO4)3 (S)	FE2O3 (S)	MOO3 (S)
300	.0000	.0000	.1719-01	.0000	.7882-05
400	.8991-04	.0000	.1719-01	.0000	.7853-05
500	.8991-04	.0000	.1719-01	.0000	.7770-05
600*	.8991-04	.0000	.1719-01	.0000	.4874-05
700	.8991-04	.0000	.1719-01	.0000	.1977-05
800	.8996-04	.0000	.1719-01	.0000	.0000
900	.8988-04	.0000	.0000	.1719-01	.0000
1000	.0000	.4492-04	.0000	.1719-01	.0000
1100	.0000	.4470-04	.0000	.1719-01	.0000
1200	.0000	.0000	.0000	.1719-01	.0000

TEMP.\COMPOUND (K)	MNCL2 (G)	FECL3 (G)	FECL2 (G)	MOO4H2 (G)	MOO2CL2 (G)
300	.1916-33	.3479-26	.0000	.3332-17	.4029-13
400	.1087-22	.9228-19	.2476-28	.2835-11	.2648-08
500	.3540-17	.9191-15	.2585-21	.9885-08	.1264-05
700	.9700-12	.1988-11	.3992-14	.1106-03	.1913-03
800	.1722-06	.3007-10	.1179-11	.9200-04	.2615-04
900	.3477-08	.3825-09	.1539-09	.1104-03	.7200-05
1000	.1604-05	.8469-09	.2203-08	.1155-03	.2249-05
1100	.8001-05	.1562-08	.1875-07	.1165-03	.8225-06
1200	.1865-04	.2420-08	.1056-06	.1172-03	.3382-06

TEMP.\COMPOUND (K)	MOO3 (G)	CRO4H2 (G)	CRO2OH (G)	CRO2CL2 (G)	CRO3 (G)
300	.0000	.5863-14	.3814-31	.4193-05	.0000
400	.7343-30	.2014-10	.5185-22	.6678-04	.0000
500	.2027-27	.2587-08	.1392-16	.2169-03	.9108-23
700	.4367-16	.7072-06	.2006-10	.1157-03	.1026-14
800	.6436-14	.4213-05	.1643-08	.6178-04	.3244-12
900	.4194-12	.1715-04	.4998-07	.3602-04	.2803-10
1000	.1043-10	.5360-04	.7628-06	.2302-04	.1043-10
1100	.1375-09	.1377-03	.7046-05	.1574-04	.1777-07
1200	.1154-08	.3048-03	.4466-04	.1102-04	.1966-06

* ESTIMATED VALUES

** CONDENSED CR2O3 AND CRO2 PHASES

TABLE 57 - FLUIDIZED-BED COMBUSTION OF C-H-N-O-S-Cl-Si-Al-K-Na-Cr-Fe-Mo-Mn-Ti FOR 100% EXCESS AIR, 90% SULFUR-REMOVAL, 1013 kPa OPERATIONS

TEMP.\COMPOUND (K)	CR203 (S)	RUTILE TIO2 (S)	AL203. TIO2 (S)	MNO. AL203 (S)	MNO2 (S)
300	.1295-04**	.1460-02	.0000	.0000	.8992-04
400	.1082-04	.0000	.1460-02	.0000	.8993-04
500	.5753-05	.0000	.1460-02	.0000	.8995-04
600	.5882-05	.0000	.1460-02	.0000	.0000
700	.9107-05	.0000	.1460-02	.0000	.0000
800	.1082-04	.0000	.1460-02	.0000	.0000
900	.1122-04	.0000	.1460-02	.0000	.0000
1000	.1043-04	.0000	.1460-02	.0000	.0000
1100	.7609-05	.0000	.1460-02	.0000	.0000
1200	.8547-06	.0000	.1460-02	.8880-04	.0000

TEMP.\COMPOUND (K)	MNSO4 (S)	MN203 (S)	FE2(SO4)3 (S)	FE203 (S)	MOO3 (S)
300	.0000	.0000	.0000	.1719-01	.7886-05
400	.0000	.0000	.0000	.1719-01	.7879-05
500	.0000	.0000	.0000	.1719-01	.7794-05
600	.8993-04	.0000	.0000	.1719-01	.4820-05
700	.8994-04	.0000	.0000	.1719-01	.1846-05
800	.8994-04	.0000	.0000	.1719-01	.0000
900	.8989-04	.0000	.0000	.1719-01	.0000
1000	.0000	.4491-04	.0000	.1719-01	.0000
1100	.0000	.4470-04	.0000	.1719-01	.0000
1200	.0000	.0000	.0000	.1719-01	.0000

TEMP.\COMPOUND (K)	MNCL2 (G)	FECL3 (G)	FECL2 (G)	MOO4H2 (G)	MOO2CL2 (G)
300	.1431-33	.3492-24	.0000	.3279-17	.3044-13
400	.2642-22	.3893-17	.1045-26	.2828-11	.2615-08
500	.8098-16	.2609-13	.7334-20	.9861-08	.1253-05
600	.5988-12	.2706-11	.1141-15	.2267-05	.3357-04
700	.4206-10	.2972-10	.5941-13	.1103-03	.1912-03
800	.8392-09	.1329-09	.5183-11	.9167-04	.2611-04
900	.4595-07	.3834-09	.1534-09	.1101-03	.7197-05
1000	.1598-05	.8490-09	.2195-08	.1154-03	.2253-05
1100	.7921-05	.1550-08	.1857-07	.1165-03	.8184-06
1200	.1702-04	.2110-08	.9603-07	.1169-03	.3082-06

TEMP.\COMPOUND (K)	MOO3 (G)	CRO4H2 (G)	CRO2OH (G)	CRO2CL2 (G)	CRO3 (G)
300	.0000	.5866-14	.3826-31	.3222-05	.0000
400	.0000	.2041-10	.5235-22	.6702-04	.7464-30
500	.2027-27	.2624-08	.1405-16	.2184-03	.9258-23
600	.8532-21	.6826-07	.5580-13	.2144-03	.4697-18
700	.4367-16	.7171-06	.2025-10	.1175-03	.1042-14
800	.6426-14	.3146-05	.4273-05	.6281-04	.3297-12
900	.4186-12	.1743-04	.5053-07	.3669-04	.2851-10
1000	.1043-10	.5441-04	.7706-06	.2342-04	.9961-09
1100	.1375-09	.1396-03	.7112-05	.1588-04	.1802-07
1200	.1152-08	.3088-03	.4506-04	.1019-04	.1992-06

* ESTIMATED VALUES

** CONDENSED CR203 AND CRO2 PHASES

TABLE 58 - FLUIDIZED-BED COMBUSTION OF C-H-N-O-S-Cl-Si-Al-K-Na-Cr-Fe-Mo-Mn-Ti FOR 100% EXCESS AIR, 99% SULFUR-REMOVAL, 1013 kPa OPERATIONS

TEMP.\COMPOUND (K) \	CR203 (S)	RUTILE TI02 (S)	AL203. TI02 (S)	MNO. AL203 (S)	MNO2 (S)
300	.1303-04**	.1460-02	.0000	.0000	.8992-04
400	.1227-04	.0000	.1460-02	.0000	.8990-04
500	.1113-04	.0000	.1460-02	.0000	.8991-04
600	.1179-04	.0000	.1460-02	.0000	.8991-04
700	.1244-04	.0000	.1460-02	.0000	.8991-04
800	.0000	.0000	.1460-02	.0000	.0000
900	.0000	.0000	.1460-02	.0000	.0000
1000*	.0000	.0000	.1460-02	.0000	.0000
1100*	.0000	.0000	.1460-02	.0000	.0000
1200	.0000	.0000	.1460-02	.8973-04	.0000

TEMP.\COMPOUND (K) \	MNSO4 (S)	MN203 (S)	FE2(SO4)3 (S)	FE203 (S)	MO03 (S)
300	.0000	.0000	.0000	.1719-01	.7878-05
400	.0000	.0000	.0000	.1719-01	.7850-05
500	.0000	.0000	.0000	.1719-01	.7831-05
600	.0000	.0000	.0000	.1719-01	.2822-04
700	.0000	.0000	.0000	.1719-01	.6079-06
800	.0000	.4496-04	.0000	.1719-01	.0000
900	.0000	.4496-04	.0000	.1719-01	.0000
1000*	.0000	.4496-04	.0000	.1719-01	.0000
1100*	.0000	.4496-04	.0000	.1719-01	.0000
1200	.0000	.0000	.0000	.1719-01	.0000

TEMP.\COMPOUND (K) \	K2CR207 (S)
300	.0000
400	.0000
500	.0000
600	.0000
700	.0000
800	.1279-04
900	.1285-04
1000*	.1190-04
1100*	.1094-04
1200	.9885-05

TEMP.\COMPOUND (K) \	MNCL2 (G)	FECL3 (G)	FECL2 (G)	MO04H2 (G)	MO02CL2 (G)
300	.3241-34	.3764-25	.0000	.3358-17	.6895-14
400	.9147-23	.7943-18	.3620-27	.2827-11	.9061-09
500	.2113-16	.3485-14	.1915-20	.9863-08	.3272-06
600	.1297-12	.1960-12	.1983-16	.2268-05	.5833-05
700	.4022-10	.1668-11	.8705-14	.1104-03	.2802-04
800	.2418-08	.7120-11	.7360-12	.1131-03	.4572-05
900	.3035-07	.2017-10	.2152-10	.1166-03	.1069-05
1200	.2663-05	.1306-09	.1502-07	.1173-03	.4831-07

TEMP.\COMPOUND (K) \	MO03 (G)	CR04H2 (G)	CR020H (G)	CR02CL2 (G)	CR03 (G)
300	.0000	.2218-14	.1429-31	.2695-06	.0000
400	.0000	.2044-10	.5241-22	.2327-04	.7477-30
500	.2027-27	.2629-08	.1407-16	.5716-04	.9274-23
600	.8532-21	.6842-07	.5588-13	.3731-04	.4705-18
700	.4367-16	.7189-06	.2029-10	.1725-04	.1044-14
800	.7922-14	.2079-05	.8064-09	.4338-05	.1603-12
900	.4429-12	.3768-05	.1091-07	.1122-05	.6157-11
1200	.1155-08	.8078-04	.1177-04	.4168-06	.5205-07

* ESTIMATED VALUES

** CONDENSED CR203 AND CR02 PHASES

C-H-N-O-S-Cl-Si-Al-K-Na-Ca-Mg-F-Be-Pb

Combustion systems that utilize sorbent materials such as dolomite or limestone for the sorption of gaseous S released from the feedstock coal introduce a different series of complex chemical reactions and interactions from those previously described. Not only is the reaction of Al with Si probable, but also the reactions of alkalis (Na, K) with clays (Al, Si), alkalis with carbonates (Ca, Mg), alkalis with both clays and carbonates, and clays with carbonates.

In order to provide a simplified view of these reactions, each element is discussed in relation to its product distribution as a function of temperature. The resulting product distributions within the various Ca and Mg fluidized-bed gaseous or solid and liquid phases are shown in Tables 59 through 61 for 0 percent S-removal and 10, 100, and 300 percent excess air operating conditions.

Calcium

At temperatures of 300 to 500 K calcium magnesium carbonate* ($CaCO_3 \cdot MgCO_3$) forms as a stable solid phase in the FBC system. Reaction with SO_x at 300 to 400 K converts 61 percent of the total Ca contained in the carbonate phase into calcium sulfate ($CaSO_4$). Similarly, at 300 K Ca also exists as gypsum ($CaSO_4 \cdot 2H_2O$), which releases water at elevated temperatures, forming $CaSO_4$. The 39 percent of Ca remaining in the $CaCO_3 \cdot MgCO_3$ phase reacts to form calcium carbonate ($CaCO_3$) and calcium magnesium silicate ($CaO \cdot MgO \cdot 2SiO_2$) at 500 K. The $CaO \cdot MgO \cdot 2SiO_2$ phase is stable to temperatures of 700 to 800 K, whereupon conversion into calcium metasilicate ($CaSiO_3$), magnesium orthosilicate (Mg_2SiO_4), and quartz results. Total removal of $CaCO_3$ is completed at 800 to 900 K by the final reaction with quartz, forming calcium orthosilicate (Ca_2SiO_4). At FBC operating temperatures of 1200 K, the major solid phases are $CaSO_4$, $CaSiO_3$, and Ca_2SiO_4.

---

*Dolomite

TABLE 59 - FLUIDIZED-BED COMBUSTION OF C-H-N-O-S-Cl-Si-Al-K-Na-Ca-Mg FOR 100% EXCESS AIR, 0% SULFUR-REMOVAL, 1013 kPa OPERATIONS

TEMP.\COMPOUND (K)	CACO3 (S)	CACO3. MGCO3 (S)	CASO4. 2H2O (S)	CASO4 (S)	CASIO3 (S)
300	.0000	.4340-01	.1079+00	.0000	.0000
400	.0000	.2650-01	.0000	.1248+00	.0000
500	.1320-01	.0000	.0000	.1248+00	.0000
600	.1320-01	.0000	.0000	.1248+00	.0000
700	.1320-01	.0000	.0000	.1248+00	.0000
800	.6553-02	.0000	.0000	.1248+00	.1995-01
900	.0000	.0000	.0000	.1248+00	.1339-01
1000	.0000	.0000	.0000	.1234+00	.1204-01
1100	.0000	.0000	.0000	.1226+00	.1117-01
1200	.0000	.0000	.0000	.1231+00	.1166-01

TEMP.\COMPOUND (K)	CA2SIO4 (S)	CAO.MGO. 2SIO2 (S)	MG(OH)2 (S)	MG(OH)CL (S)	MG2SIO4 (S)
300	.0000	.0000	.1431-01	.9244-02	.0000
400	.0000	.0000	.0000	.0000	.1655-01
500	.0000	.1330-01	.0000	.0000	.5635-01
600	.0000	.1330-01	.0000	.0000	.5635-01
700	.0000	.1330-01	.0000	.0000	.5635-01
800	.0000	.0000	.0000	.0000	.6300-01
900	.6553-02	.0000	.0000	.0000	.6300-01
1000	.7906-02	.0000	.0000	.0000	.6300-01
1100	.8781-02	.0000	.0000	.0000	.6300-01
1200	.8285-02	.0000	.0000	.0000	.6300-01

TEMP.\COMPOUND (K)	MGAL2O4 (S)	MGSIO3 (S)
300	.0000	.8294-01
400	.2391-01	.6639-01
500	.2390-01	.0000
600	.2390-01	.0000
700	.2391-01	.0000
800	.2390-01	.0000
900	.2391-01	.0000
1000	.2390-01	.0000
1100	.2391-01	.0000
1200	.2391-01	.0000

TEMP.\COMPOUND (K)	CACL2 (G)	MGCL2 (G)	MG(OH)2 (G)
300	.0000	.0000	.0000
400	.6972-33	.5234-26	.2751-34
500	.7473-23	.2508-20	.2238-26
600	.8021-18	.1164-16	.9328-21
700	.2337-14	.3715-14	.9412-17
800	.8511-12	.2681-12	.9444-14
900	.1054-10	.3849-11	.1062-11
1000	.1706-08	.5526-09	.5874-10
1100	.1518-07	.6010-08	.1158-08
1200	.3112-07	.1468-07	.1373-07

TABLE 60 - FLUIDIZED-BED COMBUSTION OF C-H-N-O-S-Cl-Si-Al-K-Na-Ca-Mg FOR 10% EXCESS AIR, 0% SULFUR-REMOVAL, 1013 kPa OPERATIONS

TEMP.\COMPOUND (K)	CACL2 (G)	MGCL2 (G)	MG(OH)2 (G)
300	.0000	.0000	.0000
400	.8717-33	.2090-25	.4945-34
500	.9565-23	.4727-20	.3293-26
600	.8327-18	.1779-16	.1373-20
700	.2358-14	.5518-14	.1386-16
800	.8573-12	.3916-12	.1371-13
900	.1887-10	.6894-11	.1896-11
1000	.1706-08	.5526-09	.1049-09
1100	.3138-07	.1242-07	.2068-08
1200	.7107-07	.3353-07	.2451-07

TABLE 61 - FLUIDIZED-BED COMBUSTION OF C-H-N-O-S-Cl-Si-Al-K-Na-Ca-Mg FOR 300% EXCESS AIR, 0% SULFUR-REMOVAL, 1013 kPa OPERATIONS

TEMP.\COMPOUND (K)	CACL2 (G)	MGCL2 (G)	MG(OH)2 (G)
300	.0000	.0000	.0000
400	.1147-32	.2198-26	.1392-34
500	.6749-23	.1437-20	.1444-26
600	.7905-18	.7278-17	.5921-21
700	.2321-14	.2341-14	.5979-17
800	.4548-12	.1392-12	.4913-14
900	.8337-11	.3046-11	.5367-12
1000	.1706-08	.5526-09	.2969-10
1100	.6179-08	.2445-08	.5855-09
1200	.1114-07	.5255-08	.6943-08

Magnesium

The major Mg phase present in the fluidized-bed combustor at low temperatures is $CaCO_3 \cdot MgCO_3$ and magnesium metasilicate ($MgSiO_3$). Reaction between both solids at 300 and 400 K leads to the formation of Mg_2SiO_4. At low temperatures magnesium hydroxide ($Mg(OH)_2$) and magnesium hydroxychloride ($Mg(OH)Cl$) are present in the fluidized bed and have the potential to react with alumina (Al_2O_3), forming magnesium aluminate ($MgAl_2O_4$).

Between 400 and 500 K 50 percent of the remaining $CaCO_3 \cdot MgCO_3$ reacts with quartz to form $CaO \cdot MgO \cdot 2SiO_2$. Simultaneously, Mg_2SiO_4 forms from the remaining Mg in the carbonate and $MgSiO_3$ phases. At 500 K $MgSiO_3$ no longer exists as a stable solid. Calcium magnesium silicate remains in the FBC system to temperatures of 700 to 800 K, prior to conversion into Mg_2SiO_4, $CaSiO_3$, and quartz.

Aluminum

The chemical reactions of Al in the fluidized bed are more basic than those of either calcium or magnesium. At 300 K aluminum is present as either $KAl(SO_4)_2 \cdot 12H_2O$ or as $Al(OH)_3$. The reaction of $KAl(SO_4)_2 \cdot 12H_2O$ with HCl produces solid KCl and Al_2O_3, in addition to gaseous SO_2 and water vapor. Alumina is then free to react with $Mg(OH)_2(s)$ and $Mg(OH)Cl(s)$ to form the $MgAl_2O_4$ phase, as previously described. Aluminum hydroxide either releases water, forming alumina, which reacts further with $MgCO_3$ to form $MgAl_2O_4$, or directly reacts with $MgCO_3$ to form the solid similar to the two-step reaction. The major phase of Al in FBC systems operating at 1200 K is $MgAl_2O_4$.

Silicon

The reactions of Si in FBC systems form various Ca and Mg phases. Magnesium metasilicate is the stable Si phase at 300 K. Eighty percent of the Si in $MgSiO_3$ is converted into Mg_2SiO_4 at 300 to 400 K. Forty percent of the remaining Si between 400 and 500 K reacts to form

$CaO \cdot MgO \cdot 2SiO_2$, while 60 percent reacts to form solid Mg_2SiO_4. Calcium magnesium silicate is stable up to 700 to 800 K, whereupon 75 percent conversion of Si into $CaSiO_3$ occurs, with the remaining 25 percent forming $MgSiO_3$. Further conversion of the $CaSiO_3$ phase results at higher reaction temperatures, with Ca_2SiO_4 forming between 800 and 900 K. In addition to these Si reactions, $2Na_2O \cdot SiO_2$ forms a stable solid phase between FBC temperatures of 300 and 1200 K. A summary of all the reactions for a combustion system containing the alkali, carbonate, and clay constituents is presented in Table 62.

A comparison of FBC systems calculations that include sorbent materials with those that do not demonstrates the S absorption capacity of the carbonate elements. At a Ca/S ratio of 1.21:1 gaseous SO_x is reduced (Table 63) to values comparable with those of 99 percent S-removal systems that have been considered thus far.

Increasing the percentage of excess air in the combustion of coal does not affect the stability of the solid compounds formed. The partial pressures exerted by the volatile hydroxides and chlorides, however, decrease as the percentage of excess air in the combustion process is increased, indicating a dilution effect. The partial pressure exerted by gaseous K_2SO_4 is unaffected in the various air:fuel ratios because of volatilization of solid K_2SO_4 and an increase in the gaseous K content from the decreased partial pressures of KOH and KCl.

The above discussion clearly projects that interaction of the clay constituents (Al and Si) with carbonates (Ca and Mg) and alkalis (Na and K) will occur within a fluidized bed. The fate of the trace elements with the minor constituents is now considered. Table 64 illustrates the compounds that may form at equilibrium within the fluidized bed. Note the Al, Si, Mg, Ca, Na, and K compounds that form, as shown in the previous discussion, are the only minor phases included in these calculations. The basis for the selectivity of the minor elements resulted from the limitations in the chemical equilibrium program. If all the phases for a C-H-N-O-S-Cl-Si-Al-K-Na-Ca-Mg-F-Be-Pb system were

TABLE 62 - SUMMARY OF THE ALKALI, CARBONATE, AND CLAY CONSTITUENT REACTIONS

Calcium*

$$CaCO_3 \cdot MgCO_3(s) \xrightarrow{300-500\ K} CaCO_3(s) + MgCO_3(s) \qquad (114)$$

$$CaCO_3(s) + SO_2(g) + 1/2\ O_2(g) \xrightarrow{300-400\ K} CaSO_4(s) + CO_2(g) \qquad (115)$$

$$CaSO_4 \cdot 2H_2O(s) \xrightarrow{300-400\ K} CaSO_4(s) + 2H_2O(g) \qquad (116)$$

$$CaCO_3 \cdot MgCO_3(s) + 2SiO_2(s) \xrightarrow{400-500\ K} CaO \cdot MgO \cdot 2SiO_2(s) + 2CO_2(g) \qquad (117)$$

$$CaO \cdot MgO \cdot 2SiO_2(s) \xrightarrow{700-800\ K} CaSiO_3(s) + MgSiO_3(s) \qquad (118)$$

$$2CaCO_3(s) + SiO_2(s) \xrightarrow{800-900\ K} Ca_2SiO_4(s) + 2CO_2(g) \qquad (119)$$

$$CaSiO_3(s) + CaCO_3(s) \xrightarrow{800-900\ K} Ca_2SiO_4(s) + CO_2(g) \qquad (120)$$

Magnesium

$$CaCO_3 \cdot MgCO_3(s) \xrightarrow{300-500\ K} CaCO_3(s) + MgCO_3(s) \qquad (121)$$

$$2MgCO_3(s) + SiO_2(s) \xrightarrow{300-500\ K} Mg_2SiO_4(s) + 2CO_2(g) \qquad (122)$$

$$2MgSiO_3(s) \xrightarrow{300-500\ K} Mg_2SiO_4(s) + SiO_2(s) \qquad (123)$$

---

*NOTE: Calcium carbonate is the favored solid phase rather than CaO in the thermodynamic equilibrium FBC calculations.

TABLE 62 (Continued)

Magnesium (Cont'd)

$$Mg(OH)_2(s) + Al_2O_3(s) \xrightarrow{300\text{-}400\ K} MgAl_2O_4(s) + H_2O(g) \quad (124)$$

$$Mg(OH)Cl(s) + Al_2O_3(s) \xrightarrow{300\text{-}400\ K} MgAl_2O_4(s) + HCl(g) \quad (125)$$

$$CaCO_3 \cdot MgCO_3(s) + 2SiO_2(s) \xrightarrow{400\text{-}500\ K} CaO \cdot MgO \cdot 2SiO_2(s) + 2CO_2(g) \quad (126)$$

$$CaO \cdot MgO \cdot 2SiO_2(s) \xrightarrow{700\text{-}800\ K} MgSiO_3(s) + CaSiO_3(s) \quad (127)$$

Aluminum

$$KAl(SO_4)_2 \cdot 12H_2O(s) \xrightarrow{300\text{-}400\ K} KAl(SO_4)_2(s) + 12H_2O(g) \quad (128)$$

$$2KAl(SO_4)_2(s) + 2HCl(g) \xrightarrow{300\text{-}400\ K} 2KCl(s) + Al_2O_3(s) + 2O_2(g) + 4SO_2(g) + H_2O(g) \quad (129)$$

$$Al_2O_3(s) + Mg(OH)Cl(s) \xrightarrow{300\text{-}400\ K} MgAl_2O_4(s) + HCl(g) \quad (130)$$

$$Al_2O_3(s) + Mg(OH)_2(s) \xrightarrow{300\text{-}400\ K} MgAl_2O_4(s) + H_2O(g) \quad (131)$$

$$2Al(OH)_3(s) \xrightarrow{300\text{-}400\ K} Al_2O_3(s) + 3H_2O(g) \quad (132)$$

$$Al_2O_3(s) + MgCO_3(s) \xrightarrow{300\text{-}400\ K} MgAl_2O_4(s) + CO_2(g) \quad (133)$$

$$2Al(OH)_3(s) + MgCO_3(s) \xrightarrow{300\text{-}400\ K} MgAl_2O_4(s) + 3H_2O(g) + CO_2(g) \quad (134)$$

TABLE 62 (Continued)

Silicon

$$MgCO_3(s) + MgSiO_3(s) \xrightarrow{300\text{-}500\ K} Mg_2SiO_4(s) + CO_2(g) \qquad (135)$$

$$CaCO_3{\cdot}MgCO_3(s) + 2SiO_2(s) \xrightarrow{400\text{-}500\ K} CaO{\cdot}MgO{\cdot}2SiO_2(s) + 2CO_2(g) \qquad (136)$$

$$CaO{\cdot}MgO{\cdot}2SiO_2(s) \xrightarrow{700\text{-}800\ K} CaSiO_3(s) + MgSiO_3(s) \qquad (137)$$

$$CaSiO_3(s) + CaCO_3(s) \xrightarrow{800\text{-}900\ K} Ca_2SiO_4(s) + CO_2(g) \qquad (138)$$

$$2CaCO_3(s) + SiO_2(s) \xrightarrow{800\text{-}900\ K} Ca_2SiO_4(s) + 2CO_2(g) \qquad (139)$$

TABLE 63 - COMPARISON OF FLUIDIZED-BED COMBUSTION SYSTEMS
CONTAINING CARBONATE SORBENTS FOR SULFUR REMOVAL
WITH PROJECTIONS FOR REDUCED SULFUR SYSTEMS

SORBENT SYSTEM

TEMP.\COMPOUND (K) \	SO2 (G)	SO3 (G)
300	.0000	.1509-32
400	.5702-32	.5738-24
500	.2944-25	.7627-20
600	.1268-19	.6195-16
700	.1337-15	.3851-13
800	.1374-12	.4760-11
900	.2241-09	.1504-08
1000	.4903-07	.8906-07
1100	.6970-05	.4363-05
1200	.4204-03	.1087-03

0% SULFUR REMOVAL CALCULATIONS

TEMP.\COMPOUND (K) \	SO2 (G)	SO3 (G)
300	.4207-32	.8747-20
400	.6806-20	.6902-12
500	.1776-12	.4638-07
600	--	--
700	.4357-04	.1264-01
800	.9021-03	.3151
900	.2068	.1399+01
1000	.6354	.1164+01
1100	.1103+01	.6971
1200	.1427+01	.3731

90% SULFUR REMOVAL CALCULATIONS

TEMP.\COMPOUND (K) \	SO2 (G)	SO3 (G)
300	.0000	.1054-33
400	.9928-23	.1018-14
500	.9237-15	.2438-09
600	.1770-09	.8809-06
700	.9930-06	.2914-03
800	.6169-03	.2179-01
900	.1549-01	.1061
1000	.4319-02	.7997-01
1100	.7543-01	.4813-01
1200	.1009	.2662-01

99% SULFUR REMOVAL CALCULATIONS

TEMP.\COMPOUND (K) \	SO2 (G)	SO3 (G)
300	.0000	.6407-34
400	.1366-24	.1402-16
500	.6024-18	.1592-12
600	.5763-14	.2872-10
700	.2463-11	.7235-09
800	.2059-09	.7283-08
900	.3412-08	.2338-07
1000	--	--
1100	--	--
1200	.1546-03	.4077-04

included, the total possible compounds would exceed 250, approximately double the current program capacity. Those phases that are found to be the most active (those most likely to form) at 1013 kPa in 0 percent S-removal systems that operate with 100 percent excess air are indicated.

The major equilibrium solid phases formed within a 1200 K fluidized bed containing clays, carbonates, and trace elements are $CaSO_4$, $2Na_2O \cdot SiO_2$, Ca_2SiO_4, Mg_2SiO_4, $CaSiO_3$, and $MgAl_2O_4$. This system is identical with that previously discussed.

The major reaction of the trace elements F and Pb in the fluidized bed at high temperatures is the formation of gaseous hydrogen fluoride (HF) and lead tetrafluoride (PbF_4). Secondary gaseous Pb compounds include lead dichloride ($PbCl_2$), lead oxide (PbO), and lead chloride (PbCl). Deposition of Pb as solid PbO is not thermodynamically projected.

TABLE 64 - CANDIDATE PHASES CONSIDERED IN THE C-H-N-O-S-Cl-Si-Al-K-Na-Ca-Mg-F-Pb FLUIDIZED-BED COMBUSTION SYSTEM

GAS PHASES

CO2
CO
H2SO4
H2O
H2
HCLO
* KOH
OH
HCL
H
N2O
N2
NO3
NO2
NO
* K2SO4
SO3
SO2
O2
CLO
KO
O
* K2CL2
* CACL2
CL2
* KCL
CL

C2HF
C2F3N
C2F4
CHCL2F
CHF3
CHF
COCLF
CF4O
COF2
CFO
CCL3F
CCL2F2
CCLF3
CF4
CF3
CF2
CF
H3SIF
SIH2F2
HSO3F
HOF
SIHF3
*HF
HPB
FNO3
FNO2
F3NO

ONF
CLO3F
SO2CLF
SO2F2
FO2
SOF2
* ALOF2
* PBO
SF6
SF5
SF4
SF3
SF2
SF
PBS
* PBCL4
ALCL2F
PBCL2
CLSIF3
ALCLF2
ALCLF
CLF5
CLF3
CLF
* PBCL
SIF4
SIF3

SIF2
SIF
AL2F6
NAALF4
ALF3
ALF2
ALF
*K2F2
*KF
NA2F2
NAF
CAF2
CAF
(MGF2)2
MGF2
MGF
*PBF4
*PBF2
*PBF
*MGCL2
*MG(OH)2

CONDENSED PHASES

* CACO3.MGCO3
* CACO3
* KAL(SO4)2.12H2O
* AL(OH)3
* MG(OH)2
* MG(OH)CL
* CAO.MGO.2SIO2
* K2SO4
* CASO4
* 2NAO.SIO2
* CA2SIO4
* MG2SIO4
* MGAL2O4
* CASIO3
* MGSIO3
* KCL
KHF2
4PBO.PBSO4
2PBO.PBSO4
4PBO.SIO2
PBO.PBSO4
PBSO4
PBSIO4
PB3O4
PBSIO3
PBO
PBS

PBCL2
K3ALF6
NA3ALF6
* ALF3
KF
NAF
* CAF2
* MGF2
PBF2
PBO2
* CASO4.2H2O

* Projected Active Phases at Equilibrium

The interaction of Pb and F occurs at high temperatures, forming gaseous lead difluoride (PbF_2). At 1200 K gaseous PbF_2 exerts a partial pressure of 10^{-10} kPa. Lowering the fluidized-bed temperature reduces the partial pressure of the PbF_2 phase.

Stable solid fluorides are formed as the bed temperature approaches 700 to 800 K. Initially, calcium fluoride (CaF_2) is formed, which is converted into magnesium fluoride (MgF_2) as the system temperature is decreased to below 500 to 600 K. The major gaseous phase formed over both carbonate fluorides is HF, with potassium fluoride (KF) as a minor, secondary phase. Sodium fluoride (NaF) does not form in this system because of the stable formation of solid $2Na_2O \cdot SiO_2$ between 300 and 1200 K.

The interaction of Pb with either the clays or carbonates is not favored. In the analysis of collected fluidized-bed solids, therefore, compounds such as lead silicates are unlikely to be detected. Fluorine, however, is projected to form a solid aluminum trifluoride complex (AlF_3) at temperatures below 500 K. Stable phases of mercury carbonate or clays are not projected to form in the fluidized bed. The reaction of Be with the clay constituents results in the formation of $BeAl_2O_4$, as shown in a previous discussion. The reaction between Be and carbonates is not favored, but the reaction of Be with F forms solid beryllium difluoride (BeF_2) at 300 K in equilibrium with gaseous BeF_2, beryllium chloride fluoride (BeClF), and aluminum oxydifluoride (AlF_2O).

Basically, the total system of carbonates, clays, and trace and minor elements is a composite of a carbonate/clay and a trace subsystem. Minor variance is shown only when elements--for example, the alkalis--are involved in both reactions, competing in the free energy minimization for the formation of either the trace or the carbonate/clay phase.

C-H-N-O-S-Cl-Si-Al-K-Na-Ti-Mo-F-Be-Pb-Hg

Although the trace and minor elements have indicated minimal reactions with either the clay or carbonate constituents at fluidized-bed temperatures of 1200 K, an interaction of the individual elements may, indeed, exist. This section considers the possible reactions among C-H-N-O-S-Cl-Si-Al-K-Na-Ti-Mo-F-Be-Pb-Hg.

Calculations indicate that interaction of these elements is limited. The compounds $PbO \cdot MoO_3$, $PbO \cdot TiO_2$, F_2OTi, FOTi, F_4MoO, Mo_3Si, F_4Ti, F_3Ti, F_2Ti, and F_6Mo considered in the thermodynamic projections are not expected to form in FBC systems. Similarly, the equilibrium projections do not predict the interaction of the trace and minor elements forming complex volatile phases. For example, F and Hg do not form stable phases of mercurous fluoride (FHg and F_2Hg_2) or mercuric fluoride (F_2Hg) as either solids, liquids, or gases. The equilibrium projections indicate that two distinct systems exist - those of the alkali-clay and of the trace reactions - both of which have been previously discussed in detail.

C-H-N-O-S-Cl-Si-Al-K-Na-Ca-Mg-Fe-Ti-Ni

A review of the thermochemical data base indicates the potential for various compounds to form between carbonate and clay constituents and the elements K, Na, Fe, Ti, and Ni. These include $4CaO \cdot 3TiO_2$, $3CaO \cdot 2TiO_2$, $Al_2O_3 \cdot TiO_2$, $MgO \cdot 2TiO_2$, $2CaO \cdot Fe_2O_3$, $2FeO \cdot SiO_2$, $FeO \cdot Al_2O_3$, $Na_2O \cdot Fe_2O_3$, $CaO \cdot Fe_2O_3$, $2MgO \cdot TiO_2$, $MgO \cdot Fe_2O_3$, $NiO \cdot Fe_2O_3$, $FeO \cdot SiO_2$, $CaO \cdot TiO_2$, $MgO \cdot TiO_2$, and $FeO \cdot TiO_2$. Table 65 illustrates the resulting active solid phases that are expected to form as a function of temperature for a combustion system with 99 percent S removal, 100 percent excess air at 1013 kPa total pressure. Many of these reactions have been described previously, and reference should be made to the appropriate sections for details of specific chemical reactions. The system does indicate, however, that additional reactions between Ti-Ca and Fe-Mg occur. Titanium at low temperatures forms the stable rutile (TiO_2) phase. As the system temperatures approach 700 K, $CaO \cdot TiO_2$ is formed, which converts into $3CaO \cdot 2TiO_2$ at temperatures between 800 and 1200 K. In FBC systems that do not contain the carbonates, Ti reacts with Al to form $Al_2O_3 \cdot TiO_2$. Due to the S-removal capabilities of the carbonates, Fe exists as iron oxide (Fe_2O_3) at low bed temperatures but is converted into $MgO \cdot Fe_2O_3$ and $NiO \cdot Fe_2O_3$ at 1100 to 1200 K fluidized-bed temperatures.

C-H-N-O-S-Cl-Si-Al-K-Na-Ca-Mg-Cr-Mn-Mo

The reaction of the alkali, clays, and carbonates with Cr, Mn, and Mo in a fluidized bed further modifies the system's chemistry, as shown in Table 66. At temperatures between 300 and 500 K, magnesium molybdate ($MgO \cdot MoO_3$) is formed. This phase is converted into calcium molybdate ($CaO \cdot MoO_3$) between 500 and 1100 K, with complete volatilization of Mo at temperatures higher than 1100 K. Molybdenum oxide (MoO_3) is not expected to form as a solid at low temperatures in a fluidized bed containing carbonates. The partial pressure of molybdenum hydroxide ($Mo(OH)_2$), the major gaseous Mo phase, is 10^{-23} kPa (10^{-25} atm) at 300 K, 10^{-17} kPa (10^{-19} atm) at 500 K, 10^{-13} kPa (10^{-15} atm) at 700 K, 10^{-10} kPa (10^{-12} atm) at 900 K, 10^{-8} kPa (10^{-10} atm) at 1100 K, and 10^{-4} kPa (10^{-6} atm) at 1200 K.

In addition to the reaction of Mo with the carbonate constituents, Cr also reacts with Mg to form magnesium chromate ($MgO \cdot Cr_2O_3$) between 300 and 700 K. Conversion of Cr into potassium chromate ($K_2Cr_2O_7$) results at higher temperatures. Neither quartz nor cristobalite are projected to form in this system.

C-H-N-O-S-Cl-Si-Al-K-Na-Co-Cr-Mg-Ni-Ca

The chemical reactions at equilibrium of Co and Cr in FBC systems containing alkali, clay, and carbonate materials indicate the formation of a stable cobalt chromate spinel structure ($CoO \cdot Cr_2O_3$) at temperatures between 300 and 1200 K, and at 1013 kPa (10 atm) total pressure for 0 percent S removal. Calcium effectively acts as a S sorbent, minimizing the potential to form cobalt sulfate ($CoSO_4$). Chromium oxide (Cr_2O_3), as opposed to chromium sulfate ($Cr_2(SO_4)_3$), forms throughout

TABLE 65 - RESULTING ACTIVE PHASES AS A FUNCTION OF TEMPERATURE FOR C-H-N-O-S-Cl-Si-Al-K-Na-Ca-Mg-Fe-Ti-Ni

	300K	500K	700K	900K	1100K	1200K
CACO3.MGCO3 (S)	●	●				
KAL(SO4)2.12H2O (S)	●					
CASO4.2H2O (S)	●					
AL(OH)3 (S)	●					
3CAO.2TIO2 (S)				●	●	●
CAO.MGO.2SIO2 (S)			●			
K2SO4 (S)						
CASO4 (S)		●	●	●	●	●
2NA2O.SIO2 (S)	●	●	●	●	●	●
CA2SIO4 (S)				●		●
MG2SIO4 (S)		●	●	●	●	●
NI2SIO4 (S)	●					
MGAL2O4 (S)		●	●	●	●	●
MGO.FE2O3 (S)				●	●	●
NIO.FE2O3 (S)		●	●		●	●
CAO.TIO2 (S)			●			
SIO2 (S)-QUARTZ	●					
FE2O3 (S)	●	●	●			
TIO2 (S)	●	●				
MGO (S)				●	●	●
NIO (S)				●		
KCL (S)	●	●	●	●		
CACO3 (S)		●	●			

TABLE 66 - RESULTING ACTIVE PHASES AS A FUNCTION OF TEMPERATURE FOR C-H-N-O-S-Cl-Si-Al-K-Na-Ca-Mg-Cr-Mn-Mo

	300K	500K	700K	900K	1100K	1200K
CACO3.MGCO3 (S)	●					
CACO3 (S)		●	●			
KAL(SO4)2.12H2O (S)	●					
CASO4.2H2O (S)	●					
AL(OH)3 (S)	●					
MG(OH)2 (S)	●					
MG(OH)CL (S)	●					
K2CR2O7 (S)				●	●	●
CAO.MGO.2SIO2 (S)		●	●			
K2SO4 (S)					●	
CASO4 (S)		●	●	●	●	●
2NA2O.SIO2 (S)	●	●	●	●	●	●
CA2SIO4 (S)				●	●	●
MG2SIO4 (S)		●	●	●	●	●
MGAL2O4 (S)		●	●	●	●	●
CAO.MOO3 (S)		●	●	●	●	
MGO.CR2O3 (S)	●	●	●			
MGO.MOO3 (S)	●					
MN3O4 (S)						
CASIO3 (S)				●	●	●
MGSIO3 (S)	●					
MN2O3 (S)				●	●	●
MNO2 (S)	●	●	●			
KCL (S)		●	●	●		

the entire operating temperature range in FBC systems, promoting reaction with cobalt oxide (CoO) to form the spinel structure. Cobalt, which does not complex with Cr, exists as the cobalt oxide spinel (Co_3O_4) at FBC temperatures between 300 and 800 K; conversion into CoO occurs as the system temperature increases. Although the equilibrium projections do not consider the formation of the solid nickel chromate ($NiO{\cdot}Cr_2O_3$) phase because of insufficient thermodynamic data for the nickel spinel structure, it is likely that $NiO{\cdot}Cr_2O_3$ forms competitively with $CoO{\cdot}Cr_2O_3$ when both metals exist within the coal or sorbent matrix.

C-H-N-O-S-Cl-Si-Al-K-Na-Ca-Mg-B-Br-V-P-Zn

The equilibrium product distribution was projected for a C-H-N-O-S-Cl-Si-Al-K-Na-Ca-Mg-B-Br-V-P-Zn FBC system using a U.S. mean 4 percent S coal for operations with 10, 100, and 300 percent excess air at 1013 kPa and temperatures between 300 and 1300 K. Approximately 250 compounds can be selected from the thermodynamic data base to illustrate the potential interactions among the various trace and minor elements. The principal chemical reactions that lead to the formation of the FBC solid or condensed phases remain unaltered from those reactions projected in the noninteractive systems. Additional phases that include magnesium orthophosphate ($Mg_3(PO_4)_2$ present at 300 to 1300 K), a magnesium vanadate complex ($2MgO{\cdot}V_2O_5$ - 300 to 1300 K), and a calcium borate complex ($3CaO{\cdot}B_2O_3$ - 900 to 1300 K) are projected to result, but only as secondary compounds with respect to Ca and Mg. Removal of B, P, and V from the gas phase, however, is achieved through the formation of the interactive complexes, as shown in Table 67. Simultaneously, volatile reactions promote the interaction of alkali with Br and B, and Zn with Br.

A review of the thermodynamic data base indicates the possibility that numerous compounds and phases could result between Br or F and the various trace and minor elements released during combustion. These reactions will be reviewed in the remaining sections.

TABLE 67 - COMPARISON OF THE PERCENT VOLATILIZATION OF TRACE AND MINOR ELEMENTS IN A NONINTERACTIVE AND INTERACTIVE FLUIDIZED-BED COMBUSTION SYSTEM

Element	Noninteractive System, % Volatilization at 1300 K*	Interactive System, % Volatilization at 1300 K	Interactive Complex Formed
B	100	0	$3CaO \cdot B_2O_3$ (s)
P	100	0	$Mg_3P_2O_8$ (s)
Br	100	100	NaBr(g), KBr(g)
V	0.06	0	$2MgO \cdot V_2O_5$ (c)
Zn	0.01	0.01	$ZnBr_2$(g)

---

*100% excess air, 0% S removal, 1013 kPa.

C-H-N-O-S-Cl-Si-Al-K-Na-Br-F-Be-Hg-Pb-(Ca-Mg)

As shown in Figure 122, the volatile K, Na, Br, F, Be, Hg, and Pb species do not exert partial pressures greater than 10^{-2} kPa (10^{-4} atm) in the 100 percent excess air, 90 percent S-removal FBC systems. Interactions among these elements are primarily through gas phase reactions. The resulting elemental percent distribution in the volatiles formed at 1200 and 1300 K is illustrated in Table 68. Minimal interaction of the trace elements with Al and Si clay constituents is projected. At 1300 K, 89.7 percent of the feedstock Be is projected to form solid $BeAl_2O_4$ and 10.3 percent as gaseous $Be(OH)_2$. The buffer gas and minor and trace element complexes do not interchange until the PFBC temperature decreases to 300 K. At ambient temperatures in the interactive system, Be is removed from the stable $BeAl_2O_4$ complex, forming solid

Curve 723290-C

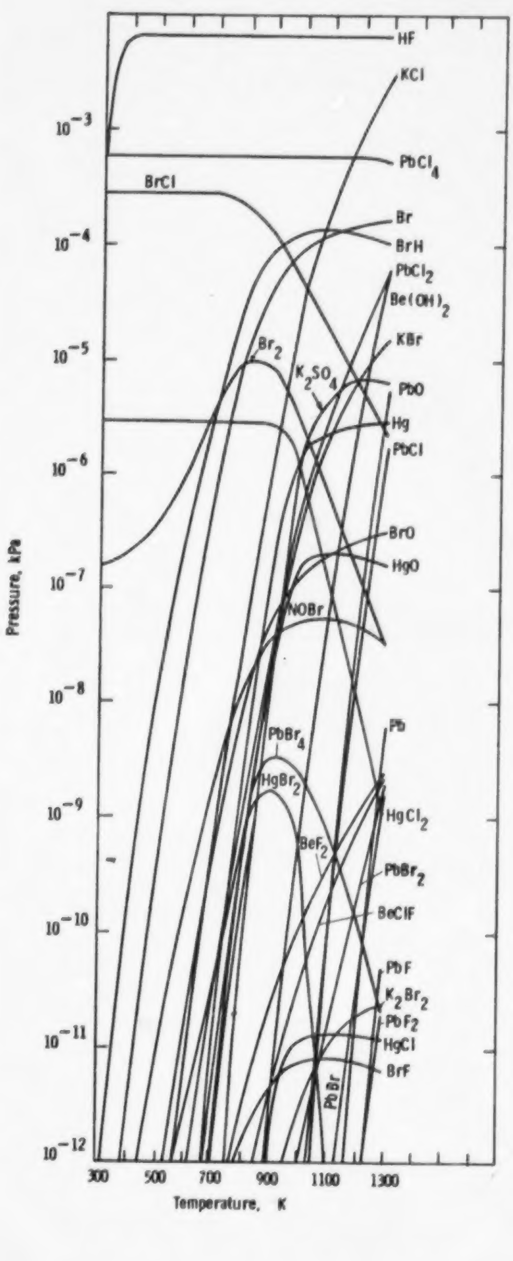

Figure 122 - Partial Pressure of Volatile Equilibrium Phases Formed in PFBC of C-H-N-O-S-Cl-Si-Al-K-Na-Br-F-Be-Hg-Pb in 100% Excess Air, 90% Sulfur Removal at 1013 kPa

TABLE 68 - FLUIDIZED-BED COMBUSTION OF C-H-N-O-S-Cl-Si-Al-K-Na-Br-F-Be-Hg-Pb-(Ca-Mg) - 100% EXCESS AIR, 90% SULFUR-REMOVAL, 1013 kPa OPERATIONS

```
      \TEMP (K)
COMPOUND\       300  400  500  600  700  800  900 1000 1100 1200 1300
---------------------------------------------------------------------
SIO2 *           ••••••••••••••••••••••••••••••••••••
SIO2 **                                                  •••••••••••
KAL(SO4)2.12H2O  •
KAL(SO4)2             •••••••••••••••••••••
AL(OH)3          •
K2SO4                 •••••••••••••••••••••••••••••••
KCL              •
ALF3             •••••••••••
KALSI3O8                                                 •••••••••••
2NA2O.SIO2       •••••••••••••••••••••••••••••••••••••••••••••••••••
AL2SIO5               ••••••••••••••••••••••••••••••••••••••••••••••
3AL2O3.2SIO2          •••••••••••••••••••••••••••••••••••••••••
BEAL2O4                                                            •
BEF2             •••••••••••••••••••••••••••••••••••••••••••••••••••
                 •
•  QUARTZ
•• CRISTOBALITE
```

ELEMENTAL PERCENT DISTRIBUTION IN GASEOUS EQUILIBRIUM PHASES

```
COMPOUND                         1200K
HF                                99.52
BE(OH)2                            2.35
PBF2                (F) 0.1072E-7, (PB) 0.5923E-7
PBF                 (F) 0.2894E-8, (PB) 0.3198E-7
PB                                 0.1316E-5
PBCL                               0.2289E-2
PBCL2                              0.4965
PBCL4                             99.50
PBO                                0.3617E-2
HG                                93.62
HGCL                               0.4532E-3
HGCL2                              0.2906
HGO                                6.09
KCL                                0.7493
K2BR2               (K) 0.3030E-7, (BR) 0.1327E-4
KBR                 (K) 0.5593E-2, (BR) 0.2449E+1
BRCL                               2.02
BRH                               42.79
BR2                                0.9486E-1
BR                                52.54
BRO                                0.9222E-1
NOBR                               0.1513E-1
BEF2                (F) 0.2913E-4, (BE) 0.1656E-3
BRF                 (F) 0.1121E-6, (BR) 0.2588E-5
BECLF               (F) 0.9889E-5, (BE) 0.1124E-3
PBBR2              (PB) 0.2504E-4, (BR) 0.1046E-3
PBBR4              (PB) 0.2073E-4, (BR) 0.1733E-3
PBBR               (PB) 0.2415E-5, (BR) 0.5048E-5
HGBR2              (HG) 0.5247E-4, (BR) 0.1096E-5
K2SO4                              0.1124E-1
ALF2O                              0.4820
```

ELEMENTAL PERCENT DISTRIBUTION IN GASEOUS EQUILIBRIUM PHASES

```
COMPOUND                         1300K
HF                                99.42
BE(OH)2                           10.27
PBF2                (F) 0.5737E-6, (PB) 0.3170E-5
PBF                 (F) 0.7394E-6, (PB) 0.8172E-5
PB                                 0.8939E-3
PBCL                               0.2987
PBCL2                             11.95
PBCL4                             86.82
```

TABLE 68 (Continued)

```
PBO                                  0.9258
HG                                  94.70
HGCL                                 0.4055E-3
HGCL2                                0.3740E-1
HGO                                  5.26
KCL                                  2.24
K2BR2                  (K) 0.3913E-7, (BR) 0.1714E-4
KBR                    (K) 0.1241E-1, (BR) 0.5435E+1
BRCL                                 0.7911
BRH                                 37.01
BR2                                  0.2403E-1
BR                                  56.61
BRO                                  0.1094
NOBR                                 0.1282E-1
BEF2                   (F) 0.7441E-4, (BE) 0.4229E-3
BRF                    (F) 0.1018E-6, (BR) 0.2352E-5
BECLF                  (F) 0.3474E-4, (BE) 0.3949E-3
PBBR2                 (PB) 0.3350E-3, (BR) 0.1400E-2
PBBR4                 (PB) 0.4004E-5, (BR) 0.3347E-4
PBBR                  (PB) 0.2763E-3, (BR) 0.5774E-3
HGBR2                 (HG) 0.3509E-5, (BR) 0.7331E-7
K2SO4                                0.1086E-1
ALF2O                                0.5777

PERCENT DISTRIBUTION OF BERQLLIUM AS A FUNCTION OF
TEMPERATURE IN PFBC SYSTEMS CONTAINING AL AND SI

   TEMPERATURE              PHASE
       (K)
   ___________        ________________
       300                100% BEF2 (S)
       400                100% BEAL2O4 (S)
       500                100% BEAL2O4 (S)
       600                100% BEAL2O4 (S)
       700                100% BEAL2O4 (S)
       800            99.9998% BEAL2O4 (S),  0.0002% BE(OH)2 (G)
       900            99.9949% BEAL2O4 (S),  0.0051% BE(OH)2 (G)
      1000            99.9413% BEAL2O4 (S),  0.0596% BE(OH)2 (G)
      1100            98.7937% BEAL2O4 (S),  1.2064% BE(OH)2 (G)*
      1200            97.6460% BEAL2O4 (S),  2.3530% BE(OH)2 (G)
      1300            89.7246% BEAL2O4 (S), 10.2737% BE(OH)2 (G)
* ESTIMATED
```

beryllium fluoride (BeF_2), while F complexes with Al as solid aluminum trifluoride (AlF_3), as shown by reactions 140 and 141:

$$BeAl_2O_4(s) + 2HF(g) \longrightarrow Al_2O_3(s) + BeF_2(s) + H_2O(g) \qquad (140)$$

$$Al_2O_3 \cdot SiO_2(s) + 6HF(g) \longrightarrow 2AlF_3(s) + SiO_2(s) + 3H_2O(g) \quad . \qquad (141)$$

When Ca or Mg are included in the chemical reactions as constituents of either the feedstock coal or the sorbent materials, F is projected to react with Ca, forming $CaF_2(s)$ at 700 K, which converts into $MgF_2(s)$ as the operating temperature decreases to 500 or 300 K. Under these conditions F is completely removed from the gas phase, forming solid carbonate species as opposed to solid Be or Al phases.

Beryllium complexes to form solid $BeAl_2O_4$ at temperatures between 300 and 700 K, above which a displacement reaction by Mg results forming solid beryllium oxide (BeO), as shown in reaction 142:

$$BeAl_2O_4(s) + MgO(s) \longrightarrow MgAl_2O_4(s) + BeO(s) \quad . \qquad (142)$$

Beryllium oxide remains as a stable solid phase at temperatures of 1100 or 1200 K, above which complete volatilization to gaseous $Be(OH)_2$ results.

Possible interactions of Ca and Mg with the trace or minor elements conceivably could lead to the formation of complexes such as $MgBr_2$, MgF_2, $CaBr_2$, MgClF, Mg_2Br_4, Mg_2F_4, MgBr, MgF, CaBr, or CaF, but these phases are not projected to form at equilibrium.

C-H-N-O-S-Cl-Si-Al-K-Na-Br-F-Fe-Mn-Ni

The projected equilibrium solids formed in the reaction of C, H, N, O, S, Cl, Si, Al, K, Na, Br, F, Fe, Mn, and Ni in a PFBC operating with 100 percent excess air and 90 percent S-removal efficiencies are illustrated in Table 69 as a function of operating temperature. Many of these interactions have been explored previously in detail, with the exception of solid iron trifluoride (FeF_3), which results between 300

TABLE 69 - FLUIDIZED-BED COMBUSTION OF C-H-N-O-S-Cl-Si-Al-K-Na-Br-F-Fe-Mn-Ni - 100% EXCESS AIR, 90% SULFUR-REMOVAL, 1013 kPa OPERATIONS

```
          \TEMP (K)
COMPOUND\            300   400   500   600   700   800   900  1000  1100  1200  1300
------------------------------------------------------------------------------------
SIO2 •                ••••••••••••••••••••••••••••••••••••••••••••
SIO2 ••                                                                ••••••••••••
KAL(SO4)2.12H2O       •
KAL(SO4)2                   ••••••••••••••••••••••••••
AL(OH)3               •
K2SO4                       ••••••••••••••••••••••••••••••••••••••
KCL                   •
KALSI3O8                                                               •••••••••••••
2NA2O.SIO2            •••••••••••••••••••••••••••••••••••••••••••••••••••••••••••••
AL2SIO5                     ••••••••••••••••••••••••••••••••••••••••••••••••••
AL6SI2O13                                                                         •
MNSO4                                   ••••••••••••••••••••
NISO4                       ••••••••••••••••••••••••••••••••••••••
NI2SIO4               •
NIO.FE2O3                                                              ••••••••••••
FE2O3                 •••••••••••••••••••••••••••••••••••••••••••••••••••••••••••••
MNO2                  •••••••••••••
MN2O3                                                            •••••••
MNO.AL2O3                                                                    ••••••
FEF3                  •••••••
•  QUARTZ
•• CRISTOBALITE
```

ELEMENTAL PERCENT DISTRIBUTION IN GASEOUS EQUILIBRIUM PHASES

```
      COMPOUND                     1200K
      NI(OH)2                       0.4384
      BRH                          42.80
      HF                           99.52
      NOBR                          0.1510E-1
      K2SO4                         0.1122E-1
      ALF2O                         0.4820
      BRO                           0.9201E-1
      NIO                           0.1262E-6
      MNCL2                         1.42
      NICL2                         2.56
      KCL                           0.7618
      BRCL                          2.05
      MNCL                          0.6156E-7
      NICL                          0.5233E-4
      K2BR2                  (K) 0.3031E-7, (BR) 0.1327E-4
      KBR                    (K) 0.5593E-2, (BR) 0.2449E+1
      FEBR2                 (FE) 0.3636E-9, (BR) 0.1296E-5
      MNBR2                 (MN) 0.3184E-5, (BR) 0.2968E-4
      NIBR2                 (NI) 0.3911E-4, (BR) 0.1455E-3
      BR2                           0.9476E-1
      NIBR                  (NI) 0.7792E-5, (BR) 0.1449E-4
      BR                           52.50
      NIF2                   (F) 0.4959E-7, (NI) 0.3079E-6
```

ELEMENTAL PERCENT DISTRIBUTION IN GASEOUS EQUILIBRIUM PHASES

```
      COMPOUND                     1300K
      NI(OH)2                       2.39
      BRH                          37.03
      HF                           99.42
      NOBR                          0.1280E-1
      K2SO4                         0.1085E-1
      ALF2O                         0.5777
      BRO                           0.1092
      NIO                           0.8214E-5
      MNCL2                         2.90
      NICL2                         5.51
      KCL                           2.27
      BRCL                          0.8024
      MNCL                          0.1630E-5
      NICL                          0.9300E-3
      K2BR2                  (K) 0.3917E-7, (BR) 0.1715E-4
      KBR                    (K) 0.1242E-1, (BR) 0.5437E+1
      FEBR2                 (FE) 0.1084E-8, (BR) 0.3861E-5
      MNBR2                 (MN) 0.4686E-5, (BR) 0.4366E-4
      NIBR2                 (NI) 0.5179E-4, (BR) 0.1926E-3
      BR2                           0.2401E-1
      NIBR                  (NI) 0.8165E-4, (BR) 0.1519E-3
      BR                           56.59
      NIF2                   (F) 0.2267E-6, (NI) 0.1407E-5
```

and 500 K* as opposed to solid AlF_3. Volatile interaction between the trace and minor constituents promotes the formation of such complexes as aluminum oxydifluoride (AlF_2O), monomeric and dimeric potassium bromide (KBr and K_2Br_2), iron dibromide ($FeBr_2$), manganese dibromide ($MnBr_2$), nickel dibromide ($NiBr_2$), nickel bromide (NiBr), and nickel difluoride (NiF_2). These interactions maintain complete volatilization of Br and F at 1200 to 1300 K combustion temperatures while slightly diminishing the stability of the Fe, Mn, and Ni complexes.

C-H-N-O-S-Cl-Si-Al-K-Na-Br-F-Ti-B-P

The resulting solid phases projected from the FBC interaction of C, H, N, O, S, Cl, Si, Al, K, Na, Br, F, Ti, B, and P, and the percent distribution in the 1200 and 1300 K volatile phases, are shown in Table 70. Once again, the solid reactions projected to occur at equilibrium in this system have been described previously in detail. Sodium, K and Ti react with either Al or Al-Si at 1200 or 1300 K combustion temperatures, forming ashlike complexes. Volatile phases result from the interaction of K, B, F, and Br, forming gaseous, potassium metaborate (KBO_2), boron oxide bromide (BOBr), monomeric and dimeric potassium bromide (KBr and K_2Br_2), and bromine monofluoride (BrF), in addition to aluminum oxydifluoride (AlF_2O).

C-H-N-O-S-Cl-Si-Al-K-Na-Br-F-Cu-Zn-Sb

A review of the thermodynamic data base indicates the possibility that compounds may form between Cu, Zn, and Sb with either Br and/or F. Table 71 shows that these interactions do not result in the formation of complex solids, but in volatile phases. Although only a limited number of these volatile complexes are projected to be stable at equilibrium (zinc dibromide ($ZnBr_2$), copper bromide (CuBr), and copper fluoride (CuF)), gaseous oxides and chlorides are the principal Cu, Zn, and Sb phases expected to form at 1200 or 1300 K combustor temperatures.

---

*Note that only 100-degree increments were selected in establishing the distribution of the trace and minor constituents within the condensed and the volatile phases.

TABLE 70 - FLUIDIZED-BED COMBUSTION OF C-H-N-O-S-Cl-Si-Al-K-Na-Br-F-Ti-B-P - 100% EXCESS AIR, 90% SULFUR-REMOVAL, 1013 kPa OPERATIONS

```
         \TEMP (K)
COMPOUND\         300  400  500  600  700  800  900  1000 1100 1200 1300
--------------------------------------------------------------------
SIO2 •            ••••••••••••••••••••••••••••••••••••
SIO2 ••
KAL(SO4)2.12H2O   •                                       •••••••••••
KAL(SO4)2              •••••••••••••••••••••
AL(OH)3           •
KCL               •
KALSI3O8                                                  •••••••••••
2NA2O.SIO2        •••••••••••••••••••••••••••••••••••••••••••••••••••
AL2SIO5                •••••••••••••••••••••••••••••••••••••••••
3AL2O3.2SIO2                                                        •
AL2O3.TIO2             ••••••••••••••••••••••••••••••••••••••••••••••
TIO2              •
ALF3              •••••••••••
H3BO3             •
H3PO4             •••••••••••••••••••••
K2SO4                  •••••••••••••••••••••••••••••••
•  QUARTZ
•• CRISTOBALITE
```

```
        ELEMENTAL PERCENT DISTRIBUTION IN GASEOUS EQUILIBRIUM PHASES

               COMPOUND                        1200K
               (HBO2)3                           0.2050E-4
               H3BO3                            85.85
               BHO2                             13.71
               BRH                              42.77
               HF                               99.52
               NOBR                              0.1512E-1
               (P2O5)2                         100.0
               K2SO4                             0.1123E-1
               KBO2                 (K) 0.1472E-1, (B) 0.1316
               ALF2O                             0.4827
               BOBR                (BR) 0.9539E-7, (B) 0.1947E-8
               BRO                               0.9218E-1
               KCL                               0.7625
               BRCL                              2.06
               K2BR2               (BR) 0.1326E-4, (K) 0.3029E-7
               KBR                 (BR) 0.2448E+1, (K) 0.5591E-2
               BR2                               0.9481E-1
               BR                               52.52
               BRF                 (BR) 0.2575E-5, (F) 0.1115E-6
```

```
        ELEMENTAL PERCENT DISTRIBUTION IN GASEOUS EQUILIBRIUM PHASES

               COMPOUND                        1300K
               (HBO2)3                           0.1081
               H3BO3                            58.77
               BHO2                             39.84
               BRH                              37.00
               HF                               99.43
               NOBR                              0.1283E-1
               (P2O5)2                         100.0
               K2SO4                             0.1087E-1
               KBO2                 (K) 0.1446   , (B) 0.1292E+1
               ALF2O                             0.5784
               BOBR                (BR) 0.5482E-6, (B) 0.1119E-7
               BRO                               0.1095
               KCL                               2.27
               BRCL                              0.8043
               K2BR2               (BR) 0.1713E-4, (K) 0.3913E-7
               KBR                 (BR) 0.5435E+1, (K) 0.1241E+1
               BR2                               0.2403E-1
               BR                               56.62
               BRF                 (BR) 0.2339E-5, (F) 0.1013E-6
```

TABLE 71 - FLUIDIZED-BED COMBUSTION OF C-H-N-O-S-Cl-Si-Al-K-Na-Br-F-Cu-Zn-Sb - 100% EXCESS AIR, 90% SULFUR-REMOVAL, 1013 kPa OPERATIONS

```
         \TEMP (K)
COMPOUND\          300   400   500   600   700   800   900  1000  1100  1200  1300
---------------------------------------------------------------------------------
SIO2 •             •••••••••••••••••••••••••••••••••••••••••••
SIO2 ••
KAL(SO4)2.12H2O    •                                               •••••••••••••
KAL(SO4)2                •••••••••••••••••••••••••
K2SO4                    •••••••••••••••••••••••••••••••••••••
KCL                •
ALF3               •••••••••••••
KALSI3O8
2NA2O.SIO2         •••••••••••••••••••••••••••••••••••••••••••••••••••••••••••••
AL2SIO5            •••••••••••••••••••••••••••••••••••••••••••••••••••••••••••••
3AL2O3.2SIO2       •••••••••••••••••••••••••••••••••••••••••••••••••••••••••
ZNSO4.7H2O         •                                                           •
ZNSO4                    •••••••••••••••••••••••••••••••••••••
ZNO
CUO-CUSO4                                                          •••••••••••••
CUSO4                    •••••••••••••••••••••••••     •
CUCL2              •
SBO2               •••••••••••••••••••••••••••••••••••••••••••••••••••••••••••••
•   QUARTZ
••  CRISTOBALITE
NOTE: AL(OH)3 SOLID IS NOT PROJECTED TO FORM AS A STABLE COMPLEX AT LOW
      TEMPERATURES
```

```
ELEMENTAL PERCENT DISTRIBUTION IN GASEOUS EQUILIBRIUM PHASES

     COMPOUND                    1200K
     BRH                          42.81
     HF                           99.52
     NOBR                          0.1514E-1
     K2SO4                         0.1124E-1
     ALF2O                         0.4824
     BRO                           0.9228E-1
     CUO                           0.6500E-1
     SBO                           0.4212E-1
     CU3CL3                        4.01
     SBCL3                         0.4759
     ZNCL2                        63.89
     KCL                           0.7175
     BRCL                          1.94
     CUCL                         95.92
     SBCL                          0.2239E-1
     K2BR2              (K) 0.3032E-7, (BR) 0.1328E-4
     KBR                (K) 0.5594E-2, (BR) 0.2450E+1
     ZNBR2             (ZN) 0.9885E-3, (BR) 0.4267E-1
     BR2                           0.9495E-1
     BRF                (F) 0.1116E-6, (BR) 0.2577E-5
     CUBR              (CU) 0.2140E-3, (BR) 0.2640E-3
     BR                           52.56
     CUF               (CU) 0.5315E-5,  (F) 0.2838E-6
     CU                            0.3849E-3
```

```
ELEMENTAL PERCENT DISTRIBUTION IN GASEOUS EQUILIBRIUM PHASES

     COMPOUND                    1300K
     BRH                          37.01
     HF                           99.42
     NOBR                          0.1283E-1
     K2SO4                         0.1087E-1
     ALF2O                         0.5780
     BRO                           0.1095
     CUO                           0.2916
     SBO                           2.65
     CU3CL3                        0.8598E-1
     SBCL3                         0.6935
     ZNCL2                        67.49
     KCL                           2.13
     BRCL                          0.7546
     CUCL                         99.62
     SBCL                          0.7030
     K2BR2              (K) 0.3913E-7, (BR) 0.1713E-4
     KBR                (K) 0.1241E-1, (BR) 0.5435E+1
     ZNBR2             (ZN) 0.5824E-3, (BR) 0.2514E-1
     BR2                           0.2404E-1
     BRF                (F) 0.1013E-6, (BR) 0.2339E-5
     CUBR              (CU) 0.3113E-3, (BR) 0.3839E-3
     BR                           56.63
     CUF               (CU) 0.1651E-4,  (F) 0.8817E-6
     CU                            0.3502E-2
```

C-H-N-O-S-Cl-Si-Al-K-Na-Br-F-Sn-Zr-As

Zirconium silicate ($ZrSiO_4$) is projected to form as a stable solid between 300 and 1200 to 1300 K in a PFBC system operating with 100 percent excess air and 90 percent S removal. The interactions of Sn and As with either the clay constituents (Al, Si), alkalis (Na, K), or halides (Br, F) do not form stable solid phases but promote gaseous phase formation of interactive species such as tin dibromide ($SnBr_2$) and arsenic trifluoride (AsF_3). Table 72 illustrates the projected solids formed as a function of temperature in the C-H-N-O-S-Cl-Si-Al-K-Na-Br-F-Sn-Zr-As system, as well as the percent distribution of the trace and minor constituents in the gas phases resulting at 1200 and 1300 K.

C-H-N-O-S-Cl-Si-Al-K-Na-Br-F-Cd-Ga-Sb

Ninety-four percent of the Cd feedstock concentration is projected to react with Br, forming gaseous cadmium bromide (CdBr) at 1200 K combustor temperatures, while only 77 percent of the feedstock Cd is released as the bromide at 1300 K (Table 73). Although Br and F are also projected to complex with Cd forming the volatiles, this reaction is projected to occur within less than 0.0001 percent of the feedstock content. Both Br and F are projected to react with Ga at combustion temperatures, forming gaseous gallium bromide (GaBr) and gallium fluoride (GaF) as trace species over solid gallium oxide (Ga_2O_3).

C-H-N-O-S-Cl-Si-Al-K-Na-Br-F-Se-Mo-Pb

Chemical reaction of Br, F, Se, Mo, or Pb with ash particles containing Si and/or Al is not anticipated for equilibrium combustor conditions, as illustrated in the solid formations of Table 74. Bromine, F, Pb, and Se are projected to volatilize completely between 300 and 1300 K, as either an oxide or a chloride, with minimal interaction

TABLE 72 - FLUIDIZED-BED COMBUSTION OF C-H-N-O-S-Cl-Si-Al-K-Na-Br-F-Sn-Zr-As - 100% EXCESS AIR, 90% SULFUR-REMOVAL, 1013 kPa OPERATIONS

```
     \TEMP (K)
COMPOUND\          300       400       500       600       700       800       900       1000      1100      1200      1300
---------------------------------------------------------------------------------------------------------------------------
SIO2 •              • • • • • • • • • • • • • • • • • • • • • • • • • • • • • • • • • • • •
SIO2 ••                                                                                     • • • • • • • • • • •
KAL(SO4)2.12H2O     •
KAL(SO4)2                     • • • • • • • • • • • • • • • • • • • • •
K2SO4                         • • • • • • • • • • • • • • • • • • • • • • • • • • • • • • •
KCL                 •
ALF3                • • • • • • • • • • •
KALSI3O8                                                                                    • • • • • • • • • • •
2NA2O.SIO2          • • • • • • • • • • • • • • • • • • • • • • • • • • • • • • • • • • • • • • • • • • • • • • • • • • •
AL2SIO5                       • • • • • • • • • • • • • • • • • • • • • • • • • • • • • • • • • • • • • • • •
3AL2O3.2SIO2                                                                                                        •
AL(OH)3             •
AS2O5               • • • • • • • • • • • • • • • • • • • • • • • • • • • • • • • • • • • • • • • • •
ZRSIO4              • • • • • • • • • • • • • • • • • • • • • • • • • • • • • • • • • • • • • • • • • • • • • •
ZRO2                                                                                                                •
SNO2                • • • • • • • • • • • • • • • • • • • • • • • • • • • • • • • • • • • • • • • • • • • • • • • • • • •
•   QUARTZ
••  CRISTOBALITE
```

```
ELEMENTAL PERCENT DISTRIBUTION IN GASEOUS EQUILIBRIUM PHASES

    COMPOUND                      1200K
    BRH                           42.78
    HF                            99.51
    NOBR                           0.1513E-1
    ASN                            0.9629E-4
    K2SO4                          0.1123E-1
    ALF2O                          0.4823
    BRO                            0.9219E-1
    SNO                            0.6793E-3
    ASO                           15.25
    SNCL4                          0.7768E-4
    ASCL3                          0.1858
    SNCL2                          0.1728E-1
    KCL                            0.7610
    BRCL                           0.2051E+1
    ASCL                          82.35
    K2BR2               (K) 0.3028E-7, (BR) 0.1326E-4
    KBR                 (K) 0.5591E-2, (BR) 0.2448E+1
    SNBR2              (SN) 0.3198E-5, (BR) 0.1337E-5
    BR2                            0.9481E-1
    BRF                 (F) 0.1115E-6, (BR) 0.2574E-5
    BR                            52.52
    ASF3                (F) 0.2786   , (AS) 0.2212E+1
    AS                             0.2589E-6
```

```
ELEMENTAL PERCENT DISTRIBUTION IN GASEOUS EQUILIBRIUM PHASES

    COMPOUND                      1300K
    BRH                           37.00
    HF                            99.42
    NOBR                           0.1283E-1
    ASN                            0.5334E-3
    K2SO4                          0.1087E-1
    ALF2O                          0.5782
    BRO                            0.1095
    SNO                           0.5031E-1
    ASO                           33.48
    SNCL4                          0.4687E-4
    ASCL3                          0.1540E-1
    SNCL2                          0.1321
    KCL                            0.2269E+1
    BRCL                           0.8030
    ASCL                          66.43
    K2BR2               (K) 0.3911E-7, (BR) 0.1713E-4
    KBR                 (K) 0.1241E-1, (BR) 0.5434E+1
    SNBR2              (SN) 0.1238E-4, (BR) 0.5179E-5
    BR2                            0.2403E-1
    BRF                 (F) 0.1013E-6, (BR) 0.2339E-5
    BR                            56.62
    ASF3                (F) 0.9645E-2, (AS) 0.7659E-1
    AS                             0.3329E-5
```

TABLE 73 - FLUIDIZED-BED COMBUSTION OF C-H-N-O-S-Cl-Si-Al-K-Na-Br-F-Cd-Ga-Sb - 100% EXCESS AIR, 90% SULFUR-REMOVAL, 1013 kPa OPERATIONS

```
         \TEMP (K)
COMPOUND\          300   400   500   600   700   800   900  1000  1100  1200  1300
-----------------------------------------------------------------------------------
SIO2 •             •••••••••••••••••••••••••••••••••••••••••••
SIO2 ••                                                            •••••••••••••
KAL(SO4)2.12H2O    •
KAL(SO4)2                •••••••••••••••••••••••••
K2SO4                    •••••••••••••••••••••••••••••••••••••
KCL                •
ALF3               •••••••••••••
KALSI3O8                                                           •••••••••••••
2NA2O.SIO2         •••••••••••••••••••••••••••••••••••••••••••••••••••••••••••••
AL2SIO5                  •••••••••••••••••••••••••••••••••••••••••••••••••
3AL2O3.2SIO2                                                                   •
AL(OH)3            •
GA2O3              •••••••••••••••••••••••••••••••••••••••••••••••••••••••••••••
SBO2               •••••••••••••••••••••••••••••••••••••••••••••••••••••••••••••
CDCL2              •••••••
CDSO4                          •••••••••••••••••••
•  QUARTZ
•• CRISTOBALITE
```

```
ELEMENTAL PERCENT DISTRIBUTION IN GASEOUS EQUILIBRIUM PHASES

         COMPOUND                      1200K
         BRH                           38.09
         HF                            99.51
         NOBR                           0.1347E-1
         K2SO4                          0.1124E-1
         ALF2O                          0.4824
         BRO                            0.8212E-1
         CDO                            5.64
         SBO                            0.4212E-1
         SBCL3                          0.5704
         KCL                            0.7622
         BRCL                           0.1829E+1
         CDCL                           0.7648E-2
         GACL                           0.1715E-2
         SBCL                           0.2378E-1
         K2BR2                  (K) 0.2401E-7, (BR) 0.1051E-4
         KBR                    (K) 0.4978E-2, (BR) 0.2180E+1
         BR2                            0.7519E-1
         BRF                    (F) 0.9928E-7, (BR) 0.2293E-5
         CDBR                     (CD) 94.30, (BR) 10.96
         GABR                  (GA) 0.1951E-5, (BR) 0.4525E-6
         BR                            46.77
         CDF                   (CD) 0.8315E-5,  (F) 0.4182E-7
         GAF                   (GA) 0.2494E-4,  (F) 0.2504E-6
         CD                             0.5172E-1
         SB                             0.1170E-6
```

```
ELEMENTAL PERCENT DISTRIBUTION IN GASEOUS EQUILIBRIUM PHASES

         COMPOUND                      1300K
         BRH                           33.71
         HF                            99.42
         NOBR                           0.1168E-1
         K2SO4                          0.1086E-1
         ALF2O                          0.5781
         BRO                            0.9968E-1
         CDO                           22.85
         SBO                            2.65
         SBCL3                          0.8400
         KCL                            2.27
         BRCL                           0.7323
         CDCL                           0.2486E-1
         GACL                           0.3961E-1
         SBCL                           0.7499
         K2BR2                  (K) 0.3245E-7, (BR) 0.1421E-4
         KBR                    (K) 0.1130E-1, (BR) 0.4950E+1
         BR2                            0.1993E-1
         BRF                    (F) 0.9222E-7, (BR) 0.2130E-5
         CDBR                     (CD) 76.70, (BR) 8.91
         GABR                  (GA) 0.3942E-4, (BR) 0.9142E-5
         BR                            51.57
         CDF                   (CD) 0.3632E-4,  (F) 0.1827E-6
         GAF                   (GA) 0.6413E-3,  (F) 0.6438E-5
         CD                             0.4230
         SB                             0.2979E-4
```

TABLE 74 - FLUIDIZED-BED COMBUSTION OF C-H-N-O-S-Cl-Si-Al-K-Na-Br-F-Se-Mo-Pb - 100% EXCESS AIR, 90% SULFUR-REMOVAL, 1013 kPa OPERATIONS

```
       \TEMP (K)
COMPOUND\       300   400   500    600   700   800    900  1000  1100   1200  1300
----------------------------------------------------------------------------------
SIO2 •            ••••••••••••••••••••••••••••••••••••••••••••••
SIO2 ••                                                              •••••••••••••
KAL(SO4)2.12H2O   •
KAL(SO4)2               •••••••••••••••••••••••••••
AL(OH)3           •
K2SO4                   ••••••••••••••••••••••••••••••••••••••••
KCL               •
ALF3              ••••••••••••••
KALSI308                                                             •••••••••••••
2NA20.SIO2        ••••••••••••••••••••••••••••••••••••••••••••••••••••••••••••••••
AL2SIO5                 •••••••••••••••••••••••••••••••••••••••••••••••••••••
3AL203.2SIO2                                                                     •
MOO3              ••••••••••••••••••••
•  QUARTZ
•• CRISTOBALITE
```

```
ELEMENTAL PERCENT DISTRIBUTION IN GASEOUS EQUILIBRIUM PHASES

     COMPOUND                    1200K
     H2MOO4                      99.70
     BRH                         42.77
     HF                          99.52
     HSE                           0.1013E-4
     NOBR                          0.1513E-1
     K2SO4                         0.1124E-1
     MOO3                          0.9830E-3
     MOO2CL2                       0.2951
     ALF2O                         0.4825
     BRO                           0.9223E-1
     SEO                        100.0
     PBO                           0.3379E-2
     PBCL4                       99.51
     PBCL2                         0.4798
     KCL                           0.7543
     BRCL                          2.05
     PBCL                          0.2174E-2
     K2BR2                (K) 0.3027E-7, (BR) 0.1326E-4
     KBR                  (K) 0.5590E-2, (BR) 0.2448E+1
     PBBR4               (PB) 0.1934E-4, (BR) 0.1031E-3
     PBBR2               (PB) 0.2336E-4, (BR) 0.6227E-4
     BR2                           0.9482E-1
     BRF                  (F) 0.1115E-6, (BR) 0.2575E-5
     PBBR                (PB) 0.2254E-5, (BR) 0.3005E-5
     BR                          52.52
     PBF2                 (F) 0.6324E-8, (PB) 0.5479E-7
     PBF                  (F) 0.1715E-8, (PB) 0.2972E-7
     PB                            0.1229E-5
```

```
ELEMENTAL PERCENT DISTRIBUTION IN GASEOUS EQUILIBRIUM PHASES

     COMPOUND                    1300K
     H2MOO4                      99.86
     BRH                         37.00
     HF                          99.42
     HSE                           0.4752E-4
     NOBR                          0.1283E-1
     K2SO4                         0.1087E-1
     MOO3                          0.5839E-2
     MOO2CL2                       0.1364
     ALF2O                         0.5784
     BRO                           0.1095
     SEO                        100.0
     PBO                           0.8724
     PBCL4                       87.22
     PBCL2                       11.62
     KCL                          2.25
     BRCL                          0.8041
     PBCL                          0.2860
     K2BR2                (K) 0.3911E-7, (BR) 0.1713E-4
     KBR                  (K) 0.1241E-1, (BR) 0.5434E+1
     PBBR4               (PB) 0.3770E-5, (BR) 0.2010E-4
     PBBR2               (PB) 0.3155E-3, (BR) 0.8409E-3
     BR2                           0.2403E-1
     BRF                  (F) 0.1013E-6, (BR) 0.2339E-5
     PBBR                (PB) 0.2602E-3, (BR) 0.3468E-3
     BR                          56.61
     PBF2                 (F) 0.3408E-6, (PB) 0.2953E-5
     PBF                  (F) 0.4416E-6, (PB) 0.7653E-5
     PB                            0.8416E-3
```

between Pb and Br or F. These interactions promote the formation of lead tetra-, di-, and monobromide, ($PbBr_4$, $PbBr_2$, PbBr) and lead di- and monofluoride (PbF_2, PbF). Molybdenum exists as a stable solid between 300 and 600 to 700 K in the PFBC system operating with 100 percent excess air and 90 percent S-removal efficiencies, prior to complete volatilization as either molybdic acid (H_2MoO_4), molybdenum trioxide (MoO_3), or molybdenum oxychloride (MoO_2Cl_2). Gaseous or condensed phase interaction of Mo with K, Na, Br, F, Se, or Pb is not projected.

C-H-N-O-S-Cl-Si-Al-K-Na-Br-F-Ge-Co

One final series of calculations is made to illustrate the possible interaction of Br and F with the trace feedstock constituents Ge and Co. Only Co is projected to react with F, forming gaseous cobalt difluoride (CoF_2) at combustion temperatures of 1200 or 1300 K. This interaction volatilizes less than 0.0001 percent of the initial feedstock content from the stable cobalt oxide solid phases (Co_3O_4 or CoO). Chemical reaction between Ge and F is not projected (Table 75).

The last seven subsystems have demonstrated the activity of both Br and F enhances volatilization of stable oxide solids in addition to complexing interactively with trace or minor constituents in the gas phase. The last three remaining subsystems will consider the interaction of the trace and minor feedstock constituents in the absence of the halides.

C-H-N-O-S-Cl-Si-Al-K-Na-Zr-B-V

The potential formation of condensed corrosive melt formations as liquid sodium sulfate (Na_2SO_4) has been demonstrated previously. Reaction of the alkali with V similarly may result in the formation of liquid vanadates in the combustor. These phases are not projected at equilibrium because of the interaction of the alkali with Al or Si. It is likely that if the alkali and V were permitted to react in the absence of the clay constituents, corrosive deposits might form.

TABLE 75 - FLUIDIZED-BED COMBUSTION OF C-H-N-O-S-Cl-Si-Al-K-Na-Br-F-Ge-Co - 100% EXCESS AIR, 90% SULFUR-REMOVAL, 1013 kPa OPERATIONS

```
        \TEMP (K)
COMPOUND\           300    400    500    600    700    800    900    1000   1100   1200   1300
---------------------------------------------------------------------------------------------
SIO2 •              ••••••••••••••••••••••••••••••••••••••••••••••••••
SIO2 ••                                                                     •••••••••••••••
KAL(SO4)2.12H2O     •
KAL(SO4)2                  •••••••••••••••••••••••••••••
AL(OH)3             •
K2SO4                      •••••••••••••••••••••••••••••••••••••••••••
KCL                 •
ALF3                •••••••••••••••
KALSI3O8                                                                    •••••••••••••••
2NA2O.SIO2          •••••••••••••••••••••••••••••••••••••••••••••••••••••••••••••••••••••••
AL2SIO5                    •••••••••••••••••••••••••••••••••••••••••••••••••••••••••
3AL2O3.2SIO2                                                                              •
CO3O4               •                                                •••••••••••••••
COO                                                                                       •
COSO4                      ••••••••••••••••••••••••••••••••••••
GEO2                •••••••••••••••••••••••••••••••••••••••••••••••••••••••••••••••••••••••
•  QUARTZ
•• CRISTOBALITE
```

```
ELEMENTAL PERCENT DISTRIBUTION IN GASEOUS EQUILIBRIUM PHASES

      COMPOUND               1200K
      BRH                      42.77
      HF                       99.52
      NOBR                      0.1513E-1
      K2SO4                     0.1124E-1
      ALF2O                     0.4824
      BRO                       0.9222E-1
      GEO                       0.4605E-1
      CO2CL4                    0.8168E-5
      COCL3                     0.2623E-2
      COCL2                    24.43
      KCL                       0.7608
      BRCL                      2.05
      COCL                      0.7490E-5
      K2BR2         (K) 0.3028E-7, (BR) 0.1326E-4
      KBR           (K) 0.5591E-2, (BR) 0.2448E+1
      BR2                       0.9482E-1
      BRF           (F) 0.1115E-6, (BR) 0.2575E-5
      BR                       52.53
      COF2          (F) 0.1723E-6, (CO) 0.4230E-5

ELEMENTAL PERCENT DISTRIBUTION IN GASEOUS EQUILIBRIUM PHASES

      COMPOUND               1300K
      BRH                      37.00
      HF                       99.42
      NOBR                      0.1283E-1
      K2SO4                     0.1087E-1
      ALF2O                     0.5781
      BRO                       0.1095
      GEO                       2.23
      CO2CL4                    0.8306E-5
      COCL3                     0.2243E-2
      COCL2                    45.08
      KCL                       2.27
      BRCL                      0.8024
      COCL                      0.1524E-3
      K2BR2         (K) 0.3911E-7, (BR) 0.1713E-4
      KBR           (K) 0.1241E-1, (BR) 0.5434E+1
      BR2                       0.2403E-1
      BRF           (F) 0.1013E-6, (BR) 0.2339E-5
      BR                       56.62
      COF2          (F) 0.6718E-6, (CO) 0.1649E-4
```

In the C-H-N-O-S-Cl-Si-Al-K-Na-Zr-B-V system zirconium silicate, ($ZrSiO_4$) is projected to form in ash particles between 300 and 1200 to 1300 K. Boron is expected to volatilize completely as either boric acid (H_3BO_3), metaboric acid (BHO_2), or potassium metaborate (KBO_2). Adsorption of the gas phase along the ash lattice may enhance secondary reactions not explored in this study. Vanadium is projected to exist primarily as liquid V_2O_5 at combustion temperatures of 1200 or 1300 K. Table 76 illustrates the stable solid phases projected to form in this PFBC subsystem and the percent distribution of the trace and minor constituents in the various volatiles that are likely to form.

C-H-N-O-S-Cl-Si-Al-K-Na-Se-Pb-Ni-Cu-Sn

In the interactive C-H-N-O-S-Cl-Si-Al-K-Na-Se-Pb-Ni-Cu-Sn subsystem only solid nickel silicate (Ni_2SiO_4) is projected to complex between the trace and minor constituents. Although 100 percent of the feedstock Se, Pb, and Cu content is projected to volatilize as either oxides or chlorides, it is unlikely that gaseous interactive phases will be formed. The stability of the projected solid phases illustrated in Table 77 has been described previously in detail.

C-H-N-O-S-Cl-Si-Al-K-Na-Se-Cu-Ge-Cr-Fe

Similarly, in the C-H-N-O-S-Cl-Si-Al-K-Na-Se-Cu-Ge-Cr-Fe subsystem interaction between the various trace and minor constituents is minimal. The feedstock Se and Cu content completely volatilizes, Ge exists principally as germanium oxide (GeO_2) at combustion temperatures of 1200 or 1300 K, and Cr and Fe exist as oxides (Cr_2O_3 and Fe_2O_3), with 22.14 percent Cr volatilizing at 1200 K and 71.68 percent at 1300 K (Table 78).

COMPARISON OF THE EQUILIBRIUM PRODUCT DISTRIBUTION IN CONDENSED AND GASEOUS PHASES FORMED DURING PFBC USING EASTERN AND WESTERN U.S. COALS

The complexity of the trace and minor element interactions has been illustrated in the preceeding subsystem calculations. Although these projections indicate the resulting product distribution in the condensed and gaseous species for specific PFB combustors utilizing a U.S. mean

TABLE 76 - FLUIDIZED-BED COMBUSTION OF C-H-N-O-S-Cl-Si-Al-K-Na-Zr-B-V - 100% EXCESS AIR, 90% SULFUR-REMOVAL, 1013 kPa OPERATIONS

```
      \TEMP (K)
COMPOUND\      300   400   500   600   700   800   900  1000  1100  1200  1300
------------------------------------------------------------------------------
SIO2 •           •••••••••••••••••••••••••••••••••••••••••••
SIO2 ••                                                          •••••••••••••
KAL(SO4)2.12H2O  •
KAL(SO4)2              •••••••••••••••••••••••••
AL(OH)3          •
K2SO4                  •••••••••••••••••••••••••••••••••••••
KCL              •
ALF3             •••••••••••••
KALSI3O8                                                         •••••••••••••
2NA2O.SIO2       •••••••••••••••••••••••••••••••••••••••••••••••••••••••••••••
AL2SIO5                •••••••••••••••••••••••••••••••••••••••••••••••••
3AL2O3.2SIO2                                                                 •
ZRSIO4           •••••••••••••••••••••••••••••••••••••••••••••••••••••••
ZRO2                                                                         •
H3BO3            •
V2O5             •••••••••••••••••••••••••••••••••••••••••••••••••••••••••••••
•  QUARTZ
•• CRISTOBALITE
```

```
      ELEMENTAL PERCENT DISTRIBUTION IN GASEOUS EQUILIBRIUM PHASES

                 COMPOUND                    1200K
                 (HBO2)3                         0.6093E-4
                 H3BO3                          85.85
                 BHO2                           13.71
                 K2SO4                           0.1124E-1
                 KBO2               (K) 0.1472E-1, (B) 0.1316
                 VO2                             0.2548E-4
                 VOCL3                           0.3157E-1
                 KCL                             0.7613
```

```
      ELEMENTAL PERCENT DISTRIBUTION IN GASEOUS EQUILIBRIUM PHASES

                 COMPOUND                    1300K
                 (HBO2)3                         0.1080
                 H3BO3                          58.77
                 BHO2                           39.84
                 K2SO4                           0.1087E-1
                 KBO2               (K) 0.1445     , (B) 0.1292E+1
                 VO2                             0.1081E-2
                 VOCL3                           0.1955E-1
                 KCL                             0.2269E+1
```

TABLE 77 - FLUIDIZED-BED COMBUSTION OF C-H-N-O-S-Cl-Si-Al-K-Na-Se-Pb-Ni-Cu-Sn - 100% EXCESS AIR, 90% SULFUR-REMOVAL, 1013 kPa OPERATIONS

```
        \TEMP (K)
COMPOUND\           300     400     500     600     700     800     900    1000    1100    1200    1300
-------------------------------------------------------------------------------------------------------
SIO2 •                •••••••••
SIO2 ••
KAL(SO4)2.12H2O       •
KAL(SO4)2                     •••••••••••••••••••••••••••••••••
AL(OH)3               •
K2SO4                         •••••••••••••••••••••••••••••••••••••••••••••••••
KALSI3O8                                                                      •••••••••••••••••
2NA2O.SIO2            •••••••••••••••••••••••••••••••••••••••••••••••••••••••••••••••••••••••••••••••••
AL2SIO5                       •••••••••••••••••••••••••••••••••••••••••••••••••••••••••••••••••
3AL2O3.2SIO2                                                                                      •
KCL                   •
NISO4                         •••••••••••••••••••••••••••••••••••••••••
NI2SIO4               •                                                       •••••••••••••••••••••••••
CUSO4                 •••••••••••••••••••••••••••••••••••••••••
CUO.CUSO4                                                     •
CUCL2                 •
SNO2                  •••••••••••••••••••••••••••••••••••••••••••••••••••••••••••••••••••••••••••••••••
*.QUARTZ
**CRISTOBALITE
        ELEMENTAL PERCENT DISTRIBUTION IN GASEOUS EQUILIBRIUM PHASES

                        COMPOUND             1200K
                        NI(OH)2                0.6438
                        HSE                    0.1014E-4
                        K2SO4                  0.1123E-1
                        SEO                  100.
                        PBO                    0.3587E-2
                        NIO                    0.1854E-6
                        CUO                    0.6208E-1
                        SNO                    0.6793E-3
                        PBCL4                 99.50
                        SNCL4                  0.7368E-4
                        CU3CL3                 4.03
                        PBCL2                  0.4944
                        NICL2                  3.65
                        SNCL2                  0.1683E-1
                        KCL                    0.7509
                        PBCL                   0.2274E-2
                        NICL                   0.7569E-4
                        CUCL                  95.91
                        PB                     0.1306E-5
                        CU                     0.3678E-3

        ELEMENTAL PERCENT DISTRIBUTION IN GASEOUS EQUILIBRIUM PHASES

                        COMPOUND             1300K
                        NI(OH)2                3.59
                        HSE                    0.4759E-4
                        K2SO4                  0.1086E-1
                        SEO                  100.
                        PBO                    0.9215
                        NIO                    0.1236E-4
                        CUO                    0.2775
                        SNO                    0.5036E-1
                        PBCL4                 86.85
                        SNCL4                  0.4447E-4
                        CU3CL3                 0.8652E-1
                        PBCL2                 11.93
                        NICL2                  8.07
                        SNCL2                  0.1288
                        KCL                    2.24
                        PBCL                   0.2978
                        NICL                   0.1380E-2
                        CUCL                  99.63
                        PB                     0.8899E-3
                        CU                     0.3336E-2
```

TABLE 78 - FLUIDIZED-BED COMBUSTION OF C-H-N-O-S-Cl-Si-Al-K-Na-Se-Cu-Ge-Cr-Fe - 100% EXCESS AIR, 90% SULFUR-REMOVAL, 1013 kPa OPERATIONS

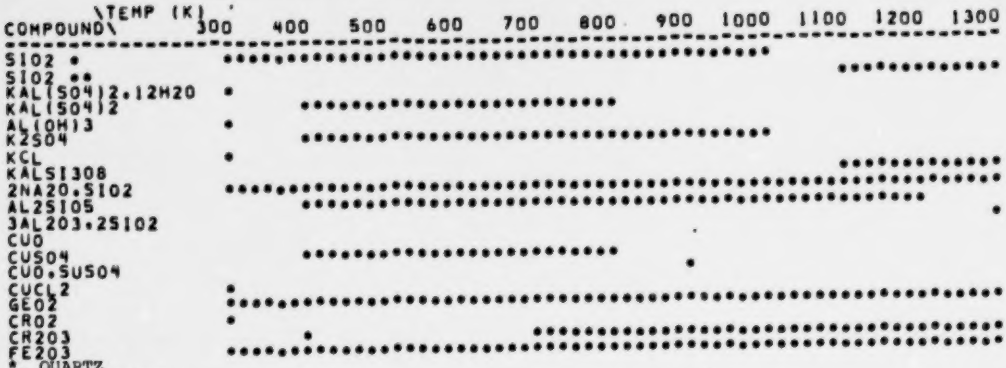

* QUARTZ
** CRISTOBALITE

ELEMENTAL PERCENT DISTRIBUTION IN GASEOUS EQUILIBRIUM PHASES

COMPOUND	1200K
CRO4H2	7.83
CRO2OH	11.43
CRO2CL2	2.88
CRO3	0.5051E-1
CRO2	0.4398E-5
SEO	100.
HSE	0.1016E-4
K2SO4	0.1123E-1
KCL	0.7591
CUO	0.6136E-1
CU3CL3	4.03
CUCL	95.91
CU	0.3640E-3
GEO	0.8247E-1

ELEMENTAL PERCENT DISTRIBUTION IN GASEOUS EQUILIBRIUM PHASES

COMPOUND	1300K
CRO4H2	15.40
CRO2OH	54.17
CRO2CL2	2.11
CRO3	0.3822
CRO2	0.1721E-3
SEO	100.
HSE	0.4767E-4
K2SO4	0.1085E-1
KCL	2.26
CUO	0.2744
CU3CL3	0.8653E-1
CUCL	99.64
CU	0.3302E-2
GEO	3.99

coal, many of the reactions are applicable to systems defining alternative feedstock compositions. This section is directed toward defining the initial chemical phases* existing in eastern and western coals containing a minimum and maximum content of the trace or minor constituents Si, Al, K, Na, Pb, Hg, F, Be, As, Cd, and Se. Combustion conditions representing 100 percent excess air operations at 1013 kPa and with 90 percent S-removal efficiencies illustrate the redistribution of the various trace and minor elements within the resulting condensed and gaseous product phases (Tables 79-82).

Initially Si is projected to exist in either solid SiO_2, $KAlSi_3O_8$, or $2Na_2O\cdot SiO_2$, and Al as $Al(OH)_3$, $KAl(SO_4)_2\cdot 12H_2O$, $KAlSi_3O_8$, AlF_3 or $Al(SO_4)_3$. The low-contaminant eastern coals (0.06 wt% K) are expected to contain K as a hydrated aluminum sulfate, aluminosilicate, or chloride at 300 K, while high-contaminant eastern coals (0.68 wt% K) favor an almost equal distribution of K between the chloride or aluminum sulfate solids. Only the aluminum sulfate solid is projected to result in western coals containing 0.01 wt% K, but at 0.32 wt%, K exists within either the chloride, aluminum sulfate, or aluminosilicate complexes. Sodium in both eastern and western coals is expected to form predominantly the water glass silicate phase ($2Na_2O\cdot SiO_2$), while 100 percent of the Pb, Hg and Se feedstock concentration volatilizes at 300 K and 1013 kPa as either gaseous tetra- and dichloride or as oxide species. Fluorine complexes initially with Al in the clay lattice as solid AlF_3, and As exists as solid As_2O_5. Conversely, the Be and Cd phases are dependent on the feedstock composition: eastern coals and maximum trace and minor element contamination in western coals favor the formation of Be as solid $Be(OH)_2$ (β), but in minimum contaminant concentrations in the western feedstock Be exists as the solid alpha sulfate; similarly, solid $CdCl_2$ is projected for the eastern coals and maximum contaminant level western materials, while $CdSO_4$ exists as the preferred phase

---

*Projected at 300 K and 1013 kPa

TABLE 79 - PFBC PROJECTIONS FOR MINIMUM TRACE AND MINOR ELEMENT CONCENTRATIONS IN EASTERN COALS[11]

Dwg. 7728A98

C	63%
H	4%
N	0.94%
O	2.5%
S	0.55%
Cl	0.01%

ELEMENT	CONCENTRATION IN COAL (%, ppm)	PROJECTED PHASES AND PERCENT DISTRIBUTION AT 300K	PROJECTED PHASES AND PERCENT DISTRIBUTION AT 1300K FOR 100% EXCESS AIR, 90% SULFUR REMOVAL 1013kPa OPERATIONS
Si	1.0%	96.08 SiO_2,* 3.31 $KAlSi_3O_8$ 0.61 $2Na_2O.2SiO_2$	49.77 SiO_2, 36.74 $3Al_2O_3.2SiO_2$, 12.88 $KAlSi_3O_8$, 0.61 $2Na_2O.SiO_2$
Al	1.1%	96.71 $Al(OH)_3$, 2.11 $KAl(SO_4)_2.12H_2O$, 0.96 $KAlSi_3O_8$, 0.22 AlF_3	96.25 $3Al_2O_3.2SiO_2$, 3.75 $KAlSi_3O_8$
K	0.06%	56.04 $KAl(SO_4)_2.12H_2O$, 25.58 $KAlSi_3O_8$, 18.38 KCl	99.62 $KAlSi_3O_8$, 0.38 KCl(g)
Na	0.01%	100 $2Na_2O.SiO_2$	100 $2Na_2O.SiO_2$
Pb	1.0 ppm	100 $PbCl_4$ (g)	97,14 PbO (g), 1.61 $PbCl_2$(g), 1.13 PbCl(g), 0.02 $PbCl_4$(g), 0.10 (Pb, PbF, PbF_2, PbF_4) (g)
Hg	0.05 ppm	100 $HgCl_2$(g)	94.81 Hg(g), 5.19 HgO(g)
F	50 ppm	100 AlF_3	100 HF (g)
Be	0.23 ppm	100 $Be(OH)_2(\beta)$	100 $Be(OH)_2$(g)
As	1.8 ppm	100 As_2O_5	93.33 AsO(g), 6.60 AsCl(g), 0.07 AsF_3(g)
Cd	0.10 ppm	100 $CdCl_2$	98.15 CdO(g), 1.85 Cd(g)
Se	1.1 ppm	100 SeO(g)	100 SeO(g)

* SOLID UNLESS OTHERWISE INDICATED

TABLE 80 - PFBC PROJECTIONS FOR MAXIMUM TRACE AND MINOR ELEMENT CONCENTRATIONS IN EASTERN COALS[11]

Dwg. 7728A97

C	80%
H	6.0%
N	1.8%
O	18%
S	5.0%
Cl	0.80%

ELEMENT	CONCENTRATION IN COAL (%, ppm)	PROJECTED PHASES AND PERCENT DISTRIBUTION AT 300K AND 1013kPa	PROJECTED PHASES AND PERCENT DISTRIBUTION AT 1300K FOR 100% EXCESS AIR, 90% SULFUR REMOVAL 1013kPa OPERATIONS
Si	6.3%	99.22 $Si0_2$*, 0.78 $2Na_20.Si0_2$	62.01 $Si0_2$, 22.66 $KAlSi_30_8$, 14.55 $3Al_20_3.2Si0_2$, 0.78 $2Na_20.Si0_2$
Al	3.1%	92.98 $Al(0H)_3$, 6.79 $KAl(S0_4)_2.12H_20$, 0.23 AlF_3	85.21 $3Al_20_3.2Si0_2$, 14.75 $KAlSi_30_8$, 0.04 $BeAl_20_4$
K	0.68%	55.12 KCl, 44.88 $KAl\ (S0_4)_2.12H_20$	97.49 $KAlSi_30_8$, 2.51 KCl(g)
Na	0.08%	100 $2Na_20.Si0_2$	100 $2Na_20.Si0_2$
Pb	18 ppm	100 $PbCl_4$ (g)	96.69 $PbCl_4$ (g), 3.22 $PbCl_2$ (g), 0.06 Pb0 (g) 0.03 $PbCl_2$ (g)
Hg	0.47 ppm	100 $HgCl_2$ (g)	94.85 Hg (g), 4.99 Hg0 (g), 0.16 $HgCl_2$ (g)
F	150 ppm	100 AlF_3	99.18 HF(g), 0.81 AlF_20 (g), 0.01 (AsF_3, BeF_2, BeClF, CdF_2) (g)
Be	2.6 ppm	100 $Be(0H)_2(\beta)$	83.10 $BeAl_20_4$, 16.89 $Be(0H)_2$(g), 0.01 ($BeCl_2$, BeClF, BeF_2) (g)
As	100 ppm	100 As_20_5	80.76 AsCl(g), 19.24 As0(g)
Cd	0.60 ppm	100 $CdCl_2$	97.86 Cd0 (g), 1.91 Cd (g), 0.23 CdCl (g)
Se	8.1 ppm	100 Se0 (g)	100 Se0 (g)

* SOLID UNLESS OTHERWISE INDICATED

TABLE 81 - PFBC PROJECTIONS FOR MINIMUM TRACE AND MINOR ELEMENT CONCENTRATIONS IN WESTERN COALS[11]

Dwg. 7728A96

C	58%
H	3.8%
N	0.59%
O	8.8%
S	0.34%
Cl	0.01%

ELEMENT	CONCENTRATION IN COAL (%, ppm)	PROJECTED PHASES AND PERCENT DISTRIBUTION AT 300K AND 1013kPa	PROJECTED PHASES AND PERCENT DISTRIBUTION AT 1300K FOR 100% EXCESS AIR, 90% SULFUR REMOVAL 1013kPa OPERATIONS
Si	0.38%	98.39 SiO_2*, 1.61 $2Na_2O.SiO_2$	65.16 SiO_2, 27.69 $3Al_2O_3.2SiO_2$, 5.54 $KAlSi_3O_8$, 1.61 $2Na_2O.SiO_2$
Al	0.31%	94.30 $Al(OH)_3$, 3.18 $Al_2(SO_4)_3$, 2.23 $KAl(SO_4)_3.12H_2O$, 0.29 AlF_3	97.82 $3Al_2O_3.2SiO_2$, 2.18 $KAlSi_3O_8$
K	0.01%	100 $KAl(SO_4)_2.12H_2O$	97.73 $KAlSi_3O_8$, 2.27 KCl (g)
Na	0.01%	100 $2Na_2O.SiO_2$	100 $2Na_2O.SiO_2$
Pb	0.70 ppm	100 $PbCl_4$ (g)	96.75 PbO (g), 1.89 $PbCl_2$ (g), 1.24 PbCl (g) 0.10 Pb (g), 0.02 $PbCl_4$ (g)
Hg	0.02 ppm	100 $HgCl_2$ (g)	94.90 Hg (g), 5.10 HgO (g)
F	19 ppm	100 AlF_3	99.83 HF (g), 0.16 AlF_2O (g) 0.01 (HSO_3F, ONF, SiF_4, AsF_3, BeF_2) (g)
Be	0.10 ppm	100 $BeSO_4$ (a)	100 $Be(OH)_2$ (g)
As	0.01 ppm	100 As_2O_5	92.81 AsO (g), 7.19 AsCl (g)
Cd	0.10 ppm	100 $CdSO_4$	98.12 CdO (g), 1.88 Cd (g)
Se	0.40 ppm	100 SeO (g)	100 SeO (g)

* SOLID UNLESS OTHERWISE INDICATED

TABLE 82 - PFBC PROJECTIONS FOR MAXIMUM TRACE AND MINOR ELEMENT CONCENTRATIONS IN WESTERN COALS[11]

Dwg.7728A95

C	74%
H	5.8%
N	1.5%
O	22%
S	1.9%
Cl	0.13%

ELEMENT	CONCENTRATION IN COAL (%, ppm)	PROJECTED PHASES AND PERCENT DISTRIBUTION AT 300K AND 1013kPa	PROJECTED PHASES AND PERCENT DISTRIBUTION AT 1300K FOR 100% EXCESS AIR, 90% SULFUR REMOVAL 1013kPa OPERATIONS
Si	4.7%	89.38 $Si0_2$*, 7.80 $2Na_20.Si0_2$, 2.82 $KAlSi_30_8$	83.03 $Si0_2$, 14.62 $3Al_20_3.2Si0_2$, 14.55 $KAlSi_30_8$, 7.80 $2Na_20.Si0_2$
Al	2.2%	94.14 $Al(0H)_3$, 3.63 $KAl(S0_4)_2.12H_20$, 1.93 $KAlSi_30_8$, 0.30 AlF_3	90.02 $3Al_20_3.2Si0_2$, 9.95 $KAlSi_30_8$, 0.03 $BeAl_20_4$
K	0.32%	44.59 KCl, 36.20 $KAl(S0_4)_2.12H_20$, 19.21 $KAlSi_30_8$	99.16 $KAlSi_30_8$, 0.84 KCl (g)
Na	0.60%	100 $2Na_20.Si0_2$	100 $2Na_20.Si0_2$
Pb	9.0 ppm	100 $PbCl_4$ (g)	39.15 $PbCl_2$ (g), 35.35 $PbCl_4$(g), 22.70 Pb0 (g) 2.78 PbCl (g), 0.02 Pb (g)
Hg	0.63 ppm	100 $HgCl_2$ (g)	95.08 Hg(g), 4.91 Hg0(g), 0.01 $HgCl_2$(g)
F	140 ppm	100 AlF_3	99.21 HF (g), 0.78 AlF_20 (g) 0.01 (BeClF, PbF_2, PbF, AsF_3, BeF_2, CdF) (g)
Be	1.4 ppm	100 $Be(0H)_2(\beta)$	69.56 $BeAl_20_4$, 30.43 $Be(0H_2)$ (g), 0.01 ($BeCl_2$, BeClF, BeF_2) (g)
As	0.07 ppm	100 As_20_5	57.17 As0 (g), 42.38 AsCl (g), 0.45 AsF_3 (g)
Cd	0.60 ppm	100 $CdCl_2$	98.01 Cd0 (g), 1.95 Cd (g), 0.04 CdCl (g)
Se	2.7 ppm	100 Se0 (g)	100 Se0 (g)

* SOLID UNLESS OTHERWISE INDICATED

in western coals containing a minimum Cd content. This heterogeneity of complexes, illustrated in the projected equilibrium phases, has resulted from the complete combustion of the feedstocks that releases Pb, Hg, and Se from inorganic or sulfur lattice in the coal particle,[15] Be from the carbon lattice, F from apatite, As and Cd from either mineral matter or inorganic association, and the alkali from the lithophilic or chloride bonds.

Combustion of eastern coals at 1300 K and 1013 kPa completely volatilizes the feedstock Se, Cd, As, F, Hg, and Pb content. Beryllium, which is released completely in the combustion of the eastern coals containing 0.23 ppm Be, complexes principally with Al to form solid $BeAl_2O_4$ when the eastern feedstock contains 2.6 ppm Be. Sodium, although projected at equilibrium to remain complexed as the silicate solid, is expected to be released from the ash, spent sorbent, and getter materials as the volatile chloride, hydroxide, and/or sulfate at approximately 1 percent of the feedstock content. Analytical characterization is required to define the actual Na content released during combustion, and X-ray diffraction analysis is essential in determining the resulting solid Na complex(es). Potassium is retained at 97 to 99 percent levels of the initial feedstock content in the solid aluminosilicate complex, with only 1 to 3 percent volatilization of the alkali as gaseous KCl.

CORROSIVE CONDENSATE FORMATIONS IN PFBC SYSTEMS

Sodium and vanadium liquids and mixed-melt phases have been projected to result at equilibrium when feedstock materials are combusted in the fluidized bed. Elimination of these corrosive deposits are essential in order to prolong the operating lifetime of the power system. Techniques that minimize the liquid or mixed-melt formations include:

- Pretreating of the feedstock or sorbent, reducing the initial alkali and V concentration in the bed

- Removing gaseous SO_x from the effluent streams through the sulfation of dolomite or limestone sorbents, reducing the potential of alkali sulfate formation
- Adding Cl to the system as either HCl or as an organic in order to drive the alkali into a more volatile phase, minimizing the formation of the sulfate condensate
- Adding aluminosilicate materials to "getter" alkali released during combustion of the feedstock or sorbent
- Increasing system operating temperatures, maintaining the alkali as a volatile species
- Developing high-temperature alloys that can withstand corrosive attack from deposited sulfate melts.

Phase diagrams have been generated to illustrate the resulting melt complexes as a function of Cl and S concentration, as well as temperature, in a 1013 kPa FBC operating with 100 percent excess air. Figure 123 indicates that solid Na phases are formed at temperatures of 1000 and 1100 K when 100 percent of the U.S. mean coal feedstock Na concentration is released during combustion. The typical U.S. mean coal Cl content (0.28 wt %) enhances the stability of the alkali chloride solid at 1000 K, in addition to the solid carbonate and sulfate phases in the 99 percent S-removal system. Chlorine does not complex with Na to form solid NaCl in systems where 90 percent S removal is achieved.

Temperatures above 1157 K are required to introduce the sulfate melt formation in the PFB combustor and effluent streams. At 1200 K in the 99 percent S-removal system, a mixture of liquid sulfate and solid carbonate are projected to coexist,* while at 90 percent S-removal capabilities only the liquid sulfate is projected to form. The concentration of ~2.7 and 4.5 percent total Cl is required by the 1200 K system to convert liquid Na_2SO_4 into volatile species in the 99 and 90 percent S-removal FBC systems. Increasing the combustor operating

---

*Typical U.S. mean coal chloride concentration is considered.

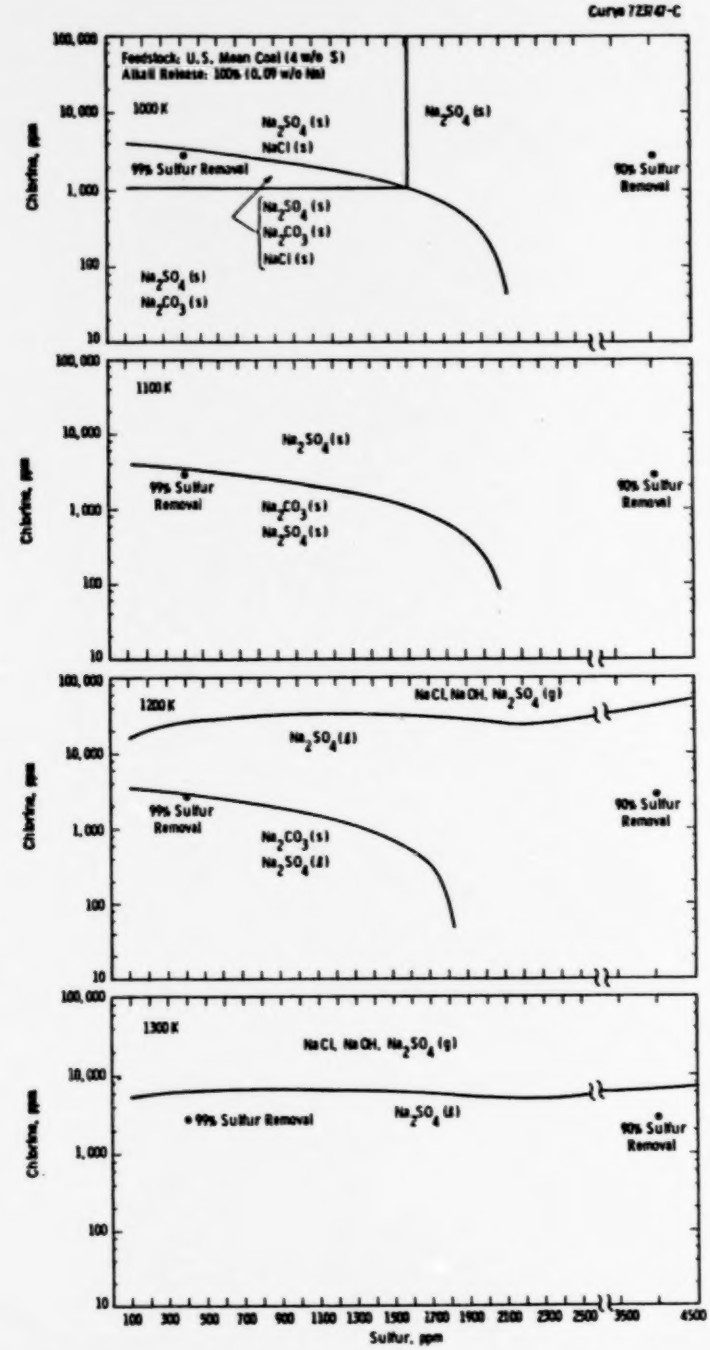

Figure 123 - Condensed Alkali Phases Formed as a Function of Temperature, Sulfur, and Chlorine Content in 1013 kPa FBC Systems Operating with 100% Excess Air and 100% Sodium Release from Feedstock Materials

temperature to 1300 K reduces the concentration of Cl required for complete volatilization of the melt to ~0.65 percent.

Although the equilibrium calculations project Na to complex as the solid water glass silicate phase, it is realistic to assume that ~1 percent of the feedstock Na concentration is released during combustion. The stability of the Na phases was reevaluated for the combustion of U.S. mean coal which releases only 1 percent of the initial Na content in 100 percent excess air and 1013 kPa operations (Figure 124). At 1000 K solid Na_2SO_4 and Na_2CO_3 in low S-containing environments are projected to exist as the principal alkali phases. Chlorine concentrations greater than 20 percent are required for sulfate sublimation and may cause severe attack to the supporting alloy materials. At 1100 K, 2 percent chlorine is required to cause sublimation of the solid Na_2SO_4 phase in the 99 percent S-removal system, while only 0.15 and 0.04 percent chlorine is required to promote volatilization of the liquid Na_2SO_4 formed at 1200 and 1300 K, respectively.

The equilibrium distribution and stability of condensed alkali and V complexes were determined as a function of Cl and S concentration for combustion of a U.S. mean coal with 100 percent excess air at 1013 kPa. We assumed that 1 percent of the feedstock Na is released from the clay aluminosilicate lattice and is available to react with the feedstock Ca and Mg. We also assumed that neither Ca nor Mg complexes with the resulting ash-containing Al and/or Si. Figure 125 illustrates the equilibrium phase diagram for these reactions at 1200 and 1300 K and 1013 kPa. Combustors operating with 99 percent S-removal efficiencies at either temperature are projected to contain condensed calcium vanadates, in addition to $CaSO_4$ and MgO. Sodium under these conditions is not projected to form the liquid sulfate melt, since S has been removed by the feedstock Ca content. It is interesting to note the complexity of the various phases expected to form at 1200 K when simpler phase interactions occur at 1300 K. Regimes within the 1200 K system promote the formation of liquid sodium vanadates (T_m $Na_2O \cdot V_2O_5$ = 903 K,

Curve 723745-B

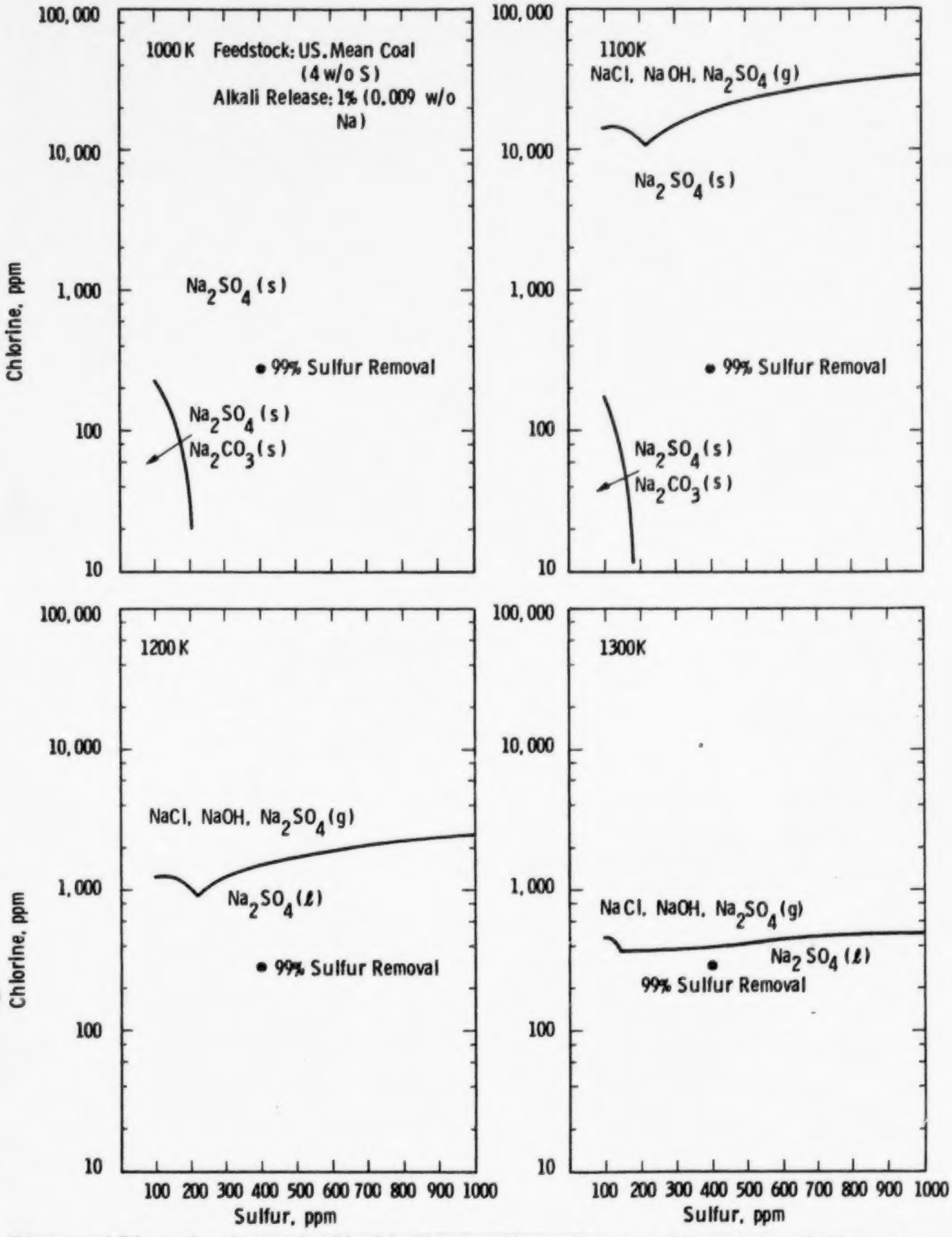

Figure 124 - Condensed Alkali Phases Formed as a Function of Temperature, Sulfur, and Chlorine Content in 1013 kPa FBC Systems Operating with 100% Excess Air and 1% Sodium Release from Feedstock Materials

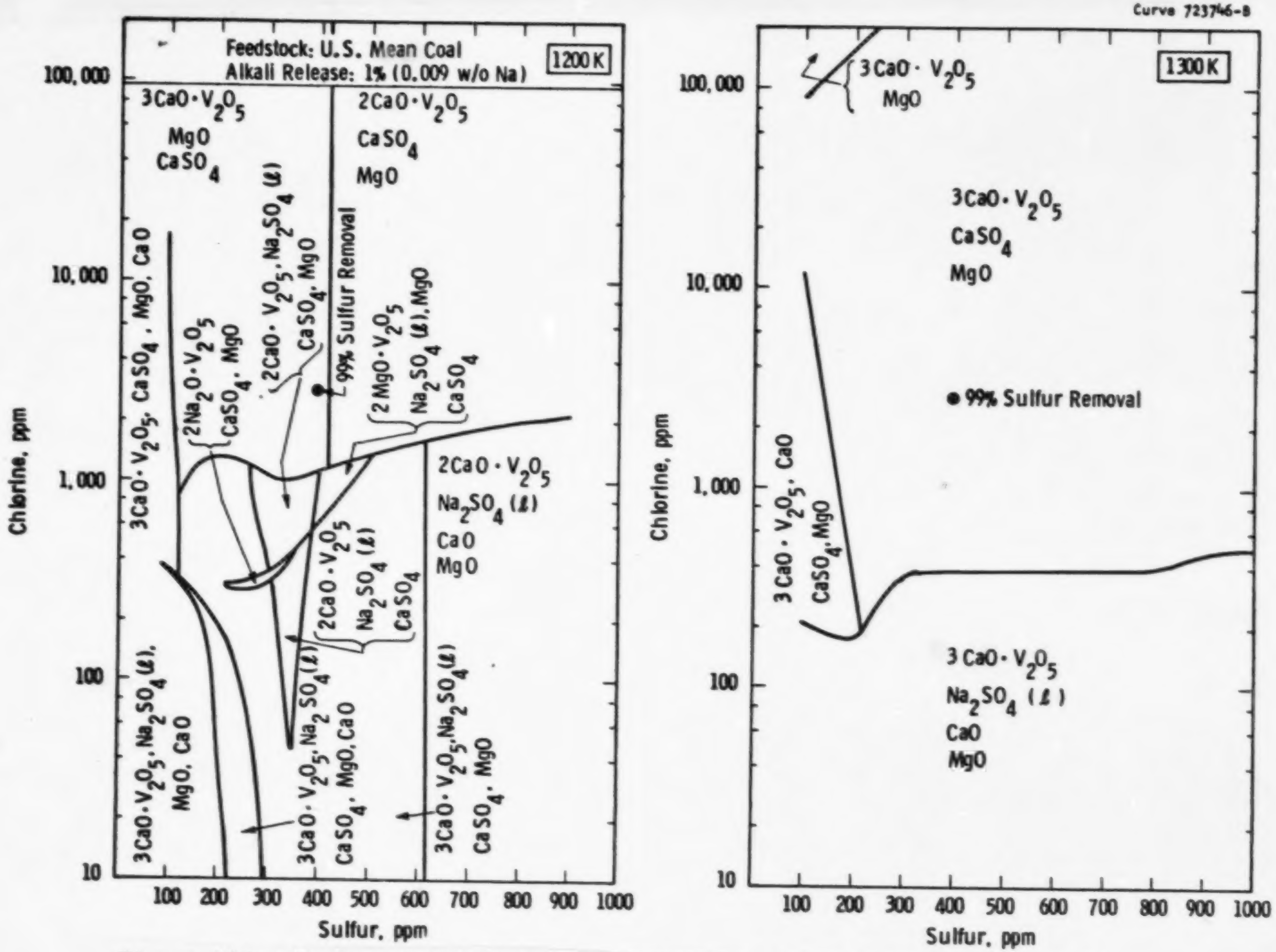

Figure 125 - Condensed Alkali and Vanadate Phases Formed as a Function of Temperature, Sulfur and Chlorine Content in 1013 kPa FBC Systems Operating with 100% Excess Air and 1% Sodium Release from Feedstock Material

T_m $2Na_2O{\cdot}V_2O_5$ = 908-926 K, T_m $3Na_2O{\cdot}V_2O_5$ = 1123 K),[87] and magnesium vanadates (T_m $2MgO{\cdot}V_2O_5$ = 1108 K, T_m $3MgO{\cdot}V_2O_5$ = 1464 K), while the projected calcium vanadate phases are expected to exist as stable solid species at combustor operating temperatures of 1300 K or below (T_m $2CaO{\cdot}V_2O_5$ = 1288 K, T_m $3CaO{\cdot}V_2O_5$ = not reported, but it is likely that the melt temperature is above 1300 K).

Exposure of high-temperature alloys to combustion gases containing SO_x, alkali metals, HCl, and various minor and trace constituents induce corrosive attack along the metal surface. Corrosion at temperatures above 1100 K is caused primarily by the condensation of volatile alkali sulfates as molten or mixed eutectics reacting with the oxidized alloy.[88] The interaction of this deposit with the oxide induces a localized reduction in the O_2 activity and increases the activity of S, which migrates through the protective oxide scale in an ionic exchange with O_2.

The acceleration of hot corrosion on the surfaces of alloys exposed to combustion gases containing Cl in addition to S has been demonstrated. Although the anion aids in the transport of volatile alkali metals, Cl in either the deposit or oxide/metal substrate has not been detected.

Current investigations[89-91] have shown that corrosion also occurs at temperatures below 1100 K. The transport and deposition of solid alkali sulfates, which react with the metal surfaces, aid in the formation of low-melting-temperature, solid-solution eutectics capable of inducing low-temperature corrosion reactions.

Parametric reactions of Na with Co, Ni, Cr, Al, and Fe assess the potential of alloy materials to withstand corrosive attack within the PFBC systems. The eutectic compositions Jones and Gadomski[89] reported (Table 83) are used in defining the effect that a variation in the S content has on the stability of the resulting condensed phases. The stability of the eutectic composition, or mixed sulfate solid solution, is then projected as a function of operating pressure. The product distribution reactions are projected for Ni- and Co-based alloys (Table 84)

TABLE 83 - MIXED SULFATE EUTECTIC COMPOSITIONS AND MELT TEMPERATURES

Eutectic Pair	Combustion mol-% 2nd Sulfate[89]	Eutectic Temperature[92]
Na_2SO_4-$CoSO_4$	47.83	848 K (575°C)
Na_2SO_4-$NiSO_4$	55	944 K (671°C)
Na_2SO_4-$Cr_2(SO_4)_3$	NR[a]	NR
Na_2SO_4-$Al_2(SO_4)_3$	17.6	913 K (640°C)
Na_2SO_4-$Fe(SO_4)_3$	18	893 K (620°C)

---

[a] NR = not reported

TABLE 84 - ALLOY COMPOSITION

Alloy	Al	B	C	Co	Cr	Fe	Mn	Mo	Ni	Ti	W
U-500	2	0.005	0.08	12	19	4	-	6	52.9	3	1
X-45	-	0.01	0.25	53.74	25.5	2	1	-	10.5	-	7

82
7728197

with combustion gases containing 100 percent Na released from a 0.05 wt % Na coal in combustion systems operating with 10, 100, and 300 percent excess air and 0, 90, and 99 percent S removal, at 700 to 1150 K and 405.2 kPa (4 atm). The concentration of Co is adjusted to promote the formation of the $Na_2SO_4 \cdot CoSO_4$ eutectic. Nickel, Cr, Al, and Fe are present as the nominal percentage in the alloys, proportioned to the total cobalt content in the system considered.

Combustion Gas Reactions with Cobalt- and Nickel-Based Alloys

Cobalt- and nickel-based alloys are generally used in the construction of low-stressed stationary vanes and high-stressed rotor blades of advanced turbine, combined-cycle power systems. Equilibrium reactions of Co or Ni with a combustion gas mixture containing S indicate that, at temperatures of 970 to 980 K, metal sulfates will form as stable solid phases at the metal/gas interface. Transition to the corresponding oxide results as the system temperature is increased. When the sulfated metal surface reacts with sodium sulfate (Na_2SO_4) deposited from the combustion gas stream, a solid solution between Na_2SO_4 and cobalt sulfate ($CoSO_4$) can result. The mixed sulfate has been identified as a low-temperature eutectic complex ($Na_2SO_4 \cdot CoSO_4$), which rapidly decomposes, leading to corrosion of the underlying alloy.

Although neither the current thermochemical data base nor the literature contains the heat of formation, entropy, or molecular constant data required to project the stability of the eutectic complex, we have assumed in the calculations that the coexisting sulfates representing the mixed solid solution phase are comparable with that of the eutectic structure. At temperature below 848 K, therefore, the resulting Na_2SO_4 and $CoSO_4$ exist as the solid eutectic complex; at elevated temperatures the sulfates favor the formation of the liquid eutectic melt. Similarly, $NiSO_4$ can exist in solid solution with $NaSO_4$, forming a stable $Na_2SO_4 \cdot NiSO_4$ eutectic at temperatures below 944 K, with melt formations resulting as temperatures increase.

The ratio of the concentration of Na to the concentration of Co or Ni at the reaction site defines the composition of the resulting products at temperature,* as shown in Figures 126 and 127. Sufficient S is present to form $NaSO_4$ if 100 percent of the Na content is released from the U.S. mean coal. In both systems a constant SO_3/SO_2 ratio for 96 percent S removal at 405.2 kPa is maintained over the condensed complexes. Where the mole ratio of Na to Co is 4:1 at temperatures below 900 K, both the alkali and the metal exist as sulfates. At the eutectic compositions ($Na_2SO_4 \cdot 47.83\%$ $CoSO_4$ and $Na_2SO_4 \cdot 55\%$ $NiSO_4$) the resulting solids contain Na and the metal sulfates, in addition to metal oxides. As the metal concentration exceeds the concentration of Na at the reaction site, the temperature at which the mixed sulfates and oxides are stable is lowered to approximately 850 K, prior to conversion into a pure Na-metal sulfate.

If we assume that Na_2SO_4 and $CoSO_4$ exist as solid eutectic solutions up to 848 K,[89] corrosion induced by the formation of $Na_2SO_4/CoSO_4$ in Co_3O_4 may occur in a 96 percent S-removal system on alloys at temperatures between 848 and 940 K. Figure 127 indicates that in a 96 percent S-removal system $Na_2SO_4/NiSO_4$ exists as a solid solution up to 900 K, where conversion into NiO occurs. This temperature of transition is 40 degrees lower than the eutectic melt temperature Jones reported. An increase in the activity of S in the combustion gas will shift the complex sulfate phase boundary to a higher temperature, thus defining a broader area that supports the eutectic formation.

The influence of the S activity in the combustion gas on the potential formation of the eutectic solids as a function of temperature at 405.2 kPa is illustrated in Figures 128 and 129. A reduction in the S content at low temperatures diminishes the stability of the sodium-metal sulfate (eutectic) and favors the mixed metal oxide-sulfate/sodium sulfate complex. Further reducing the S content in the system to levels

---

*Equilibrium calculations project phase conversion within a 10 degree temperature range.

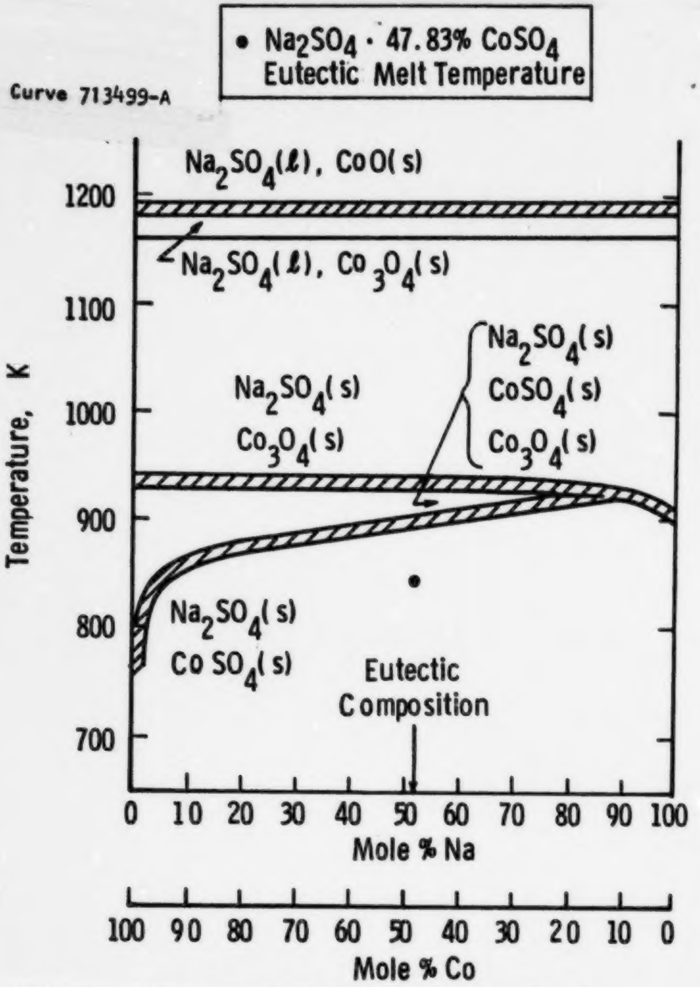

Figure 126 - Composition of Sodium-Cobalt Complexes Formed as a Function of Temperature for 96% Sulfur-Removal, 405.2 kPa Systems

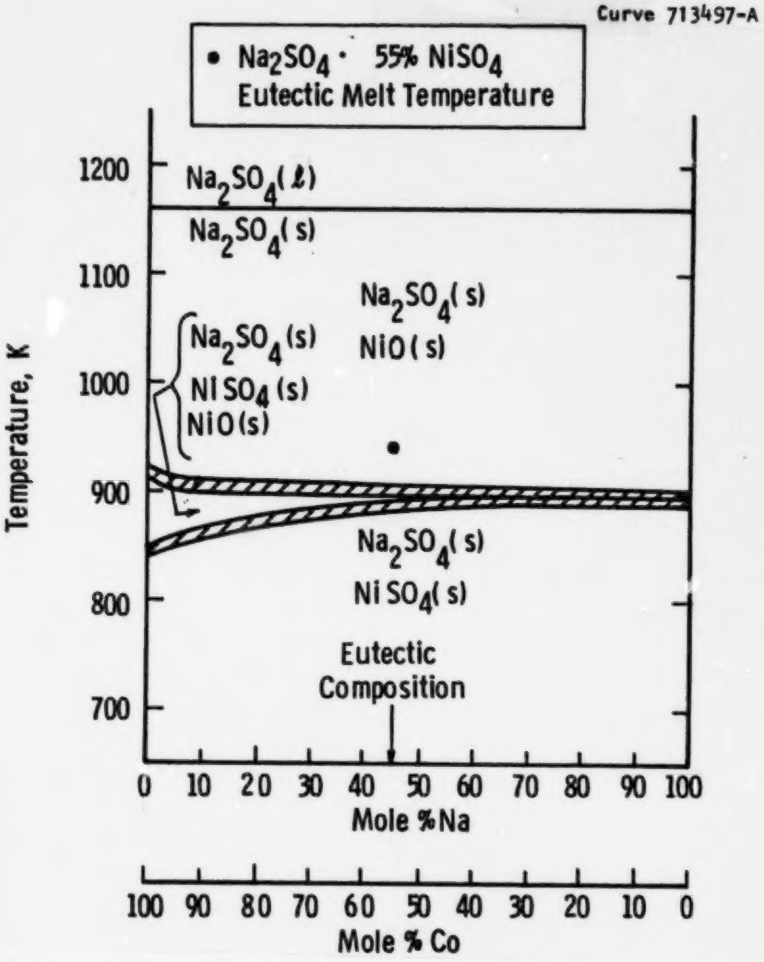

Figure 127 - Composition of Sodium-Nickel Complexes Formed as a Function of Temperature for 96% Sulfur-Removal, 405.2 kPa Systems

Curve 713492-A

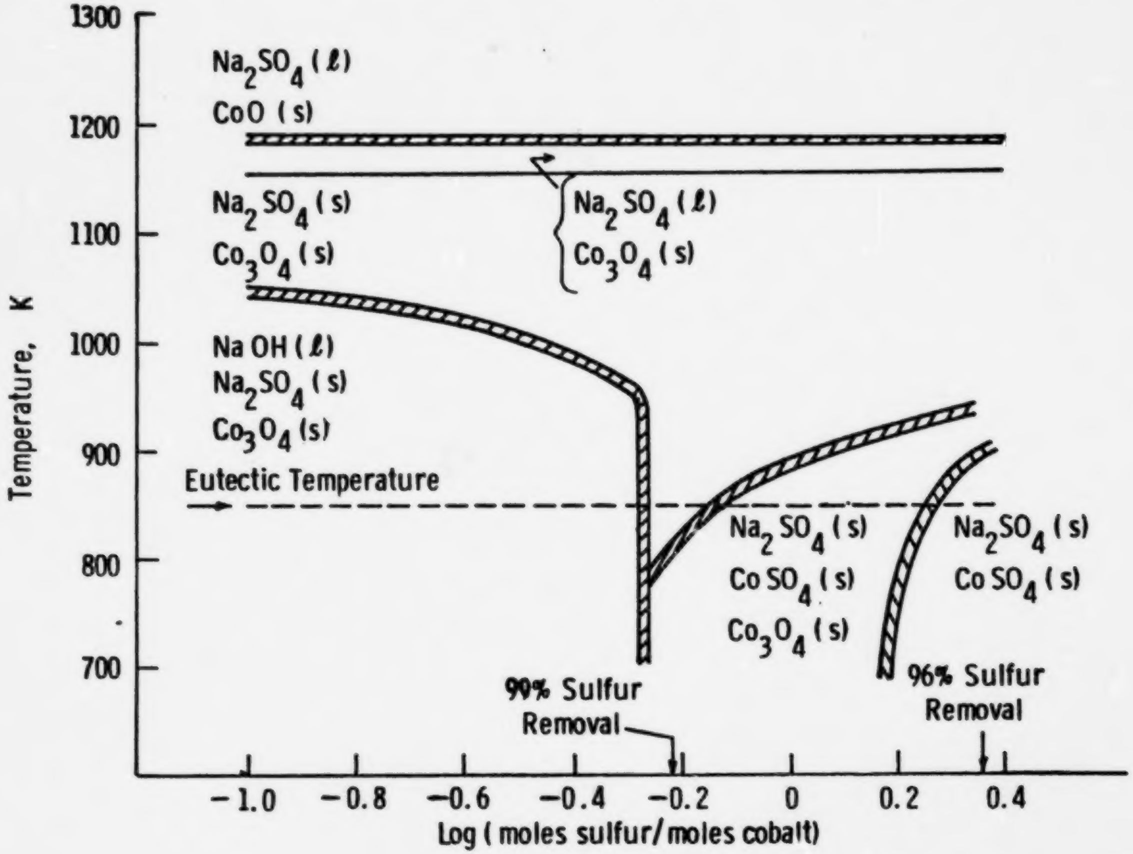

Figure 128 - Equilibrium Phase Diagram for $Na_2SO_4 \cdot 47.8\%\ CoSO_4$ Eutectic as a Function of Temperature and Sulfur Activity at 405.2 kPa

Curve 713491-A

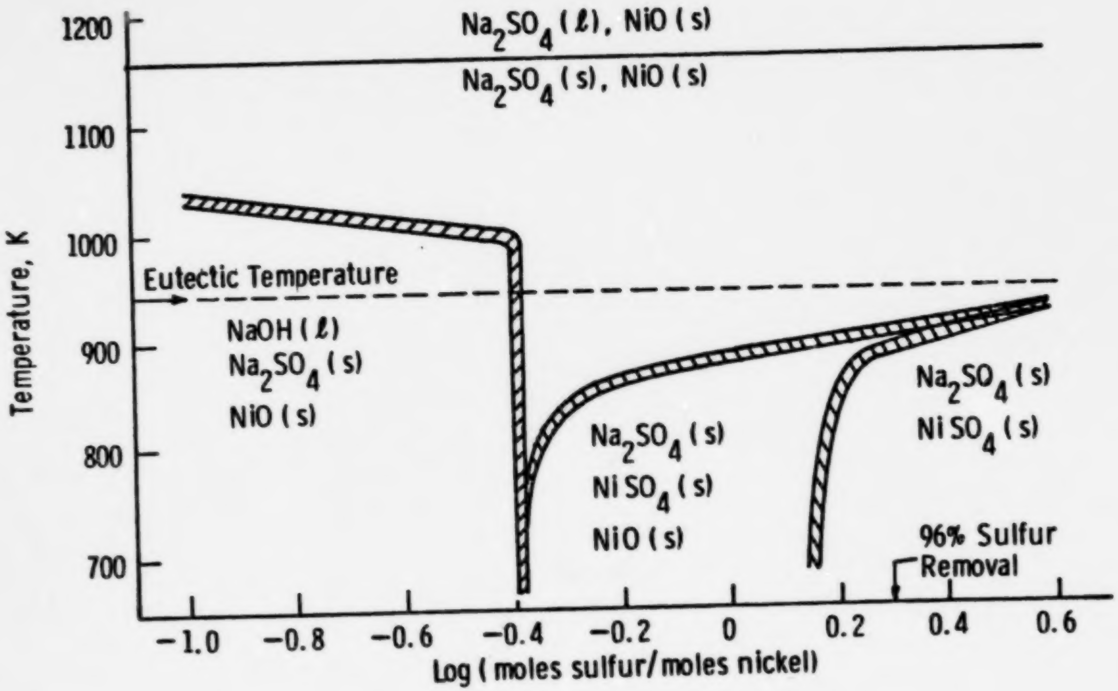

Figure 129 - Equilibrium Phase Diagram for Na_2SO_4·55% $NiSO_4$ Eutectic as a Function of Temperature and Sulfur Activity at 405.2 kPa

that do not promote the formation of the eutectic complex preferentially favors the sulfation reaction of Na. Unreacted Na in the gas phase is free to react with water vapor in the combustion gas, forming liquid sodium hydroxide (NaOH). Cobalt or nickel under these conditions exists as a stable oxide. Note that in Figure 129 the $Na_2SO_4 \cdot NiSO_4$ boundary is approaching the reported eutectic melt temperature. Systems that contain excessive S concentrations may displace the boundary above the 944 K melt line, inducing a condition that favors low-temperature corrosion.

The previous figures indicate that, as the system temperature exceeds 1000 K, Na_2SO_4 deposits on protective Co_3O_4 or NiO alloy surface. Deposition of the liquid Na_2SO_4 phase occurs at temperatures that exceed 1157 K, inducing corrosion at the liquidus/oxide interface.

The product distributions thus far have been limited to defining the Na-metal sulfate complexes that result at 405.2 kPa total pressure as a function of system temperature. The transition of the metal sulfate to the oxide phase, releasing sulfur oxides (SO_x), is a critical parameter in low-temperature corrosion. Gaseous sulfur oxides, if trapped within the eutectic complex, may diffuse to subsurface oxide layers, promoting internal sulfation or sulfidation.

Typical sulfate-oxide transition reactions include

$$CoSO_4(s) \longrightarrow CoO(s) + SO_2(g) + 1/2\ O_2(g) \qquad (143)$$

and

$$NiSO_4(s) \longrightarrow NiO(s) + SO_2(g) + 1/2\ O_2(g)\ . \qquad (144)$$

As the air: fuel ratio is increased in the FBC, an intermediate Co phase, tricobalt tetroxide (Co_3O_4), forms by the reaction

$$3CoSO_4(s) \longrightarrow Co_3O_4(s) + 3SO_2(g) + O_2(g)\ . \qquad (145)$$

The complex is reduced to cobalt oxide (CoO) as the temperature of the system increases. The exact temperature of transition between the sulfate-oxide phases is dependent on the total pressure of the system, in addition to the activities of O_2 and S in the combustion gas. Figures 130 and 131 illustrate the pressure dependency of the metal sulfates on the metal-Na eutectic in 96 percent S-removal systems. Both figures contain a region in which either $CoSO_4$ or $NiSO_4$ is stable in Na_2SO_4. The activity of S is sufficient for the Na-Co sulfate eutectic melt to form above 848 K. The eutectic melt stability temperature is increased as a function of increased systems pressure. The S content for 96 percent S-removal systems permits $NiSO_4$ to form in solid solution with Na_2SO_4 but does not approach the eutectic melt temperature of 944 K until the total pressure of the system exceeds 1013 kPa. Figures 130 and 131 indicate a zone in which S is partially released from the metal-sulfate phase, forming a mixed metal oxide-sulfate in solution with Na_2SO_4, which shifts in stability, depending on both operating temperature and pressure. The upper boundary in each diagram limits the formation of the mixed metal oxide-sulfate prior to complete conversion to the stable form of the metal oxides. As the operating temperature of the Na-Co system approaches 1200 K, Co_3O_4 is converted into CoO.

Combuston Gas Reactions with Chromium-, Aluminum-, and Iron-Containing Alloys

Cobalt- and nickel-based alloys used in the construction of turbine components typically contain additives of Cr and Al for enhanced resistance to hot corrosion. Although S is present in the combustion gases, the formation of solid chromium trisulphate ($Cr_2(SO_4)_3$) at low temperatures is not favored thermodynamically. The principal Cr solid phase that forms in the oxidizing environment is chromium oxide (Cr_2O_3). The stability of the Cr_2O_3 solid is dependent on the temperature and pressure of the system, localized Na and S activities in the combustion gas stream, and the presence of Co or Ni.

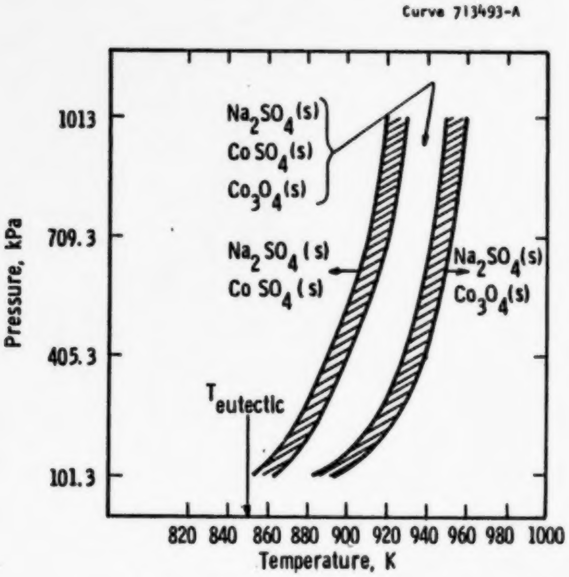

Figure 130 – Pressure Dependence on the Cobalt Sulfate-Oxide Transition in the $Na_2SO_4 \cdot CoSO_4$ Eutectic for 96% Sulfur-Removal Systems as a Function of Temperature

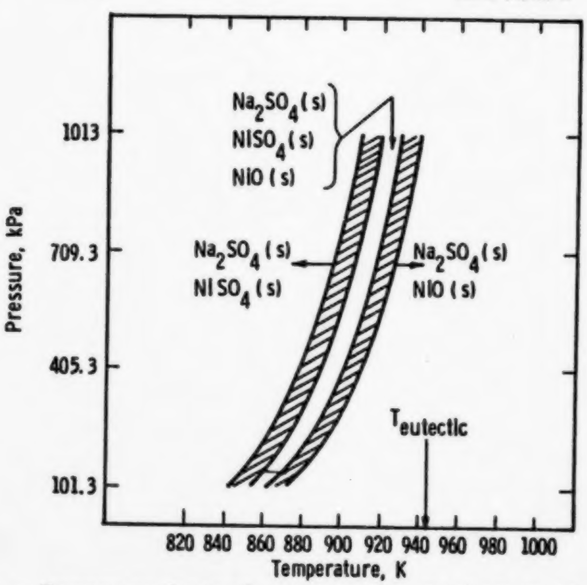

Figure 131 – Pressure Dependence on the Nickel Sulfate-Oxide Transition in the $Na_2SO_4 \cdot NiSO_4$ Eutectic for 96% Sulfur-Removal Systems as a Function of Temperature

Combustion systems that remove 96 percent of the initial S from the gas stream still contain sufficient S concentrations to promote the formation of Na_2SO_4. The interaction of Na_2SO_4 deposits with Cr_2O_3, forming low melting-temperature eutectic complexes, has not been reported in the literature. Chromium oxide volatilizes at elevated temperatures, releasing gaseous CrO_3, which in turn reduces the total volume of the Cr_2O_3 scale. Figure 132 illustrates generally the percent volatilization of solid Cr_2O_3 as a function of temperature and pressure for systems containing low concentrations of Cr. This system is comparable to alloys that form thin Cr_2O_3 surface oxide scales. Increasing the concentration of Cr in the system, typifying alloys that form thick oxide scales, lowers the percentage of volatilization.

If the concentration of S in the combustion gas were reduced to levels below that of the Na concentration, interaction of the alkali with Cr_2O_3 might result in the formation of alkali chromate complexes, as shown by the following reactions:

$$\left.\begin{array}{l} Na_2O(s) + SO_2(g) + 1/2\ O_2(g) \rightleftharpoons Na_2SO_4(s) \\ 2Cr(s) + 3/2\ O_2(g) \rightleftharpoons Cr_2O_3(s) \end{array}\right\} [S] > [Na] \qquad (146)$$

or

$$\left.\begin{array}{l} Na_2O(s) + Cr_2O_3(s) \rightleftharpoons Na_2Cr_2O_4(s) \\ 2Na_2O(s) + Cr_2O_3(s) + 3/2\ O_2(g) \rightleftharpoons 2Na_2CrO_4(s) \end{array}\right\} [S] < [Na] \qquad (147)$$

Additionally, Cr reacts with Co in oxidizing combustion gases, promoting the formation of the chromium cobalt spinel ($CoO{\cdot}Cr_2O_3$). In systems that contain Na in a mole ratio equal to the Na-to-Co concentration in the eutectic, and where the Co-to-Cr ratio is comparable to that

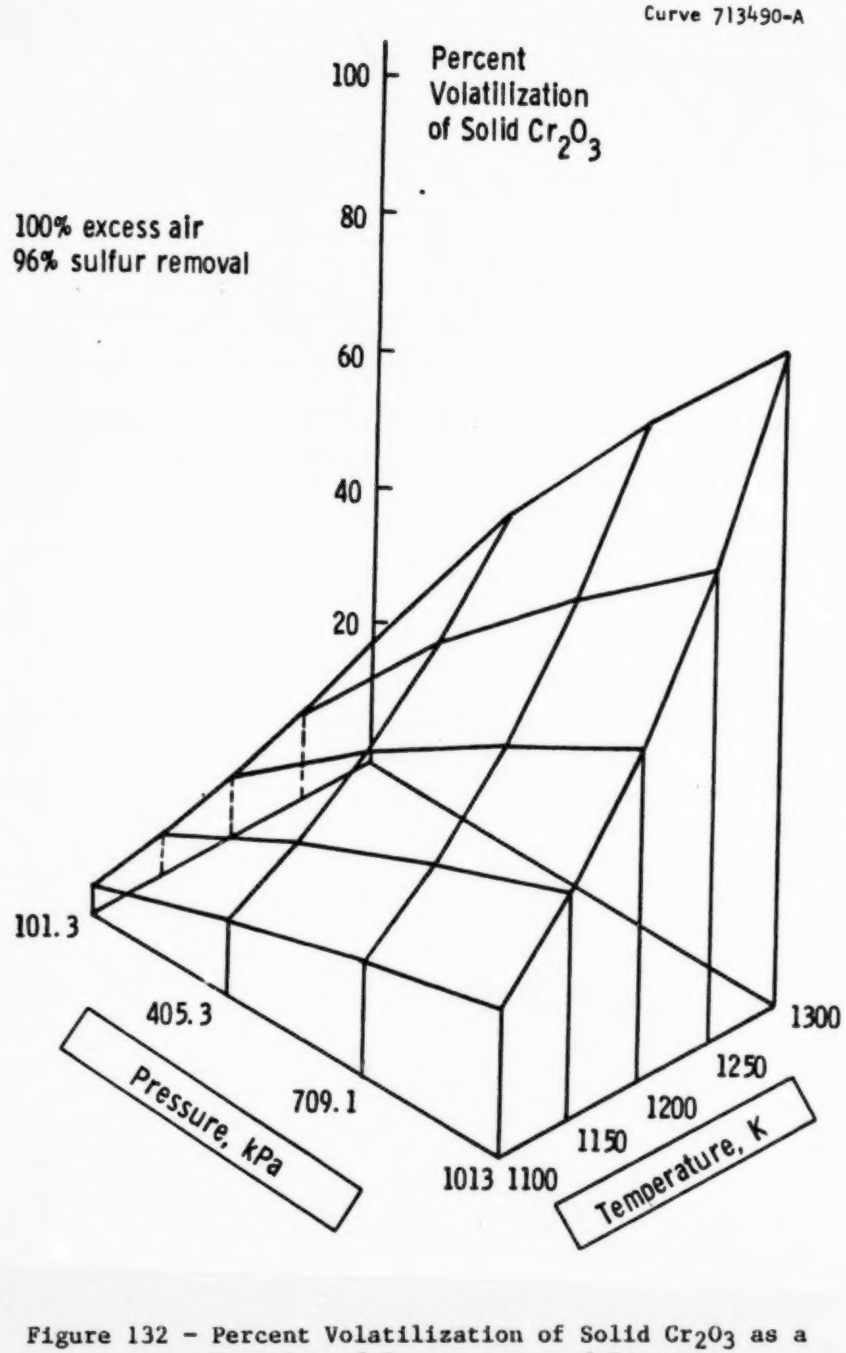

Figure 132 - Percent Volatilization of Solid Cr_2O_3 as a Function of Temperature and Pressure

of the alloy X-45, at 405.2 kPa in a 96 percent S-removal system the following phases are projected to be stable:

300 K	700-800 K	900-1000 K	1100-1200 K
Na_2SO_4 $CoSO_4$ Cr_2O_3	Na_2SO_4 $CoSO_4$ $CoO \cdot Cr_2O_3$	Na_2SO_4 Co_3O_4 $CoO \cdot Cr_2O_3$	Na_2SO_4 CoO $CoO \cdot Cr_2O_3$

The temperature zone between 700 and 1000 K is a region in which SO_2 and O_2 are released from $CoSO_4$, forming CoO, which simultaneously reacts with Cr_2O_3 to form the $CoO \cdot Cr_2O_3$ spinel. The resulting equilibrium products for the reaction of Co and Cr with Na in a 96 percent S-removal system as a function of pressure is shown in Figure 133. At low pressures the spinel $CoO \cdot Cr_2O_3$ is the candidate Cr phase at temperatures of 770 K. An increase in pressure shifts the stability of the mixed oxide/sulfate phase to higher temperatures. Alloys that contain Cr at levels promoting the formation of the $CoO \cdot Cr_2O_3$ spinel as the outer oxide scale may aid in limiting the potential for corrosion by the low-temperature eutectic melts, since the availability of Co for reaction with the alkali is reduced. Similar reactions are projected for the formation of the nickel chromate spinel ($NiO \cdot Cr_2O_3$) under similar operating conditions.

The reaction of Al with combustion gases containing S promotes the formation of aluminum trisulfate ($Al_2(SO_4)_3$) at low operating temperatures. Conversion of the trisulfate phase into aluminum oxide (Al_2O_3) is a function of the system temperature and total pressure, as shown in Figure 134. At temperatures below 740 K, the presence of Na in the 96 percent S-removal combustion gas forms the eutectic solid phase, $Na_2SO_4 \cdot 17.6\% \ Al_2(SO_4)_3$. At temperatures approaching the eutectic melt of 913 K, Na_2SO_4 is shown as a stable solid with Al_2O_3. Only extreme increases in the S activity in the gas phase would promote the formation of the stable sulfate eutectic (Figure 135). This suggests that in combustion gas systems, even at 90 percent S removal, alloys forming external Al_2O_3 scales withstand low-temperature corrosive attack because of the suppressed formation of $Al_2(SO_4)_3$.

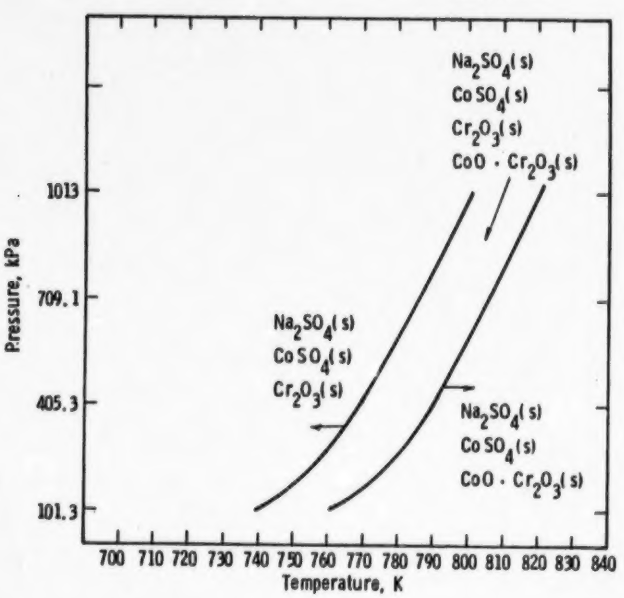

Figure 133 - Pressure Dependence on the Stability of $CoO{\cdot}Cr_2O_3$ Spinel in Na_2SO_4 for 96% Sulfur-Removal Systems as a Function of Temperature

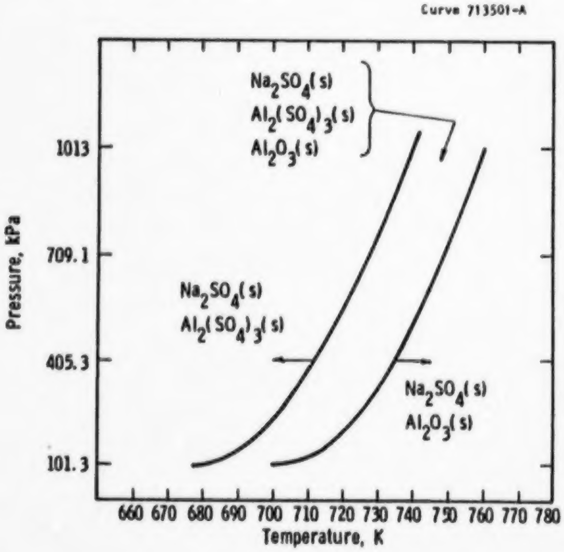

Figure 134 - Pressure Dependence on the Aluminum Sulfate-Oxide Transition in the $Na_2SO_4{\cdot}Al_2(SO_4)_3$ Eutectic for 96% Sulfur-Removal Systems as a Function of Temperature

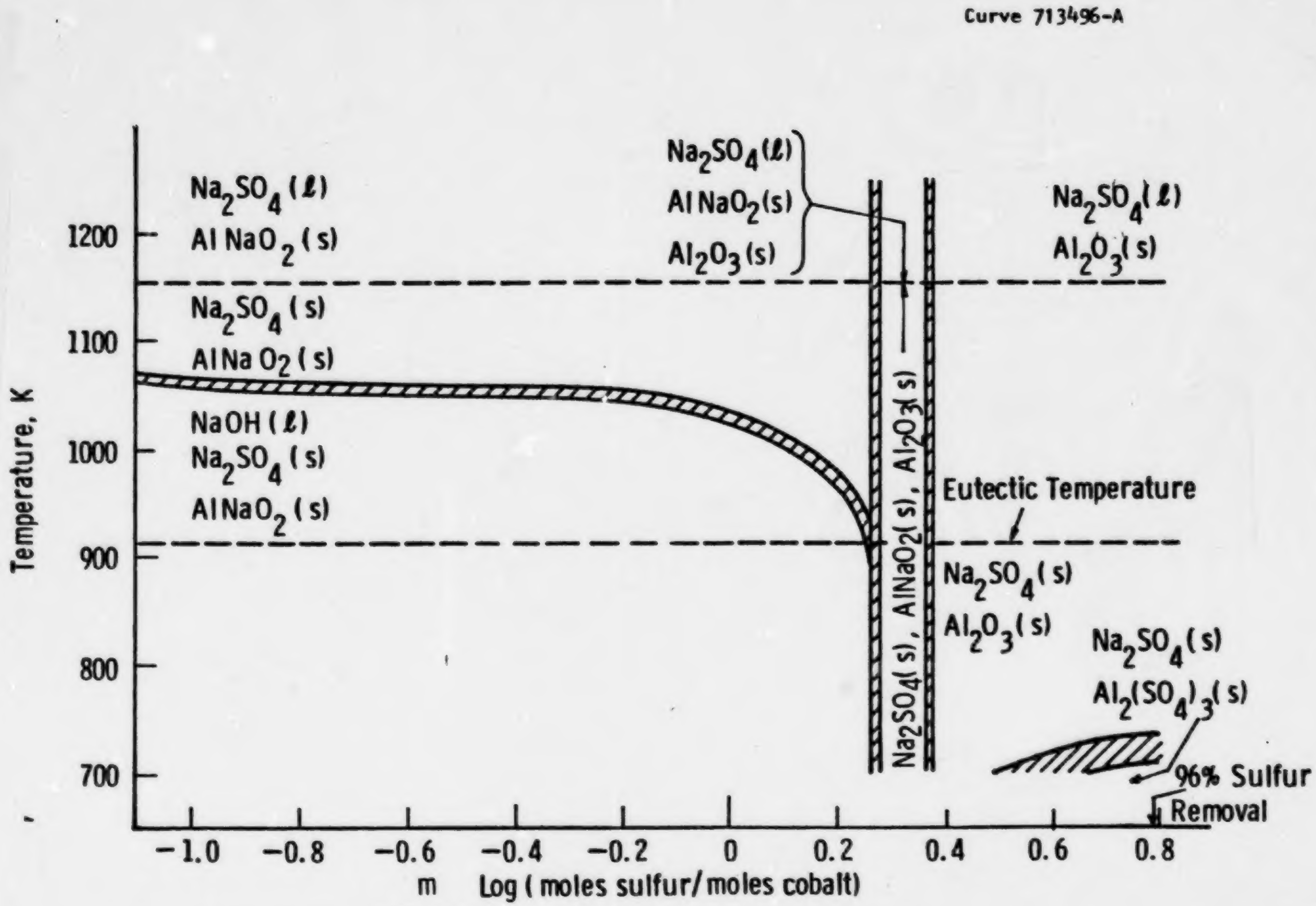

Figure 135 - Equilibrium Phase Diagram for $Na_2SO_4 \cdot 17.6\%\ Al_2(SO_4)_3$ Eutectic as a Function of Temperature and Sulfur Activity at 405.2 kPa

As the S content in the combustion gas is reduced in systems operating at temperatures of 700 K, Na_2SO_4, which exists in solid solution with $Al_2(SO_4)_3$, releases SO_2 and O_2, forming solid Na_2SO_4/Al_2O_3. Continued S reduction promotes the formation of Al_2O_3 and $AlNaO_2$ in Na_2SO_4 until complete conversion of Al into the alkali aluminate phase has occurred. The excess Na that does not complex with Al reacts with the water vapor in the combustion gas to form liquid NaOH. At temperatures of 1100 K, Na_2SO_4 can deposit on the metal substrates of either Al_2O_3, Al_2O_3 and $AlNaO_2$, or $AlNaO_2$.

At low operating temperatures the iron added to superalloys or ferritic and austenitic stainless steels used in the fabrication of blade and vane structures, forming solid iron trisulfate ($Fe_2(SO_4)_3$) when exposed to combustion gases containing S. The transition from the sulfate into the oxide releasing SO_2 and O_2 is a function of the system temperature and total pressure, as shown in Figure 136. The concentration of S that remains in the gas after 96 percent removal is sufficient to promote the formation of the solid eutectic at temperatures below that of the reported eutectic melt of 893 K.

As the S concentration in the combustion gas is reduced, the solid sulfate solution is converted into a sodium sulfate-iron oxide complex (Figure 137). As the concentration of Na exceeds that of S, Na reacts with Fe_2O_3 to form $Na_2O \cdot Fe_2O_3$ in solution with Na_2SO_4. At low temperatures in the reduced S atmospheres, Na reacts with water vapor in the combustion gas forming liquid NaOH, while at the elevated temperatures that decrease the stability of Na_2SO_4, Fe_2O_3 is formed because of the deficiency in the amount of Na required to form the double oxide structure.

Influence of Combustion Environments on Alloy-Deposit Reactions

The above discussion has presented the individual reactions of each metal in a 100 percent excess air combustion gas containing variable S activities as a function of system temperature and pressure. The alloy composition and, additionally, the interaction between the elemental

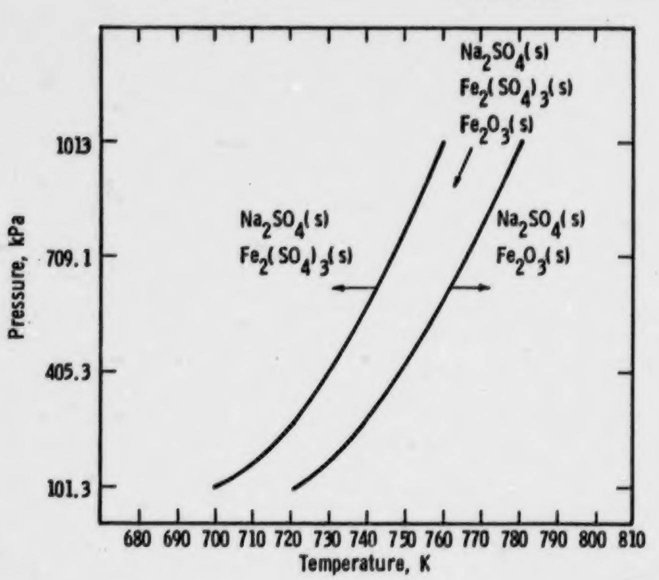

Figure 136 - Pressure Dependence on the Iron Sulfate-Oxide Transition in the $Na_2SO_4 \cdot Fe_2(SO_4)_3$ Eutectic for 96% Sulfur-Removal Systems as a Function of Temperature

constituents will further increase the number of complex reactions that simultaneously occur. This section will emphasize the reactions of Co, Ni, Cr, Al, and Fe at concentrations relative to the nominal composition of U-500 and X-45 with gases resulting from combustion in 0, 10, and 300 percent excess air, and for 0, 90, and 99 percent S-removal systems. Variations in the nature of the solids that form are a result of the total S content of the system. At a constant S activity the products formed at combustion in 10 percent excess air are identical with those formed with combustion in 300 percent excess air. Sulfur removal decreases the stability of $CoSO_4$ and $NiSO_4$ and promotes the formation of Co_3O_4, NiO, $CoO \cdot Cr_2O_3$, and $CoO \cdot Fe_2O_3$, in addition to the alkali chromates and aluminates.

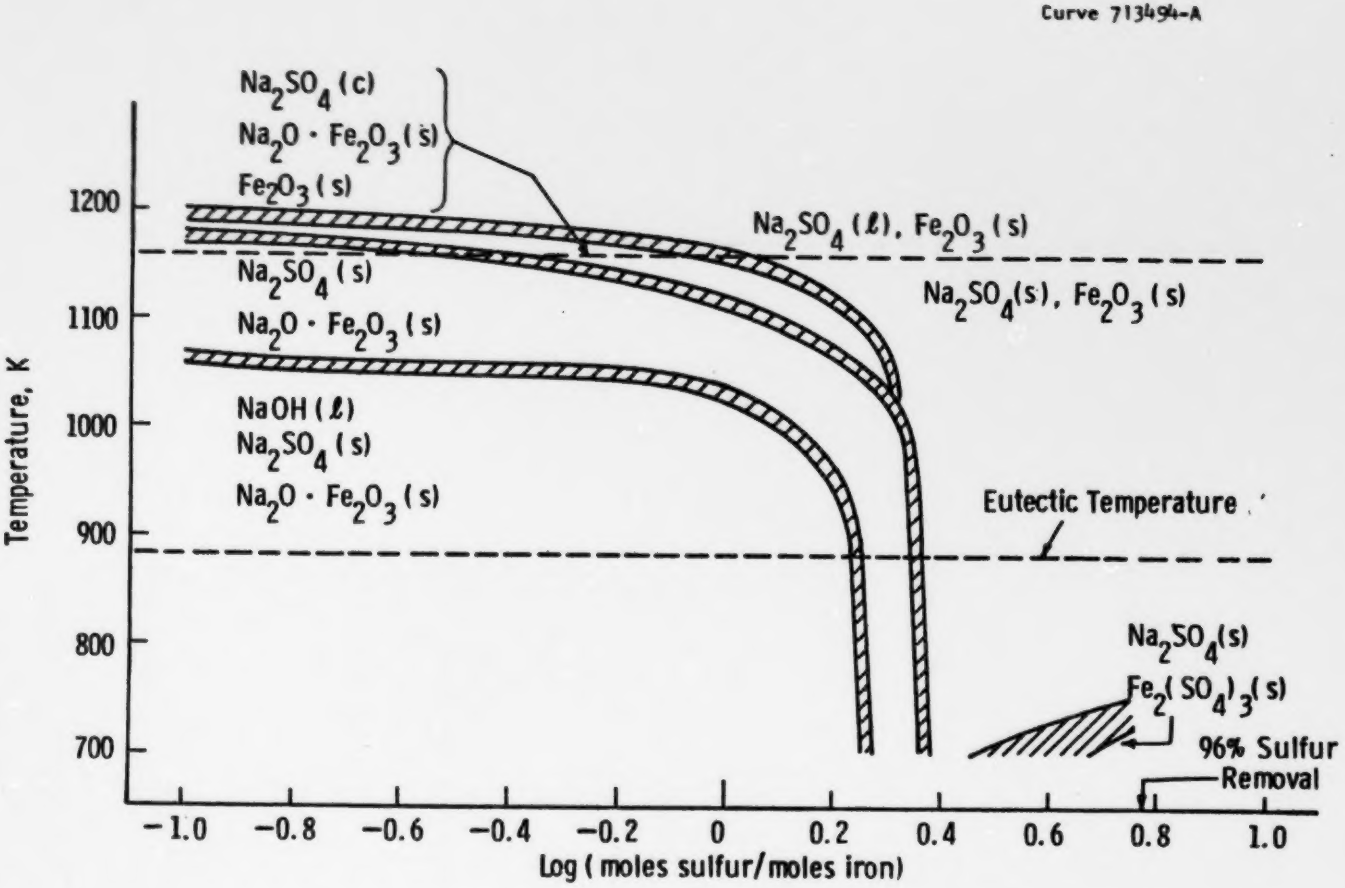

Figure 137 - Equilibrium Phase Diagram for $Na_2SO_4 \cdot 18\% \ Fe_2(SO_4)_3$ Eutectic as a Function of Temperature and Sulfur Activity at 405.2 kPa

A review of the literature indicates that scale structures for alloys containing 15 to 25 percent Cr consists of a thin layer of Cr_2O_3 initially formed on the alloy. Diffusion of Co or Ni through the Cr_2O_3 layer forms an external cobalt oxide (CoO) or nickel oxide (NiO) layer in which small quantities of Cr are dispersed. The original inner oxide layer contains $CoO \cdot Cr_2O_3$ or $NiO \cdot Cr_2O_3$ particles in a CoO or NiO matrix saturated with Cr, while an additional internal oxide zone of Cr_2O_3 particles forms at the oxide metal interface and along grain boundaries. The exact chemical structure of the scale, therefore, is dependent not only on the reactions at the alloy surface but also on the time of exposure, on the nature of the gas phases, and on possible diffusion through the scale. The thermodynamic stability of the metal phases that react with several oxidants is usually plotted on a log-log plot for two principal gaseous components, as shown in the Ellingham diagrams of Figures 138-139. The plots generally assume an internal equilibrium of the gas phase with respect to all gaseous species. The mutual phase stabilities for an alloy can be shown easily by superimposing the individual phase diagrams, neglecting the phase shifts from variation in the metal activities when metal-metal interactions occur. Although these plots do not account for the interaction of the metals, the stabilities of the oxides, sulfates, and sulfides are clearly demonstrated as a function of temperature. Chromium oxide at 894 and 1366 K is shown to be the most stable phase in combustion gases except where conditions promote a relatively high P_H/P_{H_2S} and low P_{H_2O}/P_H. Although Figures 138 and 139 illustrate the stability of Co/Ni/Cr/Al in O-S, we have assumed that complete combustion has occurred. If C were to be deposited under any test condition, additional Ellingham diagrams illustrating the metal-C reactions should be reviewed.

Using the equilibrium projections, we can illustrate the variation in the scale composition for a Co-based alloy as a function of the oxygen and sulfur activities in a combustion gas containing Na (Figure 140). At the gas/scale interface, deposits of Na_2SO_4 (ℓ) are formed at 1300 K, while the alkali sulfate eutectic melts result at 950 K. The

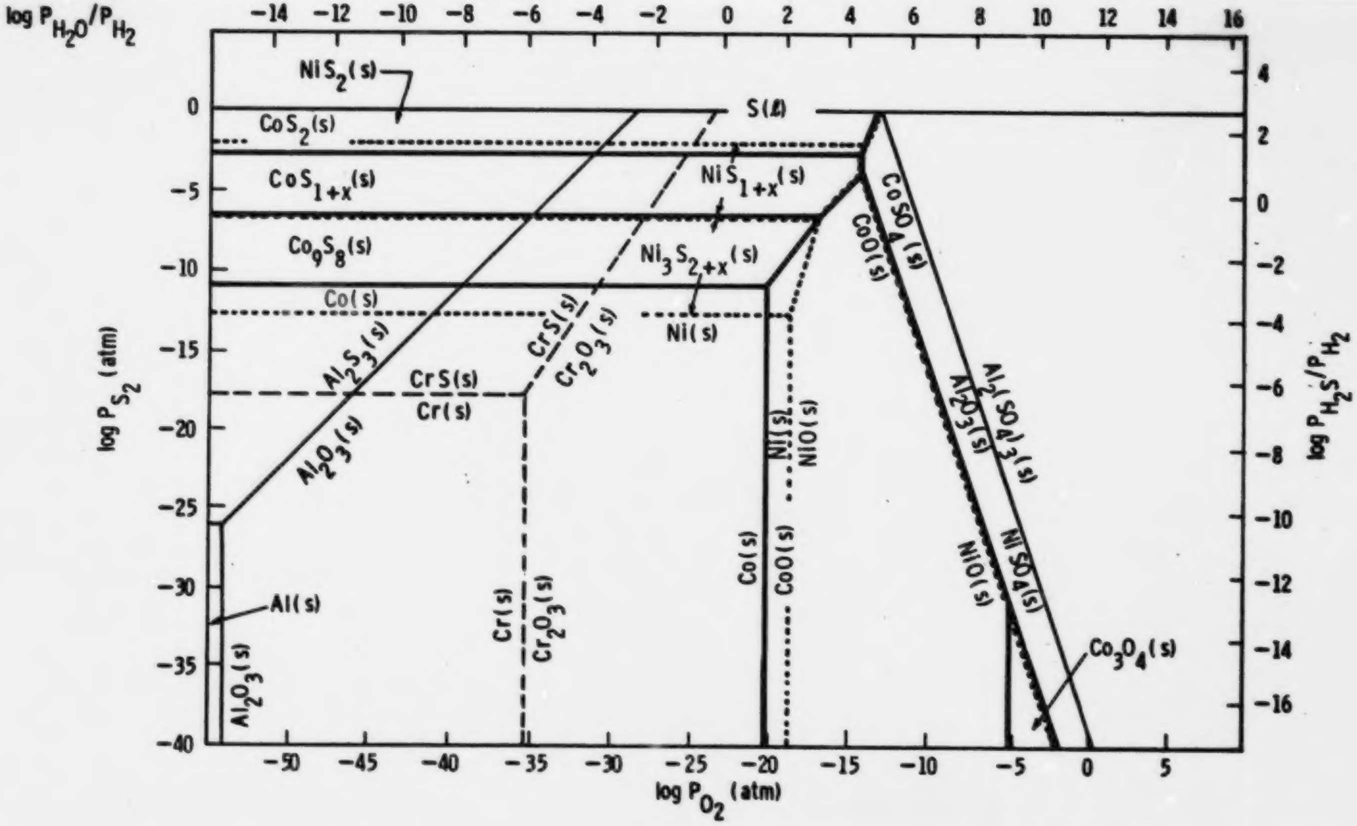

Figure 138 - Co/Ni/Cr/Al-O-S Phase Stability Diagram at 894 K[93]

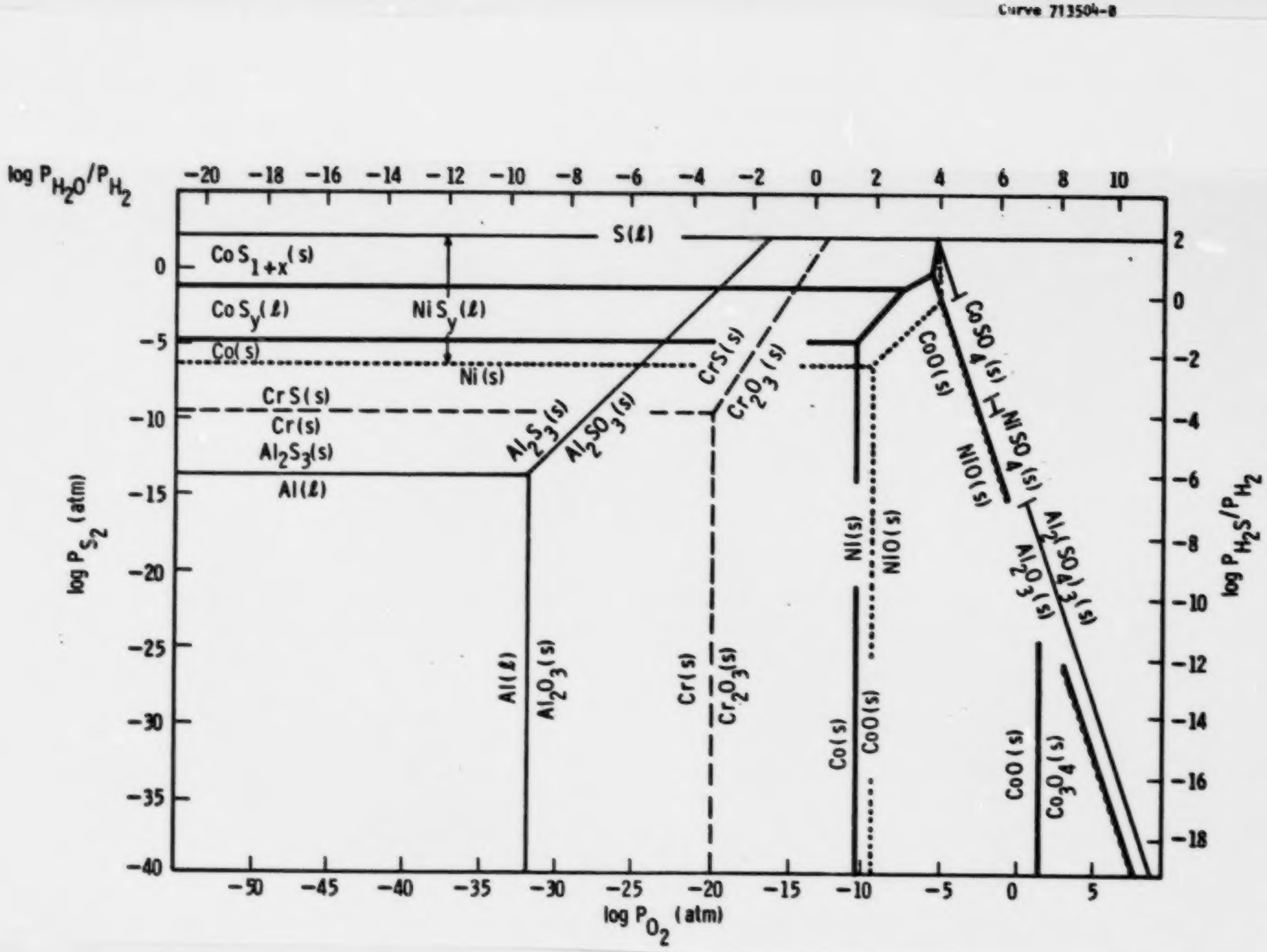

Figure 139 - Co/Ni/Cr/Al-O-S Phase Stability Diagram at 1366 K[93]

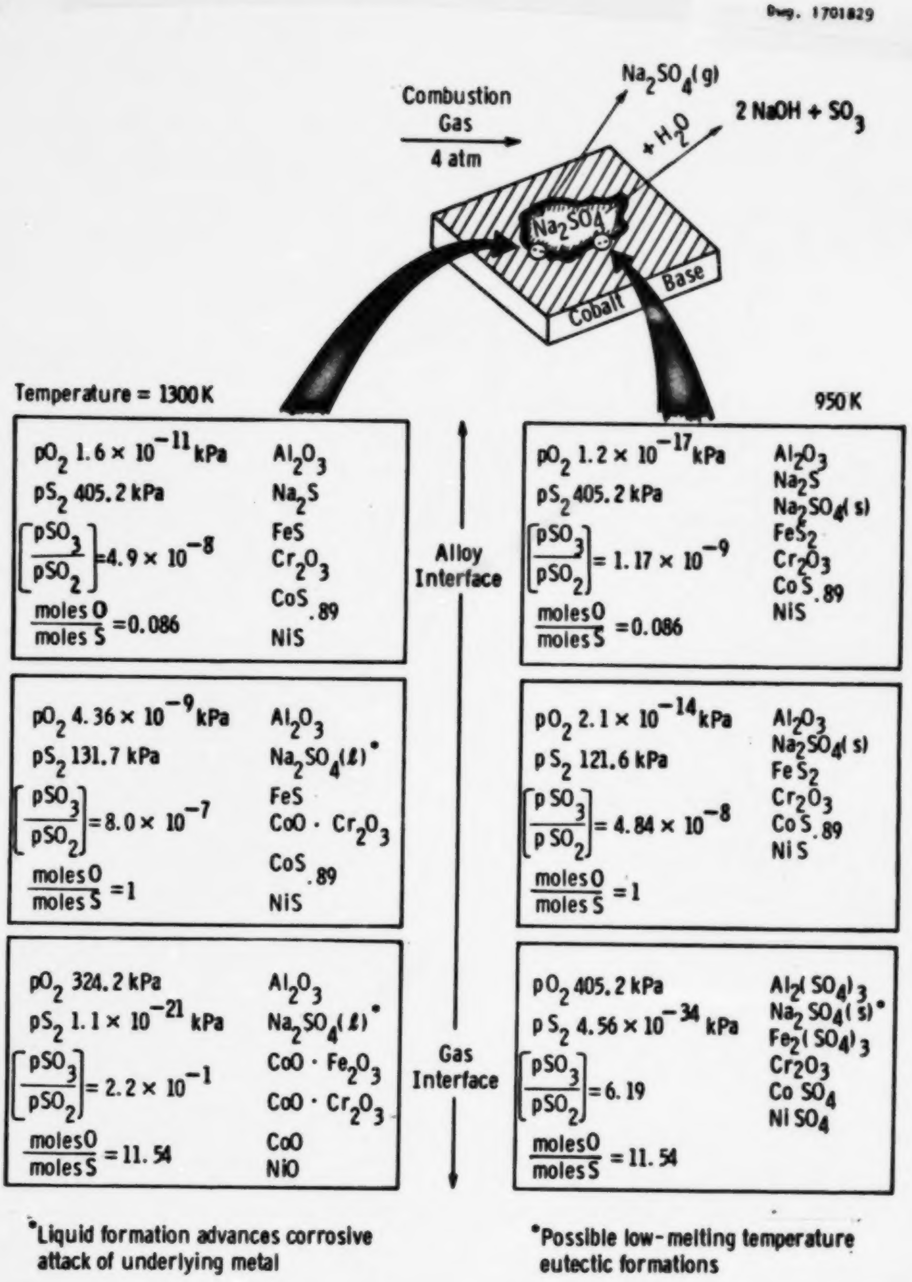
Dwg. 1701B29
Combustion Gas 4 atm
$Na_2SO_4(g)$
$+H_2O$
2 NaOH + SO_3
Na_2SO_4
Cobalt Base
Temperature = 1300 K
950 K
pO_2 1.6 × 10^{-11} kPa
pS_2 405.2 kPa
$\left[\frac{pSO_3}{pSO_2}\right]$ = 4.9 × 10^{-8}
$\frac{\text{moles O}}{\text{moles S}}$ = 0.086
Al_2O_3
Na_2S
FeS
Cr_2O_3
$CoS_{.89}$
NiS
pO_2 4.36 × 10^{-9} kPa
pS_2 131.7 kPa
$\left[\frac{pSO_3}{pSO_2}\right]$ = 8.0 × 10^{-7}
$\frac{\text{moles O}}{\text{moles S}}$ = 1
Al_2O_3
$Na_2SO_4(\ell)$*
FeS
CoO · Cr_2O_3
$CoS_{.89}$
NiS
pO_2 324.2 kPa
pS_2 1.1 × 10^{-21} kPa
$\left[\frac{pSO_3}{pSO_2}\right]$ = 2.2 × 10^{-1}
$\frac{\text{moles O}}{\text{moles S}}$ = 11.54
Al_2O_3
$Na_2SO_4(\ell)$*
CoO · Fe_2O_3
CoO · Cr_2O_3
CoO
NiO
Alloy Interface
Gas Interface
pO_2 1.2 × 10^{-17} kPa
pS_2 405.2 kPa
$\left[\frac{pSO_3}{pSO_2}\right]$ = 1.17 × 10^{-9}
$\frac{\text{moles O}}{\text{moles S}}$ = 0.086
Al_2O_3
Na_2S
$Na_2SO_4(s)$
FeS_2
Cr_2O_3
$CoS_{.89}$
NiS
pO_2 2.1 × 10^{-14} kPa
pS_2 121.6 kPa
$\left[\frac{pSO_3}{pSO_2}\right]$ = 4.84 × 10^{-8}
$\frac{\text{moles O}}{\text{moles S}}$ = 1
Al_2O_3
$Na_2SO_4(s)$
FeS_2
Cr_2O_3
$CoS_{.89}$
NiS
pO_2 405.2 kPa
pS_2 4.56 × 10^{-34} kPa
$\left[\frac{pSO_3}{pSO_2}\right]$ = 6.19
$\frac{\text{moles O}}{\text{moles S}}$ = 11.54
$Al_2(SO_4)_3$
$Na_2SO_4(s)$*
$Fe_2(SO_4)_3$
Cr_2O_3
$CoSO_4$
$NiSO_4$
*Liquid formation advances corrosive attack of underlying metal
*Possible low-melting temperature eutectic formations

Figure 140 - Direct Interaction between Gaseous Alkali, Sulfur, and Oxygen with a Cobalt-Based Alloy Demonstrating the Resulting Equilibrium Phases at Temperatures of 1300 K and 950 K as a Function of Variable Oxygen Partial Pressures

alkali sulfate or eutectic melts locally reduce the concentration of O_2 at the deposit/oxide interface. A migration of S through the scale is enhanced by an exchange of S from the deposit with oxygen from the surface oxides. In order to summarize the effect of alkali sulfate deposition or eutectic interactions, the following reactions should be considered:

High-Temperature Alkali Sulfate Deposition Reactions

$$Na_2SO_4(s) + CoO(s) \longrightarrow Na_2O(s) + CoS^*(s) + 2O_2(g) \qquad (148)$$

$$Na_2SO_4(s) + NiO(s) \longrightarrow Na_2O(s) + NiS^*(s) + 2O_2(g) \qquad (149)$$

$$2Na_2SO_4(s) + Fe_2O_3(s) \longrightarrow 2Na_2O(s) + 2FeS^*(s) + 9/2\ O_2(g) \qquad (150)$$

Low-Temperature Eutectic Reactions

$$Na_2SO_4 \cdot CoSO_4(s) + CoSO_4(s) \longrightarrow Na_2O \cdot CoO^{**}(s) + CoS(s) + 3SO_2(g) + 2O_2(g) \qquad (151)$$

$$Na_2SO_4 \cdot CoSO_4(s) + NiSO_4(s) \longrightarrow Na_2O \cdot CoO^{**}(s) + NiS(s) + 3SO_2(g) + 2O_2(g) \qquad (152)$$

$$Na_2SO_4 \cdot CoSO_4(s) + Fe_2(SO_4)_3(s) \longrightarrow Na_2O \cdot CoO^{**}(s) + 2FeS(s) + 3SO_2(g) + 6O_2(g) \qquad (153)$$

Comparable reactions can also be written for the $Na_2SO_4 \cdot NiSO_4$ and $Na_2SO_4 \cdot Fe_2(SO_4)_3$ eutectics.

In the simple Na_2SO_4 system S is exchanged with O_2 in the underlying oxide, forming Na_2O and a sulfided metal. The eutectic system has the capability of driving S into the sulfated sublayers where sulfidation occurs, thus enhancing the activity of S within the sublayer and simultaneously decreasing the oxygen activity.

---

*Complex sulfides as M_xS_y where M = Co, Ni, Fe.

**Solid solution of mixed oxides.

At 1300 K the spinel structure $CoO \cdot Cr_2O_3$ is stable when the concentration of O_2 equals or exceeds that of the S content; when the O_2 content is reduced sufficiently below that of the S, however, cobalt sulfides are formed in solution with Cr_2O_3, a condition that may permit attack when the sulfides are trapped in localized reducing sites on the alloy. Also, at conditions where the concentration of O_2 is equal to that of the S, Na_2SO_4 exists as the stable alkali phase. Conversion into the alkali sulfide occurs when O_2 is depleted within the scale, instead of a reaction promoting the formation of alkali-Cr or Al complexes.

Prevention of the initial alkali and S reaction would minimize deposition of the condensed Na_2SO_4 deposits at high temperatures and would reduce the potential formation of the low-temperature eutectic complexes. In order to limit the initial reaction, the following alternatives have been proposed:[23]

- Use of sulfur-free fuel
- Pretreatment of the feedstock material prior to combustion so as to reduce the initial alkali content
- Addition of aluminosilicate getters and chlorine to the feedstock.

Limiting the concentration of releasable S and alkali into the gas stream obviously reduces the quantity of alkali sulfates that form as either gaseous or condensed phases. The effect of adding aluminosilicate getters to the feedstock suppresses approximately 86 percent of the Na emitted into the gas stream at temperatures of 1200 K and pressures of 1013 kPa, limiting the concentration of Na for further reaction with S.

In the combustion of coal, Cl is released into the gas stream as volatile HCl. Under these conditions sodium sulfate may react with the HCl, forming gaseous NaCl, or may remain as a gaseous hydroxide or sulfate, as shown in the following reactions:

$$Na_2SO_4(c) + 2HCl(g) \longrightarrow 2NaCl(g) + SO_2(g) + 1/2\ O_2(g) + H_2O(g) \qquad (154)$$

$$Na_2SO_4(c) + 2H_2O(g) \longrightarrow 2NaOH(g) + SO_2(g) + 1/2\ O_2(g) + H_2O(g) \qquad (155)$$

$$Na_2SO_4(c) \longrightarrow Na_2SO_4(g)\ . \qquad (156)$$

The stability of the Na_2SO_4 complex, therefore, is governed by the concentration of Na, S, Cl, and water vapor in the combustion gas stream, as well as by the total pressure and temperature of the system. The effect of these parameters on the sulfate stability is illustrated in Figure 141 for combustion of a U.S. mean coal. To the left of each line of constant chloride concentration, NaCl is projected to exist as a solid when the operating temperature is lower than 1157 K and as a liquid at temperatures higher than 1157 K. Complete volatilization of the alkali sulfate is projected to the right of the concentration line. Increasing the Cl content effectively reduces the stability of $NaSO_4$ between 101.3 and 1215.6 kPa. If approximately 100 ppm Cl is released during the combustion of the feedstock material, the Na_2SO_4 stability line is displaced to below 1157 K for all operating pressures, minimizing the potential for the formation of corrosive liquid deposits.

Chlorine added to the combustion gas to quench the alkali sulfate formation may, in turn, react with the protective oxide scales of the alloys. At equilibrium the reactions of Cl at concentrations typical for release from a U.S. mean coal in a 90 percent S-removal system with an alloy, such as X-45, project the formation of Na_2SO_4, $CoSO_4$, NiO, $CoO \cdot Cr_2O_3$, and $CoO \cdot Fe_2O_3$ at 950 K. Cobalt sulfate in this system is converted into Co_3O_4 at temperatures of 960 to 970 K. Increasing the Cl concentration by a factor of 100 enhances the formation of volatile

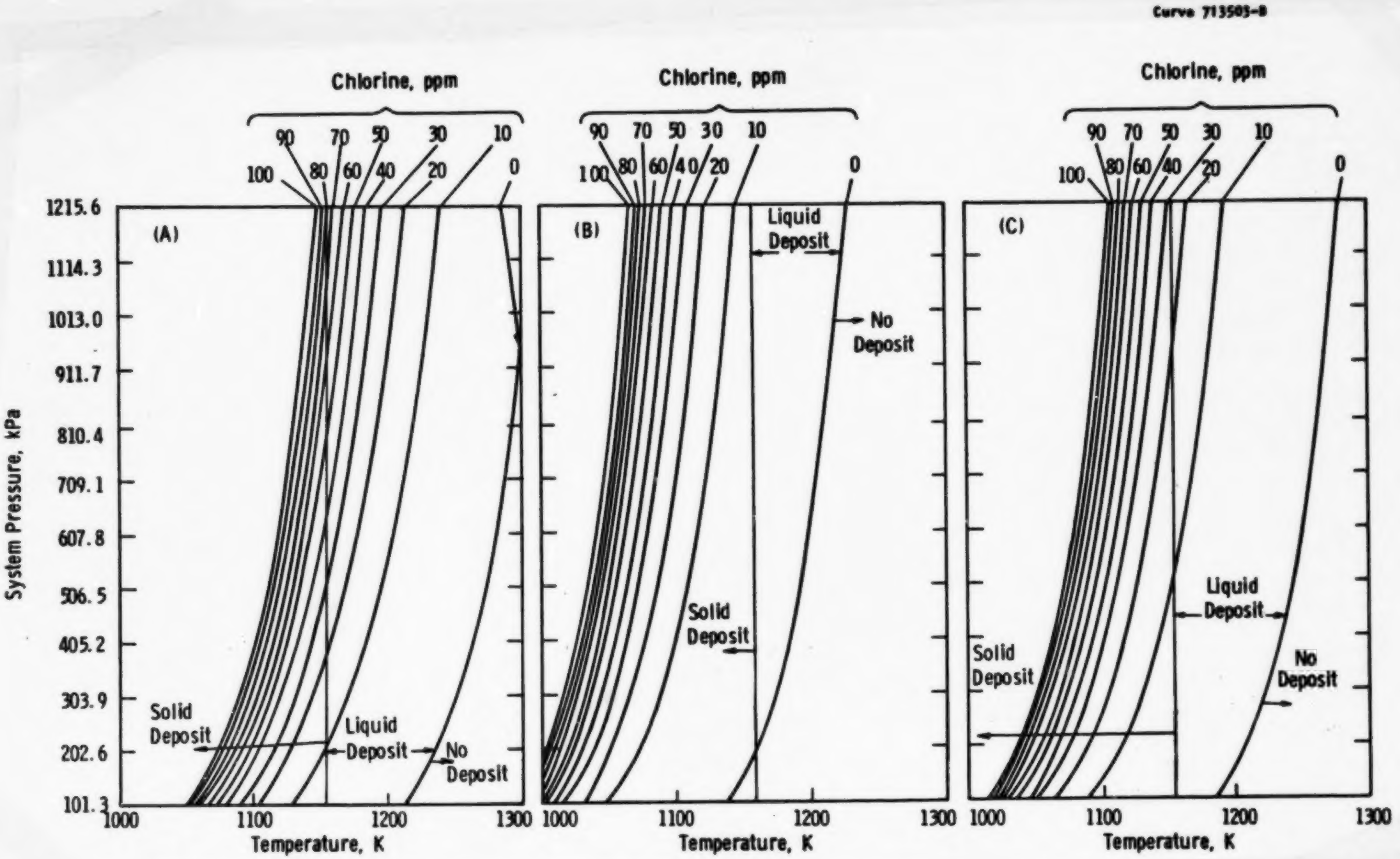

Figure 141 - Stability of Sodium Sulfate as a Function of Temperature and Pressure in Combustion Gases Containing Variable Concentrations of Sodium and Sulfur Oxides: (A) 12.54% O_2, 5.4% H_2O, 460 ppb Na, 124 ppm SO_x, (B) 12.54% O_2, 5.4% H_2O, 46 ppb Na, 124 ppm SO_x, (C) 12.54% O_2, 5.4% H_2O, 460 ppb Na, 12.4 ppm SO_x

chromium oxychloride (CrO_2Cl_2), limiting the formation of the $CoO \cdot Cr_2O_3$ spinel while increasing the concentration of $CoSO_4$ by the reactions

$$CoO \cdot Cr_2O_3(s) + 4HCl(g) + \frac{3}{2}O_2(g) \longrightarrow 2CrO_2Cl_2(g) + CoO(s) + 2H_2O(g) \quad (157)$$

and

$$CoO(s) + SO_2(g) + \frac{1}{2}O_2(g) \longrightarrow CoSO_4(s) \quad . \quad (158)$$

In the 90 percent S-removal system $NiSO_4$ is formed at temperatures below 920 to 930 K, prior to its conversion into NiO. At increased Cl concentrations in the combustion gas, NiO is no longer stable but volatilizes as nickel chlorides. Similarly, an increase in the Cl content of the combustion gas reduces the stability of $CoSO_4$, promoting the formation of volatile cobalt chlorides at temperatures between 920 and 930 K.

Sodium sulfate remains in the system as a stable solid, even though Cl has been increased by a factor of 1000 over that released by combustion. At this Cl concentration the stability of the metal oxides or sulfate is endangered by the volatilization of protective cobalt or nickel oxide or sulfate layers. Oxidation of the underlying metal may not be achieved after rapid volatilization of the outer protective oxide layer, and attack of the surface by Cl or S in the effluent gases or alkali deposits may enhance a rapid sulfidation attack of the metal substrate. Provided that a thick oxide layer has been formed on the alloy, destruction to the underlying oxide and/or metal substrate should be minimal. At low temperatures, therefore, the FBC system should contain sufficient Cl to maintain the integrity of the scale through limited volatilization of the outer alloy surface, and also to reduce the potential for the formation of metal sulfates that react with solid alkali sulfate deposits to form low-temperature eutectic melt complexes. Similarly, at higher operating temperatures the Cl concentration should be sufficient to maintain the stability of the protective metal oxide surface yet minimize the formation of the liquid sodium sulfate deposit.

The major volatile phase of Na at temperatures above 1100 K is NaCl. When the gas temperature near the alloy surface has cooled, sulfate is formed through the interaction of NaCl and gaseous SO_x, condensing out Na_2SO_4. The Cl released from the alkali chloride may react, in turn, with the surface oxide, causing volatilization of the protective scale, or may remain innocuous in the gas stream. In systems where the Cl exceeds the Na content, it may interact directly with the alkali in the gas, and also with the metal alloy. As illustrated in Figure 142, when Cl is completely released from the feedstock during combustion and the sulfur activity in the effluent gases has been reduced through the addition of sorbent materials, Na_2SO_4 and CoO form, in addition to solid NaCl. The salt is stable as a solid and does not promote corrosion of the protective oxide scale. At extremely low gaseous S concentrations the alkali is removed from the system as the volatile chloride when the system temperature approaches 1157 K. Systems that do not contain gaseous chlorides form a liquid sodium $NaOH/Na_2SO_4/CoO$ phase at temperatures below 1050 K, limiting the optimum operating condition to a narrow temperature band between 1050 and 1150 K.

Summary

The complexity of combustion gas chemistry has been demonstrated for numerous reactions that occur simultaneously in the gas stream, at the alloy/gas interface and within subscale layers. The sensitivity of the reactions is dependent not only on temperature, but also on operating pressure and on the relative composition of the combustion gas. Deposition of solids from the condensation of volatile sodium and sulfur oxides is a critical parameter that determines the stability of the alloy through the reactions of potentially corrosive sulfate complexes with protective oxide layers.

Cobalt- and nickel-based alloys used in combustion systems that operate at 0 or 90 percent S-removal capacities have an optimum operating temperature range between 980 to 1040 and 1157 K. Within this temperature zone alloys are likely to be resistant to corrosive attack

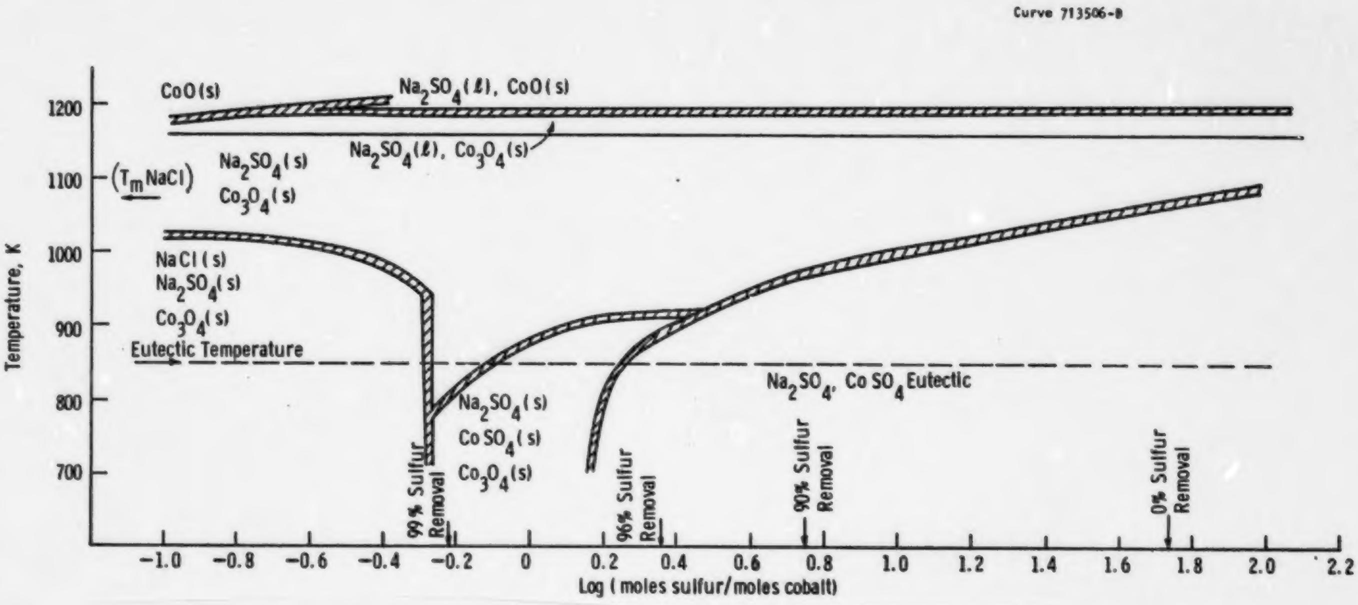

Figure 142 - Equilibrium Phase Diagram for $Na_2SO_4 \cdot 47.8\%$ $CoSO_4$ Eutectic as a Function of Temperature and Sulfur Activity at 405.2 kPa in the Presence of 100% Chlorine Release from U.S. Mean Coals

since neither liquid Na_2SO_4, responsible for high-temperature corrosion, nor the liquid eutectic sodium-cobalt-sulfate complex, responsible for initiating low-temperature corrosion, are projected to form. Continued reduction in S to 96 or 99 percent removal levels minimizes the formation of the low-temperature eutectic liquid to temperatures between 844 and 910 K while maintaining a liquid deposit of $NaSO_4$ on the surface of the alloy at temperatures above 1157 K. The formation of a stable liquid NaOH phase over solid Na_2SO_4/metal oxide at temperatures as high as 950 to 1000 K results when the combustion system operates at greater than 99 percent S-removal capacities.

The addition of chloride, as either an organic complex or as HCl, converts the liquid NaOH deposit into a stable NaCl solid in the Na_2SO_4/metal oxide phase. Additionally, Cl reduces the stability of the Na_2SO_4 complex at temperatures exceeding 1157 K. Excessive addition of Cl may endanger the stability of the protective oxide layer by leading to the formation of volatile metal chlorides and oxychlorides. A balance between the minimization of the alkali sulfate and hydroxide formation and that of surface metal volatilization must be achieved.

Alloys containing 15 to 25 percent Cr form protective oxide scales on the alloy surface, minimizing the degree of either high- or low-temperature corrosion. The Cr_2O_3 surface does not react with the S-containing combustion gas to form $Cr_2(SO_4)_3$, nor with the alkali sulfate to form an alkali-chromium-sulfate eutectic. Chromium reacts in the presence of either Co or Ni to form stable spinel structures. If the concentration of Co or Ni is limited at the alloy surface, the favored metal phase is that of the spinel instead of the alkali-metal eutectics. In this way low-temperature corrosion is minimized.

Reactions of Al- and Fe-containing alloys with combustion gases containing S form eutectics of alkali-aluminum or iron-sulfate that exist principally as solids at the alloy surface.

The stability of each phase is maintained for combustion systems operating at 0, 100, or 300 percent excess air, with variation to the resulting solid composition predominantly occurring as a function of the S content. If a reducing condition is maintained, the formation of metal sulfides results. Numerous studies are presented in the literature that demonstrate the stability of the metal complexes as a function of various gas compositions, and it is evident that Cr_2O_3 is the most stable phase formed for a combustion gas reaction with Co, Ni, Cr, or Al. Conversion into CrS results only at relatively high pH_2/pH_2S and at low pH_2O/pH_2 conditions.

Although thermodynamics provides little indication of the relative rates of the deposition or corrosion reactions, equilibrium is expected to be achieved rapidly at high temperatures. The equilibrium between the combustion gas and the alloy metals reflects the stability of the alkali sulfate or eutectic within defined operating parameters. Experimental and in-field data tend to support the predicted thermodynamic equilibrium high- and low-temperature corrosion products. The current model must be refined, however, incorporating deposition rate and sulfate-oxide reaction rates, in addition to diffusion mechanisms of elements and phases through various oxide scales in order to achieve a comprehensive understanding of the potential corrosion mechanisms.

8. SUMMARY OF THE TRACE AND MINOR ELEMENTAL INTERACTIONS - COMPARISON OF PROJECTED EMISSIONS AND PLANT DATA

The chemical equilibrium model proposes numerous pathways by which trace or minor elements react with and repartition within the clay lattice and carbonate structures of the feedstock materials during combustion (Figure 143). One hundred percent of the trace or minor elemental feedstock concentration is assumed to be available for reaction, thus illustrating the maximum concentration limit of these constituents in solid, condensed, or gaseous phases formed at temperature or pressure in fluidized-bed combustion systems using a U.S. mean coal. The current equilibrium model attempts neither to illustrate secondary chemical reactions or surface adsorption of gas phases with particulates entrained in the gas stream nor to estimate concentration gradients as a function of particle size. These reactions will be discussed when we review analytic data presented in the literature.

ELEMENTAL REACTIONS AND INTERACTIONS

An understanding of the individual trace and minor element reactions was essential before attempting to define the multichemical reactions that occur throughout the fluidized-bed combustion system. These simple reactions (C-H-N-O-S-Cl-X, where X = Be, F, Hg, Pb, Co, Cr, Fe, Mo, Mn, Ni, Ti, Na, K, Al, Si, Br, B, P, Co, V, Zn, Sb, Sn, Zr, As, Cd, Se, Ga, and Ge) that result in the fluidized-bed combustor operating with 10, 100, and 300 percent excess air, and 0, 90, and 99 percent S-removal capabilities were discussed in Section 7. At equilibrium the feedstock elements were classified as constituents that, independent of system pressure,

- Volatilize completely: Be, F, Hg, Pb, Mo, Br, B, P, Cu, As, Cd, and Se

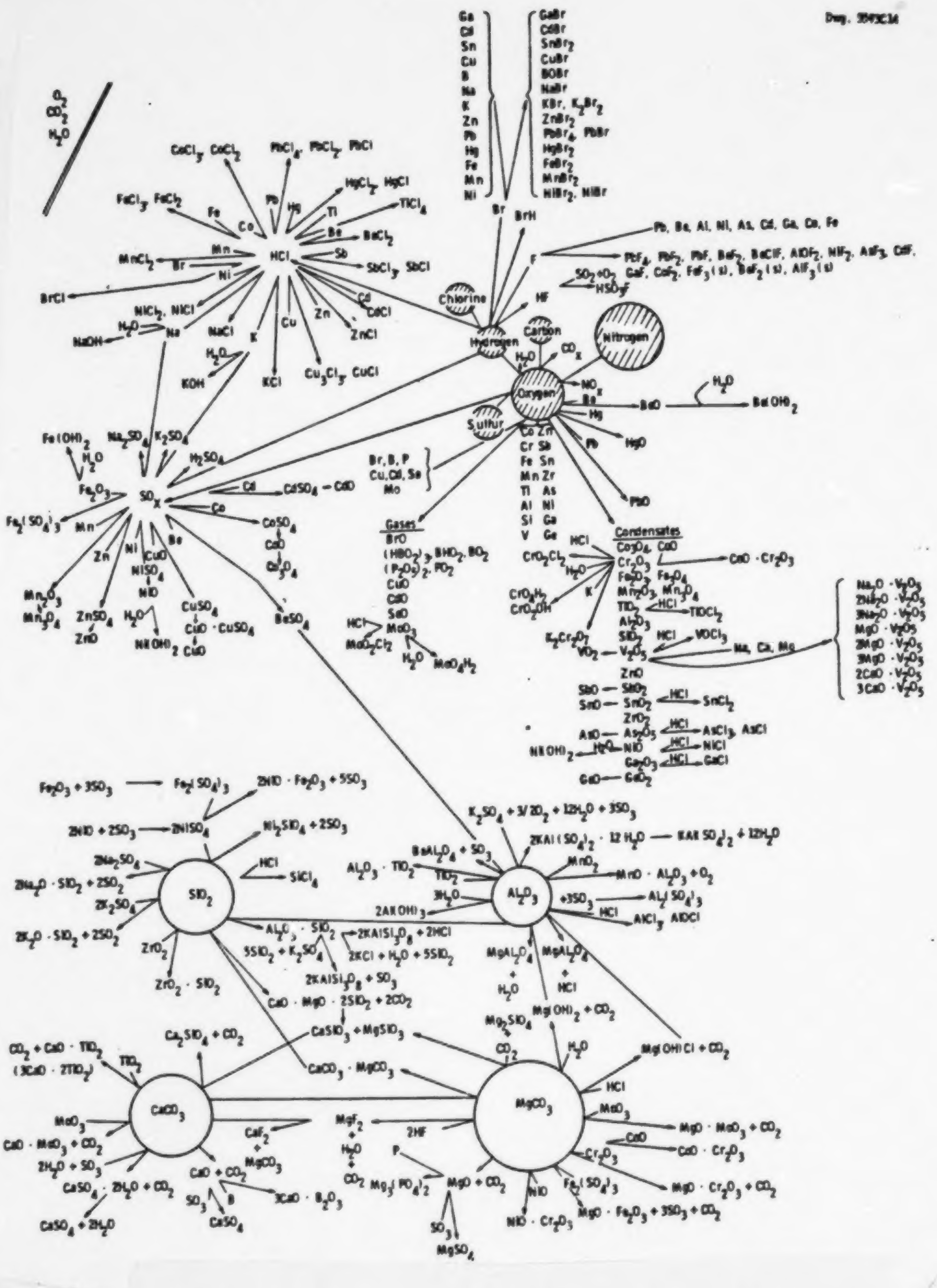
Dwg. 3549C14
O2
CO2
H2O
HCl
SOx
Chlorine
Hydrogen
Carbon
Nitrogen
Oxygen
Sulfur
Br
BrH
F
HF
Gases
Condensates
SiO2
Al2O3
CaCO3
MgCO3

Figure 143 - Principal Reaction Pathways of Trace and Minor Elements during Combustion

- Volatilize partially: Co, Cr, Mn, Ni, and Sn
- Remain as stable solid complexes: Fe, Ti, Al, Si, V, Zn, Zr, and Ga,

while the resulting phase of the Na, K, Sb, and Ge species were shown to be dependent on pressure. The parametric projections indicate the maximum concentration of the various elements emitted from the stack (no gas-solid interactions were considered from the combustor outlet to the stack), and the proposed stable solid phases formed in the fluidized-bed combustor.

The thermodynamic model utilizes the common assumption that, in high-temperature chemistry, equilibrium will be reached in the bed, and the equilibrium product distribution will be characterstic of the process effluent. It, thus, may seem unrealistic to assume that additional reactions along entrained ash particles or deposition reactions along cooler metal surfaces within either the particle collector devices or the gas turbine do not occur. The interactions of the trace and minor elements with the feedstock clay and carbonate constituents were examined in an attempt to illustrate the in-bed partitioning of the elements through the formation of stable in-bed solid phases. These interactions, if equilibrium were attained, would minimize the concentration of volatiles escaping from the bed and would serve as a second approximation for the total concentration emitted from the stack.

The mineral content in coal (Table 1) undergoes numerous conversion reactions when exposed to fluidized-bed combustion temperatures. Quartz (SiO_2 with a hexagonal lattice) remains stable throughout the low operating temperature range (300 to 1000-1100 K), prior to its conversion into cristobalite (SiO_2 with a cubic or tetragonal lattice); andalusite ($Al_2O_3 \cdot SiO_2$) releases SiO_2, forming a solid solution complex with γ-Al_2O_3, which is converted into mullite ($3Al_2O_3 \cdot 2SiO_2$) at high temperature; coal or sorbent carbonate fractions calcine and react with gaseous sulfur oxides, forming sulfates ($CaSO_4$ or anhydrite), or interact with the clay constituents, forming an anorthite ($CaAl_2Si_2O_8$) structure;

pyrites (FeS_2) oxidize, forming stable solid sulfates ($Fe_2(SO_4)_3$) at low bed temperatures and solid oxides (Fe_2O_3, Fe_3O_4) when combustion temperatures approach 1200 or 1300 K; sphalerite (ZnS) is transformed into hydrated sulfates and, as a function of the system temperature and pressure, forms zinc oxide (ZnO).

Variation in the clay content in coal (0.43-3.04 percent Al, 0.58-4.63 percent Si)[11] permits numerous minor phases to take place within the aluminosilicate lattice through either substitution or chemical bonding of the alkalis or trace and minor elements. The equilibrium projections indicate the potential for the formation of solid potassium aluminosilicate ($KAlSi_3O_8$) and disodium silicate ($2Na_2O \cdot SiO_2$) within the clay lattice containing $xAl_2O_3 \cdot ySiO_2$ complexes in addition to localized pools of SiO_2 and Al_2O_3.

Studies conducted by Gluskoter and Ruch[94] have shown the nearly total lack of water soluble potassium phases, dictating against the presence of KCl as the major potassium phase of coal. This evidence supports the thermodynamic projections that predict the formation of a relatively insoluble $KAlSi_3O_8$ complex (Appendix B). Sodium, conversely, was shown to be divided between a water soluble (possibly chloride, carbonate, or water glass) phase and an additional nonsoluble phase. The formation of the $2Na_2O \cdot SiO_2$ phase projected by the equilibrium model may in part be present in the water soluble fraction, while, depending on the concentration present and the solubility of the silicate, $2Na_2O \cdot SiO_2$ may also exist within the insoluble fraction. The degree of solubility of the alkali silicate and aluminosilicate structures needs to be established, and the exact mechanism by which the alkalis enter the clay lattice needs to be defined.

During combustion the aluminosilicate lattice undergoes a series of dehydration and devolatilization reactions that disrupt and reorient the crystal structure, exposing cavities and charged, unbalanced sites (i.e., hydroxyl groups) around the edge of the clay particle. In order to maintain the neutrality of the aluminosilicate structure, these sites must be balanced. The unbalanced charges may be satisfied through the interaction of the aluminosilicate matrix with the trace and minor elements, K, Na, Ca, Mg, Be, Ti, Mn, Ni, and Zr, as shown in the projected equilibrium solids. Physically, these elements may also substitute or be camouflaged in the clay lattice if the element has the same charge and ionic radius as the element being displaced. The trace or minor element may be captured within the lattice if it has a similar ionic radius but a higher charge than the lattice element, or it may be admitted easily into the lattice if the element has a smaller or similar ionic radius and lower charge than the displaced ion. The equilibrium calculations project the most thermodynamically stable phases formed under defined operating conditions. These phases may result along the edge of clay or spent sorbent particles or may complex internally through displacement reactions. The projected stable interactive phases include manganese aluminate ($MnO \cdot Al_2O_3$), aluminum titanate ($Al_2O_3 \cdot TiO_2$), calcium metasilicate ($CaSiO_3$), calcium orthosilicate ($CaSiO_4$), magnesium aluminate ($MgAl_2O_4$), magnesium orthosilicate (Mg_2SiO_4), magnesium metasilicate ($MgSiO_3$), calcium magnesium silicate ($Cao \cdot MgO \cdot 2SiO_2$), calcium titanates ($CaO \cdot TiO_2$, $3CaO \cdot 2TiO_2$), calcium molybdate ($CaO \cdot MoO_3$), magnesium molybdate ($MgO \cdot MoO_3$), potassium aluminosilicate ($KAlSi_3O_8$), disodium silicate ($2Na_2O \cdot SiO_2$), nickel silicate ($2NiO \cdot SiO_2$), zirconium silicate ($ZrSiO_4$), and beryllium aluminate ($BeAlO_4$). The interaction of the trace and minor constituents leads, in addition to the clay particle reactions, to the formation of stable solid compounds such as cobalt chromate ($CoO \cdot Cr_2O_3$),* potassium chromate ($K_2Cr_2O_7$), magnesium chromate ($MgO \cdot Cr_2O_3$), magnesium ferrate ($MgO \cdot Fe_2O_3$), nickel ferrate ($NiO \cdot Fe_2O_3$), magnesium phosphate ($Mg_3(PO_4)_2$), tricalcium borate ($3CaO \cdot B_2O_5$), and the potentially corrosive vanadium complexes - magnesium vanadates ($MgO \cdot V_2O_5$, $2MgO \cdot V_2O_5$, $3MgO \cdot V_2O_5$), calcium vanadates ($2CaO \cdot V_2O_5$, $3CaO \cdot V_2O_5$), and sodium vanadates ($Na_2O \cdot V_2O_5$, $2Na_2O \cdot V_2O_5$, $3Na_2O \cdot V_2O_5$). The thermodynamic projections also predict the formation of solid magnesium fluoride (MgF_2) and its conversion into solid calcium fluoride (CaF_2) in fluidized-bed combustors operating between 300 and 1000 K. The evolution of gaseous hydrogen fluoride (HF) results as a function of the combustion temperature from either the clay fraction of the feedstock material (i.e., solid AlF_3, which is stable between 300 to 500 K), the trace constituent association (i.e., solid BeF_2 and FeF_3, which are stable only between 300 and 400 K), or the carbonate-fluoride complexes (i.e., MgF_2, which is stable from 300 to 600-700 K and CaF_2, which is stable from 600-700 K to 900-1000 K).

---

*Possibly nickel chromate ($NiO \cdot Cr_2O_3$); thermodynamic data for this compound were unavailable.

The stability of the solid phases that result from the interaction of the trace or minor constituents is slightly reduced by the formation of the interactive fluoride and bromide volatile phases. These include: PbF_4, PbF_2, PbF, NaBr, KBr, K_2Br_2,$ZnBr_2$, BeF_2, BrF, BeClF, $PbBr_2$, $PbBr_4$, PbBr, $HgBr_2$, AlF_2O, $FeBr_2$, $MnBr_2$, $NiBr_2$, NiBr, NiF_2, BOBr, CuBr, CuF, $SnBr_2$, AsF_3, CdBr, GaBr, CdF, GaF, and CoF_2. These gaseous compounds are projected to form at levels of less than 1 percent of the elemental feedstock concentration, with the exception of the KBr, KBO_2, AsF_3, and CdBr phases.* These minor volatile phases, in addition to the gaseous trace and minor element chlorides, hydroxides, oxides, or nitrides, may be emitted directly from the stack or may become entrapped along the ash or carbonate particle surface through either a chemical reaction or physical adsorption mechanism.

---

*For 100 percent excess air, 90 percent S-removal, 1013 kPa FBC systems at 1200 and 1300 K, 2.4 and 5.4 percent of the feedstock Br content is present as gaseous KBr; at 1300 K, 1.3 percent of the feedstock B content is present as KBO_2; at 1200 K, 2.2 percent of the feedstock As content is present as AsF_3; and at 1200 and 1300 K, 94.3 and 76.7 percent of the feedstock Cd content and 10.9 and 8.9 percent of the feedstock Br content is present as gaseous CdBr.

ASSESSMENT OF THE POTENTIAL TOXICITY OF THE PROJECTED TRACE AND MINOR ELEMENT PHASES

Conventional Power Generating Systems

Emissions from coal combustion result when a proportion of the incombustible mineral matter in the feedstock is released into the atmosphere in the form of fly ash, small particles, and as volatile complexes. Control devices and more efficient combustion conditions reduce the emission content, lowering the potential toxicity of the stack gas phases. The trace or minor elements may deposit within the system, lowering the overall plant efficiency, may interfere with the catalytic activity in coal conversion, and may be potentially toxic or carcinogenic.[84] The literature emphasizes the possible hazardousness of the F, Be, Pb, Hg, As, Cd, Se, and Ni compound formations produced during combustion. Conclusions drawn from many of these studies, however, are only tentative and should be regarded as guidelines, subject to review and reevaluation. For example, Cowherd[9] concluded from his assessment of emissions from boiler flue gases that only Be is near the concentration of potential health concern. Although low levels of Be are known to cause berylliosis (particularly beryllium oxide (BeO)[96]), it has not been established that Be or its compounds released during combustion have any carcinogenic effect on humans.

The equilibrium estimates have projected the feedstock Hg to completely volatilize in the combustor, but measurements by Diehl[97] have shown that 7 to 19 percent of the Hg is retained in the fly ash. Presumably, Hg enrichment within the ash is enhanced during the contact of the fly ash particulate and flue gases at low temperatures. Even with 90 percent of the feedstock Hg content released during combustion[98,99] and directly emitted from the stack as a vapor, the concentration within the plume from conventional power sources did not exceed the U.S. threshold limit for Hg.[100] Although lower than the threshold limit, emitted inorganic Hg, if alkylated (i.e., by microorganisms in the environment), can be passed into the food chain (via fish) and consumed. Alkylated methyl mercury is sufficiently toxic in nature to attack the central nervous system and brain,[101-103] may be mutagenic, and, if ingested, may lead to degeneration and atrophy of the sensory cerebral cortex.[96]

Frieberg[96] has also demonstrated that As in the air is associated with particulates as arsenic trioxide (As_2O_3) and as metal arsenites. While there is little supporting evidence that coal-fired power plants raise the ambient concentration of As in the air, it is essential to establish and enforce air standard regulations on emission control and to continuously monitor the volatile and condensed As content released at the stack. Similarly, the concentration of Cd, Se, Pb, F, and Ni in the stack gas should be continuously monitored. A review of Sections 6 and 7 provides background information on the potential toxicity of each element.

Accumulation of the trace and minor elements in the soil warrents monitoring around power plants. Berry and Wallace[104] found that soils and plants one mile downstream from a Nevada power plant burning 2275 tons of coal per day are enriched in many elements, including As and F. Van Hook and Shults,[105] however, concluded that there is no consistent evidence that emissions have raised the trace or minor element content in the vicinity of the power plant. Similarly, high levels of toxic metals in the air directly linked with industrial or power plant emissions were not detected by Pierson.[106] It has been suggested that if heavy metals were deposited, the uptake by plants would depend on the soil pH. In alkaline soils the availability of Cu, Zn, Pb, and V, would decrease as much as two orders of magnitude for each pH unit increase. The long-term effects of the accumulated trace and minor elements in the soil may be affected by many factors that include: land use and weathering patterns; mineralogy; and interaction of the deposited element with the environment in which the original chemical state and bioavailability and toxicity are modified.[105] Vaughan's proposed theoretical model[107] for predicting atmospheric and hydrologic dispersion, soil/plant accumulation, and bioavailability of the trace element emissions from coal conversion processes indicates that any direct health effects resulting from emissions of an efficient, well-equipped, coal-fired power plant were unlikely, since the trace element concentrations were several orders of magnitude below the recommended standard concentration for inhalation exposure.[84]

Fluidized-Bed Combustion Systems

Analytic results of the Level 1 source test and evaluation in 1976 at the Leatherhead, England, PFBC of the National Coal Board-Coal Utilization Research Laboratory (NCB-CURL) and the Exxon facilities by both NCB and Battelle-Columbus Laboratories (Appendix C - Tables 1, 2, 3) have indicated that the trace elements shown in Table 85 exceed the land MATE concentrations. The Westinghouse thermodynamic projections for the percent volatility of the trace and minor elements at 1200-1300 K for a fluidized-bed combustor operating with 100 percent excess air and 90 percent S-removal capabilities are shown in Table 86. In additon to the projected volatility, the elemental concentration in the off-gases is estimated on the basis of volatile formation of the trace and minor constituents from combustion of 100 g U.S. mean coal with 27.6 g sorbent present. The thermodynamically proposed volatile compounds of Be, F, Hg, Pb, Co, (Cr), Br, (P), Cu, As, Cd, (Ge), and Se, if directly released from the combustor and emitted from the stack at ambient conditions, exceed the air MATE level for related species on a weight basis. Interaction of the volatiles with entrained particles, corrosion and deposition mechanisms within the fluidized-bed combustion system, dilution of the off-gas concentration in the turbine expansion gases, atmospheric diffusion and chemical reactions within the plume, rainout, washout or dry deposition of the volatile complexes from the aerosol, and meterological parameters will further minimize the concentration of the emitted trace or minor constituents. The influence of these phenomena on the final concentration of the released volatile phases will presumably be far below the air MATE level, but such an estimate is beyond the scope of this report.

TABLE 85 - TRACE ELEMENTS EXCEEDING MATE VALUES IN FLUE GAS AND SOLID EMISSIONS FROM PFBC SYSTEMS, AND CORRESPONDING PROJECTED ELEMENTAL VOLATILIZATION[111]

Dwg. 7729A02

NCB		EXXON	
FLUE GAS	SOLID EMISSIONS	FLUE GAS	SOLID EMISSIONS
LI	LI	LI	
MG	MG		
AL	AL		AL
SI	SI		SI
P	P		P
V	V	V	V
CR	CR	CR	CR
FE	FE		FE
NI	NI	NI	NI
CU	CU		CU
ZN	ZN		ZN
AS	AS	AS	AS
SE	SE		
PB	PB		PB
TL			
U			
	F		
	CA		CA
	TI		TI
	MN		MN
		BA	
		BE	

TABLE 86 - PROJECTED ELEMENTAL CONCENTRATION IN PFBC EFFLUENT GAS AND SOLID PHASES

Dwg.1714852

ELEMENT	INITIAL CONCENTRATION	PERCENT VOLATILIZATION FOR 1200–1300 K, 100% EXCESS AIR, 90% SULFUR REMOVAL FBC SYSTEMS	ESTIMATED* OFF-GAS CONCENTRATION	AIR MATE **	COMMENT ***	ESTIMATED SOLIDS CONCENTRATION	LAND MATE	COMMENT ***
Be	1.81 ppm COAL, 4 ppm SORBENT	100 (10.3)	0.14 ppm (0.014 ppm)	0.0017 ppm (Be)	E (E)	– (8.97 ppm)	0.03 ppm (Be)	– (E)
F	69.94 ppm COAL, 10 ppm SORBENT	100	3.15 ppm	1.69 ppm (HF)	E	–	–	NE
Hg	0.20 ppm COAL, 0.16 ppm SORBENT	100	0.01 ppm	0.094 ppb ($HgCl_2$)	E	–	4.0 x 10^{-7} ppm (ALKYL-Hg)	NE
Pb	34.70 ppm COAL, 18.5 ppm SORBENT	100	1.96 ppm	0.126 ppm (FUME)	E	–	6.00 ppm (PbO)	NE
Co	9.57 ppm COAL	13.76 (21.12)[a]	0.07 ppm (0.10 ppm)	0.094 ppm (FUME)	E (E)	30.46 ppm (27.98 ppm)	7.08 ppm (CoO)	E (E)
Cr	13.75 ppm COAL	78.8 (7.85[c]-22.14)	0.54 ppm (0.05 - 0.15 ppm)	0.422 ppm (SALTS)	E (NE)	10.87 ppm (46.77-39.52 ppm)	[illegible]	E (E)
Fe	1.92% COAL	0 (0)	– (–)	4.22 ppm (FUME)	NE	7.09% (7.09%)	200 ppm (Fe_2O_3)	E (E)
Mo	7.54 ppm COAL	100	0.37 ppm	4.22 ppm (SOL. MO)	NE	–	300 ppm (INSOL. Mo)	NE
Mn	48.40 ppm COAL	2.2 (1.4)	0.06 ppm (0.03 ppm)	4.22 ppm (Mn)	NE	179.34 ppm (179.80 ppm)	0.20 ppm (Mn)	E (E)
Ni	21.07 ppm COAL	5.06 (2.8)	0.06 ppm (0.03 ppm)	0.084 ppm (SOL. Ni)	NE (NE)	73.86 ppm (75.76 ppm)	2.70 ppm (NiO)	E (E)
Ti	0.07% COAL	0 (0)	– (–)	8.43 ppm ($TiCl_4$)	NE (NE)	0.28% (0.28%)	200 ppm (TiO_2)	E (E)
Br	19.298 ppm COAL	100	0.96 ppm	0.59 ppm (Br_2)	E	–	1.0 ppm (Br_2)	NE
B	102.21 ppm COAL	100 (0)	5.08 ppm (–)	75.87 ppm (B)	NE (NE)	– (377.30 ppm)	300 ppm (B_2O_3)	NE (E)
P	71.10 ppm COAL	99.99 (0)	3.53 ppm (–)	0.843 ppm (H_3PO_4)	E (NE)	– (282.46 ppm)	9.0 ppm (H_3PO_4)	NE (E)
Cu	15.18 ppm COAL	100	0.763 ppm	0.169 ppm (FUME)	E	–	106 ppm (COMPLEXED)	NE
V	32.71 ppm COAL	0.03 (0)	0.40 ppb (–)	0.42 ppm (V)	NE (NE)	303.06 ppm (120.75 ppm)	0.30 ppm (V_2O_5)	E (E)
Zn	272.29 ppm COAL	0 (0.01)	– (1 ppb)	0.57 ppm (Zn)	NE (NE)	0.10% (~ 0.10%)	1.0 ppm (Zn)	E (E)
Sb	1.26 ppm COAL	0.5 - 100[b]	0.313 ppb - 0.063 ppm	0.42 ppm (Sb)	NE (NE)	4.63 ppm	0.4 ppm (Sb)	E
Sn	4.79 ppm COAL	<3	7 ppb	1.75 ppm ($SnCl_4$)	NE	17.15 ppm	3.0 ppm (SnO)	E
Zr	72.48 ppm COAL	0	–	4.22 ppm (Zr)	NE	287.48 ppm	16.0 ppm (Zr)	E
As	14.02 ppm COAL	100	0.70 ppm	1.78 ppb (As)	E	–	0.1 ppm (As_2O_3)	NE
Cd	2.52 ppm COAL	100	0.13 ppm	0.74 ppb (Cd)	E	–	4.0 ppb (Cd)	NE
Se	2.08 ppm COAL	100	0.10 ppm	9.1 ppb (Se)	E	–	0.05 ppm (Se)	NE
Ga	3.12 ppm COAL	0.5	0.7 ppb	4.17 ppm (Ga)	NE	11.48 ppm	14.8 ppm (Ga)	NE
Ge	6.59 ppm COAL	2 - 100[b]	6.5 ppb - 0.33 ppm	0.51 ppm (GeH_4)	NE – NE[b]	23.84 ppm	18.0 (GeH_4)	E

[a] ( ) INDICATES INTERACTIVE CHEMICAL REACTION SYSTEMS

[b] SYSTEM PRESSURE DEPENDENT

[c] SPINEL INTERACTION

* ppm BY WEIGHT

** CONVERSION FROM ppm BY VOLUME TO ppm BY WEIGHT

*** E = EXCEEDED MATE LEVEL; NE = NOT EXCEEDED MATE LEVEL

Similarly, Table 86 estimates the trace and minor element concentration in solid combustor compounds. The projected concentration is based on the nonvolatile thermodynamic percentage of each element, which results in the ash/spent sorbent matrix from a coal containing 10.79 percent ash by weight, with the sorbent fully calcining. Correlation of the elemental solid concentration with the reported land MATE levels for related species shows that Be, Co, Cr, Fe, Mn, Ni, Ti, (B), (P), V, Zn, Sb, Sn, Zr, and Ge may warrant concern in the resulting combustor solid phases. It should be emphasized that for many complexes that are projected thermodynamically, corresponding MATE values are unavailable. A more definitive understanding of the ash and aerosol formation mechanisms in FBC systems and the interactions of volatile phases with entrained particles as a function of operating parameters is essential in order to define accurately the potential toxicity of solid FBC emissions. Furthermore, with the development of stringent particulate and hot-gas cleanup devices the potential toxicity level can conceivably be reduced far below levels of concern.

Potentially toxic trace and minor elements present in coal/spent sorbent wastes from FBC systems may be released into the environment through leaching processes at waste disposal sites. Although variation in the solid waste chemistry results from combustion processes, external forces such as weather, soil, topography, and groundwater at the disposal location influence the release of ions that may exceed environmental or health standards.

Incomplete combustion may be responsible for an enhanced leachability of trace and minor constituents from ash formations, while the combustion of high heat content coals produces less leachable ash fractions. Wu[112] demonstrated a higher leachability of the trace and minor elements from conventional system fly ash than from the leachable fraction in bottom ash formations, while the reverse trend was observed for solids formed in FBC operations containing sorbent materials. It has been proposed that the trace and minor elements are contained in the oxide or carbonate matrix of the sorbent, which sulfates and mixes with the bottom ash in the fluidized-bed combustor. This fraction tends to be more readily dissolved than trace or minor constituents bound within the aluminosilicate or ashlike lattice. The large concentration of calcium from the sorbent is capable of reacting with released volatiles (i.e., B, Se, F), forming calcium derivatives (calcium metaborates, soluble selenium phases or calcium difluoride) with boiling points that exceed combustion temperatures.

Westinghouse has studied extensively the composition and leachability of ions, and trace and minor elements from bed and carry-over materials obtained from ANL,[113] Exxon miniplant,[114] PER (Pope, Evans, and Robbins),[60] METC,[115] B&W (Babcock and Wilcox),[116] Battelle-Columbus Laboratories,[117] and Combustion Power Company.[118] C. C. Sun[119] has assessed these materials in terms of their ability to meet environmental and drinking water standards. The preliminary conclusions suggest the feasibility of disposing of FBC residues without indirectly polluting the environment.

ELEMENTAL CONCENTRATION IN ASH FORMATIONS

The combustion of coal in conventional systems has classified the fate of the trace and minor elements as constituents that either volatilize completely, volatilize partially, or remain nonvolatile on the basis of the proposed volatilization-condensation or adsorption model.[1] The trace and minor elements in the feedstock have previously been shown to be present as inorganic sulfides in the aluminosilicate matrix or as organic complexes. According to the volatilization-condensation model, the aluminosilicate matrix in coal does not decompose upon combustion, but rather melts and coalesces, forming slag and fly ash. It is during this melting stage that, under the reducing environment surrounding the coal particle, the chemical bonding between metallic elements and S from the sulfide mineral inclusions or between the elements associated in the organic matrix are broken, forming volatile complexes. Elements directly associated within the organic matrix become dispersed within the gas stream, as do trace and minor elements that are present in phases unstable at combustion temperatures. Once volatilized, these elements may then oxidize in the flue gases, forming less volatile species, or may condense or be adsorbed on entrained fly ash as the flue gas temperature drops.

Gas phase measurements of the volatilized trace and minor elements in the combustion zone of coal combustors and stack gas emission levels have not been made. The extent to which the trace and minor elements partially or fully volatilize on combustion, however, can be estimated from reported data by determining the depletion of the specific element in the various slag or ash formations in the particular system. The appearance of the specific element in the fly ash fines, for example, is not absolute evidence that volatilization is occurring. The element may be present in that portion of the coal mineral matter that is released as fly ash without prior volatilization and recondensation. Consistently high concentrations in increasingly finer ash particle fractions, however, certainly suggest that volatilization is a candidate initial mechanism.

The trace and minor elements that do not volatilize in the combustion zone but form a melt of uniform compositon in both the fly ash or slag formations include Al, Ba, Ca, Ce, Co, Cr, Cs, Eu, Fe, Hf, K, La, Mn, Mg, (Ni), Na, Rb, Sc, Si, Sm, Sr, Ta, Th, Ti, U and V.* The slag or bottom ash formations containing the trace or minor constituents is directly removed from the combustion zone. The elements As, Cd, Cu, Ga, Pb, (Mo), Sb, Se, and Zn** volatilize during combustion, and since the slag is removed from the combustion zone, little opportunity for condensation of these elements with the slag results. Condensation of these elements on entrained fly ash particulate, however, may occur as the flue gas cools. Therefore, the concentration of As, Cd, Cu, Ga, Pb, Sb, Se, and Zn is preferentially depleted in conventional slag formations, while partitioning of these phases, particularly as a function of decreasing particle size, results in the entrained ash fines. A third group of elements - Hg, Cl and Br - tends to remain completely in the gas phase.

---

*With the exception of Co and Fe, these elements are presumably lithophiles (associated with the aluminosilicate minerals) in crustal rock, thus demonstrating a lower volatility than the remaining trace and minor elements contained within the feedstock material.

**With the exception of Cu, these elements are chalcophiles (sulfide mineral associated) in crustal rock, which tend to volatilize more readily than the lithophilic constituents at combustor temperatures.

Many of the studies reporting the ash composition produced during conventional coal combustion support the partitioning of the trace and minor elements even though the studies were conducted on different sizes and types of systems. The results from the analytical studies conducted by the Oak Ridge National Laboratory (ORNL) at the Allen Steam Plant[99] support the previously described partitioning at the trace and minor elements in the ash and volatile phases (Appendix C, Table C-4). The elements Cr, Cs, Na, Ni, U, and V behaved as intermediary constituents, which neither partition equally between the bottom ash and fly ash nor become enriched within the fly ash fraction relative to the bottom ash concentration.

The thermodynamic equilibrium projections assume that 100 percent of the trace or minor element is available in the combustion reactions. Partitioning of the elements within ash/spent sorbent materials is established by comparing the percentage of the element forming a solid complex with the percentage of the element resulting in gaseous complexes. Although the thermodynamic model does not account for partitioning of the elements within the bed, cyclone, precipitator, or stack materials, correlation of the thermodynamic data with the published data for the conventional combustion system is evident. The elements Al, Ca, Co, Cr, Fe, K, Mn, Mg, (Ni), Na, Si, and Ti readily incorporate into the slag and inlet fly ash fraction, with no apparent tendency to concentrate in the outlet ash. These analyses are supported by the thermodynamic projections for the interactive systems through the formation of solid complexes as major phases at elevated combusted temperatures. The Allen Steam plant analysis indicates that Pb and Mo concentrate in the inlet fly ash rather than in the slag, and in the outlet ash rather than in the inlet ash. Thermodynamics indicates that 100 percent of the initial Pb or Mo content of the U.S. coal should exist as volatile complexes at 1200 K. Since the thermodynamic model does not account for the partitioning effects of volatiles with particles in the gas stream through either a chemical reaction or an adsorption mechanism, it is possible that the Pb and Mo detected as enriched in ash fractions were originally gaseous and transported with the combustion gases prior to particle interaction. The Allen steam plant data also indicate complete volatilization of Hg during combustion; thermodynamics projects 100 percent volatilization of Hg at 1200 K.

The thermodynamic projection in which 14 percent of the feedstock Co and 5 percent of the Ni content volatilize is less than the 33 and 43 percent volatility ORNL reported. The higher volatility of Co and Ni in the conventional boiler system may be attributed to higher combustion temperatures. The ORNL study also found that the fly ash was significantly enriched in Cr, even though the concentration in the slag fraction was not depleted. The ORNL sampling indicated an enrichment corresponding to between 24 and 40 percent of the original Cr content of the feedstock coal, as opposed to the thermodynamic calculations that predict 79 percent volatilization for FBC operations using a feedstock coal that contained a lower Cr content. The ORNL team suggested that Cr removed from the boiler tubes may be responsible for the enrichment. If the thermodynamic calculations were repeated using ORNL's higher-Cr coal, the adjusted equilibrium value would predict 47 percent volatilization.

According to the volatilization-condensation theory, the accumulated concentration of the trace and minor elements on smaller fly ash particles are assumed to result from the volatilization of the element or of the compound containing the element at combustion temperatures, with condensation or adsorption of these phases along the entrained ash particles as the flue gas cools. Since condensation and adsorption are both surface phenomena, the condensed concentration of the element or phase should be inversely proportional to the ash/spent sorbent particle size or increased surface area available for condensation. The elements that are enriched on smaller particles typically have boiling points lower than or comparable with the combustion zone temperature.[30] This trend was supported by Linton[120] and Keyser,[121] who demonstrated that the more volatile elements (Pb, Zn, Be, K, Mg) could be found in higher concentrations in the surface layers of fly ash than in the bulk composition of the particle. In preliminary, bench-scale experiments that simulated combustion and pyrolysis of Montana lignite in an inert atmosphere, Mims[122] demonstrated that at temperatures below 2000 K Si, Al, Mg, Fe, Ba, Sr, Ti, Na, Mn, Zn, Th, La, Hf, As, Sc, Co, Sb, and Yb vaporize slightly and that the vaporization of As, Mn, Mg, Na, and Sb are strongly enhanced as a function of increased temperature. The more refractory elements (Ti, Sc), however, vaporize to a negligible degree even at temperatures of 2673 K. The elemental concentration that could result in the aerosol, therefore, was dependent upon the degree of vaporization. When the fraction of total ash and constituent elements in the aerosol fraction was plotted against the carrier gas oxygen partial pressure, Na, Mn, and Mg showed a higher fractional vaporization than did the overall ash, while Al and Ca vaporized to a lesser extent. Using a kinetic vaporization combustion model in which the elements and individual species were assumed to vaporize from the shrinking, burning particle sphere that was assumed to be controlled by external diffusion, Mims arranged the elements as a function of the increasing fraction vaporized (Al, Sc, Sm, Ca, Fe, Mg, W, V, Cr, Mn, Co, Zn, K, As, Na, Sb). In this manner, Zn, Sb, and As, which were expected to vaporize in significant concentrations, were found to concentrate in the small particle size fractions or surface coatings, while K and Na showed varying degrees of enrichment, reflecting the possible dependence of coal composition, mineralogy, and combustion condition on release mechanisms.

The chemical characterization of four ash fractions conducted by Fischer[123] support the Mims results. In his analysis Fischer demonstrated an approximately tenfold increase of Cd, As, Se, Zn and Sb in the finest fly ash fraction (2.2 μm particles) relative to the coarsest particle size (20 μm), detected an intermediate enrichment of Sb, W, Mo, Ga, Pb, and V as a function of decreasing particle size, and observed a small but significant enrichment in the U, Cr, Ba, Cu, Be, and Mn content. Silicon was the only element in this study that demonstrated a decreasing dependence on particle size, while the concentration of Sr, Ce, La, Rb, Nd, Th, Ni, Sc, Hf, Co, Sn, Dy, Yb, Cs, Ta, Eu, and Tb was independent of particle size. Inhalation of these particles may result in the deposition of small aluminosilicate ash fines enriched with the various trace or minor phase in the pulmonary region of the respiratory tract. Once deposited, the particle may be engulfed or phagocytized by pulmonary macrophages, which provide the primary immunological defense against inhaled material. Fischer indicates that the potential antagonistic interaction of antimutagens on the fly ash surface may be responsible for the decrease in mutagenicity with increasing particle size.

Similarly to the results of Mims and Fischer, Mann[124] defined the enrichment of Sb, As, Br, Cu, Cd, Cr, Cl, F, Ga, I, Pb, Hg, Mo, Se, S, and Zn in small ash particles entrained in the flue gases from two western power plants burning low-sulfur subbituminous coals. The elements Hg, Se, Br, Zn, F, S, and Cl were shown to be emitted from the stacks either totally or partially as vapors, while Al, Ba, Ca, Fe, Mg, Si, Ru, Sr, and Sn were reported to be approximately equally distributed in all ash fractions and the variation in the enrichment tendencies of Be, Co, Mn, Ti, and V depended on system parameters.

In the 105 MW Illinois power plant, which consumes 60 tons of coal per hour, Lee[125] demonstrated that of the elements emitted from the 97.7 percent efficient electrostatic precipitator, those that concentrated on the submicron diameter particles include As, Cr, Pb, Se, and Zn. Nickel was enriched in the 5 to 10 μm diameter particle size range.

This conclusion agreed with the data reported by Davison and Natusch[13] in which a pronounced concentration of As, Cd, Pb, Se, Sb, Zn, Cr, Ni, Tl, and S was observed in the smaller fly ash particles (0.5-10 μm). The midwestern power plant burned coal from southern Indiana and was equipped with a cyclone collector. The emission control devices for fine particle collection was less effective for removing particles in the size range that contained the most toxic element. The theory that was advanced from the concentration of potentially toxic constituents on fine particles involved the volatilization of the elements in the high-temperature zone of the boiler or combustor and preferential condensation of these elements or compounds onto the surface of the fine fly ash particles in the cooler zones of the system.

Samples of pulverized coal, bottom ash, economizer fly ash, electrostatic precipitator fly ash, fly ash suspended in stack gases and particles collected from the atmosphere surrounding the 355-MW Chalk Point Station of the Potomac Electric Power Company[79] were analyzed by photon and neutron activation methods in an attempt to determine enrichment factors or the repartitioning of trace and minor elements during combustion. In these analyses Gorden categorized As, Sb, Pb, I, and Se as elements that demonstrate pronounced enrichment in smaller fly ash particles.

The 180 MW Valmont Station of the Public Service Company of Colorado employed a corner-firing method of combustion, with an attached mechanical collector and an electrostatic precipitator in parallel with a wet scrubber. The analysis by Kaakinen and Jorden,[126,127] in which the enrichment ratios for the trace elements were calculated relative to the content of Al* in the sample, indicated that the concentrations of Al, Fe, Ru, Sr, Y, and Nb were approximately constant in all of the outlet ashes, while those of Cu, Zn, As, Pb, Mo, and Sb were lowest in the bottom ash. The concentration of these elements progressively increased in the samples of fly ash collected before they entered the stack. A mathematical model was developed on the volatilization-condensation theory, in which an enrichment ratio could be determined as a function of the mass fraction of the element volatilized from the furnace, the specific area of the ash stream, and the total mass flow ratio of each ash stream. Mass imbalance closures around the plant for Rb, Nb, Cu, Zn, As, Se, Sn, Pb, and Ra were attributed to such factors as unsteady-state conditions, analytical errors in the reported concentrations, or errors in the estimated total mass flow rate.

---

*Aluminum was used as the basis for comparison because of its relatively nonvolatile nature at furnace temperatures.

The trace and minor element emissions from three coal-fired steam electricity generating plants[128-131] indicated that As, Sb, Se, V, Pb, Mo, Ni, B, Zn, Cd, Cr, Cu, Co, U, Ag, S, Hg, Cl, and F were enriched in fly ash and in flue gas samples, with S, Hg, and Cl emitted from the plant as gaseous species. Elements that were approximately equally distributed in the bottom ash and fly ash included Ba, Be, Fe, Al, Ca, Ti, Mn, and Mg. The units sampled included a balanced-draft, tangentially fired 330 MW boiler with three venturi scrubbers attached for particulate emission control, burning Wyoming subbituminous coal at a rate of 141 tons/hr; a tangentially fired 350 MW boiler with a hot-side electrostatic precipitator, utilizing Wyoming subbituminous coal at 138 tons/hr; and a 250 MW cyclone boiler with a mechanical cyclone. The concentration of each element in the various ash streams appeared to be dependent on the elemental concentration in the coal, the boiler configuration and firing conditions, the flue gas emission control device, and the properties of the element and its compounds.[16] The volatilization-condensation theory of enrichment of specific elements was demonstrated again in this study. The volatilized elements or complexes may recondense completely or partially or be emitted from the stacks (S, Hg and Cl) as a gaseous phase. Condensation of the volatiles in the cooler gas streams enhances the elemental concentration in the fine particulate fly ash fractions because:

- Condensation occurs either by nucleation or by deposition on previously formed particles. Since residence times between volatilization and condensation are relatively low, any nucleation will produce relatively small particles.

- Deposition occurs on the particle surface and, therefore, is dependent on particle surface area. Since surface area is greater for finer particles, small particles display increased concentrations of elements that tend to recondense.

Cowherd's[9] analysis of pollutant formations in the 125 MW tangentially fired boiler equipped with a mechanical fly ash collector at the Widows Creek Power Plant evaluated 22 trace elements, nitrates, sulfates, POM, and PCB as potentially hazardous emissions resulting from coal combustion. The analytical results shown in Appendix C (Table C-5) indicate that, with the exception of Sb, Ba, Be, Mn, Te, Ti, and V, the elements tend to concentrate in ash downstream of the boiler, enriching particularly the fine particles. The greatest degree of enrichment in the particles is by Be, Cd, Co, and Zn. According to this report, Be is the only potentially hazardous element emitted into the gas stream at a concentration near its TLV. In addition to these results, the POM concentration was shown to be approximately evenly distributed between the bottom ash and the collector ash, while PCB was present in all of the ash streams.

Fennelly[132] viewed the chemical structure of coal as a network of interconnected, aromatic hydrocarbon compounds that upon combustion directly formed small hydrocarbon fractions (less than three C atoms) from the direct cleavage of substituted alkyl groups in the organic matrix of the coal particle. The polynuclear aromatic hydrocarbons (PAH) were proposed to result from condensation reactions of various hydrocarbon decompositional products. Estimates of the concentration range of the organic and inorganic potential pollutants from coal-fired, fluidized-bed combustion systems are illustrated in Appendix C (Table C-6). Lee[134] demonstrated the presence of short-chain alkyl sulfates as dimethyl sulfate ($(H_3CO)_2SO_2$) and its hydrolysis product monomethyl sulfate (H_3COSO_3) in fly ash and airborne particulate matter formed during the combustion of an 0.5 percent S southern Utah coal in a stoker-type plant. Although these organic phases constitute only 0.5 percent of the total S present in the sample, these constituents have been proved to be mutagenic and carcinogenic.[135-139]

Werner[140] showed the concentration of gaseous C_1-C_6 organic emissions from chemically active fluidized-bed (CAFB) processes to be equivalent to those formed during conventional combustion and emissions of heavier organics to be lower than the average of those from conventional boilers. Functional groups identified in condensible CAFB air samples include esters, hydrocarbons, ketones, amides, alcohols, phenols, amines, nitro-compounds, ethers, substituted aromatics and organosilicon compounds. Ash particulate emissions that form in the lignite gasification/combustion of the oil-fired CAFB contain concentrations of Ba, As, Ni, Cr, Ti, P, Si, Mg, B, Be, Cd, Sr, Cu, and Li that exceed MATE levels. Reducing particulate emissions by 99.8 percent through stringent cleanup control devices will lower the trace and minor emission concentration to below the reported MATE value.

In the ANL study Swift[141] estimated that the projected trace and minor element emissions from conventional combustion systems typically operating between 1473-1873 K exceed emissions from the 1200-1300 K fluidized-bed combustion systems (Appendix C, Table C-7).

Fluidized-bed combustion, because of its lower combustion temperature, has the potential for reducing the volatility of the trace and minor elements, thereby retaining a higher concentration of the elements in the ash while simultaneously reducing stack-gas emission concentrations. Particulate fines that escape removal in cleaning systems are similarly expected to contain a lower concentration of trace and minor elements than conventional boiler fines. Swift reports an average retention of 23 percent of the feedstock Hg content in the solid effluent materials formed from the combustion of high-volatile bituminous Pittsburgh seam coal with Tymochtee dolomite and high-purity type 38 Alundum. Arsenic was recovered at 85 percent levels in the FBC system but completely volatilized in the conventional combustion system. Fluorine was retained in concentrations of 5 to 23 percent in the solid phase leaving the combustor, without the addition of the sorbent material, and in concentrations of 56 to 62 percent when the sorbent was included in the combustor. These results reflect the thermodynamic projections for the formation of the CaF_2 or MgF_2 phases. Bromine retention was also enhanced in the presence of the sorbent.

From the ANL analysis of a 10 sulfation/regeneration cycle of Tymochtee dolomite, the concentration of Cr, Tl, V, Mo, Zn, Ba, Fe, In, and Sr was shown to be enriched in the resulting spent sorbent solid, possibly because of the buildup of coal ash on the dolomite particle surface through repeated utilization. No trace or minor element appeared to be depleted in the dolomite after 10 cycles, and As, Cd, Cr, Pb, Ni, Se, Tl, and Zr, which tend to volatilize in conventional systems, were either enriched or remained stable within the dolomite during the 10 combustion cycle exposures.

The apparent differences reported in these few studies indicate the possible variation in the ash morphology and formation mechanism in FBC systems as compared with those occurring during conventional combustion. Mazza,[142] in the 18-in. AFBC unit at METC, in which 1/4 in. Montana Rosebud subbituminous coal particles and limestone were combusted at temperatures of 1089 to 1144 K, indicated that the fluidized-bed fly ash was composed not of spherical, homogeneous particles, but of irregularly shaped, heterogeneous ones. The particle size distribution of the aerosol formed in the METC unit exhibited a multimodal behavior, and, with the presence of excess Ca in the bed, the aluminosilicate fly ash matrix contained crystalline forms of calcium aluminosilicate, with calcium sulfate present as a major constituent phase of small particles. Reference to Section 7 supports these reported reactions on the basis of the simple thermodynamics of the FBC system.

The current work on the pressurized FBC at the Exxon miniplant provides additional information that illustrates the fate of the trace and minor elements during combustion and the projected flue gas emission concentration.[108,109] Analytical techniques determining the trace and minor element concentration in the feedstock materials and resulting ash include ICP (inductively coupled plasma emission spectroscopy), NAA (neutron activation analysis), and SSMS (spark source mass spectroscopy). The percent ratio of the elemental mass in the flue gases to the total mass of the element in all streams (Appendix C, Table C-1) can be correlated with the proposed volatility of the trace and minor species. Bromine and Co are detected in the flue gases at concentrations of between 40 and 80 percent of the total mass load, as compared with 100 and 13.76 to 21.12 percent volatility projected at thermodynamic equilibrium. Volatile hydroxide phases of Co may be responsible for the enhanced Co concentration observed in the flue gases as compared with the thermodynamic projections, which lack data for these species. Thirty to forty percent of the F, Mn, and B feedstock concentration is observed to be released into the flue gas stream, while between 10 and 20 percent of the feedstock Mo, Sn, Cd, and Ge, and between 0 to 10 percent of the feedstock Be, Hg, Pb, Cr, Fe, Ni, Ti, Na, K, Al, Si, P, Cu, V, Zn, Sb, Zr, As, and Ga are observed in the flue gases. The flue gas release data support the interaction of F and B, possibly with the Ca fraction of the feedstock or sorbent material, forming CaF_2 or $3CaO.B_2O_5$, which minimizes the 100 percent volatility projection in a noninteractive system.

From the release data it is apparent that Be does not simply volatilize, but complexes with solids, possibly forming the thermodynamically projected $BeAl_2O_4$ phase. The concentration of Mn in the flue gas, however, exceeds the projected level, possibly because either a kinetic reaction mechanism enhances the volatility of the combusted Mn phases or the flue gas-contained elutriated fines contain a high Mn content. The flue gas data indicate that an adsorption mechanism may be responsible for the suppressed concentration of Hg, Pb, P, Cu, Mo, Cd, Ge, (Sb), Se, and As in the effluent streams, while Cr, Fe, Ni, Ti, Na, K, Zr, Al, Si, V, Zn, Sn, and Ga closely parallel the thermodynamic projections, forming stable solids that can be retained in the bed or removed by gas cleaning.

In the vaporization-condensation model Davison and Natusch[13] originally assumed that the condensation of a surface layer would result along the entrained particle, with a thickness that was independent of particle size. This model, according to Smith,[143] must obviously fail at some minimum particle size where the size of the surface layer approaches the particle radius. The chemical composition in the resulting particles is subject to change, not only from variation within the feedstock composition and combustion parameters, but also with the actual formation mechanism. Four mechanisms for the formation of submicron and micron particles include:

- Formation by homogeneous nucleation,[29] in which particles form from completely volatilized materials. This mechanism is expected to yield an extremely large concentration of particles <0.01 μm. Coalescence of these submicron particles into particles ranging from 0.1 to 1 μm in diameter is considered unlikely in pulverized coal plants, which demonstrate a concentration gradient as a function of the particle size profile.
- Formation by condensation of volatilized materials on smaller particles, composed primarily of soot from incomplete combustion under reducing condition.

- Formation by condensation of volatilized material on substrate particles resulting from submicron mineral inclusions in coal. Although heterogeneity is expected in the mineral inclusions of the feedstock, relatively homogeneous fly ash particles are formed within a uniform size fraction.
- Formation by bursting or fracturing of larger particles during rapid gas release and subsequent coalescence of smaller fragments. Condensation of the volatilized material may occur before, during, and/or after coagulation. The mechanism favors the coalescence or agglomeration of many small, liquid particles forming spherical particles in the 0.1 to 1.0 μm range, leading to interparticle homogeneity. The 5 to 100 μm cenospheres or plerospheres result from release of water vapor, sulfur oxides, and carbon dioxide from the feedstock particle, causing an initial ballooning of the liquid particle. Inner, smaller spheres result from an internal process also related to the release of gaseous phases. With temperatures in the combustor exceeding the temperature for cenosphere formation,* the low viscosity of the small particle causes it to burst into a shower of small particles.

Extension of the volatilization-condensation models needs to account for the relative concentration of potentially volatile and nonvolatile phases in the original feedstock material as well as a diffusion-limited volatility process and the transport process of phases from the particle surface. Potentially volatile phases may become entrapped within the aluminosilicate matrix and appear to enhance the elemental concentration in the resulting solids.

---

*Padia[144] demonstrated the formation of cenospheres at 1498 K. The calculated time for the formation of a 40 μm cenosphere from a 12 μm particle was on the order of 0.03 s at 1398 K, and 0.002 s at 1598 K.

CONTROL ALTERNATIVES

A substantial fraction of the trace and minor element concentration present in coal, limestone, or dolomite during combustion is retained with the fly ash and spent sorbent solids removed from the combustor and by emission control devices. However, significant quantities may still be emitted from the stack as vapors or in association with submicron particles. The trace and minor element concentration in the feedstock and in the resulting combustion products must not only be environmentally acceptable (below the hazardous or toxic pollutant level), but sufficiently low to minimize the potential formation of corrosive deposits within the fluidized-bed combustion system. Control alternatives include:

- Use of feedstocks containing low concentrations of potentially toxic trace or minor elements (Hg, Be, Pb, F, Cd, Se, As, Ni) and alkali (Na, K - the major constituents in corrosion).
- Pretreatment of the feedstock through water washing to dissolve and remove suspendable mineral matter or through a mild acid treatment, stripping Fe, Al, Ca, Mg, and SO_4 ions from the matrix. Preheating of the feedstock enhances devolatilization of many trace and minor elements and phases, permitting substitution of nonbonded, less-volatile elements or phases within the aluminosilicate matrix.
- A reduction of SO_x and alkali concentration in the effluent stream through the use of sorbent materials (limestone or dolomite) and aluminosilicate additives in order to minimize the potential for the formation of corrosive alkali sulfates. Liquid deposits of these materials can be eliminated if the combustor and, consequently, the turbine are operated at temperatures below the corrosive phase melt temperatures. Although this option prolongs system life, plant efficiencies are reduced.

- Particulate removal gas-cleaning devices have been proposed to reduce simultaneously the concentration of entrained ash/spent sorbent particulate material and volatiles released from the combustor. Particulate control equipment includes:[84]
    - Settling chambers in which larger pollutants and agglomerates are removed by gravity
    - Centrifugal collectors in which particulate matter is separated from the carrier gas by cyclones or mechanical precipitators
    - Electrostatic precipitators in which particles (particularly submicron ash) are electrically charged and collected on an earthed surface, which can then be removed through either a wet or dry process
    - Wet scrubbers, operating on the theory that gas streams carrying particulates and liquid droplets from flue gases impinge upon a surface and are removed, while small particles are collected after being electrically charged
    - Fabric or baghouse filters, removing solid particulate matter from gas streams by filtration. Fabric filters have an efficiency of more than 99.9 percent for particles down to 1 μm in diameter and 98 percent for particles down to 0.05 μm.[53] Control of Hg, As, and Se is enhanced when baghouse filters are used.[53]

Conventional equipment can be advantageously used in the fluidized-bed combustion system as a means of minimizing trace and minor element emissions. The lower combustion temperatures of the fluidized-bed combustion systems further reduce the volatility of the trace metals and, consequently, stack gas concentration levels below the conventional combustor levels. Similarly, the high pressures employed by PFBC raise the boiling point of many trace metals, thus decreasing emission via volatilization and/or condensation. With combustion of larger sized coal particles in the fluidized bed, a reduction in the emission of fine particulates containing higher concentrations of potentially hazardous or toxic trace and minor elements results.

9. REFERENCES

1. Lyon, W. S., Trace Element Measurements at the Coal-Fired Steam Plant. Cleveland: CRC Press; 1977.

2. Magee, E. M., H. J. Hall, and G. M. Varga, Jr., Potential Pollutants in Fossil Fuels. Report to EPA, Esso Research & Engineering Co., Linden, NJ, June 1973, NTIS PB 225-039.

3. Klein, D. H., A. W. Andren, and N. Bolton, Mass Balance for Thirty-three Elements at a Coal Fired Power Plant, Oak Ridge National Laboratories, Oak Ridge, TE, 1974.

4. Wewerka, E. M., J. M. Williams, P. L. Wanek, and J. D. Olsen, Environmental Contamination from Trace Elements in Coal Preparation Wastes. A Literature Review, Los Alamos Scientific Laboratory, Los Alamos, NM, NTIS PB 267-339.

5. Weir, A., The Environmental Effects of Trace Elements in the Pond Disposal of Ash and Flue Gas Desulfurizaton Sludge. Report to EPRI, Research Project 202, Southern California Edison Co., Rosemead, CA, September 1975.

6. Kaakinen, J. W., Trace Element Study in a Pulverized-Coal-Fired Power Plant, Dissertation, Boulder, CO: University of Colorado; 1974.

7. Bertine, K. K., and E. P. Goldberg, Fossil Fuel Combustion and the Major Sedimentary Cycles, Science, 173: 233-35; July 1971.

8. Merryman, E. L., A. Levy, G. W. Felton, K. T. Liu, Method for Analyzing Emissions from Atmospheric Fluidized Bed Combustors. Report to EPA, Battelle Memorial Laboratories, Columbus, OH, April 1977, EPA-600/7-77-034, NTIS PB 271-514.

9. Cowherd, C. M., M. Marcus, C. M. Guenther, J. L. Spigarelli, Hazardous Emisson Characteristics of Utility Boilers. Report to EPA, Midwest Research Institute, Kansas City, MO, July 1975, EPA-650/2-75-066, NTIS PB 245-017.

10. Cato, G. A., Field Testing, Trace Element and Organic Emissions from Industrial Boilers. Report to EPA, KVB Engineering Inc., Tustin, CA, October 1976, EPA-600/2-76-086b.

11. Ruch, R. R., H. J. Gluskoter, and N. F. Shimp, Occurrence and Distribution of Potentially Volatile Trace Elements in Coal. Report to EPA, Illinois State Geological Survey, July 1974, EPA-640/2-74-054, NTIS PB 238-091.

12. Gluskoter, H. J., An Introduction to the Occurrence of Mineral Matter in Coal, Illinois State Geological Survey, Urbana, Illinois. Proceedings of the International Conference on Ash Deposits and Corrosion from Impurities in Combustion Gases, New England College, Henniker, NH, June 26 - July 1, 1977.

13. Davison, R. L., D. F. S. Natusch, J. R. Wallace, and C. A. Evans, Jr., Trace Elements in Fly Ash - Dependence of Concentration on Particle size. Envi. Sci. and Techn., 8 (13): 1107-1113; December 1974.

14. Miller, W. G., Relationships between Minerals and Selected Trace Elements in Some Pennsylvanian Age Coals of Northwestern Illinois. University of Illinois, Urbana, IL, MS Thesis, 1974.

15. Gluskoter, H. J., R. R. Ruch, W. G. Miller, R. A. Cahill, G. B. Dreher, and J. K. Kuhn, Trace Elements in Coal: Occurrence and Distribution, Illinois State Geological Survey, Circular 499, Urbana, IL, 1977.

16. Ray, S. S., F. G. Parker, Characterization of Ash from Coal-Fired Power Plants, Tennessee Valley Authority, Chattanooga, TN, January 1977, NTIS PB 265-374.

17. Wender, I., Catalytic Synthesis of Chemicals from Coal, Catalysis Reviews Science and Engineering, 14 (1): 101; 1976.

18. Keller, W. D. Systematic Chemical Trace Element Study of a Producing Agstone Quarry, Pit and Quarry, 42 (11): 118-24; 1950.

19. Hoke, R., Emissions from Pressurized Fluidized Bed Combustion, Proceedings of the Fourth International Conference on Fluidized Bed Combustion. McLean, VA: The Mitre Corporation; 1976.

20. Swift, W. M., G. J. Vogel, A. F. Panek, and A. A. Jonke, Trace Element Mass Balances around a Bench-Scale Combustor, Proceedings of the Fourth International Conference on Fluidized Bed Combustion, McLean, VA: The Mitre Corporation; 1976.

21. Alvin, M. A., E. P. O'Neill, L. N. Yannopoulos, and D. L. Keairns, Evaluation of Trace Element Release from Fluidized-Bed Combustion Systems, Report to EPA, Westinghouse Research and Development Center, Pittsburgh, PA, March 1978, EPA-600/7-78-050, NTIS PB 281-321.

22. O'Neill, E. P., D. L. Keairns, and M. A. Alvin, Sorbent Selection for the CAFB Residual Oil Gasification Demonstration Plants, Report to EPA, Westinghouse Research Laboratory, Pittsburgh, PA, March 1977, EPA-600/7-77-029, NTIS PB 266-827.

23. Chamberlin, R. M., An Investigation of Hot Corrosion and Erosion Occurring in a Fluid Bed Combustor - Gas Turbine Cycle Using Coal as Fuel, Final report to Combustion Power, Westinghouse Research and Development, Pittsburgh, PA, May 5, 1977.

24. Ciliberti, D. F., A. Y. Ranadive, M. A. Alvin, and D. L. Keairns, Hot Gas Cleanup Using Ceramic Cross Flow Membrane Filters, Report to DOE, Westinghouse Research and Development Center, Pittsburgh, PA, Contract No. DE-AC01-ET 15491.

25. Mulik, P. R., D. F. Ciliberti, M. A. Alvin, and D. L. Keairns, Simultaneous High-Temperature Removal of Alkali and Particulates in a Pressurized Gasification System, Annual Technical Progress Report to DOE, Westinghouse Research and Development Center, Pittsburgh, PA, October 1978 - September 1979. Contract No. DE-AC21-78E11026.

26. Grim, R. E., Applied Clay Mineralogy, New York: McGraw Hill Book Company, Inc.; 1962.

27. Deer, W. A., R. A. Howie, and J. Zussman, An Introduction to the Rock-Forming Minerals, New York: John Wiley and Sons, Inc.; 1966.

28. Levin, E. M., C. R. Robbins and H. F. McMurdie, Phase Diagrams for Ceramists, Columbus, OH: The American Chemical Society; 1964.

29. Ulrich, G. D., An Investigation of the Mechanism of Fly-Ash Formation in Coal-Fired Utility Boilers, Quarterly and Annual Report for DOE February 1, 1977 - January 31, 1978; November 1, 1977 - January 31, 1978 and Quarterly Report, February 1 - April 30, 1978, Department of Chemical Engineering, University of New Hampshire, Durham, NH, Contract No. EX-76-C-01-2205.

30. Natusch, D. F. S., J. R. Wallace, and C. A. Evans, Jr., Toxic Trace Elements: Preferential Concentration in Respirable Particles, Science, 183:202; 1974.

31. Yannopoulos, L. N., J. L. Toth, and A. Pebler, Experimental Determination of Alkali Impurity Release from Various Dolomites, Combustion and Flame, 30: 61-69; 1977.

32. Lee, S. H. D., and I. Johnson, Removal of Gaseous Alkali Metal Compounds from Hot Flue Gas by Particulate Sorbents, Argonne National Laboratory, Paper presented at the 24th International Gas Turbine Conference, March 11-15, 1979, San Diego, CA.

33. Christensen, H. E. (ed.), et al., The Toxic Substance List, 1974 edit., U.S. Dept. of HEW, Public Health Service, Center for Disease Control, NIOSH, Rockville, MD.

34. Carpenter, R. L., and G. J. Newton, Variation in the Physical Characteristics of Fluidized Bed Combustor Exhaust Aerosol Arising from Combustion of Different Fuels, Annual Report of the Inhalation Toxicology Research Institute, Edited by R. F. Henderson, J. H. Diel, and B. S. Martinez, Lovelace Biomedical and Environmental Institute, Inc., Albuquerque, NM, October 1, 1977 - September 30, 1978, for DOE, Contract Number EY-76-C-04-1013.

35. Weissman, S. H., R. L. Carpenter, and G. J. Newton, Inorganic Composition of Particles Collected from Low Btu Gasifier Exhaust Streams, in Henderson, op. cit.

36. Weissman, S. H., R. L. Carpenter, G. J. Newton, and C. H. Hobbs, Elemental Profile of Fluidized Bed Coal Combustor Fly Ash: Effect of Fuel, Bed Material and Operating Parameters, in Henderson, op. cit.

37. Sheridan, C. J., R. C. Pfleger, and R. O. McClellan, Cytotoxicity of Vanadium Pentoxide on Pulmonary Aveolar Macrophages from Dog, Rabbit, and Rat: Effect on Viability and Effect on Lipid Metabolism, in Henderson, op. cit.

38. Hill, J. O., Immunotoxicology of Fossil Fuel Effluents: Complement Activation, in Henderson, op. cit.

39. Clark, C. R., R. L. Hanson, and A. Sanchez, Mutagenicity of Effluents Associated with Fluidized Bed Combustion of Coal, in Henderson, op. cit.

40. Royer, R. E., C. E. Mitchell,and R. L. Hanson, Chemical Characterization and Mutagenicity of Potential Low Btu Gasifier Effluents, in Henderson, op. cit.

41. Hill, J. O., and C. E. Mitchell, In Vitro Cytotoxicity Testing of Potential Effluents from the Fluidized Bed Combustion and Low BTU Gasification of Coal, in Henderson, op. cit.

42. Cleland, J. G., G. L. Kingsbury, Minimum Acute Toxicity Effluent (MATE) Values for Organic and Inorganic Compound from Fossil Energy Processes, A Subset of Multimedia Goals for Environmental-Assessment Use in Rapid Screening of Effluents, Research Triangle Institute, Research Triangle Park, NC, EPA 68-02-2612, draft 5/10-77. RTI Project No. 41U-1430-10.

43. Greenwood, D. R., G. L. Kingsbury, and J. G. Cleland, A Handbook of Key Federal Regulations and Criteria for Multimedia Environmental Control, Research Triangle Institute, Research Triangle Park, NC, August 1979, EPA-600/7-79-175.

44. Berry, L., and A. Wallace, Trace Elements in the Environment -- Their Role and Potential Toxicity as Related to Fossil Fuels -- A Preliminary Study, University of California, Los Angeles, CA, January 1974.

45. Mitchell, J. E., Fluidized Bed Combustor Monthly Progress Report for October 1978, Exxon Research and Engineering Company, Linden, NJ (Ref. No.: 78FR1347).

46. Carpenter, L., H. Weissman, G. J. Newton, R. L. Hanson, and E. R. Peele, Characterization of Aerosols Produced by an Experimental Fluidized-Bed Coal Combustor Operated with Sub-bituminous Coal, Lovelace Biomedical and Environmental Research Institute, Albuquerque, NM, February 1978.

47. Forney, A. J., W. R. Haynes, S. J. Gasior, R. M. Kornosky, C. E. Schmidt, and A. G. Sharkey, Trace Element and Major Component Balances around the Synthane PDU Gasifier, Pittsburgh Energy Research Center, Pittsburgh, PA, August 1975.

48. Lee, S. H., I. Johnson, and J. Fischer, A Study of the Volatility of Minor and Trace Elements in Illinois Coal, Argonne National Laboratory, Argonne, IL, August 1977, ANL/CEN/FE-77-4.

49. Raridon, R. J., Pathways of Trace Elements in the Environment, Union Carbide Corporation, Oak Ridge, TN, Presidential Address to the Association of Academies of Science, February 21, 1977, Denver, CO.

50. Werner, A. S., Inorganic and Trace Element Emissions from the Chemically Active Fluid Bed (CAFB) Process, GCA Technology Division, Contract Number 68-02-1316, T. O. No. 14.

51. Ragaini, R. C., and J. M. Ondov, Trace-Element Emissions from Western U. S. Coal-Fired Plants, Lawrence Laboratory, University of California, Livermore, CA, October 11, 1976.

52. Wilde, K. A., and M. E. Halbrook, Thermodynamic Distribution of Trace Elements by Minimization of Free Energy, Ind. Eng. Chem. Fundam., 16 (4): 489-92; 1977.

53. Yeh, J. T., C. R. McCann, J. J. Demeter, and D. Bienstock, Removal of Toxic Trace Elements from Coal Combustion Effluent Gas, Pittsburgh Energy Research Center, Pittsburgh, PA, September 1976, PERC/RI-76/5.

54. Argonne National Laboratory, Argonne, IL, Reduction of Atmospheric Pollution by the Application of Fluidized-Bed Combustion, Monthly, Quarterly, and Annual Reports, 1970-1975.

55. Argonne National Laboratory, Argonne, IL, Supportive Studies in Fluidized-Bed Combustion, July 1976 - June 1977.

56. Babcock & Wilcox, Fluidized-Bed Combustion Development Facility and Commercial AFBC Design Assessment, Quarterly Technical Progress Report, April-June 1978.

57. National Coal Board, London, UK, Reduction of Atmospheric Pollutants, June 1970-1971.

58. Pope, Evans and Robbins, Characterization and Control of Gaseous Emissions from Coal-Fired Fluidized-Bed Boiler, October 1970.

59. Pope, Evans and Robbins, Study of the Characterization and Control of Air Pollutants from a Fluidized-Bed Boiler - The SO_2 Acceptor Process, July 1972.

60. Pope, Evans and Robbins, Multicell Fluidized-Bed Boiler Design, Construction and List Program, August 1974.

61. Attari, A., J. Paw, and M. Mensinger, Fate of Trace and Minor Constituents of Coal during Gasification, Institute of Gas Technology, September 1976.

62. Swift, W. M., G. W. Smith, and F. G. Teats., Supportive Studies on Fluidized-Bed Combustion. Task C. Trace Pollutant Control in FBC, Argonne Quarterly Report for Jan-March, 1978, ANL-CEN/FE-8-3.

63. Coleman, W. M., P. Perfetti, H. C. Dorn, and L. T. Taylor, Trace-Element Distribution in Various Solvent Fractions as a Function of Coal Feed, Fuel, 57: 612-16; 1978.

64. Mroz, E. J., The Study of the Elemental Composition of Particulate Emissions from an Oil-Fired Power Plant, University of Maryland, College Park, MD, PhD Thesis, 1976.

65. Alvin, M. A., E. P. O'Neill, and D. L. Keairns, Thermodynamic Projections of Trace Element Release in Fluidized-Bed Combustion Systems, Proceedings of the 5th International Conference on Fluidized-Bed Combustion, McLean, VA: The Mitre Corporation; 1978.

66. Ciliberti, D. F., M. M. Ahmed, N. H. Ulerich, M. A. Alvin, and D. L. Keairns, Experimental/Engineering Support for EPA's FBC Program: Final Report - Volume II. Particulate, Nitrogen Oxide, and Trace Element Control. Report to EPA, Westinghouse Research and Development Center, Pittsburgh, PA, January 1980, EPA-600/7-80-015b.

67. Duffin, R. J., E. L. Peterson, and C. Zener, Geometric Programming, New York: John Wiley and Sons; 1967.

68. Chase, M. W., J. L. Curnutt, H. Prophet, R. A. McDonald, and A. N. Syverud, JANAF Thermochemical Tables, Journal of Physical and Chemical Reference Data, National Bureau of Standards, 2nd Edition, and 1974-1975 supplements.

69. Hertzberg, G., Molecular Spectra and Molecular Structure I-III, New York: D. Van Nostrand Co., Inc.; 1945, 1950, 1966.

70. Glassner, A., The Thermochemical Properties of the Oxides, Fluorides and Chlorides to 2500 K, Argonne National Laboratory, Argonne, IL, ANL-5750, 1957.

71. Barin, J., and O. Knacke, Thermochemical Properties of Inorganic Substances, Berlin: Springer-Verlag; 1973.

72. Oppermann, Von H., Fur Anorzanische und Allgemeine Chemie, Band 359 (52); 1968.

73. Krasnov, K. S., Handbook: Molecular Constants of Inorganic Compound, Khumiya, 1968.

74. National Bureau of Standards, NBS TN 270-3, Selected Values of Chemical Thermodynamic Properties, 1968.

75. Feber, R. C., Heats of Dissociation of Gaseous Halide, Los Alamos Scientific Laboratory, Los Alamos, NM, LA-4163, TSC-4, Chemistry TID-3500 (40th ed.), 1965.

76. Schick, H. L., Thermodynamics of Certain Refractory Compounds, New York: Academic Press; 1966.

77. Robie, R., and D. R. Waldbaum, Thermodynamic Properties of Minerals and Related Substances at 298.15 K (25.0 C) and One Atmosphere (1.013 Bars) Pressure and at Higher Temperatures, Geological Survey Bulletin 1259, U.S. Government Printing Office, Washington, D.C., 1968.

78. Spencer, F. E., J. C. Hendrie, Jr., and D. Bienstock, A Ternary Margules-Type Model for Plasma/Slag Equilibrium in Potassium Seeded Coal Combustion for Magnetohydrodynamic Power Generation: Calculations and Comparison with Experiments, U.S. Energy Research and Development Administration, Paper presented at the Sixth International Conference on Magnetohydrodynamic Electrical Power Generation, Washington, D.C., June 9-13, 1975.

79. Gordon, G. E., D. D. Davis, G. W. Israel, H. E. Landsberg, T. C. O'Haver, S. W. Staley, and W. H. Zoller, Study of the Emissions from Major Air Pollution Sources and Their Atmospheric Interactions, University of Maryland, College Park, MD, Prepared for the National Science Foundation for the period November 1, 1972 - October 31, 1974.

80. Torrey, S. ed., Trace Contaminants from Coal, Pollution Technology Review No 50, Park Ridge, NJ: Noyes Data Corporation; 1978.

81. Cox, J. A., G. L. Lundquist, A. Przyjazny, and C. D. Schmulbach, Leaching of Boron from Coal Ash, Environmental Science and Technology, June 1978.

82. Weast, R. C., Handbook of Chemistry and Physics, Forty-Ninth Edition, Cleveland, OH: The Chemical Rubber Co.; 1968.

83. A Review of Current Information on Some Ecological and Health Related Aspects of Trace Metals Into the Environment Associated with the Combustion of Coal, S. Torrey ed., Trace Contaminants from Coal, Pollution Technology Review No. 50, Park Ridge, NJ: Noyes Data Corporation; 1978.

84. Lim, M. Y., Trace Elements From Coal Combustion, IEA Coal Research, London, Report Number ICTIS/TR05, May 1979.

85. Hall, H. J., G. M. Varga, and E. M. Magee, Trace Elements and Potential Pollutant Effects in Fossil Fuels. Proceedings of Symposium on Environmental Aspects of Fuel Conversion Technology, St. Louis, MO, May 1974.

86. Piperno, E., Trace Element Emissions; Aspects of Environmental Toxicology, Trace Elements in Fuels, (ed. S. P. Babu) Advances in Chemistry Series, American Chemical Society, Washington, D.C., 1975.

87. Reid, W. T., External Corrosion and Deposits, Boilers and Gas Turbines, New York: American Elsevier Publishing Co., Inc.; 1971.

88. Stringer, J., Hot Corrosion of High Temperature Alloys, Department of Metallurgy and Material Science, University of Liverpool, Liverpool, England; August 20, 1976. (Contract/Grant Number: AFOSR-72-2388)

89. Jones, R. L., and S. T. Gadomski, Mixed Sulfate/SO_3 Reactions in Low Power Hot Corrosion: A Possible Harmful Effect of Platinum Coatings, NRL letter report 6170-773a:RLJ:blr, sponsored under NAVSEA Program for Advanced Materials Development to Support Marine Gas Turbine Engines, November 1, 1977.

90. Barkalow, R. H., and F. S. Pettit, Marine Gas Turbine Hot Corrosion Dependence on Ingested Salt Levels, First Quarterly Report by Materials Engineering and Research Laboratory at Pratt and Whitney Aircraft, Naval Research Laboratories, Washington, D.C. (Contract Number N00173-77-C-0206).

91. Aprigliano, L. F., Burner-Rig Simulation of Low-Temperature Hot Corrosion, Materials Department at David W. Taylor Naval Ship Research and Development Center, Bethesda, MD, November 1977, MAT-77-68.

92. Clark, P. U., Fused Salt Mixtures: Eutectic Compositions and Melting Points, Sandia Corp., Albuquerque, NM, 1968, SC-R-68-1680.

93. Hemmings, P. L., and R. A. Perkins, Thermodynamic Phase Stability Diagrams for the Analysis of Corrosion Reactions in Coal Gasification/Combustion Atmospheres. Interim Report FP-539, Research Project 716-1, to EPRI, Lockheed Palo Alto Research Laboratories, Palo Alto, CA, December 1977.

94. Gluskoter, H. J., and R. R. Ruch, Chlorine and Sodium in Illinois Coals as Determined by Neutron Activation Analysis, Fuel, 1971.

95. Spengler, C. J., The Upper Three-Phase Region in a Portion of the System $KAlSi_2O_6$-SiO_2-H_2O at Water Pressures from Two to Seven Kilobars, Pennsylvania State University, College Park, PA, PhD Thesis, June 1965.

96. Frieberg, L., Toxicity of Metals, Volume II, Research Triangle Park, Subcommittee on the Toxicology of Metals, Permanent Commission and International Association of Occupational Health, EPA, May 1977, NTIS PB 268-324.

97. Diehl, R. C., E. A. Hattman, H. Schultz, and R. J., Haren, Fate of Trace Mercury in the Combustion of Coal, Report on Managing Coal Wastes and Pollution Program, Technical Progress Report, Pittsburgh Energy Research Center, Pittsburgh, PA, May 1972, NTIS PB 210-226.

98. Bolton, N., R. Van Hook, W. Fulkerson, W. Lyon, and A. Andren, Trace Element Measurements at the Coal-Fired Allen Steam Plant, Progress Report June 1971 -January 1973, Oak Ridge National Laboratory, Oak Ridge, TN, March 1973, ORNL-NSF-EP-43.

99. Klein, D. H., A. W. Andren, J. A. Carter, J. F. Emery, C. Feldman, W. Fulkerson, W. S. Lyon, J. C. Ogle, Y. Talmi, R. I. Van Hook, and N. Bolton, Pathways of Thirty-Seven Trace Elements through Coal-Fired Plant, Envi. Sci. and Techn., 9 (10): 973-79; 1975.

100. Schroeder, H. A., Metals in Air, Environment, 13 (8): 18-31; October 1971.

101. Dunlap, L., Mercury: Anatomy of a Pollution Problem, Chem. Eng. News, 49 (27): 22-34; July 1971.

102. Environmental Mercury and Man, Report of an Interdepartmental Working Group on Heavy Metals, Central Unit an Environmental Pollution, Department of Environment, Pollution Paper 10, HMSO, 1974.

103. Grant, N., Mercury in Man, Environment, 13 (4): 2-15; May 1971.

104. Berry, W. L., and A. Wallace, Trace Elements in the Environment, Their Role and Potential Toxicity as Related to Fossil Fuels: A Preliminary Study. Los Angeles, California University, Laboratory of Nuclear Medicine and Radiation Biology, January 1974, Report No. UCLA-12-946.

105. Van Hook, R. I., and W. D. Shults, Effects of Trace Contaminants from Coal Combustion, Proceedings of a Workshop, Knoxville, TN, August 2-6, 1976, ERDA, Division of Biomedical and Environmental Research, June 1977.

106. Pierson, D. H., P. A. Cawse, L. Salmon and R. S. Cambray, Trace Elements in the Atmospheric Environment, Nature, 241 (5387): 252-56; January 26, 1973.

107. Vaughan, B. E., K. H. Abdel, D. A. Cataldo, J. M. Hales, C. E. Hanes, L. A. Rancitelli, R. C. Rouston, R. E. Wildung, and E. G. Wolf, Review of Potential Impact on Health and Environmental Quality from Metals Entering the Environment as a Result of Coal Utilization, Battelle Energy Program Report, Richland Battelle Memorial Institute, August 1975.

108. Bertrand, R. R., et al., A Regenerative Limestone Process for Fluidized Bed Coal Combustion and Desulfurization, Monthly Report No. 65, Exxon Research and Engineering Company to EPA, Linden, NJ, January 1-31, 1978, Contract No. 68-02-1312.

109. Hoke, R. C., Fluidized Bed Combustor Monthly Progress Report, Task 3 Comprehensive Analysis, Exxon Research and Engineering Company, to EPA, December 1978, Ref. No. 78 GR 1347.

110. Merryman, E. L., A. Levy, G. W. Felton, K. T. Liu, J. M. Allen, and H. Nack, Method for Analyzing Emissions from Atmospheric Fluidized-Bed Combustor, Final Report to EPA, Battelle-Columbus Laboratory, Columbus, OH, April 1977, EPA-600/7-77-034.

111. Private Communication, P. F. Fennelly, GCA Corporation, Technology Division, Bedford, MA, December 4, 1979.

112. Wu, E. J., W. W. Choi, and K. Y. Chen, Chemical Affiliation of Trace Metals in Coal Ash, Environmental Engineering Program, University of Southern California, Los Angeles, CA, Paper presented at the 87th AIChE National Meeting, Boston, MA, August 19-22, 1979.

113. Jonke, A. A. et al., Annual Report on a Development Program in Pressurized Fluidized-Bed Combustion, Argonne National Laboratories, Argonne, IL, July 1976, ANL/ES-CEN-1016.

114. Studies of the Pressurized Fluidized-Bed Coal Combustion Process, Office of Research and Development. Report to EPA, Exxon Research and Engineering Co., Linden, NJ, September 1977, EPA-600/7-77-107, NTIS PB 272-722.

115. Wilson, J. S., and R. Rice, EPA-sponsored FBC run, Morgantown Energy Research Center (MERC),* Morgantown, WV; March 31, 1977.

116. SO_2 Absorption in Fluidized-Bed Combustion of Coal-Effect of Limestone Particle Size. Report to EPRI, Babcock and Wilcox Company, March 31, 1977, RP719-1.

117. Hall, A. M., Testing, Identification, and Evaluation of Commercial and "Advanced Experimental" Materials and Coatings under Design Conditions Simulating Fuel Power Cycle Combinations, Task II. Monthly Technical Progress Report No. 12 to ERDA, Battelle Columbus Laboratories, Columbus, OH; June 6, 1977, FE-2325-12.

118. Energy Conversion from Coal Utilizing CPU-400 Technology, Combustion Power Company, Contract No. E(49-18)-1536, March 1976.

119. Sun, C. C., C. H. Peterson, and D. L. Keairns, Experimental/ Engineering Support for EPA's FBC Program: Final Report - Volume III. Solid Residue Studies, Report to EPA, Westinghouse Research and Development Center, Pittsburgh, PA, January 1980, EPA-600/7-80-015c.

120. Linton, R. W., P. Williams, C. A. Evans, Jr., and D. F. S. Natusch, Analytic Chemistry, 49: 1514; 1977.

121. Keyser, T. R., D. F. S. Natusch, C. A. Evans, Jr., and R. W. Linton, Environmental Science Technology, 12: 769; 1978.

---

*Now Morgantown Energy Technology Center (METC).

122. Mims, C. A., M. Neville, R. J. Quann, and A. F. Sarofim, Laboratory Studies of Trace Element Transformations During Coal Combustion, Massachusetts Institute of Technology, Paper presented at the National 87th AIChE Meeting, Boston, MA, August 19-22, 1979.

123. Fischer, G. L., Potential Health Significance of Coal Fly Ash, Radiobiology Laboratory, University of California, Davis, CA, prepared for the Symposium of Trace Metals and Toxic Substances from Coal Combustion, 87th National AIChE Meeting, Boston, MA, August 19-22, 1979.

124. Mann, R. M., R. A. Magee, R. V. Collins, M. R. Fuchs, and F. G. Mesich, Final Report - Trace Elements of Fly Ash: Emissions from Coal-Fired Steam Plants Equipped with Hot-Side and Cold-Side Electrostatic Precipitators for Particulate Control, Report to EPA, Radian Corporation, Austin, TX, December 1978, EPA 908/4-78-008, DCN 78-216-137-09.

125. Lee, R. E., Jr., H. L. Crist, A. E. Riley, and K. E. Macleod, Concentration and Size of Trace Metal Emissions from a Power Plant, a Steel Plant, and a Cotton Gin. Envi. Sci. and Techn., 9 (7): 643-47; July 1975.

126. Kaakinen, J. W., R. M. Jorden, M. H. Lawasani, and R. E. West, Trace Element Behavior in Coal-Fired Power Plant. Envi. Sci. and Techn., 9 (9): 862-69; September 1975.

127. Kaakinen, J. W., and R. M. Jorden, Determination of a Trace Element Mass Balance for a Coal-Fired Power Plant, Presented at First Annual National Science Foundation Conference on Trace Contaminants, Oak Ridge, TN. August 1973.

128. Magee, R. A., F. B. Meserola, and R. G. Oldham, Coal Fired Power Plant Trace Element Study. Vol. I: A Three Station Comparison. Report to EPA, Radian Corporation. Austin, TX. September 1975.

129. Magee, R. A., et al., op. cit., Vol. II: Station I.

130. Magee, R. A., et al., op. cit., Vol. III: Station II.

131. Magee, R. A., et al., op. cit., Vol. IV: Station III.

132. Fennelly, P. F., Emission Estimates of Organic and Inorganic Compounds from Coal Fired Fluidized Bed Combustion, GCA/Technology Division, Bedford, MA, Presented at the 70th Annual Meeting of the Air Pollution Control Association, Toronto, Ont., Canada, June 20-24, 1977.

133. Fennelly, P. F., D. F. Durocher, R. Hall, and H. Klemm, Preliminary Environmental Assessment of Coal-Fired Fluidized Bed Combustion. Draft Report to EPA, GCA/Technology Division, June 1976, Contract No. 68-02-1316.

134. Lee, M. L., D. W. Later, D. K. Rollins, D. J. Eatough, and L. D. Hansen, Dimethyl and Monomethyl Sulfate: Presence in Coal Fly Ash and Airborne Particulate Matter, Science, 207: 186-87; January 11, 1980.

135. Druckrey, H., R. Preussmann, N. Nashed, and S. Ivankovic, Z. Krebsforsch, 68: 103; 1966.

136. Druckrey, H., H. Kruse, R. Preussmann, S. Ivankovic, and C. Landshutz, Z. Krebsforsch, 74: 241; 1970.

137. Couch, D. B., N. L. Forbes, and A. W. Hsie, Mutat. Res. 57: 217; 1978.

138. Hollaender, A. (ed.), Chemical Mutagens: Principles and Methods for Their Detection, Vols. 1-3, New York: Plenum Press; 1971.

139. Lowley, P. D., in Chemical Carcinogens, C. E. Searle (ed.), Monograph 173, American Chemical Society, Washington, D.C., 1976.

140. Werner, A. S., C. W. Young, W. Piispanen, and B. M. Myatt, Preliminary Environmental Assessment of the Lignite-Fired CAFB, report to EPA, GCA Corporation, Bedford, MA, February 1979, EPA-600/7-79-048.

141. Swift, W. M., G. J. Vogel, A. F. Panek, and A. A. Jonke, Trace-Element Mass Balance around a Bench-Scale Combustor, Paper presented at the 68th Annual Meeting of the Air Pollution Control Association, Boston, MA, June 15-20, 1975.

142. Mazza, M. H., D. A. Green, M. W. Paris, and G. J. Newton, Mineral Characterization of Fluidized-Bed Combustion Aerosol Ash -- Montana Rosebud Sub-bituminous Coal, Morgantown Energy Research Center, and Lovelace Biomedical and Environmental Research Institute, MERC/TPR-78/1, Distribution Category UC-90, April 1978.

143. Smith, R. D., The Trace Element Chemistry of Coal During Combustion and the Emissions From Coal-Fired Plants, Progress in Energy and Combustion Science, 6 (1): 53-119; 1980.

144. Padia, A. S., The Behavior of Ash in Pulverized Coal under Simulated Combustion Conditions, Massachusetts Institute of Technology, Cambridge, MA, PhD Thesis, 1976.

APPENDIX A

SUMMARY OF THE ELEMENTAL CONCENTRATIONS, CONSIDERED PHASES AND EQUILIBRIUM REACTIONS

TABLE A1 - ELEMENTAL CONCENTRATION AND CONSIDERED PHASES

```
                            GAS PHASES          SOLID/CONDENSED PHASES
C   70.28%                    BEC2                   BE
H    4.95%                    BECL                   BECL2
N    1.30%                    BECL2                  BEO
O    8.68%                    BE2CL4                *BESO4
S    4.00%                    BEH                    BE2C
CL   0.28%                    BEH2                   BE3N2
BE   1.61 PPM (COAL)          BEN
       4 PPM (SORBENT)        BEO
                             *BE(OH)2
                              BE2O
                              BE2O2
*PROJECTED ACTIVE FBC EQUILIBRIUM PHASES

MAJOR VOLATILE PHASES:BE(OH)2
MAJOR SOLID PHASES:BESO4, BEO.AL2O3
PRINCIPAL REACTIONS:
                                  700-800K
                         BESO4 (S)----------> BEO (S) + SO2 (G)  + 1/2O2 (G)
                         BESO4 (S) + H2O (G)----> BE(OH)2(G) + SO2 (G)  + 1/2O2 (G)
                                                 OR
                         BEO (S) + H2O (G)------> BE(OH)2 (G)
                         THE REACTION OF BE WITH AL RESULTS IN THE FORMATION OF
                           BEO.AL2O3 (S) AT TEMPERATURES  >500K.

MINIMUM ACUTE TOXICITY EFFLUENT LEVEL (PPM):
      BE AND COMPOUNDS:  2.00E0
PERCENT BERYLLIUM VOLATILIZATION AT EQUILIBRIUM
  FOR 1200-1300K OPERATIONS: 100%
```

TABLE A2 - ELEMENTAL CONCENTRATION AND CONSIDERED PHASES

```
                         GAS PHASES                     SOLID/CONDENSED PHASES
C   70.28%               CF        *FNA     SF4           FK
H    4.95%               CFO       FN       SF5           FNA
N    1.30%               CFN       FNO      SF6           F2NK
O    8.68%               CF2       FNO2    *HSO3F
S    4.00%               CF2O      FNO3
CL   0.28%               CF3       FO
F   60.94 PPM (COAL)     CF4       FO2
    10 PPM (SORBENT)     CF4O      F2
                         CHCLF2    F2K2
                         CHCL2F    F2N
                         CHFO      F2N2
                         CHF3      F2NA2
                         CH2CLF    F2O
                         CH2F2     F2OS
                         C2F3N     F2O2S
                         C2HF      F3CL
                         CCLFO     F3N
                         CCLF3     F3NO
                         CCL2F2    F4N2
                         CCL3F     F5CL
                         F        *HF
                         FCL       SF
                         FHO       SF2
                        *FK        SF3
*PROJECTED ACTIVE FBC EQUILIBRIUM PHASES

MAJOR VOLATILE PHASES:HF, KF, NAF, HSO3F
MAJOR SOLID PHASES:--
PRINCIPAL REACTIONS:
                                 >1000K
                         HSO3F (G) ---------> HF (G) + 1/2O2 (G) + SO2 (G)
                         FOR  99% SULFUR REMOVAL SYSTEMS:
                                         300-800K
                         HF (G) + NACL (S)----------> NAF (S) + HCL (G)
                         THE REACTION OF GASEOUS F WITH CA OR MG  RESULTS IN
                           THE FORMATION OF  CAF2 (S) (600-1000K) AND MGF2(S)
                           (<600K).  SIMILARLY THE MAJOR REACTIONS OF F WITH
                           PB IN FBC SYSTEMS LEAD TO THE FORMATION OF PBF4 (G) AND
                           PBF2 (G).  IN THE PRESENCE OF SI AT 300K, REACTION
                           WITH F LEADS TO THE FORMATION OF GASEOUS SIF4. SI
                           ALSO COMPLEXES WITH NA IN THE SYSTEM TO FORM THE
                           WATER GLASS PHASE, MINIMIZING THE POTENTIAL OF
                           FORMING EITHER SOLID OR VOLATILE NAF.
                           VOLATILE NIF2, CDF, ALF2O, GAF, BECLF, CUF, ASF3,
                           PBF2, PBF, COF2 PHASES ARE PROJECTED IN THE
                           INTERACTIVE EQUILIBRIUM SYSTEMS.
                           SOLID ALF3 FORMS BETWEEN 300 AND 600K IN PFBC SYSTEMS.
MINIMUM ACUTE TOXICITY EFFLUENT LEVEL (PPM):
      F(-):   2.50E3
PERCENT FLUORINE VOLATILIZATION AT EQUILIBRIUM
  FOR 1200-1300K OPERATIONS: 100%
```

TABLE A3 - ELEMENTAL CONCENTRATIONS AND CONSIDERED PHASES

```
C    70.28%           GAS PHASES          SOLID/CONDENSED PHASES
H     4.95%            *HG                     HG
N     1.30%            *HG2                    HGS
O     8.68%            *HGCL                   HGCL2
S     4.00%            *HGCL2                  HG2CL2
CL    0.28%            *HGH                    HGO
HG    0.20 PPM (COAL)  *HGO
      0.16 PPM (SORBENT)
*PROJECTED ACTIVE FBC EQUILIBRIUM PHASES

MAJOR VOLATILE PHASES:HG, HGCL2, HGO, HG2, HGCL
MAJOR SOLID PHASES:--
PRINCIPAL REACTIONS:
                         T>900K
                HGCL2 (G)------> HG (G) + 2CL (G)
                HG (G) + 1/2O2 (G)------> HGO (G)
MINIMUM ACUTE TOXICITY EFFLUENT LEVEL (PPM):
     ALKYL MERCURY:   1.00E1
PERCENT MERCURY VOLATILIZATION AT EQUILIBRIUM
  FOR 1200-1300K OPERATIONS: 100%
```

TABLE A4 - ELEMENTAL CONCENTRATION AND CONSIDERED PHASES

```
C   70.28%                GAS PHASES          SOLID/CONDENSED PHASES
H    4.95%                   PB                        PB
N    1.30%                   PB2                       PBCO3
O    8.68%                  *PBCL                      PBCL
S    4.00%                  *PBCL2                     PBO
CL   0.28%                  *PBCL4                     PBO2
PB  34.78 PPM (COAL)         PBH                       PB3O4
    18.5 PPM (SORBENT)      *PBO                       PBS
                             PBS                       PBSO4
                                                       PBO.PBSO4
                                                       2PBO.PBSO4
*PROJECTED ACTIVE FBC EQUILIBRIUM PHASES               4PBO.PBSO4

MAJOR VOLATILE PHASES:PBCL4, PBCL2,PBO,PBCL
MAJOR SOLID PHASES:--
PRINCIPAL REACTIONS:
                 PBCL4 (G) + 2H2O (G) ----> PBO (G) + 4HCL (G) + 1/2O2 (G)
                            1000-1100K
                 PBCL4 (G) -------------> PBCL2(G) + 2CL (G)
                 PBCL2 (G) ---> PBCL (G) + CL (G)
MINIMUM ACUTE TOXICITY EFFLUENT LEVEL (PPM):
     PBO:                  2.00E2
     PBS:                  1.50E2
     PB ARSENATE:          1.50E2
     PB INORGANIC FUME:    1.50E2
PERCENT LEAD VOLATILIZATION AT EQUILIBRIUM
  FOR 1200-1300K OPERATIONS: 100%
                 THE REACTION OF GASEOUS F AND PB RESULTS IN THE
                   FORMATION OF PBF4 AND PBF2 GASES.
                 NOTE THAT IN PRESSURIZED SYSTEMS PBCL4 GAS IS THE
                   PREDOMINANT VOLATILE PHASE, WHILE AT AMBIENT
                   CONDITIONS PBO IS FAVORED.
```

TABLE A5 - ELEMENTAL CONCENTRATION AND CONSIDERED PHASES

```
                            GAS PHASES          SOLID/CONDENSED PHASES
C   70.28%                    CO                       CO
H    4.95%                  *COCL                      COCL2
N    1.30%                  *COCL2                    *COO
O    8.68%                  *COCL3                    *COSO4
S    4.00%                  *COCL4                    *CO3O4
CL   0.28%                   CO2CL4                    COS.89
CO   9.57 PPM
*PROJECTED ACTIVE FBC EQUILIBRIUM PHASES

MAJOR VOLATILE PHASES:COCL2, COCL3, CO2CL4, COCL
MAJOR SOLID PHASES:COSO4, CO3O4, COO
PRINCIPAL REACTIONS:
                                            900-1100K
                         3COSO4 (S) + 1/2O2 (G) -------------> CO3O4 (S) + 3SO2 (G)
                                                                   + 3/2O2 (G)
                         AND
                         COSO4 (S) ----> COO (S) + SO2 (G) + 1/2O2 (G)
                         CO3O4 (S) ----> 3COO (S) + 1/2O2 (G)
                         COSO4 (S) + 2HCL (G) ----> COCL2 (G) + H2SO4 (G)
                         CO3O4 (S) + 6HCL (G) ----> 3COCL2 (G) + 3H2O (G)
                                                              + 1/2O2 (G)
                         COO (S) + CL2 (G) ----> COCL2 (G) + 1/2O2 (G)
                         2COCL2 (G) + CL2 (G) ----> 2COCL3 (G)
                         THE EQUILIBRIUM REACTION OF CR WITH CO IN FBC SYSTEMS
                           LEADS TO THE FORMATION OF THE STABLE COBALT CHROMATE
                           (COO.CR2O3) AT TEMPERATURES BETWEEN 300K AND 1200K.

MINIMUM ACUTE TOXICITY EFFLUENT LEVEL (PPM):
      CO FUME:     1.00E2
      COCL2:       1.60E3
      CO(CO)4:     1.40E5
      COS          3.15E3
      CO(NO3)2:    2.70E2
      COO:         2.36E3
PERCENT COBALT VOLATILIZATION AT EQUILIBRIUM
  FOR 1200-1300K OPERATIONS: 13.76%; FOR REACTION WITH
  CR IN AN INTERACTIVE SYSTEM 21.12% VOLATILIZATION OF
  COAL-CONTAINED COBALT IS PROJECTED.
```

TABLE A6 - ELEMENTAL CONCENTRATION AND CONSIDERED PHASES

```
C   70.28%              GAS PHASE              SOLID/CONDENSED PHASES
                         •CR                          CR
H    4.95%               •CRCL                        CR(CO)6
N    1.30%               •CRCL2                       CRCL2
O    8.68%               •CRCL3                       CRN
S    4.00%               •CRCL4                       CRO2
CL   0.28%                CRN                         CRO3
CR  13.75 PPM            •CRO                         CRS3
                         •CRO2                        CR2(CO3)3
                         •CRO2CL2                     CR2N
                         •CRO3                       •CR2O3
                         •CRO2(OH)2                   CR2S3
                         •CRO2OH                      CR2(SO3)3
                          CRS                         CR2(SO4)3
                          CR2                         CR3C2
                          CR(CO)6                     CR4C
                                                      CR7C3
                                                      CR23C6
•PROJECTED ACTIVE FBC EQUILIBRIUM PHASES              CRCL3

MAJOR VOLATILE PHASES:CRO4H2, CRO2CL2, CRO2OH,CRO3 (GREATER THAN 1OE-10 ATM)
MAJOR SOLID PHASES:CR2O3
PRINCIPAL REACTIONS:
                                                   >1000K
                 CR2O3 (S) + 2H2O (G) + 3/2O2 (G) -----------> 2CRO4H2 (G)
                                                  400-800K
                 CR2O3 (S) + 4HCL (G) + 3/2O2 (G)----------> 2CRO2CL2 (G) +
                                                                 2H2O (G)
                 IN SULFUR FREE FBC SYSTEMS K IS NO LONGER PRESENT AS
                    K2SO4, BUT REACTS WITH CR TO FORM K2CR2O7 AT
                    TEMPERATURES GREATER THAN 800K. SIMILAR REACTIONS
                    ARE PROJECTED FOR NA.
                 IN THE PRESENCE OF MG, CR REACTS TO  FORM MGO.CR2O3
                    (S) AT TEMPERATURES BELOW 700K.
                 REACTIONS OF CR WITH NI OR CO IN AN INTERACTIVE SYSTEM
                    LEADS TO THE FORMATION OF NIO.CR2O3 AND COO.CR2O3.
MINIMUM ACUTE TOXICITY EFFLUENT LEVEL (PPM):
      CR INSOLUBLE:        1.00E3
      CR SALTS SOLUBLE:    5.00E2
      CR CHROMATE          9.55E0
      CR IV OXIDE:         1.10E1
PERCENT CHROMIUM VOLATILIZATION AT EQUILIBRIUM
  FOR 1200-1300K OPERATIONS: 78.6%; FOR REACTION WITH
  CO OR NI IN AN INTERACTIVE SYSTEM 7.85% VOLATILIZATION OF
  COAL-CONTAINED CHROMIUM IS PROJECTED.
```

TABLE A7 - ELEMENTAL CONCENTRATION AND CONSIDERED PHASES

```
C   70.28%             GAS PHASES        SOLID/CONDENSED PHASES
H    4.95%              *FE                     FECL2
N    1.30%              *FECL                   FECL3
O    8.68%              *FECL2                  FE
S    4.00%              *FECL3                  FEH202
CL   0.28%              *FE2CL4                 FEH303
FE   1.92%              *FE2CL6                 FE0.947
                        *FEH202                 FEO
                        *FEO                   *FE203
                                                FESO4
                                               *FE(SO4)3
                                                FES
                                                FE304
                                                FECO3
                                                FE3C
                                                FE4N
                                                FE2N
                                                FEOCL
*PROJECTED ACTIVE FBC EQUILIBRIUM PHASES        FES2

MAJOR VOLATILE PHASES:FECL2, FE(OH)2, FECL3, FEO, FE2CL4, FECL, (FECL3)2, FE
MAJOR SOLID PHASES:FE203, FE2(SO4)3
PRINCIPAL REACTIONS:
                                     T>800K
                       FE2(SO4)3 (S)---------> FE203(S) + 3SO2 (G) + 3/2O2 (G)
                                  T>1735K
                       6FE203 (S) ---------> 4FE304 (S) + O2 (G)
                       FE203 (S) + 2H20 (G)---> 2FE(OH)2 (G) + 1/2O2 (G)
                       FE203 (S) + 4HCL (G)----> 2FECL2 (G) + 2H20 (G) + 1/2O2(G)
                       FE203 (S) + 6HCL (G)----> 2FECL3 (G) + 3H20 (G)
                       THE REACTION OF NI WITH FE RESULTS IN THE FORMATION OF
                         NIO.FE203 (S) BY THE REACTION
                                                1000-1100K
                       NISO4 (S) + FE203 (S)----------> NIO.FE203 (S) + SO2 (G) +
                                                                  1/2O2 (G)
                       REACTION OF FE WITH MG RESULTS IN THE FORMATION OF
                         MGO.FE203 AT TEMPERATURES GREATER THAN 900K.
MINIMUM ACUTE TOXICITY EFFLUENT LEVEL (PPM):
       FE SOLUBLE SALTS:  1.00E3
       FEO FUME:          5.00E3
       FE(CO)5:           7.00E2
       FE304:             9.33E3
PERCENT IRON VOLATILIZATION AT EQUILIBRIUM
  FOR 1200-1300K OPERATIONS: 0%
```

TABLE A8 - ELEMENTAL CONCENTRATION AND CONSIDERED PHASES

```
                               GAS PHASES       SOLID/CONDENSED PHASES
C   70.28%                      MO                        MO
H    4.95%                     •MOO                       MOS2
N    1.30%                     •MOO2                      MOS3
O    8.68%                     •MOO3                      MOC
S    4.00%                     •MOO2CL2                   MOO2
CL   0.28%                     •MOCL4                    •MOO3
MO   7.54 PPM                  •MOCL5                     MOCL4
                               •MOCL6                     MOCL5
                               •MOO4H2                    MOCL6
                                                          MO(CO)6
                                                          MO2O
                                                          MO2N
                                                          MO2S3
                                                          MO3C2
•PROJECTED ACTIVE FBC EQUILIBRIUM PHASES

MAJOR VOLATILE PHASES:MOO4H2, MOO2CL2, MOO3 (GREATER THAN  10E-10ATM)
MAJOR SOLID PHASES:MOO3
PRINCIPAL REACTIONS:
                                                T<600K
                      MOO3 (S) + H2O (G) ----------> MOO2(OH)2 (G)
                      MOO3 (S) + 2HCL (G) ----------> MOO2CL2 (G) + H2O(G) OR
                      MOO3 (S) + CL2 (G) ----------> MOO2CL2 (G) + 1/2O2 (G)
                      AT TEMPERATURES BETWEEN 300 AND 500K MGO.MOO3 (S) IS
                         FORMED. THIS PHASE IS CONVERTED INTO CAO.MOO3 (S)
                         BETWEEN 500 AND 1100K, WITH COMPLETE VOLATILIZATION
                         OF MO AT TEMPERATURES GREATER THAN 1100K.

MINIMUM ACUTE TOXICITY EFFLUENT LEVEL (PPM):
      MO SOLUBLE:     5.00E3
      MO INSOLUBLE:  1.00E4
PERCENT MOLYBDENUM VOLATILIZATION AT EQUILIBRIUM
  FOR 1200-1300K OPERATIONS: 100%
```

TABLE A9 - ELEMENTAL CONCENTRATION AND CONSIDERED PHASES

```
                     GAS PHASES       SOLID/CONDENSED PHASES
C  70.28%              •MN                   MN
H   4.95%              •MNO                  MNCO3
N   1.30%              •MNCL                 MNC2
O   8.68%              •MNCL2                MNO
S   4.00%               MNS                  MNO2
CL  0.28%               MN2                  MNS
MN 49.40 PPM                                •MNSO4
                                             MNCL2
                                            •MN2O3
                                             MN3C
                                             MN7C3
                                            •MN3O4
                                             MNS2
•PROJECTED ACTIVE FBC EQUILIBRIUM PHASES

MAJOR VOLATILE PHASES:MNCL2, MNCL, MNO, MN
MAJOR SOLID PHASES:MNSO4, MN2O3, MN3O4
PRINCIPAL REACTIONS:
                                            T<900-1100K
                     2MNSO4 (S) + 1/2O2 (G)-------------> MN2O3 (S) + 2SO2 (G)
                                                                + O2 (G)
                                 T> 1300K
                     3MN2O3 (S) ----------> 2MN3O4 (S) + 1/2O2 (G)
                     MNSO4 (S) + 2HCL (G)----> MNCL2 (G) + H2SO4 (G)
                     MANGANESE AT LOW TEMPERATURES IN 99% SULFUR REMOVAL
                        SYSTEMS FORMS MNO2(S) RATHER THAN MNSO4. CONVERSION
                        OF MNO2 INTO MN2O3 RESULTS BETWEEN 700 AND 800K.
                        A FINAL REACTION OF MN WITH AL OCCURS AT 1100-1200K
                        FORMING MNO.AL2O3 (S) BY THE REACTION
                     MN2O3 (S) + 2(AL2O3.SIO2) (S) ----> 2(MNO.AL2O3) (S)
                                                      + 2SIO2 (S) + 1/2O2 (G)

MINIMUM ACUTE TOXICITY EFFLUENT LEVEL (PPM):
      MN:  5.00E3
PERCENT MANGANESE VOLATILIZATION AT EQUILIBRIUM
  FOR 1200-1300K OPERATIONS: 2.2%; FOR REACTION WITH
  AL IN AN INTERACTIVE SYSTEM 1.4% VOLATILIZATION OF
  COAL-CONTAINED MANGANESE IS PROJECTED.
```

TABLE A10 - ELEMENTAL CONCENTRATION AND CONSIDERED PHASES

```
C   70.28%                  GAS PHASES         SOLID/CONDENSED PHASES
H    4.95%                   •NI                        NI
N    1.30%                   •NIO                       NIS
O    8.68%                   •NICL                     •NIO
S    4.00%                   •NICL2                    •NISO4
CL   0.28%                   •NIH                       NICL2
NI 21.07 PPM                  NI(CO4)2                  NI3S2
                             •NI(OH)2
•PROJECTED ACTIVE FBC EQUILIBRIUM PHASES

MAJOR VOLATILE PHASES:NICL2, NI(OH)2, NICL, NIO, NI, NIH
MAJOR SOLID PHASES:NISO4, NIO
PRINCIPAL REACTIONS:
                              800-1000K
                    NISO4 (S)------------> NIO (S) + SO2 (G) + 1/2O2 (G)
                             T>1100K
                    NIO (S) -----------> NIO (G)
                    NISO4 (S) + 2HCL(G)----> NICL2 (G) + H2SO4 (G)
                    NIO (S) + 2HCL (G) ----> NICL2 (G) + H2O (G)
                    NISO4 (S) + H2O (G)----> NI(OH)2 (G) + SO2 (G) + 1/2O2 (G)
                    NIO (S) + H2O (G) ----> NI(OH)2 (G)
                    ADDITIONAL REACTIONS IN INTERACTIVE FBC SYSTEMS INCLUDE:
                                                1000-1100K
                    NISO4 (S) + FE2O3 (S) ------------> NIO.FE2O3 (S) + SO2 (G)
                                                                      + 1/2O2 (G)
                    AND
                                                400-500K
                    2NISO4 (S) + SIO2 (S) ----------> NI2SIO4 (S) + 2SO2 (G)
                                                                  + O2 (G)
                                                  700-800K
                    NI2SIO4 (S) + 2FE2O3 (S) -----------> 2(NIO.FE2O3) (S)
                                                                    + SIO2 (S)
                    REACTION OF NI WITH CR IN AN INTERACTIVE SYSTEM LEADS TO
                       THE FORMATION OF NIO.CR2O3.

MINIMUM ACUTE TOXICITY EFFLUENT LEVEL (PPM):
      NI SOLUBLE:    1.00E2
      NI(CO)4:       7.00E0
      NI3S2:         1.50E1
      NIO            9.00E2
PERCENT NICKEL VOLATILIZATION AT EQUILIBRIUM
  FOR 1200-1300K OPERATIONS: 5.05%; FOR REACTION WITH
  FE IN AN INTERACTIVE SYSTEM 2.6% VOLATILIZATION OF
  COAL-CONTAINED NICKEL IS PROJECTED.
```

TABLE A11 - ELEMENTAL CONCENTRATION AND CONSIDERED PHASES

```
C   70.28%               GAS PHASE              SOLID/CONDENSED PHASES
H    4.95%                 TI                        TI
N    1.30%                 TIS                       TIS2
O    8.68%                *TIO                       TIO
S    4.00%                *TIO2                     *TIO2
CL   0.28%                 TICL                      TICL3
TI   0.07%                *TICLO                     TICL4
                          *TIOCL2                    TI2O3
                          *TICL2                     TI3O5
                          *TICL3                     TI4O7
                          *TICL4                     TIH2
                           TIN                       TIC
                                                     TIN
                                                     TI2S3
                                                     TIS3
                                                     TI2S
                                                     TIS
*PROJECTED ACTIVE FBC EQUILIBRIUM PHASES             TICL2

MAJOR VOLATILE PHASES:TIOCL2, TICL3, TICL2, TICL, TICL4, TIOCL, TIO2, TIO
MAJOR SOLID PHASES:TIO2
PRINCIPAL REACTIONS:

                     TIO2 (S) + 2HCL (G) ---------> TIOCL2 (G) + H2O (G)
                                          T>1000K
                     TIO2 (S) + 4HCL (G) ---------> TICL4 (G) + 2H2O (G)
                                          T<1000K
                                             T>1000K
                     TICL4 (G) + 1/2O2 (G) ---------> TIOCL2 (G) + 2CL(G)
                     TIO2 (S) ----> TIO2 (G)
                     IN THE PRESENCE OF CA, 3CAO.TIO2 FORMS BETWEEN TEMPERATURES
                        OF 800 AND 1200K. TEMPERATURES OF 700K FAVOR THE
                        FORMATION OF CAO.TIO2,WHILE TIO2 IS THE PREDOMINANT
                        PHASE BELOW 700K. IN SYSTEMS THAT DO NOT
                        CONTAIN THE CARBONATES, TI REACTS WITH AL TO FORM
                        AL2O3.TIO2 AS SHOWN IN THE FOLLOWING REACTION:
                                                   300-400K
                     2AI(OH)3 (S) + TIO2 (S) --------> AL2O3.TIO2(S) + 3H2O (G)
MINIMUM ACUTE TOXICITY EFFLUENT LEVEL (PPM):
      TI(+4):   2.53E2
      TICL4:    1.00E4
      TIO2:     1.00E4
PERCENT TITANIUM VOLATILIZATION AT EQUILIBRIUM
  FOR 1200-1300K OPERATIONS: 0%
```

TABLE A12 - ELEMENTAL CONCENTRATION AND CONSIDERED PHASES

```
                              GAS PHASES               SOLID/CONDENSED PHASES
C   70.28%                     •NA2SO4                          •NA2SO4
H    4.95%                     •NAOH                             NAOH
N    1.30%                     •NACL                             NACL
O    8.68%                      NA                               NA
S    4.00%                      NACN                             NA2CO3
CL   0.28%                      NAH                              NACN
NA   0.09% (COAL)               NAO                              NAH
     0.03% (SORBENT)            NA2                              NAO
                                NA2O                             NA2CL2
                                NA2CL2                           NA2O2H2
                                NA2C2N2                          NA2S
                                NA2O2H2
•PROJECTED ACTIVE FBC EQUILIBRIUM PHASES

MAJOR VOLATILE PHASES:NACL, NAOH, NA2SO4
MAJOR SOLID PHASES:NA2SO4
PRINCIPAL REACTIONS:
                             2NACL (G) + H2O (G) + SO2 (G) + 1/2 O2 (G)------->
                                    NA2SO4 (S,L,G) + 2HCL (G)
                             2NAOH (G) + SO2 (G) + 1/2 O2 (G)------->
                                    NA2SO4 (S,L,G) + 2HCL (G)
                             NA2SO4 (S)<--> NA2SO4 (L)<--> NA2SO4 (G)
                             REACTION OF NA WITH SI IN AN INTERACTIVE SYSTEM
                                LEADS TO THE FORMATION OF SOLID 2NA2O.SIO2.

MINIMUM ACUTE TOXICITY EFFLUENT LEVEL (PPM):
      NA+:         5.31E4
      NAOH:        2.00E3
PERCENT SODIUM VOLATILIZATION AT EQUILIBRIUM
  FOR 1200-1300K OPERATIONS: 0-100%; FOR REACTION OF NA
  WITH SI IN AN INTERACTIVE SYSTEM LESS THAN 1% VOLATILIZATION OF
  COAL AND SORBENT-CONTAINED SODIUM IS PROJECTED.
```

TABLE A13 - ELEMENTAL CONCENTRATION AND CONSIDERED PHASES

```
                                 GAS PHASES               SOLID/CONDENSED PHASES
C   70.28%                        •K2SO4                        •K2SO4
H    4.95%                        •KOH                           KOH
N    1.30%                        •KCL                           KCL
O    8.68%                         K                             K
S    4.00%                         KCN                           K2CO3
CL   0.28%                         KH                            KCN
K    0.22% (COAL)                  KO                            KH
     0.44% (SORBENT)               K2                            KO2
                                   K2O                           K2O2
                                   K2CL2                         K2CL2
                                   K2C2N2                        K2O2H2
                                   K2O2H2                        K2S
                                                                 K2O
•PROJECTED ACTIVE FBC EQUILIBRIUM PHASES

MAJOR VOLATILE PHASES:KCL, KOH, K2SO4
MAJOR SOLID PHASES:K2SO4
PRINCIPAL REACTIONS:
                          2KCL (G) + H2O (G) + SO2 (G) + 1/2O2 (G)------>
                                K2SO4 (S,L,G) + 2HCL (G)
                          2KOH (G) + SO2 (G) + 1/2 O2 (G)------>
                                K2SO4 (S,L,G) + 2HCL (G)
                          K2SO4 (S)<--> K2SO4 (L)<--> K2SO4 (G)
                          REACTION OF K WITH SI AND AL IN AN INTERACTIVE
                             SYSTEM LEADS TO THE FORMATION OF SOLID KALSI3O8.

MINIMUM ACUTE TOXICITY EFFLUENT LEVEL (PPM):
      K+:          5.73E4
      KOH:         2.00E4
PERCENT POTASSIUM VOLATILIZATION AT EQUILIBRIUM
  FOR 1200-1300K OPERATIONS: 0-100%; FOR REACTION OF K
  WITH AL AND SI IN AN INTERACTIVE SYSTEM LESS THAN 5% VOLATILIZATION OF THE
  COAL AND SORBENT-CONTAINED POTASSIUM IS PROJECTED.
```

TABLE A14 - ELEMENTAL CONCENTRATION AND CONSIDERED PHASES

```
                          GAS PHASES                SOLID/CONDENSED PHASES
C    70.28%          CH3BR          •BRH                   CBR4
H     4.95%         •CH2BR2         •BRNO                  BRH4N
N     1.30%          CHBR3          •BRN                   BR2
O     8.68%         •CBRN           •SOBR2
S     4.00%         •CCL2BR2        •BRO
CL    0.28%          CCLBR3         •BRCL
BR   19.298PPM       CBR4           •BR2
                    •CBR3           •BR
                    •CBR2            CCL3BR
                     CBR
•PROJECTED ACTIVE FBC EQUILIBRIUM PHASES

MAJOR VOLATILE PHASES:BRCL, BRH, BR2, BR, BRO (GREATER THAN 10E-8 KPA)
MAJOR SOLID PHASES:--
PRINCIPAL REACTIONS:  NABR AND KBR GASES RESULT IN FBC EFFLUENT IN THE
                      PRESENCE OF ALKALI.
                      THE REACTION OF BR WITH ZN RESULTS IN THE FORMATION OF
                      VOLATILE ZNBR2.
                      VOLATILE FEBR2, BRF, CUBR, MNBR2, NIBR2, NIBR, BOBR,
                      SNBR2, CDBR, GABR, HGBR2, PBBR, PBBR2, PBBR4 PHASES ARE
                      PROJECTED IN INTERACTIVE EQUILIBRIUM SYSTEMS.

MINIMUM ACUTE TOXICITY EFFLUENT LEVEL (PPM):
      BR2:  7.00E2
      HBR:  1.00E4
PERCENT BROMINE VOLATILIZATION AT EQUILIBRIUM
  FOR 1200-1300K OPERATIONS : 100%
```

TABLE A15 - ELEMENTAL CONCENTRATION AND CONSIDERED PHASES

```
                                GAS PHASES               SOLID/CONDENSED PHASES
C     70.28%             BC               BOCL                   B4C
H      4.95%             B10H14           B2O                    B10H14
N      1.30%             B5H9             BO                     B5H9
O      8.68%             B2H6             BS                     B2(OH)4
S      4.00%             B2(OH)4          B2CL4                  B3O3H3
CL     0.28%            •(HBO2)3          BCL3                  •H3BO3
B    102.21PPM           B3O3H3           BCL2                   HBO2
                        •H3BO3            BCL                    BN
                         BH3              B2                     B2O3
                         BH2O2            B                      B
                         BH2              B3H6N3
                        •BHO2
                         HBO
                         HBS
                         BCL2H
                         BH
                         BN
                         (BOCL)3
                         B2O3
                         B2O2
                        •BO2
•PROJECTED ACTIVE FBC EQUILIBRIUM PHASES

MAJOR VOLATILE PHASES:H3BO3, BHO2, (HBO2)3, BO2
MAJOR SOLID PHASES:H3BO3
PRINCIPAL REACTIONS:
                                         300-500K
                               H3BO3 (S)----------> H3BO3 (G)
                               3H3BO3 (G)----> (HBO2)3 (G) + 3H2O (G)
                                          T>1200K
                               H3BO3 (G)------------> BHO2 (G) + H2O (G)
                               THE REACTION OF CA WITH GASEOUS B RESULTS IN THE
                                 FORMATION OF 3CAO.B2O3(S) BETWEEN 900 AND 1300K.
MINIMUM ACUTE TOXICITY EFFLUENT LEVEL (PPM):
      B:      9.00E4
      B2O3:   1.00E4
PERCENT BORON VOLATILIZATION AT EQUILIBRIUM
  FOR 1200-1300K OPERATIONS: 100%; FOR REACTION WITH CA
  IN AN INTERACTIVE SYSTEM 0% VOLATILIZATION OF COAL-CONTAINED
  BORON IS PROJECTED.
```

TABLE A16 - ELEMENTAL CONCENTRATION AND CONSIDERED PHASES

```
                               GAS PHASES              SOLID/CONDENSED PHASES
C     70.28%                     CHP                           •H3PO4
H      4.95%                    •HP                             P4O10
N      1.30%                    •H2P                            P4S3
O      8.68%                    •H3P                            P3N5
S      4.00%                     NP                             P
CL     0.28%                    •P4O10
P     71.10PPM                   P4O6
                                •PO2
                                •PO
                                •POCL3
                                 P4S3
                                 PSCL3
                                 PS
                                •PCL5
                                •PCL3
                                •PCL
                                 P4
                                 P2
                                 P
•PROJECTED ACTIVE FBC EQUILIBRIUM PHASES

MAJOR VOLATILE PHASES:(P2O5)2, PO2 (GREATER THAN 10E-8 KPA)
MAJOR SOLID PHASES:H3PO4
PRINCIPAL REACTIONS:                MELT TEMP: 316K
                          H3PO4 (S)-------------------> H3PO4 (L)
                                     316-900K
                          H3PO4 (L)--------------->(P2O5)2 (G) + 6H2O (G)
                          THE REACTION OF P WITH MG RESULTS IN THE FORMATION OF
                            MG3(PO4)2 (S).

MINIMUM ACUTE TOXICITY EFFLUENT LEVEL (PPM):
      H3PO4:   1.00E3
      PH3:     4.00E2
      P2S5:    1.00E3
PERCENT PHOSPHOROUS VOLATILIZATION AT EQUILIBRIUM
  FOR 1200-1300K OPERATIONS: 99.99%; FOR REACTION WITH MG
  IN AN INTERACTIVE SYSTEM 0% VOLATILIZATION OF COAL-CONTAINED PHOSPHORUS
  IS PROJECTED.
```

TABLE A17 - ELEMENTAL CONCENTRATION AND CONSIDERED PHASES

```
                           GAS PHASES          SOLID/CONDENSED PHASES
C   70.28%                  •CUH                       CUCN
H    4.95%                  •CUO                       CU(OH)2
N    1.30%                  •CUS                      •CUO.CUSO4
O    8.68%                  •CU3CL3                   •CUSO4
S    4.00%                  •CUCL                      CU2O
CL   0.28%                  •CU2                      •CUO
CU  15.16 PPM               •CU                        CU2S
                                                       CUS
                                                       CUCL2
                                                       CUCL
                                                       CU
•PROJECTED ACTIVE FBC EQUILIBRIUM PHASES

MAJOR VOLATILE PHASES:CU3CL3, CUCL, CUO (AT FBC TEMPERATURES OF 1200-1300K)
MAJOR SOLID PHASES:CUSO4, CUO.CUSO4, CUO (BELOW 900K)
PRINCIPAL REACTIONS:
                                  DISSOCIATION TEMP  >1078K
                         2CUSO4 (S) ------------------------------> CUO.CUSO4 (S)
                                                         + SO2 (G)+ 1/2O2 (G)
                         CUO.CUSO4 (S) ----> 2CUO (S) + SO2 (G) + 1/2O2 (G)
                         CUO (S) ------> CUO (G)
                         3CUSO4 (S) + 6HCL (G) ----> CU3CL3 (G) + 3H2SO4 (G) + 3CL(G)
                         CU3CL3 (G)----> 3CUCL (G)

MINIMUM ACUTE TOXICITY EFFLUENT LEVEL (PPM):
      COMPLEXED COPPER: 3520
      CU FUME:           200
      CU SALTS, DUST:   1000
PERCENT COPPER VOLATILIZATION AT EQUILIBRIUM
  FOR 1200-1300K OPERATIONS: 100%
```

TABLE A18 - ELEMENTAL CONCENTRATION AND CONSIDERED PHASES

```
                           GAS PHASES             SOLID/CONDENSED PHASES
C    70.28%                 •VN                 V2C        VOCL3
H     4.95%                 •VO2                VC.8       VO
N     1.30%                 •VO                 VN         VCL4
O     8.68%                 •VOCL3              VN.465     VCL3
S     4.00%                 •VCL4              •V2O5       VCL2
CL    0.28%                 •V                  V2O4       V
V    32.71                                      V2O3
•PROJECTED ACTIVE FBC EQUILIBRIUM PHASES

MAJOR VOLATILE PHASES:VOCL3, VCL4, VO2 (GREATER THAN 10E-8 KPA)
MAJOR SOLID PHASES:V2O5
PRINCIPAL REACTIONS:              MELT TEMP: 943K
                           V2O5 (S)-----------------> V2O5 (L)
                           THE REACTION OF V WITH MG RESULTS IN THE FORMATION OF
                             2MGO.V2O5 (S); SIMILARLY WITH NA, NA2O.V2O5 IS PROJECTED

MINIMUM ACUTE TOXICITY EFFLUENT LEVEL(PPM):
      V2O5:  5.00E2
PERCENT VANADIUM VOLATILIZATION AT EQUILIBRIUM
  FOR 1200-1300K OPERATIONS: 0.03%; FOR REACTION WITH MG OR NA
  IN AN INTERACTIVE SYSTEM 0% VOLATILIZATION OF COAL-CONTAINED VANADIUM
  IS PROJECTED
```

TABLE A19 - ELEMENTAL CONCENTRATION AND CONSIDERED PHASES

```
                         GAS PHASES        SOLID/CONDENSED PHASES
C    70.28%               •ZNH                      ZNCO3
H     4.95%               •ZNS                     •ZNSO4.7H2O
N     1.30%               •ZNCL                     ZNSO4.6H2O
O     8.68%               •ZN2                     •ZNSO4.H2O
S     4.00%               •ZN                      •ZNSO4
CL    0.28%                                        •ZNO
ZN 272.29 PPM                                       ZNS (WURTZITE)
                                                    ZNS (SPHALERITE)
                                                    ZNCL2
                                                    ZN
•PROJECTED ACTIVE FBC EQUILIBRIUM PHASES

MAJOR VOLATILE PHASES:ZNCL (GREATER THAN 10E-8 KPA)
MAJOR SOLID PHASES:ZNO, ZNSO4, ZNSO4.H2O, ZNSO4.7H2O
PRINCIPAL REACTIONS:
                                   300-400K
                         ZNSO4.7H2O (S)-----------> ZNSO4.H2O (S) + 6H2O (G)
                                   400-500K
                         ZNSO4.H2O (S) -----------> ZNSO4 (S) + H2O (G)
                               500-1200K
                         ZNSO4 (S) ----------> ZNO (S) + SO2 (G) + 1/2O2 (G)
                         THE REACTION OF GASEOUS BR AND ZN RESULTS IN THE
                           FORMATION OF ZNBR2(G).
MINIMUM ACUTE TOXICITY EFFLUENT LEVEL (PPM):
       ZN:      6.75E2
       ZNCL2:   1.00E3
       ZNO:     5.00E3
PERCENT ZINC VOLATILIZATION AT EQUILIBRIUM
  FOR 1200-1300K OPERATIONS: <1%; FOR REACTION WITH BR
  IN AN INTERACTIVE SYSTEM 0.01% VOLATILIZATION OF
  COAL-CONTAINED ZINC IS PROJECTED.
```

TABLE A20 - ELEMENTAL CONCENTRATION AND CONSIDERED PHASES

```
                         GAS PHASES        SOLID/CONDENSED PHASES
C   70.28%                 SBH3                     SB2O5
H    4.95%                 SBN                      SB2O4
N    1.30%                •SBO                      SB2O3
O    8.68%                •SBCL3                   •SBO2
S    4.00%                •SBCL                     SB2S3
CL   0.28%                 SB4                      SBCL3
SB   1.26 PPM              SB2                      SB
                          •SB
•PROJECTED ACTIVE FBC EQUILIBRIUM PHASES

MAJOR VOLATILE PHASES:SBO, SBCL3, SBCL, SB
MAJOR SOLID PHASES:SBO2
PRINCIPAL REACTIONS: SBO2 (S) ---> SBO (G) + 1/2O2 (G)  (HIGH TEMPERATURE)
                     SBO2 (S) + 3HCL (G)---> SBCL3 (G) + 3/2H2O (G)
                                           + 1/2O2 (G) (LOW TEMPERATURE)

MINIMUM ACUTE TOXICITY EFFLUENT LEVEL (PPM):
      SB    5.00E2
      SBH3  5.00E2
PERCENT ANTIMONY VOLATILIZATION AT EQUILIBRIUM
  FOR 1200-1300K OPERATIONS: 4-100%; FOR ATMOSPHERIC FBC SYSTEMS: 0.5-4.9%
  VOLATILIZATION FOR 1519.5 KPA FBC SYSTEMS.
```

TABLE A21 - ELEMENTAL CONCENTRATION AND CONSIDERED PHASES

```
                         GAS PHASES        SOLID/CONDENSED PHASES
C   70.28%                 SNH4                   •SNO2
H    4.95%                 SNH                     SNS2
N    1.30%                •SNO                     SNS
O    8.68%                 SNS                     SNCL4
S    4.00%                •SNCL2                   SNCL2
CL   0.28%                 SNCL                    SN
SN   4.79PPM               SN2
                           SN
                          •SNCL4
•PROJECTED ACTIVE FBC EQUILIBRIUM PHASES

MAJOR VOLATILE PHASES:SNO, SNCL2, SNCL4
MAJOR SOLID PHASES:SNO2
PRINCIPAL REACTIONS:  SNO2 (S) ---> SNO(G) + 1/2O2 (G)
                      SNO2 (S) + 2HCL (G) ---> SNCL2 (G) + H2O (G) + 1/2O2 (G)

MINIMUM ACUTE TOXICITY EFFLUENT LEVEL (PPM):
      SNO   1.00E2
      SNCL4 2.07E3
      ORGANOTIN  1.00E2
PERCENT TIN VOLATILIZATION AT EQUILIBRIUM
  FOR 1200-1300K OPERATIONS:  <3%
```

TABLE A22 - ELEMENTAL CONCENTRATION AND CONSIDERED PHASES

```
                         GAS PHASES          SOLID/CONDENSED PHASES
C   70.28%                 ZRH                      ZRC4
H    4.95%                 ZRN                      ZRC
N    1.30%                 ZRO2                     ZRN
O    8.68%                 ZRO                     •ZRO2
S    4.00%                •ZRCL4                    ZRCL4
CL   0.28%                 ZRCL3                    ZRCL3
ZR  72.46 PPM              ZRCL2                    ZRCL2
                           ZRCL                     ZR
                           ZR
•PROJECTED ACTIVE FBC EQUILIBRIUM PHASES

MAJOR VOLATILE PHASES:(ZRCL4)
MAJOR SOLID PHASES:ZRO2
PRINCIPAL REACTIONS:  ZRO2 (S) + 4HCL (G) ---> ZRCL4 (G) + 2H2O (G)
                      SOLID ZRSIO4 FORMS BETWEEN 300 AND 1200-1300K IN
                      INTERACTIVE PFBC SYSTEMS.

MINIMUM ACUTE TOXICITY EFFLUENT LEVEL(PPM):
     ZR      5.00E3
PERCENT ZIRCONIUM VOLATILIZATION AT EQUILIBRIUM
  FOR 1200-1300K OPERATIONS:  0%
```

TABLE A23 - ELEMENTAL CONCENTRATION AND CONSIDERED PHASES

```
                        GAS PHASES          SOLID/CONDENSED PHASES
C   70.28%                ASH3                      •AS205
H    4.95%                ASH                        AS203
N    1.30%                ASN                        ASCL3
O    8.68%               •ASO                        AS
S    4.00%               •ASCL3
CL   0.28%               •ASCL
AS  14.02 PPM             AS4
                          AS2
                          AS
•PROJECTED ACTIVE FBC EQUILIBRIUM PHASES

MAJOR VOLATILE PHASES:ASCL, ASO, ASCL3
MAJOR SOLID PHASES:AS205
PRINCIPAL REACTIONS:
                                             1000-1200K
                    AS205 (S) + 2HCL(G)----------->2ASCL(G) + H2O(G) + 2O2(G)
MINIMUM ACUTE TOXICITY EFFLUENT LEVEL (PPM):
      AS:      2.00E0
      AS2O3:   2.00E0
      ASH3:    2.00E0
PERCENT ARSENIC VOLATILIZATION AT EQUILIBRIUM
  FOR 1200-1300K OPERATIONS: 100%
```

TABLE A24 - ELEMENTAL CONCENTRATION AND CONSIDERED PHASES

```
                        GAS PHASES          SOLID/CONDENSED PHASES
C   70.28%                CDH                       •CDSO4
H    4.95%               •CDO                        CDO
N    1.30%               •CDCL                       CDS
O    8.68%                CD2                        CDCL2
S    4.00%               •CD                         CD
CL   0.28%
CD   2.52 PPM
•PROJECTED ACTIVE FBC EQUILIBRIUM PHASES

MAJOR VOLATILE PHASES:CDO, CD, CDCL
MAJOR SOLID PHASES:CDSO4
PRINCIPAL REACTIONS:              900-1100K
                        CDSO4(S) ------------> CDO(G) + SO2(G)+ 1/2O2(G)
                        SOLID CDCL2 IS PROJECTED AS A STABLE SOLID AT 300K.

MINIMUM ACUTE TOXICITY EFFLUENT LEVEL (PPM):
      --
PERCENT CADMIUM VOLATILIZATION AT EQUILIBRIUM
  FOR 1200-1300K OPERATIONS: 100%
```

TABLE A25 - ELEMENTAL CONCENTRATION AND CONSIDERED PHASES

```
                           GAS PHASES          SOLID/CONDENSED PHASES
C   70.28%                   H2SE                    SE
H    4.95%                  *HSE
N    1.30%                   NSE
O    8.68%                  *SEO
S    4.00%                   SE2
CL   0.28%                   CSE
SE  2.08 PPM
*PROJECTED ACTIVE FBC EQUILIBRIUM PHASES

MAJOR VOLATILE PHASES:SEO
MAJOR SOLID PHASES:--
PRINCIPAL REACTIONS:
                         -STABLE FORMATION OF SEO(G)-

MINIMUM ACUTE TOXICITY EFFLUENT LEVEL (PPM):
     SE:      1.08E1
     H2SE:    1.08E1
PERCENT SELENIUM VOLATILIZATION AT EQUILIBRIUM
  FOR 1200-1300K OPERATIONS: 100%
```

TABLE A26 - ELEMENTAL CONCENTRATION AND CONSIDERED PHASES

```
                         GAS PHASES          SOLID/CONDENSED PHASES

C   70.28%                GA2C2                   *GA203
H    4.95%                GAH                      GA
N    1.30%                GAO
O    8.68%                *GACL
S    4.00%                GA
CL   0.28%
GA   3.12 PPM

*PROJECTED ACTIVE FBC EQUILIBRIUM PHASES
MAJOR VOLATILE PHASES:GACL
MAJOR SOLID PHASES:GA203
PRINCIPAL REACTIONS:
                         GA203 (S) + 2HCL (G)---> 2GACL (G) + H20 (G) + 02 (G)

MINIMUM ACUTE TOXICITY EFFLUENT LEVEL (PPM):
     GA:  4.95E3

PERCENT GALLIUM VOLATILIZATION AT EQUILIBRIUM
  FOR 1200-1300K OPERATIONS: 0-0.66% (0-0.021 PPM)
```

TABLE A27 - ELEMENTAL CONCENTRATION AND CONSIDERED PHASES

```
                         GAS PHASES         SOLID/CONDENSED PHASES

C   70.28%                GEH                   *GEO2
H    4.95%               *GEO                    GE
N    1.30%                GES
O    8.68%                GECL
S    4.00%                GE2
CL   0.28%
GE   6.59 PPM

*PROJECTED ACTIVE FBC EQUILIBRIUM PHASES
MAJOR VOLATILE PHASES:GEO
MAJOR SOLID PHASES:GEO2
PRINCIPAL REACTIONS:
                   GEO2 (S) ----> GEO (G) + 1/2O2 (G)

MINIMUM ACUTE TOXICITY EFFLUENT LEVEL (PPM):
      GE(+4):   2.34E4
      GEH4:     6.00E2

PERCENT GERMANIUM VOLATILIZATION AT EQUILIBRIUM
  FOR 1200-1300K OPERATIONS: 0-100%
```

TABLE A28 - ELEMENTAL CONCENTRATION AND CONSIDERED PHASES

```
C   70.28%
H    4.95%
N    1.30%
O    8.68%
S    4.00%
CL   0.28%
AL   1.29%
SI   2.49%
CA   0.77%  (COAL)
    21.70%  (SORBENT)
MG   0.05%  (COAL)
    13.19%(SORBENT)
```

```
GAS PHASES
  AL
 •ALCL
 •ALCLO
 •ALCL2
 •ALCL3
  ALH
 •ALHO
  ALHO2
  ALN
 •ALO
 •ALO2
  ALS
 •AL2CL6
  AL2O
  AL2O2
  AL2CL8NI
  ALBO2
  ALCLF
  ALCLF2
  ALCL2F
  ALF
  ALF2
  ALF3
  ALF4NA
  AL2F6
  SIC4H12
  SIC2
  SICH3CL3
  SI2C
  SIC
  SIH4
  SIH3CL
  SIH2CL2
  SIHCL3
  SIH
  SIN
 •SIO
 •SIO2
  SIS
  SI
  SI2
  SI3
 •SICL
 •SICL2
 •SICL3
 •SICL4
  CAH
  CAO
  CAS
 •CACL2
  CACL
  CAF2
  CAF
  CA
 •MG(OH)2
  MG(OH)CL
  MGH
  MGO
  MGS
  MG2CL4
 •MGCL2
  MGFCL
  MGCL
  MG2F4
  MGF2
  MGF
  MG
```

```
SOLID/CONDENSED PHASES
  AL
  ALCLO
  ALCL3
  ALCL4K
  ALCL6K3
  ALCL4NA
  ALCL6NA
 •AL(OH)3
  ALN
  ALNAO2
  AL2CL9K3
 •AL2O3
  AL2O3.MNO
 •AL2(SO4)3
  AL2O3.FEO
 •ALF3
  ALF6K3
  ALF6NA3
 •AL2BEO4
 •AL2MGO4
  AL2O3.MNO
 •AL2O3.SIO2
  AL6BEO10
  AL6O13SI2
  AL2O3.FEO
  AL4C3
  AL2O3.3H2O
  AL2O3.2SIO2.2H2O
 •AL2O3.H2O
 •AL2O3.TIO2
  AL2O3.FEO
  AL2O3.MNO
 •KAL(SO4)2.12H2O
 •KAL(SO4)2
 •KALSI3O8
  SIC
  SI3N4
  SI2N
 •SIO2
  SI
  SIS
  K2SIO3
  3NA2O.2SIO2
  NA2O5SI
 •2NA2O.SIO2
  NA2SIO3
  SIO3MO
 •CACO3.MGCO3
  4CAO.AL2O3.13H2O
  5CAO.6SIO2.5/2H2O
  3CAO.AL2O3.6H2O
  5CAO.6SIO2.3/2H2O
  5CAO.6SIO2.3H2O
  3CAO.2SIO2.3H2O
  2CAO.3SIO2.5/2H2O
  CAO.2SIO2.2H2O
 •CASO4.2H2O
  4CAO.3SIO2.3/2H2O
  6CAO.6SIO2.H2O
  CA(OH)2
  CAC2
 •CACO3
  CASO4.1/2H2O
  CA(NO3)2
  CA3N2
  12CAO.7AL2O3
  CAO.AL2O3.2SIO2
  2CAO.AL2O3.SIO2
  3CAO.2SIO2
```

TABLE A28 (Continued)

```
                                             2CAO.AL2O3.SIO2
                                             CAO.2AL2O3
                                            •CAO.MGO.2SIO2
                                             3CAO.AL2O3
                                             3CAO.SIO2
                                            •CASO4
                                            •2CAO.SIO2
                                             CAO.MGO.SIO2
                                             CAO.AL2O3
                                             CASO3
                                            •CASIO3
                                             CAO
                                            •CAF2
                                             CAS
                                             CACL2
                                             4CAO.3TIO2
                                            •3CAO.2TIO2
                                             2CAO.FE2O3
                                             CAO.FE2O3
                                            •CAO.TIO2
                                            •CAO.MOO3
                                            •MG(OH)2
                                             MG2C3
                                             MGC2
                                             MGCO3
                                             MGH2
                                            •MG(OH)CL
                                             MG(NO3)2
                                             MG3N2
                                             MGSO4
                                            •MG2O4SI
                                            •MGO3SI
                                             MGO
                                             MGS
                                             MGCL2
                                             MG2SI
                                             MG2O4TI
                                            •MGO.FE2O3
                                             MGO3TI
                                            •MGO.CR2O3
                                            •MGO.MOO3
                                             MGH2
                                            •MGF2
                                             MG2CA
                                             MGO.2TIO2
                                             MGO.TIO2
                                             CAO.MGO.2SIO2
                                            •NI2SIO4
•PROJECTED ACTIVE FBC EQUILIBRIUM PHASES

MAJOR VOLATILE PHASES:ALCL3, ALOCL, ALCL2, ALO2, ALOH, ALCL, ALO, AL2CL6,
      SIO2, SICL4, SICL3, SIO, SICL2, SICL, CACL2, MG(OH)2, MGCL2
MAJOR SOLID PHASES AL2O3, AL2(SO4)3, AL2SIO5, (K,NA)ALSI3O8, SIO2,
      AL2BEO4, AL2MGO4, AL2O3.SIO2, AL2O3.TIO2, KAL(SO4)2.12H2O, KAL(SO4)2,
      2NA2O.SIO2, CACO3.MGCO3, CASO4.2H2O, CACO3, CAO.MGO.2SIO2, CASO4,
      2CAO.SIO2, CASIO3, CAF2, 3CAO.2TIO2, CAO.TIO2, CAO.MOO3, MG(OH)2, MG(OH)CL
      MGO3SI, MGO.FE2O3, MGO.CR2O3, MGO.MOO3, MGF2, NI2SIO4, MG2O4SI
PRINCIPAL REACTIONS:
                                  T>800K
                     AL2(SO4)3 (S) ---------> AL2O3 (S) + 3SO2 (G) + 3/2O2 (G)
                     AL2O3 (S) + 6HCL (G)----> 2ALCL3 (G) + 3H2O (G)
                     AL2O3 (S) + 2HCL (G)----> 2ALOCL (G) + H2O (G)
                                            101 KPA
                     AL2(SO4)3 (S) + H2O (G) --------> AL2O3.H2O (S)
                                           + 3SO2 (G) + 3/2O2 (G)
                                            >101 KPA
                     AL2(SO4)3 (S) + 3H2O (G) ------> 2AL(OH)3 (S)
                                           + 3SO2 (G) + 3/2O2 (G)
                             1000-1100K
                     SIO2 (S) ------------> SIO2 (S)
                      (QUARTZ)                (CRISTABOLITE)
                                         300-400K
                     KAL(SO4)2.12H2O (C) ----------> KAL(SO4)2 (C) + 12H2O (G)
                                             800-1000K
                     2KAL(SO4)2 (C) + SIO2 (C) -------------> AL2O3.SIO2(C) +
                                              K2SO4 (C) + 3SO2 (G) + 3/2O2 (G)
```

TABLE A28 (Continued)

```
                                               700-800K
                      AL2(SO4)3 (S) + SIO2 (C)----------->AL2O3.SIO2 (C) +
                                                       3SO2 (G) + 3/2O2 (G)
                      2NA2O (S) + SIO2 (S)----> 2NA2O.SIO2 (S)
                      SIO2 (C) ----> SIO2 (G)
                      SIO2 (C) + 4HCL (G) ----> SICL4 (G) + 2H2O (G)
                                              300-400K
                     2AL(OH)3 (S) + SIO2 (S)-----------> AL2O3.SIO2 (S) +
                                                       3H2O (G)
                      K2SO4 (S) + AL2O3.SIO2 (S) + 5SIO2 (S)----> 2KALSI3O8 (S)+
                                                       SO2 (G) + 1/2O2 (G)
                                        T>1200K
                      3(AL2O3.SIO2) (S)----------> 3AL2O3.2SIO2 (S) + SIO2(S)
                                            300-400K
                      AL2O3 (S) + BESO4 (S)----------> BEAL2O4 (S) + SO2(G)
                                                                + 1/2O2 (G)
                                            400-500K
                      BEAL2O4 (S) + H2O (G)----------> BE(OH)2 (G) + AL2O3 (S)
                                            400-500K
                      SIO2 (S) + 2NISO4 (S) ----------> NI2SIO4(S) + 2SO2(G)
                                                                + O2 (G)
                                                1100-1200K
                      2AL2O3.SIO2 (S) + MN2O3 (S) -----------> 2MNO.AL2O3 (S) +
                                                       2SIO2 (S) + 1/2O2 (G)
                                            700-800K
                      AL2O3 (S) + TIO2 (S)------------> AL2O3.TIO2 (S)
                                            300-400K
                      2AL(OH)3 (S) + TIO2 (S) -----------> AL2O3.TIO2(S) + 3H2O(G
                                       300-500K
                      CACO3.MGCO3 (S)----------> CACO3 (S) + MGCO3 (S)
                                                      300-400K
                      CACO3 (S) + SO2 (G) + 1/2O2 (G) ----------> CASO4 (S)
                                                               + CO2 (G)
                                     300-400K
                      CASO4.2H2O (S) ----------> CASO4 (S) + 2H2O (G)
                                                 400-500K
                      CACO3.MGCO3 (S) + 2SIO2 (S) ------------> CAO.MGO.2SIO2(S)
                                                       + 2CO2 (G)
                                         700-800K
                      CAO.MGO.2SIO2 (S) -----------> CASIO3 (S) + MGSIO3 (S)
                                             800-900K
                      2CACO3 (S) + SIO2 (S) ------------>CA2SIO4 (S) + 2CO2 (G)
                                           800-900K
                      CASIO3 (S) + CACO3(S) ---------> CA2SIO4 (S) + CO2 (G)
                                            300-500K
                      2MGCO3 (S) + SIO2 (S) ---------> MG2SIO4 (S) + 2CO2 (G)
                                  300-500K
                      2MGSIO3 (S) ----------> MG2SIO4(S)  +  SIO2 (S)
                                             300-400K
                      MG(OH)2 (S) + AL2O3 (S) ----------> MGAL2O4 (S) + H2O(G)
                                              300-400K
                      MG(OH)CL (S) + AL2O3 (S) ----------> MGAL2O4 (S) + HCL (G)
                                            T<700K
                      CASO4 (S) + TIO2 (S) ----------> CAO.TIO2(S)
                                       T>800K
                      3(CAO.TIO2) (S) ---------> 3CAO.2TIO2 (S) + TIO2 (S)
                      ADDITIONAL REACTIONS INCLUDE:
                        MGO.FE2O3 (S)   T>900K
                        CAO.MOO3 (S)      500-1100K
                        MGO.CR2O3 (S)     300-700K
                        MGO.MOO3 (S)      300K
                        CAF2 (S)          600-1000K
                        MGF2 (S)        T>700K
MINIMUM ACUTE TOXICITY EFFLUENT LEVELS (PPM):
      AL(+3):  5.30E3
      AL2O3:   1.00E4
      SI:      1.00E4
      SIH4:    7.00E2
      SIC:     1.00E4
      CA(+2):  1.62E4
      CAO:     5.00E3
      MG(+2):  3.22E4
      MGO:     1.00E4
PERCENT AL, SI, CA, MG VOLATILIZATION AT EQUILIBRIUM
  FOR 1200-1300K OPERATIONS: AL= 0.02%; SI= 0%; CA= 0%; MG= 0%
```

APPENDIX B

SOLUBILITY OF ALUMINOSILICATE COMPLEXES[95]

Solubility of Water in $KAlSi_3O_8$ (ℓ):

18.1 ± 0.3 mol % at 1283 K and 2430 kPa
25.9 ± 0.2 mol % at 1231 K and 6250 kPa

Solubility of water in $KAlSi_2O_6$ (ℓ):

26.8 ± 0.2 mol % at 1228 K and 4000 kPa
32.1 mol % at 1194 K and 6150 kPa

Solubility of water $0.75KAlSi_3O_8$-$0.25SiO_2$:

17.6 ± 1.3 mol % at 1184 K and 3000 kPa
23.3 mol % at 1185 K and 4960 kPa

Composition of aqueous phases in equilibrium with:

Liquid $KAlSi_2O_6$

at 1206 K and 4000 kPa:
0.13 mol % K_2O, 0.12 mol % Al_2O_3, 0.49 mol % SiO_2, 99.26 mol % H_2O
at 1187 K and 6000 kPa:
0.41 mol % K_2O, 0.44 mol % Al_2O_3, 1.69 mol % SiO_2, 97.46 mol % H_2O

Crystalline $KAlSi_2O_6$

at 1123 K and 4000 kPa:
0.15 mol % K_2O, 0.12 mol % Al_2O_3, 0.42 mol % SiO_2, 99.31 mol % H_2O
at 1011 K and 6550 kPa:
0.44 mol % K_2O, 0.56 mol % Al_2O_3, 1.18 mol % SiO_2, 97.82 mol % H_2O

Composition of aqueous phases in equilibrium with:
Liquid $KAlSi_3O_8$
at 1238 K and 3000 kPa:
0.034 mol% K_2O, 0.031 mol % Al_2O_3, 0.343 mol % SiO_2, 99.59 mol% H_2O
at 1153 K and 6200 kPa:
0.26 mol % K_2O, 0.22 mol % Al_2O_3, 1.42 mol % SiO_2, 98.10 mol % H_2O
Crystalline $KAlSi_3O_8$
at 1111 K and 2800 kPa:
0.02 mol % K_2O, 0.02 mol % Al_2O_3, 0.20 mol % SiO_2, 99.76 mol % H_2O
at 1035 K and 5900 kPa:
0.15 mol % K_2O, 0.15 mol % Al_2O_3, 1.02 mol % SiO_2, 98.68 mol % H_2O

Composition of aqueous phases at equilibrium with:
Liquid 0.75 $KAlSi_3O_8$-0.25 SiO_2
at 1179 K and 3000 kPa:
0.018 mol % K_2O, 0.016 mol % Al_2O_3, 0.561 mol % SiO_2, 99.405 mol % H_2O
at 1121 K and 6700 kPa:
0.23 mol % K_2O, 0.22 mol % Al_2O_3, 2.33 mol % SiO_2, 97.22 mol % H_2O

COMMENT AND CONCLUSIONS

Data show an increase in the water solubility of the akali aluminosilicate phases with increasing $K_2O/(Al_2O_3 + SiO_2)$ ratio in the melt. The increase is linearly proportional to the increase in the $K_2O/(Al_2O_3 + SiO_2)$ mole ratio, suggesting either that the increasing mol percent of alkali cations permits the hydroxyl ions to penetrate the Si-O bond more easily or that the alkali cations are hydrated directly, accounting for the increase in phase solubility.

APPENDIX C

CHEMICAL ANALYSIS OF TRACE AND MINOR ELEMENTS IN COMBUSTION PRODUCTS

TABLE C-1 - EXXON MINIPLANT SSMS COAL, SORBENT AND ASH ANALYSIS FROM RUN 50.5[108] , wt%

Dwg. 7729A03

ELEMENT	COAL	DOLOMITE	BED REJECT	2° CYCLONE	COARSE PARTICLES >3μm	FINE PARTICLES <3μm	FLUE GAS **
Be*	0.1	0.01	0.3	0.15	3	4	<0.13 (1.42)
F*	0.2	10	0.3	3	15	15	58.0 (38.22)
Hg*	0.2	<0.4	<0.3	<0.4	<0.4	<0.4	1.116 (4.79)
Pb*	32	1.5	1	20	40	40	2.01 (0.07)
Co*	3	<1	1.5	3	20	30	122.8 (43.42)
Cr*	36	5	30	200	200	300	250 (7.57)
Fe	0.64	0.1	1	10	2	6	9702 (1.65)
Mo*	2	1	2	7	3	5	29.0 (15.02)
Mn*	5	100	100	300	50	200	583 (33.88)
Ni*	6	100	150	700	100	400	136.2 (7.26)
Ti	0.04	0.003	0.02	0.7	0.3	0.7	37.95 (0.10)
Na	0.028	0.1	0.03	0.1	0.07	0.15	388.4 (1.01)
K	0.2	0.5	1	0.6	0.15	0.30	58.04 (0.02)
Al	2.4	0.06	1.5	15	20	20	776.9 (0.04)
Si	6.4	0.15	0.15	15	20	20	5,822 (0.10)
Br*	16	6	3	1.5	2.5	10	1,165 (76.75)
B*	5	10	30	30	50	50	194.2 (33.31)
P	0.0032	0.0001	0.0050	0.03	0.05	0.1	6.697 (0.23)
Cu*	16	3	15	50	30	70	11.16 (0.75)
V*	16	1	20	200	50	200	4.46 (0.31)
Zn*	32	2	400	40	20	70	29.0 (1.00)
Sb*	1	<0.1	1	0.4	0.7	2	0.67 (0.73)
Sn*	0.2	<0.2	2	1	2	6	2.23 (10.80)
Zr*	4	0.3	10	200	100	100	0.27 (0.07)
As*	10	20	20	40	10	30	6.697 (0.57)
Cd*	0.05	<0.5	<0.5	<1.5	<1.5	<1.5	1.339 (11.97)
Se*	3	0.6	3	1.5	5	15	82.60 (29.75)
Ga*	3	0.2	7	70	10	60	0.67 (0.25)
Ge*	0.3	0.7	40	20	3	15	4.46 (12.28)

* μg/g

**μg/m^3, 298 K, 101.3 kPa

( ) PERCENT RATIO OF MASS OF THE ELEMENT IN THE STREAM TO THE TOTAL MASS OF THE ELEMENT IN ALL OF THE INPUT STREAMS

Dwg. 7728A99

TABLE C-2 - EXXON MINIPLANT SSMS COAL AND ASH ANALYSIS FROM RUN 109 , μg/g

ELEMENT	LAND MATE	ILLINOIS COAL	PFIZER DOLOMITE	INITIAL BED	FINAL BED	BED OVERFLOW	2^0 CYCLONE
Be	0.03	▨ 3	0.01	▨ 0.5	▨ 0.5	▨ 0.8	▨ 2
F	75	<2	34	17	30	17	17
Hg	0.02	▨ <10	▨ <1	▨ <1	▨ <1	▨ <1	▨ <1
Pb	0.10	▨ <2	0.1	0.1	0.1	0.1	▨ 14
Co	3	▨ 30	3	2	1	2	3
Cr	0.5	▨ 130	▨ 12	▨ 40	▨ 40	▨ 120	▨ 40
Fe	0.5	▨ ~7%	▨ 180	▨ 6000	▨ 6000	▨ 6000	▨ 6000
Mo	14	12	2	8	8	8	8
Mn	0.2	▨ 200	▨ 40	▨ 40	▨ 40	▨ 120	▨ 40
Ni	0.02	▨ 200	▨ 3	▨ 100	▨ 100	▨ 100	▨ 100
Ti	2	▨ 210	▨ 15	▨ 300	▨ 400	▨ 300	▨ 1000
Na	90	▨ 5000	▨ 350	▨ 1000	▨ 3500	▨ 1000	▨ 1000
K	1720	▨ ~1%	300	1000	▨ 2000	500	▨ 3000
Al	2	▨ ~10%	▨ 500	▨ ~1%	▨ ~1%	▨ 5000	▨ ~2%
Si	21	▨ ~8%	▨ 2000	▨ ~2%	▨ ~2%	▨ ~2%	▨ ~2%
Br	1	0.3	▨ 5	▨ 2	▨ 2	▨ 2	▨ 2
B	324	▨ 400	5	100	100	100	100
P	0.001	▨ 300	▨ 0.2	▨ 120	▨ 120	▨ 120	▨ 120
Cu	1	▨ 70	▨ 4	▨ 20	▨ 20	▨ 35	▨ 35
V	0.30	▨ 130	▨ 2	▨ 30	▨ 30	▨ 40	▨ 100
Zn	1	▨ 30	▨ 10	▨ 20	▨ 10	▨ 4	▨ 10
Sb	0.40	▨ 4	0.2	0.4	0.4	▨ 1	▨ 1
Sn	3	1	0.8	0.8	2	2	2
Zr	15	▨ 20	0.1	8	▨ 40	14	▨ 40
As	0.1	▨ 10	▨ 8	▨ 8	▨ 2	▨ 8	▨ 8
Cd	0.004	▨ 2	▨ <0.2	▨ <0.2	▨ <0.2	▨ <0.3	▨ <0.7
Se	0.05	▨ <5	▨ <0.1	▨ <1	▨ <1	<0.03	<0.03
Ga	14.9	▨ 30	0.2	2	2	3	3
Ge	18	▨ 30	0.1	15	15	▨ 40	10

▨ MATE EXCEEDED

COMMENTS AND CONCLUSIONS

SSMS analysis of the feedstock and resulting solid formations from the Exxon miniplant run 50 series and run 69 indicate that Be, As, Se, Cd, Sb, Hg, and Pb exceed the determined land MATE values. With the exception of that of As, the concentration of the elements are three times higher in the 2° cyclone material than in that determined for the bed overflow material of run 50. A similar correlation was observed between the ash content formed at each location. From run 69 the concentrations of Be, Cd, and Sb were twice as high in the 2° cyclone material as in the bed overflow material. Again, the ash content of the 2° cyclone material was approximately twice that of the bed overflow. No correlation was observed between the resulting toxic trace element concentrations and the different operating conditions, as shown below.

MINIPLANT COMBUSTOR OPERATING CONDITIONS

Conditions	Run 50.2	Run 50.4	Run 50.5	Run 69
Date	3/30/77	3/31/77	3/31/77	3/16/78
Pressure, kPa	900	900	900	930
Bed Temperature, °C	805	890	890	947
2nd Cyclone Temperature, °C	743	816	831	910
Particulate Temperature, °C	204	204	204	427
Superficial Velocity, m/s	1.2	1.3	1.4	1.8
Expanded Bed Height, m	3.2	3.3	3.3	3.0
Excess Air, %	63	40	40	14
Coal Feed Rate, kg/hr	71.0	83.5	86.3	132
Sorbent Feed Rate, kg/hr	10.9	12.8	13.2	48
Coal Type	CH	CH	CH	IL
Sorbent Type	P.D.	P.D.	P.D.	P.D.

CH - Champion Coal (2% S) + Kentucky Coal (0.6% S) impurities

IL - Illinois Coal No. 6 (4% S)

P.D. - Pfizer No. 1337 Dolomite

From the analytical results obtained in the run 50 series, Be, As, Se, Cd, Sb, and Pb are more concentrated in the finer particulate (<10μm) than in the coarser 2° cyclone particulate (>10μm).

TABLE C-3 - CONCENTRATION OF MAJOR, MINOR AND TRACE ELEMENTS IN SOLID STREAMS IN THE 6-INCH FBC UNIT AT BATTELLE-COLUMBUS LABORATORY[110], ppmw

Dwg. 1714B51

ELEMENT	ILLINOIS #6 COAL	GROVE LIMESTONE	BED MATERIAL	PARTICULATES	
				>27μm	<27μm
Be	0.17, (2)	<0.18, (<0.006)	<0.18, (<0.006)	2.6, (0.2)	6.0, (2)
F	110, (<3)	140, (<10)	170, (<3)	290, (<5)	450, (<20)
Hg	0.16, (<2)	<0.01, (<0.3)	<0.01, (<0.3)	<0.01, (<0.3)	14, (<0.3)
Pb	0.47, (<1)	0.86, (3)	1.9, (1)	4.3, (20)	43, (100)
Co	4.0, (10)	0.14, (0.3)	0.14, (0.3)	2.1, (10)	14, (10)
Cr	13, (100)	0.87, (5)	1.3, (10)	15, (100)	87, (100)
Fe	>1%, (~5%)	~1200, (~0.02%)	~4600, (~0.1%)	>1%, (~2%)	>1%, (~2%)
Mo	2.9, (30)	0.67, (<3)	1.2, (<3)	3.3, (20)	14, (10)
Mn	80, (100)	15, (100)	26, (20)	60, (200)	60, (500)
Ni	33, (<10)	0.69, (<2)	23, (<2)	23, (200)	99, (100)
Ti	240, (5000)	87, (2)	130, (2)	870, (1000)	~2200, (~1%)
Na	890, (~2%)	140, (200)	320, (200)	~1400, (3000)	>0.5%, (5000)
K	~1200, (~0.6%)	>0.5%, (~0.3%)	~1600, (~0.2%)	>0.5%, (~1%)	>1%, (~2%)
Al	>1%, (~5%)	~3000, (~0.1%)	~3000, (~0.1%)	>1%, (~5%)	>1%, (~5%)
Si	>1%, (~20%)	<1%, (~1%)	>0.5%, (~0.5)	>1%, (~20%)	>1%, (~20%)
Br	4.7, (10)	1.2, (0.5)	4.5, (1)	6.0, (0.5)	60, (1)
B	93, (0.03)	6.2, (1)	33, (5)	500, (50)	~2000, (300)
P	3.2, (100)	140, (10)	310, (20)	310, (50)	310, (200)
Cu	9.0, (30)	2.2, (2)	78, (3)	66, (50)	120, (50)
V	20, (500)	7, (10)	7, (10)	25, (500)	140, (1000)
Zn	37, (<10)	4.0, (<3)	17, (<3)	6.7, (<3)	140, (<3)
Sb	0.56, (<0.5)	N.R. , (<0.1)	N.R. , (<0.2)	0.67, (0.2)	1.4, (1)
Sn	0.28, (<1)	0.12, (<1)	0.55, (<1)	1.2, (<2)	12, (10)
Zr	10, (300)	7.0, (3)	28, (20)	35, (200)	120, (200)
As	2.7, (<3)	<0.61, (<0.5)	0.67, (1)	4.1, (1)	6.1, (3)
Cd	0.10, (<30)	N.R. (<3)	0.14, (<10)	0.67, (<3)	1.0, (<3)
Se	0.29, (<5)	N.R., (<1)	N.R., (<2)	0.94, (<5)	8.4, (<5)
Ga	1.7, (<5)	0.23, (<0.5)	1.1, (<0.5)	2.3, (<5),	11, (<10)
Ge	2.0, (100)	N.R., (<0.2)	1.4, (10)	3.0, (3)	14, (10)

• RUN 1, (RUN 2)

N.R. – NOT REPORTED

COMMENTS AND CONCLUSIONS

Test Parameters for the 6 in FBC unit at the Battelle-Columbus Laboratory, Ohio

Conditions		Run 1	Run 2
Coal feed rate, lb/hr		15.9	8.8
Limestone feed rate, lb/hr		15.4	4.3
Air feed rate, lb/hr		145.0	87.3
Bed height:	expanded, in	48	48
	settled, in	12.6	21.6
Bed Temperature, °F		1538	1655
Superficial gas velocity, ft/s		9.1	6.0
Ca/S ratio		6.7:1	2.9:1
Particulate loading, g/m^3		1.44	1.64

A net increase in the trace element concentration is observed as a function of decreasing particle size.

Dwg.7729A01

TABLE C-4 - TRACE AND MINOR ELEMENT CONCENTRATION IN COAL, SLAG, INLET AND OUTLET FLY ASH FORMATIONS AT THE ALLEN STEAM PLANT [99] , μg/g

ELEMENT	COAL	SLAG	PRECIPITATOR INLET	PRECIPITATOR OUTLET
Be				
F				
Hg	99* (0.122)	0.08 (0.028)	0.06 (0.050)	–
Pb	7.4 (4.9)	4.5 (6.2)	142 (80)	– (650)
Co	3.95 (2.9)	20.3 (20.8)	38 (39)	42 (65)
Cr	22 (18)	160 (152)	255 (300)	300 (900)
Fe	15890 (10850)	111300 (112000)	111000 (121000)	165000 (150000)
Mo	34 (9)	(21)	(210)	(450)
Mn	53 (33.8)	420 (295)	328 (298)	460 (430)
Ni	(16)	(85)	(210)	(220)
Ti	550 (506)	2930 (410)	276 (5980)	2950 (10000)
Na	677 (696)	3160 (5000)	58.20 (10100)	3400 (11300)
K	2180 (1540)	11650 (15800)	15500 (20000)	10600 (24000)
Al	11290 (10440)	78195 (102300)	65450 (90900)	200000 (76000)
Si	(23100)	(229000)	(196000)	
Br	2.3 (3.7)	<0.5 (2)	<5 (~4)	10
B				
P				
Cu	66 (8.3)	233 (20)	333 (140)	333 (170)
V	37 (28.5)	256 (260)	420 (440)	230 (1180)
Zn	97	22.6	1420	–
Sb	>1 (0.5)	>2 (0.64)	3.2 (12)	– (55)
Sn				
Zr				
As	4.3 (5)	3.8 (18)	32 (110)	94 (440)
Cd	0.46 (0.47)	3.2 (11)	5.5 (8.0)	5.2 (51)
Se	3.0 (2.2)	12 (0.08)	24 (25)	500 (88)
Ga	(4.5)	(5)	71 (81)	93
Ge				

* 1972 DATA; ( ) INDICATE 1973 DATA

COMMENTS AND CONCLUSIONS

Results by neutron activation analysis of coal, slag, and precipitator inlet and outlet ash formation from the 290 MW cyclone unit burning 106 tons/hr of coal from Kentucky and southern Illinois (moisture = 9.5-13.4%; volatile material = 34.0-35.7%; fixed carbon = 40.5-43.1%; ash = 10.4-13.4%; Btu/g = 10740-11390; sulfur = 3.1 - 3.5%) at the Allen Steam Plant, Memphis, TN[99] are shown in Table G-4. These results categorize the elements as:

- Class I - Elements that showed approximately equal concentrations in all phases of the ash sample. This class included Al, Ba, Ca, Ce, Co, Eu, Fe, Hf, K, La, Mg, Mn, Rb, Sc, Si, Sn, Sr, Ta, Th, and Ti.
- Class II - Elements that showed enrichment in the fly ash. This class included As, Cd, Cu, Ga, Pb, Sb, Se, and Zn. These elements were concentrated in the inlet fly ash as compared to the bottom ash, and in the outlet fly ash as compared with the inlet fly ash.
- Class III - Elements that remained essentially completely in the vapor phase. This class included Hg, Cl, and Br.

The other elements analyzed in this study (Cr, Cs, Na, Ni, U, and V) could not be assigned to a specific class on the basis of the data alone, but, they seem to be intermediate between Class I and Class II.

Soil compositions were sampled at 1-mile intervals from 20 miles south to 20 miles north of the plant. The elements that are concentrated in the plant's fly ash above the values for Memphis area soils or similar soils around the world are Se, B, Cu, Ni, Cd, Pb, As, V, Zn, Ga, Ge, and Li. If the high concentrations of trace elements in the soil near Allen were due to fly ash fallout, a sharp decrease in concentration with depth might be expected. However, there was no appreciable concentration change with soil depth for Cd, Zn, Pb, Cu, As, and V. For the remaining elements the background data for soils was limited. Although inconclusive data were presented, the environmental samples did not indicate any major impact of emissions from the plant on the trace element concentration in the surrounding environment.

Partitioning of the trace and minor elements as a function of particle size for the Allen Steam Plant is illustrated in Figures C-1 and C-2. Neutron activation analyses demonstrate neither a significant enrichment nor a depletion of the elements, as particle size is varied between 1 and 15 µm for both the inlet and the outlet precipitator ash.

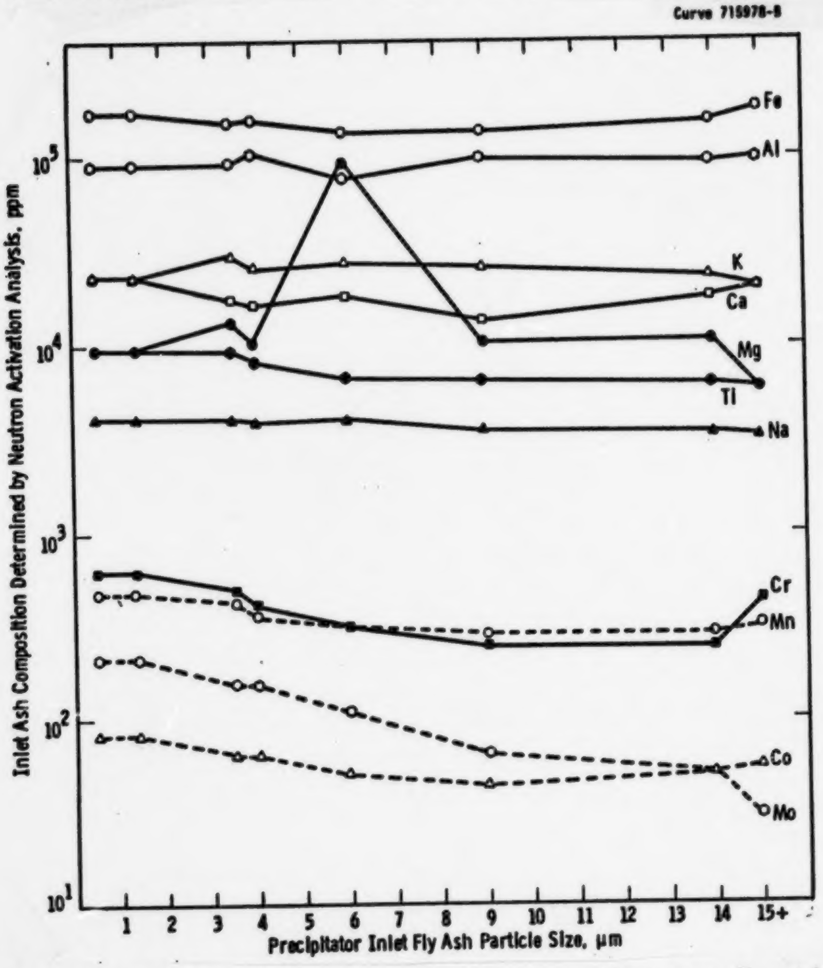

Figure C-1 - Trace and Minor Element Concentration as a Function of Precipitator Inlet Fly Ash Particle Size at the Coal-Fired Allen Steam Plant, Memphis, Tennessee [1]

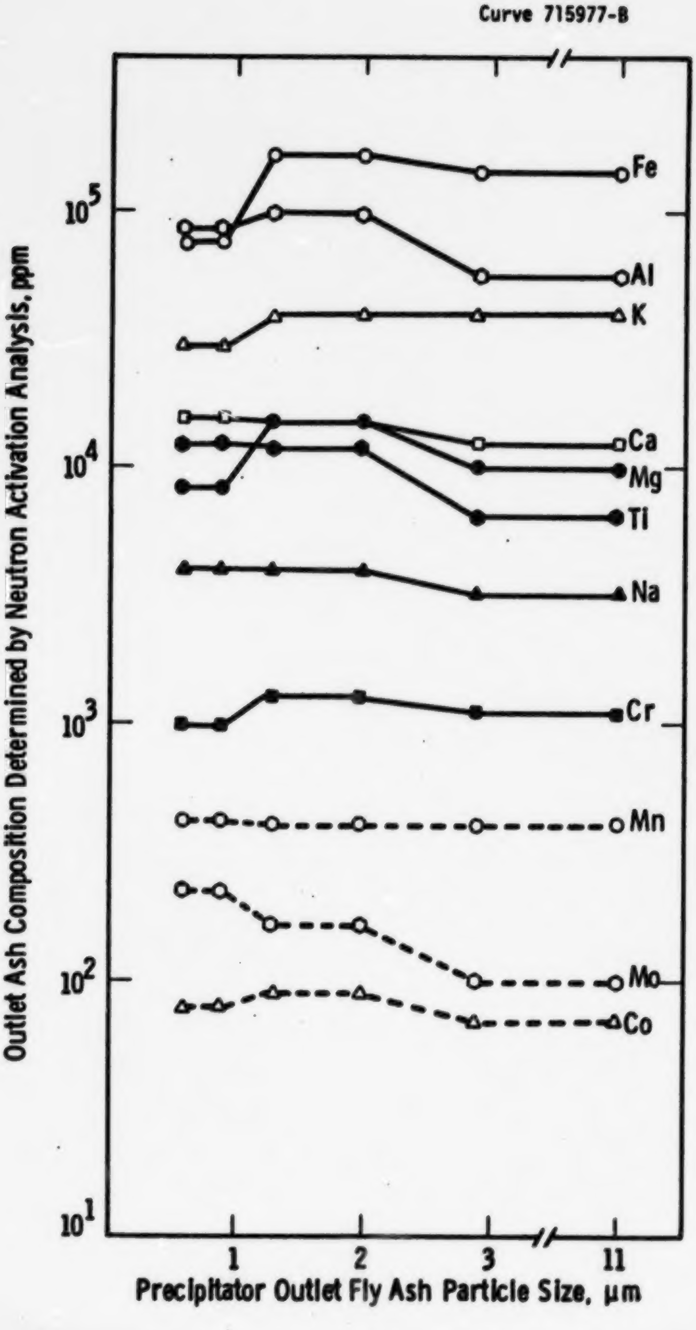

Figure C-2 - Trace and Minor Element Concentration as a Function of Precipitator Outlet Fly Ash Particle Size at the Coal-Fired Allen Steam Plant, Memphis, Tennessee[1]

TABLE C-5 - POLLUTANT CONCENTRATION (AVERAGE PPM) IN COAL, ASH AND FLUE GAS STREAMS AT THE WIDOWS CREEK STEAM PLANT[9]

Dwg.7729A04

ELEMENT	COAL	BOTTOM ASH	SUPERHEATER ASH	INLET FLY ASH	DUST COLLECTOR ASH	OUTLET FLY ASH
Be	1.5	7.3	6.1	8.0	7.9	9.3
F	121	10.6	42.2	624	29.5	671
Hg	1.91	<0.51	<18.0	20.0	<1.18	17.0
Pb	3.72	8.10	10.6	32.0	14.9	36.6
Co	1.45	3.63	4.75	5.98	7.93	3.69
Cr	24	124	115	206	151	220
Fe	23200	212900	254400	142600	129900	113000
Mo						
Mn	35	229	269	249	241	201
Ni	15	62	101	134	82	126
Ti	895	6150	5370	6450	5120	6890
Na						
K						
Al						
Si						
Br						
P						
Cu	10	48	48	68	57	74
V	62	353	262	341	235	415
Zn	55	150	143	352	150	366
Sb	<1.1	1.3	0.90	<0.95	<0.9	1.5
Sn	1.69	2.03	1.93	2.81	2.89	1.92
Zr						
As	14.3	5.8	7.0	8.4		8.3
Cd	0.99	1.08	1.60	6.44	2.01	8.09
Se	<6.1	<5.6	<5.8	26.5	<12.5	<16.7
Ga						
Ge						
POM (1)	4.7	<0.2			0.2	
POM (2)		<0.2				
POM (3)		<0.2				
PCB		0.02	0.09		0.07	

(1) 7, 12 – DIMETHYLBENZ[a] ANTHRACENE

(2) 3, 4 – BENZOPYRENE

(3) 3 – METHYLCHOLANTHRENE

COMMENTS AND CONCLUSIONS

Major findings of this study were as follows:

- The mass balance for approximately half the elements was closed within acceptable limits of 20 to 25 percent. The causes of the imbalance were inefficient collection of the vaporous metals in the flue gases and analytical errors, particularly in the analysis of coal.

- An enrichment of the various trace constituents occurred to a moderate degree in the cooler ash streams and to a higher degree in the finer particles of the fly ash.

TABLE C-6 - ESTIMATED CONCENTRATION RANGES OF POTENTIAL POLLUTANTS FROM COAL-FIRED FLUIDIZED-BED COMBUSTION[133,134]

Gas phase	
Several hundred ppm:	CH_4, CO, HCl, SO_2, NO
Ten ppm:	SO_3, C_2H_4, C_2H_6
One ppm:	HF, HCN, NH_3, $(CN)_2$, COS, H_2S, H_2SO_4, HNO_3, F, Na
One ppb:	Diolefins, aromatic hydrocarbons, phenols, azoarenes, As, Pb, Hg, Br, Cr, Ni, Se, Cd, U, Be
One-tenth (0.1) ppb:	Carboxylic acids, sulfonic acids, chlorinated hydrocarbons, alkynes, cyclic hydrocarbons, amines, pyridines, pyroles, furans, ethers, esters, epoxides, alcohols, ozone, aldehydes, ketones, thiophenes, mercaptans
Solids	
One ppm:	Al, Ca, Fe, K, Mg, Si, Ti, Cu, Zn, Ni, U, V
One ppb:	Ba, Co, Mn, Rb, Sc, Sr, Cd, Sb, Se, Ca
One-tenth (0.1) ppm:	Eu, Hf, La, Sn, Ta, Th

COMMENTS AND CONCLUSIONS

Sparse experimental information is available for most of these compounds, and the estimates based on simple thermodynamic considerations and empirical correlation with conventional combustion systems are probably good only within an order of magnitude. Nitrogen oxide, sulfur dioxide, and carbon monoxide are the only compounds generated in quantities high enough to be of concern, yet they are significantly less than those generated in conventional combustion systems.

TABLE C-7 - PROJECTED EMISSIONS OF TRACE ELEMENTS FROM CONVENTIONAL AND FLUIDIZED-BED COMBUSTORS EXPRESSED AS PERCENTAGES OF ELEMENTS ENTERING THE SYSTEM[141]

Element	Conventional Combustion, %	Fluidized-Bed Combustion, %
Hg	90-100	80
F	90-100 (estimated)	40
Br	90-100	65
As	0-60	15
Pb	10	0-20
Be	Not available	20-40
Sc	10	0
Cr	0	25
Co	10-20	0-20
Na	0-10	5
K	0-10	10
Fe, La, Mn	0	0

COMMENTS AND CONCLUSIONS

ANL results indicate that trace element emissions to the environment from fluidized-bed combustions would be less than that expected from a conventional coal-fired boiler. This conclusion was based on a comparison of

- Open mass balance made around the ANL 15.2-cm-dia. pressurized, fluidized-bed combustor, with
- Similar mass balances reported for conventional coal-fired boilers.

The following observations were reported:

- No enrichment of Pb or Be is indicated to result in FBC fine fly ash. Conventional power plant studies have shown enrichment of Pb an order of magnitude higher in fine ESP ash than in coarser ash removed from a mechanical collector.

- The Cr concentration in the combustion ash products is lower than the concentration in the feedstock material. There appears to be no significant increase in the Cr concentration in the fly ash with decreasing particle size, as would be expected if Cr were lost through volatilization.

- Sodium and K show no increase in concentration in fly ash formed from the combustion of coal at bed temperatures of 1116 K, suggesting that neither Na nor K was volatilized during combustion. At 1172 K the concentration of Na does appear to increase significantly with decreasing particle size.

- The concentration of Ba, Co, La, Sb, Sc, and Ta showed slight tendencies to increase with decreasing ash particle size.

- The concentration of Fe in the primary cyclone fly ash is approximately the same as in the feedstock content. With succeeding stages of particulate removal the Fe content decreases by a factor of two, suggesting the possibility that the segregation of certain trace and minor elements by particle size in the resulting fly ash might be a function of the "grain" size of the discrete phases of mineral matter that host the various trace elements in the coal instead of being simply the consequence of volatilization during combustion.